

Improving Magnetic Particle Technology (MPT) for the Rehabilitation of Oiled Wildlife

Linda Diep

Bachelor of Science (Biological Sciences)

Bachelor of Science (Honours)

Thesis submitted in fulfilment of the requirements for the degree of

Doctor of Philosophy

Victoria University, Australia

Institute for Sustainable Industries & Liveable Cities

December 2023

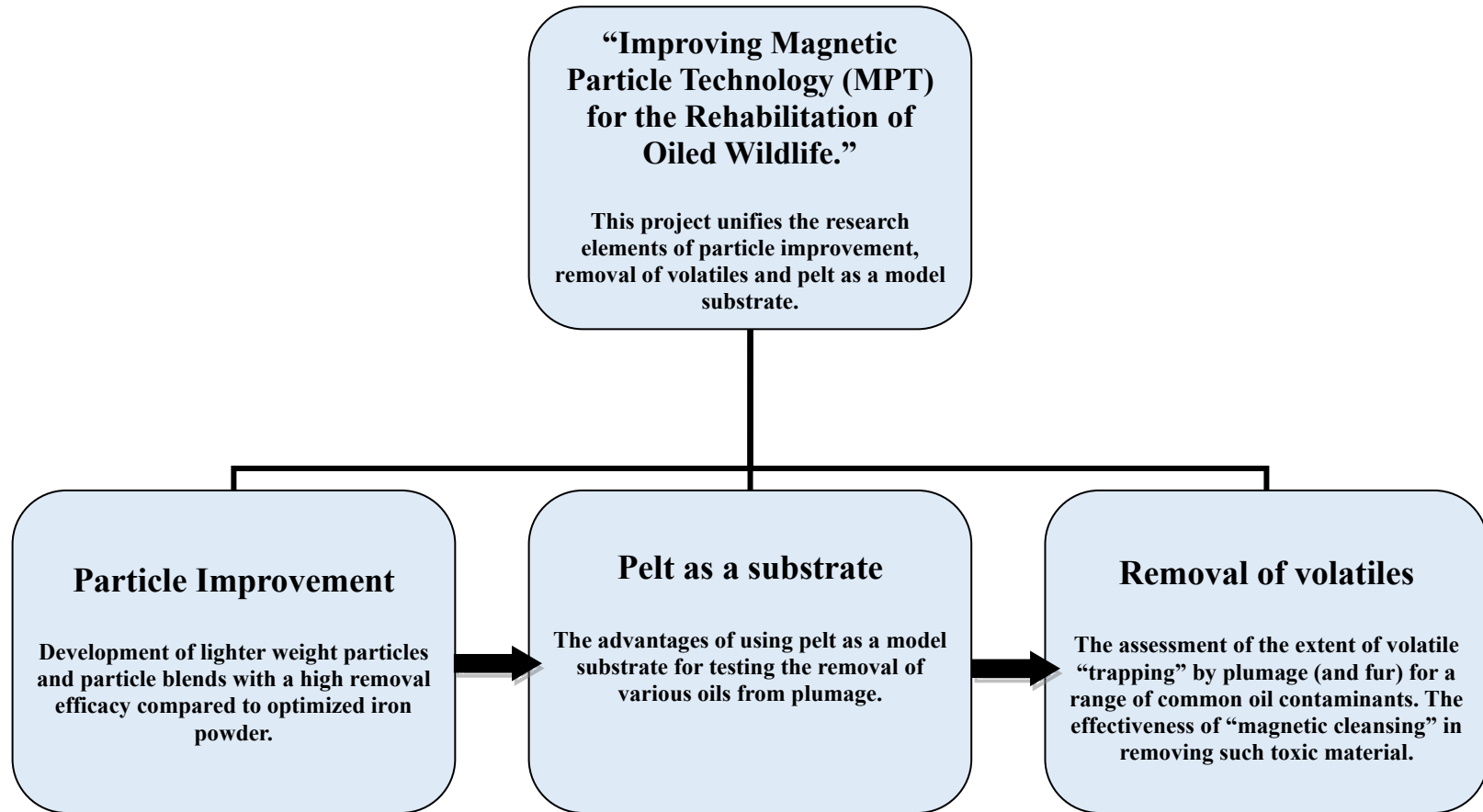
Abstract

The traditional method for cleaning and rehabilitating oil contaminated wildlife involves the capture of the animal, an initial stabilization protocol, transportation to a treatment facility, cleansing with surfactant/warm water, and a recovery process. Despite numerous successes using this approach, it is extremely time and labor intensive and is stressful to the animal. Unfortunately, there remains a paucity of research into advancing the science and technology associated with the rescue and rehabilitation of oiled wildlife. In this regard, the Animal Rehabilitation Technology (ART) group at Victoria University, Melbourne, Australia, has developed oil adsorbing magnetic particles that effectively provide a “dry clean”. This method, referred to as “magnetic cleansing”, offers advantages over the traditional method. For example, it is relatively low cost, is more benign with respect to feather damage and is highly portable. Potentially, this technology will benefit the survival of affected wildlife worldwide but is of particular significance with respect to the protection of Victoria’s iconic Little Penguin population. The famous “Penguin Parade” at the Phillip Island Nature Parks is an important contributor to Victoria’s economy, providing significant employment in the region. Given the ever-present threat of oil contamination, it is crucial that all measures are taken to prepare for such events and that the finest available technology is in place to best deal with such challenges, when they occur.

The overall aim of this project is to further improve the application of this novel technology. Therefore, an existing database related to the removal of different % coverages of Diesel Fuel Oil from carcasses of Little Penguin has been analyzed with respect to generating logistical information on providing a “quick clean” to remove the most volatile and corrosive components, upon first encounter. Thus, several contamination-event scenarios have been assessed for a two-person team and relevant parameters, including the number of contaminated animals, the average % coverage, the % removal after 1 and 2 treatments, the time taken for 1 and 2 treatments, the mass of magnetic particles required, and the mass of oil-laden particles to be transported post-treatment. This analysis has demonstrated the feasibility of incorporating a magnetic cleansing “quick clean” into existing stabilization protocols for the rapid on-site removal (i.e., within minutes) of the most toxic and corrosive components. In this context, an attempt has also been made to improve the magnetic particles themselves, by making them lighter in weight but retaining

sufficient magnetic susceptibility. This has been shown to be possible by synthesizing and testing magnetic particles from different combinations of nanoparticulate magnetite and zeolite or sawdust. To quantitatively assess the efficacy of removal of different contaminants from feather and fur substrates, an assay has been developed and tested, based on quantifying the removal of different oils from Little Penguin pelt. This substrate has been demonstrated to be superior to feather clusters or whole animal carcasses. Finally, the relative physical characteristics of the evaporation of up to eleven different oils from Little Penguin pelt has been investigated. For each oil these studies have revealed a novel volatile fraction that evaporates within a ten-hour period, accompanied by an initial latency period (plateau). Weathering then continues for up to twenty days, whereby a new plateau is established that defines the total volatile fraction. Notably, it has also been revealed that some volatile components become trapped in the plumage. This is an important finding that supports the application of a “quick clean” to remove such chemicals as soon as possible.

Conceptual Framework



Declaration

“I, Linda Tu-Nhi Diep, declare that the PhD thesis entitled “**Improving the Magnetic Particle Technology (MPT) for the Rehabilitation of Oiled Wildlife**” is no more than 80,000 words in length including quotes and exclusive of tables, figures, appendices, bibliography, references and footnotes. This thesis contains no material that has been submitted previously, in whole or in part, for the award of any other academic degree or diploma. Except where otherwise indicated, this thesis is my own work”.

“I have conducted my research in alignment with the Australian Code for the Responsible Conduct of Research and Victoria University’s Higher Degree by Research Policy and Procedures”.

A solid black rectangular box used to redact the signature of Linda Diep.

Linda Diep

28/12/23

Date

***DEEPEST GRATITUDE AND DEDICATION TO MY BELOVED
FAMILY***

Acknowledgements

First of all, I would like to express my gratitude and thank you Buddha, God of the Soil and my Ancestors for giving me the strength, granting countless blessings and guiding me to achieve my goals.

I would like to dedicate, this special acknowledgment to my principal supervisor, Professor John Orbell and co-supervisor Dr. Lawrence Ngeh at Victoria University. Their excellent guidance and expert advice of Professor John and Dr. Lawrence has helped me overcome this challenging nature in completing my PhD Thesis. Without the support of my two great supervisors I wouldn't have acquired the skills necessary to conduct this research. I really appreciate all of the skills that I have gained and it was a privilege to work with both of my supervisors. Thank you Professor John and Dr. Lawrence for their endless support, encouragement and continual care that you have provided me during my PhD journey which I will always keep in memory.

I sincerely would like to thank all of my supervisors and VU technical staff for their exceptional support and assistance throughout the course of my research project. I would also like to take this opportunity to thank Dr. Peter Dann at Phillip Island Nature Parks for providing biological specimens to conduct my research and thank you Professor Stephen Bigger at Victoria University for developing the mathematical modelling software.

I am very grateful and would like to express my gratitude to my Grandparents, Mum and Dad, Little Brother, relatives and friends for their endless love, unconditional care and support that you have provided me. Thank you Dad, Mum and brother Danny for always being there for me and all the love you have given.

Journal Publications, Conference Presentations and Awards

Refereed Journal Articles

1. Diep, L., Bigger, S.W., Dann, P., Ngeh, L.N., Dao, H.V., Shewan, A., & Orbell, J.D. 2024. The use of Little Penguin pelt as a model substrate for the assessment of the efficacy of oil removal via ‘magnetic cleansing’. *Methods in Ecology and Evolution*, in preparation.
2. Diep, L., Bigger, S.W., Dann, P., Ngeh, L.N., Dao, H.V., Shewan, A., & Orbell, J.D. 2024. A novel “quick clean” technology for the rapid removal of volatiles from contaminated wildlife. *Marine Pollution Bulletin*, in preparation.
3. Diep, L., Bigger, S.W., Dann, P., Ngeh, L.N., Dao, H.V., Shewan, A., & Orbell, J.D. 2024. The existence of two distinct volatile fractions in the evaporation of oil contamination from plumage. *Journal of Hazardous Materials*, in preparation.

Presentations at International Conferences

1. Orbell, JD, Dann, P, Bigger, SW, Ngeh, LN, Diep, L, Shewan, A, ‘*Penguin pelt as a substrate for the testing of oil contamination removal efficacy via magnetic particle technology (MPT)*’, the 10th International Penguin Conference, Dunedin, New Zealand, 24 August – 28 August, 2020.
2. Orbell, JD, Dann, P, Bigger, SW, Ngeh, LN, Diep, L, Shewan, A, ‘*Novel “quick clean” technology for the rapid removal of volatiles from contaminated wildlife*’, the 14th International effects of Oiled on Wildlife (EOW) Conference, Long Beach Hilton, California, USA, 26 September – 30 September, 2022.

Other Presentations

1. Diep, L, '*Advancing the Science and Technology of Oiled Wildlife Treatment – During a Pandemic*', Victoria University ISILC HDR Student Research Conference, Victoria University, Melbourne, Australia, 3 December, 2020.
2. Diep, L, '*Improving Magnetic Particle Technology (MPT) for the Rehabilitation of Oiled Wildlife*', Three Minute Thesis (3MT) Competition Victoria University, Victoria University, Melbourne, Australia, 10 August, 2022 (3MT Heats Showcase) and 7 September, 2022 (3MT VU Finals Showcase).

Awards

1. Winner of Best Talk for Technology Stream Award, 2020 Victoria University ISILC HDR Student Research Conference, Victoria University, Melbourne, Australia, 3 December, 2020.
2. Winner of Overall Best Presentation Talk Award, 2020 Victoria University ISILC HDR Student Research Conference, Victoria University, Melbourne, Australia, 3 December, 2020.
3. People's Choice Winner, Victoria University 3 Minute Thesis competition (3MT Heats Showcase), Victoria University, Melbourne, Australia, 10 August, 2022.
4. Runner Up, Victoria University 3 Minute Thesis competition (3MT VU Finals Showcase), Victoria University, Melbourne, Australia, 7 September, 2022.
5. People's Choice Winner, Victoria University 3 Minute Thesis competition (3MT VU Finals Showcase), Victoria University, Melbourne, Australia, 7 September, 2022.

Table of Contents

Abstract.....	ii
Declaration.....	v
Acknowledgements.....	vii
Journal Publications, Conference Presentations and Awards.....	viii
Table of Contents.....	x
List of Tables.....	xvi
List of Figures.....	xix
List of Abbreviations and Symbols.....	xxvii
Chapter 1: Introduction.....	1
1.1 The effect of oil spills on the environment.....	3
1.1.1 Oil Spill Sources and Spill Rates.....	5
1.1.2 Major Oil Spills in the Ocean.....	6
1.1.3 Oil Spill Statistics.....	7
1.1.4 Major Oil Spills in History.....	8
1.1.5 Global Oil Spill Trend.....	10
1.2 The impact of oil spills on wildlife.....	11
1.3 Traditional techniques for environmental remediation.....	13
1.4 Rehabilitation of oiled wildlife.....	14
1.4.1 Current stabilization protocols for oiled birds.....	14

1.4.2	Stabilization and treatment protocols used at Phillip Island Nature Parks.....	15
1.4.3	Existing methods for cleaning and rehabilitation.....	17
1.4.4	Disadvantages of existing methods for cleaning and rehabilitation....	17
1.5	The “Magnetic Cleansing” method.....	17
1.5.1	Advantages of the “Magnetic Cleansing” method.....	19
1.6	Significance of the research.....	21
1.7	Aims and objectives.....	21
1.8	References.....	23
Chapter 2: An analysis of the logistics of providing an MPT "quick clean" to contaminated Little Penguins in the field.....		29
2.1	Introduction.....	30
2.2	Methodology - exploiting the AMSA database for logistical Information.....	37
2.3	Results and Discussion.....	39
2.4	Conclusion.....	47
2.5	References.....	47
Chapter 3: Improving the efficacy of oil-sequestering magnetic particles.....		50

3.1 Introduction.....	51
3.2 Materials and Methods.....	56
3.2.1 Chemicals.....	56
3.2.2 Preparation of "Magnetic Zeolite" (MZ) particles.....	56
3.2.3 Preparation of "Magnetic Sawdust" (MS) particles.....	57
3.2.4 Characterization of the magnetic particles.....	59
3.2.4.1 Particle size analysis.....	59
3.2.4.2 Particle flow characteristics.....	60
3.2.4.3 Magnetic "pull" experiments.....	62
3.2.4.4 Oil pick-up isotherms.....	63
3.3 Results and Discussion.....	65
3.3.1 "Magnetic Zeolite" (MZ) particles.....	65
3.3.2 "Magnetic Sawdust" (MS) particles.....	67
3.3.3 MZ particle analysis.....	68
3.3.4 MS particle analysis.....	71
3.3.5 The relative Particle Size Analyser (PSA) parameters.....	73
3.3.6 Compressibility and flow parameters.....	74
3.3.7 Magnetic pull experiments.....	75
3.3.8 Isotherms.....	76
3.4 Conclusions.....	91
3.5 References.....	92

Chapter 4: Penguin Pelt as a model substrate for the MPT assessment of oil removal from plumage.....100

4.1 Introduction.....102

4.1.1 Oil removal from a glass substrate.....104

4.1.2 Oil removal from feather clusters.....105

4.1.3 Oil removal from plumage (carcass).....105

4.1.4 Oil removal from pelt.....106

4.2 Methodology for the removal of different oil types.....109

4.2.1 Removal from feather clusters.....109

4.2.2 Removal from pelt.....109

4.2.3 Removal from whole bird model (carcass).....110

4.3 Materials and equipment.....111

4.3.1 Materials.....111

4.3.2 Equipment.....112

4.4 Results and Discussion.....112

4.4.1 The importance of pelt sample size in relation to oil type.....112

4.4.1.1 Removal of Gippsland crude oil.....112

4.4.1.2 Removal of Diesel oil.....115

4.4.1.3 Removal of Engine oil.....117

4.4.1.4 Removal of Bunker oil 1 (BO1).....117

4.4.2 Recycling of pelt samples.....121

4.4.2.1 Experimental method.....121

4.4.2.2	The recycling ('washing') process.....	121
4.4.2.3	Removal of Gippsland Crude Oil from recycled penguin pelt.....	121
4.4.2.4	Removal of Diesel Fuel Oil from recycled penguin pelt.....	121
4.4.2.5	Removal of Engine Oil from recycled penguin pelt.....	125
4.4.2.6	Removal of Bunker Oil (BO1) from recycled penguin pelt.....	126
4.4.3	Mimicking the penguin's body temperature – removal from pelt at 40°C.....	128
4.4.4	The relationship between the removal isotherm profile and the percentage coverage of Diesel Fuel Oil on a Little Penguin plumage (carcass).....	130
4.5	References.....	134

Chapter 5: The characterization of the evaporation of crude oils from penguin pelt.....139

5.1	Introduction.....	140
5.1.1	Weathering.....	140
5.1.2	Volatiles in different oils.....	143
5.1.3	Research plan/experimental overview.....	150
5.2	Materials and Equipment.....	152
5.2.1	Crude oils investigated.....	152
5.2.2	Facilities.....	152
5.2.3	Equipment and substrate materials.....	153

5.3 Methodology and experiments conducted.....	154
5.4 Mathematically modelling the data.....	159
5.5 Results and Discussion.....	160
5.5.1 Block 1 (Experiments 1 & 2).....	169
5.5.2 Block 2 (Experiments 1 & 3).....	170
5.6 The discovery of the “Highly Volatile Fraction” (HVF).....	174
5.7 References.....	180
Chapter 6: Overview.....	187
Appendices.....	191

List of Tables

Table 1.1: North America Spill Statistics.....	7
Table 1.2: Major tanker spills since 1967.....	8
Table 1.3: Historical major oil spills in or near Australian waters, and several smaller offshore spills (AMSA, 2020).....	9
Table 1.4: The number of Little Penguins treated annually at the animal rehabilitation facility of PINP from 1994 to 2000.....	12
Table 2.1: Scenario (10 birds), and for hypothetical 100 and 1000 birds (blue – one treatment; red – two treatments).....	40
Table 2.2: Logistical analysis – “In the field” scenario based on 10 birds.....	42
Table 2.3: Logistical analysis – “In the field” scenario based on 100 based birds.....	43
Table 2.4: Logistical analysis – “In the field” scenario based on 1000 based birds.....	44
Table 2.5: Cumulative time (h), total mass of powder (kg) and total mass of waste (kg) as a function of 1 treatment for 10% Diesel Oil coverage based on 10, 100 and 1000 birds.....	45
Table 2.6: Cumulative time (h), total mass of powder (kg) and total mass of waste (kg) as a function of 1 treatment for 20% Diesel Oil coverage based on 10, 100 and 1000 birds.....	45
Table 2.7: Cumulative time (h), total mass of powder (kg) and total mass of waste (kg) as a function of 1 treatment for 50% Diesel Oil coverage based on 10, 100 and 1000 birds.....	45
Table 2.8: Cumulative time (h), total mass of powder (kg) and total mass of waste (kg) as a function of 1 treatment for 70% Diesel Oil coverage based on 10, 100 and 1000 birds.....	45
Table 2.9: Cumulative time (h), total mass of powder (kg) and total mass of waste (kg) as a function of 1 treatment for 100% Diesel Oil coverage based on 10, 100 and 1000 birds.....	45
Table 2.10: Cumulative time (h), total mass of powder (kg) and total mass of waste (kg) as a function of 2 treatments for 10% Diesel Oil coverage based on 10, 100 and 1000 birds.....	46
Table 2.11: Cumulative time (h), total mass of powder (kg) and total mass of waste (kg) as a function of 2 treatments for 20% Diesel Oil coverage based on 10, 100 and 1000 birds.....	46

Table 2.12: Cumulative time (h), total mass of powder (kg) and total mass of waste (kg) as a function of 2 treatments for 50% Diesel Oil coverage based on 10, 100 and 1000 birds.....	46
Table 2.13: Cumulative time (h), total mass of powder (kg) and total mass of waste (kg) as a function of 1 treatment for 70% Diesel Oil coverage based on 10, 100 and 1000 birds.....	46
Table 2.14: Cumulative time (h), total mass of powder (kg) and total mass of waste (kg) as a function of 2 treatments for 100% Diesel Oil coverage based on 10, 100 and 1000 birds.....	46
Table 3.1: Composition of the eight magnetic zeolite (MZ) particle types and the two magnetic sawdust (MS) particle types that were formulated.....	58
Table 3.2: Parameters measured by the PSA instrument, together with their definitions....	60
Table 3.3: Interpretation of the Carr index and Hausner ratio with respect to flowability...	62
Table 3.4: PSA output parameters for the Fe powder control (blue), the MZ particles (black) and the MS particles (red).....	73
Table 3.5: Compressibility and flow parameters calculated as described in Section 3.2.4.2 for the Fe powder and the Fe ₃ O ₄ nanoparticle controls, pastes MZ 1 – 5 and MS 1 – 2.....	74
Table 3.6: Magnetic pull parameters were determined as described in Section 3.2.4.2 for the Fe powder, the Fe ₃ O ₄ nanoparticle controls and pastes M 1 – 5.....	75
Table 3.7: A comparative tabulation of the isotherm data from Figure 3.17 (yellow – glass substrate) and Figure 3.18 (green – feather clusters) respectively. P ₀ – P ₃ % is the oil removal (%), N ₀ is the total number of treatments.....	80
Table 4.1: Oil contaminants utilised in the experiment.....	111
Table 4.2: Comparison of the removal of Gippsland crude oil between plumage, pelt (large and small size) and feather cluster.....	113
Table 4.3: Comparison of the removal of Diesel oil between plumage and pelt (large and small size).....	115
Table 4.4: Comparison of the removal Engine oil between plumage, pelt (large and small size) and feather cluster.....	117
Table 4.5: Comparison of the removal of Bunker oil 1 (BO1) between plumage, pelt (large and small size) and feather cluster.....	119
Table 4.6: The removal of Gippsland crude oil, P (%), comparison between original pelt and recycled pelt. Recycling of the pelt experiments were conducted in five replicates.....	122
Table 4.7: The removal of Diesel Fuel oil, P (%), comparison between original pelt and recycled pelt. Recycling of the pelt experiments were conducted in five replicates.....	123

Table 4.8: The removal of Engine oil, P (%), comparison between original pelt and recycled pelt. Recycling of the pelt experiments were conducted in five replicates.....	125
Table 4.9: The removal of Bunker oil 1 (BO1), P (%), comparison between original pelt and recycled pelt. Recycling of the pelt experiments were conducted in five replicates.....	127
Table 4.10: Magnetic cleansing experiments with different levels of Diesel fuel oil coverage.....	131
Table 4.11: Magnetic cleansing experiments with different levels of Diesel fuel oil coverage including the average of 10%, 20%, 50%, 70% and 100% and average of percentage error.....	132
Table 5.1: Crude oils used in the evaporation experiments, showing their sources and relative viscosities. For the experiments conducted at ~20 °C and ~16 °C in the “Potter Lab”, over a period of up to 21 days, the six oils used are marked with an asterisk and highlighted in green. For the experiments conducted at ~20 °C in the “Ambient Lab”, over a period of up to 10 hours, all eleven oils were used.....	152
Table 5.2. OilVap Parameters for ~20 °C “Potter Lab” Experiment 1 for Little Penguin Pelt and (Glass), experiments up to 21 days.....	160
Table 5.3. OilVap Parameters for ~21 °C Ambient Lab Experiments for Little Penguin Pelt and (Glass). Experiment 2 up to ~ 10 hours.....	161
Table 5.4. OilVap Parameters for 16 °C “Potter Lab” Experiment 3 for Little Penguin Pelt and (Glass), experiments up to ~21 days.....	162
Table 5.5. A summary of the average -c and r ² parameters for Experiments 1 to 3 extracted from the data provided in Tables 5.2 to 5.4	162
Table 5.6. The Total Volatile Fraction (TVF) for evaporation of the oils shown from Penguin Pelt after 21 days, at ~20 °C compared to ~16 °C.....	170
Table 5.7. The Total Volatile Fraction (TVF) for the evaporation of the oils shown from Glass after 21 days at 20 °C, compared to 16 °C.....	171
Table 5.8. Total Volatile Fraction (TVF) from Penguin Pelt after 21 days at 20 °C, compared to Glass.....	172
Table 5.9. Total Volatile Fraction (TVF) from Penguin Pelt after 21 days at 16 °C, compared to Glass.....	173
Table 5.10. A tabulation of the relative parameters (derived from Tables 5.2 and 5.3) relating to the evaporation of Diesel, Kerosene, Bohai Bay, Ikan Pari, Bunker 180 and Bunker 380 contaminants from Little Penguin Pelt (P) and Glass (G).....	178

List of Figures

Figure 1.1: Percentage of Products made from a Barrel of Crude Oil.....	5
Figure 1.2: Number of medium (7-700 tonnes) and large (>700 tonnes) tanker spills from 1970-2021.....	11
Figure 1.3: Methods for treating oil spills depending on oil recovery or degradation.....	13
Figure 1.4: State of the art review and future directions in oil spill modelling.....	13
Figure 1.5: Percentage (F%) of oil removed from duck feather clusters as a function of the number of treatments. Error bars represent 95% confidence intervals for five replicates.....	18
Figure 1.6: (Ngeh 2002), provides a schematic representation of the utilization of magnetic particles to remove a contamination from a substrate.....	18
Figure 2.1: Contaminated Little Penguins in holding bays.....	30
Figure 2.2: Electron micrographs of oil sequestering particles (a) polymer-coated and (b) finely divided iron powder.....	32
Figure 2.3: Magnetic “wand”.....	33
Figure 2.4: A illustration of the removal of Diesel oil (100% coverage – worst case scenario) from a Little Penguin carcass.....	35
Figure 2.5: Simulating a “quick clean” for a Little Penguin Carcass contaminated with (a) 20% coverage (by mass) of engine oil (b) after magnetic particle application (c) 82% removal is achieved.....	35
Figure 2.6: Representative data for the “magnetic wand” removal of Diesel and engine oil from carcass of the Little Penguin to the extent of 20% (by mass).....	36
Figure 2.7: The “backpack” design, based on MPT, for a portable “Quick Clean” Kit.....	37
Figure 2.8: Histogram of Diesel removal (%) versus number of treatments (N), cleansing time (min) and magnetic particle consumption (g) as a function of the number of treatments, for the removal of 50% Diesel Oil coverage (by mass) from plumage. Error bars represent the standard error for three replicates.....	38
Figure 2.9: A potential pollution event scenario. Ten fully contaminated (100% coverage) brown pelicans from the Deepwater Horizon oil spill being held, awaiting treatment in a small holding bay.....	40
Figure 3.1: Anton Paar PSA 990 Particle Size Analyzer (PSA).....	59

Figure 3.2: Magnetic “pull” experiments (a) portable electronic weighing scale (b) for “magnetic zeolite” and (c) for iron powder (control).....	63
Figure 3.3: The formulated MZ particles.....	65
Figure 3.4: The formulated MS particles.....	67
Figure 3.5: Particle size measurement for iron powder.....	68
Figure 3.6: Particle size measurement for developed iron oxide nanoparticle with 1 gram zeolite added.....	69
Figure 3.7: Particle size measurement for developed iron oxide nanoparticle with 2 grams zeolite added.....	69
Figure 3.8: Particle size measurement for developed iron oxide nanoparticle with 3 grams zeolite added.....	69
Figure 3.9: Particle size measurement for developed iron oxide nanoparticle with 4 grams zeolite added.....	70
Figure 3.10: Particle size measurement for developed iron oxide nanoparticle with 5 grams zeolite added.....	70
Figure 3.11: Particle size measurement for developed iron oxide nanoparticle with 6 grams zeolite added.....	70
Figure 3.12: Particle size measurement for developed iron oxide nanoparticle with 7 grams zeolite added.....	71
Figure 3.13: Particle size measurement for developed iron oxide nanoparticle with 8 grams zeolite added.....	71
Figure 3.14: Particle size measurement for iron powder.....	72
Figure 3.15: Particle size measurement for developed iron oxide nanoparticle with 1 gram sawdust added.....	72
Figure 3.16: Particle size measurement for developed iron oxide nanoparticle with 2 grams sawdust added.....	72
Figure 3.17: Comparison of the oil pick-up, P (%), from a glass substrate as a function of the number of treatments, N, amongst different powder compositions.....	78
Figure 3.18: Comparison of the oil removal (%), from duck feathers as a function of the number of treatments, N, amongst different powder compositions.....	78

Figure 3.19: Examining the developed Magnetic Particles under an optical microscope (Olympus) of: **(a)** Control – no zeolite (only Fe₃O₄ added), **(b)** Magnetic Zeolite 1, **(c)** Magnetic Zeolite 2, **(d)** Magnetic Zeolite 3, **(e)** Magnetic Zeolite 4, **(f)** Magnetic Zeolite 5, **(g)** Magnetic Zeolite 6, **(h)** Magnetic Zeolite 7, **(i)** Magnetic Zeolite 8, **(j)** Control – no sawdust (only Chitosan and Fe₃O₄ added), **(k)** Magnetic Sawdust1 and **(l)** Magnetic Sawdust 2.....79

Figure 3.20: The P₀% oil pick-up from a glass and feathers for different powder compositions.....81

Figure 3.21: The P₁% oil pick-up from a glass and feathers for different powder compositions.....82

Figure 3.22: The P₂% oil pick-up from a glass and feathers for different powder compositions.....83

Figure 3.23: The P₃% oil pick-up from a glass and feathers for different powder compositions.....84

Figure 3.24: **(a)** Comparison of the P₁% removals versus Pull per gram ($\times 10^{-3}$) for glass and **(b)** Comparison of the P₁% removals versus Pull per gram ($\times 10^{-3}$) for feathers.....85

Figure 3.25: **(a)** Comparison of the P₂% removals versus Pull per gram ($\times 10^{-3}$) for glass and **(b)** Comparison of the P₂% removals versus Pull per gram ($\times 10^{-3}$) for feathers.....85

Figure 3.26: **(a)** Comparison of the P₃% removals versus Pull per gram ($\times 10^{-3}$) for glass and **(b)** Comparison of the P₃% removals versus Pull per gram ($\times 10^{-3}$) for feathers.....86

Figure 3.27: **(a)** Comparison of the P₀% removals versus Pull per gram ($\times 10^{-3}$) for glass and **(b)** Comparison of the P₀% removals versus Pull per gram ($\times 10^{-3}$) for feathers.....86

Figure 3.28: **(a)** Comparison of the P₁% removals versus Mean size for glass and **(b)** Comparison of the P₁% removals versus Mean size for feathers.....87

Figure 3.29: **(a)** Comparison of the P₂% removals versus Mean size for glass and **(b)** Comparison of the P₂% removals versus Mean size for feathers.....87

Figure 3.30: **(a)** Comparison of the P₃% removals versus Mean size for glass and **(b)** Comparison of the P₃% removals versus Mean size for feathers.....88

Figure 3.31: **(a)** Comparison of the P₀% removals versus Mean size for glass and **(b)** Comparison of the P₀% removals versus Mean size for feathers.....88

Figure 3.32: **(a)** Comparison of the P₁% removals versus Span for glass and **(b)** Comparison of the P₁% removals versus Span for feathers.....89

Figure 3.33: **(a)** Comparison of the P₂% removals versus Span for glass and **(b)** Comparison of the P₂% removals versus Span for feathers.....89

Figure 3.34: (a) Comparison of the P ₃ % removals versus Span for glass and (b) Comparison of the P ₃ % removals versus Span for feathers.....	90
Figure 3.35: (a) Comparison of the P ₀ % removals versus Span for glass and (b) Comparison of the P ₀ % removals versus Span for feathers.....	90
Figure 4.1: Isotherm for oil removal from a glass substrate. The contaminant is Arab medium oil, and the ideal grade of iron powder used for such experiments is Höganäs MH300.29. The 95% confidence intervals are shown by error bars, for five replicates.....	104
Figure 4.2: Typical ab(d)sorption isotherm for oil removal from a cluster of feathers. The contaminant is Arab medium oil. The confidence intervals are 95% for five replicates.....	105
Figure 4.3: The sorption isotherm for oil pick-up from plumage. The contaminant used is Gippsland crude oil, and the iron powder is grade MH300.29. The confidence intervals are 95% for five replicates.....	106
Figure 4.4: (a) Histogram representation (b) Curve representation comparing the removal percentages (P%) of three different contaminants (Jasmine Crude Oil, Engine Oil and Diesel Fuel Oil) from rabbit fur (RF) as a function of the number of treatments (N). The SE for five replicates is shown by error bars.....	107
Figure 4.5: (a) Histogram representation (b) Curve representation comparing the removal percentages (P%) of three different contaminants (Jasmine Crude Oil, Engine Oil and Diesel Fuel Oil) from seal fur (RF) as a function of the number of treatments (N). The SE for five replicates is shown by error bars.....	107
Figure 4.6: Breast pelt and back pelt from Little Penguin (<i>Eudyptula minor</i>).....	111
Figure 4.7: Magnetic Tester employed for performing MPT oil removal experiments.....	112
Figure 4.8: Comparison between penguin carcass (plumage), large penguin pelt size, small penguin pelt size and a penguin feather cluster for the removal of Gippsland crude oil as a function of the number of treatments, N. Error bars represent the 95% confidence intervals for five replicates.....	114
Figure 4.9: Comparison between penguin carcass (plumage), large penguin pelt size, small penguin pelt size and a penguin feather cluster for the removal of Gippsland crude oil as a function of the number of treatments, N. Error bars represent the 95% confidence intervals for five replicates.....	114
Figure 4.10: Comparison between penguin carcass (plumage), large penguin pelt size and small penguin pelt size for the removal of Diesel oil as a function of the number of treatments, N. Error bars represent the 95% confidence intervals for five replicates.....	116
Figure 4.11: Comparison between penguin carcass (plumage), large penguin pelt size and small penguin pelt size for the removal of Diesel oil as a function of the number of treatments, N. Error bars represent the 95% confidence intervals for five replicates.....	116

Figure 4.12: Comparison between penguin carcass (plumage), large penguin pelt size, small penguin pelt size and a penguin feather cluster for the removal of Engine oil as a function of the number of treatments, N. Error bars represent the 95% confidence intervals for five replicates.....118

Figure 4.13: Comparison between penguin carcass (plumage), large penguin pelt size, small penguin pelt size and a penguin feather cluster for the removal of Engine oil as a function of the number of treatments, N. Error bars represent the 95% confidence intervals for five replicates.....118

Figure 4.14: Comparison between penguin carcass (plumage), large penguin pelt size, small penguin pelt size and a penguin feather cluster for the removal of Bunker oil 1 (BO1) as a function of the number of treatments, N. Error bars represent the 95% confidence intervals for five replicates.....119

Figure 4.15: Comparison between penguin carcass (plumage), large penguin pelt size, small penguin pelt size and a penguin feather cluster for the removal of Bunker oil 1 (BO1) as a function of the number of treatments, N. Error bars represent the 95% confidence intervals for five replicates.....120

Figure 4.16: Comparison between original pelt and recycled pelt for the removal of Gippsland crude oil as a function of the number of treatments, N. Error bars represent the 95% confidence intervals for five replicates.....122

Figure 4.17: Comparison between original pelt and recycled pelt for the removal of Gippsland crude oil as a function of the number of treatments, N. Error bars represent the 95% confidence intervals for five replicates.....123

Figure 4.18: Comparison between original pelt and recycled pelt for the removal of Diesel fuel oil as a function of the number of treatments, N. Error bars represent the 95% confidence intervals for five replicates.....124

Figure 4.19: Comparison between original pelt and recycled pelt for the removal of Diesel fuel oil as a function of the number of treatments, N. Error bars represent the 95% confidence intervals for five replicates.....124

Figure 4.20: Comparison between original pelt and recycled pelt for the removal of Engine oil as a function of the number of treatments, N. Error bars represent the 95% confidence intervals for five replicates.....125

Figure 4.21: Comparison between original pelt and recycled pelt for the removal of Engine oil as a function of the number of treatments, N. Error bars represent the 95% confidence intervals for five replicates.....126

Figure 4.22: Comparison between original pelt and recycled pelt for the removal of Bunker oil 1 (BO1) as a function of the number of treatments, N. Error bars represent the 95% confidence intervals for five replicates.....127

Figure 4.23: Comparison between original pelt and recycled pelt for the removal of Bunker oil 1 (BO1) as a function of the number of treatments, N. Error bars represent the 95% confidence intervals for five replicates.....	128
Figure 4.24: Nested isotherms for the removal of Gippsland Crude Oil (left) and Diesel Fuel Oil (right) from penguin pelt at pelt temperatures of 40 °C and 22 °C.....	129
Figure 4.25: Histograms of Diesel Fuel Oil removal (%), as a function of the number of treatments, N; for the removal of 10%, 20%, 50%, 70% and 100% Diesel Oil coverage (by mass) from plumage. Error bars represent the standard error for three replicates for the removal of 10%, 20%, 50% and 70% Diesel Oil coverage (by mass) from plumage.....	131
Figure 4.26: Sorption isotherm of oil removal (%), as a function of the number of treatments, N, for the removal of 10%, 20%, 50%, 70% and 100% Diesel Oil coverage (by mass) from plumage. Error bars represent the standard error for three replicates for the removal of 10%, 20%, 50% and 70% Diesel Oil coverage (by mass) from plumage.....	132
Figure 4.27: Oil removal (%), as a function of the number of treatments, N, for the average removal of 10%, 20%, 50%, 70% and 100% Diesel Oil coverage (by mass) from plumage. Error bars represent the average standard error for three replicates.....	133
Figure 5.1: Weathering of oil spilled in the marine environment.....	142
Figure 5.2: Weathering process of a typical crude oil.....	143
Figure 5.3: Here, the air boundary layer regulating method is depicted. The rate of evaporation is regulated by diffusion into the air layer, which is the limiting factor. Turbulence in the air affects this rate by increasing the transport of molecules over the boundary layer. For pure liquids with a high evaporative rate, this regulation mechanism is true. Water is the most commonly help concept and is an example of such a liquid.....	147
Figure 5.4: Here, the diffusion-controlled regulatory mechanism is depicted. The limiting factor and thus the regulation mechanism is diffusion through the evaporating liquid. This technique applies to oils, fuels, and a variety of other liquid mixes that both evaporate more slowly than water.....	148
Figure 5.5. Weight of oiled breast feathers of the domestic duck (<i>Ana platyrhychos</i>) over time.....	148
Figure 5.6: Weight versus time of weathering for oiled duck feather clusters.....	149
Figure 5.7. Typical weighing experiments, showing (a) an oil sample on a glass substrate (Petri dish) and (b) an oiled pelt sample, contained in a petri dish.....	153
Figure 5.8. Breast and back pelt from Little Penguin (<i>Eudyptula minor</i>), supplied by the Phillip Island Nature Parks.....	153

Figure 5.9. Comparative evaporation profiles of Diesel from pelt and glass over ~21 days, at a controlled temperature of 20 ± 1 °C, in the “Potter Lab”. Note that 1 day = 1,440 minutes, 21 days = 30,240 min.....	155
Figure 5.10. Comparative evaporation profiles of Diesel from glass and pelt over ~21 days, at a controlled temperature of 20 ± 1 °C, in the “Potter Lab”, showing the OilVap fit curves for the data presented in Figure 5.9	156
Figure 5.11. Comparative evaporation profiles of Diesel from pelt and glass over hours, at a controlled temperature of 21 ± 1 °C. Note that 10 hours = 600 min.....	157
Figure 5.12. Comparative evaporation profiles of Diesel from glass and pelt over hours, at a controlled temperature of 21 ± 1 °C, showing the OilVap fit curves for the data presented in Figure 5.11	157
Figure 5.13. Comparative evaporation profiles of Diesel from glass over ~21 days, at a controlled temperature of 20 ± 1 °C and 16 ± 1 °C. Note that 1 day = 1,440 minutes, 21 days = 30,240 min.....	158
Figure 5.14. Comparative evaporation profiles of Diesel from pelt over ~21 days, at a controlled temperature of 20 ± 1 °C and 16 ± 1 °C. Note that 1 day = 1,440 minutes, 21 days = 30,240 min.....	159
Figure 5.15. Comparative %wL(inf) (plateau) parameters for the evaporation of six oils from Little Penguin Pelt and Glass at ~20 °C up to ~21 days in the “Potter Lab” – Experiment 1	163
Figure 5.16. Comparative %wL(inf) parameter for the evaporation of all eleven oils from Little Penguin Pelt and Glass at ~21 °C up to 10 hours in the “Ambient Lab” – Experiment 2	164
Figure 5.17. Comparative %wL(inf) parameter for the evaporation of six oils from Little Penguin Pelt and Glass at ~16 °C up to ~21 days in the “Potter Lab” – Experiment 3	164
Figure 5.18. Comparative k parameter with reference to the evaporation profile for Little Penguin Pelt and Glass at ~20 °C – Experiment 1	165
Figure 5.19. Comparative v₀ parameter with reference to the evaporation profile for Little Penguin Pelt and Glass at ~20 °C – Experiment 1	166
Figure 5.20. Comparative k parameter with reference to the evaporation profile for Little Penguin Pelt and Glass at ~21 °C.....	167
Figure 5.21. Comparative v₀ parameter with reference to the evaporation profile for Little Penguin Pelt and Glass at ~21 °C – Experiment 2	167
Figure 5.22. Comparative k parameter with reference to the evaporation profile for Little Penguin Pelt and Glass at ~16 °C – Experiment 3	168

Figure 5.23. Comparative v_0 parameter with reference to the evaporation profile for Little Penguin Pelt and Glass at $\sim 16^\circ\text{C}$168

Figure 5.24. Comparative **Total Volatile Fraction (TVF)** profiles of light, medium and heavy crude oils from penguin pelt after 21 days, at controlled temperatures of 20°C and 16°C ...170

Figure 5.25. Comparative **Total Volatile Fraction (TVF)** profiles of light, medium and heavy crude oils from Glass after 21 days, at a controlled temperature of 20°C and 16°C171

Figure 5.26. Comparative Total Volatile Fraction (TVF) profiles of light, medium and heavy crude oils from Penguin Pelt and Glass after 21 days, at a controlled temperature of 20°C ..172

Figure 5.27. Comparative Total Volatile Fraction (TVF) profiles of light, medium and heavy crude oils from Penguin Pelt and Glass after 21 days, at a controlled temperature of 16°C ..173

Figure 5.28 The above two graphs provide a representative example of the existence of the **Highly Volatile Fraction (HVF)** for the initial evaporation of Diesel from Little Penguin pelt.....175

Figure 5.29. A schematic representation of the various fractions during the evaporation of a crude oil from a given surface.....176

Figure 5.30. Results of an experiment to estimate the duration of the “latency period” associated with the Highly Volatile Fraction (HVF) for the evaporation of diesel from a glass surface.....177

Figure 5.31. Comparative values of **NVF**, **RF** and **HVF** for the evaporation the light, medium and heavy pairs of oil from plumage and glass at $\sim 20^\circ\text{C}$179

List of Abbreviations and Symbols

AMSA	Australian Maritime Safety Authority
BO1	Bunker Oil 1
BO2	Bunker Oil 2
C	Carr Index
<i>c</i>	closeness to fit to first order kinetics
C (%)	Percentage of oil removed from carcass
DO	Diesel Oil
DFO	Diesel Fuel Oil
<i>d_o</i>	Maximum days
EO	Engine Oil
F (%)	Percentage removal of contaminants for feathers
<i>f₁</i>	Mass of feather cluster
<i>f₂</i>	Mass of feather cluster and excess contaminant
<i>f₃</i>	Mass of contaminated feather cluster
<i>f₄</i>	Mass of magnetically stripped feather cluster
GCO	Gippsland Crude Oil
H	Hausner Ratio
HVF	Highly Volatile Fraction
IP	Iron Powder
JCO	Jasmine Crude Oil
<i>k</i>	rate constant
MPT	Magnetic Particle Technology

MS	Magnetic Sawdust
MZ	Magnetic Zeolite
N	Number of treatments
N^T	The total number of treatments
NVF	Normal Volatile Fraction
N_{99}	Effective number of treatments to achieve 99% of contaminant removal
N_{90}	Effective number of treatments to achieve 99% of contaminant removal
N_{75}	Effective number of treatments to achieve 75% of contaminant removal
OWCN	Oiled Wildlife Care Network
P (%)	Percentage of contaminant removal
P_o (%)	Percentage of contaminant removal (plateau)
$P\%$ (N_1)	Percentage removal by weight after 1 st treatment
$P\%$ (N_2)	Percentage removal by weight after 2 nd treatment
$P\%$ (N_3)	Percentage removal by weight after 3 rd treatment
PINP	Phillip Island Nature Parks
PSA	Particle Size Analyzer
RT	Room Temperature
r^2	Regression coefficient
R	Particle to contaminant ratio
R_o	Maximum particle-to-oil Ratio

RF	Recalcitrant Fraction
S	Standard Deviation
SE	Standard Error
T	Temperature
TVF	Total Volatile Fraction
v_0	Initial evaporation rate
w_1	Mass of pelt
w_2	Mass of pelt and contaminant
w_3	Mass of oil
w_4	Mass of pelt, contaminant, and iron powder
w_5	Mass of iron powder
w_6	Mass of treated pelt
ZVI	Zero Valent Iron
95%	95% Interval Confidence
%wt	Percentage weight loss
%wL(inf)	Plateau

Chapter 1: Introduction

1.1 Oil spills' effects on the environment

1.1.1 Oil Spill Sources and Spill Rates

1.1.2 Major Oil Spills in the Ocean

1.1.3 Oil Spill Statistics

1.1.4 Major Oil Spills in History

1.1.5 Global Oil Spill Trend

1.2 The impact of oil spills on wildlife

1.3 Traditional techniques for environmental remediation

1.4 Rehabilitation of oiled wildlife

1.4.1 Current stabilization protocols for oiled birds

1.4.2 Stabilization and treatment protocols used at Phillip Island Nature Parks

1.4.3 Existing methods for cleaning and rehabilitation

1.4.4 Disadvantages of existing methods for cleaning and rehabilitation

1.5 The “Magnetic Cleansing” method

1.5.1 Advantages of the “Magnetic Cleansing” method (MC leads to a / furthermore of a quick clean approach – AMSA report – remove volatiles essentially)

1.6 Significance of the research

1.7 Aims and objectives

1.8 References

Chapter 1: Introduction

1.1 The effect of oil spills on the environment

Oil spills are extremely harmful to the environment. The risk of oil spills is higher than ever, with large oil companies operating all over the world. Oil spills in recent decades have caused damage to reef ecosystems, wildlife breeding grounds and coastal environments. They cause food chains to become unbalanced and species growth slows in the affected ecosystem (Ecospill, 2021).

Crude oil is a fossil that is used to create a variety of products, including fuels. It is the liquid by-product of extinct plants and animals. Oil is found in reservoirs below or beneath the surface of the ocean, where oil droplets live in “pores” or holes in the rocks. Oil corporations drill down and pump out crude oil, then carry it to refineries using pipes, ships, trucks, or trains for processing. Oil needs to be refined to create various petroleum products, including gasoline and other fuels, as well as items we use daily, such plastics, soaps, and paints, the oil needs to be refined. However, whether intentionally or accidentally, oil is released into the water causing severe environmental harm. Each year, 706 million gallons (2.673×10^9 litres) of used oil spill into the ocean, often with damaging effects (Wong, 2022).

The most harmful oil spills, however, are caused by human activity, specifically leaks and spills from handling, transport, storage, and use of crude oil and any of its distillation products. Many of them are essentially accidental spills, which can happen under numerous conditions. For instance, oil may spill from the containers when inadequately maintained and stored. Large and unexpected spills are typically caused by mishaps during offshore drilling operations and ruptures of large transport vessels like oil tankers.

Additionally, there are deliberate oil spills, such as when tanker ship commanders clean their vessels and discharge any leftover oil into the sea. This might seem unimportant but considering the quantity of ships involved and the size of the tankers, the amount of oil that is released can end up being significant (Wong, 2022).

Plants, animals, and their ecosystems are harmed when oil spills into the environment. Plankton, plants, invertebrates, fish, birds, and mammals all live in ecosystems such as water, sediments, beaches, wetlands, and forests. The level of influence of the oil relies on a variety of factors, including the organism's life stage (egg, larvae, juvenile, adult), the time of year (wet or dry season), and other disruptions, such as the existence of invasive species and the long-term impacts of the spilt oil. Although the whole extent of oil's environmental impact may not be known, certain generalisations can be made. The following information provides an overview of the potential consequences of an oil spill (Department of Ecology State of Washington, 2019).

According to the Department of Ecology State of Washington (2019), **Figure 1.1**, Oil has three major environmental effects:

- Acute (immediate toxicity) – A measure of the quantity of volatile compounds in the oil that easily dissolve in water and have the potential to damage plants and animals.
- Mechanical injury – A measure of the physical impact of oil on species and environments (coating and smothering).
- Persistence – A measure of how long oil will remain in the environment before it degrades.

The environmental impacts of oil vary based on the environmental circumstances and the type of oil spilt. The history of oil can also be important. Used oils, waste oils, and oil combinations may provide different results than fresh products.

Crude oil is refined into several products with variable qualities. Toxic components are more concentrated in lighter, more refined oils. Heavier oils have lower levels of harmful components but are more persistent in the environment (Department of Ecology State of Washington, 2019).

For reference, the percentage of products produced from a Barrel of Crude Oil are shown in **Figure 1.1**.

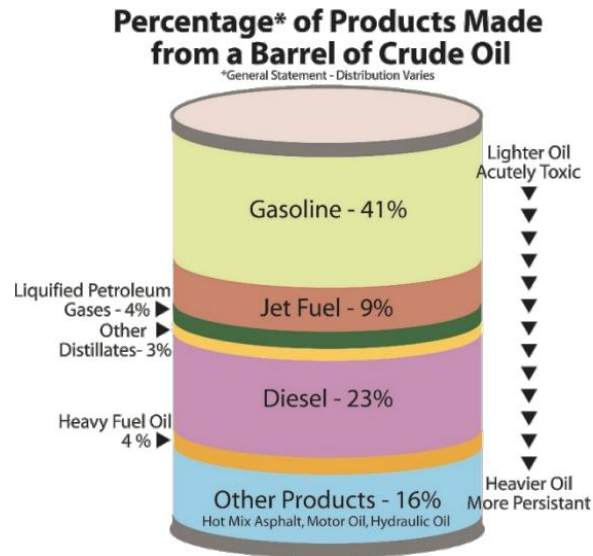


Figure 1.1: Percentage of Products made from a Barrel of Crude Oil (Department of Ecology State of Washington, 2019).

The effects of oil are influenced by environmental factors. Higher temperatures and/or winds provide circumstances that accelerate the evaporation of volatile products. Higher wind and wave conditions can mix water into certain oils, resulting in a viscous mousse (thick, sticky).

Larger waves will also mix more oil into the water column, increasing hazardous effects, making it critical to understand both the kind of oil spilt as well as current environmental factors such as air and water temperature, wind speed, wave height, salt, humidity, and direct sunlight (Department of Ecology State of Washington, 2019).

1.1.1 Oil Spill Sources and Spill Rates

Exploration, production, and consumption of oil and petroleum products are increasing globally, as is the threat of oil pollution. The transportation of petroleum from the oil fields to the consumer involves as many as 10-15 transfers between various modes of transport, including tankers, pipelines, railcars, and tank trucks. Along the way, oil is stored at transfer points, terminals, and refineries. Accidents can occur during any of the exploration, production, transportation, or storage steps (Michel and Fingas, 2016).

Obviously, keeping spills to a minimum is an important aspect of environmental protection. With the introduction of strict new legislation and stringent operating codes, both the government and industry are working to reduce the risk of oil spills. Many operating and maintenance procedures have been implemented by industry to reduce accidents that could result in spills. In fact, spillage has decreased over the last 20 years. This is especially true in the case of tanker accidents at sea. To reduce the possibility of human error, intensive training programmes have been developed. Despite these efforts, experts estimate that 30-50% of oil spills are either directly or indirectly caused by human error, with equipment failure or malfunction accounting for 20-40% of all spills (Michel and Fingas, 2016).

1.1.2 Major Oil Spills in the Ocean

Oil spills were common in the past, with an average of 78.8 spills per year in the 1970s (Wong, 2022). The Amoco Cadiz oil spill occurred in 1978, when a very large crude carrier carrying nearly 69 million gallons (2.611×10^8 litres) of light crude oil ran aground on shallow rocks off the coast of Brittany, France. The impact slashed holes in the ship's hull and container tanks, allowing the oil to escape. The oil slick polluted 321 kilometres of the French coast, killing millions of invertebrates such as molluscs and crustaceans, as well as an estimated 20,000 birds, and contaminated oyster beds in the area (Wong, 2022).

Oil spills have decreased dramatically due to improved control and care, from an average of 78.8 in the 1970s to 6.2 spills per year in the 2010s. However, the few spills that have occurred in recent years have had significant environmental consequences. On April 20, 2010, a surge of natural gas blasted through a cement well cap that had recently been installed to seal a well drilled by the Deepwater Horizon oil platform, resulting in the largest accidental oil spill in history. About 206 million gallons of oil were released, coating approximately 2,100 kilometres of the US Gulf Coast from Texas to Florida (Wong, 2022). Currently, oil spills are caused by accidents at oil wells or on the pipelines, ships, trains, and trucks that transport oil from wells to refineries (U.S. Energy Information Administration, 2022).

1.1.3 Oil Spill Statistics

Oil Spills are a common occurrence, owing to the widespread use of oil and petroleum products in our daily lives. In relation to North America, for example, approximately 450,000 tonnes of oil and petroleum products are used in Canada on a daily basis. The United States of America consumes roughly ten times this amount and, for reference, approximately 20 million tonnes are consumed globally each day. Notably, more than half of the approximately four million tonnes of oil and petroleum products consumed in the United States each day is imported, primarily from Canada, Saudi Arabia, and Africa. Of this, automotive gasoline accounts for approximately 40% of daily demand, while diesel fuel accounts for approximately 15%. Thus, petroleum accounts for approximately 40% of US energy consumption, natural gas 25% and coal 20%. Much of the refined oil in both Canada and the United States is used to power transportation (Michel and Fingas, 2016). Spill statistics associated with this consumption is summarized in **Table 1.1**.

Table 1.1: North America Spill Statistics (Michel and Fingas, 2016).

Source	Percentage of total spills	
	Volume	Numbers
Land spills (85% volume, 90% numbers)		
Pipelines	40	20
Wells, production and storage facilities	25	25
Storage refineries	12	25
Retail and delivery	5	10
Trucks	6	11
Rail	7	4
other	5	5
On-water spills (15% volume, 10% numbers)		
Non tank vessels	25	30
Tank barges	15	10
terminals/refineries	25	30
tankers	20	20
platforms and pipelines	15	10
Types of oil spilled		
Crude oil	35	
Diesel and No. 2 fuel oils	20	
Bunkers	15	
Marine	10	
Gasoline	8	
Condensates	3	
Waste and residuals	3	
Other oils	6	

1.1.4 Major Oil Spills in History

Table 1.2 summarises the 20 largest oil spills that have occurred worldwide since the Torrey Canyon spill in 1967. It is worth noting that the 19th and 20th largest spills occurred before the year 2000. Sanchi, the most recent addition to the top 20, is the only major spill of non-persistent oil featured here, and it had fewer environmental consequences than some of the crude oil spills listed. Despite their size, a few of these accidents required little or no response because the oil was split some way offshore and did not harm coasts. For comparison, Prestige, Exxon Valdez, and Hebei Spirit are included (ITOPF, 2022). **Table 1.3** shows the major historical oil spills in or near Australian waters, and several smaller offshore spills.

Table 1.2: Major tanker spills since 1967 (ITOPF, 2022).

Position	Shipname	Year	Location	Spill size (tonnes)
1	ATLANTIC EMPRESS	1979	Off Tobago, West Indies	287,000
2	ABT SUMMER	1991	700 nautical miles off Angola	260,000
3	CASTILLO DE BELLVER	1983	Off Saldanha Bay, South Africa	252,000
4	AMOCO CADIZ	1978	Off Brittany, France	223,000
5	HAVEN	1991	Genoa, Italy	144,000
6	ODYSSEY	1988	700 nautical miles off Nova Scotia, Canada	132,000
7	TORREY CANYON	1967	Scilly Isles, UK	119,000
8	SEA STAR	1972	Gulf of Oman	115,000
9	SANCHI*	2018	Off Shanghai, China	113,000
10	IRENES SERENADE	1980	Navarino Bay, Greece	100,000
11	URQUIOLA	1976	La Coruna, Spain	100,000
12	HAWAIIAN PATRIOT	1977	300 nautical miles off Honolulu	95,000
13	INDEPENDENTA	1979	Bosphorus, Turkey	95,000
14	JAKOB MAERSK	1975	Oporto, Portugal	88,000
15	BRAER	1993	Shetland Islands, UK	85,000
16	AEGEAN SEA	1992	La Coruna, Spain	74,000
17	SEA EMPRESS	1996	Milford Haven, UK	72,000
18	KHARK 5	1989	120 nautical miles off Atlantic coast of Morocco	70,000
19	NOVA	1985	Off Kharg Island, Gulf of Iran	70,000
20	KATINA P	1992	Off Maputo, Mozambique	67,000
21	PRESTIGE ⁺	2002	Off Galicia, Spain	63,000
36	EXXON VALDEZ ⁺	1989	Prince William Sound, Alaska, USA	37,000
132	HEBEI SPIRIT ⁺	2007	South Korea	11,000

Table 1.3: Historical major oil spills in or near Australian waters, and several smaller offshore spills (AMSA, 2020).

Date	Vessel	Location	Oil amount
28 November 1903	Petriana	Port Phillip Bay, Victoria	1,300 tonnes
03 March 1970	Oceanic Grandeur	Torres Strait, Queensland	1,100 tonnes
26 May 1974	Sygna	Newcastle, New South Wales	700 tonnes
14 July 1975	Princess Anne Marie	Offshore, Western Australia	14,800 tonnes
10 September 1979	World Encouragement	Botany Bay, New South Wales	95 tonnes
29 October 1981	Anro Asia	Bribie Island, Queensland	100 tonnes
22 January 1982	Eso Gippsland	Port Stanvac, South Australia	unknown
03 December 1987	Nella Dan	Macquarie Island	125 tonnes
06 February 1988	Sir Alexander Glen	Port Walcott, Western Australia	450 tonnes
20 May 1988	Korean Star	Cape Cuvier, Western Australia	600 tonnes
28 July 1988	Al Qurain	Portland, Victoria	184 tonnes
21 May 1990	Arthur Phillip	Cape Otway, Victoria	unknown
14 February 1991	Sanko Harvest	Esperance, Western Australia	700 tonnes
21 July 1991	Kirki	Western Australia	17,280 tonnes
30 August 1992	Era	Port Bonython, South Australia	300 tonnes
10 July 1995	Iron Baron	Hebe Reef, Tasmania	325 tonnes

28 June 1999	Mobil Refinery	Port Stanvac, South Australia	230 tonnes
26 July 1999	MV Torungen	Varanus Island, Western Australia	25 tonnes
03 August 1999	Laura D'Amato	Sydney, New South Wales	250 tonnes
18 December 1999	Sylvan Arrow	Wilson's Promontory, Victoria	less than 2 tonnes
02 September 2001	Pax Phoenix	Holbourne Island, Queensland	less than 1000 litres
25 December 2002	Pacific Quest	Border Island, Queensland	greater than 70 km slick
24 January 2006	Global Peace	Gladstone, Queensland	25 tonnes
11 March 2009	Pacific Adventurer	Cape Moreton, Queensland	270 tonnes
21 August 2009	Montara Wellhead oil platform	NW Australian coast	Approx 4,750 tonnes
03 April 2010	Shen Neng 1	Great Keppel Island, Queensland	4 tonnes
09 January 2012	MV Tycoon	Christmas Island	102 tonnes

1.1.5 Global Oil Spill Trend

Statistics regarding the frequency of spills of more than 7 tonnes from tankers have shown a clear downward trend over the last half-century. As shown in **Figure 1.2**, the average number of spills per year in the 1970s was around 79, but it fell by more than 90 percent to 6 in the 2010s. So far, this decade, the annual average number of oil spills has been 5, one less than the previous decade's average (ITOPF, 2022).

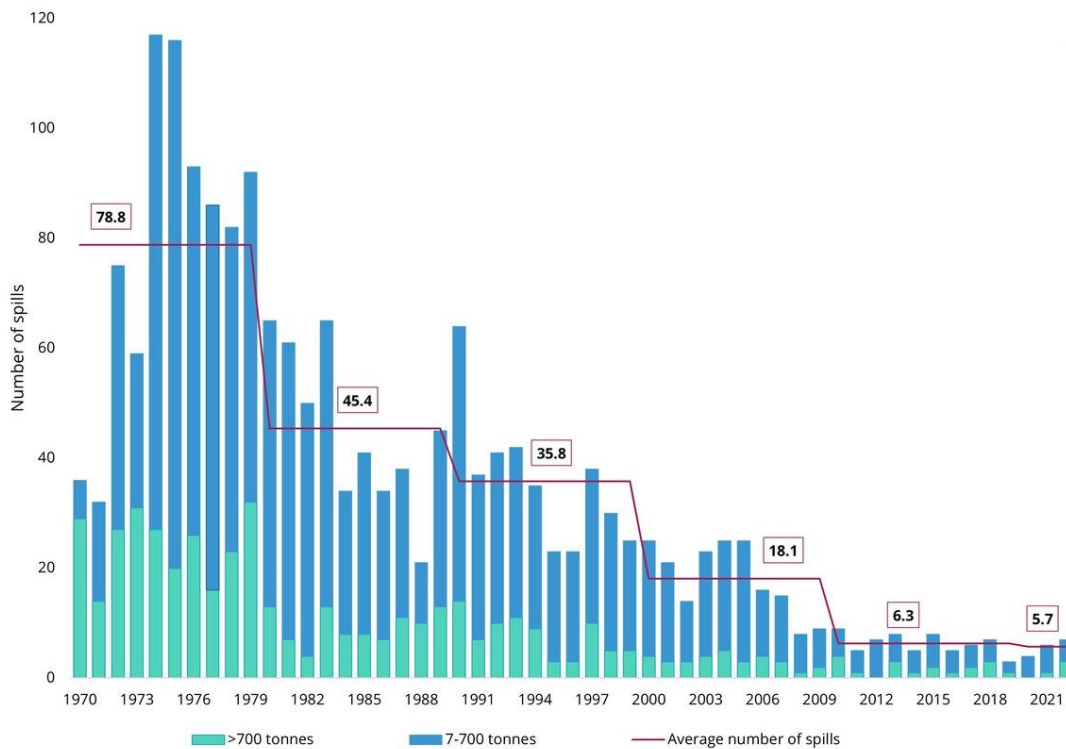


Figure 1.2: Number of medium (7-700 tonnes) and large (>700 tonnes) tanker spills from 1970-2021 (ITOPF, 2022).

1.2 The impact of oil spills on wildlife

Oil pollution is a global issue that has a harmful influence on ecosystems and wildlife (ITOPF, 2004). Contamination of marine animals and birds is one of the ecological repercussions of an oil spill (Michael, 1977). The effects of such pollution on birds include plumage matting and subsequent loss of heat, resulting in hypothermia (Clark & Gregory, 1971; Jenssen & Ekker, 1989). Ingestion of oil while preening can be lethal in several cases (Hartung & Hunt 1966). The problem is frequently worsened when the petroleum products are hazardous and toxic, such as diesel oil, which contains a number of damaging aromatic components (Hartung & Hunt, 1966; Peakall *et al.*, 1982). Some hazardous components can also be absorbed through the skin (Perry *et al.*, 1978). According to Dennis (1959), a one-inch-diameter patch of oil is enough to separate the insulation of the plumage and expose the bird to hypothermia and pneumonia. These facts call for a thorough first clean-up (stabilization) of the bird, ideally involving the removal of the most toxic and corrosive components as quickly as possible. The removal of the tarrier components is saved for later further

treatments since it is impractical to deliver conventional detergent-based cleaning equipment to the location. In a few circumstances (including Phillip Island Nature Parks, PINP) the treatment centre is close enough to the scene of an incident that the distinction between initial and subsequent treatments is not as important. However, there is still a genuine need for technology that can be utilized as part of field stabilization to remove the most of the most toxic contamination upon first encounter (Ngeh, 2002).

Phillip Island Nature Parks (PINP) is internationally known for the “Fairy Penguin Parade” and is a crucial nesting ground for the Little Penguins (*Eudyptula minor*). Currently, there are approximately 26,000 Little Penguins in the region of Phillip Island (Ngeh, 2002).

The mortality of Little Penguins on Phillip Island has been reported (Obendorf & McColl, 1980; Harrigan, 1992). The primary cause of Little Penguins dying is due to road accidents and predation. A moderately small number are the victims of oil pollution and the PINP treatment facility has developed successful techniques and facilities for managing these causalities. Many animals including wallabies, koalas, opossums, mutton birds, seals, albatross, gannets and seagulls have also been treated at the PINP animal rehabilitation facility. At PINP, the methodology utilized for the removal of oil and chemical contamination from feathers is the conventional detergent techniques (Jessop & Healy, 1997). From 1994 to 2000, several Little Penguins were treated for oil contamination and a number were treated for fox bites, starvation and heat stress at the PINP animal rehabilitation facility.

Table 1.4: The number of Little Penguins treated annually at the animal rehabilitation facility of PINP from 1994 to 2000 (Healy, 1999).

Year	Little Penguins treated for oil contamination/annually	Little Penguins treated for other conditions/annually
1994-1995	118	106
1995-1996	301	205
1996-1997	24	128
1997-1998	36	142
1998-1999	23	92
1999-2000	236	110

1.3 Traditional techniques for environmental remediation

Oil spills have long been recognized as having substantial environmental implications, and much research and technology development has been conducted to establish acceptable cleanup procedures (Suni *et al.*, 2004; Ventikos *et al.*, 2004). Mechanical/physical recovery (booms, skimmers, sorbents), chemical treatment (dispersants, emulsion breakers; gelling agents, sinking agents), bioremediation, and in-situ burning are the four broad categories of these approaches (Mullin and Champ, 2003; Ventinkos *et al.*, 2004). Such oil spill treatment methods are shown in **Figure 1.3** and **Figure 1.4**.

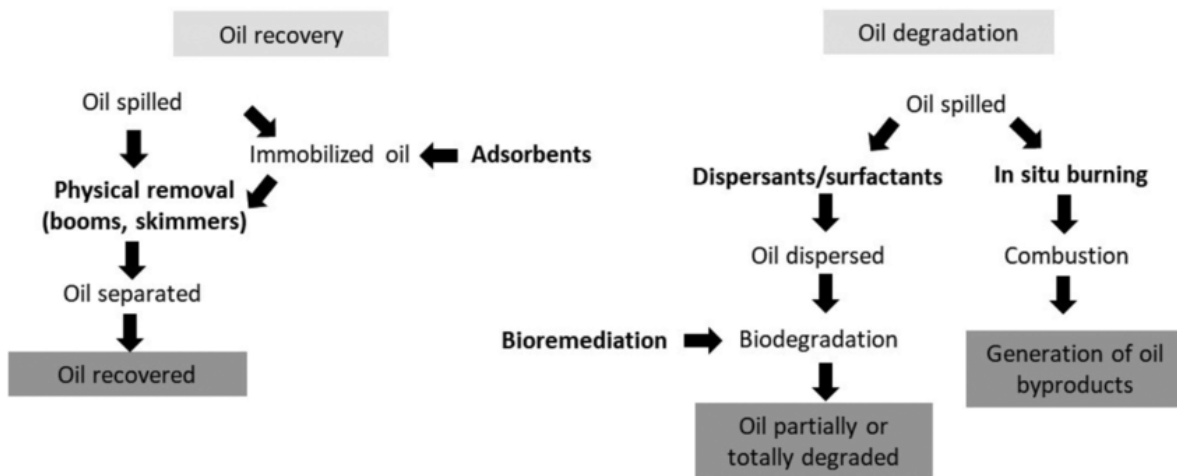


Figure 1.3: Methods for treating oil spills depending on oil recovery or degradation (Silva *et al.*, 2022).

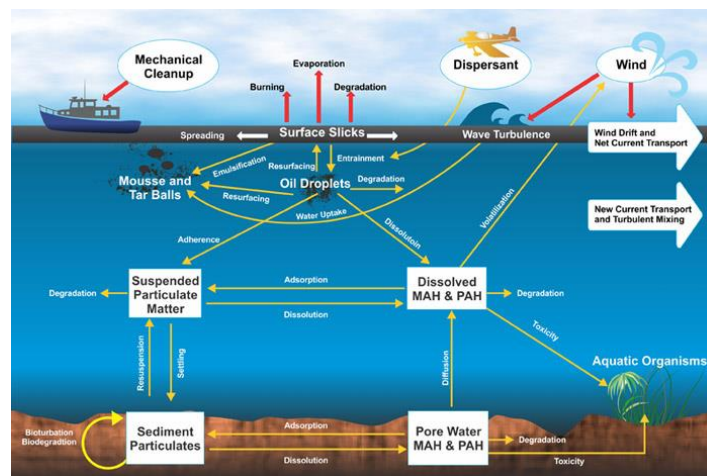


Figure 1.4: State of the art review and future directions in oil spill modeling (Spaulding, 2017).

1.4 Rehabilitation of oiled wildlife

The principle objectives of oiled bird rehabilitation are to rescue, treat, and clean the animals before releasing them back into the natural environment (Dao, 2007).

1.4.1 Current stabilization protocols for oiled birds

Current practices in rehabilitation may vary according to the nature of the event. Established wildlife rescue associations have existing protocols, which may vary to some degree. Some of these associations have created standard protocols for stabilizing or cleansing oiled birds (Gilbert, 1999; Miller, 1999). There are several factors which may influence whether the adjustment protocols are carried out on site or at a treatment centre. These include: (i) the distance to a treatment centre, (ii) manpower requirements, and (iii) accessibility of equipment on site.

The current general guidelines which are adopted for stabilizing oiled birds involves: (i) physical examination, (ii) removal of excess oil, (iii) administering rehydration liquid, (iv) administering an activated charcoal suspension, (v) keeping the bird warm, and (vi) transporting it to a treatment centre (Miller, 1999).

The stabilization of an oiled bird should ideally be commenced within 8-24 hours of when the oil has come into contact with the bird (Miller, 1999). The physical examination is normally performed on all oiled birds. Seriously contaminated birds are given first aid which incorporates cleaning their eyes and mouth. Excess oil will then be removed from the body with an absorbent cloth (Miller, 1999). If the birds are critically dehydrated, rehydration solutions are administered. A rehydration solution comprises glucose, salts and other mineral ingredients. This is followed by administering an activated charcoal suspension to coagulate and ingest oil into the stomach (Holcomb & Russell, 1999). The contaminated birds are appropriately dressed in a paper or woollen poncho to keep them warm and to prevent additional poisoning by preening (Harris & Smith, 1997; Stocker, 2000). The birds are then transported in cardboard boxes, which contains no more than three birds, towards the treatment facility for further treatments. If the transporting time is longer than one-hour,

hot water bottles can be used to prevent from hypothermia (Stocker, 2000).

Upon the arrival at the treatment centre all birds are transported to warm surroundings. They are again reviewed for any signs of stress and hypothermia. Most birds usually remain dehydrated upon first arrival at the treatment facility and are commonly re-administered a rehydration solution, followed by an activated charcoal suspension (Schmidt, 1997; Stocker, 2000). At this point, if the birds present no sign of stress and are eating normally, the bird can then be ready for cleaning using detergents.

The conventional methodology of the cleansing of live oiled birds, typically involves the utilization of detergents and a large quantity of warm water (35°C to 40°C). If a detergent becomes unavailable, dishwashing liquid has been found to be an appropriate alternative.

1.4.2 Stabilization and treatment protocols used at Phillip Island Nature Parks

According to Ngeh (2002), the treatment facility of PINP is near the site of many incidents so that the initial stabilization is generally accomplished at the animal rehabilitation facility. Its accessibility is close to the foreshore of Phillip Island which enables the oil-contaminated birds, mainly penguins, to be transported towards the treatment facility for stabilization and washing without any significant delay. Cardboard boxes are normally used for transporting penguins towards the facility. The stabilization and treatment for oiled penguins are similar to the existing standard stabilization and treatment protocols that have been described previously but can vary to some degree. The approach involves the following procedures. When oiled penguins are rescued around their nestling place, they are normally placed with no more than three penguins in a carton. The birds are then delivered to the treatment facility for further investigation. Upon the arrival at the treatment facility the birds are usually moved towards a warm surrounding. They are then carefully inspected for any signs of stress and hypothermia. Heaters are used to warm up chilled birds. If the penguins are very weak and presenting stress, they are then dressed in woollen ponchos prior to the stabilization and cleansing (Ngeh, 2002).

All the penguins are treated with a rehydration solution, which is prepared from the Vytrate™ concentrate. This solution is prepared by diluting 5mL of Vytrate concentrate with 45 mL of luke-warm water. A flexible plastic tube is then carefully and gently fed down the bird's throat, close to the vicinity of the penguin's stomach. A 50 mL syringe is then connected towards the tube and can be mainly used to administer the Vytrate™ solution. The Vytrate™ solution is normally administered twice per day until the penguin is eating 150-250 g of fish per day, especially pilchard (Ngeh, 2002).

Each bird will also be fed with a Tympanyl™ formulation, which is a vegetable oil that emulsifies the ingested oil. Following this treatment plan the bird is required to be fed with four fishes, feeding twice a day. When the penguin appears calm and not under-weight, washing may then be commenced. The methodology of washing the contaminated penguins at PINP. The methodology of washing the contaminated penguins at PINP using DivoPlusV2™ detergent has been developed based on a series of trial and error experiments and found to be the optimal cleansing agent for procedure. If the DivoPlusV2™ becomes unavailable, Sunlight™ dishwashing liquid would be a suitable alternative. Two people are usually required to wash each bird. Normally 20 minutes is the maximum time authorized to carry out a washing session of the bird. However, if the penguins present any signs of stress, washing will then be immediately terminated (Ngeh, 2002).

The cleansing procedure is mainly repeated until all traces of oil are removed from the penguins. Commonly the washing sessions range from a few days to a few weeks depending among the condition of the bird and the severity of the contamination. There are no attempts to restore the preening oils of the penguin. According to Naviaux & Pittman, (1973) the totally cleansed feathers regain water-repellency, and the natural oils return to the feathers, mostly through the preening procedure. The time that was taken to regain waterproofing primarily depends on the extent of oil contamination and on the efficiency of the washing process. The precise stabilization and treatment methods employed at PINP have been published elsewhere (Jessop & Healy, 1997).

1.4.3 Existing methods for cleaning and rehabilitation

The standard method for the removal of oil from birds involves the use of surfactants and, more recently, the possible use of magnetic cleansing has been suggested. In spite of the fact that surfactant-based techniques have obtained some degree of accomplishment, it is very time-consuming and labour intensive and does not allow for oil to be removed upon first encountering the bird. It is obligatory to transport the contaminated bird to a suitable treatment centre (Orbell *et al.*, 2007).

1.4.4 Disadvantages of existing methods for cleaning and rehabilitation

Even though the conventional surfactant-based methodology of cleansing has accomplished commendable success at a number of treatment centres worldwide, there remain issues associated with time and cost, and the detergents themselves can be detrimental. A considerable amount of the cost results from the fact that the feathers may be remained damaged for a prolonged period subsequent to cleansing, demanding further protection of the animals in specialized facilities up to the scheduled time of release. Even though the costs for standard rehabilitation fluctuate widely, depending on the environment and place of the event, such long-established detergent-based methodologies are inherently costly and generate considerable wastewater. In addition it is not possible to utilise these methods within the initial stabilization formalities (in the field) since the facilities are not transportable, and most of the contamination must remain on the bird until the bird can be transported to a suitable treatment facility (Orbell *et al.*, 2007).

1.5 The “Magnetic Cleansing” method

During the late 1990’s it was demonstrated that finely divided iron powder was efficient for absorbing a wide variety of oils and chemical contaminants from birds. This opened the possibility of ‘magnetically harvesting’, both the iron powder together with the adsorbed contaminant, from various substrates. It was noted that up to 97% of a variety of oils, and an oil/seawater emulsion, could be removed from *feathers* (Orbell *et al.*, 1999). **Figure 1.5** illustrates a typical *in vitro experiment* whereby progressive treatments of a cluster of duck

feathers saturated with crude oil are essentially restored to their original condition (visually and texturally) via “magnetic cleansing”. An especially promising part of this strategy is the fact that iron powder is non-toxic and a non-irritant (Orbell *et al.*, 2007).

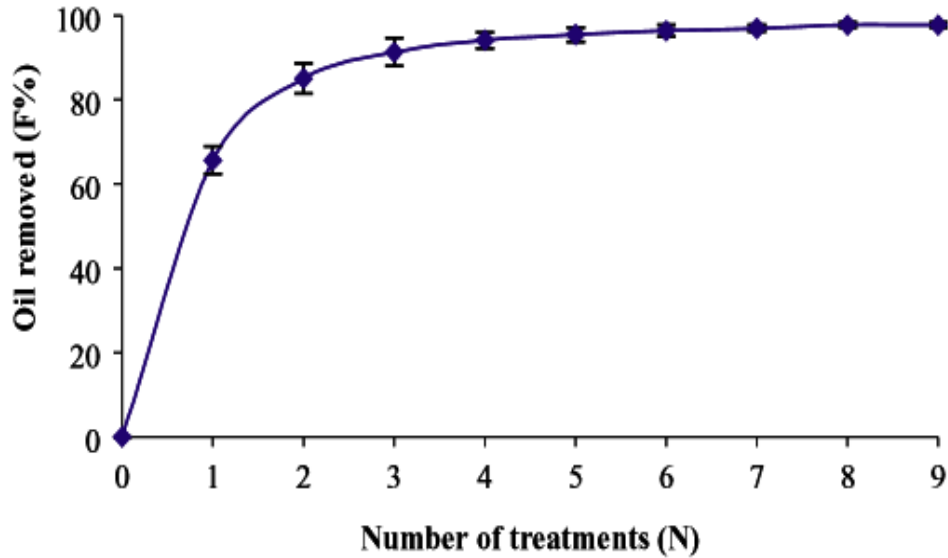


Figure 1.5: Percentage (F%) of oil removed from duck feather clusters as a function of the number of treatments. Error bars represent 95% confidence intervals for five replicates (Orbell *et al.*, 2007).

Magnetic particles have an affinity for an oil contaminated substrate (e.g. feathers).

Figure 1.6 illustrates the principle behind “magnetic cleansing”. The contaminant-laden particles which are subsequently “harvested” with a magnetic device.

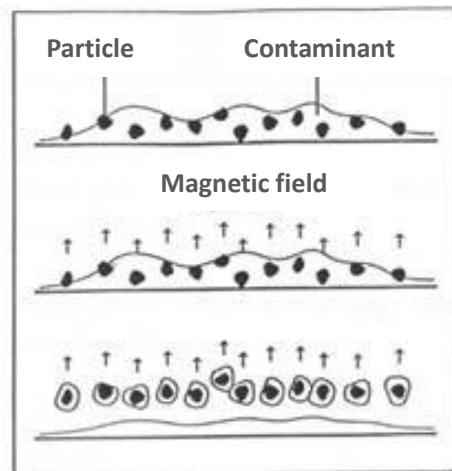


Figure 1.6: (Ngeh 2002), provides a schematic representation of the utilization of magnetic particles to remove a contamination from a substrate.

The application of magnetic particle technology (MPT) towards environmental remediation and wildlife rehabilitation has been under investigation for a number of years, at Victoria University (VU), in collaboration with the PINP. For example, iron powder has been used for the removal of oil contamination from various substrates (Ngeh, 2002), including feathers and plumage (Orbell *et al.*, 1999; 2004; 2006).

The application of MPT in the biosciences is well-established (Safarikova *et al.*, 2001). During recent years, the application of MPT to environmental remediation has also been considered. For example, the use of MPT to remove heavy metals from water (Phanapavudhikul *et al.*, 2003; Oliveira *et al.*, 2004; Hu *et al.*, 2004) and soil (Rikers *et al.*, 1998) has been studied. MPT has also been applied towards the removal of radionuclides from contaminated soil (Macasek *et al.*, 2000) and contaminated water (Kochen *et al.*, 1997), and for the removal phosphate from wastewater (Franzreb *et al.*, 1998). According to previous research (Orbell *et al.*, 1999) MPT is equally effective in the presence of water and for the removal of oil/water emulsions.

Magnetic cleansing involves the application of MPT to environmental remediation and wildlife rehabilitation. Magnetic cleansing is aimed at advancing the science and technology of wildlife remediation and raising the awareness of the problem of oil-spills within the environment. It has been adapted to the rescue and rehabilitation of oiled wildlife, particularly in relation to the Little Penguins. The MPT development involves the use of oil sequestering magnetic particles for the removal of contaminants from wildlife, effectively via a benign dry cleansing process. This research at Victoria University has had an international profile for many years achieving The Banksia Sustainability Award 2013 and The Google Challenge Award with a \$250,000 grant in 2015.

1.5.1 Advantages of the “Magnetic Cleansing” method

The magnetic cleansing method offers several advantages over the conventional detergent-based method such as providing a “quick clean” to the animal upon first encounter. This “quick clean” method removes toxic and/ or corrosive materials from the feathers. This

method could also be useful as part of a stabilization protocol when large numbers of affected animals are awaiting treatments. This “quick clean” method compared to the detergent-based method assures many advantages, particularly with regards to oil removal, handling time (only for “quick clean” in the field), and cost of materials, recycling of waste and highly portable. A traditional detergent-based cleansing method shows greater damage to plumage and requires lots of warm water (Ngeh, 2012).

The methodology of magnetic cleansing additionally provides the possibility of superior equipment portability. Also, it has demonstrated that finely divided iron powder is practically ideal, supporting the removal (via magnetic harvesting) of different oil types and oil/seawater emulsions from both feather clusters and plumage of whole bird models (Ngeh, 2012), with minimal harm towards the feathers compared to detergent-based cleansing (Orbell *et al.*, 1999; 2004). After the bird has been stabilized and transferred to a treatment facility, magnetic cleansing is applied in conjunction with detergent cleansing.

Research (Ngeh, 2012) has shown that magnetic cleansing research involves the development and optimization, not only of the particles themselves, but also of the equipment and protocols that are appropriate for application in the field. Development of the oil-sequestering magnetic particles themselves with various approaches have been under investigation, including the coating of iron particles with hydrophobic (or super-hydrophobic) surfaces (Ngeh, 2012). More recently this technique has been demonstrated to be capable of achieving 100% removal within experimental error (Dao *et al.*, 2006). It has also been demonstrated to be effective with respect to weathered/tarry contamination (Orbell *et al.*, 2005) and (Dao *et al.*, 2006).

With the increasing availability of new methods and materials for the removal of oil contamination from wildlife, it is important to develop laboratory, as well as field techniques, for assessing relative removal efficacies. This may be done using substrates such as single feathers, feather clusters, whole bird carcasses or animal pelt. As part of these experiments, other variables such as the contaminant type, the cleansing agents (such as detergent type or magnetic particle type), the use of different pre-treatment agents and variants of the hardware/equipment or conditions (such as temperature), may be examined

1.6 Significance of the research

Like all wildlife, Victoria's iconic Little Penguin population is vulnerable to oil spills. Researchers at Victoria University and the PINP have developed a novel technology, based on oil ab(d)sorbing magnetic particles, for providing a "quick clean" to oil contaminated wildlife in the field, upon first encounter. Incorporating this technology into existing stabilization protocols promises to remove the more volatile toxic and/or corrosive components in a matter of minutes, potentially improving the animal's survivability and long-term health prospects. Thus, it is possible to effectively dry-clean a contaminated animal. This is dubbed "magnetic cleansing" and offers a range of advantages over traditional detergent-based methods (e.g., portability). The main purpose of this project is to further improve this technology and its application, to better understand the logistics of implementing it in the field and to further investigate the science of the evaporation of oil from different substrates, including plumage, particularly with respect to the phenomenon of "weathering". In the context of this research program, it should be emphasized that the iconic "Penguin Parade" at PINP is an important contributor Victoria's economy and provides significant employment towards the region. The continuing viability and sustainability of Victoria's Little Penguin population is obviously dependent upon their ongoing survival. Although rare, oil contamination presents a serious threat to the Little Penguins population. It is crucial that all measures should be taken to prepare for such events and that the finest available technology is in place to encounter such challenges and when they occur.

1.7 Aims and objectives

These aims and objectives are unified and represented schematically in the Conceptual Framework Schematic on page iv of the thesis.

- (1) To collate and analyze an existing database, resulting from a previous project within our research group, on the quantification of the magnetic cleansing of Diesel Fuel Oil from whole bird models (Little Penguin carcasses) for a range of % oil coverage. In this way, logistical information on the provision of a "quick clean" of Little Penguins in the field may be established.

- (2) In conjunction with the above logistical information, to investigate the synthesis of lighter weight magnetic particles and their efficacy in the removal of contamination from plumage.
- (3) To investigate an established gravimetric method, the use of MPT to provide relative quantitative assays for the comparative removals of oil contamination from Little Penguin pelt as a substrate, as opposed to feather clusters or carcasses. To investigate the feasibility of recycling the pelt substrate via the quantification of the oil removal.
- (4) The physical characteristics of oil evaporation (“weathering”) from Little Penguin pelt (representing plumage) will be investigated for eleven different oils, including light, medium and heavy. Thus, weathering experiments will be carried out for periods of up to 21 days and more detailed investigations of the evaporation profiles will be investigated over the first 10 hours of the process. The effect of temperature on the weathering profiles will also be investigated. Curve fitting software developed within our group will be employed in the analysis of this data.

References

- Australian Maritime Safety Authority (AMSA), *Major historical incidents*, viewed 11 October 2024, <<https://www.amsa.gov.au/marine-environment/incidents-and-exercises/major-historical-incidents>>.
- Clark, RB & Gregory, KG 1971, 'Feather-wetting in cleaned birds', *Mar. Pollut. Bull.*, vol. 2, pp. 78-79.
- Dao, HV, Ngeh, LN, Bigger, SW & Orbell, JD 2006, 'Achievement of 100% removal oil from feathers employing magnetic particle technology', *J. Environ. Eng.*, vol. 132, no. 5, pp. 555-559.
- Dao, HV, Maher, LA, Ngeh, LN, Bigger, SW, Orbell, JD, Healy, M, Jessop, R., Dann, P 2006, 'Removal of petroleum tar from bird feathers utilizing magnetic particles', *Environ. Chemistry Letters*, vol. 4, no. 2, pp. 111-113.
- Dao, HV, Ngeh, LN, Bigger, SW, Orbell, JD, Healy, M, Jessop, Dann, P 2006, 'Magnetic cleansing of weathered/tarry oiled feathers – The role of pre-conditioners', *Marine Pollution Bulletin*, vol. 52, pp. 1591-1594.
- Dao, HV 2007, 'An investigation into factors affecting the efficacy of oil removal from wildlife using magnetic particle technology', PhD Thesis, Victoria University, Melbourne Australia.
- Dennis, JV 1959, *Oil pollution survey of the United States Atlantic coast*. American Petroleum Institute, Divisional Transportation, Washington D. C.
- Department of Ecology State of Washington 2019, *Focus on: Environmental Harm from Oil Spills*, viewed 28 January 2023, <Focus on: Environmental Harm from Oil Spills (wa.gov)>.

Ecospill 2021, *What are the environmental effects of an oil spill*, viewed 24 January 2023, <<https://www.ecospill.com.au/what-are-the-environmental-effects-of-an-oil-spill/>>.

Franzreb, M, Kampeir, P, Franz, M, Eberle, HS 1998, 'Use of magnetic technology for phosphate elimination from municipal sewage', *Journal of Acta hydrochimica et Hydrobiological*, vol. 26, no. 4, pp. 213-217.

Gilbert, T 1999, *Oiled wildlife issues*, National Oiled Wildlife Response Plan (NOWRP).

Harrigan, KE 1992, 'Causes of mortality of Little Penguins *Eudyptula minor* in Victoria', EMU, *J. Roy. Australasian Ornithol. Union.*, vol. 91, pp. 273-277.

Harris, JM & Smith, DC 1997, 'Treatment husbandry and rehabilitation of oil-soaked birds', *Current. Vet. Ther.*, vol. 6, pp. 694-697.

Hartung, R, Hunt, GS 1966, 'Toxicity of some oils to waterfowl', *J. Wild. Manage.*, vol. 30, pp. 564-570.

Healy, M 1999, *Personal communication*, Phillip Island Nature Park, Melbourne, Australia.

Holcomb, J & Russell, M 1999, 'New breakthroughs in oiled bird rehabilitation', *J. Wildl. Rehabil.*, vol. 22, no. 4, pp. 6-8.

Hu, J, Lo, IMC, Chen, G 2004, 'Removal of Cr (VI) by magnetite', *Water Sci. & Technol.*, vol. 50, no. 12, pp. 139-146.

International Tanker Owners Pollution Federation Limited (ITOPF) 2004, *ITOPF Handbook 2004/2005*, viewed 14 December 2023, <<http://www.itopf.com/itopfhandbook2004.pdf>>.

International Tanker Owners Pollution Federation Limited (ITOPF) 2022, *ITOPF Statistics 2022*, viewed 14 December 2023, <<https://www.itopf.org/knowledge-resources/documents-guides/oil-tanker-spill-statistics-2022/>>.

Jenssen, BM & Ekker, M 1989, 'Rehabilitation of oiled birds: A physiological evaluation of four cleansing agents', *Mar. Pollut. Bull.*, vol. 20, pp. 509-512.

Jessop, R & Healy, M 1997, '*Techniques for the treatment of sick, injured or oiled penguins*', viewed 14 December 2023, <oiled-seabirds-jessop-and-healy.pdf (seabirdrescue.org.au)>

Kochen, RL & Navratil, JD 1997, *Removal of radioactive materials and heavy metals from water using magnetic resin*, US Patent, 5, 595, 666.

Macasek, F & Bartos, P 2000, 'A Magnetic Sorbent for Radiocesium and Radiostrontium Removal from Clay and Soil Suspensions', *J. Radioanalytical and Nuclear Chemistry*, vol. 246, no. 3, pp. 565-569.

Michael, AD 1977, 'Fate and effects of petroleum hydrocarbons in marine ecosystems and organisms', *Pergamon Press*, pp. 129-137.

Michel, J & Fingas, M 2016, 'Oil Spills: Causes, Consequences, Prevention, and Countermeasures', *Fossil Fuels*, pp. 159-201.

Miller, EA 1999, *Oil spill medical protocols*, Tri-state Bird Rescue & Research, Incorporation.

Mullin, JV & Champ, MA 2003, 'Introduction/overview of *in-situ* burning of oil spills', *Spill Sci. & Technol. Bull.*, vol. 8, no. 4, pp. 323-330.

Naviaux, J & Pittman, A 1973, 'Cleaning of oil-covered birds', *Biol. Conserv.*, vol. 5, pp. 292-294.

Ngeh, LN 2002, 'The development of magnetic particle technology for application to environmental remediation', PhD Thesis, Victoria University, Melbourne, Australia.

Ngeh, LN, Orbell, JD, Bigger, SW, Munaweera, K, Dann, P 2012, 'Magnetic cleansing for the provision of a quick clean to oiled wildlife', *World of Academy of Science and Technology*, vol. 72, pp. 1091-1093.

Obendorf, DL, McColl, K 1980, 'Mortality in Little Penguins *Eudyptula minor* along the coast of Victoria', *J. Wildl. Disease*, vol. 16, pp. 251-259.

Oliveira, LCA, Rios, RVRA, Fabris, JD, Lago, RM 2004, 'Magnetic particle technology: A simple preparation of magnetic composites for the adsorption of water contaminants', *J. Chem. Edu.*, vol. 81, no. 2, pp. 248-250.

Orbell, JD, Tan, EK, Coutts, MC, Bigger, SW, Ngeh, LN 1999, 'Cleansing oiled feathers-magnetically', *Mar. Pollut. Bull.*, vol. 38, no. 3, pp. 219-221.

Orbell, JD, Ngeh, LN, Bigger, SW, Zabinskas, M, Zheng, M, Healy, M, Jessop, R, Dann, P 2004, 'Whole-bird models for the magnetic cleansing of oiled feathers', *Mar. Pollut. Bull.*, vol. 38, no. 48, pp. 336-340.

Orbell, JD, Dao, HV, Ngeh, LN, Bigger, SW, Healy, M, Jessop, R, Dann, P 2005, 'Acute temperature dependency in the cleansing of tarry feathers utilizing magnetic particles', *Environ. Chem. Letters*, vol. 3, no. 1, pp. 25-27.

Orbell, JD, Dao, HV, Maher, LA, Ngeh, LN, Bigger, SW, Healy, M, Jessop, R, Dann, P 2006, 'Removal of petroleum tar from bird feathers utilizing magnetic particles', *Environ. Chem. Letters*, vol. 4, no. 2, pp. 111-113.

Orbell, JD, Dao, HV, Ngeh, LN, Bigger, SW, Healy, M, Jessop, R, Dann, P 2006, 'Magnetic cleansing of weathered/tarry oiled feathers – the role of pre-conditioners', *Mar. Pollut. Bull.*, vol. 52, pp. 1591-1594.

Orbell, JD, Dao, HV, Ngeh, LN, Bigger, SW 2007, 'An investigation into the feasibility of applying magnetic particle technology to the cleansing of oiled wildlife in the field', *The*

technical Report Prepared for the Australian Marine Safety Authority (National Plan Environment Working Group) and the Phillip Island Nature Parks.

Orbell, JD, Dao, HV, Ngeh, LN, Bigger, SW 2007, 'Magnetic particle technology in environmental remediation and wildlife rehabilitation', *Environmentalist*, vol. 27, pp. 175-182.

Orbell, JD, Dao, HV, Kapadia, J, Ngeh, LN, Bigger, SW, Healy, M, Jessop, R, Dann, P 2007, 'An investigation into the removal of oil from rock utilizing magnetic particle technology', *Mar. Pollut. Bull.*, vol. 54, pp. 1958-1961.

Peakall, DB, Hallet, DJ, Bend, JR, Foureman, GL 1982, 'Toxicity of Prudhoe Bay Crude oil and its aromatic fractions to nestling herring gulls', *Environ. Res.*, vol. 27, pp. 206-215.

Perry, MC, Ferrigno, F, Settle, FH 1978, 'Rehabilitation of birds oiled on two mid-Atlantic estuaries', *Proceedings of the Annual Conference South-eastern Association of Fish and Wildlife Agencies*, Hot Springs, VA, USA, pp. 318-324.

Phanapavudhikul, P, Waters, AJ, Perez de Ortiz, ES 2003, 'Design and Performance of Magnetic Composite Particles for the Separation of Heavy Metals from Water', *J. Environ. Sci. Health, Part A-Toxic/Hazardous Substances and Environmental Engineering*, vol. A38, no. 10, pp. 2277-2285.

Rikers RA, Voncken, JHL, Dalmijn, WL 1998, 'Cr-polluted Soil Studied by High Gradient Magnetic Separation and Electron Probe', *J. Environ. Eng.*, vol. 124, no. 12, pp. 1159-1164.

Safarikova, M & Safarik, I 2001, 'The Application of Magnetic Techniques in Biosciences', *Magn. Electro. Sep.*, vol. 10, pp. 223-252.

Schmidt, K 1997, 'A drop in the ocean', *New Scientist*, vol. 3, pp. 41-44.

Silva, IA, Almeida, FCG, Souza, TC, Bezerra, KGO, Durval, IJB, Converti, A, Sarubbo, L 2022, 'Oil spills: impacts and perspectives of treatment technologies with focus on the use of green surfactants', *Environ, Monit, Assess.*, vol. 194, no. 143.

Spaulding, ML 2017, 'State of the art review and future directions in oil spill modelling', *Mar. Pollut. Bull.*, vol. 115, no. 1-2, pp. 7-19.

Stocker, L 2000, Practical wildlife care, *Blackwell Science*, London.

Suni, S, Kosunen, AL, Hautala, M, Pasila, A, Romantschuk, M 2004, 'Use of a by-product of peat excavation, cotton grass fibre, as a sorbent for oil spills', *Mar. Pollut. Bull.*, vol. 49, no. 11-12, pp. 916-921.

U.S. Energy Information Administration 2022, *Oil and petroleum products explained*, viewed 28 January 2022, <<https://www.eia.gov/energyexplained/oil-and-petroleum-products/oil-and-the-environment.php>> .

Ventikos, NP, Vergetis, E, Psaratifs, HN, Triantafyllou, G 2004, 'A high level synthesis of oil spill response equipment and countermeasures', *J. Hazard. Mater.*, vol. 107, pp. 51-58.

Wong, C 2022, *How do oil spills affect the environment*, viewed 28 January 2023, <How Do Oil Spills Affect the Environment | Earth.Org>.

Chapter 2: An analysis of the logistics of providing an MPT “quick clean” to contaminated Little Penguins in the field.

2.1 Introduction

2.2 Methodology – exploiting the AMSA database for logistical information

2.3 Results and Discussion

2.4 Conclusion

2.5 References

2.1 Introduction

Oil spill events are very diverse in terms of their location, contaminant types, affected wildlife, weather conditions and available resources (Wilhelmsson *et al.*, 2013). Worldwide, there tends to be a standard response to such events based on stabilizing affected wildlife, transporting them to treatment facilities, “traditional” surfactant-based cleansing and subsequent rehabilitation and release (Ngeh *et al.*, 2012). For events that occur in remote locations or when large numbers of contaminated birds must be contained in holding bays, there may be a considerable delay in both the stabilization of the animal and its subsequent treatment (Ngeh *et al.*, 2012). Most oil contaminants have a “volatile” fraction that is usually toxic and/or corrosive and it is desirable to remove this fraction as soon as possible upon first encountering the animal. Indeed, anecdotal evidence suggests that fumes from such volatile components can even present a health risk to animal rescuers/rehabilitators in a holding bay environment. This problem is difficult to address via conventional treatment protocols.

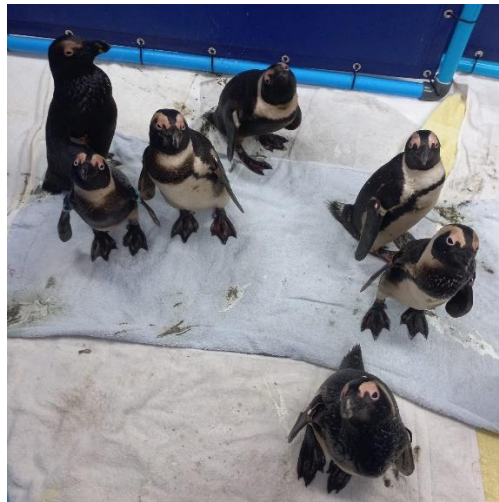


Figure 2.1: Contaminated Little Penguins in holding bays (SANCCOB, 2024).

Since several decades, scientists at Victoria University and the PINP have collaborated on a program aimed at advancing the science and technology involved in the rescue and rehabilitation of oiled wildlife (Ngeh *et al.*, 2012). This study has received significant international interest (Copley, 1999; Pilcher, 2004) and is now at the level where proof of principle work has been accomplished and peer reviewed (Orbell *et al.*, 1999; 2004; 2005; 2007; Dao *et al.*, 2006-a; 2006-b; 2006-c). The application of oil ab(d)sorbing magnetic

particles to the cleansing and rehabilitation of oiled wildlife is at the core of the research presented in this thesis.

The use of oil sequestering magnetic particles for the removal of contaminants from plumage is a promising development (Orbell *et al.*, 1999; 2007). In contrast to detergent-based cleaning, this method of dry-cleaning causes less harm to the feathers. Furthermore, due to its portability, the use of magnetic particle technology (MPT) to remove oil contamination from plumage (and fur) can provide a “quick clean” to the animal upon first encounter. This could be especially useful if the contaminant is toxic and/or corrosive, as many of these chemicals are, or if transporting the victim to a treatment facility is delayed. Notably, when many affected animals are awaiting treatment, the method could be an important part of a stabilization protocol (Ngeh *et al.*, 2012). Penguins, in particular, that are exposed to oil spills are at risk of hypothermia because the oil affects the waterproofing and insulating characteristics of their plumage. They can also absorb the oil while preening themselves, resulting in toxicity and internal organ damage (Victoria University, 2014).

The “magnetic cleansing” technique, including the magnetic particles used and associated equipment for use in the field, are now well-developed and have been deployed at the PINP. However, the logistics for applying this technology to an actual event is still under development. Work is also underway to further develop the magnetic particles themselves, including within this project, Chapter 3. This research is ongoing and diverse methods have been investigated for the development of the oil-sequestering magnetic particles themselves, from the coating of iron particles with hydrophobic (or super-hydrophobic) surfaces, as shown in **Figure 2.2(a)**, to the identification and characterization of highly ab(d)sorbent grades of iron powder, **Figure 2.2(b)**. In relation to the latter, it has been shown that specific grades of finely divided iron powder are very effective for “magnetic harvesting,” which is the removal of a variety of different oils and oil/seawater emulsions from both feather clusters and from the plumage of whole birds (Orbell *et al.*, 2004). More recently, it has been shown that this method is effective in removing weathered/tarry contamination, with 100% removal achieved within experimental error (Dao *et al.*, 2006; Orbell *et al.*, 2005; Dao *et al.*, 2006).

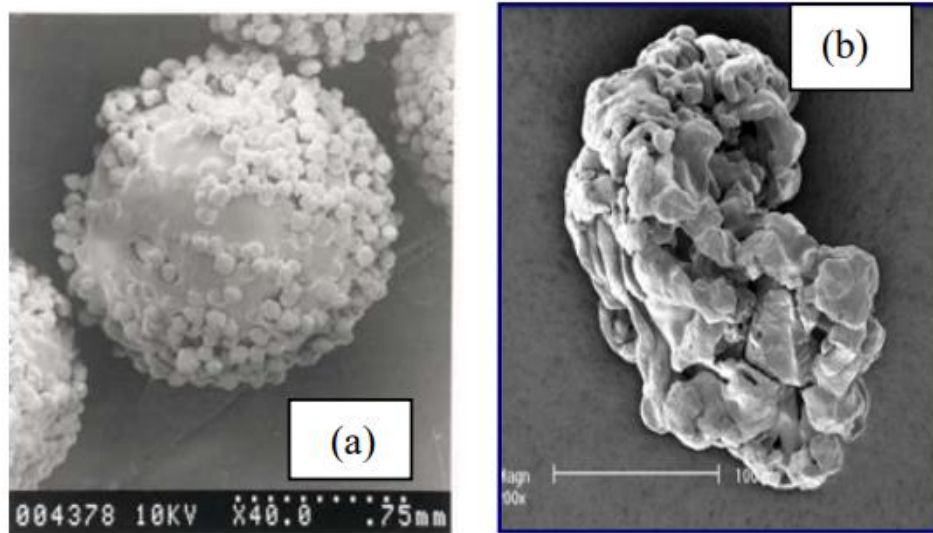


Figure 2.2: Electron micrographs of oil sequestering particles **(a)** polymer-coated and **(b)** finely divided iron powder (Ngeh *et al.*, 2012).

The design and development of appropriate magnetic harvesting equipment for different situations is also ongoing, and includes the design and testing of a portable, hand-held magnetic device (the “magnetic harvester”) that can safely and efficiently strip the oil-laden magnetic particles from the animal and allow the waste to be disposed of in a controlled way (Ngeh, 2012). The development of such devices within Victoria University Research Group evolved through four generations of construction and testing (Ngeh, 2012):

- a. First Generation:** a standard “magnetic tester” the magnetic field of which can be mechanically turned on and off by moving the plunger. Although appropriate for routine laboratory experiments, this device requires two hands to operate and is not considered suitable for “field” work.
- b. Second Generation:** a one-handed magnetic harvester with a compressed air-operated mechanical on-off switch. Although effective, this device is deemed too cumbersome for use in the field.
- c. Third Generation:** an electromagnetic device that has since been proven unsuitable due to an inability to achieve a magnetic field strength in the desired range of 5,000-10,000 Gauss.

- d. Fourth Generation:** a “magnetic wand” designed with a “quick clean” in mind. This is built on a meticulously planned array of rare earth magnets inside a 100 mm stainless steel tube with a non-magnetic 35 mm tip. The non-magnetic tip of this device makes it easy to wipe off oil-laden particles into a waste container while simultaneously producing a strong, highly localized magnetic field. This is an essential component of any field equipment (Ngeh, 2012).

An investigation into the feasibility of applying MPT to the cleansing of oiled wildlife in the field (Orbell *et al.*, 2007), sponsored by the Australian Maritime Authority (AMSA), demonstrated the potential for MPT to provide an effective solution to this problem by providing a “quick clean” to contaminated animals upon first encounter in the field, or within holding bays, via the use of oil absorbing magnetic particles and a specifically developed “magnetic wand”, **Figure 2.3**.



Figure 2.3: Magnetic “wand” (Ngeh *et al.*, 2012).

This technology has been shown to remove the volatile components from feathers and plumage within minutes and, furthermore, the technology is highly portable (Orbell *et al.*, 1999; 2004; 2005; 2007; Ngeh *et al.*, 2012; Dao *et al.*, 2006). The 35 mm non-magnetic tip allows the oil-laden particles to be wiped off the tube into a container and another cycle of removal can immediately be commenced. This “wand” technology for providing a “quick clean” in the field won the 2013 Banksia Sustainability Award - in partnership with the Phillip Island Nature Parks and the 2014 Google Impact Challenge Award - in partnership with the Penguin Foundation.

Concurrent with the development of the previous mentioned technology, an experimental program was carried out to investigate the feasibility of applying MPT to the cleaning of oiled wildlife in the field by removing different coverage (% by mass) of various oil types from the plumage of the Little Penguin (*Eudyptula minor*) (Orbell *et al.*, 2018). These ongoing investigations are designed to estimate the logistical requirements for such potential operations, such as the time taken, the mass of particles required per bird, the mass of waste per bird, costs relating to materials, waste disposal, and personnel, in addition to establishing important methodologies for conducting complex experiments of this type. Other considerations, such as the use of pre-treatment agents, have also been addressed (Orbell *et al.*, 2018).

Figure 2.4 illustrates an example of data collected in these experiments. The first investigations were conducted using a laboratory magnetic tester so that the highest percentage of contamination can eventually be removed. However, the most intriguing discovery at this point is that a large fraction of contamination can be removed after only one or two treatments (taking only 5-10 minutes). This observation led to the notion that MPT could be used to provide a “quick clean” upon initial encounter in the field (Ngeh *et al.*, 2012).

As a result of the subsequent development of the magnetic wand device, **Figure 2.3**, a program was carried out to produce a prototype set of equipment to allow a “quick clean” to be trialed. **Figure 2.5** depicts such experiments.

Data analysis of such experiments reveals that the initial removal increases as the percentage coverage decreases. Recent experiments have also shown that using the magnetic wand device rather than the magnetic tester improves the initial removal. **Figure 2.6** depicts some representative data. Notably, for 20% coverage (by mass) of diesel and engine oil, respectively, 85% and 93% removal of these contaminants can be accomplished following just two treatments, requiring around 5 minutes in each case (Ngeh *et al.*, 2012). This represents primarily the volatile fractions of these oils, that are removed preferentially.

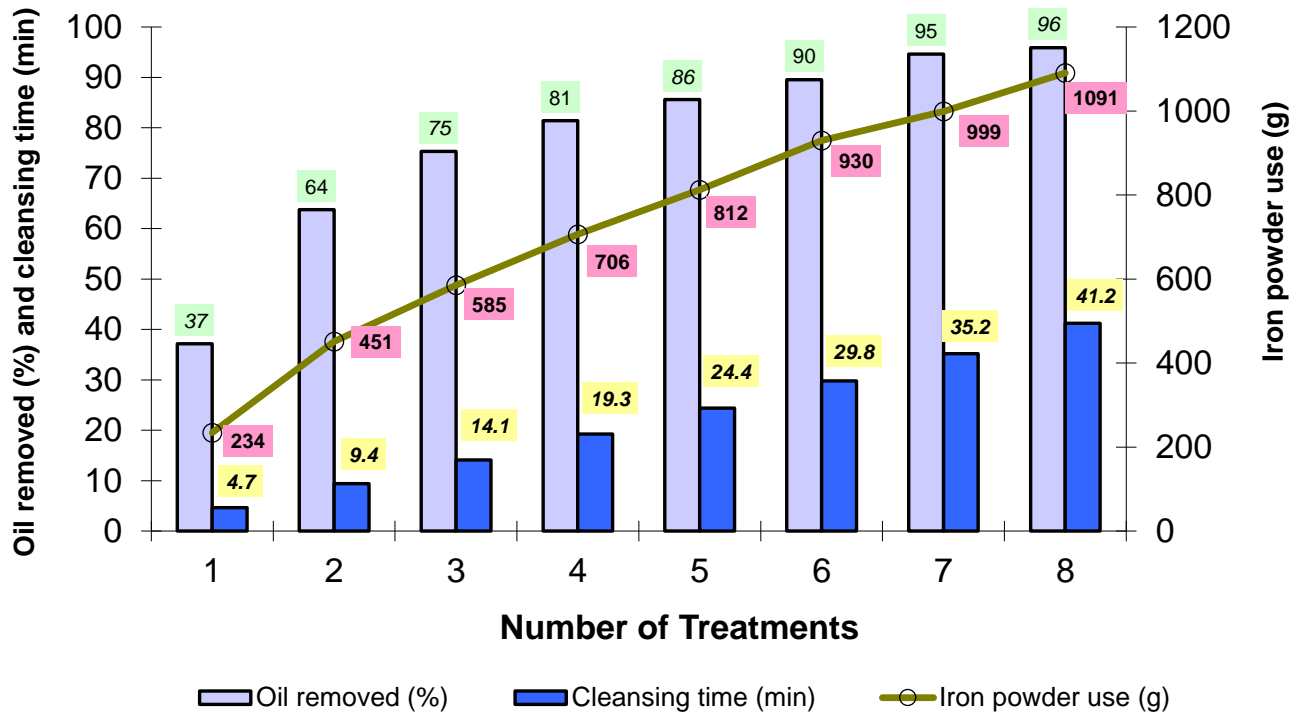


Figure 2.4: An illustration of the removal of Diesel oil (100% coverage – worst case scenario) from a Little Penguin carcass. It should be noted that in this experiment, a “first generation” magnetic tester was utilized, and that 37% removal could be accomplished in 4.7 minutes and 64% removal in 9.4 minutes (Ngeh *et al.*, 2012).

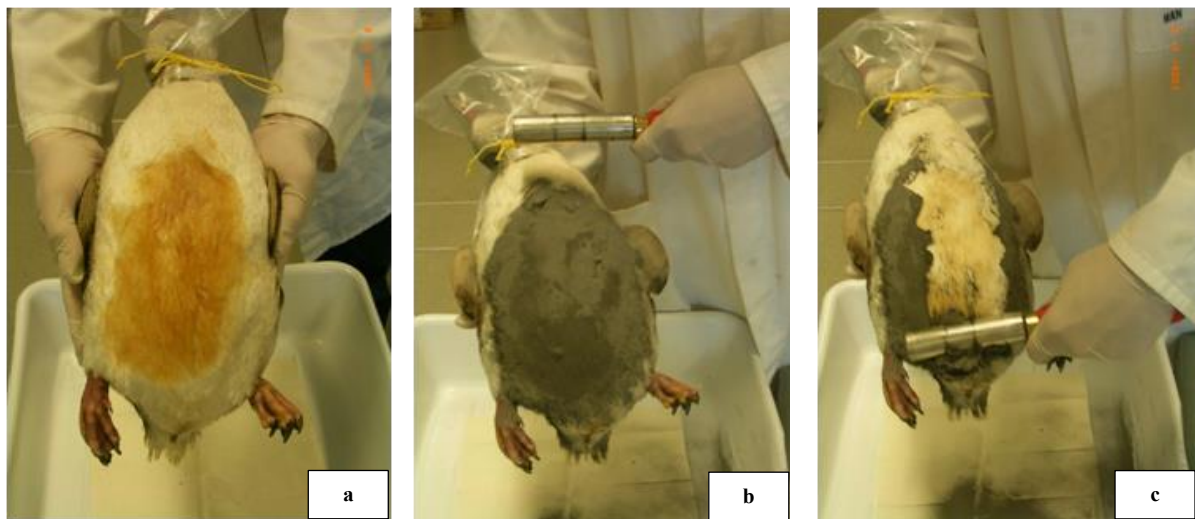


Figure 2.5: Simulating a “quick clean” for a Little Penguin Carcass contaminated with (a) 20% coverage (by mass) of engine oil (b) after magnetic particle application (c) 82% removal is achieved (Ngeh *et al.*, 2012).

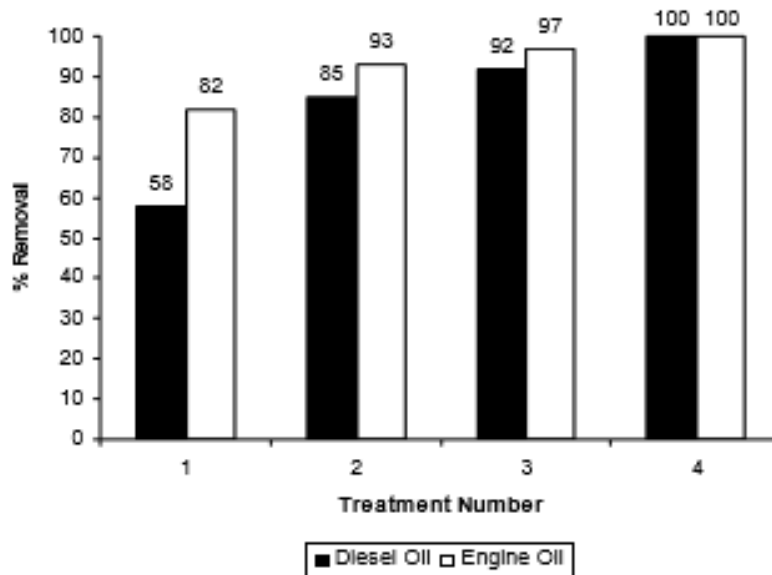


Figure 2.6: Representative data for the “magnetic wand” removal of Diesel and engine oil from carcass of the Little Penguin to the extent of 20% (by mass) (Ngeh *et al.*, 2012).

To further advance this concept, a collaboration between Victoria University’s College of Engineering and Science, the Phillip Island Nature Parks Research Centre, and Monash University’s Department of Design with the goal of applying industrial design expertise to designing a prototype field kit for providing contaminated wildlife in the field a “quick clean”, **Figure 2.7.**

The design of such an integrated portable kit must consider factors such as the weight of the various components, including the weight of particles required, the amount of waste produced, particle and waste storage, ergonomic factors, the number of people required in the quick clean team (e.g. one person would be required to handle the animal while the other performs the operation) and their specific roles etc. Other factors to consider include the requirement for additional products and equipment, such as appropriate gear. Then, both in the lab and in the field, any such prototype would need to be tested and assessed (Munaweera, 2015). A “proof of principle” analysis of such logistical parameters is carried out in this Chapter based on an existing database generated by our research group.



Figure 2.7: The “backpack” design, based on MPT, for a portable “Quick Clean” Kit (Orbell *et al.*, 2022).

2.2 Methodology – exploiting the AMSA database for logistical information

The AMSA report (Orbell *et al.*, 2007) contains a large database on the magnetic cleansing removal characteristics and parameters, *vide supra*, of Diesel fuel oil from Little Penguin carcasses, that have been contaminated at plumage coverages¹ of 10, 20, 50, 70 and 100%. Other important parameters that have been documented include the % removal at each treatment, the cumulative treatment time and the cumulative mass of magnetic powder used. The amount of waste generated at each treatment can also be calculated from this data.

For example, representative data for the magnetic cleansing removal of Diesel from a Little Penguin carcass for 50% contaminant coverage, is shown in **Figure 2.8**, below. From such plots and their associated data, the essential logistical data may be extracted. Of course, other contaminants and species are possible, provided the same exhaustive experiments have been conducted for a given oil and bird, but the data provided by the AMSA study is sufficient to

¹ The methodology for the determination of % oil coverage of a carcass is given in the AMSA report, pages 16 – 17.

provide a “ballpark” estimate of the logistics that might be involved in providing a general quick clean in the field. Thus, the parameters of interest that have been extracted from this data for logistical analysis include, more specifically: the % coverage; the number of treatments; the cumulative time at each treatment per bird; the cumulative mass of powder used at each treatment per bird; the cumulative amount of oil removed at each treatment per bird (%); the cumulative mass of magnetic particles used at each treatment per bird and the cumulative mass of waste produced at each treatment per bird.

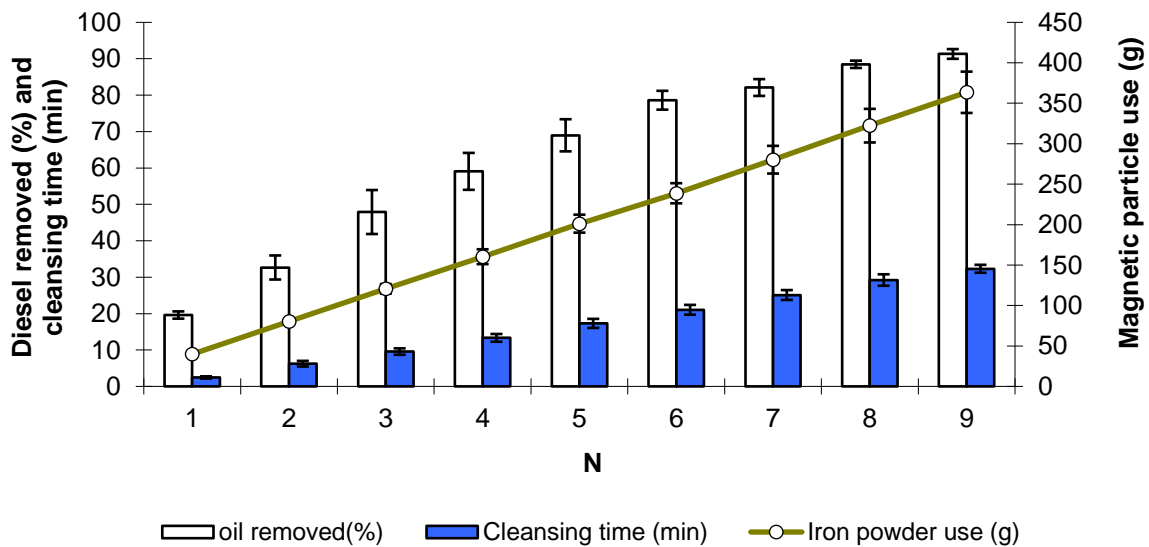


Figure 2.8: Histogram of Diesel removal (%) versus number of treatments (N), cleansing time (min) and magnetic particle consumption (g) as a function of the number of treatments, for the removal of **50% Diesel Oil coverage** (by mass) from plumage. Error bars represent the standard error for three replicates (Orbell *et al.*, 2007).

Thus, the AMSA database described above has been employed in this study to investigate the logistics of providing a “quick clean” based on MPT to contaminated Little Penguins in the field. In this regard, several “in-field scenarios” are proposed, documented, and discussed below.

Removal data for 1 and 2 treatments (N = 1 or 2 are considered a “quick clean”) has been documented for 10, 100 and 1000 Little Penguins that are contaminated to different extents with Diesel fuel oil. Namely, “average coverages” of 10%, 20%, 50%, 70% and 100% are considered in turn for each population. In practice, for a given oil spill, an “average coverage”

would have to be estimated (possibly using drone technology), prior to determining the resources required.

2.3 Results and Discussion

Table 2.2 shows a collation of the essential logistical data from the AMSA project for the removal of Diesel from Little Penguin plumage for 10, 20, 50, 70 and 100% coverages, for 1 and 2 treatments, respectively (representing a “quick clean”) as applied to *10 birds*. **Table 2.3** contains a summary of the essential logistical data for the removal of Diesel from Little Penguin plumage for 10, 20, 50, 70 and 100% coverages for 1 and 2 treatments respectively (representing a “quick clean”) as applied to *100 birds*. **Table 2.4** contains a summary of the essential logistical data for the removal of Diesel from Little Penguin plumage for 10, 20, 50, 70 and 100% coverages for 1 and 2 treatments respectively (representing a “quick clean”) as applied to *1000 birds*. This data will allow different scenarios to be assessed with respect to the feasibility of providing an MPT “quick clean” in the field. In this regard, the data has been further summarized into **Tables 2.5 to 2.14** to facilitate logistical analysis. Thus, three key parameters have been considered: cumulative treatment times for N = 1 or 2; total mass of powder required for N = 1 or 2 and total mass of waste (oil-laden particles) for N = 1 or 2. A “team” is considered to consist of 2 persons, one person to handle the animal and the other person to conduct the removal. A minimum of one team is required.

The following example illustrates how this data might be applied to a real-life scenario. Thus, consider the follow scenario based on the Deepwater Horizon oil spill on April 20, 2010 (National Oceanic and Atmospheric Administration, 2010), when an explosion damaged the Deepwater Horizon oil rig resulting in a massive discharge of oil into the Gulf of Mexico (https://en.wikipedia.org/wiki/Deepwater_Horizon_oil_spill) resulting in extensive pollution of wildlife, including brown pelicans, as shown in **Figure 2.9** (Encyclopedia Britannica, 2010; 2023). In this picture there are approximately 10 birds that are, obviously, 100% covered. The nature of the contamination is not clear, although it is likely to be a combination of light crude plus dispersant, both of which are potentially toxic and corrosive². This small holding bay is

² Note that MPT will just as effectively remove the dispersant.

an ideal opportunity for a “quick clean” utilizing the wand and MPT. The question is, would this be feasible in terms of resources and logistics and how many two-person teams would be required? Based on the whole carcass experiments described previously and the data generated, it is possible to estimate the logistics of this (and other) scenario(s). Based on the data in **Tables 2.9 and 2.14**, specifically, it is possible to determine the logistical requirements for this particular scenario, by extracting the relevant data. This data for this scenario (10 birds), and for a hypothetical 100 and 1000 birds, are summarized in **Table 2.1**.



Figure 2.9: A potential pollution event scenario. Ten fully contaminated (100% coverage) brown pelicans from the Deepwater Horizon oil spill being held, awaiting treatment in a small holding bay (Encyclopedia Britannica, 2010; 2023).

Table 2.1 (blue – one treatment; red – two treatments)

Birds	10	100	1000
Cumulative time (h)	0.8 (1.6)	7.7 (15.4)	78.5 (157.0)
Total mass of powder (kg)	2.3 (4.5)	23.4 (45.1)	234.3 (450.9)
Total mass of waste (kg)	2.9 (5.4)	28.7 (54.2)	287.4 (542.1)
	<i>Suggest 1 team</i>	<i>Suggest 4 teams</i>	<i>Suggest 10 teams</i>

Thus, the number of 2 person teams required for a given scenario can be determined. For example, for 10 birds, each being 100% covered, the time required to perform 1 treatment each for all the birds would be about 48 minutes (0.8 h), the total mass of magnetic particles to be carried would be 2.3 kg (~1.2 kg per person) and the total mass of waste would be around 2.9 kg (~1.5 kg per person). These numbers are approximately doubled for two treatments. Therefore, for this scenario, it is reasonable to conclude that one two-person team is sufficient to apply the quick clean technique in the field to these birds. A similar analysis for the 100 and 1000 bird scenarios suggests 4 and 10 teams, respectively. Therefore, if necessary, and if costs allow, more than one trained team may be employed. In such an instance, the relevant logistical statistics are easily adjusted proportionally. For example, the calculated time required for one team would be halved for two teams.

To illustrate the practicality of a quick clean consider the following scenarios – *Oil type: Diesel, immediate access and 1 team (initially):*

“In the field” scenario – 10%, 20%, 50%, 70% and 100% Coverage

Based on 10 birds for 1 (blue) treatment and 2 (red) treatments

Table 2.2: Logistical analysis – “In the field” scenario based on 10 birds.

Coverage	10%		20%		50%		70%		100%	
Treatment	Treatment 1	Treatment 2								
Number of birds	10	10	10	10	10	10	10	10	10	10
Coverage (%)	10	10	20	20	50	50	70	70	100	100
Treatments per bird	1	2	1	2	1	2	1	2	1	2
Cumulative time per treatment per bird (min)	2.3	5.4	2.3	4.2	2.5	6.2	3.1	6.4	4.7	9.4
Cumulative mass of powder used per treatment per bird (g)	20.6	41.2	28.1	52.0	39.9	80.4	50.8	101.9	234.3	450.9
Cumulative oil removal per treatment per bird (%)	32.7	56.0	29.5	46.0	19.6	32.7	17.1	31.3	37.2	63.8
Cumulative mass of oil removed per bird (g)	4.4	7.6	8.4	13.2	14.0	23.4	17.1	31.3	53.1	91.2
Cumulative time for 10 birds (min)	23.1	53.7	23.2	42.5	24.5	62.4	30.5	63.7	46.6	94.1
Total mass of powder (kg)	0.21	0.41	0.28	0.52	0.39	0.80	0.50	1.01	2.34	4.50
Total mass of oil removed (kg)	0.04	0.08	0.08	0.13	0.14	0.23	0.17	0.31	0.53	0.91
Total mass of waste (kg)	0.25	0.49	0.36	0.65	0.53	1.03	0.67	1.33	2.87	5.42

“In the field” scenario – 10%, 20%, 50%, 70% and 100% Coverage

Based on 100 birds for 1 (blue) treatment and 2 (red) treatments

Table 2.3: Logistical analysis – “In the field” scenario based on 100 based birds.

Coverage	10%		20%		50%		70%		100%	
Treatment	Treatment 1	Treatment 2								
Number of birds	100	100	100	100	100	100	100	100	100	100
Coverage (%)	10	10	20	20	50	50	70	70	100	100
Treatments per bird	1	2	1	2	1	2	1	2	1	2
Cumulative time per treatment per bird (min)	2.3	5.4	2.3	4.2	2.5	6.2	3.1	6.4	4.7	9.4
Cumulative mass of powder used per treatment per bird (g)	20.6	41.2	28.1	52.0	39.9	80.4	50.8	101.9	234.3	450.9
Cumulative oil removal per treatment per bird (%)	32.7	56.0	29.5	46.0	19.6	32.7	17.1	31.3	37.2	63.8
Cumulative mass of oil removed per bird (g)	4.4	7.6	8.4	13.2	14.0	23.4	17.1	31.3	53.1	91.2
Cumulative time for 100 birds (hr)	3.85	8.94	3.87	7.09	4.09	10.4	5.08	10.6	7.7	15.6
Total mass of powder (kg)	2.06	4.12	2.81	5.2	3.98	8.04	5.08	10.19	23.43	45.09
Total mass of oil removed (kg)	0.44	0.76	0.84	1.32	1.40	2.34	1.71	3.13	5.31	9.11
Total mass of waste (kg)	2.5	4.88	3.65	6.51	5.39	10.38	6.79	13.32	28.74	54.21

“In the field” scenario – 10%, 20%, 50%, 70% and 100% Coverage

Based on **1000 birds** for 1 (blue) treatment and 2 (red) treatments

Table 2.4: Logistical analysis – “In the field” scenario based on 1000 based birds.

Coverage	10%		20%		50%		70%		100%	
Treatment	Treatment 1	Treatment 2								
Number of birds	1000	1000	1000	1000	1000	1000	1000	1000	1000	1000
Coverage (%)	10	10	20	20	50	50	70	70	100	100
Treatments per bird	1	2	1	2	1	2	1	2	1	2
Cumulative time per treatment per bird (min)	2.3	5.4	2.3	4.2	2.5	6.2	3.1	6.4	4.7	9.4
Cumulative mass of powder used per treatment per bird (g)	20.6	41.2	28.1	52.0	39.9	80.4	50.8	101.9	234.3	450.9
Cumulative oil removal per treatment per bird (%)	32.7	56.0	29.5	46.0	19.6	32.7	17.1	31.3	37.2	63.8
Cumulative mass of oil removed per bird (g)	4.4	7.6	8.4	13.2	14.0	23.4	17.1	31.3	53.1	91.2
Cumulative time for 1000 birds (hr)	38.5	89.5	38.7	70.9	40.9	104.0	50.8	106.1	77.7	156.8
Total mass of powder (kg)	20.6	41.2	28.1	52.0	39.9	80.4	50.8	101.9	234.3	450.9
Total mass of oil removed (kg)	4.4	7.6	8.4	13.2	14.0	23.4	17.1	31.3	53.1	91.2
Total mass of waste (kg)	25.0	48.9	36.5	65.1	53.9	103.8	67.9	133.2	287.4	542.1

“In the field” scenario – 10%, 20%, 50%, 70% and 100% Coverage – 1 Treatment

Based on 10 birds, 100 birds and 1000 birds

Table 2.5: Cumulative time (h), total mass of powder (kg) and total mass of waste (kg) as a function of 1 treatment for 10% Diesel Oil coverage based on 10, 100 and 1000 birds.

Birds	10	100	1000
Cumulative time (hr)	0.4	3.9	39
Total mass of powder (kg)	0.2	2.1	21
Total mass of waste (kg)	0.3	2.5	25

Table 2.6: Cumulative time (h), total mass of powder (kg) and total mass of waste (kg) as a function of 1 treatment for 20% Diesel Oil coverage based on 10, 100 and 1000 birds.

Birds	10	100	1000
Cumulative time (hr)	0.4	3.9	39
Total mass of powder (kg)	0.3	2.8	28
Total mass of waste (kg)	0.4	3.7	37

Table 2.7: Cumulative time (h), total mass of powder (kg) and total mass of waste (kg) as a function of 1 treatment for 50% Diesel Oil coverage based on 10, 100 and 1000 birds.

Birds	10	100	1000
Cumulative time (hr)	0.4	4.1	41
Total mass of powder (kg)	0.4	4.0	40
Total mass of waste (kg)	0.5	5.4	54

Table 2.8: Cumulative time (h), total mass of powder (kg) and total mass of waste (kg) as a function of 1 treatment for 70% Diesel Oil coverage based on 10, 100 and 1000 birds.

Birds	10	100	1000
Cumulative time (hr)	0.5	5.1	51
Total mass of powder (kg)	0.5	5.1	51
Total mass of waste (kg)	0.7	6.8	68

Table 2.9: Cumulative time (h), total mass of powder (kg) and total mass of waste (kg) as a function of 1 treatment for 100% Diesel Oil coverage based on 10, 100 and 1000 birds.

Birds	10	100	1000
Cumulative time (hr)	0.8	7.7	78
Total mass of powder (kg)	2.3	23.4	234
Total mass of waste (kg)	2.9	28.7	287

“In the field” scenario – 10%, 20%, 50%, 70% and 100% Coverage – 2 Treatments

Based on 10 birds, 100 birds and 1000 birds

Table 2.10: Cumulative time (h), total mass of powder (kg) and total mass of waste (kg) as a function of 2 treatments for 10% Diesel Oil coverage based on 10, 100 and 1000 birds.

Birds	10	100	1000
Cumulative time (hr)	0.9	8.9	90
Total mass of powder (kg)	0.4	4.1	41
Total mass of waste (kg)	0.5	4.9	49

Table 2.11: Cumulative time (h), total mass of powder (kg) and total mass of waste (kg) as a function of 2 treatments for 20% Diesel Oil coverage based on 10, 100 and 1000 birds.

Birds	10	100	1000
Cumulative time (hr)	0.7	7.1	71
Total mass of powder (kg)	0.5	5.2	52
Total mass of waste (kg)	0.7	6.5	65

Table 2.12: Cumulative time (h), total mass of powder (kg) and total mass of waste (kg) as a function of 2 treatments for 50% Diesel Oil coverage based on 10, 100 and 1000 birds.

Birds	10	100	1000
Cumulative time (hr)	1.0	10.4	104
Total mass of powder (kg)	0.8	8.0	80
Total mass of waste (kg)	1.0	10.4	104

Table 2.13: Cumulative time (h), total mass of powder (kg) and total mass of waste (kg) as a function of 1 treatment for 70% Diesel Oil coverage based on 10, 100 and 1000 birds.

Birds	10	100	1000
Cumulative time (hr)	1.1	10.6	106
Total mass of powder (kg)	1.0	10.2	102
Total mass of waste (kg)	1.3	13.3	133

Table 2.14: Cumulative time (h), total mass of powder (kg) and total mass of waste (kg) as a function of 2 treatments for 100% Diesel Oil coverage based on 10, 100 and 1000 birds.

Birds	10	100	1000
Cumulative time (hr)	1.6	15.7	157
Total mass of powder (kg)	4.5	45.1	451
Total mass of waste (kg)	5.4	54.2	542

2.4 Conclusion

The primary advantages of the magnetic cleansing method are its portability, combined with its ability to rapidly remove up to 100% of the more toxic and corrosive volatile contaminants upon first encounter in the field. Another advantage is that the method lends itself to the quantification of important parameters that relate to the logistics of its implementation. The analysis conducted in this investigation demonstrates the feasibility of incorporating this technology via a “quick clean” approach into existing stabilization controls.

2.5 References

Copley, J 1999, ‘Squeaky-clean: Magnets could help wildlife recover from oil slicks’, *New Scientist*, vol. 162, p.11.

Dao, HV, Ngeh, LN, Bigger, SW & Orbell, JD 2006, ‘Achievement of 100% removal oil from feathers employing magnetic particle technology’, *J. Environ. Eng.*, vol. 132, no. 5, pp. 555-559.

Dao, HV, Maher, LA, Ngeh, LN, Bigger, SW, Orbell, JD, Healy, M, Jessop, R., Dann, P 2006, ‘Removal of petroleum tar from bird feathers utilizing magnetic particles’, *Environ. Chemistry Letters*, vol. 4, no. 2, pp. 111-113.

Dao, HV, Ngeh, LN, Bigger, SW, Orbell, JD, Healy, M, Jessop, Dann, P 2006, ‘Magnetic cleansing of weathered/tarry oiled feathers – The role of pre-conditioners’, *Marine Pollution Bulletin*, vol. 52, pp. 1591-1594.

Encyclopedia Britannica 2010, *Deepwater Horizon oil spill: brown pelican*, viewed 19 December 2023, <<https://www.britannica.com/topic/2023-The-Year-in-Review>>.

Encyclopedia Britannica 2023, *Oil Spill*, viewed 19 December 2023, <<https://www.britannica.com/science/oil-spill>>.

Munaweera, K 2015, 'The rational development of improved methods for the removal of oil contamination from wildlife and rocky foreshore utilizing magnetic particle technology', PhD Thesis, Victoria University, Melbourne, Australia.

National Oceanic and Atmospheric Administration 2010, *Deepwater Horizon; Gulf of Mexico*, viewed 19 December 2023, <<https://incidentnews.noaa.gov/incident/8220>>.

Ngeh, LN, Orbell, JD, Bigger, SW, Munaweera, K, Dann, P 2012, 'Magnetic cleansing for the provision of a quick clean to oiled wildlife', *World of Academy of Science and Technology*, vol. 72, pp. 1091-1093.

Orbell, JD, Tan, EK, Coutts, MC, Bigger, SW, Ngeh, LN 1999, 'Cleansing oiled feathers-magnetically', *Mar. Pollut. Bull.*, vol. 38, no. 3, pp. 219-221.

Orbell, JD, Ngeh, LN, Bigger, SW, Zabinskas, M, Zheng, M, Healy, M, Jessop, R, Dann, P 2004, 'Whole-bird models for the magnetic cleansing of oiled feathers', *Mar. Pollut. Bull.*, vol. 38, no. 48, pp. 336-340.

Orbell, JD, Dao, HV, Ngeh, LN, Bigger, SW, Healy, M, Jessop, R, Dann, P 2005, 'Acute temperature dependency in the cleansing of tarry feathers utilizing magnetic particles', *Environ. Chem. Letters*, vol. 3, no. 1, pp. 25-27.

Orbell, JD, Dao, HV, Ngeh, LN, Bigger, SW 2007, 'Magnetic particle technology in environmental remediation and wildlife rehabilitation', *Environmentalist*, vol. 27, pp. 175-182.

Orbell, JD, Dao, HV, Ngeh, LN, Bigger, SW 2007, 'An investigation into the feasibility of applying magnetic particle technology to the cleansing of oiled wildlife in the field', The technical Report Prepared for the Australian marine Safety Authority (National Plan Environment Working Group) and the Phillip Island Nature Parks.

Orbell, JD, Bigger, SW, Ngeh, LN, Diep, L 2018, 'The development of a "quick clean" stabilization method based magnetic particle technology (MPT)', *International Effects of Oil on Wildlife (EOW) Conference 2018*, Royal Sonesta Harbor Court in Baltimore, Maryland, USA.

Orbell, JD, Dann, P, Bigger, SW, Ngeh, LN, Diep, L, Shewan, A 2022, 'Novel "quick clean" technology for the rapid removal of volatiles from contaminated wildlife', *the 14th International effects of Oiled on Wildlife (EOW) Conference 2022*, Long Beach Hilton, California, USA.

Pilcher, HR 2004, *Oil-drenched birds get dry cleaned*, viewed 18 December 2023, <<https://www.nature.com/articles/news040322-2>>.

SANCCOB, 2024, *Update on Oiled African Penguin Recovery in Algoa Bay*, viewed 26 September 2024, <<https://sancob.co.za/news/update-on-oiled-african-penguin-recovery-in-algoa-bay/>>.

Victoria University 2014, *Award-winning invention saves oiled wildlife*, viewed 18 December 2023, <<https://www.vu.edu.au/node/10900271>>.

Wilhelmsson, D, Thompson, RC, Nolmstrom, K, Linden, O, Hagg, HE 2013, 'Managing Ocean Environments in a Changing Climate', *Sustainability and Economic Perspectives.*, pp. 127-169.

Chapter 3: Improving the efficacy of oil-sequestering magnetic particles

3.1 Introduction

3.2 Materials and Methods

3.2.1 Chemicals

3.2.2 Preparation of “Magnetic Zeolite” (MZ) particles

3.2.3 Preparation of “Magnetic Sawdust” (MS) particles

3.2.4 Characterization of the magnetic particles

3.2.4.1 Particle size analysis

3.2.4.2 Particle flow characteristics

3.2.4.3 Magnetic “pull” experiments

3.2.4.4 Oil pick-up isotherms

3.3 Results and Discussion

3.3.1 MZ particles

3.3.2 MS particles

3.3.3 MZ particle analysis

3.3.4 MS particle analysis

3.3.5 The relative Particle Size Analyzer (PSA) parameters

3.3.6 Compressibility and flow parameters

3.3.7 Magnetic pull experiments

3.3.8 Oil removal isotherms

3.4 Conclusions

3.5 References

3.1 Introduction

To date, magnetic cleansing research within our group has relied upon commercially available zero valent iron (ZVI) powder (oil-absorbing magnetic particles), for which an optimum particle grade has been previously established (Orbell *et al.*, 2004). This grade of iron powder has subsequently been utilized to develop the concept of a “quick clean” of oiled wildlife (Ngeh *et al.*, 2012) and has been recommended by our group for incorporation into existing stabilization protocols (Orbell *et al.*, 2022). This highly portable method promises to be particularly advantageous for the rapid removal of toxic and corrosive volatile components upon first encounter (Ngeh *et al.*, 2012).

A potential limiting factor for the above technique, particularly for larger and more remote events, is the weight of the iron powder and the oil-laden iron powder waste that has to be transported to and from the scenario. Therefore, to improve this aspect of the logistics, the current project will investigate modification of the magnetic particles so that they weigh less for a comparable oil sequestering capability. Other factors that could be considered with respect to the development of magnetic particles include increasing their versatility with respect to the range of contaminants absorbed, increasing their pick-up efficacy and reducing their cost. This project has specifically focused reducing their weight for a given settled volume (particularly for applications in the field) whilst maintaining their magnetic susceptibility.

Modifications of contaminant ad(b)sorbing magnetic particles may be achieved in terms of altering either their surface characteristics, such as surface hydrophobicity, roughness, or by attaching specific molecules to their surface, or by altering their particle size distribution and/or porosity (Munaweera, 2015) or by changing their chemical composition, e.g., ZVI powder *versus* magnetite, or by blending various materials such as zeolite with iron oxide nanoparticles or other magnetic material, e.g. “magnetic zeolites” (Oliveira *et al.*, 2004). Such materials have been previously developed for a wide range of applications such as the removal of metallic contaminants from water (Oliveira *et al.*, 2004). Other examples of the use of appropriately modified magnetic particles include sewage treatment (Booker *et al.*, 1991), the removal of radionuclides from milk (Sing, 1994), the adsorption of organic dyes (Safarik *et*

al., 1995) and the remediation of small-scale oil spills (Orbell *et al.*, 1997). High adsorption capacity magnetic composites based on activated carbon/iron oxide and clay/iron oxide have been reported to remove contaminants from aqueous effluents (Oliveira *et al.*, 2003). Other research has combined the adsorption characteristics of zeolites with iron oxide magnetic properties to generate a magnetic adsorbent. Zeolites themselves offer an affordable option for the removal of organic and inorganic contaminants (Murray, 2000). For example, zeolites are effective cation exchangers, which can be implemented to adsorb metallic contaminants. With respect to the heavy metals, adsorption capacity results from a high surface area and a net negative charge within their channel structures (Cadena *et al.*, 1990). Zeolite itself is used as a commercial product *per se* for the mopping up of oil spills. Natural zeolites are readily available and inexpensive materials. They have a high surface area, which attracts and retains cations like heavy metals, and a net negative charge in their channel structure, which contributes to their capacity for adsorption (Cadena *et al.*, 1990). NaY zeolites have been investigated as heavy metal adsorbents (Ryachi and Bencheikh, 1998; Barbier *et al.*, 2000; De Pena *et al.*, 2000; Trgo and Peric, 2003) and have one of the greatest surface areas and highest cation exchange capacities (Bailey *et al.*, 1999). “Magnetic zeolites” and blends with magnetic iron-based powders are therefore good candidates for potentially improved magnetic particles for use in magnetic cleansing technology. This approach has been utilized in the present research project with specific reference to the work of Gupta *et al.*, 2011; 2012. A number of research groups have been working to create magnetic composites with a high surface area and high adsorption capacity based on activated carbon/iron oxide and clay/iron oxide to remove pollutants from aqueous effluents in particular. For example, a novel magnetic adsorbent was created by combining the magnetic properties of iron oxides with the adsorption characteristics of zeolites (Oliveira *et al.*, 2004). Zeolites have been described as a desirable and affordable alternative for the elimination of both organic and inorganic pollutants (Murray, 2000). Recently, the literature has reported on the adsorption by zeolites of a number of organic pollutants in water, including pesticides, phenols, and chlorophenols (Shu *et al.*, 1997; Torrents and Jayasundera, 1997; Danis *et al.*, 1998; Konstantinou *et al.*, 2000).

There is a wide range of natural adsorbents reported in the literature that could be candidates for blends with magnetic iron material. For example, the scavenging of radioactive waste, in

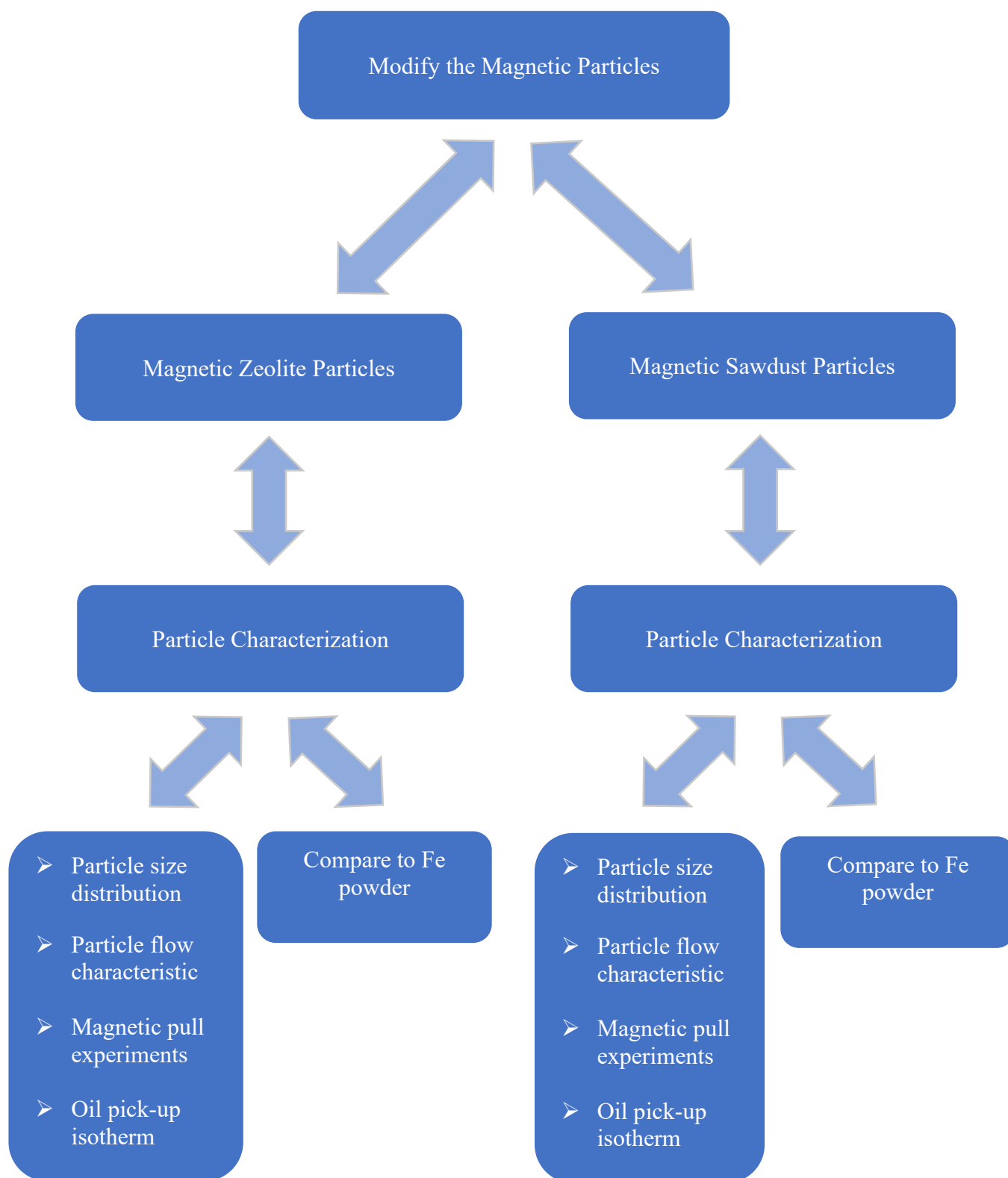
particular strontium-90, has received much attention. Any “new built” reactors contribute to the extensive and complicated legacy of radioactive waste that China, and many other nations, have accumulated over the course of several decades of military and civilian nuclear technology. These pollutants are among the most dangerous substances that humanity ever produced, thus proper management and safe disposal are essential (Cheng *et al.*, 2012). Strontium-90, for example, which has a long half-life of 28 years and is which is environmentally harmful, is the radionuclide that is most frequently found nuclear waste sites and nuclear power plants (Trivedi *et al.*, 1999). Due to its chemical similarity to calcium, it is easily incorporated into bone of humans and animals, irradiating the bone marrow (Chen, 1997; Wang *et al.*, 2009). In some accident scenarios such as earthquakes, radioactive waste can leak into and contaminate water systems. Therefore, it is of great importance to investigate methods that can effectively and conveniently remove strontium ions from aqueous solutions (Cheng *et al.*, 2012). Many such methods, including solvent extraction (Law *et al.*, 1999), membrane filtration (Raut *et al.*, 2012), ion exchange (Cho *et al.*, 2009), and electrocoagulation (Murthy *et al.*, 2011), have been suggested to remove strontium ions from aqueous solutions. The high cost, poor efficiency, and secondary contamination of many of these methods, however, make them impractical to implement. It appears that the best methods for removing metal ions from wastewater are adsorption and electrochemical precipitation. In this regard, numerous adsorbents have been studied by researchers to extract strontium from aqueous solutions, including multiwall carbon nanotube/iron oxide magnetic composites (Chen *et al.*, 2009), minerals (Ghaemi *et al.*, 2011; Kutahyali *et al.*, 2012; Bascetin *et al.*, 2010; Kamel, 2010), silica materials (Zhang *et al.*, 2008; Carroll *et al.*, 2008), gel (Wang *et al.*, 2009; Li *et al.*, 2010), oxides (Trivedi *et al.*, 1999; Valsala *et al.*, 2010; Langley *et al.*, 2009; Tel *et al.*, 2010), and biomass (Chen, 1997; Chakraborty *et al.*, 2007; Ahmadpour *et al.*, 2010; Maresova *et al.*, 2011; Chen *et al.*, 2012). These studies represent a valuable resource for the further development of composite magnetic particles.

One such absorbent, namely sawdust, is frequently used by itself to remove pollution from wastewater, including dye (Witek-Krowiak *et al.*, 2011; Sidiras *et al.*, 2011; Ahmad *et al.*, 2009; Dulman *et al.*, 2009), paraquat (Nanseu-Njiki *et al.*, 2010), oil mill wastewater (Chouchene *et al.*, 2010), ammonium (Wahab *et al.*, 2010), and heavy metals (Gupta *et al.*,

2009; Vinodhini *et al.*, 2009; Semerijian, 2010; Rahman *et al.*, 2009). The advantage of sawdust is that it is a plentiful, renewable and affordable lignocellulosic waste material. However, when utilising sawdust itself as an ad(b)sorbent, it is challenging and time-consuming to extract the sawdust from aqueous solution after ad(b)sorption. Fe_3O_4 magnetic materials are widely known for their simplicity of preparation for application to magnetic separation (Cheng *et al.*, 2012). The challenge here is to combine the magnetic particle and the sawdust into a homogenous blend where the separation of the components does not occur. It is also a challenge to produce particles that have a sufficiently high magnetic susceptibility, a greater specific surface area and easier surface modification/manipulation (Tian *et al.*, 2011; Fan *et al.*, 2011; Ye *et al.*, 2008). Lysozyme removal using magnetic Fe_3O_4 /chitosan nanoparticles has been researched by Lin *et al.*, 2012. Cheng *et al.*, 2012 have investigated the combining of sawdust with magnetic Fe_3O_4 particles with respect to the sequestration of Strontium-90 from aqueous solution. Here, the sawdust was modified and combined with Fe_3O_4 particles using chitosan as the bridging agent.

In this chapter, a research program is described that was specifically designed to improve existing oil absorbing magnetic particles (i.e. zero valent iron powder), particularly with respect to the application of MPT to a “quick clean” of contaminated wildlife upon first encounter. Therefore, the improved particles should exhibit a magnetic susceptibility and oil absorbing capacity that is comparable to our already optimized grade of zero-valent iron powder (ZVIP) but which are significantly lighter in weight (for a given settled volume). This will reduce the weight of material required to transport to a contamination site. Thus, zeolites and sawdust particles were infused with Fe_3O_4 nanoparticles in different proportions and their magnetic harvesting potential determined. Therefore, it is hypothesized that such oil absorbing magnetic particles will have sufficient oil sequestering capability and magnetic susceptibility to be comparable in efficacy to ZVIP particles, albeit significantly lighter in weight for a given settled volume.

Schematic Methodology



3.2 Materials and methods

3.2.1 Chemicals

The following materials were used for the synthesis of the “magnetic zeolite” particles. Iron (III) chloride, $\text{FeCl}_3 \cdot 6\text{H}_2\text{O}$, supplied by Merck; Iron (II) sulphate, $\text{FeSO}_4 \cdot 7\text{H}_2\text{O}$, supplied by Unilab; 25% ammonia solution, supplied by Univar; Zeolite, supplied by Zorbe. The following materials were used for the preparation of the “magnetic sawdust” particles. The following materials were used for the synthesis of the magnetic sawdust particles. $\text{FeCl}_3 \cdot 6\text{H}_2\text{O}$, supplied by Sigma-Aldrich; $\text{FeCl}_2 \cdot 6\text{H}_2\text{O}$, supplied by Sigma-Aldrich; 25% ammonia solution supplied by Univar; 1% acetic acid supplied by Victoria University Laboratory Technical Services; Chitosan powder supplied by Sigma-Aldrich; and sawdust, supplied by Pollard’s Sawdust Supplies. During the preparation of iron oxide nanoparticles with added sawdust (magnetic sawdust), a control was also developed by only producing iron oxide nanoparticles without adding sawdust. Due to COVID restrictions on laboratory access, only two variations of magnetic sawdust were made. The contaminant used was “Engine Oil (BP Vanellus)”.

3.2.2 Preparation of “magnetic zeolite” (MZ) particles

The “recipe” for the magnetization of zeolite is a variation of a literature method (Gupta, *et al.*, 2012) and is described as follows. Note that this method involves the intimate mixing of iron oxide nanoparticles with crushed zeolite particles to give a homogeneous composite.

Using an analytical balance, 12.2 g of $\text{FeCl}_3 \cdot 6\text{H}_2\text{O}$ and 8.4 g of $\text{FeSO}_4 \cdot 7\text{H}_2\text{O}$ were weighed into an 800 mL beaker. 200 mL of deionised water was then used to dissolve both the $\text{FeCl}_3 \cdot 6\text{H}_2\text{O}$ and $\text{FeSO}_4 \cdot 7\text{H}_2\text{O}$. The beaker was then placed inside the fume hood on top of a hot plate and a magnetic flea was added into the beaker. The mixture was then heated to 90 °C. When the mixture had reached 90 °C, the heating mode of the hot plate was adjusted to low. During this stage, the mixture inside the beaker was a dark orange. 20 mL of an ammonia solution (25% v/v) was then added into the beaker and the mixture turned black. 1 g of zeolite was then weighed out and pulverized using a pestle and mortar. 200 mL of deionized water

was then added to the 1 g of crushed zeolite. This solution was poured into the $\text{FeCl}_3 \cdot 6\text{H}_2\text{O}$ and $\text{FeSO}_4 \cdot 7\text{H}_2\text{O}$ beaker and stirred thoroughly using magnetic flea. A pH meter was used to maintain a pH of approximately 10. The mixture was then stirred at 80 °C for 30 minutes and then cooled to room temperature. The resulting black precipitate (Fe_3O_4 nanoparticles/Zeolite) was then collected by filtration and washed to neutrality with deionized water and then dried at 50 °C for 24 h. The dry black Fe_3O_4 /Zeolite precipitate was then pulverized into a powder crushed using a pestle and stored for use. Following the above method, the relative proportions of the Fe_3O_4 nanoparticles and zeolite were varied. Thus, eight different variations were prepared as shown in **Table 3.1**. These products were subsequently characterized in terms of their relative particle size distributions, magnetic susceptibilities, settled volumes/densities and their oil pick-up characteristics (isotherms). The Fe_3O_4 nanoparticles and ZVI powder were used as controls in subsequent experiments.

3.2.3 Preparation of “magnetic sawdust” (MS) particles

The “recipe” for the magnetization of sawdust is a variation of a literature method (Cheng *et al.*, 2012) and is described as follows. 5.406 g of $\text{FeCl}_3 \cdot 6\text{H}_2\text{O}$ and 1.988 g of $\text{FeCl}_2 \cdot 6\text{H}_2\text{O}$ were dissolved in 80 mL deionized water in a three-neck flask and the temperature was slowly increased to 70 °C under reflux in a nitrogen atmosphere with constant mechanical stirring. The temperature was maintained at 70 °C for 30 minutes and then 20 mL 25% v/v ammonia solution was added instantaneously to the resultant solution, keeping the temperature at 70 °C for another 30 minutes. Then the temperature was slowly raised to 90 °C for 60 minutes, with continuous stirring. The obtained black precipitate (Fe_3O_4 nanoparticles) was thoroughly rinsed with deionized water and separated magnetically. Sawdust was washed several times with deionized water to remove surface impurities and dried at 80 °C for 12 hours. 10 grams of the sawdust was then added in 100 mL of 1% v/v acetic acid and stirred for 1 hour. Chitosan acetic acid solution was prepared by dissolving 1 gram of chitosan powder in 100 mL acetic solution and stirred for 1 hour. These 2 solutions were mixed together and stirred for 30 minutes. One gram of the Fe_3O_4 nanoparticles was added to the solution which was then stirred for 3 hours. The solution was then poured into 250 mL of 1M NaOH solution at 50 °C and stirred for 5 hours. The magnetic products were harvested magnetically with a “magnetic

tester” (3000-5000 Gauss) and was then washed with deionized water until the wash-water had a neutral pH. Finally, the “magnetic sawdust” was dried at 80 °C for 24 hours.

A summary of the composition of the MZ and MS particles is given in **Table 3.1**.

Table 3.1: Composition of the eight magnetic zeolite (MZ) particle types and the two magnetic sawdust (MS) particle types that were formulated, see **Section 3.2.2/3**.

Magnetic Zeolites (MZ)	Mass of iron oxide nanoparticles (g)	Mass of crushed zeolite or sawdust (g)	Total mass of composite (g)	% by weight of the iron oxide nanoparticles	% by weight of crushed zeolite or sawdust
Control (no zeolite)	9.2	0	9.2	100	0
MZ 1	9.2	1	10.2	90.19	9.80
MZ 2	9.2	2	11.2	82.14	17.85
MZ 3	9.2	3	12.2	75.40	24.59
MZ 4	9.2	4	13.2	69.69	30.30
MZ 5	9.2	5	14.2	64.78	35.21
MZ 6	9.2	6	15.2	60.52	39.47
MZ 7	9.2	7	16.2	56.79	43.20
MZ 8	9.2	8	17.2	53.48	46.51
MS 1	1	10	11	9.09	90.90
MS 2	2	10	12	16.66	83.33

3.2.4 Characterization of the magnetic particles

3.2.4.1 Particle size analysis

An Anton Paar PSA 990 Particle Size Analyzer (PSA), **Figure 3.1**, was used to measure the particle size distribution of the developed magnetic particles. Using the PSA requires loading the sample and adjusting the “dispersion parameters”. The developed particles were measured in dry mode and the samples carried by compressed air. Adjusting the compressed air pressure should be undertaken before measuring the sample in order to achieve a satisfactory dispersion. This can be completed by modulating the mass distributor, air pressure and vibrator settings, while the level of sensor obscuration is observed. The following flowchart summarizes the operation of the PSA 990.

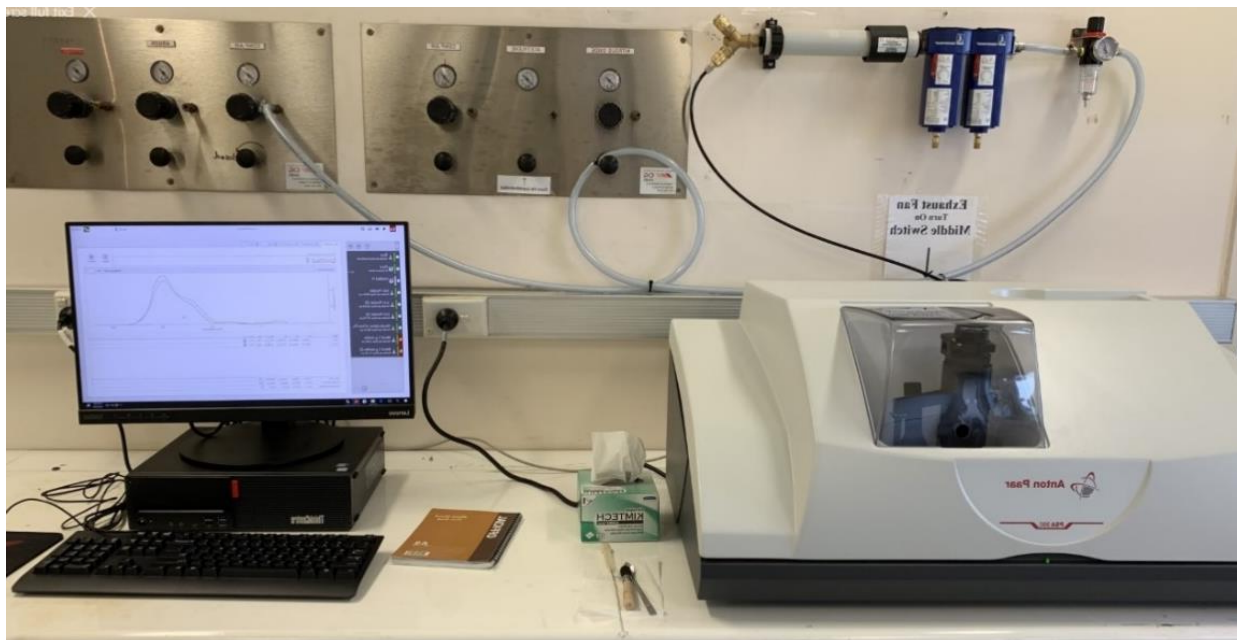


Figure 3.1: Anton Paar PSA 990 Particle Size Analyzer (PSA). The parameters that are measured with this instrument are given in **Table 3.2** below:

Table 3.2: Parameters measured by the PSA instrument, together with their definitions.

Parameters	Definition
D₁₀	Percentile value, D ₁₀ indicates the size below which 10% of all particles are found. The length unit, D ₁₀ , represents the 10% of particles in a powder that are smaller than this size (Microtrac, 2023).
D₅₀	Percentile value, D ₅₀ indicates the size below which 50% of all particles are found. The length unit, D ₅₀ , represents the 50% of particles in a powder that are smaller than this size (Microtrac, 2023).
D₉₀	Percentile value, D ₉₀ indicates the size below which 90% of all particles are found. The length unit, D ₉₀ , represents the 90% of particles in a powder that are smaller than this size (Microtrac, 2023).
Mean size	This is the value of the particle size which divides the population exactly into two equal halves (i.e., there is 50% of the distribution above this value and 50% below) (Microtrac, 2023).
Span	Volume-based size distribution is defined as $\text{span} = (D_{90} - D_{10})/D_{50}$ (Burgess <i>et al.</i> , 2004; Microtrac, 2023). The span value denotes the degree of consistency in the particle size. If the span approaches zero, it indicates that the granularity is more uniform, and the size consistency is better (ACTTR Technology, 2020).
Obscuration	The detector measures the reduction in light intensity and, employing a calibration curve, processes the signal to determine particle size (Bettersize Instruments, 2022).

3.2.4.2 Particle flow characteristics

The flow characteristics of the developed particles are of interest, not just for assessing their handling properties, but also for their relationship to the particle size distribution and surface roughness properties of the particles - which are in turn related to their efficacy of contaminant pick-up.

A simple method for assessing the flow characteristics of particles involves the use of the Carr Index³, C, and the closely related Hausner Ratio, H, (Hadjittofis *et al.*, 2018). The Carr Index

³ Also called “Carr’s Compressibility Index”

refers to an indication of the compressibility of a powder (Gibson, 2001). The Carr Index is expressed as follow:

$$C = 100 \times [(d_T - d_B) / d_T] \quad \text{Equation (1)}$$

Where:

$$d_T = m/V_T$$

$$d_B = m/V_B$$

C = The Carr Index

m (g) = mass of particles

d_T (g/mL) = the tapped bulk density of the powder after “tapping down”

d_B (g/mL) = the freely settled bulk density of the powder

V_B (mL) = the freely settled bulk volume

V_T (mL) = the “tapped down” bulk volume

The Hausner ratio is referred to as the number that is correlated to the flowability of a powder or granular material (Gibson, 2001). The Hausner Ratio, H, is given by the equation:

$$H = d_T/d_B \quad \text{Equation (2)}$$

When exactly the same mass is used throughout, the equations for C and H reduce to:

$$C = 100 \times [(V_B - V_T)/V_B]$$

$$H = V_B/V_T$$

Equations (1) and (2) are the two equations that have been used in this thesis. In order to measure the C and H values, the volumes V_B (mL) and V_T (mL) need to be measured. Therefore, for each powder, a weighed amount of a powder was placed into a measuring cylinder and the volume recorded before and after “tapping down”. The tapping of the graduated cylinder containing the sample was carried out until no further change of volume was observed (Particle Analytical, 2018). The calculated values of these parameters may be interpreted as follows:

Table 3.3: Interpretation of the Carr index and Hausner ratio with respect to flowability (Powder Process, 2023).

Flowability expected	Hausner Ratio	Carr Index
Excellent / Very Free Flow	1.00 - 1.11	<10
Good / Free Flow	1.12 - 1.18	11-15
Fair	1.19 - 1.25	16-20
Passable	1.26 - 1.34	21-25
Poor Flow / Cohesive	1.35 - 1.45	26-31
Very Poor Flow / Very Cohesive	1.46 - 1.59	32-37
Approximatively no flow	> 1.60	> 38

3.2.4.3 “Magnetic pull” experiments

The so-called “magnetic pull” of the particles, related to their magnetic susceptibility, was measured for all the magnetic zeolite formulations and controls (iron powder and iron oxide nanoparticles). A simple apparatus was devised for making such measurements that is described as follows.

Identical tapped (settled) volumes of each powder were placed in sample vials and suspended from an electronic weighting scale, as indicated in **Figure 3.2**. These samples were then subjected to a constant magnetic field from the tip of a magnetic testing device (approximately 3000 Gauss). The device was maintained at a constant distance from the vial for each measurement. The relative magnetic pull (a simple measure of relative magnetic susceptibility) was determined from the weight reading on the electronic weighing scale. Relative values and their interpretation are given in section 3.3 below.

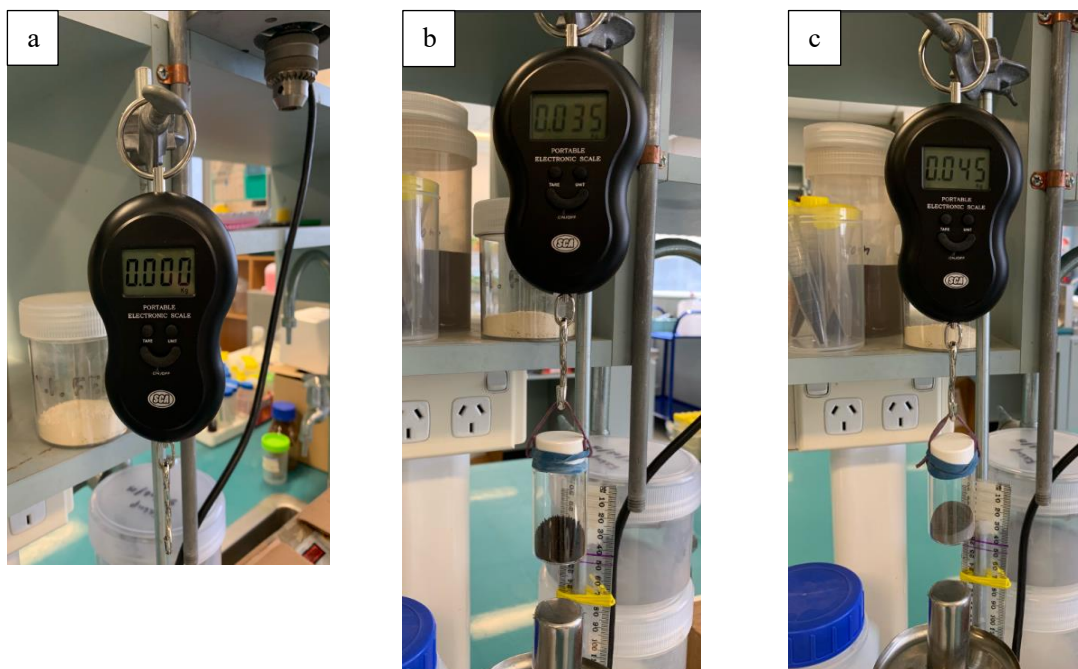


Figure 3.2: Magnetic “pull” experiments (a) portable electronic weighing scale (b) for “magnetic zeolite” and (c) for iron powder (control). Note that the iron powder presents a greater pull (0.045 vs 0.035 kg) than an equivalent settled volume of the magnetic zeolite sample.

3.2.4.4 Oil pick-up isotherms⁴

In this research an existing gravimetric method by Orbell *et al.* (1997; 1999), was employed to determine the magnetic removal of contaminants from a given substrate such as glass and feather clusters. This is described below:

Glass substrate

A pre-weighed (w_1) petri dish was loaded with a fixed mass of a contaminant and then weighed again (w_2). After applying a mass of magnetic particles to the contaminant, the petri dish was re-weighed (w_3). The particle-to-contaminant ratio, R , is defined as the mass of particles divided by the mass of interest contaminant, and it can be calculated using the following equation:

⁴ The term “isotherm” is frequently used to refer to plots of this mathematical form.

$$R = (w_3 - w_2)/(w_2 - w_1)$$

To ensure sorption, the contaminant and magnetic particles were thoroughly mixed and left for one minute. Previous experiments (Godhino, 1993) demonstrated that adsorption occurs almost instantly. The contaminant-laden magnetic particles were collected using a magnetic tester. The petri dish was then re-weighed (w_4). The following equation is used to calculate the percentage of contaminant removal, P (%):

$$P (\%) = [(w_2 - w_4)/(w_2 - w_1)] \times 100\%$$

The harvesting procedure was repeated until a constant P (%) value was obtained. P_o (%) denotes the maximum removal P_o (%) is obtained at a specific R-ratio called R_o .

Feather clusters

A cluster of feathers (usually 4) were tied and weighed (f_1). The feathers were then dipped into a beaker (100 mL) of contaminant to allow saturation. The feathers were then allowed to drain on a tared petri dish for approximately 10 minutes until being re-weighed (f_2). The feathers are then removed from the petri dish and residual quantity, r , is recorded. The weight of contaminant-laden feathers, f_3 , is given by:

$$f_3 = f_2 - r$$

Contaminated feathers were then covered with the oil ad(b)sorbing magnetic particles. A previous study (Godinho, 1993) has noted that the ad(b) sorption process is effectively instantaneous. Using a magnetic tester, the contaminant-laden particles are harvested from the feathers. The feather cluster was then reweighed (f_4). The percentage of oil removal (F%) was calculated as follows:

$$F (\%) = [(f_3 - f_4)/(f_3 - f_1)] \times 100\%$$

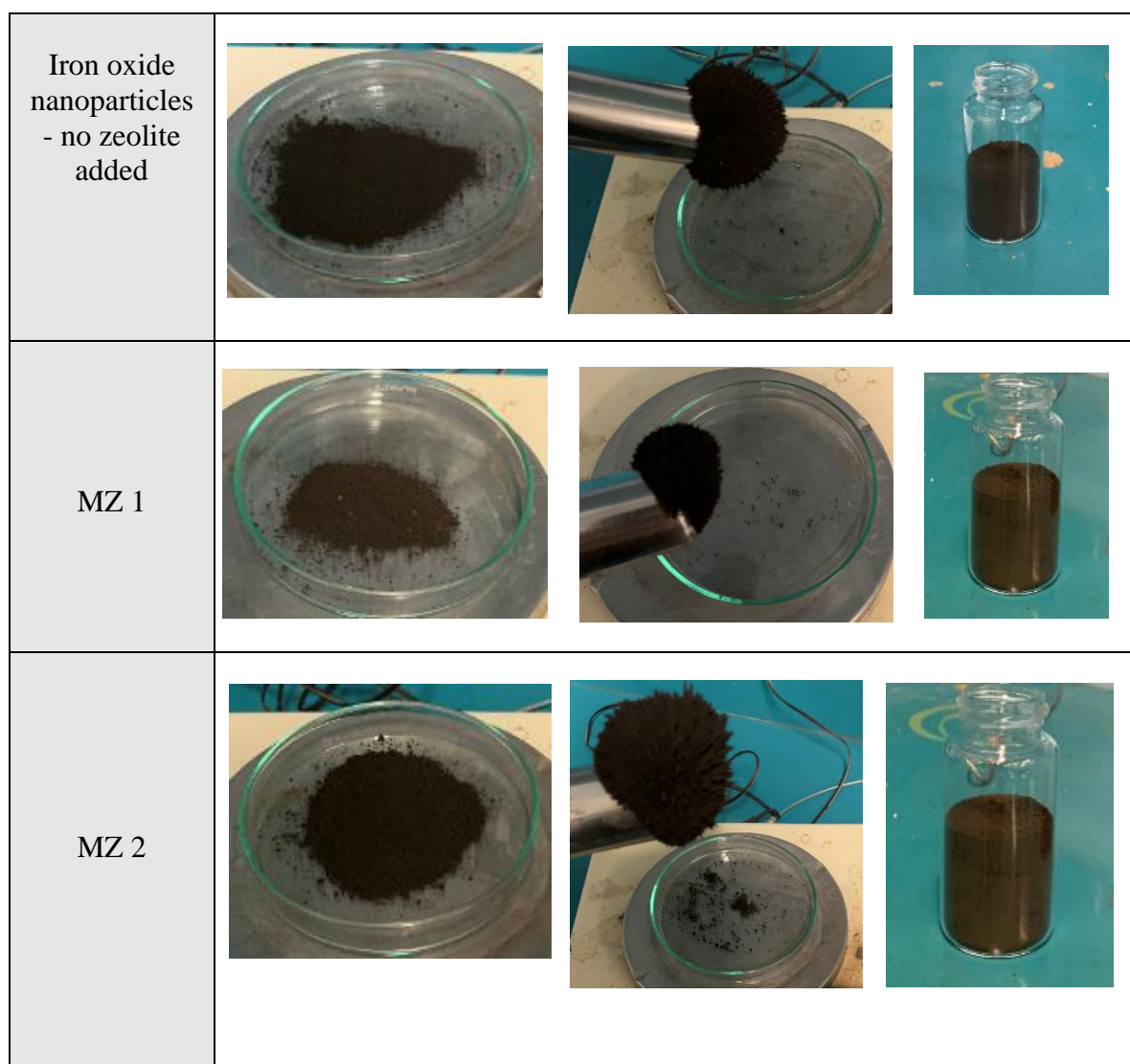
The above removal procedure was repeated until a maximum oil pick-up was achieved. A

graph of percentage pick-up (F%) versus number of treatments (N) was then plotted. This plot is referred to as an “isotherm”.

3.3 Results and Discussion

3.3.1 “Magnetic Zeolite” (MZ) particles

The different formulations of MZ particles, prepared as described in Section 3.2.2 and listed in Table 3.1, are shown in Figure 3.3, below:



MZ 3			
MZ 4			
MZ 5			
MZ 6			
MZ 7			



Figure 3.3: The formulated MZ particles.

3.3.2 “Magnetic Sawdust” (MS) particles

The different formulations of MS particles, prepared as described in Section 3.2.3 and listed in **Table 3.1**, are shown in **Figure 3.4**, below:

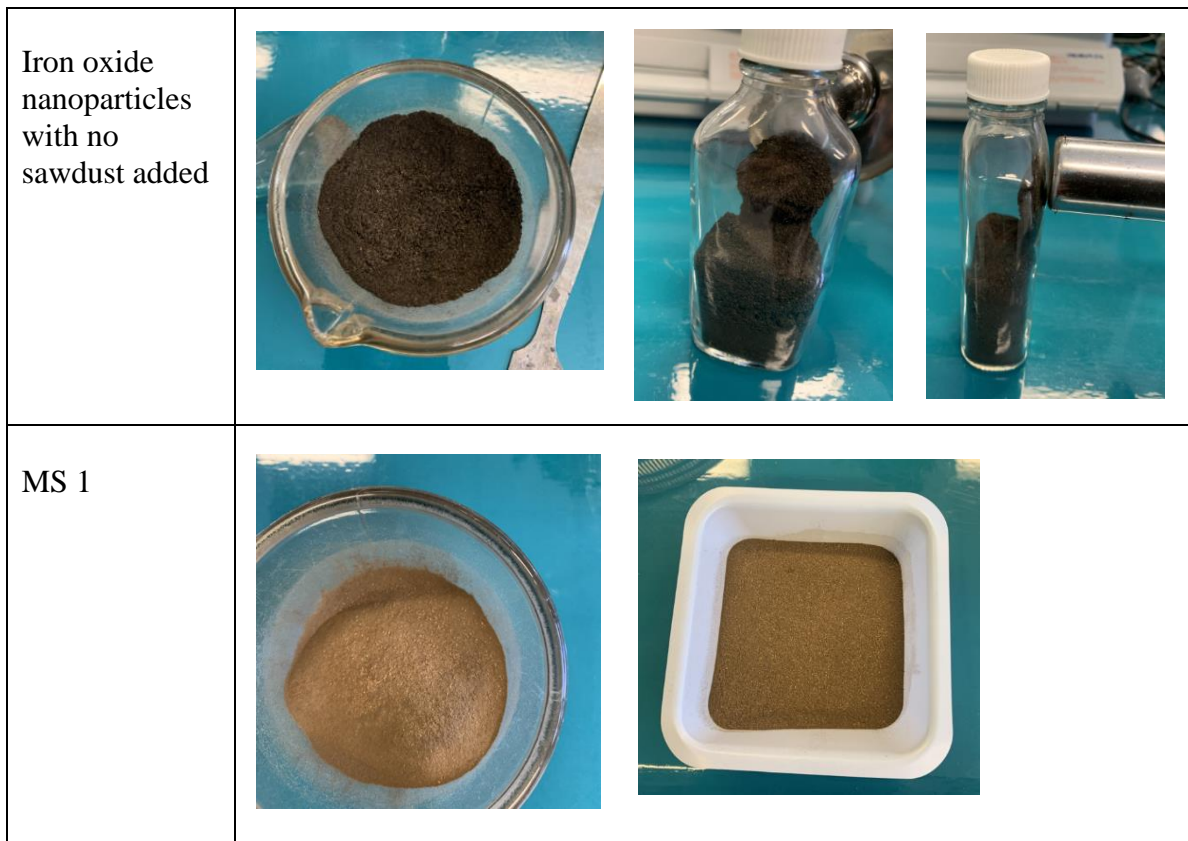




Figure 3.4: The formulated MS particles.

3.3.3 MZ particle analysis

Figures 3.5 to 3.13 show the Anton Paar PSA 990 Particle Size Analyzer (PSA) data output for the Fe powder control and the eight MZ particle formulations. The parameters that are measured with this instrument are listed and defined in **Table 3.2** to facilitate their comparison.

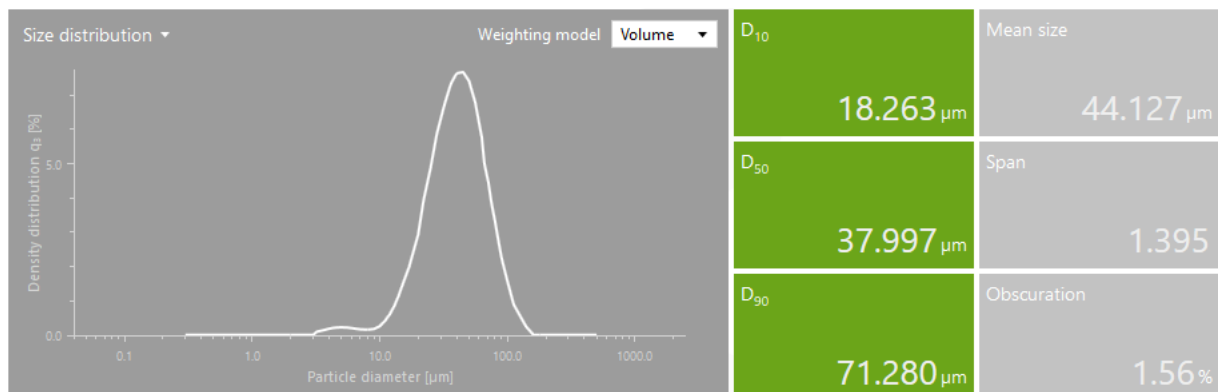


Figure 3.5: Particle size measurement for iron powder.

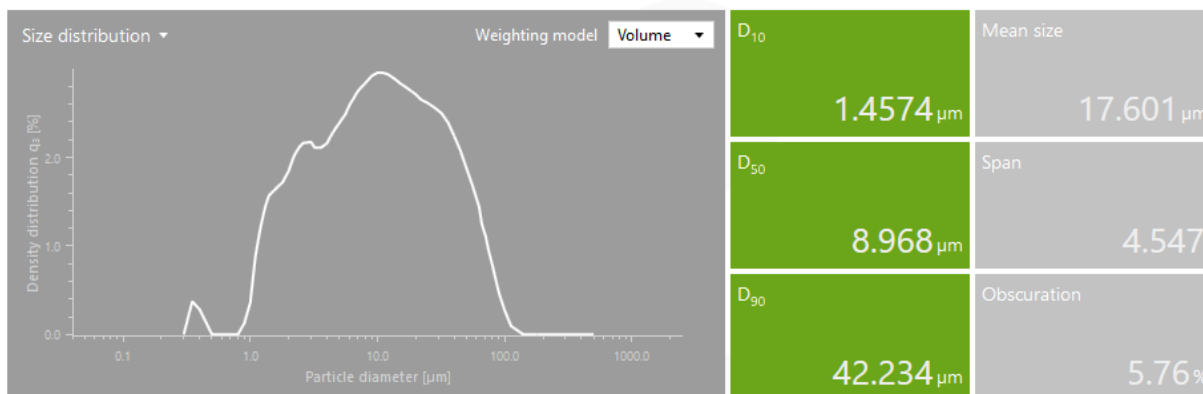


Figure 3.6: Particle size measurement for developed iron oxide nanoparticle with 1 gram zeolite added.

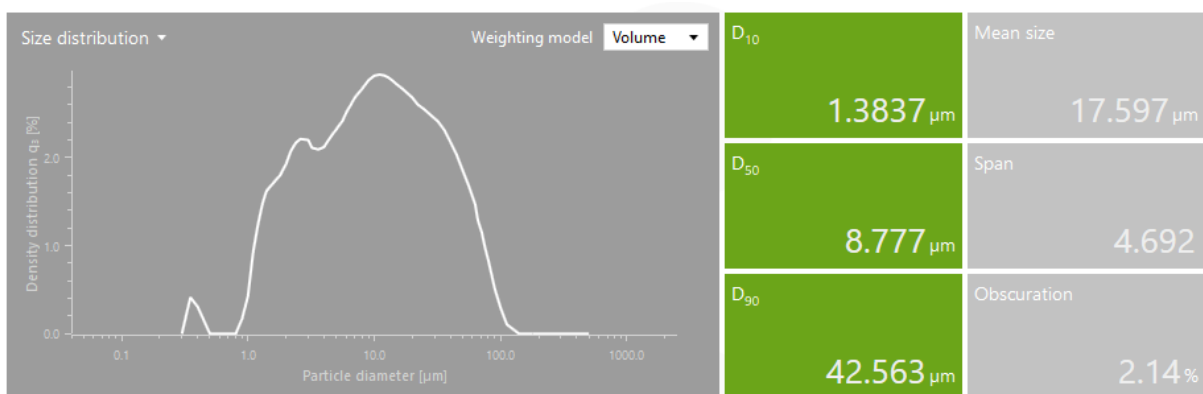


Figure 3.7: Particle size measurement for developed iron oxide nanoparticle with 2 grams zeolite added.

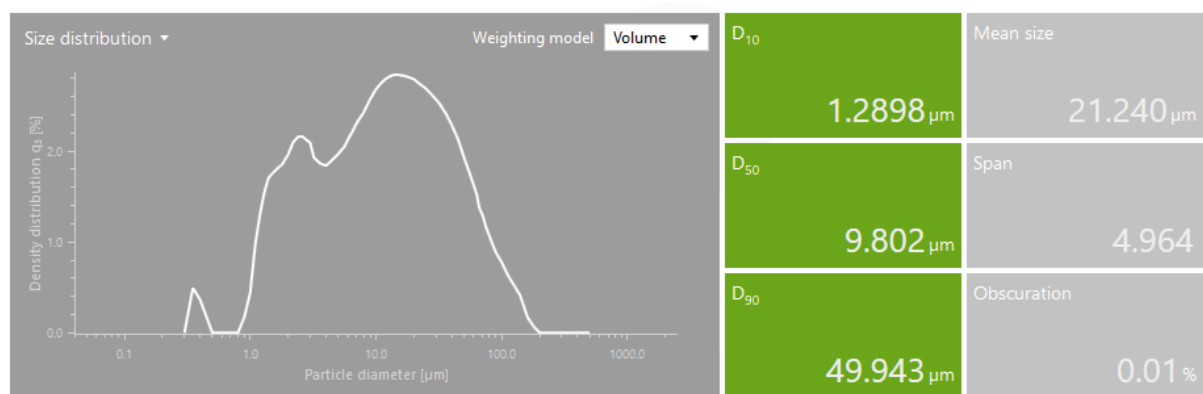


Figure 3.8: Particle size measurement for developed iron oxide nanoparticle with 3 grams zeolite added.

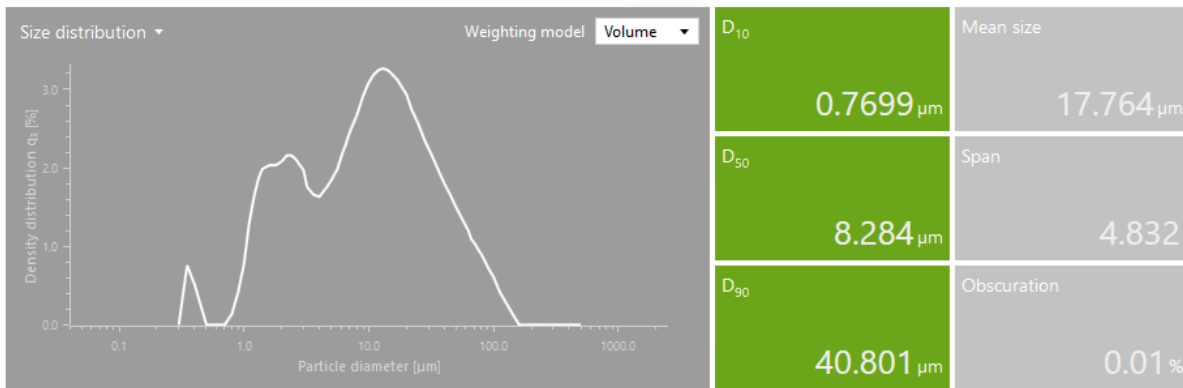


Figure 3.9: Particle size measurement for developed iron oxide nanoparticle with 4 grams zeolite added.

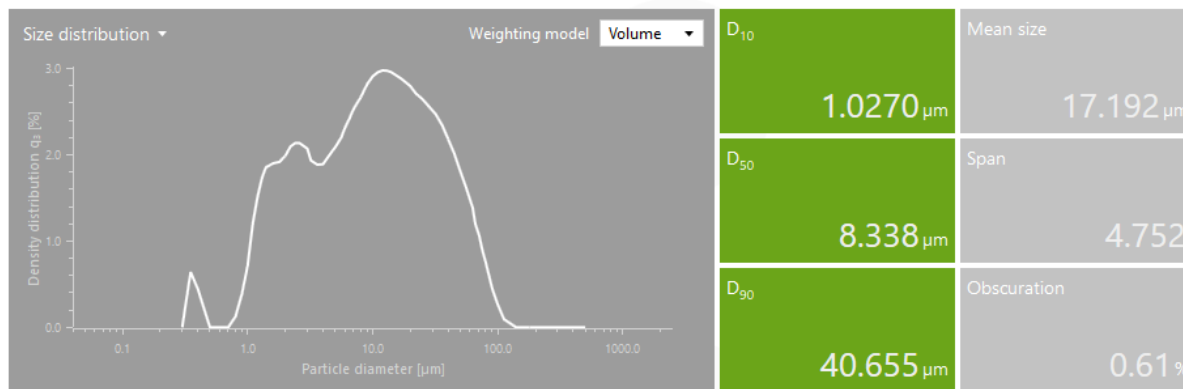


Figure 3.10: Particle size measurement for developed iron oxide nanoparticle with 5 grams zeolite added.

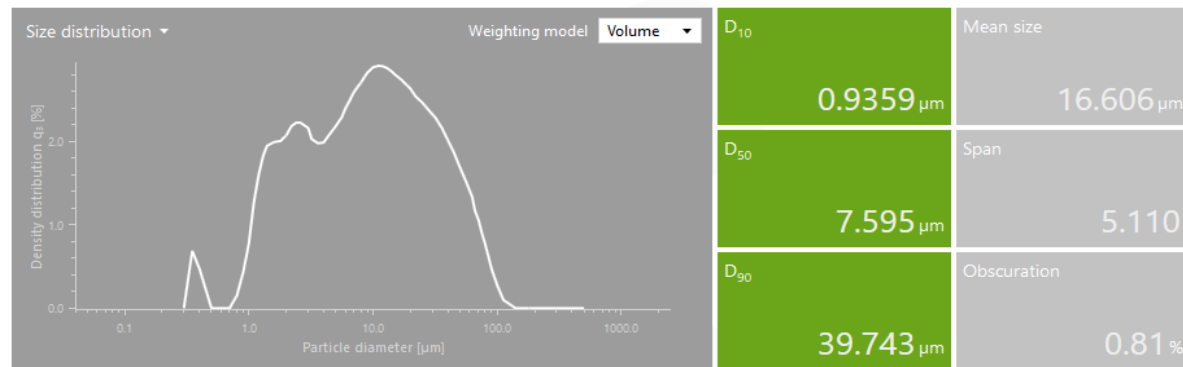


Figure 3.11: Particle size measurement for developed iron oxide nanoparticle with 6 grams zeolite added.

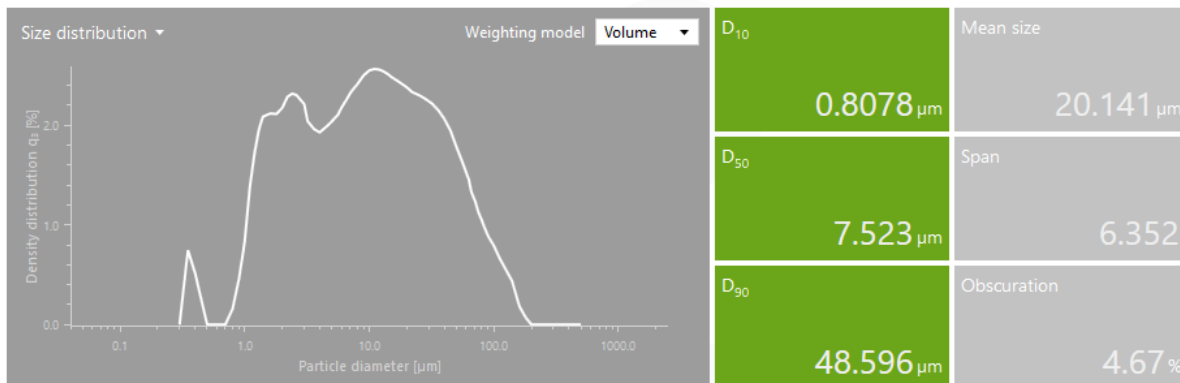


Figure 3.12: Particle size measurement for developed iron oxide nanoparticle with 7 grams zeolite added.

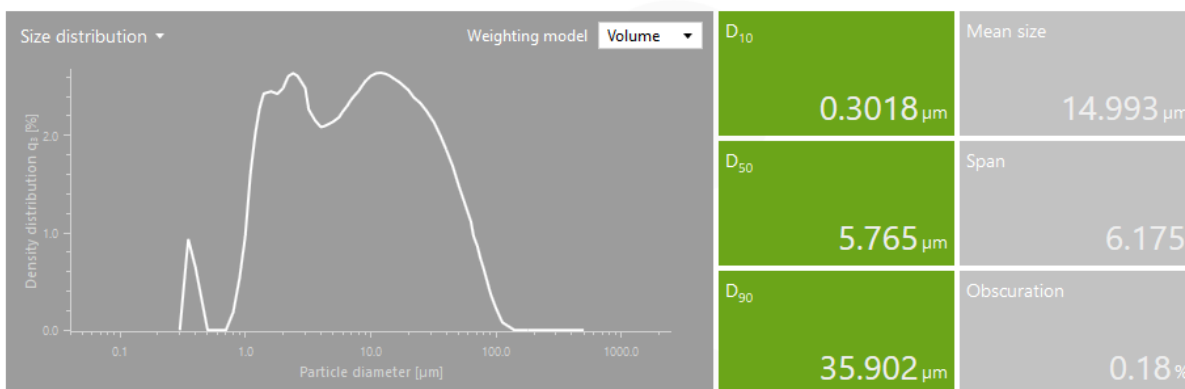


Figure 3.13: Particle size measurement for developed iron oxide nanoparticle with 8 grams zeolite added.

3.3.4 MS particle analysis

Figures 3.14 to 3.16 show the Anton Paar PSA 990 Particle Size Analyzer (PSA) data output for the Fe powder control and the two MS particle formulations. The parameters that are measured with this instrument are also given in **Table 3.2** to facilitate comparison.

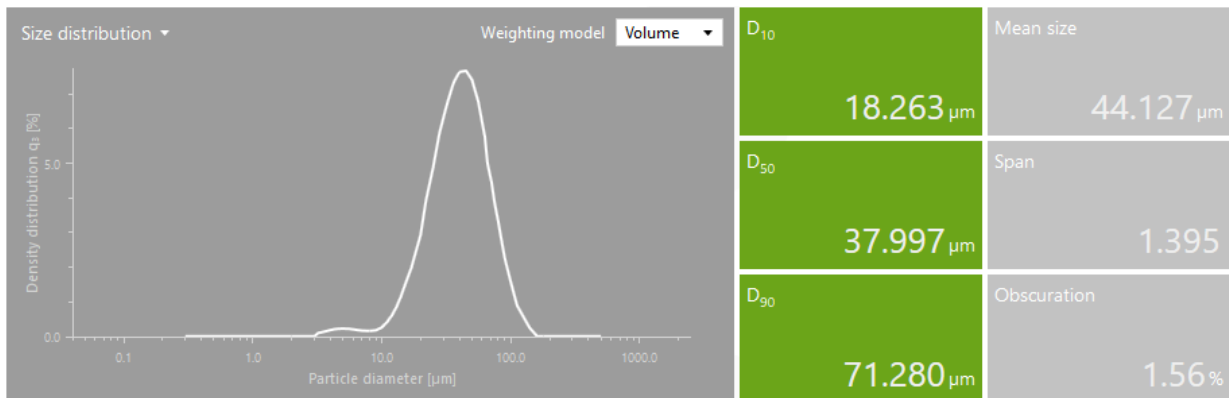


Figure 3.14: Particle size measurement for iron powder.

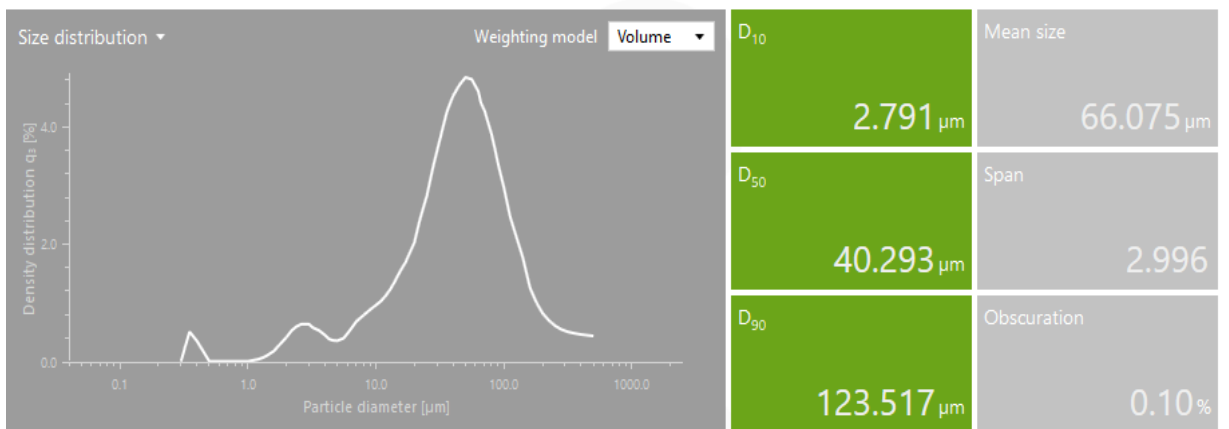


Figure 3.15: Particle size measurement for developed iron oxide nanoparticle with 1 gram sawdust added.

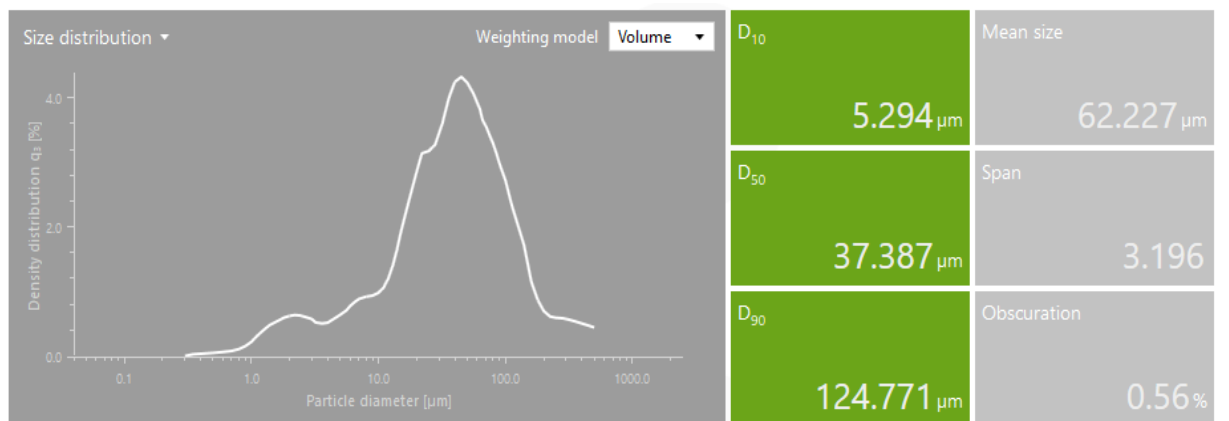


Figure 3.16: Particle size measurement for developed iron oxide nanoparticle with 2 grams sawdust added.

The data in **Figures 3.5 to 3.13** (Magnetic Zeolite – MZ) and **Figures 3.14 to 3.16** (Magnetic Sawdust – MS) are tabulated in **Table 3.4**, below:

3.3.5 The relative PSA characteristics

The PSA output parameters for the MZ and MS particles and the Fe powder control are given in **Table 3.4**.

Table 3.4: PSA output parameters for the Fe powder control (blue), the MZ particles (black) and the MS particles (red). The parameters are defined in **Table 3.2**.

Magnetic particle type	D10 (µm)	D50 (µm)	D90 (µm)	“Mean” Size (µm)	Span	Obscuration (%)
Fe powder	18.263	37.997	71.280	44.127	1.395	1.56
MZ 1	1.4574	8.968	42.234	17.601	4.547	5.76
MZ 2	1.3837	8.777	42.563	17.597	4.692	2.14
MZ 3	1.2898	9.802	49.943	21.240	4.964	0.01
MZ 4	0.7699	8.284	40.801	17.764	4.832	0.01
MZ 5	1.0270	8.338	40.655	17.192	4.752	0.61
MZ 6	0.9359	7.595	39.743	16.606	5.110	0.81
MZ 7	0.8078	7.523	48.596	20.141	6.352	4.67
MZ 8	0.3018	5.765	35.902	14.993	6.175	0.18
MS 1	2.791	40.293	123.517	66.075	2.996	0.10
MS 2	5.294	37.387	124.771	62.227	3.196	0.56

As can be seen from the above table, the mean particle size for iron powder is ~ 2.5 x higher than the mean values for MZ 1 to MZ 8. Thus, the mean particle size for iron powder is 44.127 µm whereas the mean values for MZ 1 to MZ 8 range from 14.993 to 21.240 µm, with an average mean size of 17.891. In the case of the developed MZ particles, MZ 3 and MZ 7 attained higher mean sizes of 21.240 µm and 20.141 µm respectively. MZ 1, MZ 2, MZ 4, MZ 5 and MZ 6 had lower, more consistent, values ranging from, 16.606 to 17.764 µm, with MZ 8 being the lowest at 14.993 µm. These size differences in the MZ particles could be relevant to their relative pick-up characteristics. A focus of further work in developing such particles might be to create a more uniform particle size. Notably, the MS particles are substantially bigger than both the iron and the MZ particles at an average mean size of 64.151 µm. Referring to the span measurements, iron powder is 1.395 whereas the span values for MZ 1 to MZ 8 range from 4.547 to 6.352, with an average span value of 5.178. In reference to the developed MZ particles, MZ 7 and MZ 8 show higher span values of 6.352 and 6.175 respectively. MZ 1 to MZ 6 attained more consistent, values ranging from, 4.547 to 5.110. In

particular, the MS particles have a smaller span value than the MZ particles at an average span value of 3.096.

The MZ peaks are broader than the iron powder peak and the MS peaks as indicated in the relative span values **Table 3.4**. MZ peaks are slightly bimodal becoming more pronounced with increasing zeolite content. However, the particle size distribution for MS particles presents a uniform bell-shaped curve peak.

3.3.6 Compressibility and flow parameters

Compressibility and flow parameters for the Fe powder and Fe₃O₄ nanoparticle controls, pastes MZ 1 – 5 and MS 1-2 were calculated as described in **Section 3.2.4.2** - and are given in **Table 3.5**.

Table 3.5: Compressibility and flow parameters calculated as described in **Section 3.2.4.2** for the Fe powder and the Fe₃O₄ nanoparticle controls, pastes MZ 1 – 5 and MS 1 – 2. Note that the sawdust data is in red.

Magnetic Powder	Mass of particles (g)	Unsettled Volume, V _B (mL)	Tapped Volume, V _T (mL)	d _B = m/V _B g/mL	d _T = m/V _T g/mL	Hausner Ratio	Carr Index, (%)	Flow
Fe Powder	13.62 (97.14)	4.7 (32.0)	3.8 (26)	2.9 (3.0)	3.6 (3.7)	1.2 (1.0)	19 (19)	Fair (Fair)
Fe ₃ O ₄ Nanoparticles	4.65 (12.67)	4.8 (32)	3.9 (22)	1.0 (0.4)	1.2 (0.6)	1.2 (1.5)	17 (33)	Fair (Poor)
MZ 1	4.36	4.7	3.7	0.9	1.2	1.3	25	Passable
MZ 2	4.26	4.9	4.0	0.9	1.1	1.1	18	Fair
MZ 3	5.60	5.0	4.0	1.1	1.4	1.3	21	Fair
MZ 4	4.33	4.7	3.8	0.9	1.1	1.2	20	Fair
MZ 5	4.39	5.1	4.1	0.9	1.1	1.2	20	Fair
MS 1	10.52	32	21	0.33	0.49	1.5	33	(Poor)
MS 2	11.73	33	22	0.35	0.53	1.5	34	(Poor)

It can be seen from **Table 3.5** that Fe powder and Fe₃O₄ Nanoparticles have the same Hausner Ratio values and a slight difference for the Carr Index (%). Notably, for the Hausner Ratio and Carr Index (%) MZ 1 attained the highest values 1.3 and 25% respectively, achieving passable flow. MZ 3, MZ 4 and MZ 5 presented lower and more consistent, values for the

Hausner Ratio and Carr Index (%) with MZ 2 being the lowest at 1.1 and 18% respectively, demonstrating a fair flow from MZ 2 – MZ 5. Referring to the MS particles, the Hausner Ratio and Carr Index (%) indicate a poor flow characteristic. This could be due to their bigger particle size. Although for MS particles, if the Hausner Ratio and Carr Index (%) parameters are poor this would not matter if the particles are being applied by hand rather than sprayed on by a device.

3.3.7 Magnetic pull experiments

The magnetic pull parameters for the Fe powder and Fe₃O₄ nanoparticle controls and pastes MZ 1 – 5, were determined as described in **Section 3.2.4.3** and the results are given in **Table 3.6**. There was insufficient lab time (due to COVID) to conduct magnetic pull experiments on the MS particles.

Table 3.6: Magnetic pull parameters were determined as described in **Section 3.2.4.2** for the Fe powder, the Fe₃O₄ nanoparticle controls and pastes M 1 – 5.

Magnetic Powder	Magnetic Pull (kg)	Mass of Powder (g)	Pull per g (x 10 ⁻³)
Fe Powder	0.045	13.62	3.3
Fe ₃ O ₄ nanoparticles	0.030	4.65	6.5
MZ 1	0.030	4.36	6.9
MZ 2	0.030	4.26	7.0
MZ 3	0.035	5.60	6.3
MZ 4	0.025	4.33	5.8
MZ 5	0.025	4.39	5.7

3.3.8 Isotherms

Nested isotherms for the magnetic removal of a contaminant Engine oil (BP Vanellus) from a glass substrate and from feather clusters is shown in **Figure 3.17** and **Figure 3.18** respectively. These plots enable the removal efficacy for MZ 1 to MZ 8 particles to be

compared with each other and to the Fe powder control. A notable difference between these two sets of nested isotherms is that the curves representing removal from a glass substrate are noticeably more clumped together than the curves representing removal from feather clusters. This suggests that the surface texture of the particles has an important role to play in the removal of oil from feathers since this substrate is more complex and intricate, which places more demands on the surface characteristics of the particles. This shows that the surface characteristic of the particles, such as roughness, are an important characteristic in optimizing contaminant removal from complex substrates such as plumage and feathers.

In order to investigate these findings further, the surfaces of the particles MZ 1 to MZ 8, MS 1 to MS 2 and the Fe powder control have been examined under a microscope and the images obtained in **Figure 3.19**.

The relevant removal data from **Figures 3.17** and **3.18** is provided in **Table 3.7**.

From the images in **Figure 3.19**, the following qualitative assessment may be made in terms of surface “roughness”. Note that this analysis is done relative to MZ1 since this has inflated values of the Hausner and Carr indices, **Tables 3.3** and **3.4**.

MZ 1 > Fe₃O₄; MZ 1 > MZ 2; MZ 1=MZ 3; MZ 1 > MZ 4; MZ 1 = MZ 5; MZ 1 >MZ 6;
MZ 1 = MZ 7; MZ 1 > MZ 8.

These inequalities are consistent with the measured Hausner and Carr indices in **Table 3.5** and demonstrate that the surface roughness is directly related to the flowability of the particles. The particle flowability is important to consider with respect to how the particles are to be applied to the contaminated substrate. For example, this parameter might not be so important for the implementation of quick clean technology utilizing the magnetic wand where the particle are best applied by hand but could be very important for other applications of MPT, such as the magnetic sweeper (Personal Communication), where the particles, are best sprayed onto an oil slick.

Figures 3.17 and 3.18 show the comparison of the oil pick-up, from glass and feathers as a function of the number of treatments, N, for iron powder and the different MZ particles. The purpose of this experiment is to investigate which proportion of zeolite has achieved the highest oil pick-up and the relative effectiveness of all existing particles. The relevant data from these curves is summarized in **Table 3.7**.

In terms of the isotherms depicted in **Figures 3.17 and 3.18** show that after the first treatment, removal of engine oil from glass using MZ 4 and removal from feathers using MZ 6 achieved high initial oil pick-up of 84.9% and 51.7% respectively, compared to MZ 8 (removal from glass) and MZ 1 (removal from feathers) which achieved lower initial removals of 57.7% and 19.7% respectively. With respect to the maximum removal glass, iron powder and MZ 5 have achieved high removals of 98.1% (N=10) and 98.0% (N=8) respectively. Thus, the maximum removal from feathers, a removal exceeding 99.5% (N=13) and 99.4% (N=12) were achieved for MZ 1 and iron powder. However, MZ 8 (from glass) and MZ 6 (from feathers) obtained lower final removals of 90.6% and 83.0% respectively.

Figure 3.17 and **Figure 3.18** show the following nested removal isotherms. This is the data created for the removal of Engine Oil (BP Vanellus) from both glass and duck feathers.

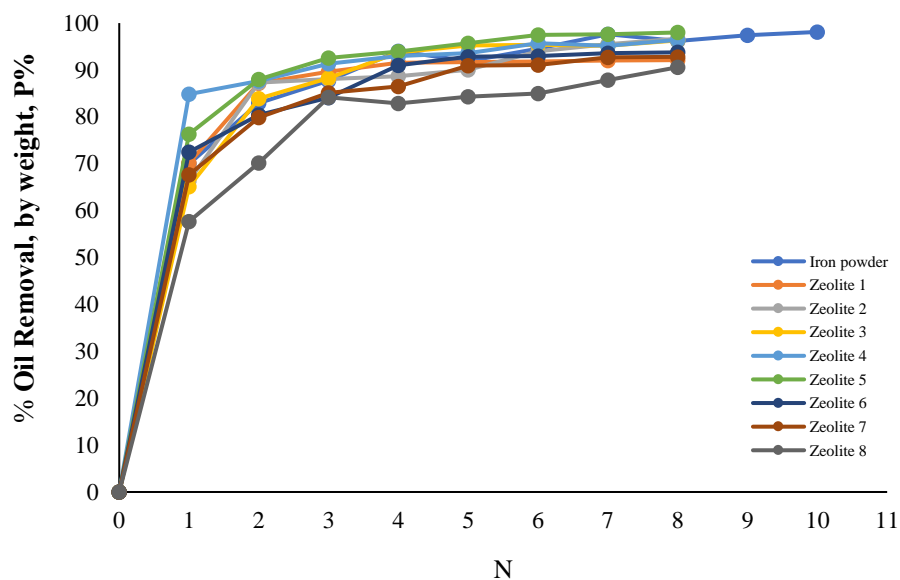


Figure 3.17: Comparison of the % Oil Removal, by weight, P%, from a glass substrate as a function of the number of treatments, N, amongst different powder compositions. The estimated average % error (with respect to the SE) is 10.5%.

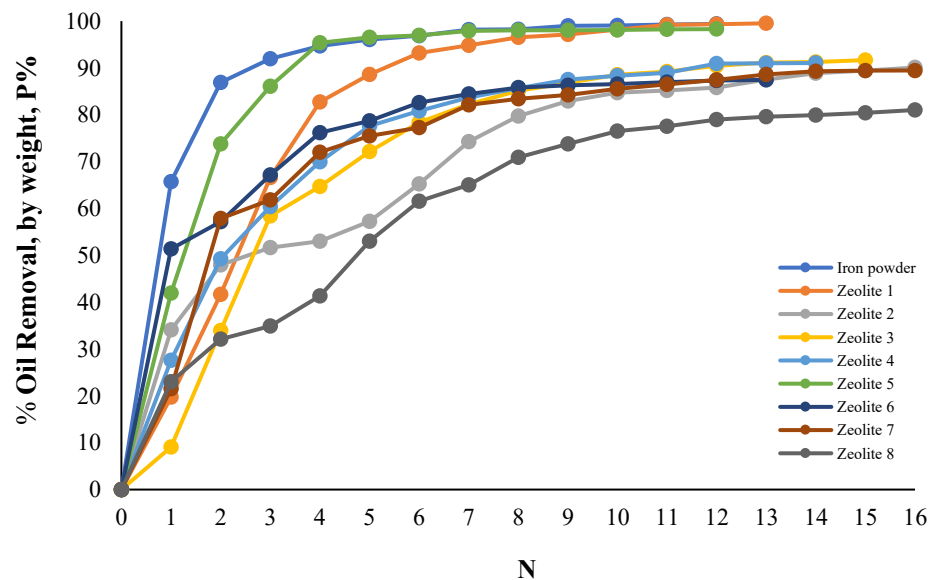


Figure 3.18: Comparison of the % Oil Removal, by weight, P%, from duck feathers as a function of the number of treatments, N, amongst different powder compositions. The estimated average % error (with respect to the SE) is 8.23%.

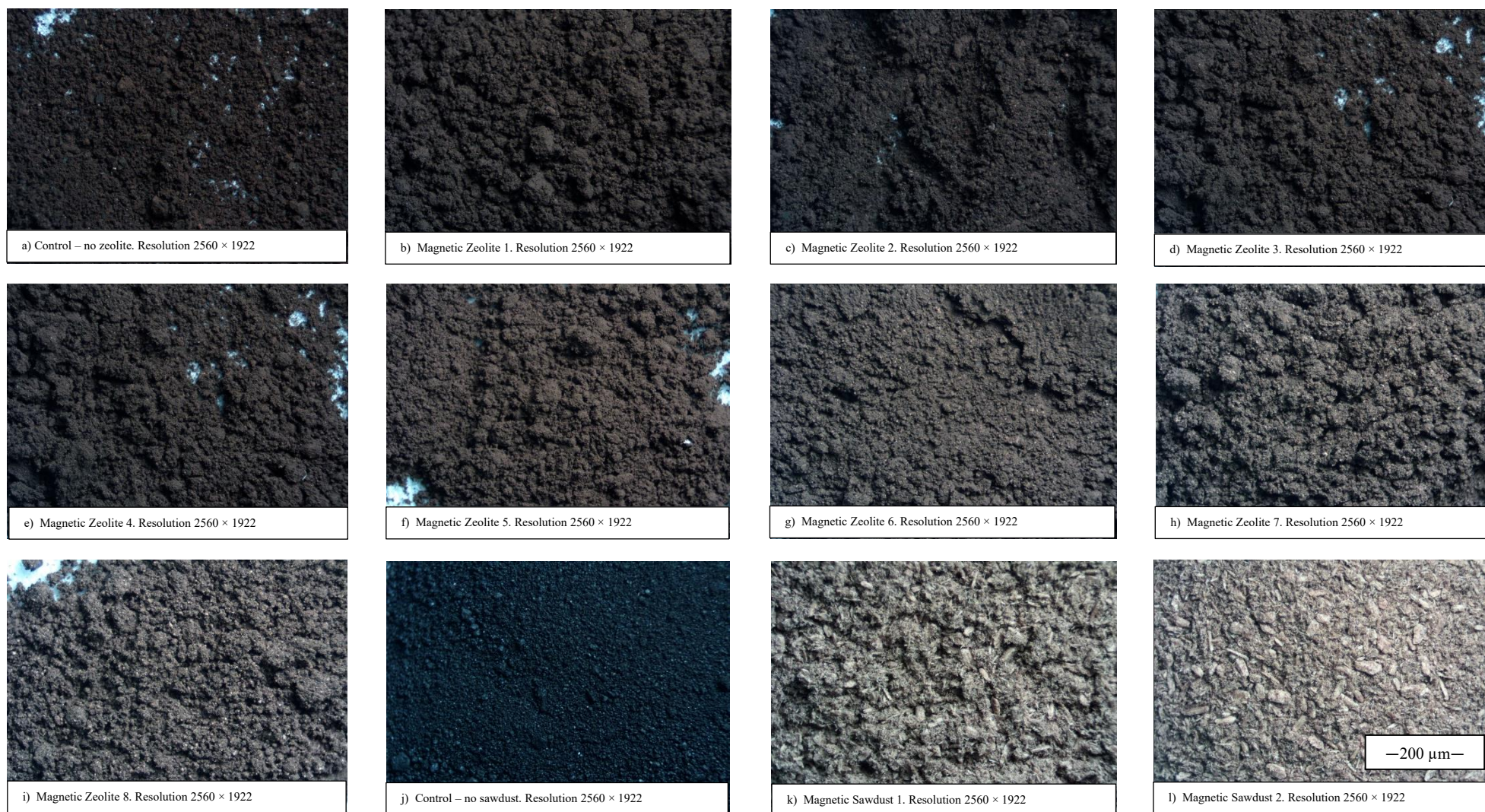


Figure 3.19: Examining the developed Magnetic Particles under an optical microscope (Olympus) of: **(a)** Control – no zeolite (only Fe_3O_4 added), **(b)** Magnetic Zeolite 1, **(c)** Magnetic Zeolite 2, **(d)** Magnetic Zeolite 3, **(e)** Magnetic Zeolite 4, **(f)** Magnetic Zeolite 5, **(g)** Magnetic Zeolite 6, **(h)** Magnetic Zeolite 7, **(i)** Magnetic Zeolite 8, **(j)** Control – no sawdust (only Chitosan and Fe_3O_4 added), **(k)** Magnetic Sawdust1 and **(l)** Magnetic Sawdust 2. The approximate scale (overall) is shown in Box 1.

Table 3.7: A comparative tabulation of the isotherm data from **Figure 3.17** (yellow – glass substrate) and **Figure 3.18** (green – feather clusters) respectively. P₀% – P₃% is the oil removal (%), N_T is the total number of treatments. The estimated average % error (with respect to the SE for glass substrate) is 10.5% and the estimated average % error (with respect to the SE for feather clusters) is 8.23%.

Powder	P ₀ %	N _T	P ₁	P ₂	P ₃	Powder	P ₀ %	N _T	P ₁	P ₂	P ₃
Fe	98.1	10	70.0	82.9	87.7	Fe	99.4	12	65.7	86.9	92.0
MZ 1	92.1	8	70.2	87.2	89.7	MZ 1	99.5	13	19.7	41.7	66.6
MZ 2	96.7	8	66.4	87.3	88.0	MZ 2	95.8	16	36.1	50.8	59.7
MZ 3	96.3	8	65.2	83.9	88.3	MZ 3	95.6	15	20.8	42.7	56.4
MZ 4	96.4	8	84.9	87.6	91.3	MZ 4	91.1	14	27.6	49.2	60.4
MZ 5	98.0	8	76.3	88.0	92.6	MZ 5	98.3	12	41.9	73.8	86.1
MZ 6	93.8	8	72.5	80.4	84.1	MZ 6	83.0	14	51.7	64.0	68.0
MZ 7	92.8	8	67.7	79.8	85.1	MZ 7	90.8	14	20.2	56.6	64.1
MZ 8	90.6	8	57.7	70.2	84.2	MZ 8	85.5	17	22.4	37.5	51.5

As can be seen from **Table 3.7**, the final removal of engine oil from glass using iron powder achieved a higher removal compared to the removal from feathers, except for MZ 1. The removal from feathers using MZ particles shows an erratic pattern, particularly for MZ 5 and MZ 6 particles. In fact, the pickup of engine oil using MZ 5 particles for the removal of feathers is as efficient as compared to the removal of oil using iron powder from glass and feathers (see Figure 3.20). It appears MZ 5 formulation is the best composition in terms of removal efficiency of engine oil using both glass and feathers.

Comparison between the P_o% amongst iron powder and different MZ Powder Type from glass and feathers.

Note: For Figures 3.20 to 3.23 the estimated average % error (with respect to the SE for glass substrate) is 10.5% and the estimated average % error (with respect to the SE for feather clusters) is 8.23%. These represent small errors that do not detract from the trend analyses shown.

The comparison between the P_o% from glass and feathers for iron powder and different MZ Powder Type is shown in Figure. 3.20.

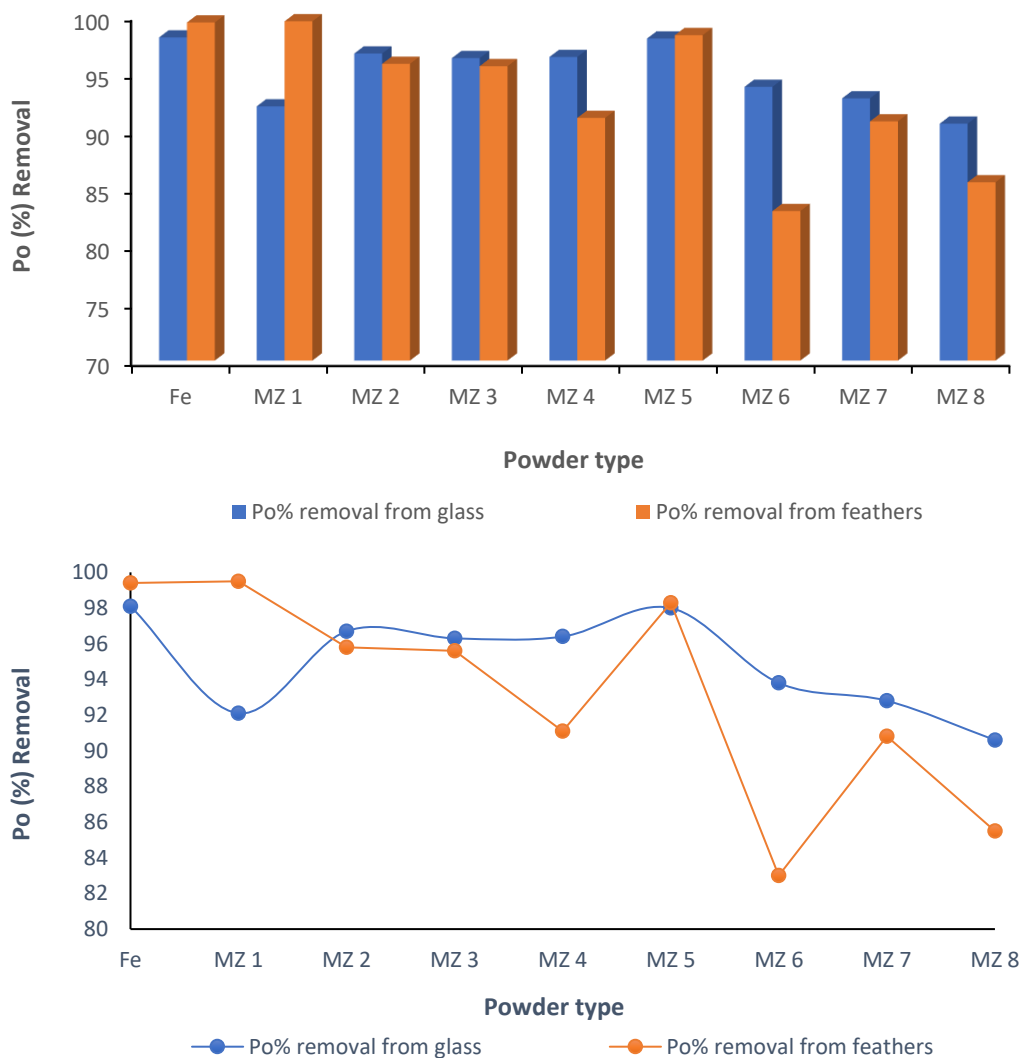


Figure 3.20: The P_o% oil pick-up from glass and feathers for different powder compositions. The line representations of the histograms provided a clearer representation of the trends, especially as to where the maximums occur.

Comparison between the P₁% amongst iron powder and different MZ Powder Type from glass and feathers.

The comparison between the P₁% from glass and feathers for iron powder and different MZ Powder Type is shown in Figure. 3.21.

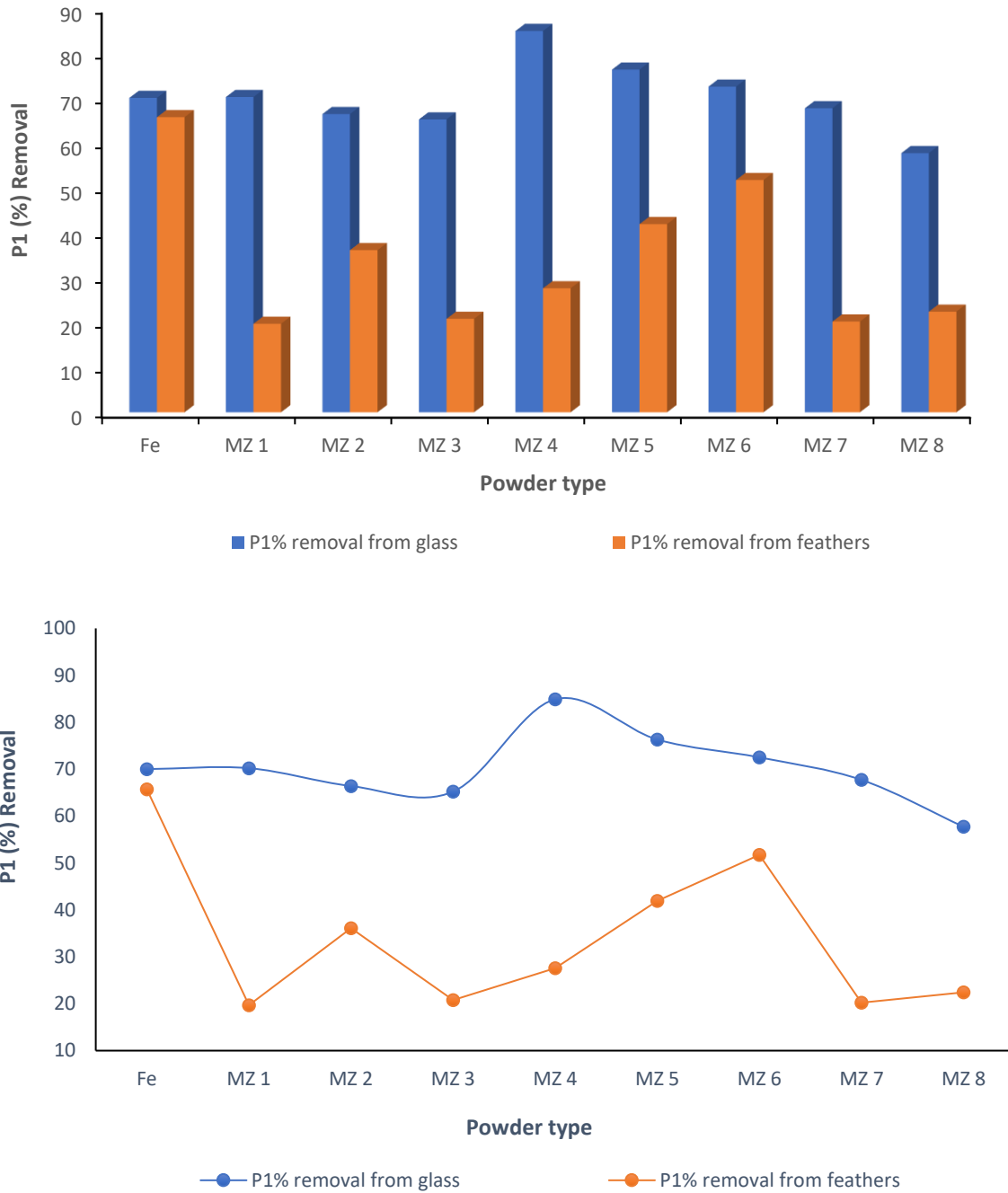


Figure 3.21: The P₁% oil pick-up from glass and feathers for different powder compositions. The line representations of the histograms provided a clearer representation of the trends, especially as to where the maximums occur.

Comparison between the P₂% amongst iron powder and different MZ Powder Type from glass and feathers.

The comparison between the P₂% from glass and feathers for iron powder and different MZ Powder Type is shown in Figure. 3.22.



Figure 3.22: The P₂% oil pick-up from glass and feathers for different powder compositions. The line representations of the histograms provided a clearer representation of the trends, especially as to where the maximums occur.

Comparison between the P₃% amongst iron powder and different MZ Powder Type from glass and feathers.

The comparison between the P₃% from glass and feathers for iron powder and different MZ Powder Type is shown in Figure. 3.23.

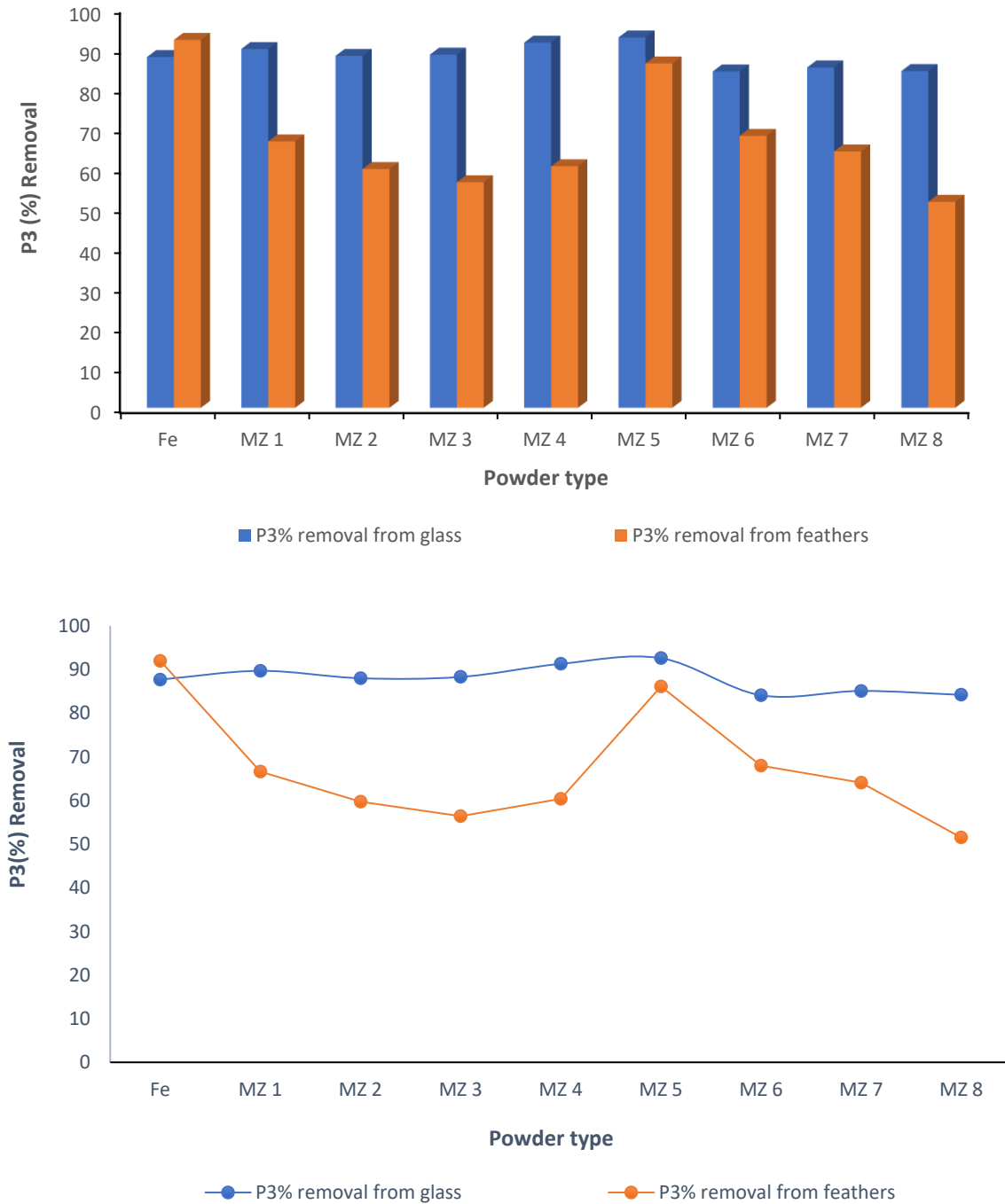


Figure 3.23: The P₃% oil pick-up from glass and feathers for different powder compositions. The line representations of the histograms provided a clearer representation of the trends, especially as to where the maximums occur.

Figures 3.20 to Figure 3.23 compare the first three oil % pick-ups ($P_1\%$, $P_2\%$, $P_3\%$) and the final pick-up ($P_0\%$) for eight different zeolite powders.

Comparison between $P_1\%$, $P_2\%$, $P_3\%$ and $P_0\%$ versus Pull per g ($\times 10^{-3}$) for glass and feather substrates

This comparison is depicted in Figure 3.24 to Figure 3.27 for the particles listed in Tables 3.6 and 3.7.

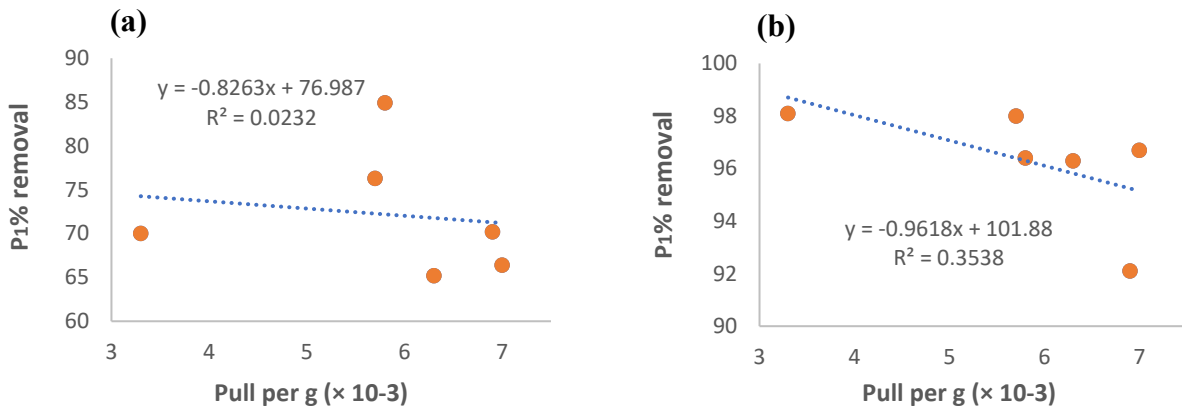


Figure 3.24: (a) Comparison of the $P_1\%$ removals versus Pull per gram ($\times 10^{-3}$) for glass and (b) Comparison of the $P_1\%$ removals versus Pull per gram ($\times 10^{-3}$) for feathers.

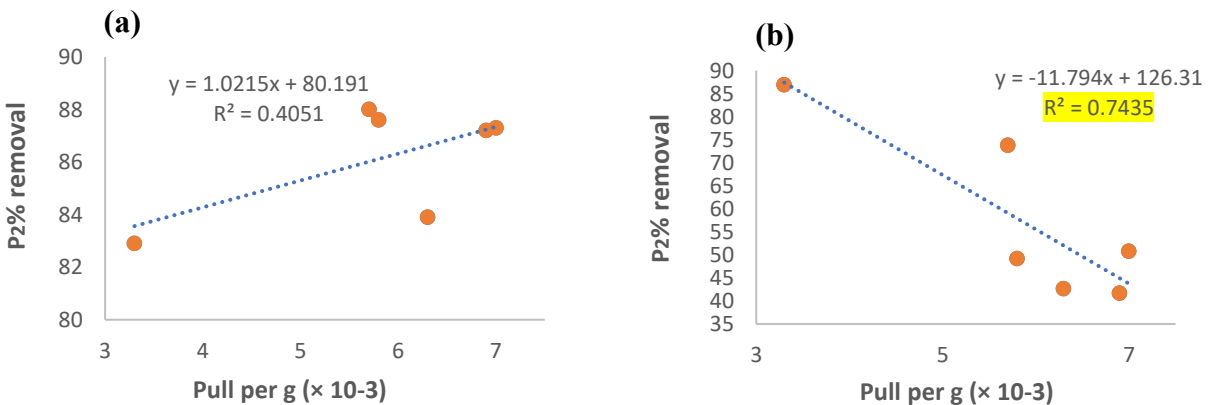


Figure 3.25: (a) Comparison of the $P_2\%$ removals versus Pull per gram ($\times 10^{-3}$) for glass and (b) Comparison of the $P_2\%$ removals versus Pull per gram ($\times 10^{-3}$) for feathers.⁵

⁵ $P_1\%$, $P_2\%$ and $P_3\%$ have previously been defined as representing the “initial” removal and $P_0\%$, the “final” removal.

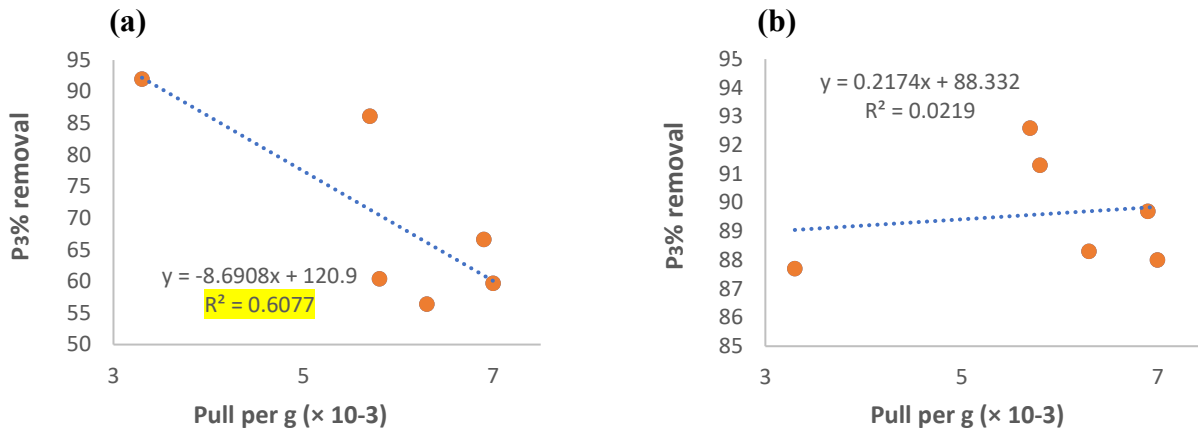


Figure 3.26: (a) Comparison of the P₃% removals versus Pull per gram (× 10⁻³) for glass and (b) Comparison of the P₃% removals versus Pull per gram (× 10⁻³) for feathers.

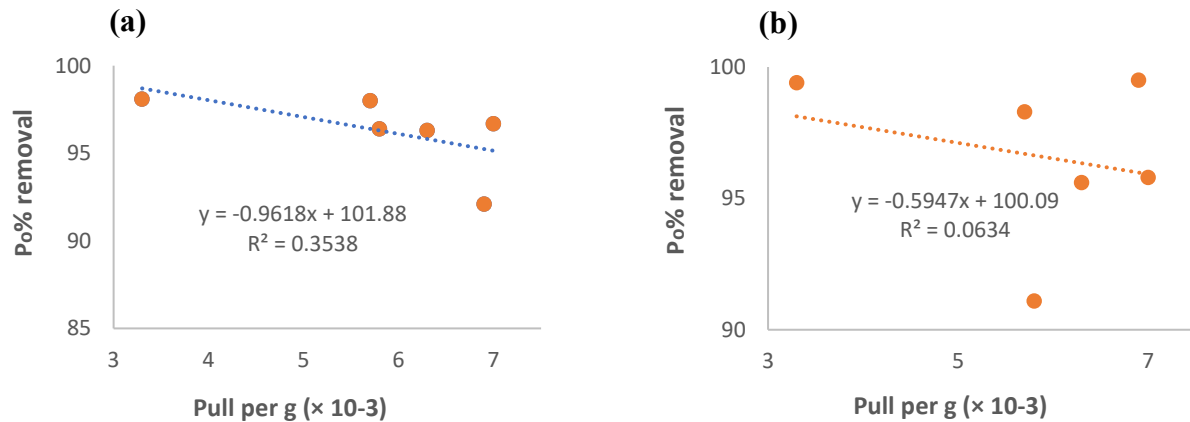


Figure 3.27: (a) Comparison of the P₀% removals versus Pull per gram (× 10⁻³) for glass and (b) Comparison of the P₀% removals versus Pull per gram (× 10⁻³) for feathers.

For both glass and feathers there appears to be some anomalies in the data. For example, for the P₃% removal from glass it appears that these decrease with increasing magnetic pull, and similarly for P₂% removal from feathers. This is the opposite of what would be expected and suggests a problem with the recording of the data. More experimentation would be required to resolve this. However, given that overall the correlations are very low, it is concluded that the magnetic pull range of between 3 and 7 (per g × 10⁻³) results in a P₀% removal range of between 90 and 100% values is sufficient for the particles studied.

Comparison between the P₁%, P₂%, P₃% and P₀% versus Mean size for glass and feathers

This is depicted in **Figures 3.28** to **Figure 3.31**.

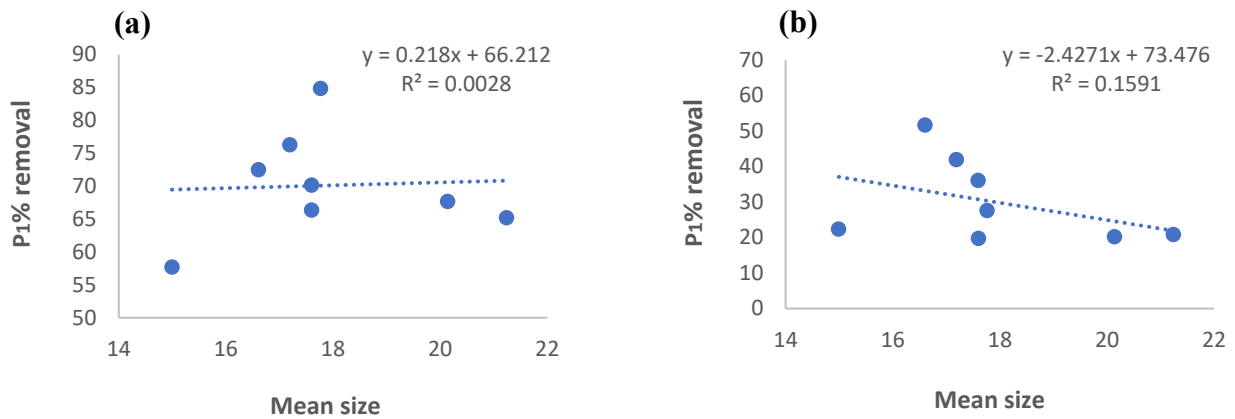


Figure 3.28: (a) Comparison of the P₁% removals versus Mean size for glass and (b) Comparison of the P₁% removals versus Mean size for feathers.

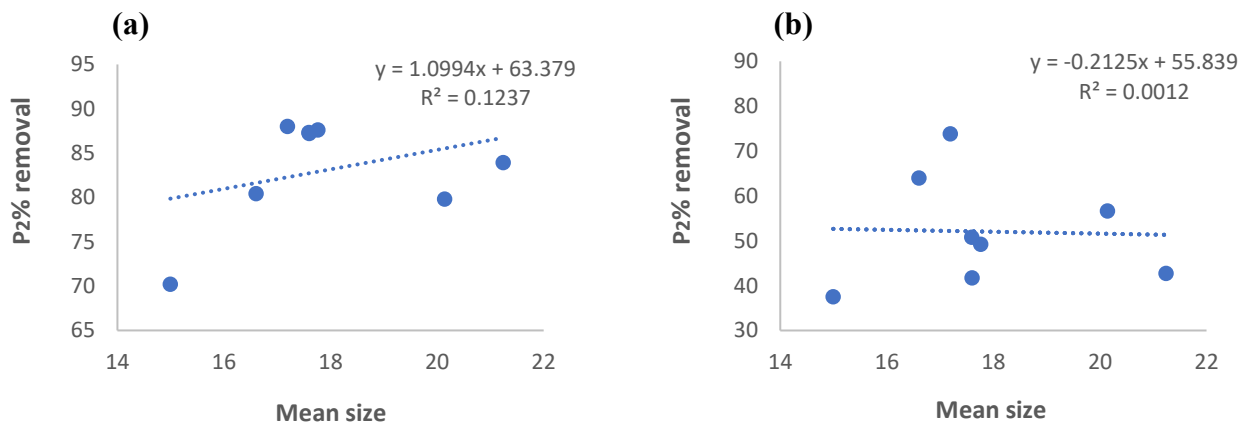


Figure 3.29: (a) Comparison of the P₂% removals versus Mean size for glass and (b) Comparison of the P₂% removals versus Mean size for feathers.

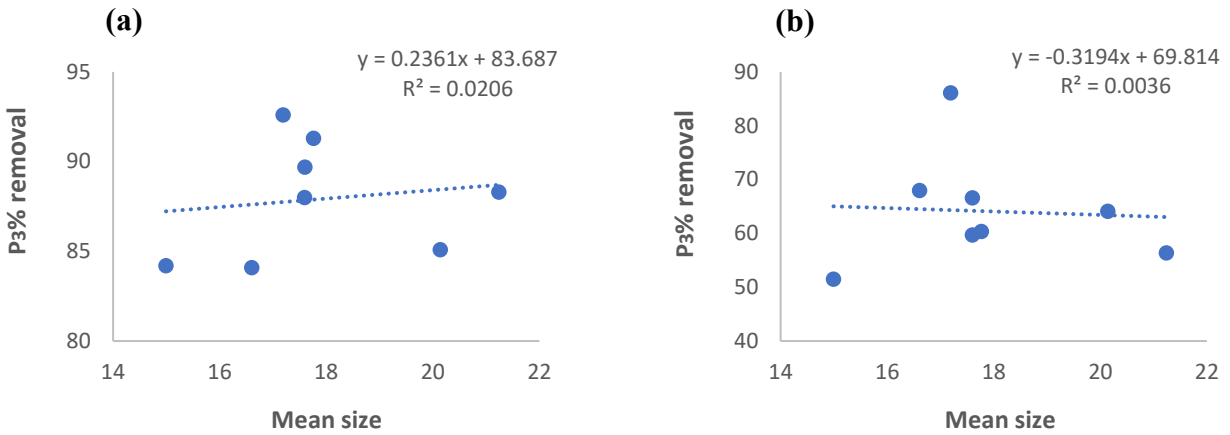


Figure 3.30: (a) Comparison of the P₃% removals versus Mean size for glass and (b) Comparison of the P₃% removals versus Mean size for feathers.

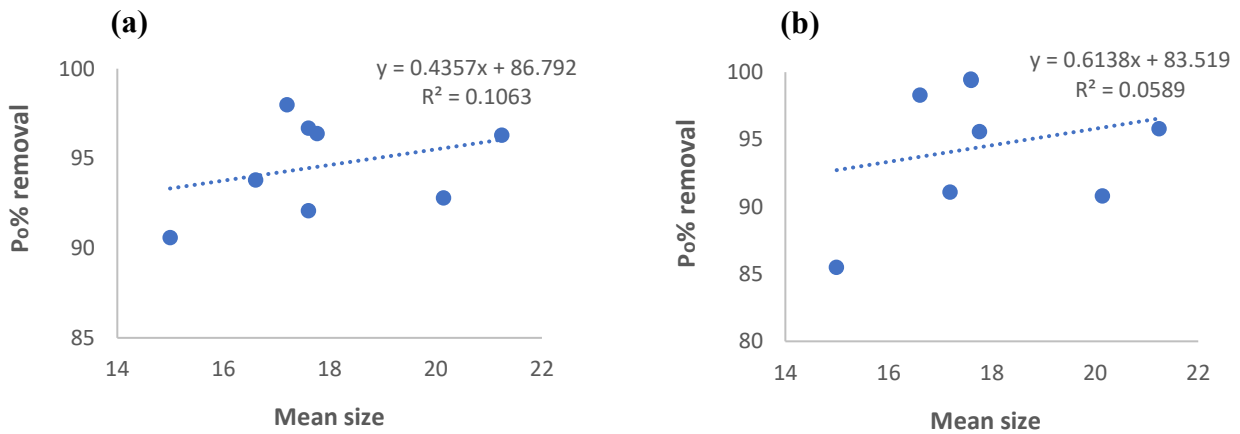


Figure 3.31: (a) Comparison of the P₀% removals versus Mean size for glass and (b) Comparison of the P₀% removals versus Mean size for feathers.

With respect to the above plots for a glass substrate, there is barely any correlation at all, with the slopes being very slightly positive. Therefore, it is inconclusive as to whether the P% values have any dependency on the mean particle size. The same situation is also true for feathers.

Comparison between the P₁%, P₂%, P₃% and P₀% versus Span for glass and feathers.

This is depicted in Figure 3.32 to Figure 3.35.

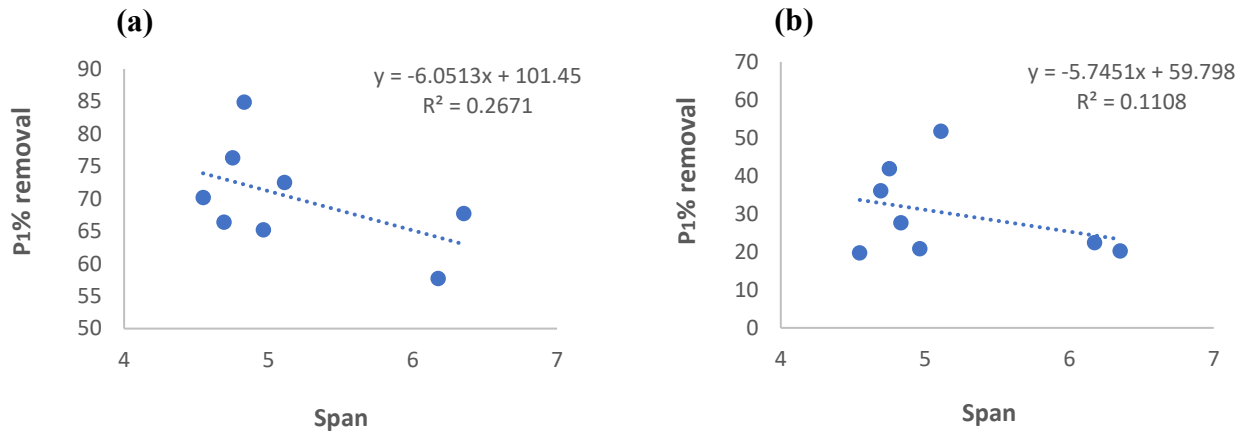


Figure 3.32: (a) Comparison of the P₁% removals versus Span for glass and (b) Comparison of the P₁% removals versus Span for feathers.

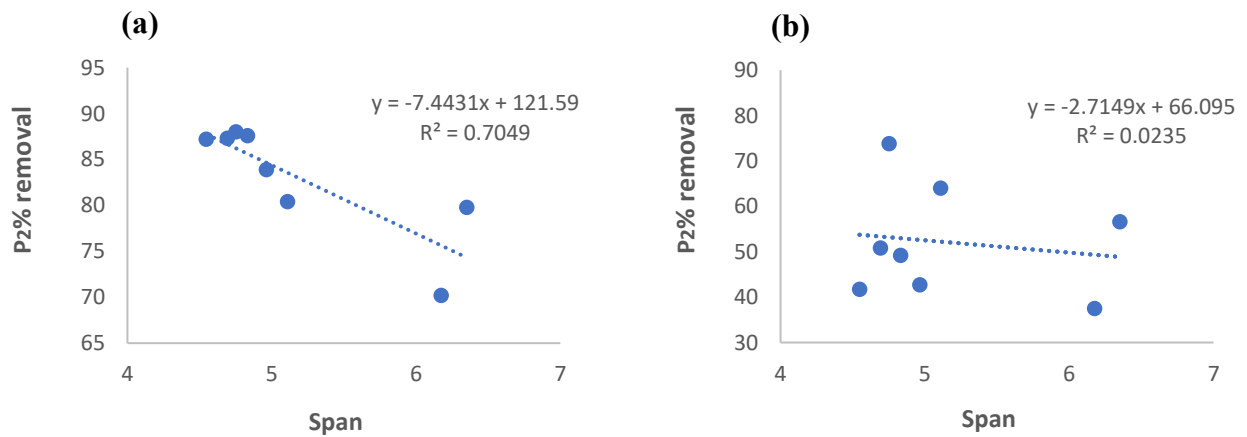


Figure 3.33: (a) Comparison of the P₂% removals versus Span for glass and (b) Comparison of the P₂% removals versus Span for feathers.

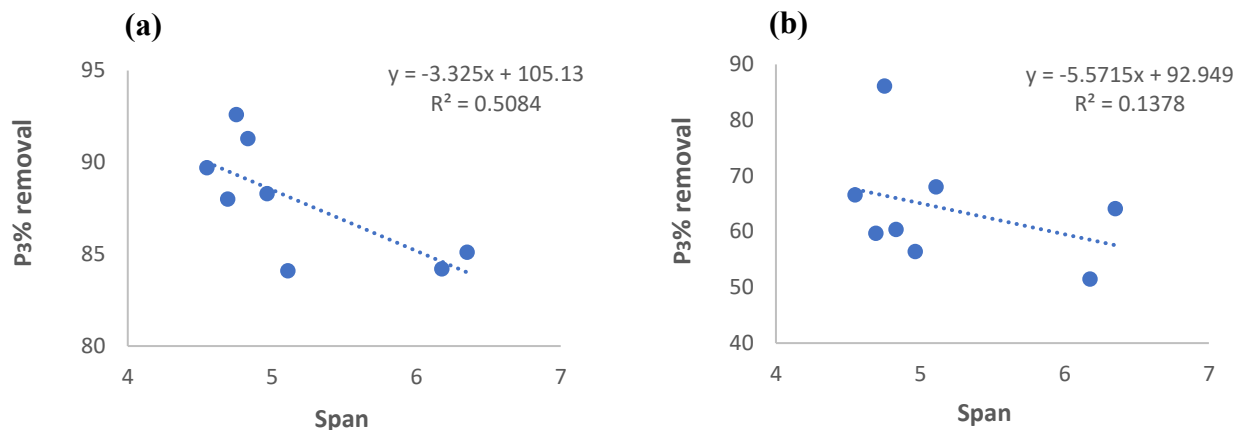


Figure 3.34: (a) Comparison of the P₃% removals versus Span for glass and (b) Comparison of the P₃% removals versus Span for feathers.

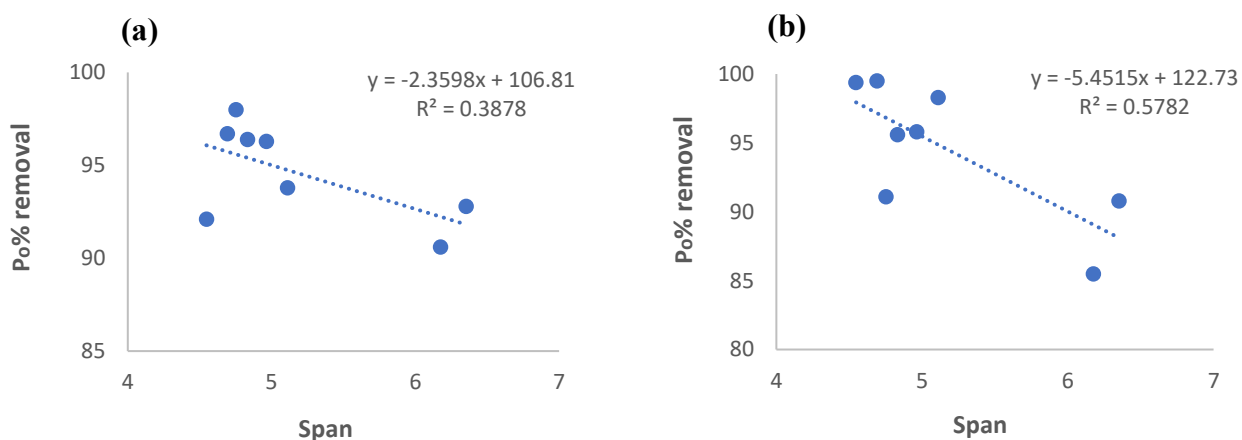


Figure 3.35: (a) Comparison of the P₀% removals versus Span for glass and (b) Comparison of the P₀% removals versus Span for feathers.

According to the Span results, there is evidence for some correlation between the P% values and the span parameter with respect to a glass substrate. The best correlations are for P₂% and P₃% based on the R² values. The negative slopes suggest that the P% values decrease with increasing span. For a feather substrate this is also evidence for some correlation but P₁% to P₃% the correlation coefficients are rather low compared to glass. Notably, there is also a negative slope in these curves suggesting that a smaller span is an advantage with respect to removal.

Thus, it would appear from the above results that a smaller span is more important for the degree of removal (initial and final) than a small particle size.

3.4 Conclusions

The research described in this chapter is within the context of the “quick clean” approach utilizing magnetic particle technology. The research has shown that it is feasible to create oil ad(b)sorbing magnetic particles that are lighter in weight and with equivalent effectiveness to existing zero valent iron powder magnetic particles. The possible advantage of such particles is that a lower weight of material will need to be transported to and from a pollution event. In this regard, the zeolite and sawdust particles that were infused with Fe_3O_4 nanoparticles in different proportions to create improved oil ad(b)sorbing magnetic particles has been found to be lighter in weight than iron powder but can remove equivalent amounts of oil contamination from a feather substrate. Furthermore, these studies have shown that some particle compositions are better than others and hence there is scope for further optimization. For example, from the eight MZ and two MS particle types investigated, the particle designated MZ5 has been identified as being the most effective, showing approximately a removal efficacy of ~ 98.0% from both glass and feather substrates. Further improvement of such oil sequestering particles will undoubtedly improve the logistics for a quick clean in the field by reducing the weight of oil sequestering particles for a given % removal in the field and by reducing the weight of the oil laden particles to be transported back to be disposed.

3.5 References

ACTTR Techology 2023, *How Does A Particle Size Analyzer Measures & Report*, viewed 22 December 2023, <<https://www.acttr.com/en/en-faq/en-faq-particle-size-analyzer/401-en-faq-particle-measure-expression.html>>.

Ahmad, A, Rafatullah, M, Sulaiman, O, Ibrahim, MH, Hashim, R 2009, 'Scavenging behavior of meranti sawdust in the removal of methylene blue from aqueous solution', *J. Hazard. Mater.*, vol. 170, pp. 357–365.

Ahmadpour, A, Zabihi, M, Tahmasbi, M, Bastami, TR 2010, 'Effect of adsorbents and chemical treatments on the removal of strontium from aqueous solutions', *J. Hazard. Mater.*, vol. 182 pp. 552–556.

Bailey, SE, Olin, TJ, Bricka, RM, Adrian, DD 1999, 'A review of potentially low-cost sorbents for heavy metals', *Water Res.*, vol. 33, pp. 2469.

Barbier, F, Duc, G, Ramel, MP 2000, 'Adsorption of Pb and Cd ions from aqueous solution to the montmorillonite/water interface', *Colloid. Surf. A: Physicochem. Eng. Aspects.*, vol. 166, pp. 153-159.

Bascetin, E & Atun, G 2010, 'Adsorptive removal of strontium by binary mineral mixtures of montmorillonite and zeolite', *J. Chem. Eng.*, vol. 55, pp. 783–788.

Better Particle Size Solution (Bettersize) 2022, *What is obscuration*, viewed 22 December 2023, <<https://www.bettersizeinstruments.com/learn/bettersize-wiki/what-is-obscuration/>>.

Booker, NA, Keir, D, Priestley, A, Rithchie, CD, Sudarmana, DL, Woods, MA 1991, 'Sewage clarification with magnetite particles', *Water Science, Technology*, vol. 123, pp. 1703-1712.

Burgess, DJ, Duffy, E, Etzler, F, Hickey, AJ 2004, 'Pharmaceutical Preformulation and Formulation: A Practical Guide from Candidate Drug Selection to Commercial Dosage Form', *J. AAPS.*, vol. 6, no. 3, pp. 23-24.

Cadena, F, Rizvi, R & Peter, RW 1990, 'Feasibility studies for the removal of heavy metal from solution using Tailored bentonite, hazardous and industrial wastes', *Proceedings 22nd Midi Atlantic Industrial Waste Conference, Drexel University*, p. 77.

Carroll, SA, Roberts, SK, Criscenti, LJ, O'Day, PA 2008, 'Surface complexation model for strontium sorption to amorphous silica and goethite', *Geochem. Trans.*, vol. 9, pp. 2–27.

Chakraborty, D, Maji, S, Bandyopadhyay, A, Basu, S 2007, 'Biosorption of cesium-137 and strontium-90 by mucilaginous seeds of *Ocimum basilicum*', *Bioresour. Technol.*, vol. 98, pp. 2949–2952.

Chen, JP 1997, 'Batch and continuous adsorption of strontium by plant root tissues', *Bioresour. Technol.*, vol. 60, pp. 185–189.

Chen, C, Jun, H, Shao, D, Li, J, Wang, X 2009, 'Adsorption behavior of multiwall carbon nanotube/iron oxide magnetic composites for Ni (II) and Sr (II)', *J. Hazard. Mater.*, vol. 164 pp. 923–928.

Chen, Y & Wang, J 2012, 'Removal of radionuclide Sr^{2+} ions from aqueous solution using synthesized magnetic chitosan beads', *Nucl. Eng. Des.*, vol. 242, pp. 445–451.

Cheng, Z, Gao, Z, Ma, W, Sun, Q, Wang, B, Wang, X 2012, 'Preparation of magnetic Fe_3O_4 particles modified sawdust as the adsorbent to remove strontium ions', *J. Chem. Eng.*, vol. 209, pp. 451-457.

Cho, Y & Komarneni, S 2009, 'Cation exchange equilibria of cesium and strontium with K-depleted biotite and muscovite', *Appl. Clay Sci.*, vol. 44, pp. 15– 20.

Chouchene, A, Jeguirim, M, Trouve, G, Favre-Reguillon, A, Buzit, GL 2010, 'Combined process for the treatment of olive oil mill wastewater: absorption on sawdust and combustion of the impregnated sawdust', *Bioresour. Technol.*, vol. 101, pp. 6962–6971.

Danis, TG, Albanis, TA, Petrakis, D, Pomonis, PJ 1998, 'Removal of chlorinated phenols aqueous solutions by adsorption on alumina pillared clays and mesoporous alumina aluminum phosphates', *Water Research*, vol. 32, pp. 295–302.

De Pena, YP, Lopez, W, Burguera, JL, Burguera, M, Gallignani, M, Brunetto, R, Carrero, P, Rondon, C, Imbert, F 2000, 'Synthetic zeolites as sorbent material for on-line preconcentration of copper traces and its determination using flame atomic absorption spectrometry', *Anal. Chim. Acta.*, vol. 403, pp. 249–258.

Dulman, V & Cucu-Man, SM 2009, 'Sorption of some textile dyes by beech wood sawdust', *J. Hazard. Mater.*, vol. 162, pp. 1457–1464.

Fan, L, Luo, C, Lv, Z, Fuguang, L, Qiu, H 2011, 'Preparation of magnetic modified chitosan and adsorption of Zr^{2+} from aqueous solutions', *Colloids Surf. B.*, vol. 88, pp. 574–581.

Ghaemi, A, Torab-Mostaedi, M, Ghannadi-Maragheh, M 2011, 'Characterization of strontium (II) and barium (II) adsorption from aqueous solutions using dolomite powder', *J. Hazard. Mater.*, vol. 190, pp. 916–921.

Gibson, M 2001, *Pharmaceutical Preformulation and Formulation: A Practical Guide from Candidate Drug Selection to Commercial Dosage Form*, CRC Press, Boca Raton.

Godhino, L 1993, 'A physical method for the removal of oil contamination', Honours Thesis, Victoria University, Melbourne, Australia.

Gupta, S & Babu, BV 2009, 'Modeling, simulation, and experimental validation for continuous Cr (VI) removal from aqueous solutions using a sawdust as an adsorbent', *Bioresour. Technol.*, vol. 100, pp. 5633–5640.

Gupta, VK, Agarwal, S, Saleh, TA 2011, 'Chromium removal by combining the magnetic properties of iron oxide with adsorption properties of carbon nanotubes', *Water Research*, vol. 45, pp. 2207-2212.

Gupta, VK & Nayak, A 2012, 'Cadmium removal and recovery from aqueous solutions by novel adsorbents prepared from orange peel and Fe₂O₃ nanoparticles', *J. Chem. Eng.*, vol. 180, pp. 81-90.

Hadjittofis, E, Das, SC, Zhang, GGZ, Heng, JYY 2017, 'Developing Solid Oral Dosage Forms (Second Edition)', *Academic Press*, pp. 225-252.

Kamel, NHM 2010, 'Adsorption models of Cs radionuclide and Sr (II) on some Egyptian soils', *J. Environ. Radioact.*, vol. 101, pp. 297–303.

Konstantinou, IK, Albanis, TA, Petrakis, DE, Pomonis, PJ 2000, 'Removal of herbicides from aqueous solutions by adsorption on Al-pillared clays', *Water Research*, vol. 34, pp. 3123–3136.

Kutahyali, C, Cetinkaya, B, Bahadir Acar, M, Olcay, NI, Cireli, I 2012, 'Investigation of strontium sorption onto Kula volcanics using central composite design', *J. Hazard. Mater.*, vol. 201–202, pp. 115–124.

Langley, S, Gault, AG, Ibrahim, A, Takahashi, Y, Renaud, R, Fortin, D, Clark, ID, Ferris, FG 2009, 'Sorption of strontium onto bacteriogenic iron oxides', *Environ. Sci. Technol.*, vol. 43 pp. 1008–1014.

Law, JD, Brewer, KN, Herbst, RS, Todd, TA, Wood, DJ 1999, 'Development and demonstration of solvent extraction processes for the separation of radionuclides from acidic radioactive waste', *Waste Manage.*, vol. 19, pp. 27–37.

Li, Q, Liu, HN, Liu, TY, Guo, M, Qing, BJ, Ye, XS, Wu, ZJ 2010, 'Strontium and calcium ions adsorption by molecularly imprinted hybrid gel', *J. Chem. Eng.*, vol. 157, pp. 401–407.

Lin, YL, Wang, R, Ma, W, Cheng, ZH 2012, 'Characteristics of lysozyme adsorption on magnetic Fe₃O₄/chitosan nanoparticles at fixed pH', *Adv. Mater. Res.*, vol. 343–344, pp. 909–913.

Maresova, J, Pipiska, M, Rozloznik, M, Hornik, M, Remenarova, L, Augustin, J 2011, 'Cobalt and strontium sorption by moss biosorbent: modeling of single and binary metal systems', *Desalination*, vol. 266, pp. 134–141.

Microtrac 2023, *Particle Size Distribution: Particle Analyzers :: Microtrac*, viewed 22 December 2023, <<https://www.microtrac.com/knowledge/particle-size-distribution/>>.

Munaweera, K 2015, 'The rational development of improved methods for the removal of oil contamination from wildlife and rocky foreshore utilizing magnetic particle technology', PhD Thesis, Victoria University, Melbourne, Australia.

Murray, HH 2000, 'Traditional and new applications for kaolin, smectite and palygorskite: a general overview', *Appl. Clay. Sci.*, vol. 17, pp. 207-221.

Murthy, ZVP & Parmar, S 2011, 'Removal of strontium by electrocoagulation using stainless steel and aluminum electrodes', *Desalination*, vol. 282, pp. 63–67.

Nanseu-Njiki, CP, Dedzo, GK, Ngameni, E 2010, 'Study of the removal of paraquat from aqueous solution by biosorption onto Ayous (*Triplochiton schleroxylon*) sawdust', *J. Hazard. Mater.*, vol. 179, pp. 63– 71.

Ngeh, LN, Orbell, JD, Bigger, SW, Munaweera, K, Dann, P 2012, 'Magnetic cleansing for the provision of a quick clean to oiled wildlife', *World of Academy of Science and Technology*, vol. 72, pp. 1091-1093.

Oliveira, LCA, Rios, RVRA, Fabris, JD, Sapag, K, Garg, VK, Lago, RM 2003, 'Clay-iron oxide magnetic composites for the adsorption of contaminations in water', *Appl. Clay Sci.*, vol. 22, pp. 169-177.

Oliveira, LCA, Petkowicz, DI, Smaniotto, A, Pergher, SBC 2004, 'Magnetic zeolites: a new adsorbent for removal of metallic contaminants from water', *Water Research*, vol. 38, pp. 3699-3704.

Orbell, JD, Godhino, L, Bigger, SW, Nguyen, TM, Ngeh, LN 1997, 'Oil spill remediation using magnetic particles', *J. Chem. Edu.*, vol. 74, no. 12, pp. 1446-1448.

Orbell, JD, Tan, EK, Coutts, MC, Bigger, SW, Ngeh, LN 1999, 'Cleansing oiled feathers-magnetically', *Mar. Pollut. Bull.*, vol. 38, no. 3, pp. 219-221.

Orbell, JD, Ngeh, LN, Bigger, SW, Zabinskas, M, Zheng, M, Healy, M, Jessop, R, Dann, P 2004, 'Whole-bird models for the magnetic cleansing of oiled feathers', *Mar. Pollut. Bull.*, vol. 38, no. 48, pp. 336-340.

Orbell, JD, Dann, P, Bigger, SW, Ngeh, LN, Diep, L, Shewan, A 2022, 'Novel "quick clean" technology for the rapid removal of volatiles from contaminated wildlife', *the 14th International effects of Oiled on Wildlife (EOW) Conference 2022*, Long Beach Hilton, California, USA.

Particle Analytical 2018, *Bulk and tapped density*, viewed on 25 December 2023, <<https://particle.dk/physical-characterization/bulk-and-tapped-density/>>.

Powder Process 2023, *Carr Index and Hausner Ratio*, viewed on 25 December 2023, <https://powderprocess.net/Powder_Flow/Carr_Index_Hausner_Ratio.html>.

Rahman, MS & Islam, MR 2009, 'Effect of pH on isotherms modeling for Cu (II) ions adsorption using maple wood sawdust', *J. Chem. Eng.*, vol. 149, pp. 273– 280.

Raut, DR, Mohapatra, PK, Manchanda, VK 2012, 'A highly efficient supported liquid membrane system for selective strontium separation leading to radioactive waste remediation', *J. Membr. Sci.*, vol. 390–391, pp. 76–83.

Ryachi, K & Bencheikh, A 1998, 'Characterization of some materials applied to depollution of waste liquid', *Ann. Chim. Sci. Mat.*, vol. 23, pp. 393-396.

Safarikova, M & Safarik, I 2001, 'The Application of Magnetic Techniques in Biosciences', *Magn. Electro. Sep.*, vol. 10, pp. 223-252.

Semerjian, L 2010, 'Equilibrium and kinetic of cadmium adsorption from aqueous solutions using untreated *Pinus halepensis* sawdust', *J. Hazard. Mater.*, vol. 173, pp. 236-242.

Shu, HT, Li, D, Scala, AA, Ma, YH 1997, 'Adsorption of small organic pollutant from aqueous streams by aluminosilicate-based microporous materials', *Sep. Purif. Technol.*, vol. 11, pp. 27-36.

Sidiras, D, Batzias, F, Schroeder, E, Ranjan, R, Tsapatsis, M 2011, 'Dye adsorption on autohydrolyzed pine sawdust in batch and fixed-bed systems', *J. Chem. Eng.*, vol. 171, pp. 883-896.

Sing, KS 1994, 'Ground water monitor', *Technology Profile*, vol. 21, p. 60.

Tel, H, Altas, Y, Eral, M, Sert, S, Cetinkaya, B, Inan, S 2010, 'Preparation of ZrO_2 and ZrO_2 - TiO_2 microspheres by the sol-gel method and an experimental design approach to their strontium adsorption behaviours', *J. Chem. Eng.*, vol. 161, pp. 151-160.

Tian, Y, Min, W, Lin, X, Huang, P, Huang, Y 2011, 'Synthesis of magnetic wheat straw for arsenic adsorption', *J. Hazard. Mater.*, vol. 193, pp.10-16.

Torrents, A & Jayasundera, S 1997, 'The sorption of non-ionic pesticides onto clays and influence of natural organic carbon', *Chemosphere*, vol. 35, pp. 1549-1565.

Trgo, M & Peric, J 2003, 'Interaction of the zeolitic tuff with Zn containing simulated pollutant solutions', *J. Colloid Interface Sci.*, vol. 260, pp. 166-175.

Trivedi, P & Lisa, A 1999, 'A comparison of strontium sorption to hydrous aluminum, iron, and manganese oxides', *J. Colloid Interf. Sci.*, vol. 218, pp. 554–563.

Valsala, TP, Joseph, A, Sonar, NL, Sonavane, MS, Shah, JG, Raj, K, Venugopal, V 2010, 'Separation of strontium from low level radioactive waste solutions using hydrous manganese dioxide composite materials', *J. Nucl. Mater.*, vol. 404, pp. 138–143.

Vinodhini, V & Das, N 2009, 'Packed bed column studies on Cr (VI) removal from tannery wastewater by neem sawdust', *Desalination*, vol. 264, pp. 9–14.

Wahab, MA, Jellali, S, Jedidi, N 2010, 'Ammonium biosorption onto sawdust: FTIR analysis, kinetics and adsorption isotherms modeling', *Bioresour. Technol.*, vol. 101, pp. 5070–5075.

Wang, M, Ling, X, Peng, J, Zhai, Mao, Li, J, Wei, G 2009, 'Adsorption and desorption of Sr (II) ions in the gels based on polysaccharide derivatives', *J. Hazard. Mater.*, vol. 171, pp. 820–826.

Witek-Krowiak, A 2011, 'Analysis of influence of process conditions on kinetics of malachite green biosorption onto beech sawdust', *J. Chem. Eng.*, vol. 171, pp. 976–985.

Ye, XS, Liu, TY, Li, Q, Liu, HN, Wu, ZJ 2008, 'Comparison of strontium and calcium adsorption onto composite magnetic particles derived from Fe₃O₄ and bis(trimethoxysilylpropyl) amine', *Colloids Surf. A.*, vol. 330, pp. 21–27.

Zhang, AY, Chen, CM, Kuraoka, E, Kumagai, M 2008, 'Impregnation synthesis of a novel macroporous silica-based crown ether polymeric material modified by 1-dodecanol and its adsorption for strontium and some coexistent metals', *Sep. Purif. Technol.*, vol. 62, pp. 407–414.

Chapter 4: Penguin Pelt as a model substrate for the MPT assessment of oil removal from plumage

4.1 Introduction

- 4.1.1 Oil removal from a glass substrate
- 4.1.2 Oil removal from feather clusters
- 4.1.3 Oil removal from plumage (carcass)
- 4.1.4 Oil removal from pelt

4.2 Methodology for the removal of different oil types

- 4.2.1 Removal from feather clusters
- 4.2.2 Removal from pelt
- 4.2.3 Removal from whole bird model (carcass)

4.3 Materials and equipment

- 4.3.1 Materials
- 4.3.2 Equipment

4.4 Results and Discussion

- 4.4.1 The importance of pelt sample size in relation to oil type
 - 4.4.1.1 Removal of Gippsland crude oil
 - 4.4.1.2 Removal of Diesel oil
 - 4.4.1.3 Removal of Engine oil
 - 4.4.1.4 Removal of Bunker oil 1 (BO1)
- 4.4.2 Recycling of pelt samples
 - 4.4.2.1 Experimental method
 - 4.4.2.2 The recycling ('washing') process

- 4.4.2.3 Removal of Gippsland Crude Oil from recycled penguin pelt
- 4.4.2.4 Removal of Diesel Fuel Oil from recycled penguin pelt
- 4.4.2.5 Removal of Engine Oil from recycled penguin pelt
- 4.4.2.6 Removal of Bunker Oil 1 (BO1) from recycled penguin pelt
- 4.4.3 Mimicking the penguin's body temperature – removal from pelt at 40 °C.
- 4.4.4 The relationship between the removal isotherm profile and the percentage coverage of Diesel Fuel Oil on a Little Penguin plumage (carcass).

4.5 References

4.1 Introduction

Marine oil spills are a major source of water contamination, causing massive environmental and economic damage. They disrupt the biological framework of the seas and other bodies of water, causing significant losses in aquatic biodiversity. Effective spill clean-up is critical for the protection of the maritime environment (Singh *et al.*, 2020). In the 1960s, oil spills in the ocean became a significant environmental issue, mostly because of increased petroleum exploration and production on continental shelves and the usage of supertankers capable of delivering more than 500,000 metric tons of oil (Britannica, 2017). Most oil spills that occur in rivers, bays, and the ocean are brought on by mishaps involving tankers, barges, pipelines, refineries, drilling rigs, and storage facilities, but they can also result from recreational boats and marinas (NOAA, 2016).

The impacts of oil pollution on wildlife are the most observable and intensively scrutinized, particularly during acute oil spills (Piatt *et al.*, 1990; Furness & Camphuysen, 1997; Henkel & Ziccardi, 2018). Oil spills have the greatest conspicuous effects on larger species of wildlife, such as marine animals and seabirds (Ober, 2019). Direct and indirect effects of oil on wildlife include harm via physical contact, ingestion, inhalation, and absorption. All kinds of oil, including light (such as petrol and diesel), medium, and heavy (such as crude and bunker), interfere with the ability of animal fur and feathers to repel water. When birds and mammals come into contact with oil, they lose their ability to fly, dive, swim, float, and thermoregulate (manage their own body temperature), which can result in hypothermia, drowning, and death (Burger & Fry, 1993; Heubeck *et al.*, 2003; Helm *et al.*, 2015). Similarly, when animals with feathers and fur preen, or groom, they consume and inhale the oil on their bodies, which can cause internal pollution and disruption to their hormonal and endocrine systems (Altamirano 1983; Eppley & Rubega, 1990; Mearns *et al.*, 1999).

Thus an animal can be harmed by oil exposure in several different ways. Aside from toxicity, oil lowers heat insulation and water proofing capabilities in mammals, allowing water to penetrate (Davies *et al.*, 1998; Massey, 2006). As a result, contaminants on feathers and fur must be removed as part of the rescue and rehabilitation process. Warm water and detergent are traditionally used to clean oiled wildlife (Hill 1999; USFWS 2002; OWCN 2003; IPIECA

2004, Parsons & Underhill 2005; Gregory 2006; Davis *et al.*, 2011). Pre-treatment agents are sometimes required (Jessup *et al.*, 2012). Although these strategies have advanced significantly and achieved notable outcomes (Newman *et al.*, 2003; Parsons and Underhill 2005; Massey, 2006), they are time-consuming and labor intensive. The practicalities for rescuing oiled land mammals utilizing the surfactant and warm water method are particularly difficult in remote locations such as Australia's deserts, Alaska's wilderness, or Antarctica. Therefore, it is critically necessary to develop new, portable technologies for removing the more toxic and corrosive contaminants from wildlife. In this regard, a novel method based on oil-ab(d)sorbing magnetic particle technology has been devised by researchers at Victoria University that is efficient and effective at removing fresh, tarry, and weathered oil from feathers and plumage (Orbell *et al.*, 1999; Orbell *et al.*, 2004; 2005; Dao *et al.*, 2006).

Magnetic cleansing lends itself to conducting highly reproducible, quantitative, oil removal experiments from almost any substrate (Dao, 2007). Thus, it is an ideal method for assaying relative oil removal efficacies for a wide variety of oils and substrates (e.g., rock, fur, plumage). It may also be applied to assaying the relative effectiveness of pre-treatment agents and for differentiating between initial and overall removal efficacies (Orbell *et al.*, 2006; 2007; Dao, 2006; Munaweera *et al.*, 2012; 2015). The ideal substrate to conduct such quantitative assays is obviously the live animal itself. However, this is not practical and, in the past, the most common model substrate has been either a single feather or feather clusters (Orbell *et al.*, 1999; 2004; 2005; 2007; Dao *et al.*, 2006; 2007). Unfortunately, feathers and feather clusters are not an ideal model for real plumage as the oil removal tends to be overestimated. Consequently, oil removal experiments have previously been carried out on animal carcasses (Orbell *et al.*, 2007), specifically Little Penguin carcasses obtained from The PINP (victims of fox predation or road kill). However, such experiments are difficult to carry out in the laboratory, since the carcasses are a limited resource that need to be stored, thawed, and plugged for leaks of bodily fluids. In addition, given the very low oil to substrate mass ratio, the quantitative oil removal experiments are subject to inherently high experimental errors. This chapter investigates the feasibility of using a compromise substrate for assay experiments of this kind, namely pelt. In this case, the pelt of the Little Penguin has been supplied by the PINP and oil removal assays have been conducted by an established methodology and the results have been compared to oil removal from feather clusters and

carcasses. Since pelt is also a limited resource attention has been given to the recycling of this substrate.

The replicate assays were conducted by standard gravimetric techniques that originated and were developed by our research group (Orbell *et al.*, 1997; 2007; Ngeh, 2002; Dao *et al.*, 2006; 2007). Thus, so-called isotherms are constructed from quantitative removal data and are subsequently analyzed, either directly or by a computer modelling technique, also developed by our group (see Chapter 5). Before the methodologies for characterizing the removal of oil from various substrates (including pelt) are described in detail, the following representative isotherms are presented that illustrate the characteristic mathematical form of the removal isotherms, as well as illustrating the high reproducibility that is possible for such experiments.

4.1.1 Oil removal from a glass substrate

Figure 4.1 depicts a typical isotherm for the removal of a contaminant from a glass substrate (glass petri dish surface). In **Figure 4.1**, P (%) represents the percentage of contaminants picked up by weight, and R represents the particle-to-contaminant ratio by weight⁶. Standard errors (SE) or 95% confidence intervals (error bars) are used in all studies whenever possible. The contaminant pick-up ultimately reaches a plateau that is described by the parameters P_o (%) and R_o , as shown in **Figure 4.1**. These values are characteristic of a particular oil and substrate (Dao, 2007).

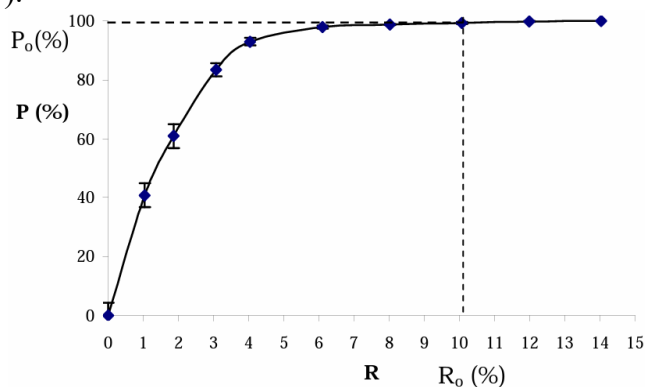


Figure 4.1: Isotherm for oil removal from a glass substrate. The contaminant is Arab medium oil, and the ideal grade of iron powder used for such experiments is Höganäs MH300.29. The 95% confidence intervals are shown by error bars, for five replicates.

⁶ This represents a variation on the common method, where the horizontal axis is the particle-to-contaminant ratio, R , rather than the number of treatments, N .

4.1.2 Oil removal from feather clusters

Figure 4.2 shows an illustration of a representative isotherm for the removal of contaminants from a cluster of feathers. The value F (%) represents the percentage removal of contaminants by weight, and N represents the number of treatments. Error bars represent 95% confidence intervals for five replicates. Typically, the contaminant pick-up approaches a plateau after a given number of treatments. As with pick-up from a glass surface, reproducibility increases as optimum pick-up is reached (Dao, 2007). Note that the final removal approaches 100%.

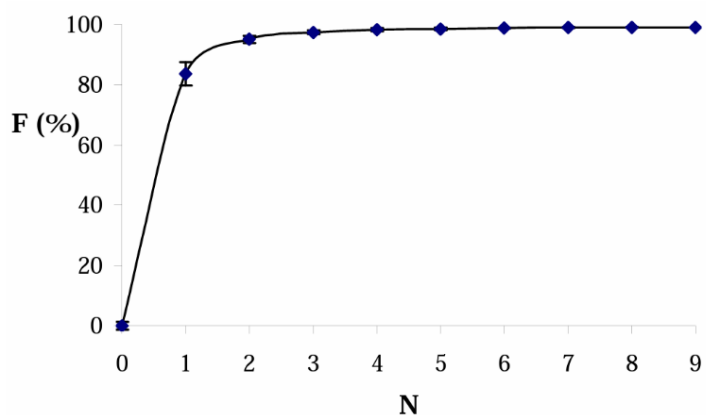


Figure 4.2: Typical adsorption isotherm for oil removal from a cluster of feathers. The contaminant is Arab medium oil. The confidence intervals are 95% for five replicates.

4.1.3 Oil removal from plumage (carcass)

Figure 4.3 shows a typical isotherm for the removal of contaminants from Little Penguin carcass, i.e., a whole bird model. The parameter C (%) represents the percentage removal of contaminants that are picked up (by weight), and N represents the number of treatments. It is clear that the removal of contaminants from plumage reaches its maximum more gradually than when contaminants are removed from a glass surface or from feathers, although a plateau is reached after about the same number of treatments. Again, as the optimal pick-up is approached, reproducibility increases (Dao, 2007).

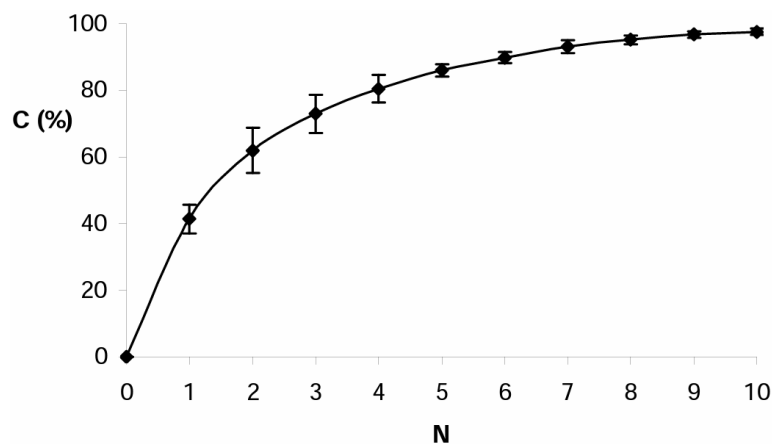


Figure 4.3: The sorption isotherm for oil pick-up from plumage. The contaminant used is Gippsland crude oil, and the iron powder is grade MH300.29. The confidence intervals are 95% for five replicates.

4.1.4 Oil removal from pelt

Experiments on the removal of different oils from a pelt substrate have also been previously carried out in our group (Munaweera, 2015). **Figures 4.4** and **4.5** show sets of histograms⁷ and nested isotherm curves for the removal of Jasmine Crude Oil (JCO), Engine Oil (EO) and Diesel Fuel Oil (DFO) from rabbit and seal pelt, respectively. These oils were chosen to represent heavy, medium, and light oils. P% represents the percentage by weight of contaminants removed, and N represents the number of treatments. This data has been reproduced here to illustrate the sensitivity of the MPT assay for distinguishing between different oil ‘types’ and different kinds of pelt. It is anticipated that a similar sensitivity would be obtained in assays involving avian pelt, and an analogous methodology is employed in this project. Therefore, in this project, penguin pelt was used as a model substrate for the assessment of oil removal from plumage. The core of this study is trying to establish an assay that is as representative of the live animal as possible, since there are three possible substrates that are possible; namely, feathers, whole bird model – (carcass) and pelt (in between feathers and carcass). However, both pelt and carcass may be taken as being more representative of actual plumage. Pelt was selected as being a more satisfactory substrate than feathers or carcass for the following reasons.

⁷Sometimes the removal isotherms are represented by histograms, especially for the comparison of relative error bars.

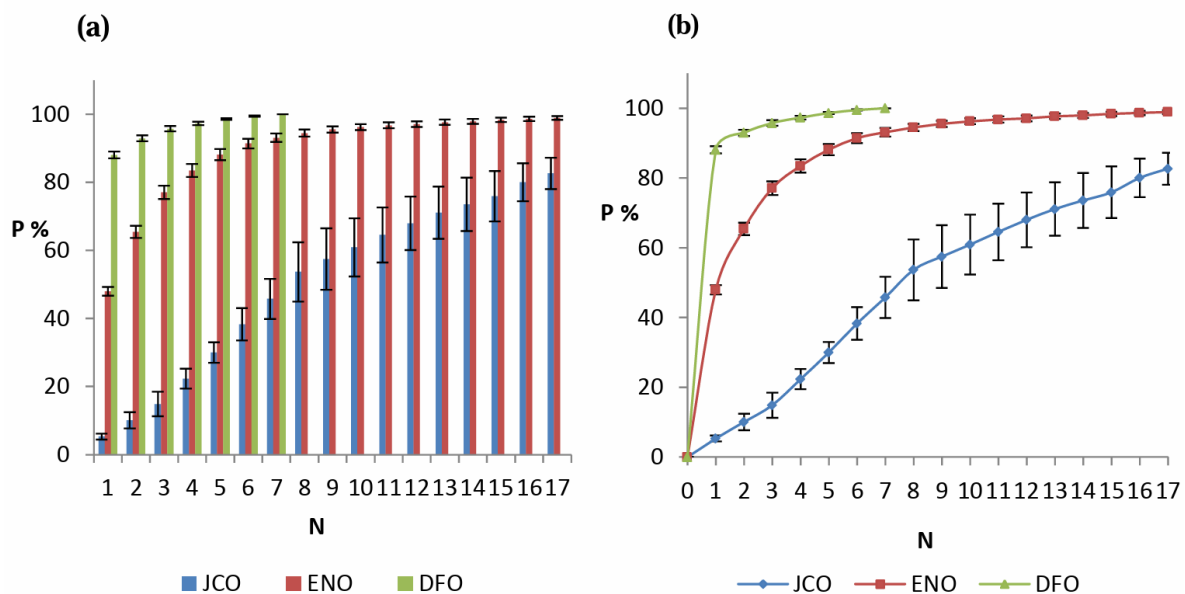


Figure 4.4: (a) Histogram representation (b) Curve representation comparing the removal percentages (P%) of three different contaminants (Jasmine Crude Oil, Engine Oil and Diesel Fuel Oil) from rabbit fur (RF) as a function of the number of treatments (N). The SE for five replicates is shown by error bars (Munaweera, 2015).

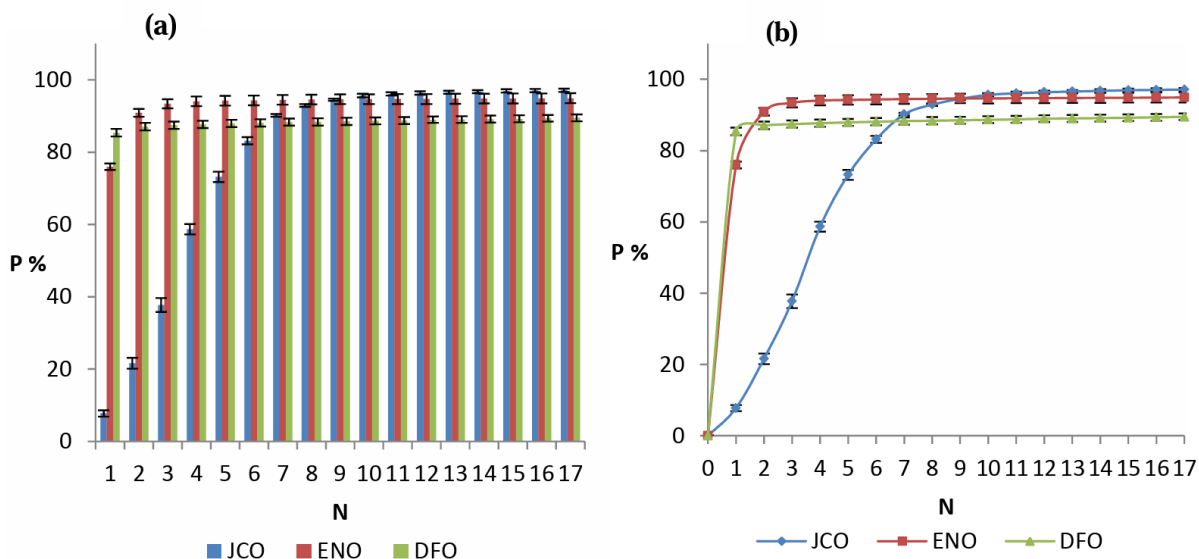


Figure 4.5: (a) Histogram representation (b) Curve representation comparing the removal percentages (P%) of three different contaminants (Jasmine Crude Oil, Engine Oil and Diesel Fuel Oil) from seal fur (SF) as a function of the number of treatments (N). The SE for five replicates is shown by error bars (Munaweera, 2015).

Feathers are only an approximation of the carcass (plumage) and a carcass is not a live animal. Carcasses are problematic for an experimental point of view. When using the carcasses to test for oil removal efficiency they must be thawed out (from refrigerated storage), dried, drained, and the orifices must be covered to prevent leakage of bodily fluids - since accurate gravimetric experiments are to be carried out. Such experiments are very labour intensive and are very difficult experiments to carry out in the laboratory. Also, a very small oil-to-substrate ratio increases the errors when conducting gravimetric experiments. In contrast, feather clusters as a substrate are simple to use and provide highly reproducible removal results, although this substrate is only an approximation of a bird's plumage. Given the problems with using carcasses, it was assessed that the best substrate to use is "in-between" feathers and plumage, namely the pelt of the Little Penguin. Therefore, penguin pelt (obtained from PINP) was used to conduct a series of experiments. Indeed, it has been subsequently found that pelt is a superior substrate to conduct such assays, *vide infra*.

The existing methodology described above for generating oil removal isotherms for the removal of different oil types from Little Penguin pelt has been implemented in this chapter. A series of experiments have been carried out whereby the removal isotherms from feather clusters, whole bird models (carcass) and different pelt sample sizes have been determined and directly compared for different oil types. The oils used are the light oils (Gippsland Crude and Diesel), the medium oil (Engine oil) and the heavy oil (Bunker Oil). Experiments have also been carried out to test the feasibility of recycling the pelt since, like carcasses, it is also a limited resource. All experiments have been performed in five-fold replicate and the data represent with 95% confidence intervals.

Note: *An important consideration in the application of MPT to oil removal "assays" is the extent to which the oil the removal efficacy, as determined by MPT, carries over with fidelity to the detergent-based removal efficacy. Previous work by this group (Kasup et al., 2015) has addressed this problem and has shown that there is an excellent correspondence between MPT and detergent based efficacies ($r^2 > 90\%$ correlation).*

4.2 Methodology for the removal of different oil types

In this research existing gravimetric methods devised by Orbell *et al.* (1997; 1999), were employed to determine the isotherms for the removal of contaminants from various substrates including feather clusters, pelt, and whole bird models (carcass). These methods are described below:

4.2.1 Removal from feather clusters

A cluster of feathers (usually 4) were tied and weighed (f_1). The feathers were then dipped into a beaker (100 mL) of contaminant to allow saturation. The feathers were then allowed to drain on a tared petri dish for approximately 10 minutes until being re-weighed (f_2). The feathers are then removed from the petri dish and residual quantity, r , recorded. The weight of contaminant-laden feathers, f_3 , is given by:

$$f_3 = f_2 - r$$

Contaminated feathers were then covered with the oil ad(b)sorbing magnetic particles. A previous study (Godinho, 1993) has noted that the ad(b)sorption process is effectively instantaneous. Using a magnetic tester, the contaminant-laden particles are harvested from the feathers. The feather cluster was then reweighed (f_4). The percentage of oil removal (F%) was calculated as follows:

$$F (\%) = [(f_3 - f_4)/(f_3 - f_1)] \times 100\%$$

The above removal procedure was repeated until a maximum oil pick-up was achieved. A graph of percentage pick-up (F%) versus number of treatments (N) was then plotted. This plot is referred to as an “isotherm”.

4.2.2 Removal from pelt

A piece of pelt was placed onto a tared petri dish and weighed (w_1). An approximate amount of oil was applied on top of the pelt and left for approximately 5 minutes. The pelt was then re-weighed (w_2). The amount of oil (w_3) was calculated as ($w_2 - w_1$).

Immediately, iron powder was applied, and the oil contaminated pelt was re-weighed (w_4). The mass of iron powder (w_5) was calculated as ($w_4 - w_2$).

The iron powder was left in the oil for approximately 2 minutes and then magnetically harvested using a magnetic tester. The mass of the treated pelt was determined (w_6). The percentage of oil removal (P%) was calculated as follows:

$$P\% = (w_2 - w_6) / (w_2 - w_1) \times 100$$

The above removal procedure was repeated until maximum oil pick-up was achieved. A graph of percentage pick-up (P%) versus number of treatments (N) was then plotted.

4.2.3 Removal from whole bird model (carcass)

The gravimetric determination method for removal of contaminants from a whole bird model (carcass) has previously been developed by (Ngeh, 2002). This method is described below:

Using a top pan balance, a whole bird (carcass) was weighed (p_1). Onto the plumage (breast feathers) an amount of contaminant was carefully poured, and the carcass was then carefully re-weighed (p_2). On top of the feathers and carcass, iron powder was applied and left for approximately 1.5 minutes to allow absorption and adsorption of oil contaminants to occur (Tan, 1998). Using a magnetic tester, the contaminants and iron powder was removed, and the carcass was weighed (p_3). The percentage of oil removal C (%) from carcass is determined as follow:

$$C (\%) = [(p_2 - p_3) / (p_2 - p_1)] \times 100\%$$

It usually takes 35-40 minutes to meticulously perform 10 magnetic cleansing treatments on an oiled bird carcass (Dao, 2007). Additionally, it is noteworthy that solvent extraction can be used to recycle oil-laden iron powder (Ngeh, 2002).

4.3 Materials and equipment

4.3.1 Materials

Iron powder (Höganäs Pty. Ltd), grade MH300.29, spongy annealed superfine powder, was used in all experiments. Four different types of oil have been used, see **Table 4.1**.

Table 4.1: Oil contaminants utilised in the experiment⁸.

Light Oils	Heavy Oils
Gippsland Crude Oil (GCO)	Engine Oil (EO)
Diesel Oil (DO)	Bunker Oil 1 (BO1)

Breast and back pelt of the Little Penguin (*Eudyptula minor*) was supplied by the Phillip Island Nature Parks, **Figure 4.6**.



Figure 4.6: Breast pelt and back pelt from Little Penguin (*Eudyptula minor*).

⁸ Diesel and Engine Oils may also be considered “medium viscosity”.

4.3.2 Equipment

The equipment that is required for this research includes a magnetic tester (Alpha Magnetics, Victoria, Australia). This magnetic device is designed so magnetic fields can be mechanically switched off and on by moving the plunger up and down.



Figure 4.7: Magnetic Tester employed for performing MPT oil removal experiments.

The testing procedure is described in the methodology, Section 4.2.

4.4 Results and Discussion

4.4.1 The importance of pelt sample size in relation to oil type

4.4.1.1 Removal of Gippsland Crude Oil

For the Little Penguin, **Table 4.2** and **Figures 4.8 & 4.9**, compare data for the removal of Gippsland Crude Oil from feather clusters, pelt (of two different sample sizes) and carcass (plumage)⁹. The pelt sample sizes tested were large (17 cm long × 10 cm wide) and small (5 cm long × 5 cm wide).

⁹ The data for removal from the carcass of Little Penguin was drawn from the work of Dao *et al.*, 2007.

Table 4.2: Comparison of the removal of Gippsland Crude Oil between plumage, pelt (large and small size) and feather cluster.

N	Plumage		Pelt (large size)		Pelt (small size)		Feather cluster	
	P%	95%	P%	95%	P%	95%	F%	95%
1	41.37	4.34	67.90	4.12	85.51	1.49	98.12	0.16
2	61.96	6.74	73.12	3.31	87.62	0.69	98.54	0.10
A 3	72.94	5.72	78.04	2.53	89.38	0.98	98.84	0.18
4	80.50	4.20	82.34	3.09	90.34	1.09	99.03	0.12
5	86.01	1.91	87.27	2.88	91.75	0.97	99.11	0.20
6	89.84	1.69	91.65	2.36	92.88	1.22	99.12	0.12
7	93.11	2.01	94.05	1.82	94.54	0.79	99.16	0.11
8	95.18	1.33	95.44	1.55	95.27	2.31		
9	96.76	0.96	96.68	2.09	95.30	2.31		
10	97.60	0.97	97.27	2.18				

From this data it can be seen that, for this oil, the removal profile from a feather cluster substrate is significantly higher than for the carcass (whole bird) substrate. This is not unexpected and demonstrates how removal from a feather cluster substrate gives exaggerated results. However, when pelt is used, the removal profile becomes more aligned to that of the carcass. Furthermore, this alignment is dependent on the pelt sample size – a larger size being preferred. This is because this oil is of a low viscosity and readily spreads over the side of the patch. Notably, this effect is not encountered with higher viscosity contaminants, as will be seen later in this chapter. Therefore, to assay more volatile oils with respect to pelt, a judicious choice of pelt sample size is recommended depending on the viscosity of the contaminant.

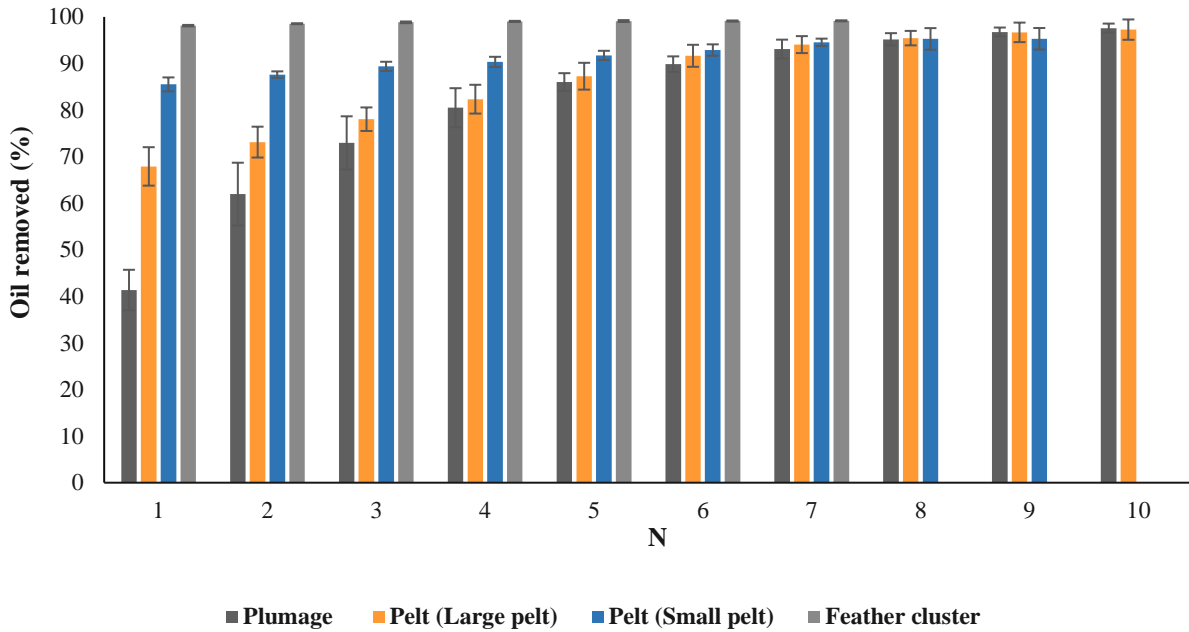


Figure 4.8: Comparison between penguin carcass (plumage), large penguin pelt size, small penguin pelt size and a penguin feather cluster for the removal of Gippsland Crude Oil as a function of the number of treatments, N. Error bars represent the 95% confidence intervals for five replicates.

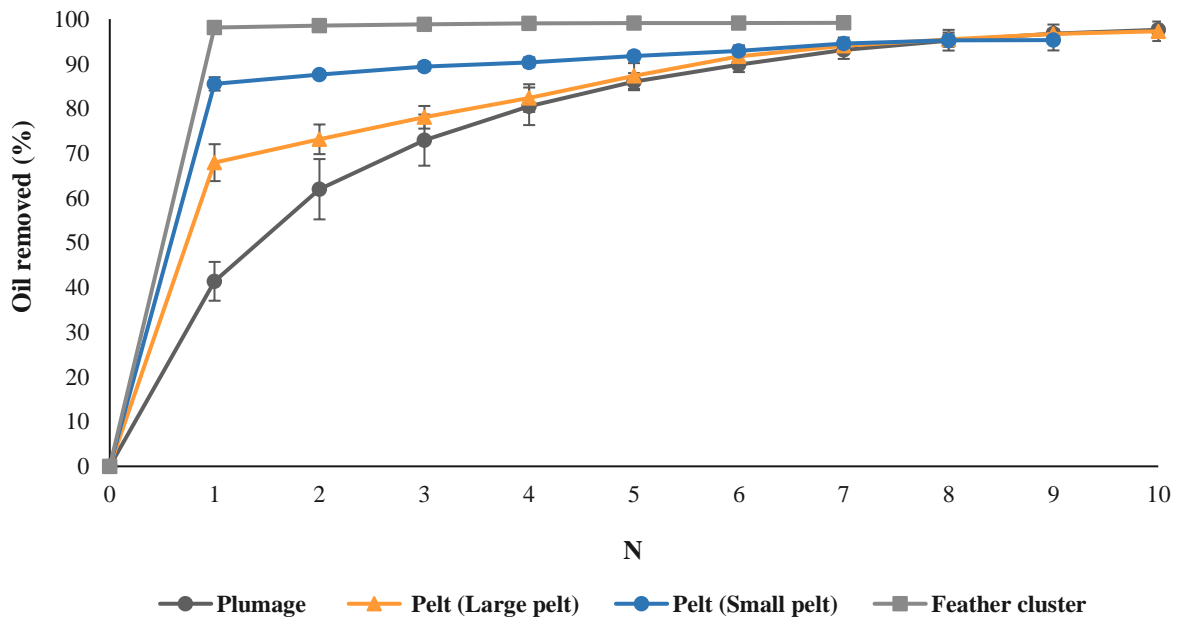


Figure 4.9: Comparison between penguin carcass (plumage), large penguin pelt size, small penguin pelt size and a penguin feather cluster for the removal of Gippsland Crude Oil as a function of the number of treatments, N. Error bars represent the 95% confidence intervals for five replicates. These error bars are too small to be seen on the graph. These are behind the dots. However, they can be seen in the corresponding histogram plot.

4.4.1.2 Removal of Diesel Oil

Table 4.3 and **Figures 4.10 & 4.11**, compare data for the removal of Diesel Oil from pelt (of two different sample sizes) and carcass (plumage)¹⁰. The pelt sample sizes tested were large (17 cm long × 10 cm wide) and small (5 cm long × 5 cm wide).

Table 4.3: Comparison of the removal of Diesel Oil between plumage and pelt (large and small size).

N	Plumage		Pelt (large size)		Pelt (small size)	
	P%	95%	P%	95%	P%	95%
1	27.19	10.65	23.23	2.17	78.59	5.56
2	45.93	17.65	36.54	2.18	81.22	3.46
3	60.35	14.24	53.27	3.16	83.32	3.65
4	70.23	10.76	64.17	4.68	84.59	3.43
5	77.26	7.52	73.81	3.26	86.47	3.95
6	82.95	5.05	80.68	2.44	88.47	4.50
7	87.21	5.69	85.15	2.61	90.11	4.33
8	90.76	3.68	89.39	1.83	92.16	2.89
9	93.11	2.36	90.75	1.35	93.35	3.21
10			91.55	1.19	93.75	3.25

These results further illustrate the importance of a judicious choice of pelt sample size depending on the viscosity of the contaminant. Indeed, for the larger size pelt sample, the removal profile for the pelt and the carcass are essentially the same, within experimental error. This supports our contention that both the pelt and the carcass may be described as “plumage”.

¹⁰ The data for removal of all oils from the carcass of Little Penguin was drawn from the work of Dao *et al.*, 2007.

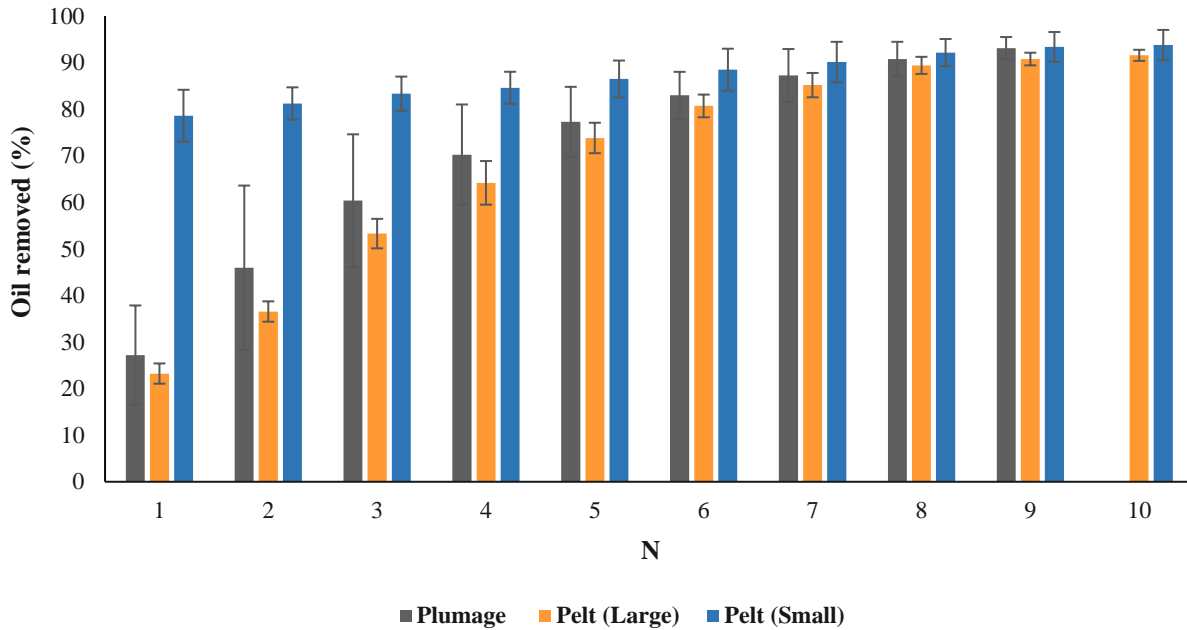


Figure 4.10: Comparison between penguin carcass (plumage), large penguin pelt size and small penguin pelt size for the removal of Diesel Oil as a function of the number of treatments, N. Error bars represent the 95% confidence intervals for five replicates.

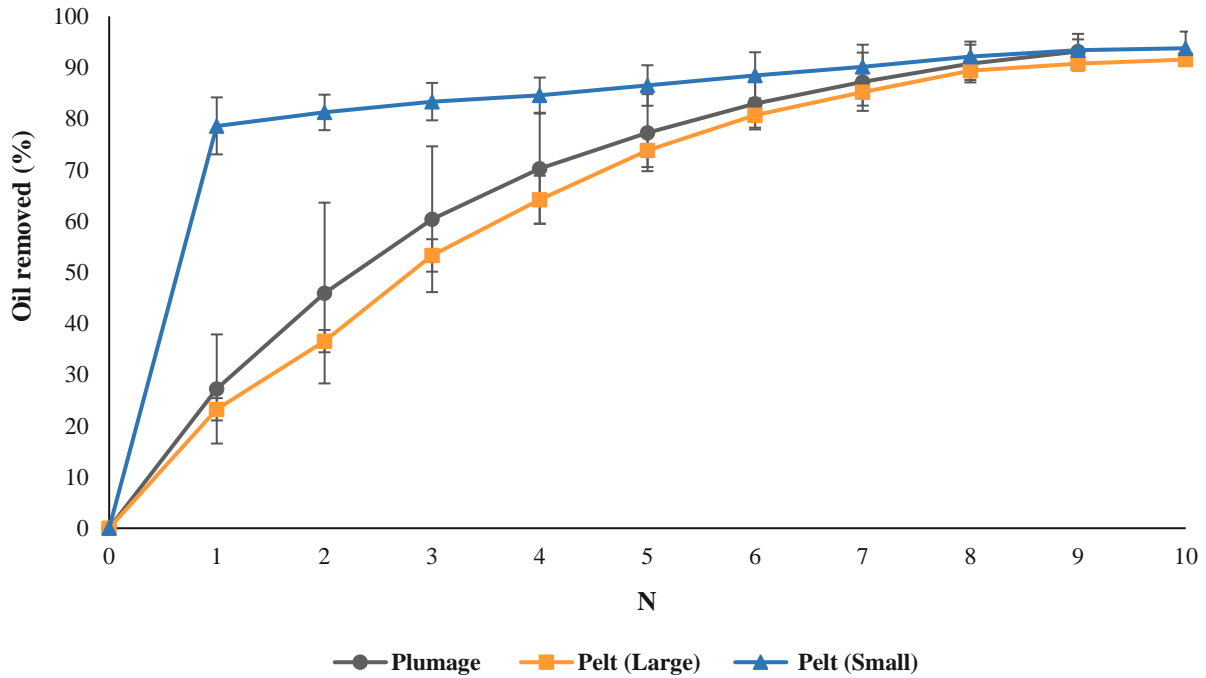


Figure 4.11: Comparison between penguin carcass (plumage), large penguin pelt size and small penguin pelt size for the removal of Diesel Oil as a function of the number of treatments, N. Error bars represent the 95% confidence intervals for five replicates. These error bars are too small to be seen on the graph. These are behind the dots. However, they can be seen in the corresponding histogram plot.

4.4.1.3 Removal of Engine Oil

Table 4.4 and **Figures 4.12 & 4.13**, compare data for the removal of Engine Oil from pelt (of two different sample sizes) and carcass (plumage)¹¹. The pelt sample sizes tested were large (17 cm long × 10 cm wide) and small (5 cm long × 5 cm wide).

Table 4.4: Comparison of the removal of Engine Oil between plumage, pelt (large and small size) and feather cluster.

N	Plumage		Pelt (large size)		Pelt (small size)		Feather cluster	
	P%	95%	P%	95%	P%	95%	F%	95%
1	38.23	4.80	40.23	2.20	48.34	1.63	96.65	2.14
2	53.97	11.64	54.27	4.86	61.33	2.79	99.18	0.67
3	66.23	8.11	67.00	5.39	72.32	3.34	99.43	0.43
4	75.23	5.52	78.50	3.51	80.81	3.94	99.53	0.35
5	81.44	5.02	85.87	3.73	86.01	3.33	99.63	0.27
6	86.58	4.91	89.23	4.15	89.98	2.27	99.71	0.21
7	90.88	3.65	91.31	3.30	92.92	1.69	99.74	0.21
8	93.74	2.40	93.99	1.33	94.81	1.70		
9	95.89	1.30	95.48	0.79	96.17	2.24		
10	96.98	1.45	95.94	1.16	97.47	2.27		
10	96.98	1.45	95.94	1.16	97.47	2.27		

4.4.1.4 Removal of Bunker Oil 1

Table 4.5 and **Figures 4.14 & 4.15**, compare data for the removal of Bunker Oil 1 from pelt (of two different sample sizes) and carcass (plumage)¹². The pelt sample sizes tested were large (17 cm long × 10 cm wide) and small (5 cm long × 5 cm wide).

¹¹ The data for removal of all oils from the carcass of Little Penguin was drawn from the work of Dao *et al.*, 2007.

¹² The data for removal of all oils from the carcass of Little Penguin was drawn from the work of Dao *et al.*, 2007.

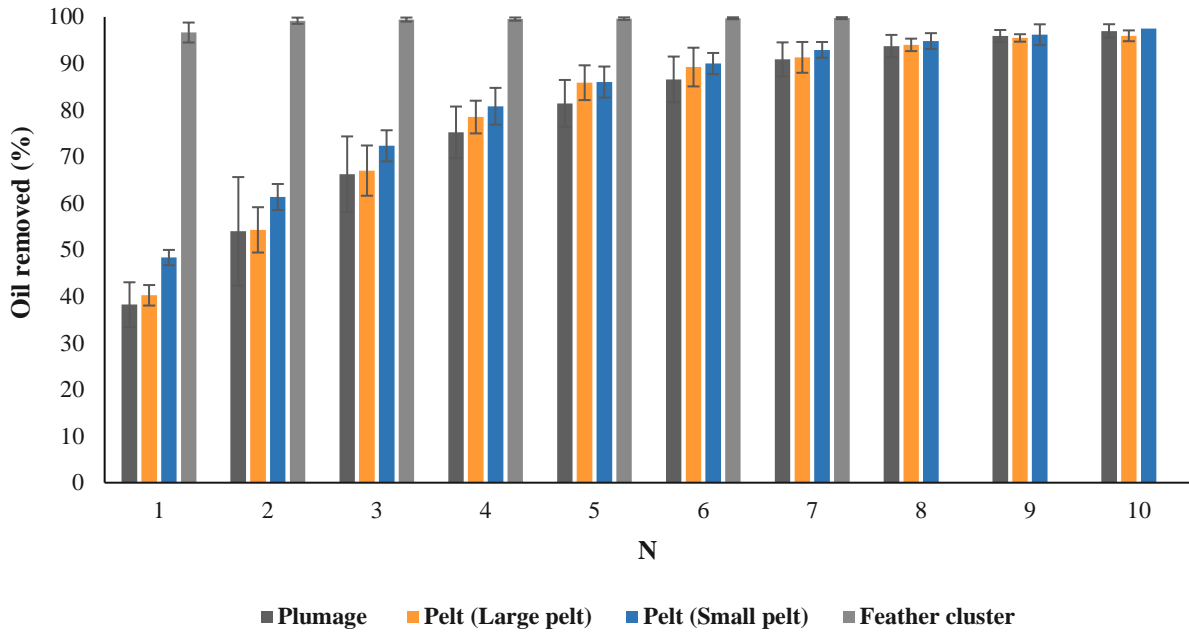


Figure 4.12: Comparison between penguin carcass (plumage), large penguin pelt size, small penguin pelt size and a penguin feather cluster for the removal of Engine oil as a function of the number of treatments, N. Error bars represent the 95% confidence intervals for five replicates.

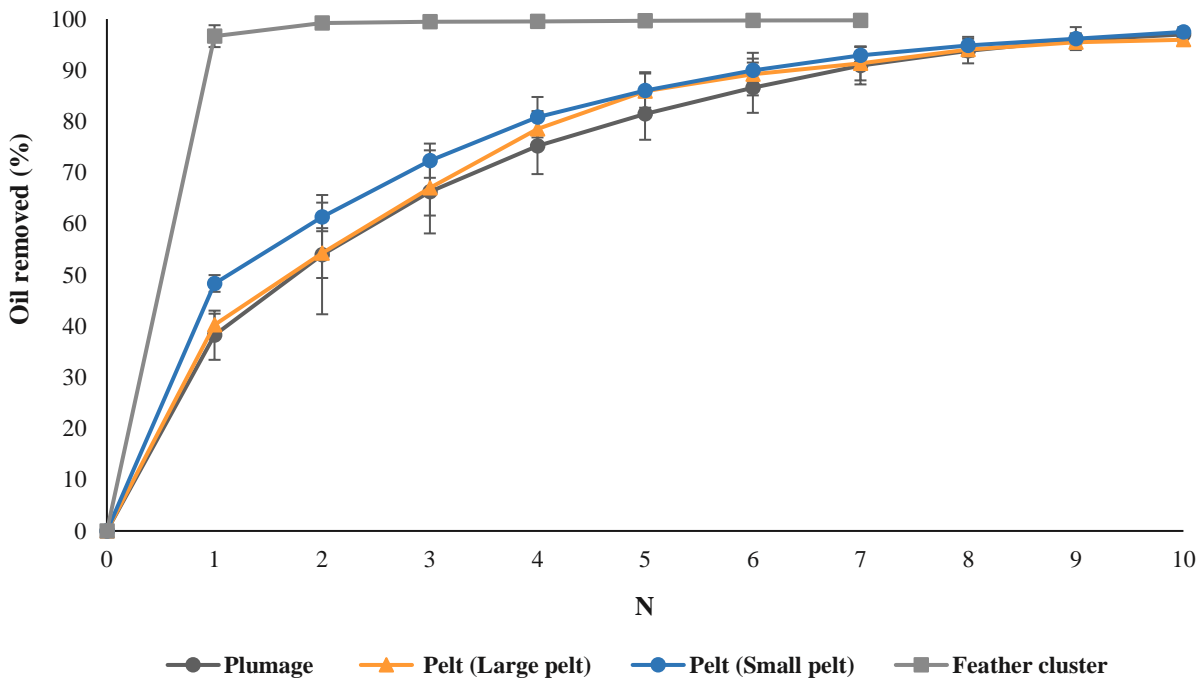


Figure 4.13: Comparison between penguin carcass (plumage), large penguin pelt size, small penguin pelt size and a penguin feather cluster for the removal of Engine Oil as a function of the number of treatments, N. Error bars represent the 95% confidence intervals for five replicates. These error bars are too small to be seen on the graph. However, they can be seen in the corresponding histogram plot.

Table 4.5: Comparison of the removal of Bunker Oil 1 (BO1) between plumage, pelt (large and small size) and feather cluster.

N	Plumage		Pelt (large size)		Pelt (small size)		Feather cluster	
	P%	95%	P%	95%	P%	95%	F%	95%
1	35.07	5.46	38.38	6.04	45.44	3.09	82.23	5.38
2	51.80	7.67	52.62	7.71	56.35	1.85	94.26	1.78
3	66.99	3.40	69.33	3.36	66.73	3.40	97.01	1.88
4	75.03	2.83	77.10	3.12	75.80	2.18	98.25	1.39
5	84.30	2.94	85.61	3.76	84.37	3.45	98.91	0.63
6	88.66	2.88	88.52	2.93	89.93	1.67	99.01	0.37
7	91.16	2.66	92.85	2.22	91.79	0.98	99.26	0.40
8	93.61	2.27	94.21	1.82	93.30	1.42		
9	95.0	1.70	94.76	1.72	93.95	1.94		
10	95.98	1.79	95.15	1.67	94.28	1.98		
11					94.41	2.00		
12					94.49	1.98		

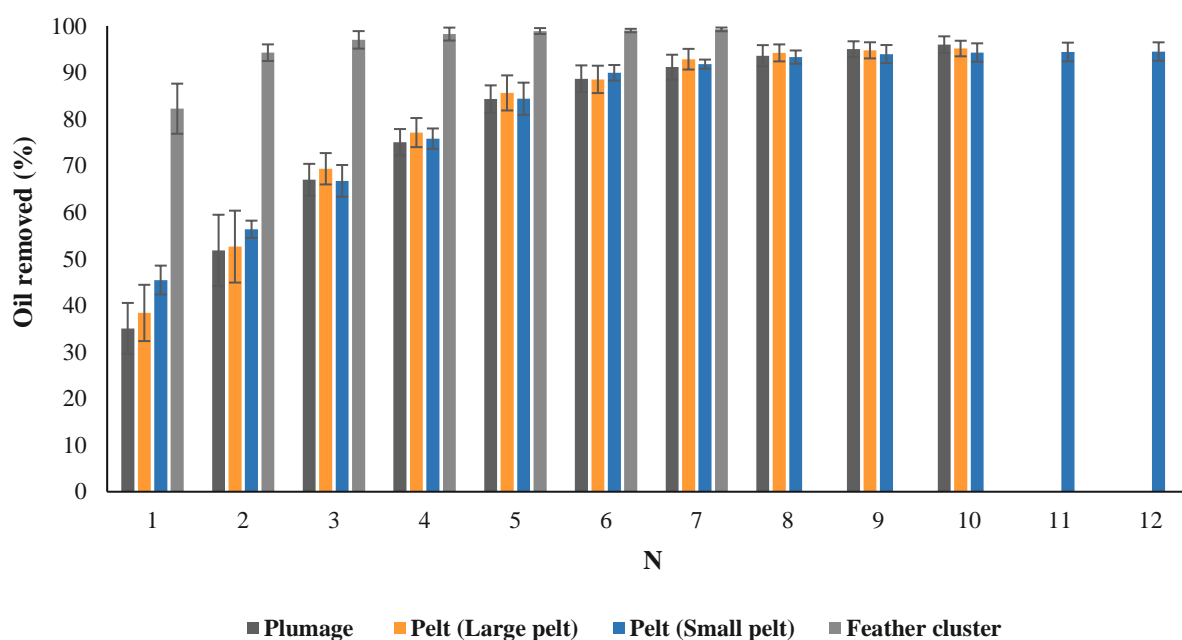


Figure 4.14: Comparison between penguin carcass (plumage), large penguin pelt size, small penguin pelt size and a penguin feather cluster for the removal of Bunker Oil 1 (BO1) as a function of the number of treatments, N. Error bars represent the 95% confidence intervals for five replicates.

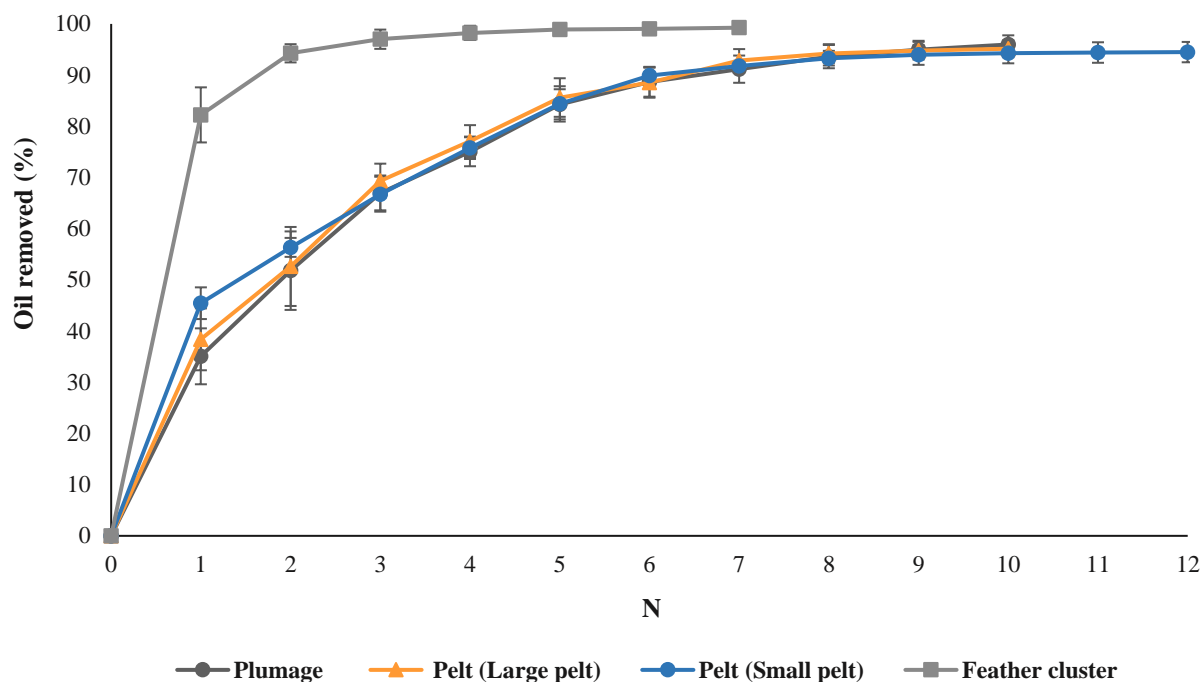


Figure 4.15: Comparison between penguin carcass (plumage), large penguin pelt size, small penguin pelt size and a penguin feather cluster for the removal of Bunker Oil 1 (BO1) as a function of the number of treatments, N. Error bars represent the 95% confidence intervals for five replicates. These error bars are too small to be seen on the graph. These are behind the dots. However, they can be seen in the corresponding histogram plot.

For this, more viscous, contaminant, the removal profile for a feather cluster remains highly exaggerated compared to pelt and plumage, whereas the profiles for both pelt sample sizes and for carcass are all effectively equivalent within experimental error.

In general, for the three oils (Gippsland Crude Oil, Engine Oil and Bunker Oil 1) investigated, a feather cluster achieved the highest initial removals compared to plumage, pelts (small and large size). These high initial removals are understandable due to feather clusters being more open and having a greater surface allowing easy accessibility. Plumage has the lowest initial oil removal as its feathers are very closely packed and more difficult to access. These studies show that pelt is the preferred substrate as it is truly representative of the whole animal. Moreover, pelt substrate is easier to handle and to conduct removal experiments in the laboratory. Also, as will be demonstrated later, pelt can be recycled for further experimentation which overcomes, to some extent, the fact that it is a limited resource.

4.4.2 Recycling of pelt samples

4.4.2.1 Experimental method

Previous research within this group has demonstrated that recycled seal pelt (fur) can be used successfully to assess oil removal, compared to the virgin pelt (Munaweera, 2015). Therefore, analogous experiments have been carried out to determine whether recycled penguin pelt mimics the virgin material, across a range of oils. Thus, used penguin pelts were washed with detergent/water and the oil removal isotherms were statistically compared to those for the virgin pelt. Four oils; namely, Gippsland Crude Oil, Diesel Fuel Oil, Engine Oil and Bunker Crude Oil, were evaluated compared to their respective removals from virgin pelt.

4.4.2.2 The recycling ('washing') process

A 'used' penguin pelt was dipped into a warm dilute detergent solution for approximately 5 minutes. This was followed by finger-rubbing the surface for 1-2 minutes and rinsing with warm de-ionised water. This process was repeated until the pelt was (subjectively) considered clean. This recycled penguin pelt was then dried gently using a blow dryer.

4.4.2.3 Removal of Gippsland Crude Oil from recycled penguin pelt

Table 4.6 show the comparison between original pelt and recycled pelt for the removal of Gippsland Crude Oil. These results are represented by histograms and curves in **Figure 4.16** & **Figure 4.17**. The results show that, within experimental error, the recycled pelt is effectively equivalent to the original pelt.

4.4.2.4 Removal of Diesel Fuel Oil from recycled penguin pelt

Table 4.7 shows the comparison between original pelt and recycled pelt for the removal of Diesel Fuel Oil. These results are represented by histograms and curves in **Figure 4.18** & **Figure 4.19**. The results show that, within experimental error, the recycled pelt is effectively equivalent to the original pelt.

Table 4.6: The removal of Gippsland Crude Oil, P (%), comparison between original pelt and recycled pelt. Recycling of the pelt experiments were conducted in five replicates.

N	Original	Five replicates (P%)					P% (mean)	95%
1	68.06	63.95	69.34	68.61	65.32	72.30	67.90	4.12
2	73.45	69.93	74.44	73.81	70.94	76.49	73.12	3.31
3	79.19	76.97	80.25	77.51	75.49	79.99	78.04	2.53
4	83.89	81.88	84.82	81.21	79.0	84.79	82.34	3.09
5	88.03	86.2	90.40	86.24	84.63	88.88	87.27	2.88
6	92.35	90.92	94.89	90.89	89.96	91.60	91.65	2.36
7	93.95	92.97	95.91	93.16	92.86	95.38	94.05	1.82
8	95.92	95.11	96.30	94.92	93.85	97.05	95.44	1.55
9	97.19	97.20	97.26	95.80	94.35	98.82	96.68	2.09
10	98.02	97.34	98.84	96.12	94.98	99.09	97.27	2.18

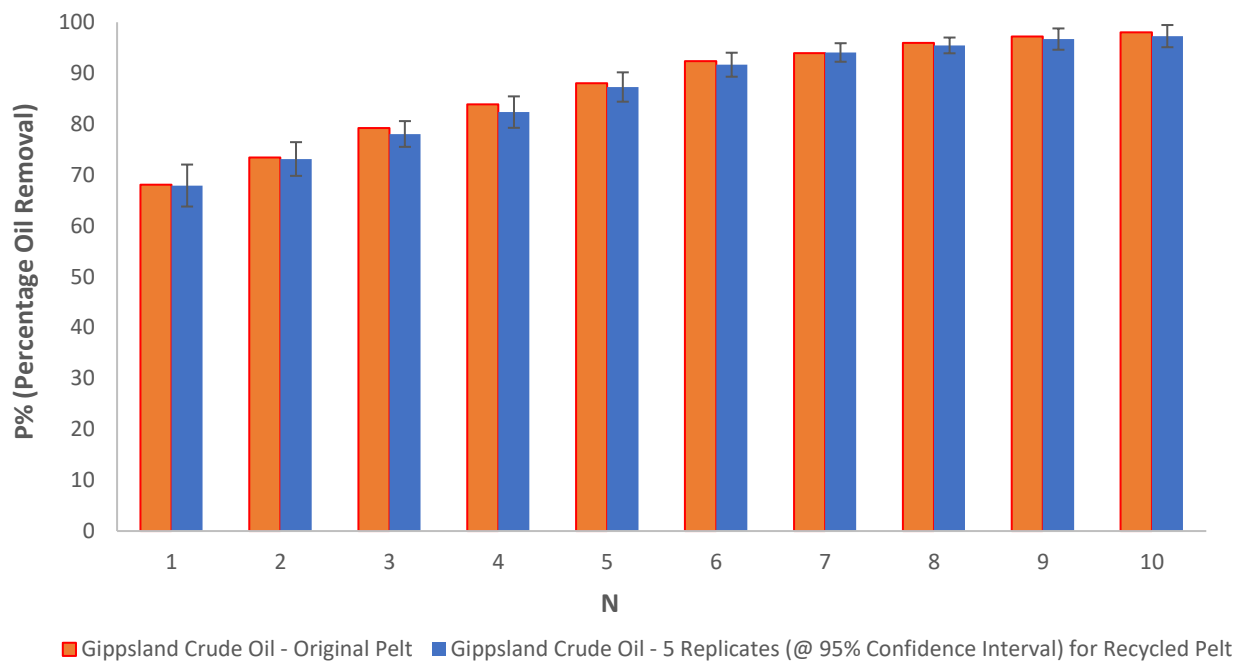


Figure 4.16: Comparison between original pelt and recycled pelt for the removal of Gippsland Crude Oil as a function of the number of treatments, N. Error bars represent the 95% confidence intervals for five replicates.

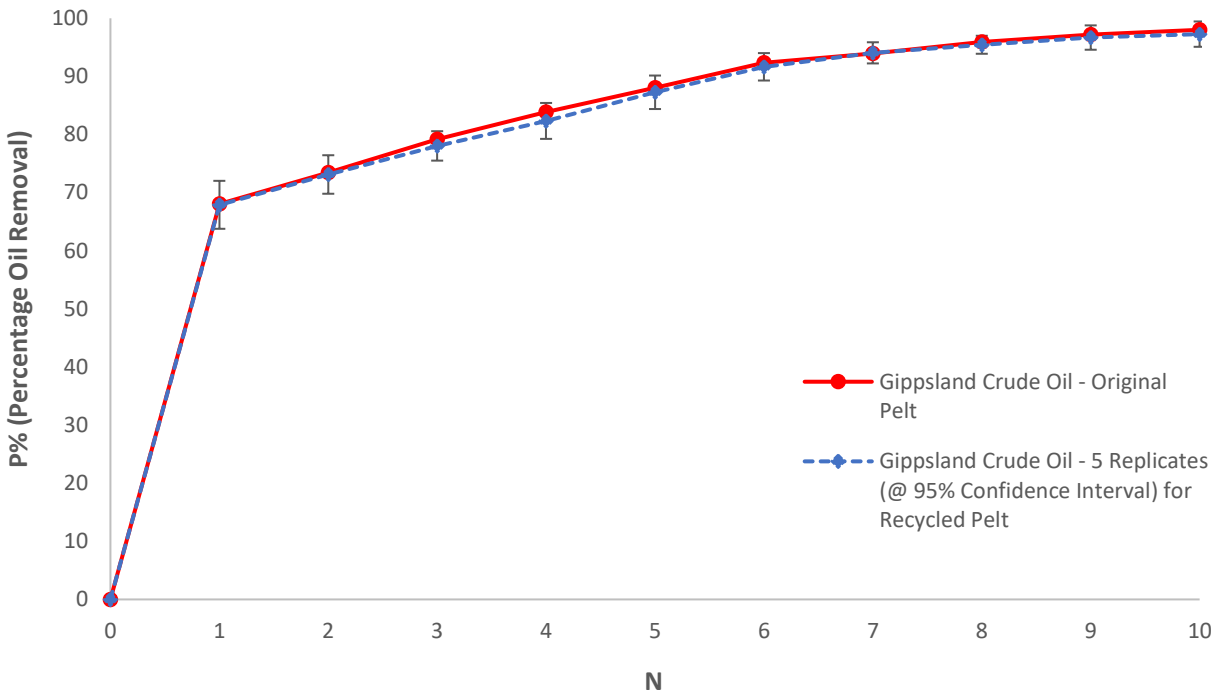


Figure 4.17: Comparison between original pelt and recycled pelt for the removal of Gippsland Crude Oil as a function of the number of treatments, N. Error bars represent the 95% confidence intervals for five replicates.

Table 4.7: The removal of Diesel Fuel Oil, P%, comparison between original pelt and recycled pelt. Recycling of the pelt experiments were conducted for five replicates.

N	Original	Five replicates (P%)					P% (mean)	95%
1	23.42	25.7	24.23	21.25	22.2	22.78	23.23	2.17
2	36.73	38.5	37.36	33.81	37.0	36.07	36.54	2.18
3	53.41	55.01	54.4	49.22	55.4	52.36	53.27	3.16
4	64.67	67.57	66.58	58.31	62.58	65.83	64.17	4.68
5	73.19	76.29	75.09	69.49	73.36	74.82	73.81	3.26
6	79.25	82.76	81.26	77.48	81.43	80.5	80.68	2.44
7	84.5	86.97	86.75	81.72	85.02	85.33	85.15	2.61
8	88.98	89.82	91.56	87.5	89.19	88.9	89.39	1.83
9	91.48	91.52	92.22	89.5	90.21	90.33	90.75	1.35
10	91.71	91.94	92.7	90.06	91.59	91.46	91.55	1.19

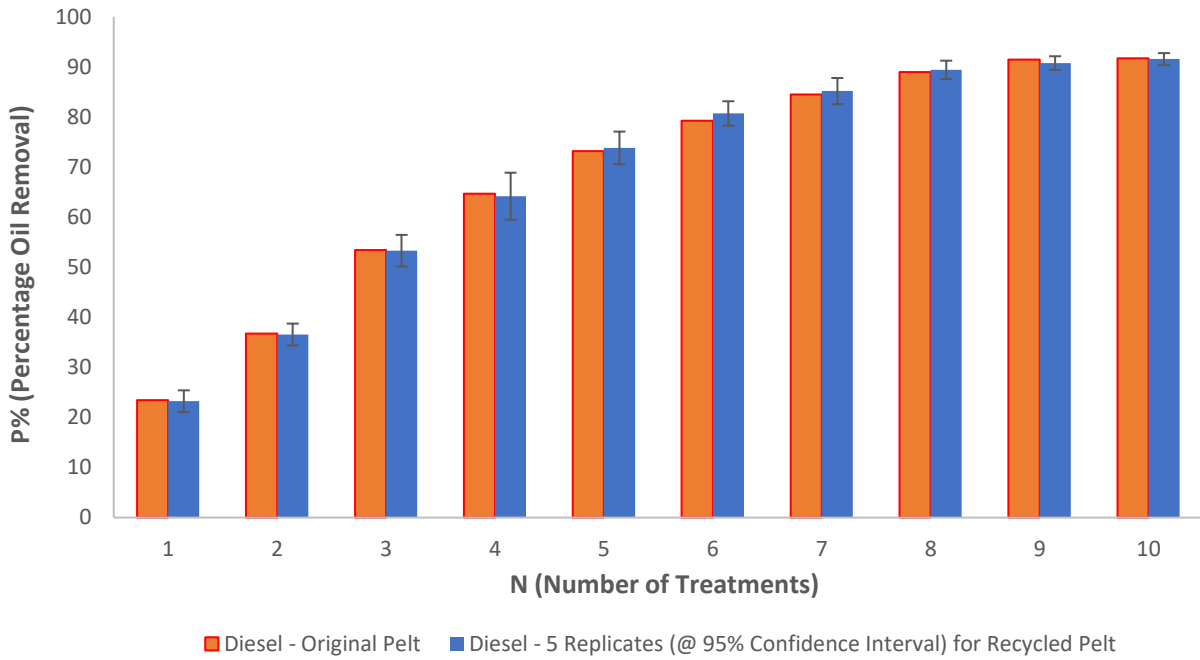


Figure 4.18: Comparison between original pelt and recycled pelt for the removal of Diesel Fuel Oil as a function of the number of treatments, N. Error bars represent the 95% confidence intervals for five replicates.

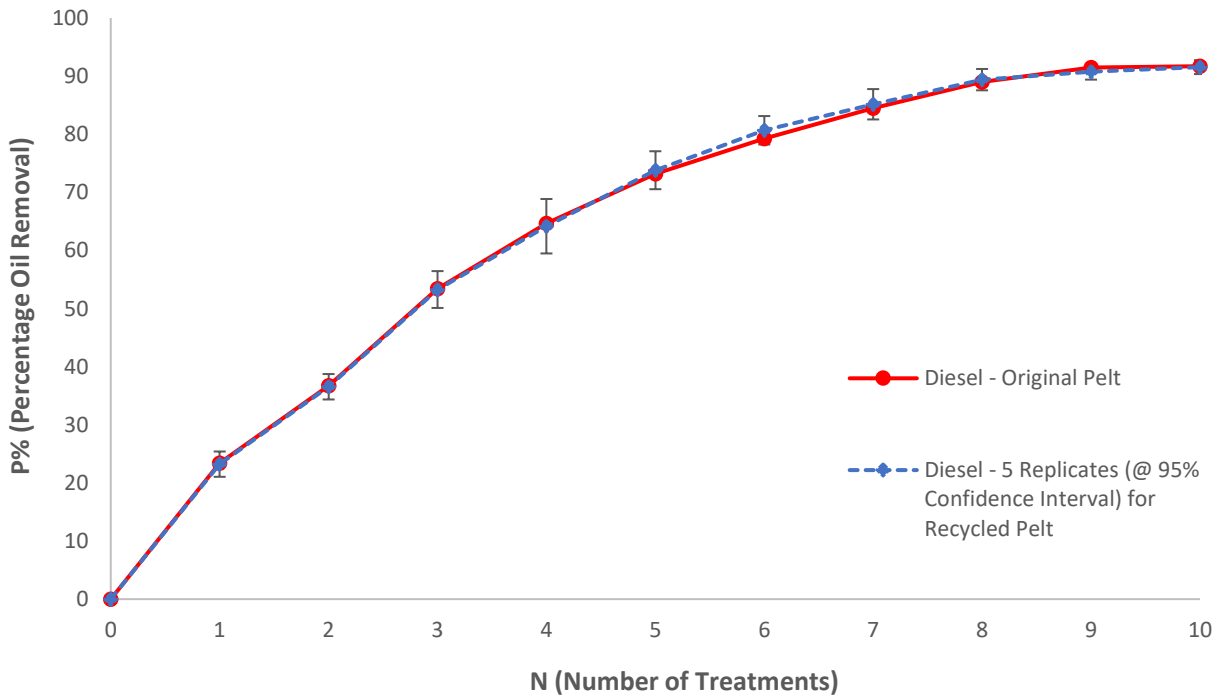


Figure 4.19: Comparison between original pelt and recycled pelt for the removal of Diesel Fuel Oil as a function of the number of treatments, N. Error bars represent the 95% confidence intervals for five replicates.

4.4.2.5 Removal of Engine Oil from recycled penguin pelt

Table 4.8 shows the comparison between original pelt and recycled pelt for the removal of Engine Oil. These results are represented by histograms and curves in **Figure 4.20 & Figure 4.21**. The results show that, within experimental error, the recycled pelt is effectively equivalent to the original pelt.

Table 4.8: The removal of Engine Oil, P (%), comparison between original pelt and recycled pelt. Recycling of the pelt experiments were conducted in five replicates.

N	Original	Five replicates (P%)					P% (mean)	95%
1	41.22	40.81	39.83	37.35	41.34	41.83	40.23	2.20
2	57.77	55.63	54.14	47.61	56.62	57.39	54.27	4.86
3	68.52	69.14	67.04	59.49	69.31	70.04	67.00	5.39
4	77.86	78.32	82.18	74.25	78.7	79.06	78.50	3.51
5	83.33	83.21	90.8	83.67	85.8	85.91	85.87	3.73
6	87.79	89.55	94.87	86.41	87.96	87.39	89.23	4.15
7	89.44	92.67	95.15	90.83	89.48	88.45	91.31	3.30
8	92.14	94.08	95.78	93.01	93.79	93.33	93.99	1.33
9	95.09	95.31	96.14	94.63	95.23	96.12	95.48	0.79
10	95.29	95.59	96.48	94.67	95.83	97.15	95.94	1.16

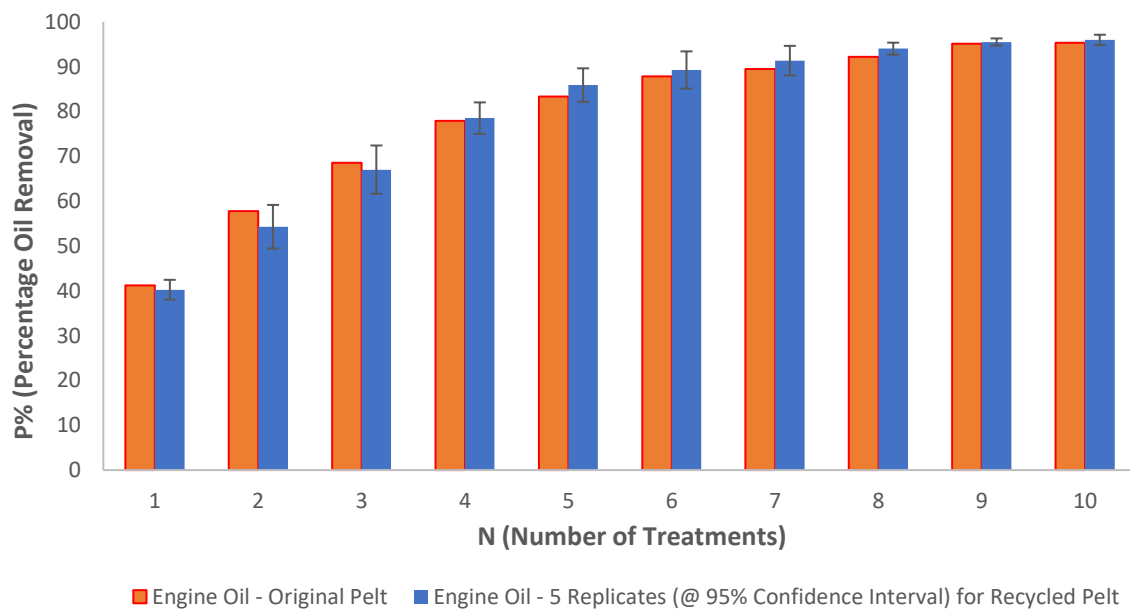


Figure 4.20: Comparison between original pelt and recycled pelt for the removal of Engine Oil as a function of the number of treatments, N. Error bars represent the 95% confidence intervals for five replicates.

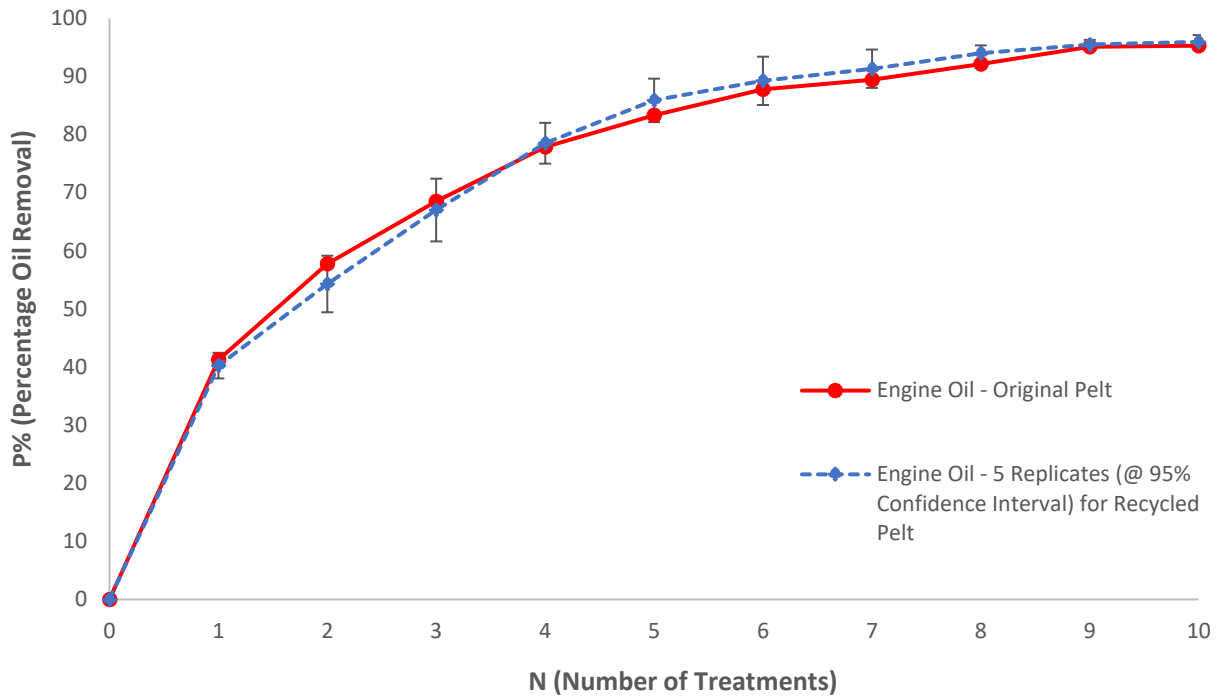


Figure 4.21: Comparison between original pelt and recycled pelt for the removal of Engine Oil as a function of the number of treatments, N. Error bars represent the 95% confidence intervals for five replicates.

4.4.2.6 Removal of Bunker Oil 1 (BO1) from recycled penguin pelt

Table 4.9 shows the comparison between original pelt and recycled pelt for the removal of Bunker Oil (BO1). These results are represented by histograms and curves in **Figure 4.22** & **Figure 4.23**. The results show that, within experimental error, the recycled pelt is effectively equivalent to the original pelt.

Table 4.9: The removal of Bunker Oil 1 (BO1), P (%), comparison between original pelt and recycled pelt. Recycling of the pelt experiments were conducted in five replicates.

N	Original	Five replicates (P%)					P% (mean)	95%
1	37.17	38.26	39.01	30.61	43.95	40.09	38.38	6.04
2	53.88	52.07	57.1	42.25	54.13	57.56	52.62	7.71
3	66.89	67.09	71.83	65.81	70.6	71.36	69.33	3.36
4	75.53	75.67	80.16	74.21	76.2	79.28	77.10	3.12
5	84.41	84.02	87.44	81.1	86.95	88.58	85.61	3.76
6	87.88	88.85	89.44	84.51	89.06	90.77	88.52	2.93
7	91.36	91.28	93.64	90.67	93.86	94.84	92.85	2.22
8	93.66	93.55	95.56	91.95	94.88	95.13	94.21	1.82
9	94.95	95.18	95.83	92.32	95.17	95.32	94.76	1.72
10	95.27	95.82	96.18	92.8	95.35	95.61	95.15	1.67

The results of the removal of Bunker Oil 1 (BO1) for original pelt and recycled pelt are shown in **Figure 4.22** and **Figure 4.23**.

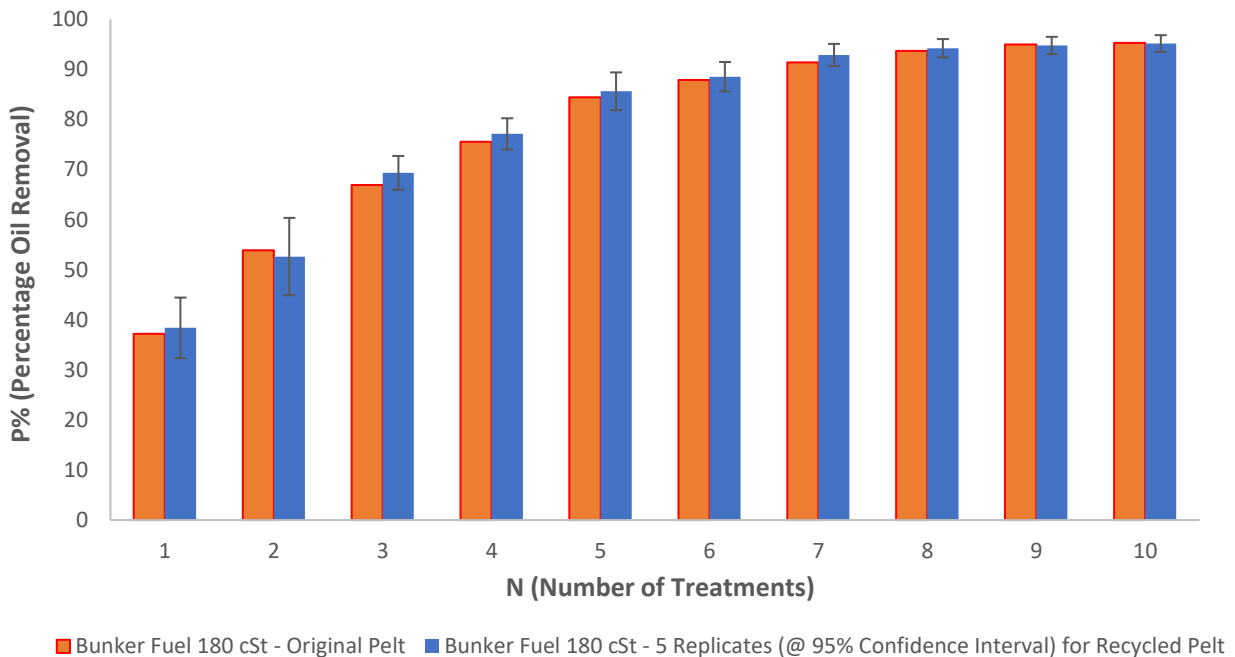


Figure 4.22: Comparison between original pelt and recycled pelt for the removal of Bunker Oil 1 (BO1) as a function of the number of treatments, N. Error bars represent the 95% confidence intervals for five replicates.

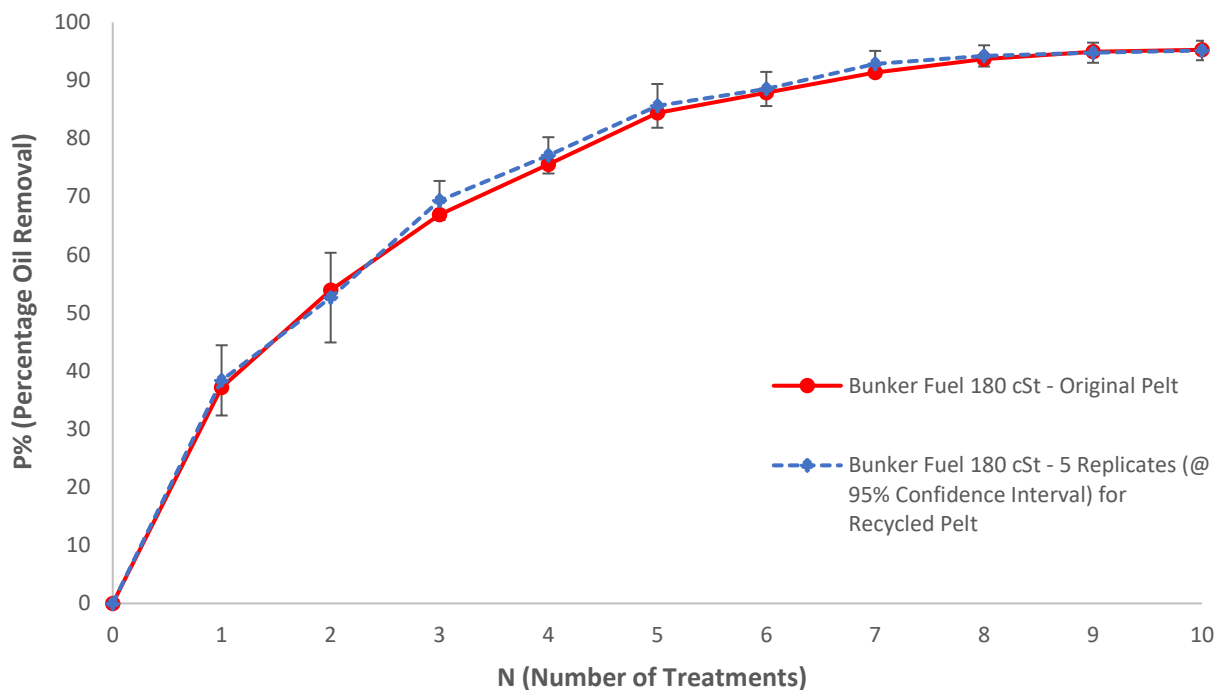


Figure 4.23: Comparison between original pelt and recycled pelt for the removal of Bunker Oil 1 (BO1) as a function of the number of treatments, N. Error bars represent the 95% confidence intervals for five replicates.

In conclusion, for all four oils studies, the removal isotherms for recycled penguin pelt are identical, within experimental error, to those for the virgin material. What remains to be done in the future is to see whether this is also the case for multiple recycles. However, these results are extremely encouraging and further strengthen the case for pelt as a superior substrate.

4.4.3 Mimicking the penguin’s body temperature - removal from pelt at 40 °C.

An additional advantage of pelt as a substrate is that, unlike feather clusters and carcass as substrates, pelt allows contaminant removal experiments to be conveniently conducted at different temperatures. Thus, experiments have been conducted whereby the removal of two light oils, Gippsland Crude and Diesel, from penguin pelt have been carried out at room temperature 22 °C and at 40 °C (to mimic the live penguin body temperature). Here, the pelt was heated on a temperature controlled hot plate that can be maintained at the live animal’s body temperature of 40 °C. The oil removal experiments can then be effectively conducted

at this temperature. The results of these experiments are shown in **Figure 4.24**. These graphs show the percentage removal (P%) versus the number of treatments (N) for the removal of these light to medium contaminants from the pelt of Little Penguin at 22 °C and 40 °C, respectively. Counterintuitively perhaps, both graphs show that the initial removals are higher and more rapid for the lower temperature. However, the final removals are higher for the higher temperature. Interestingly, these experiments demonstrate that the more volatile components are preferentially removed by the magnetic cleansing process, since these can be seen to have been evaporated away before the first treatment at 40 °C. It may also be indicating that the more volatile components are being lost from a warm animal making the task of cleaning an impacted animal more hazardous for the wildlife officer (Personal Communication). This preferential removal of the more volatile and usually more toxic/corrosive components is the essence of our recently developed “quick clean” stabilization technique based on magnetic cleansing (Ngeh *et al.*, 2012). The ‘hysteresis’ from N = 0 to 3 represents the components that have already evaporated at 40 °C prior to the magnetic cleansing (after ~ 5 min).

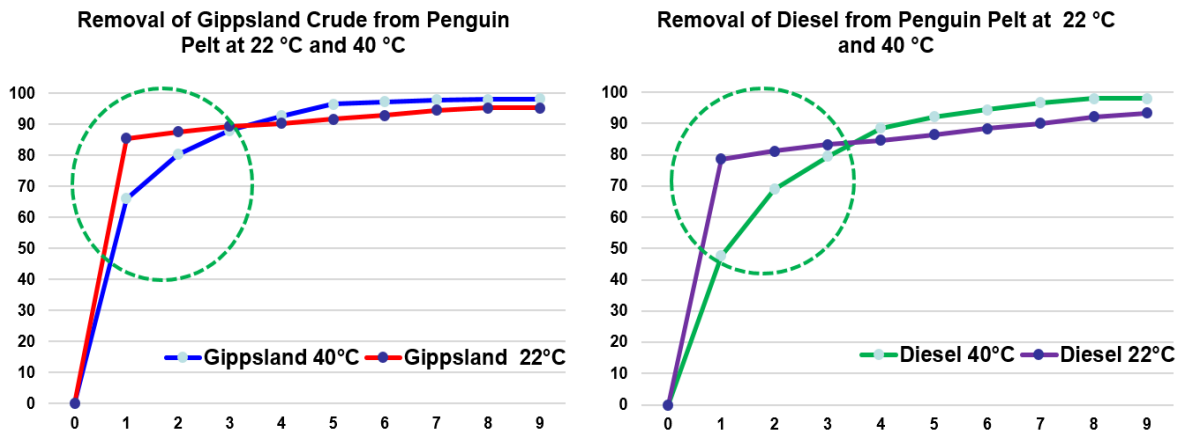


Figure 4.24: Nested isotherms for the removal of Gippsland Crude Oil (left) and Diesel Fuel Oil (right) from penguin pelt at pelt temperatures of 40 °C and 22 °C. These experiments were not conducted in replicate. However, from previous studies such curves are highly reproducible. The estimated average percentage SE is ~ 8%. This will not make a significant difference to the relative trend comparisons.

Yet another ‘bonus’ of the above experiments is that the relative hysteresis areas indicate the relative amounts of such volatile constituents in these two oils. Here, this ratio is 1.82 : 1 (Diesel Fuel Oil : Gippsland Crude Oil). This ratio was calculated by a “cut and weigh” method of the relative hysteresis areas. Thus, Diesel can be said to contain almost twice the amount of these (more dangerous) volatiles than Gippsland Crude. This could be very useful for the assessment of the relative toxicity threats of different oils, since it is these components that represent the greatest initial threat to the bird (and to rehabilitators - when birds are in holding bays).

4.4.4 The relationship between the removal isotherm profile and the percentage coverage of Diesel Fuel Oil on a Little Penguin plumage (carcass).

From an assay point of view, especially in relation to a whole bird, it is important to ascertain how the removal isotherm profile is related to the extent (%) of contaminant coverage on the bird. A previous study by our group (Orbell *et al.*, 2007) devised a method for experimentally quantifying (for Diesel Fuel Oil) the % coverage for Little Penguin Carcasses. The same study generated removal isotherms for coverages of 10%, 20%, 50% 70 % and 100% coverages. This data has been extracted from the report and is summarized in **Table 4.10**. This data is represented by the sets of histograms in **Figure 4.25** and by the nested isotherms in **Figure 4.26**. These experiments on carcasses were particularly difficult to conduct in the laboratory and consequently the experimental errors were high. However, within experimental error, it may be concluded from **Figures 4.25 & 4.26** that the removal isotherm profile for plumage is essentially independent of the % contamination coverage on the bird. Therefore, assays based on pelt samples can be confidently related to real life scenarios where the % contamination coverage on the birds is highly variable.

Table 4.10: Magnetic cleansing experiments with different levels of Diesel Fuel Oil coverage.

N	10% Coverage		20% Coverage		50% Coverage		70% Coverage		100% Coverage
	P%	95%	P%	95%	P%	95%	P%	95%	P%
1	32.69	9.30	29.47	8.39	19.60	4.288	17.05	10.65	37.15
2	55.97	10.10	46.02	9.11	32.66	14.21	31.28	16.71	63.75
3	67.94	11.37	59.69	3.41	47.90	25.99	50.91	13.86	75.32
4	75.69	13.80	69.44	7.84	59.07	21.82	65.58	8.69	81.38
5	79.45	13.51	77.16	4.23	68.97	18.98	75.14	5.20	85.57
6	83.33	10.51	81.94	4.02	78.60	11.11	81.31	11.96	89.56
7	87.17	13.38	85.55	2.64	82.09	9.93	86.61	12.01	94.61
8	90.07	7.86	89.10	2.20	88.47	4.32	90.26	10.72	95.91
9	92.46	5.37	91.79	1.45	91.32	5.76	93.99	9.79	96.01

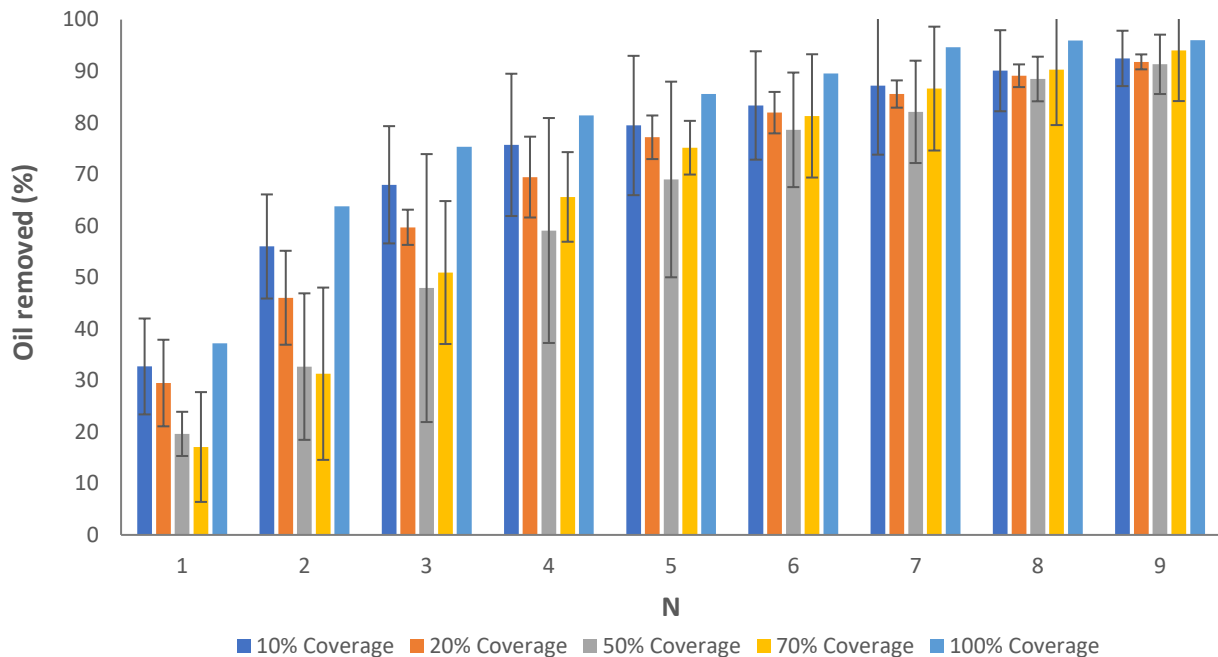


Figure 4.25: Histograms of Diesel Fuel Oil removal (%), as a function of the number of treatments, N; for the removal of 10%, 20%, 50%, 70% and 100% Diesel Oil coverage (by mass) from plumage. Error bars represent the standard error for three replicates for the removal of 10%, 20%, 50% and 70% Diesel Oil coverage (by mass) from plumage.

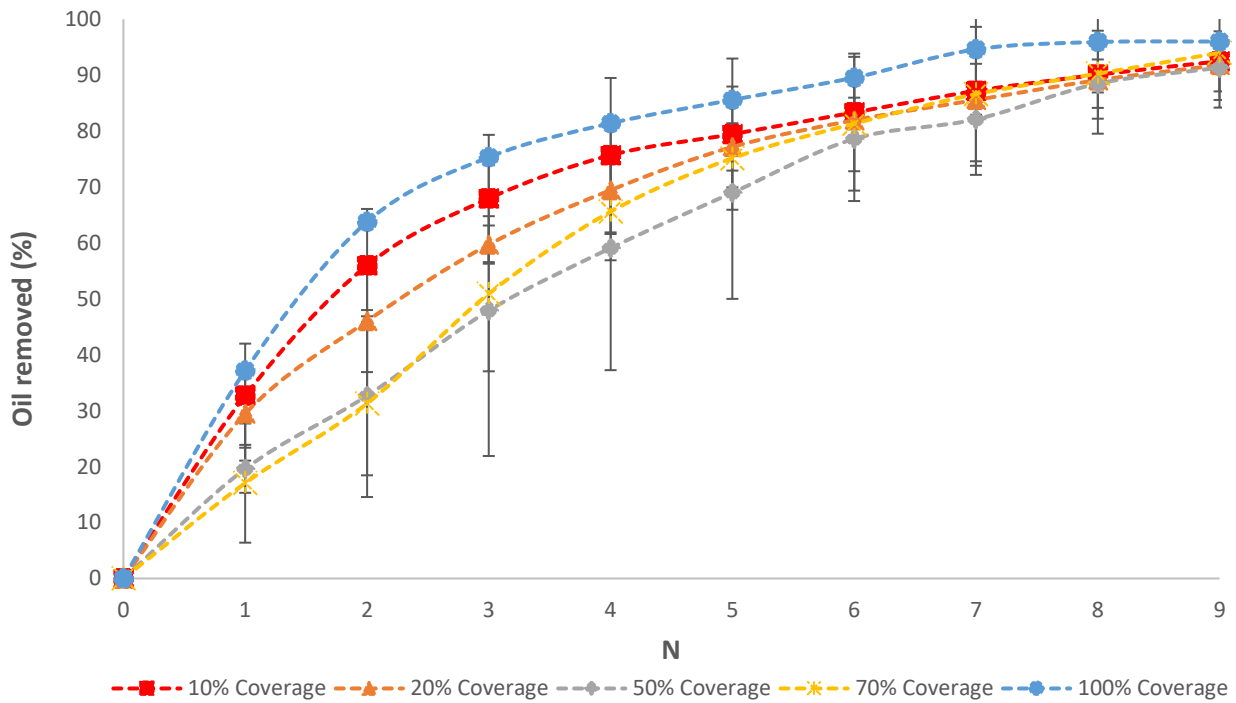


Figure 4.26: Sorption isotherm of oil removal (%), as a function of the number of treatments, N, for the removal of 10%, 20%, 50%, 70% and 100% Diesel Oil coverage (by mass) from plumage. Error bars represent the standard error for three replicates for the removal of 10%, 20%, 50% and 70% Diesel Oil coverage (by mass) from plumage.

This data may be averaged, **Table 4.11**, to give a generic removal isotherm with appropriate error bars as shown in **Figure 4.27**.

Table 4.11: Magnetic cleansing experiments with different levels of Diesel Fuel Oil coverage including the average of 10%, 20%, 50%, 70% and 100% and average of percentage error.

N	10% Coverage		20% Coverage		50% Coverage		70% Coverage		100% Coverage	Average of % Coverage	Average of Percentage Error
	P%	95%	P%	95%	P%	95%	P%	95%	P%		
										0	0
1	32.69	9.30	29.47	8.39	19.60	4.28	17.05	10.65	37.15	27.19	35.32
2	55.97	10.10	46.02	9.11	32.66	14.21	31.28	16.71	63.75	45.93	33.70
3	67.94	11.37	59.69	3.41	47.90	25.99	50.91	13.86	75.32	60.35	25.99
4	75.69	13.80	69.44	7.84	59.07	21.82	65.58	8.69	81.38	70.23	19.93
5	79.45	13.51	77.16	4.23	68.97	18.98	75.14	5.20	85.57	77.26	14.23
6	83.33	10.51	81.94	4.02	78.60	11.11	81.31	11.96	89.56	82.95	11.59
7	87.17	13.38	85.55	2.64	82.09	9.93	86.61	12.01	94.61	87.21	11.10
8	90.07	7.86	89.10	2.20	88.47	4.32	90.26	10.72	95.91	90.76	6.99
9	92.46	5.37	91.79	1.45	91.32	5.76	93.99	9.799	96.01	93.11	6.03

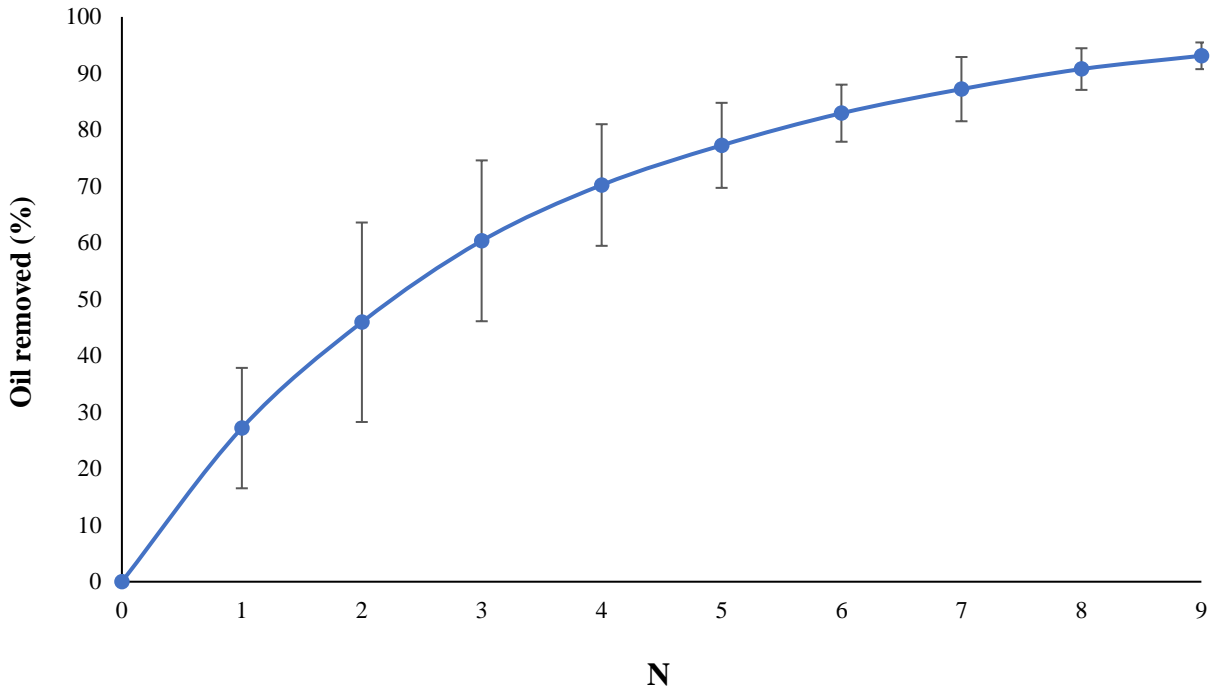


Figure 4.27: Oil removal (%), as a function of the number of treatments, N, for the average coverage of 10%, 20%, 50%, 70% and 100% Diesel Oil coverage (by mass) from plumage. Error bars represent the average standard error for three replicates.

The data in **Figure 4.27** show the average results for all 10%, 20%, 50%, 70% and 100% Diesel Oil coverages (generic). Here a “quick clean” using MPT would remove ~46% after 2 treatments (estimated 34% error) that would capture most of the most highly volatile, toxic, and corrosive components and would take less than ~10 min. Notably, after 9 treatments a maximum value of ~93% removal of contaminants is achieved, but the time required for this in the field would be prohibitive. A final clean would best be achieved by the traditional aqueous surfactant method after the stabilized bird has been transported to a treatment facility.

4.5 References

Altamirano, C 1983, *Water quality in aquatic: chemical and physical parameters affecting recreation and wildlife*, U.C. Berkley Environmental Sciences Senior Seminar Report.

Britannica 2017, *Oil spill*, viewed 24 September 2023, <<https://www.britannica.com/science/oil-spill>>.

Burger, AE & Fry, DM 1993, *Effects of oil pollution on seabirds in the northeast Pacific*, viewed 24 September 2023, <INIS Repository Search - Single Result (iaea.org)>.

Dao, HV, Maher, LA, Ngeh, LN, Bigger, SW, Orbell, JD, Healy, M, Jessop, R., Dann, P 2006, 'Removal of petroleum tar from bird feathers utilizing magnetic particles', *Environ. Chemistry Letters*, vol. 4, no. 2, pp. 111-113.

Dao, HV, Ngeh, LN, Bigger, SW, Orbell, JD, Healy, M, Jessop, Dann, P 2006, 'Magnetic cleansing of weathered/tarry oiled feathers – The role of pre-conditioners', *Marine Pollution Bulletin*, vol. 52, pp. 1591-1594.

Dao, HV, Ngeh, LN, Bigger, SW & Orbell, JD 2006, 'Achievement of 100% removal oil from feathers employing magnetic particle technology', *J. Environ. Eng.*, vol. 132, no. 5, pp. 555-559.

Dao, HV 2007, 'An investigation into factors affecting the efficacy of oil removal from wildlife using magnetic particle technology', PhD Thesis, Victoria University, Melbourne Australia.

Davies, L, Lewis, A, Lunel, T, Crosbie, A 1998, *Dispersion of Emulsified Oils at Sea – Laboratory Study*, National Environmental Technology Centre, Technical Report, AEAT-4347.

Davis, RW, Williams TM, Thomas, JA, Kastelein, RA 2011, 'The effect of oil contamination and cleaning on sea otters (*Enhydra lutris*) II', *Can. J. Zool.*, vol. 66, no. 12, pp. 2782-2790.

Eppley, ZA, Rubega, MA 1990, 'Indirect effects of an oil spill: reproductive failure in a population of South Polar skuas following the 'Bahia Paraiso' oil spill in Antarctica', *Marine Ecology Progress Series*, vol. 67, pp. 1-6.

Furness, RW & Camphuysen, CJ 1997, 'Seabirds as monitors of the marine environment', *ICES Journal of Marine Science*, vol. 54, no. 4, pp. 726-737.

Helm, RC, Carter, HR, Ford, RG, Fry, DM, Moreno, RL, Sanpera, C, Tseng, FS 2015, 'Overview of efforts to document and reduce impacts of oil spills on seabirds', *Handbook of Oil Spill Science and Technology*, pp. 429-453.

Henkel, LA, Ziccardi, MH 2018, 'Life and death: How should we respond to oiled wildlife?', *Journal of Fish Wildlife Management*, vol. 9, no. 1, pp. 296-301.

Heubeck, M, Camphuysen, KCJ, Bao, R, Humple, D, Rey, AS, Cadiou, B, Brager, S, Thomas, T 2003, 'Assessing the impact of major spills on seabird populations', *Marine Pollution Bulletin*, vol. 46, no. 7, pp. 900-902.

Hill, JF 1999, *Oil spills and Marine Wildlife: Guidelines for a response plan for the Isle of Mull*, Project Report commissioned by the Hebridean Whale and Dolphin Trust.

International Petroleum Industry Environmental Conservation Association (IPIECA) 2004, *A guide to oiled wildlife response planning*, viewed 23 December 2023, <www.ipieca.org/downloads/oil_spill/oilspill_reports/Vol.13_OiledWildlife.pdf>.

Jessup, DA, Yeates, LC, Toy-Choutka, S, Casper, D, Murray, MJ, Ziccardi, MH 2012, 'Washing oiled sea otters', *Wild. Soc. Bull.*, vol. 36, no. 1, pp. 6-15.

Massey, JG 2006, 'Summary of an oiled bird response', *J. Exotic Pet Medicine*, vol. 15, no. 1, pp. 33-39.

Mearns, AJ, Levine E, Yender R, Helton, D, Loughlin, T 1999, 'Protecting fur seals during spill response lessons from the San Jorge (Uruguay) oil spill', *International Oil Spill Conference Proceedings*, vol. 1, pp. 467-470.

Munaweera, K, Ngeh, LN, Bigger, SW, Orbell, JD, Dann, P 2012, 'Towards a rational choice of pre-treatment agents for the cleansing of oiled wildlife', *Australian Wildlife Rehabilitation Conference*, Townsville, Australia.

Munaweera, K 2015, 'The Rational development of improved methods for the removal of oil contamination from wildlife and rocky foreshore utilizing magnetic particle technology', PhD Thesis, Victoria University, Melbourne, Australia.

National Oceanic Atmospheric Administration (NOAA) 2016, *A major marine ecosystem threat*, viewed 24 September 2023, <Oil spills: A major marine ecosystem threat | National Oceanic and Atmospheric Administration (noaa.gov)>.

Newman, SH, Ziccardi, MH, Berkner, AB, Holcomb, J, Clumpner, C, Mazet, JAK 2003, 'A historical account of oiled wildlife care in California', *Marine Ornithology*, vol. 31, pp. 59-64.

Ngeh, LN 2002, 'The development of magnetic particle technology for application to environmental remediation', PhD Thesis, Victoria University, Melbourne, Australia.

Ngeh, LN, Orbell, JD, Bigger, SW, Munaweera, K, Dann, P 2012, 'Magnetic cleansing for the provision of a quick clean to oiled wildlife', *World of Academy of Science and Technology*, vol. 72, pp. 1091-1093.

Ober, HK 2019, *Effects of oil spills on marine and coastal wildlife*, viewed 24 September 2023, <<https://edis.ifas.ufl.edu/publication/UW330>>.

Orbell, JD, Godinho, L, Bigger, SW, Nguyen, TM, Ngeh, LN 1997, 'Oil spill remediation using magnetic particles: An experiment in environmental technology', *J. Chem. Edu.*, vol. 74, no. 12, pp. 1446-1448.

Orbell, JD, Tan, EK, Coutts, MC, Bigger, SW, Ngeh, LN 1999, 'Cleansing oiled feathers-magnetically', *Mar. Pollut. Bull.*, vol. 38, no. 3, pp. 219-221.

Orbell, JD, Ngeh, LN, Bigger, SW, Zabinkas, M, Zheng, M, Healy, M, Jessop, R, Dann, P 2004, 'Whole-bird models for the magnetic cleansing of oiled feathers', *Mar. Pollut. Bull.*, vol. 38, no. 48, pp. 336-340.

Orbell, JD, Dao, HV, Ngeh, LN, Bigger, SW, Healy, M, Jessop, R, Dann, P 2005, 'Acute temperature dependency in the cleansing of tarry feathers utilizing magnetic particles', *Environ. Chem. Letters*, vol. 3, no. 1, pp. 25-27.

Orbell, JD, Dao, HV, Maher, LA, Ngeh, LN, Bigger, SW, Healy, M, Jessop, R, Dann, P 2006, 'Removal of petroleum tar from bird feathers utilizing magnetic particles', *Environ. Chem. Letters*, vol. 4, no. 2, pp. 111-113.

Orbell, JD, Dao, HV, Ngeh, LN, Bigger, SW, Healy, M, Jessop, R, Dann, P 2006, 'Magnetic cleansing of weathered/tarry oiled feathers – the role of pre-conditioners', *Mar. Pollut. Bull.*, vol. 52, pp. 1591-1594.

Orbell, JD, Dao, HV, Ngeh, LN, Bigger, SW 2007, 'Magnetic particle technology in environmental remediation and wildlife rehabilitation', *Environmentalist*, vol. 27, pp. 175-182.

Orbell, JD, Dao, HV, Kapadia, J, Ngeh, LN, Bigger, SW, Healy, M, Jessop, R, Dann, P 2007, 'An investigation into the removal of oil from rock utilizing magnetic particle technology', *Mar. Pollut. Bull.*, vol. 54, pp. 1958-1961.

Orbell, JD, Dao, HV, Ngeh, LN, Bigger, SW 2007, 'An investigation into the feasibility of applying magnetic particle technology to the cleansing of oiled wildlife in the field', The technical Report Prepared for the Australian marine Safety Authority (National Plan Environment Working Group) and the Phillip Island Nature Parks.

Oiled Wildlife Care Network (OWCN) 2003, *Protocol for the care of oil affected marine mammals*, Wildlife Health Centre, University of California, Davis, U.S.A.

Parsons, NJ & Underhill, LG 2005, 'Oiled and injured African penguins *Spheniscus demersus* and other seabirds admitted for rehabilitation in the Western Cape, South Africa, 2001 and 2002', *African Journal of Marine Science*, vol. 27, no. 1, pp. 289-296.

Piatt, JF, Lensink, CJ, Butler, W, Kendziorek, M, Nysewander, DR 1990, Immediate impact of the 'Exxon Valdez' oil spill on marine birds, *The Auk.*, vol. 107, pp. 387-397.

Singh, H, Bhardwaj, N, Arya, SK, Khatri, M 2020, 'Environmental impacts of oil spills and their remediation by magnetic nanomaterials', *Environmental Nanotechnology, Monitoring & Management.*, vol. 14, 100305.

Tan, EK 1998, 'Oil spill remediation using magnetic particles', Honours Thesis, Victoria University, Melbourne, Australia.

US Fish and Wildlife Service (USFWS) 2002, *Best practices for migratory bird care during oil spill response*, US Fish and Wildlife Service, USA.

Chapter 5: The characterization of the evaporation of crude oils from penguin pelt

5.1 Introduction

5.1.1 Weathering

5.1.2 Volatile in different oils

5.1.3 Research plan/experimental overview

5.2 Materials and Equipment

5.2.1 Crude oils investigated

5.2.2 Facilities

5.2.3 Equipment and substrate materials

5.3 Methodology and experiments conducted

5.4 Mathematically modelling the data

5.5 Results and Discussion

5.5.1 Block 1 (Experiments 1 & 2)

5.5.2 Block 2 (Experiments 1 & 3)

5.6 The discovery of the “Highly Volatile Fraction” (HVF)

5.7 References

5.1 Introduction

5.1.1 Weathering

During recent years, increased consumption of petroleum has led to larger oil exploration and oil transportation activities in the marine environment (O'Rourke & Connolly, 2003; National Research Council, 2003). Crude oil production and transport on the sea surface always poses a risk of spills (Michel & Fingas, 2016). As a result of human errors and mechanical failures, incidents such as collision of ships, pipeline explosions, and oil rig failures release tons of crude oil into the marine environment (Adofo *et al.*, 2002). Crude oil in the marine environment exhibits detrimental and long-term effects (Zhang *et al.*, 2019). Flowing oil into the sea can contaminate the food chain of marine animals, sink to the sea bed affecting marine life, pollutes harbor facilities, and ruins eco sensitive near shore resources (Kennish, 1997; 2002). Due to the unpredictable nature of sea surfaces and weather conditions, oil spills on the sea surface are difficult to recover. Therefore, oil spills pose a threat to marine life (Gin *et al.*, 2001; Thakur & Koul, 2022).

Crude oils spilling onto the sea surface form a thin layer called an oil slick. The oil slick is then degraded by several natural processes referred to as oil weathering processes (OWP). Weathering has a significant impact on crude oil properties, especially in terms of viscosity and density (Mishra & Kumar, 2015). There have been several studies of oil weathering processes (Sebastiao and Soares, 1995; ASCE, 1996; Reed *et al.*, 1999; Lehr, 2001; Azevedo *et al.*, 2014; Fingas, 2014). Researchers have found that changes in slick properties over time could affect slick lifespan on the sea surface. Initial spill conditions and oil properties can also have a substantial impact on slick evolution. Prior understanding of oil properties is crucial when responding to an oil spill or planning a countermeasure.

Oil weathering processes (OWP) occur naturally as part of oil slicks generated by oil spills on the sea surface (Keramea *et al.*, 2023). They include spreading, evaporation, dissolution, dispersion, and emulsification (Mishra & Kumar, 2015). These processes are complex, self-competing and simultaneous. Even though the evaporation process removes a significant fraction of volatile components, residue still remains on the sea surface as a result of emulsification, which leads to increased oil volume (Xie *et al.*, 2007). However, not all oils

have the ability to emulsify; some may separate into distinct oil and water phases (Zolfaghari *et al.*, 2016).

Weathering changes the physical properties, chemical activities, and toxic chemical content of oil over a wide range of timescales. As a result of evaporation, light, low boiling hydrocarbon compounds can be rapidly removed in hours, while biodegradation can take longer and follow a degradation succession mostly determined by the compound class (Tarr *et al.*, 2016). Although weathering progressions occur naturally, anthropogenic factors may augment the process, including burning, dispersants, shoreline washing, and fertilization (Beyer *et al.*, 2016; Asif *et al.*, 2022).

During spills, fresh crude oil contains relatively high proportions of low boiling point compounds that are more water soluble than other components, fresh crude oil floats, and at its lowest viscosity, spreads easily (Adofo *et al.*, 2002; Wang *et al.*, 2003; Tarr *et al.*, 2016). Therefore, fresh oil spills generally pose the highest level of environmental risk. As a result of weathering, oil initially loses its average molecular weight, losing volatile and water-soluble components, resulting in the residual becoming more viscous and making it more likely to accumulate in wind rows rather than to spread out in a thin film (Tarr *et al.*, 2016). Over time, as the weathering process continues, the oil residue may become reduced to small quantities of solid residue, like tar balls (Warnock *et al.*, 2015).

In most cases, oil residues mix with water and emulsify to form a viscous emulsion that is resistant to further weathering (Khan *et al.*, 1995; Fingas *et al.*, 2003). Emulsification inhibits subsequent remediation methods, such as skimming, dispersing, or burning (Hubbe *et al.*, 2013; Pete *et al.*, 2021; Silva *et al.*, 2022). However, in general, emulsified oil poses fewer environmental hazards because it transforms into a sticky material that smothers and covers instead of producing toxic reactions (Tarr *et al.*, 2016). Ingestion of emulsified oil (e.g., through preening of feathers), can have a significant toxic effect (Morandin & Hara, 2016; King *et al.*, 2021). Heavily emulsified oil residues degrade slowly, so they persist in the environment longer (Tarr *et al.*, 2016).

As can be seen in **Figure 5.1**, there are various types of weathering processes that act on the initially released oil (#1), along with the variation of oil residues (#2 through to #6) that occur in the environment because of weathering. Chemical, microbial and photo-induced

degradations (notably oxidation) occur on both oil residues and on individual hydrocarbon and non-hydrocarbon molecules that have been released into the environment (Tarr *et al.*, 2016).

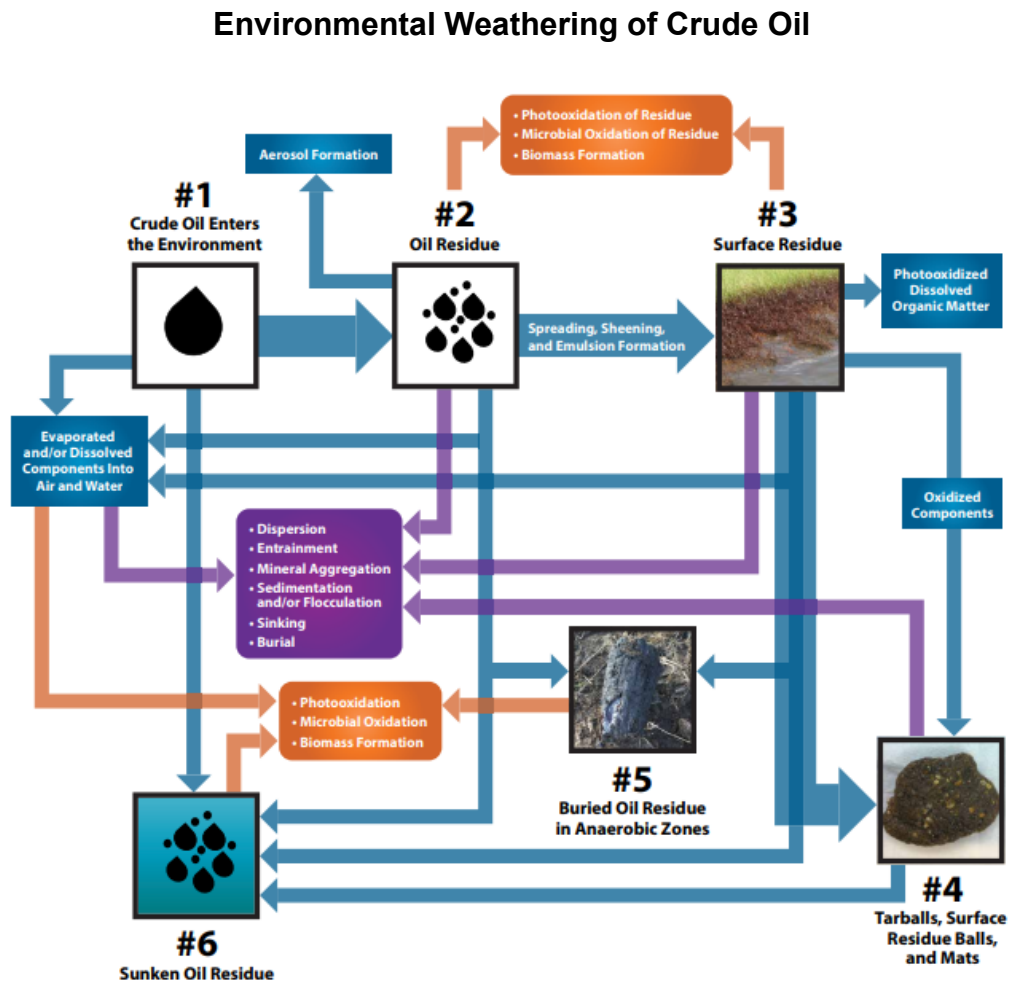


Figure 5.1: Weathering of oil spilled in the marine environment (Tarr *et al.*, 2016).

There are up to eight main weathering processes involved in the weathering of oil spills, including spreading, evaporation, dispersion, emulsification, dissolution, oxidation, sedimentation, sinking and biodegradation (Lehr, 2001; Tarr *et al.*, 2016; Bacosa *et al.*, 2022). Each of these processes can be classified into one to two chronological categories, based on when their effect is most significant. Therefore, the early stage of a spill involves spreading, evaporation, dispersion, emulsification and dissolution. The later stage of a spill includes oxidation, sedimentation, and biodegradation. The longer-term processes tend to define the final outcome of a particular oil spill (Tarr *et al.*, 2016).

The diagram below illustrates the outcome of a typical crude oil spill, demonstrating how the relative importance of the weathering process changes over time (from hours to years). The width of the band represents the significance of the process (Fernandes, 2018).

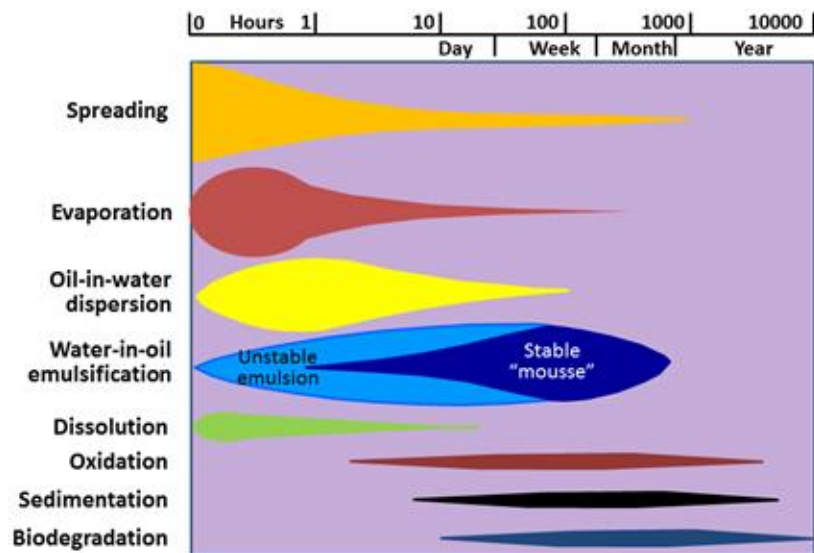


Figure 5.2: Weathering process of a typical crude oil (Fernandes, 2018).

Since the 1970s, numerous studies have published on the role of evaporation after an oil spill (Mackay and Shiu, 1976; Fingas, 1995; Gros *et al.*, 2014). Fingas (1995), when modelling crude oil evaporation rates and mechanisms, discovered that up to 75% of a light crude oil volume evaporates after the first few days following an oil spill. Evaporation was shown to be the major fractionation process in a mass transfer model developed by Gros *et al.* (2014) to specify the first day of an oil spill. Wind and wave activity can potentially transport oil components into the atmosphere by forming aerosols (Arey *et al.*, 2007; Aeppli *et al.*, 2013).

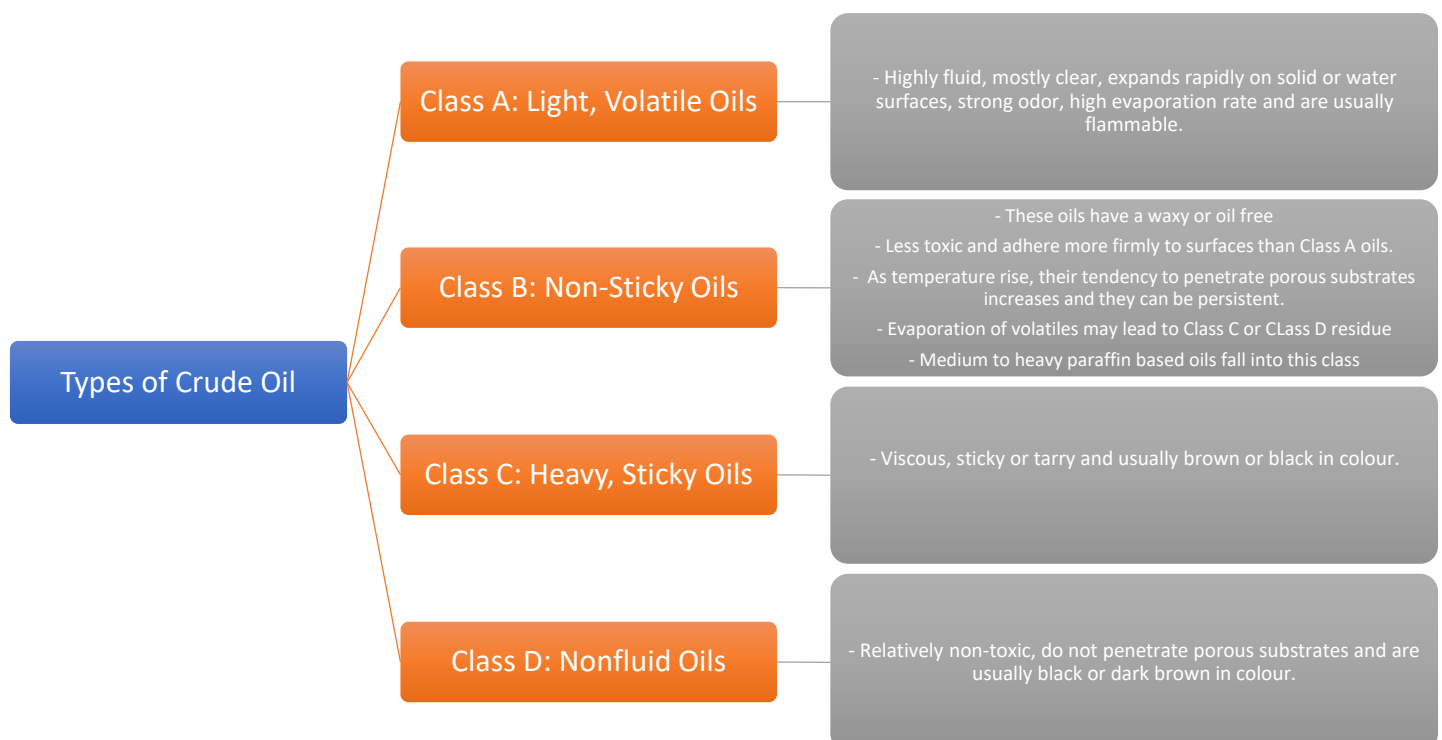
5.1.2 Volatiles in different oils

There are many different types of crude oil. Crude oil ranges in density and consistency in its natural, unrefined, state from very thin, light, and volatile fluidity to extremely thick, semi-solid heavy oil (Murty & Kaufman, 2020). There is also a gradation in the color of oil extracted from the ground, ranging from a light, golden yellow to the deepest, darkest black imaginable (The No. 1 Source for Oil and Energy News, 2009).

According to the No. 1 Source for Oil and Energy News (2009), the four major types of oil are as follows:

- (1) Very Light Oils/Light Distillates - including Jet Fuel, Gasoline, Kerosene etc. These oils are highly volatile and can evaporate in a matter of days, allowing them to diffuse quickly and reduce toxicity levels.
- (2) Light Oils/Middle Distillates, which include the majority of so-called Grade 1 and Grade 2 fuel oils, including Diesel fuel oils, domestic fuels and light crude marine gas oils. These oils are mildly volatile, less evaporative, and mildly toxic.
- (3) Medium Oils: these have a lower volatility, resulting in messier and more complex “clean ups”.
- (4) Heavy Fuel oils: so-called Grades 3, 4, 5, and 6 fuel oils (Bunker B and C), along with intermediate and heavy marine fuels. Due to the slow and limited evaporation of these oils, their toxicity is enhanced. This means not only potentially severe contamination for fish, fowl, and fur-bearing creatures, but also potentially “long-term” contamination of water and soil (The No. 1 Source for Oil and Energy News, 2009; Ndimele, 2017; Chizoba, 2021).

According to the classification of crude oil types by (United States Environmental Protection Agency, 2021; DeMarco, 2022):



For most oil spills, evaporation is an important process (Fingas, 1999). Light crude oils can be decreased by up to 75% of their original volume in a few days, whereas medium crudes can be reduced by up to 40%. In the first several days after a spill, heavy or residual oils will only lose roughly about 5% of their volume. Evaporation is a component of the process and common to most oil spill behavior models. Despite the importance of the subject, only a small amount of research has been carried out on the fundamental physics and chemistry of oil spill evaporation (Fingas, 1995). Oil evaporation is complicated by the fact that oil is a combination of hundreds of components that varies from source to source and even over time (Fingas 2004; 2011). Much of the research mentioned in the literature focuses on ‘calibrating’ equations originally established for water evaporation (Singh and Xu, 1997; Xu and Singh, 2000). Similarly, there is a scarcity of published empirical data on oil evaporation (Fingas, 1999; 2004).

Water evaporation has been studied scientifically and quantitatively for many years (Brutsaert, 1982; Jones, 1992). Water evaporation also serves as the foundation for the oil work in the literature. However, the evaporation of a multi-component system such as crude oil compared to a pure substance like water, result in fundamental differences (Fingas, 1999). Firstly, the evaporation rate of a single liquid, such as water, is constant across time. For crude oils and other multi-component fuel mixes, evaporative loss by total weight or volume is logarithmic with time. This is due to the more volatile components are being depleted that are depleted dramatically over time. The influence of atmospheric conditions is the second major difference. Wind speed and relative humidity have a significant impact on water evaporation. Water can only be held in air to a certain extent. The rate of evaporation is governed by the boundary layer above an evaporating water mass. Evaporation stops once this air layer is saturated with water (or any other evaporating component). Normal air does not contain a high concentration of benzene and other oil components and the saturation level of these in air is frequently well above the concentrations achievable from an evaporating slick (Fingas, 1995).

Evaporation is a critical mechanism in most oil spills. Typical crude oils can lose up to 45 percent of their volume in just a few days (Fingas, 2011). Previous research (Fingas, 2011) has shown that Macondo oil lost up to approximately 60% in a short period of time when released under water at high pressure. Evaporation is included as a process and output in almost all oil spill models. Evaporation is a major factor for most oils. Furthermore, many crude oils must evaporate before forming water-in-oil emulsions (Fingas, 2011). Light oils will undergo a drastic transition from fluid to viscous and heavy oils will solidify. Many oils generate tar balls

or thick tar mats after prolonged evaporative exposure. Despite its relevance, little research has been carried out on the fundamental physics and chemistry of oil spill evaporation (Fingas, 1995). It is worth reiterating that the complexity of studying oil evaporation derives from the fact that oil is a diverse mixture of hundreds of components, and the composition of oil fluctuates from source to source and even over time. Much of the research described in previous literature focuses on calibrating equations derived for water evaporation (Fingas, 1995; 2011).

The processes that control evaporation are critical (Brutsaert, 1982; Jones, 1992). The transition of molecules from the surface of a liquid into the vapor phase above it is referred to as evaporation (Fingas, 2011). The boundary layer is known as the immediate layer of air above the evaporation surface (Monteith & Unsworth, 2008; 2013). This boundary layer is the intermediary interface between the air and the liquid and potentially can be as thin as one millimeter. The properties of this air boundary layer might have an impact on evaporation. Mostly, in the case of water, the boundary layer controls the rate of evaporation. The relative humidity of air may store a varied amount of water depending on temperature. Under weather conditions when the air boundary layer is not moving (no wind) or has minor turbulence, the air immediately above the water becomes saturated rapidly and evaporation decelerates. According to the saturation of the boundary layer, real water evaporation occurs at a small fraction of the maximum evaporation rate. The physics of the air-boundary layer is thus said to govern water evaporation. This regulation appears as an increase in evaporation caused by wind or turbulence (Fingas, 2011). When there is little turbulence, evaporation can be slowed by orders of magnitude. Monteith and Unsworth (2008) found that molecular diffusion of water molecules through air is at least 10 times slower than turbulent diffusion (Fingas, 2011).

The air-boundary-layer regulating mechanism is depicted schematically in **Figure 5.3**. If it was not for the regulation caused by the slow transfer of vapor into the air boundary layer, the liquid may evaporate at a very quick rate. Water is the most typical example of this form of control. Water evaporation may be increased by spreading it out or accelerating wind speed or air turbulence. The transport of water across the air border layer is accelerated by wind speed or turbulence in the air boundary layer (Fingas, 2011; 2014).

Some liquids are not controlled by the air boundary layer due to the rate of evaporation is too slow for the vapors to permeate the air boundary layer above them (Fingas, 2011). Most mixtures are driven by the diffusion of molecules from within the liquid to the liquid's surface.

Figure 5.4 depicts this regulating process. Slowly evaporating mixtures of substances, such as oils and fuels, exhibit this process. Some of the outputs of this mechanism may appear counterintuitive to some, such as the fact that increasing area does not always increase the evaporation rate. More significantly, raising the wind speed has only a slight effect on evaporation. Combinations of the two regulatory mechanisms are feasible. If a combination contains volatile components, for example, the volatile components may evaporate via an air boundary-layer-regulated process, whereas the remainder of components evaporate via a diffusion-regulated mechanism (Fingas, 2011; 2014).

Water evaporation research dates back decades and served as the foundation for early oil evaporation research (Fingas, 2011). The evaporation of a pure liquid like water differs significantly from that of a multi-component system like crude oil for various reasons. The rate of evaporation for a single liquid, such as water, is constant across time (Monteith & Unsworth, 2008; 2013). For crude oils, petroleum products, and other multi-component fuel mixtures, evaporative loss is not linear with time, either in terms of weight or volume (Fingas, 1997).

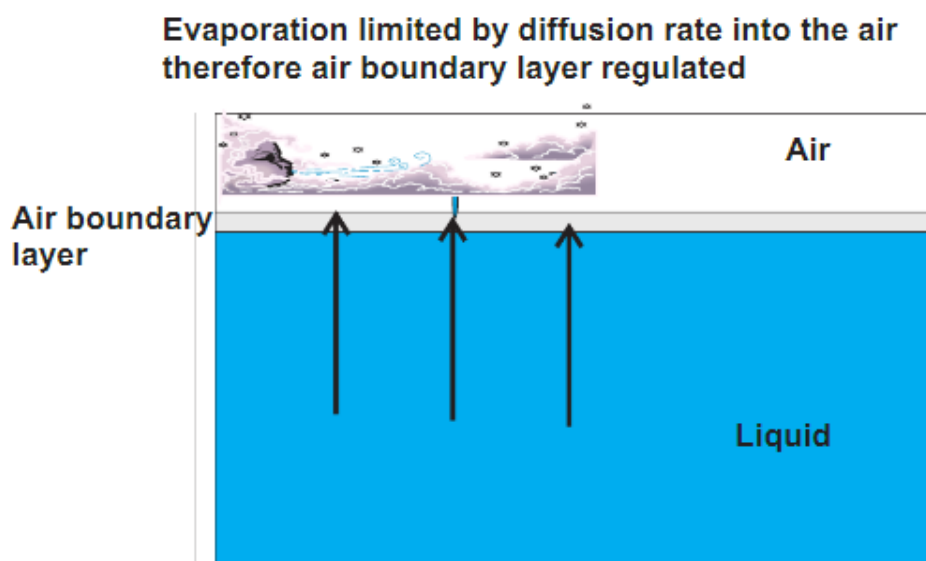


Figure 5.3: Here, the air boundary layer regulating method is depicted. The rate of evaporation is regulated by diffusion into the air layer, which is the limiting factor. Turbulence in the air affects this rate by increasing the transport of molecules over the boundary layer. For pure liquids with a high evaporative rate, this regulation mechanism is true. Water is the most commonly help concept and is an example of such a liquid (Fingas, 2011).

Evaporation limited by diffusion rate through liquid and through surface layer - therefore diffusion regulated

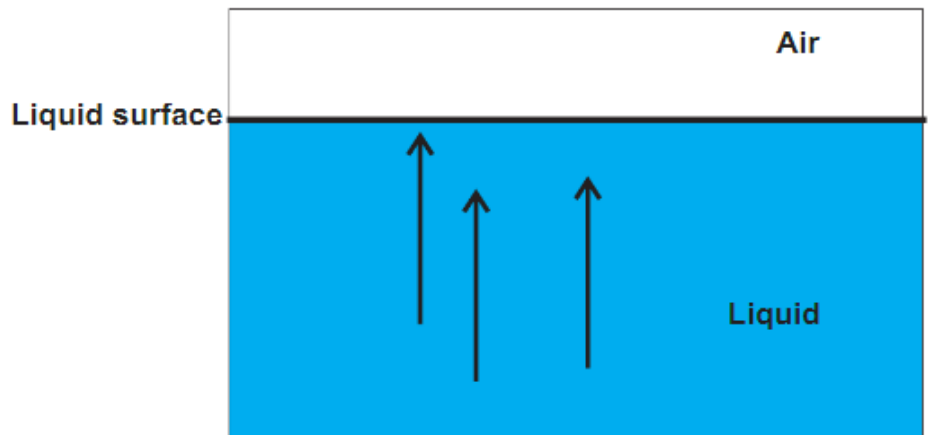


Figure 5.4: Here, the diffusion-controlled regulatory mechanism is depicted. The limiting factor and thus the regulation mechanism is diffusion through the evaporating liquid. This technique applies to oils, fuels, and a variety of other liquid mixes that both evaporate more slowly than water (Fingas, 2011).

Previous studies on oil weathering were also undertaken by Ngeh (2002), “Preparation of Feathers Contaminated with Weathered Oil”. **Figure 5.5** depicts the oiled feathers mass loss over time. The figure demonstrates the loss of the more volatile components and the “weathering” of the heavier components onto the feathers (Ngeh, 2002).

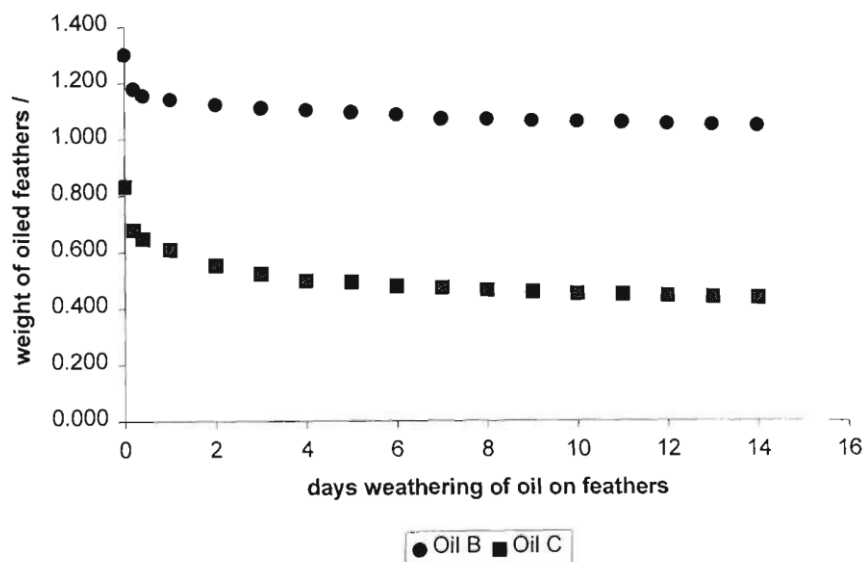


Figure 5.5: Weight of oiled breast feathers of the domestic duck (*Ana platyrhychos*) over time (Ngeh, 2002).

Ngeh (2002) has shown that a light Oil C evaporates faster than a viscous Oil B. After fourteen days, the percentage by weight of Oil C evaporated is around 50%, while the percentage by weight of Oil B evaporated is approximately 20%. The data reveals that the rate of evaporation for both oils has decreased significantly after 5 days. The feathers are deemed fully weathered, under the conditions specified, when the graph becomes parallel to the time axis (Ngeh, 2002).

Another previous study conducted by Dao (2007), also monitored the weight loss of weathered oiled feathers over time. For the purpose of these experiments, weathering is defined as the rate of evaporation over time for the more volatile components. Accordingly, evaporation is thought to be the main weathering mechanism (Mullin & Champ, 2003), which causes heavy crude oil spills to lose 5-10% of its weight and lighter spills to lose 20-60% (NOAA, 1997). Furthermore, for wildlife contamination, long-term, non-evaporative weathering processes should not be considered since they would continue beyond the animal's survival span. A comparable approach for simulating oil weathering has been described (Urum *et al.*, 2004; 2005).

Bunker oil (BO2) and Shell crude oil (SO) were the contaminants used in the authors' (Ngeh and Dao) experiments. At room temperature, SO is tarry and semi-solid oil with a viscosity of 3000 to 4000 cSt at 100 °C. Therefore, it is deemed appropriate to describe it as a "worst case scenario" involving a tarry contaminant. BO2 is a very sticky oil (222 cSt at 40 °C) that is occasionally discovered as a contaminant at the PINP, posing a threat to the resident little penguins (Dao, 2007). Clusters of breast/contour feathers from the Mallard Duck (*Anas platyrhynchos*) were used in the above authors experiments (Dao, 2007).

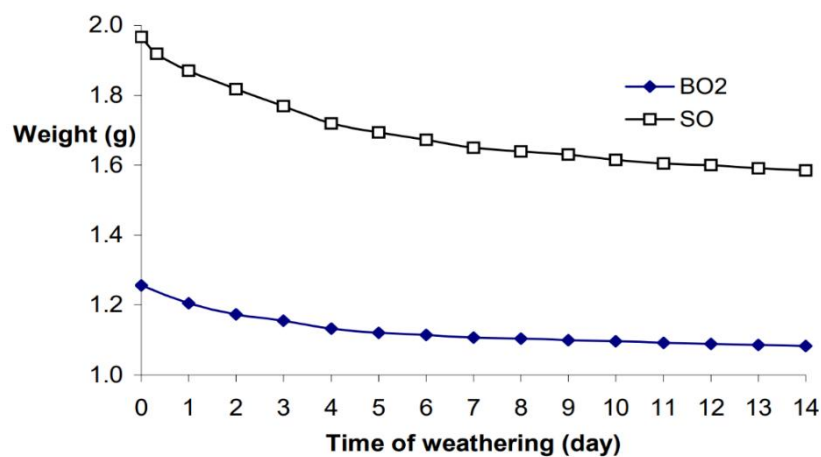


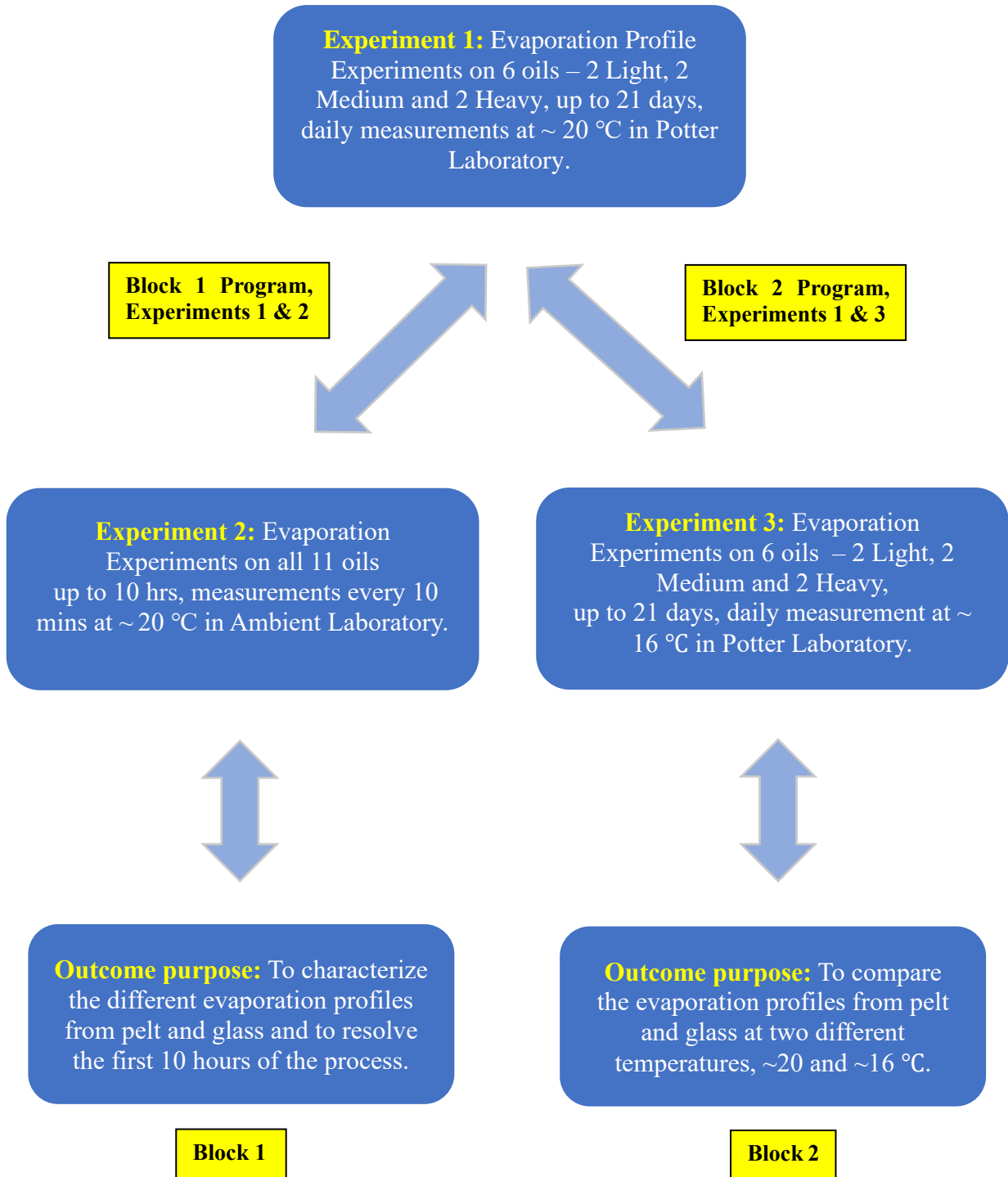
Figure 5.6. Weight versus time of weathering for oiled duck feather clusters (Dao, 2007).

In the experiments of Dao, 2007, the weathering of oil was mimicked and tested in the laboratory using feather clusters that were submerged in a melt of the oil and then allowed to solidify into a tarry deposit (Orbell *et al.*, 2005; 2007; Dao *et al.*, 2006-a; 2006-b). The resulting tarry feathers were allowed to hang in the air for up to 14 days at room temperature. The amount of weathering was determined by tracking the weight loss of the oiled feathers over time. As can be observed in **Figure 5.6**, for crude oil (SO), the evaporation rate is rather high for the first five days, resulting in a weight loss of around 14%. The evaporation rate slows down considerably after seven days, and at this point the oil is thought to have weathered significantly (losing about 16% of its weight). Following fourteen days of weathering, subsequent oil loss is relatively small, and the oil is regarded almost fully weathered (representing approximately 19% weight loss). **Figure 5.6** shows that fourteen days of weathering resulted in a 14% weight loss in Bunker Oil (BO2).

5.1.3 Research plan/experimental overview

In the current project, a series of evaporation experiments has been designed to assess the relative evaporation profiles (% wt. loss vs time) for the evaporation of a range of crude oils, **Table 5.1**, from the pelt of the Little Penguin. For each oil evaporation experiment, the evaporation profile from a glass surface has also been determined, as a control. After preliminary experiments to establish facilities and parameters, two “Blocks” of experiments were designed and conducted. **Block 1** consists of **Experiments 1 & 2** and **Block 2** consists of **Experiments 1 & 3**, as shown in the **Experimental Design Schematic**, below. The rationale for the **Block 1** experiments is to fully characterize the relative evaporation profiles from pelt (and glass) for six oils (2 light, 2 medium and 2 heavy – asterisked in **Table 5.1**) at ~20 °C, up to a 21-day period (**Experiment 1**) - and to further resolve these evaporation profiles up to the first 10 hours (**Experiment 2**). To the best of the author’s knowledge, *the detailed evaporation behaviour* up to the first 10 hours has not been previously investigated or characterized. The purpose of examining the evaporation profile over the first 10 hours or so, is predicated by the fact that the removal of volatiles over this period is critical for the health of a contaminated animal. The rationale for the **Block 2** experiments is to compare the evaporation profiles from Little Penguin pelt (and glass) for up to 21 days at ~20 °C and at ~16 °C for all the 11 oils in **Table 5.1**, to ascertain the effect on the evaporation profile of a lower temperature. The details of these experiments are described in the **Methodology 5.4 section**, below.

Experimental Design Schematic



5.2. Materials and equipment

5.2.1 Crude oils investigated

A range of light, medium and heavy crude oils were used in these experiments. These are listed, together with their relative viscosities, in **Table 5.1**.

Table 5.1: Crude oils used in the evaporation experiments, showing their sources and relative viscosities. For the experiments conducted at ~ 20 °C and at ~ 16 °C in the “Potter Lab”, over a period of up to 21 days, the six oils used are marked with an asterisk and highlighted in green. For the experiments conducted at ~ 20 °C in the “Ambient Lab”, over a period of up to 10 hours, all eleven oils were used.

	Oil	Source	Viscosity (cP)
Light	Sakhalin	Lytton Oil Refinery, Caltex Australia Ltd., Lytton, QLD 4178	7
Light	Tapis	Lytton Oil Refinery, Caltex Australia Ltd., Lytton, QLD 4178	6
Light	Margham Condensate	Lytton Oil Refinery, Caltex Australia Ltd., Lytton, QLD 4178	4
Light	Merine	Exxon/Mobil Oil Pty. Ltd., Australia	9
Light	Murban	Lytton Oil Refinery, Caltex Australia Ltd., Lytton, QLD 4178	8
Light	Diesel*	Shell local service station	7
Light	Kerosene*	Diggers brand, Recochem Inc., Australian Division, Brisbane, QLD.	1.64
Medium	Bohai Bay Crude*	Lytton Oil Refinery, Caltex Australia Ltd., Lytton, QLD 4178	394
Medium	Ikan Pari Crude*	Lytton Oil Refinery, Caltex Australia Ltd., Lytton, QLD 4178	46
Heavy	Bunker Oil 180*	Industrial and Bearing Supplies (IBS), Gulf Western Oil, Australia.	32040
Heavy	Bunker Oil 380*	Industrial and Bearing Supplies (IBS), Gulf Western Oil, Australia.	70320

5.2.2 Facilities

For the experiments conducted at ~ 20 °C and at ~ 16 °C over a period of ~ 21 days, a temperature-controlled room (the “Potter Lab”) was established on the Werribee Campus of

Victoria University, whereby the temperature could be controlled to within ± 1 °C. For the experiments conducted at ~ 20 °C, over a period of ~ 10 hours, an empty office (the “Ambient Lab”) was adapted to mimic ambient conditions. Here, the temperature was subject to normal air conditioning control to within ± 1.5 °C. Disturbances, including *in situ* weighing, and air drafts were carefully kept to a minimum during the above experiments.

5.2.3 Equipment and substrate materials

All weighing, from both a glass and a pelt substrate, was conducted using a Mettler Toledo Analytical Balance, **Figure 5.7**, for both venues.

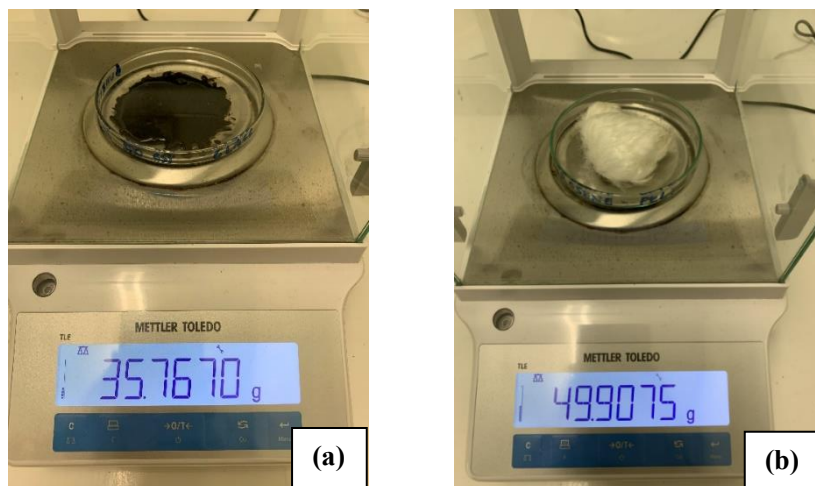


Figure 5.7. Typical weighing experiments, showing (a) an oil sample on a glass substrate (Petri dish) and (b) an oiled pelt sample, contained in a petri dish.



Figure 5.8. Breast and back pelt from Little Penguin (*Eudyptula minor*) were supplied by the PINP.

The glass substrate used was the surface of a standard Petri dish and the pelt substrate was cut from Little Penguin (*Eudyptula minor*) pelt samples provided by the PINP, Victoria, Australia, **Figure 5.8**.

5.3. Methodology and experiments conducted

Experiments were carried out to quantify the evaporation, over time, of the oils listed in **Table 5.1**, from two different substrates, namely, Little Penguin pelt and Petri dish glass (the control). Thus, initial trials and three experiments (within two blocks), *vide supra*, were conducted over two different time periods, ~10 hours and ~21 days, and at two different temperatures, ~16 and ~20 °C, as follows:

Initial trials: Trial evaporation experiments from Little Penguin pelt and a glass surface (control) were carried out in the Group’s “Ambient Laboratory” (Room 2131, Werribee Campus) that was subjected to conventional air conditioning, at ~20 °C. Initially, these evaporation experiments were conducted for all the oils in **Table 5.1**, for up to ~ 5 hours each, with measurements made every 10 minutes. The purpose of these trials was to test the equipment, assess the effects of drafts and traffic, test temperature stability and determine the best pelt size. Based on these trials, it was decided to conduct **Experiments 1 and 3** in a dedicated temperature-controlled lab, dubbed the “The Potter Lab”, at a thermostated temperatures of ~20 °C and ~16 °C, for experiments of up to 21 days duration, and to conduct **Experiment 2** in the dedicated “Ambient Lab” at ~20 °C for experiments of up to 10 hours duration.

Experiments 1 and 2, below, were conducted to explore the evaporation profiles of crude oils from pelt and glass, where both the short (up to 10 hours) and long term (up to 21 days) profiles are revealed. *Most evaporation profiles in the literature take measurements daily over a period of weeks and do not reveal any information on the initial stage of this process.* Such initial information is vital for understanding the effects of volatiles on wildlife, since the first hours are a crucial period with respect to health effects. Thus, the data obtained from **Experiments 1 and 2** are complementary. **Experiment 3**, has been conducted to assess the effect of a lower ambient temperature on the evaporation profiles of different oils from plumage, again referenced to a glass surface as a control. Here the data from **Experiment 1** may be directly

compared to the data from **Experiment 3**, and, in this regard, these two experiments are also complementary.

Experiment 1: Oil evaporation from a penguin pelt and a glass surface (control) over ~21 days at 20 ± 1 °C in the “Potter Lab”.

These experiments were conducted for the six (asterisked/highlighted) oils described in **Table 5.1**, *vide supra*. A section of penguin pelt was placed into a petri dish and approximately 1 g of an oil was dispensed onto the centre of the pelt. The weight of the oiled pelt plus the Petri dish was immediately measured and recorded *daily* until the weight became constant, this took up to ~21 days. Simultaneously, a standard Petri dish was weighed using the analytical balance. Approximately 1 g of a particular oil was then dispensed onto the centre of the petri dish, **Figure 5.7**. The weight of the oil plus the Petri dish was then immediately measured and recorded *daily* until the weight became constant; this also took up to 21 days. The results were plotted as the % wt. loss vs time (days), as nested curves to reveal the relative evaporation profiles for the different oils, in relation to the pelt and the glass control surface. **Figures. 5.9 and 5.10**¹³ show representative sets of such curves for Diesel. All other such curves are given in the **Appendix 5**.

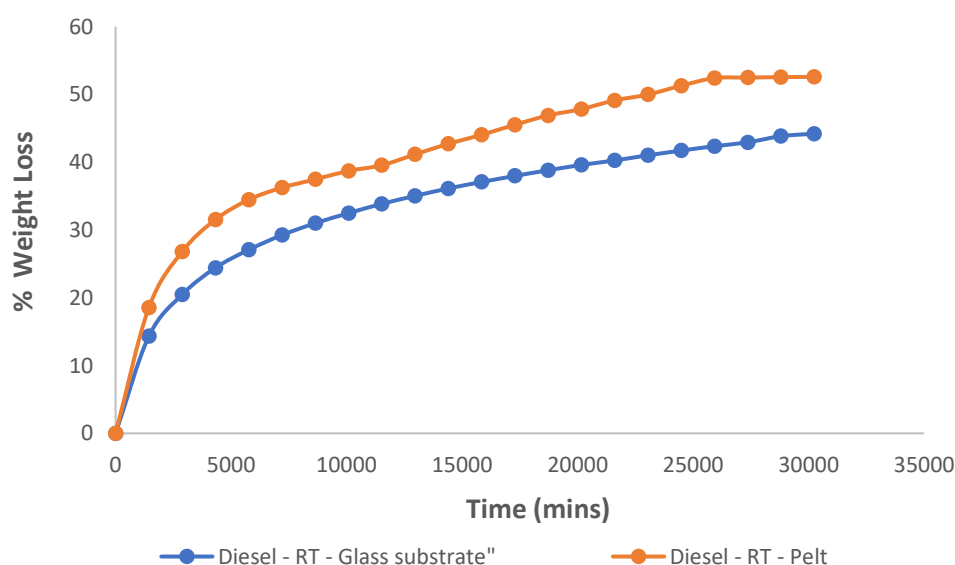


Figure 5.9. Comparative evaporation profiles of Diesel from pelt and glass over ~21 days, at a controlled temperature of 20 ± 1 °C, in the “Potter Lab”. Note that 1 day = 1,440 minutes, 21 days = 30,240 min.

¹³ The details of the mathematical modelling of the data are discussed later in Section 5.4.

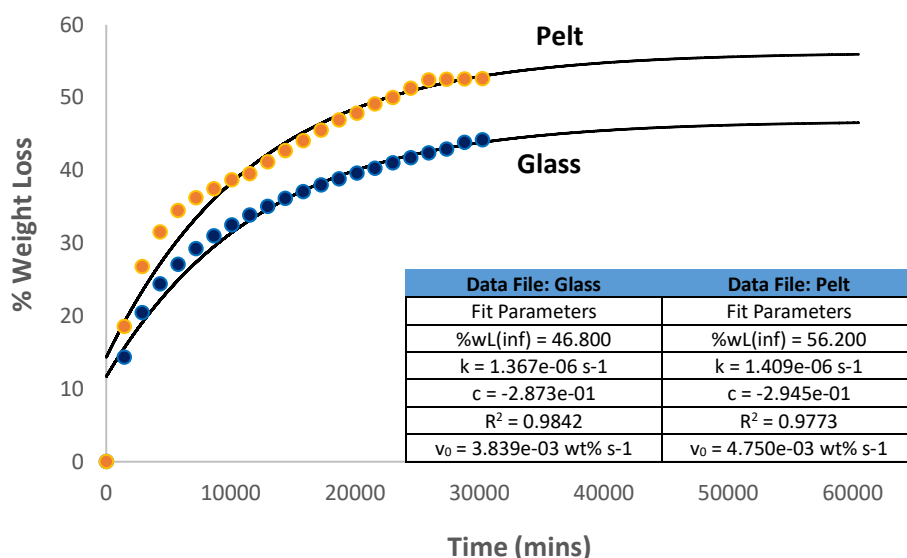


Figure 5.10. Comparative evaporation profiles of Diesel from glass and pelt over ~21 days, at a controlled temperature of 20 ± 1 °C, in the “Potter Lab”, showing the OilVap fit curves for the data presented in **Figure 5.9**. Note that 1 day = 1,440 minutes, 21 days = 30,240 min. The inset gives the OilVap output data for the relevant: plateau, fit and rate parameters for each curve. This is discussed further in the text in Section 5.4.

Experiment 2: Oil evaporation from penguin pelt and a glass surface (control) over ~10 hours at 20.0 ± 1.5 °C in the “Ambient Lab”.

These experiments were conducted for all eleven oils described in **Table 5.1**, *vide supra*. A section of penguin pelt was placed into a petri dish and approximately 1 g of an oil was dispensed onto the centre of the pelt. The weight of the oiled pelt plus the Petri dish was immediately measured and recorded *every 10 minutes* until the weight became constant, this took up to 10 hours. Simultaneously, a 100mm Petri dish was weighed using the analytical balance. Approximately 1 g of a particular oil was then dispensed onto the centre of the petri dish. The weight of the oil plus the Petri dish was then immediately measured and recorded *every 10 minutes* until the weight became constant; this also took up to 10 hours. The results were plotted as the % wt. loss vs time (days), as nested curves, to reveal the relative evaporation profiles for the different oils, in relation to the pelt and the glass control surface. **Figures 5.11 and 5.12** show representative sets of such curves for Diesel. All other such curves are given in the **Appendix 5**.

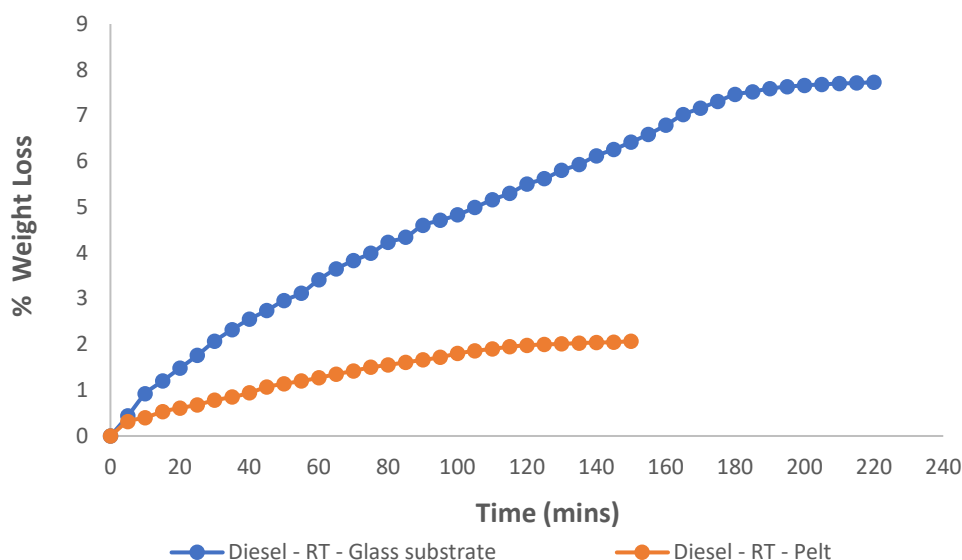


Figure 5.11. Comparative evaporation profiles of Diesel from pelt and glass over hours, at a controlled temperature of 21 ± 1 °C. Note that 10 hours = 600 min.

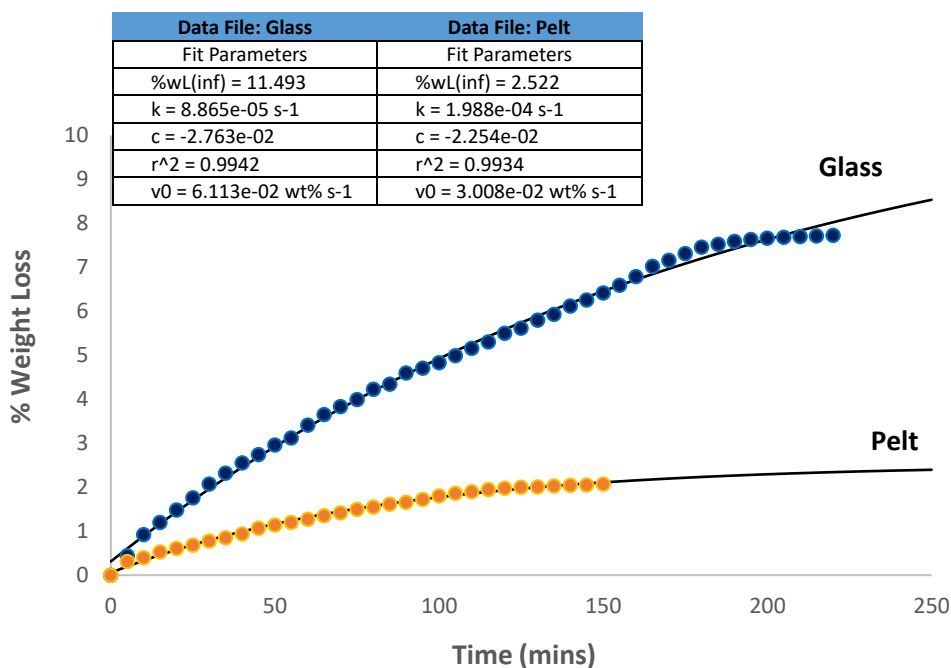


Figure 5.12. Comparative evaporation profiles of Diesel from glass and pelt over hours, at a controlled temperature of 21 ± 1 °C, showing the OilVap fit curves for the data presented in **Figure 5.11**. The inset gives the OilVap output data for the relevant plateau, fit and rate parameters for each curve. This is discussed further in the text in Section 5.4.

Experiment 3: Oil evaporation from penguin pelt and a glass surface (control) over ~21 days at 16 ± 1 °C in the “Potter Lab”.

These experiments were conducted for the six (asterisked/highlighted) oils described in **Table 5.1**, *vide supra*. A section of penguin pelt was placed into a petri dish and approximately 1 g of an oil was dispensed onto the centre of the pelt. The weight of the oiled pelt plus the Petri dish was immediately measured and recorded *daily* until the weight became constant, this took up to 21 days. Simultaneously, a standard Petri dish was weighed using the analytical balance. Approximately 1 g of a particular oil was then dispensed onto the centre of the petri dish. The weight of the oil plus the Petri dish was then immediately measured and recorded *daily* until the weight became constant; this also took up to 21 days. The results were plotted as the %weight loss vs time (days), as nested curves, to reveal the relative evaporation profiles for the different oils, in relation to the two different temperatures. **Figure 5.13** and **Figure 5.14** shows representative sets of such curves for Diesel. All other such curves are given in the **Appendix 5**.

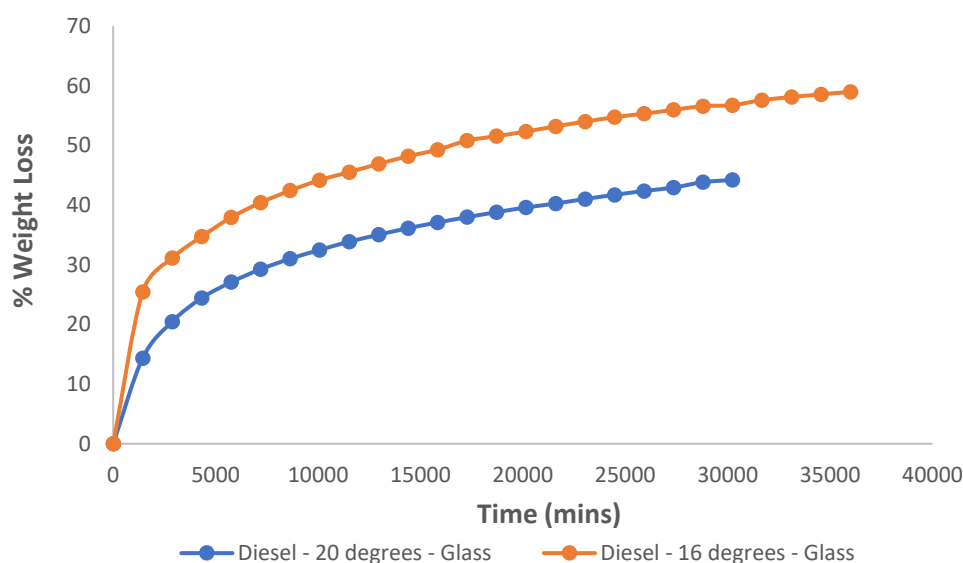


Figure 5.13. Comparative evaporation profiles of Diesel from glass over ~21 days, at a controlled temperature of 20 ± 1 °C and 16 ± 1 °C. Note that 1 day = 1,440 minutes, 21 days = 30,240 min.

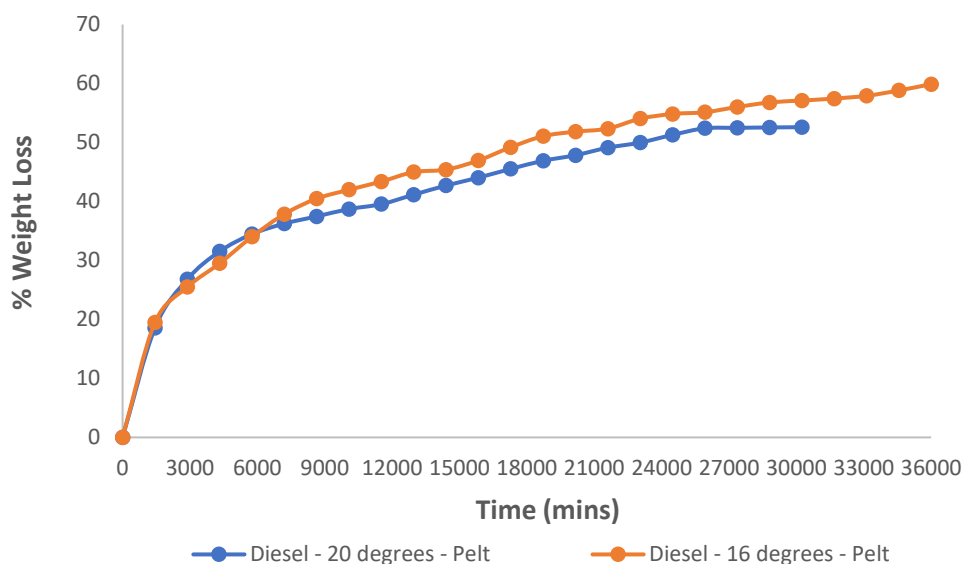


Figure 5.14. Comparative evaporation profiles of Diesel from pelt over ~21 days, at a controlled temperature of 20 ± 1 °C and 16 ± 1 °C. Note that 1 day = 1,440 minutes, 21 days = 30,240 min.

5.4. Mathematically modelling the data

The above evaporation data from **Experiments 1, 2 & 3** are given by 23 nested curves in total, including the representative curves shown in **Figures 5.9 to 5.14**, *vide supra*. The full set of such curves is provided in the **Appendix**. The observed logarithmic form of these curves is well established in the literature (Fingus, 2014).

To analyse and compare these curves, all such data has been fitted to a first order kinetics equation utilizing the **OilVap-v1** software developed by Professor Stephen Bigger of Victoria University¹⁴. The software is designed to fit the %wt. loss versus time by an iterative process. Representative examples of such “fitted” curves, for the Diesel data, is shown in **Figures 5.10 and 5.12**, *vide supra*. The full set of these fitted curves is provided in the **Appendix 5**.

¹⁴ User information on this software is provided in the Appendix.

For the OilVap software, the relevant first order equation is as follows:

$$\%wL = \%wL_{inf}[1 - \exp(-kt + c)]$$

where $\%wL_{inf}$ is the asymptotic value of the percentage weight loss after infinite time (the plateau), k is the first-order rate constant, and c is a constant that indicates how closely the model fits to first-order kinetics. Therefore, if $c = 0$, the fit is perfectly characterised by the first-order kinetic equation:

$$\%wL = \%wL_{inf}[1 - \exp(-kt)]$$

The software also calculates the linear regression coefficient fit parameter, r^2 , and the initial rate, v_0 , according to the equation:

$$v_0 = k \times \%wL_{inf}$$

5.5. Results and discussion

The five relevant parameters, namely, $\%wL(\mathbf{inf})$ (the plateau), k , (rate constant), c (closeness of fit to first order kinetics), r^2 (regression coefficient) and v_0 (initial evaporation rate) for each curve are given in **Tables 5.2 to 5.4**.¹⁵

Table 5.2. OilVap Parameters for ~20 °C “Potter Lab” **Experiment 1** for Little Penguin Pelt and (Glass), experiments up to 21 days.

Oil	$\%wL(\mathbf{inf})$	k (e-06 s-1)	$-c$ (e-01)	r^2	v_0 (e-03 wt% s-1)
Diesel	56.200 (46.800)	1.409 (1.367)	2.945 (2.873)	0.9773 (0.9842)	4.750 (3.839)
Kerosene	99.923 (99.891)	7.154 (4.425)	9.487 (4.027)	0.9012 (0.9975)	42.89 (26.52)
Bohai Bay Crude	21.900 (15.000)	1.655 (1.434)	7.189 (6.483)	0.9312 (0.9576)	2.174 (1.291)
Ikan Pari Crude	53.0000 (31.500)	1.922 (1.364)	7.101 (3.978)	0.9429 (0.9757)	6.112 (2.578)
Bunker 180	21.400 (11.200)	1.459 (1.325)	4.680 (3.521)	0.9559 (0.9733)	1.873 (0.8906)
Bunker 380	22.000 (10.600)	1.682 (1.382)	5.184 (3.892)	0.9467 (0.9801)	2.220 (0.8790)

¹⁵ All decimal places have been retained in these tables as this represents the software output.

Table 5.3. OilVap Parameters for ~21 °C Ambient Lab Experiments for Little Penguin Pelt and (Glass). **Experiment 2** up to ~ 10 hours.

Oil	%wL(inf)	k (e-04 s-1)	-c (e-01)	r ²	v ₀ (e-02 wt% s-1)
Sakhalin Crude	33.781 (29.919)	2.636 (3.194)	1.472 (2.187)	0.9908 (0.9943)	53.42 (57.34)
Tapis Crude	21.692 (17.127)	1.570 (5.778)	0.9971 (4.849)	0.9940 (0.9725)	20.44 (59.37)
Margham Condensate Crude	32.697 (39.653)	1.943 (2.123)	1.312 (2.308)	0.9951 (0.9965)	38.12 (50.50)
Merinie Crude	18.233 (21.577)	1.497 (1.958)	1.140 (3.253)	0.9983 (0.9917)	16.38 (25.35)
Murban Crude	21.800 (24.800)	1.622 (2.725)	1.459 (3.848)	0.9953 (0.9870)	21.22 (40.55)
Diesel	2.522 (11.493)	1.988 (0.8865)	0.2254 (0.2763)	0.9934 (0.9942)	3.008 (6.113)
Kerosene	17.823 (35.200)	1.922 (1.661)	0.08949 (0.2791)	0.9930 (0.9875)	20.55 (35.08)
Bohai Bay Crude	3.393 (5.511)	1.588 (2.621)	1.012 (0.7424)	0.9947 (0.9960)	3.233 (8.668)
Ikan Pari Crude	16.857 (14.212)	2.632 (1.770)	0.01683 (1.078)	0.9888 (0.9958)	26.63 (15.09)
Bunker 180	1.193 (1.134)	1.796 (2.071)	0.1503 (0.5708)	0.9989 (0.9945)	1.286 (1.409)
Bunker 380	1.500 (1.291)	0.8206 (1.449)	0.08321 (0.07270)	0.9982 (0.9983)	0.7386 (1.122)

Table 5.4. OilVap Parameters for 16 °C “Potter Lab” **Experiment 3** for Little Penguin Pelt and (Glass), experiments up to ~21 days.

Oil	%wL(inf)	k (e-06 s-1)	-c (e-01)	r ²	v ₀ (e-03 wt% s-1)
Diesel	63.000 (61.000)	1.171 (1.313)	3.018 (4.086)	0.9864 (0.9840)	4.427 (4.806)
Kerosene	95.900 (98.600)	9.268 (24.04)	3.696 (0.1358)	0.9830 (0.9999)	53.33 (142.2)
Bohai Bay Crude	13.100 (18.400)	1.124 (1.234)	3.149 (7.559)	0.9514 (0.9552)	0.8832 (1.362)
Ikan Pari Crude	39.000 (37.000)	1.248 (1.119)	3.735 (2.652)	0.9810 (0.9889)	2.921 (2.485)
Bunker 180	10.500 (10.200)	0.5885 (0.8105)	0.6472 (1.093)	0.9475 (0.9965)	0.3708 (0.4960)
Bunker 380	-	-	-	-	-

For the data presented in **Tables 5.2 to 5.4**, there are *three categories of parameter* to consider. Firstly, %wL(inf) represents the “plateau” for a given logarithmic curve. The second category, containing the parameters -c and r², represent how well the data is modelled by first order kinetics and the goodness of fit of the modelled curve (ideally with values of 0 and 1 respectively). The third category of parameters includes k and v₀ and are “rate of evaporation” parameters, i.e., the **first order rate constant** and the **initial rate parameter**, respectively. The parameters -c and r² are discussed first since they provide a validation for the use of first order kinetics modelling. **Table 5.5** summarizes the average parameters for the three experiments. This data shows that, overall, the first order kinetics model is an accurate representation, and that the goodness of fit is generally excellent.

Table 5.5. A summary of the average -c and r² parameters for **Experiments 1 to 3** extracted from the data provided in **Tables 5.2 to 5.4**.

Experiment 1 - Table 5.2			
Parameter	Little Penguin Pelt	Glass	
-c	0.61	0.41	Ideally 0
r ²	0.94	0.98	Ideally 1.0
Experiment 2 - Table 5.3			
	Little Penguin Pelt	Glass	
-c	0.07	0.18	Ideally 0
r ²	1.00	0.99	Ideally 1.0
Experiment 3 - Table 5.4			
	Little Penguin Pelt	Glass	
-c	0.29	0.31	Ideally 0
r ²	0.97	0.99	Ideally 1.0

With respect to the relative %wL(inf) parameters (the plateau values), for evaporation from Little Penguin Pelt and Glass, for the three experiments, this data is represented by the histograms shown in **Figures 5.15 to 5.17**. Thus **Figure 5.15** shows the comparative %wL(inf) parameters for the evaporation of six oils from Little Penguin Pelt and Glass at ~20 °C, up to ~21 days, **Experiment 1**. Under these experimental conditions, for all the oils except kerosene, the **Total Volatile Fraction (TVF)**, see **Figure 5.25**, is greater for the evaporation from pelt than it is for glass. Correspondingly, the residual contaminant, i.e., the **Recalcitrant Fraction (RF)**, is less for the evaporation from pelt than it is for glass. This demonstrates that the evaporation profile is substrate specific. The actual comparative TVF and RF values are summarized in **Table 5.6**.

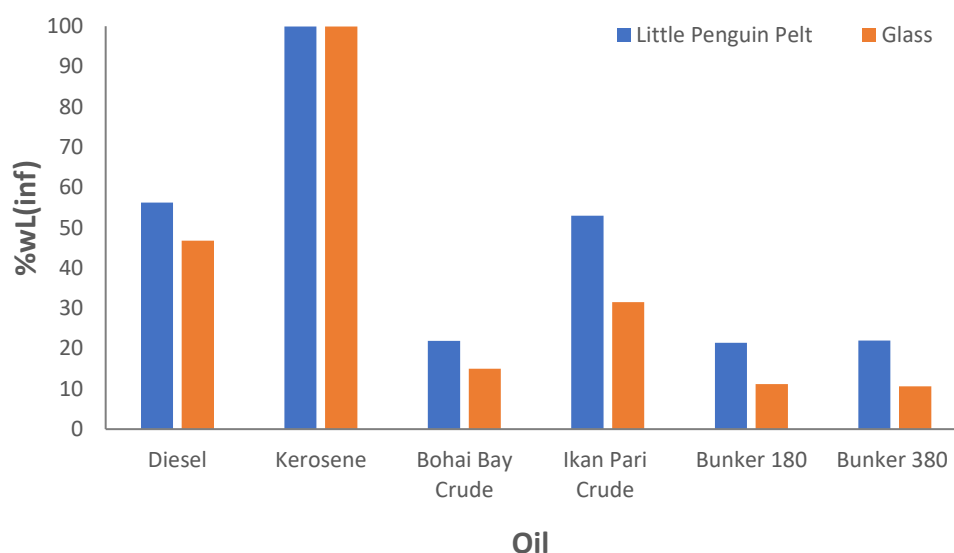


Figure 5.15. Comparative %wL(inf) (plateau) parameters for the evaporation of six oils from Little Penguin Pelt and Glass at ~20 °C up to ~21 days in the Potter Lab – **Experiment 1**.

Figure 5.16 shows the comparative %wL(inf) parameters for the evaporation of all eleven oils from Little Penguin Pelt and Glass at ~21 °C, up to ~10 h – **Experiment 2**. Under these experimental conditions, for all the oils, except Sakhalin and Tapis, the **Highly Volatile Fraction (HVF)**¹⁶, **Figure 5.25**, is greater for the evaporation from glass than it is for pelt. This is an interesting observation since it suggests that for these nine oils, the volatiles are trapped within the plumage, the opposite of what is observed in **Experiment 1**. This % trapping may then be calculated, **Table 5.6**. Notably, trapping is very high for Diesel, Kerosene and Bohai Bay.

¹⁶ The so-called Highly Volatile Fraction (HVF) refers to the plateau that is formed during the initial evaporation phase, a new discovery, that is described in detail later, see **Figure 5.25**.

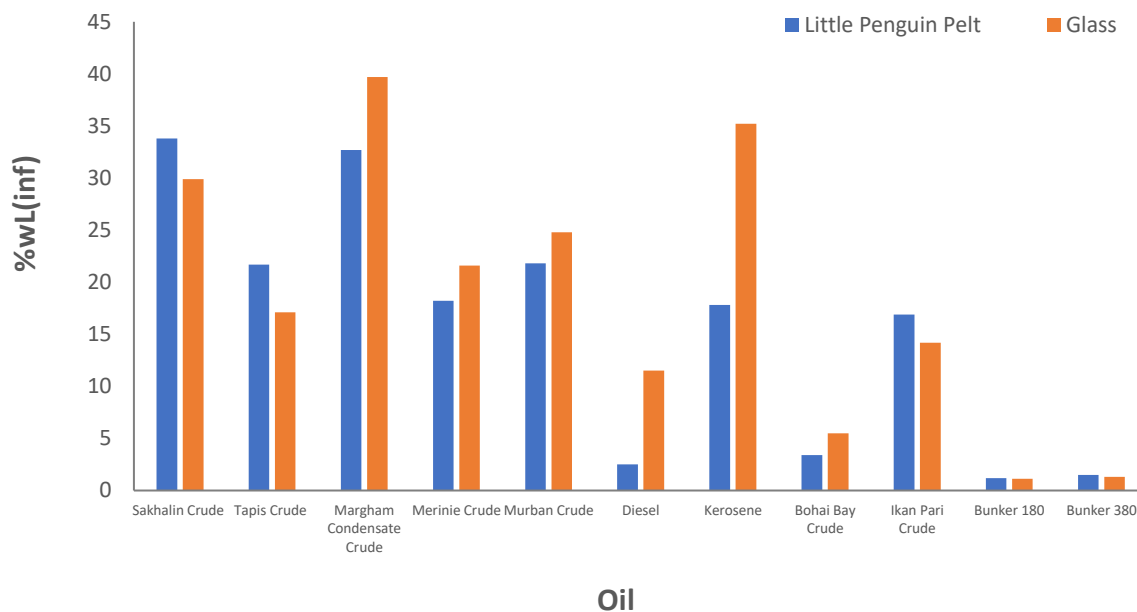


Figure 5.16. Comparative %wL(inf) parameter for the evaporation of all eleven oils from Little Penguin Pelt and Glass at ~21 °C up to 10 hours in the “Ambient Lab” – **Experiment 2.**

Figure 5.17 shows the comparative %wL(inf) parameters for the evaporation of all five oils from Little Penguin Pelt and Glass at ~16 °C, up to ~21 days – **Experiment 3.** Under these experimental conditions, for all the oils, except Sakhalin and Tapis, the **Total Volatile Fraction (TVF)**, **Figure 5.25**, is greater for the evaporation from glass than it is for pelt for Kerosene and Bohai Bay, but less from glass compared to pelt for Diesel, Ikan Pari and Bunker180. This suggests that, at lower temperatures, trapping of volatiles in the plumage can also occur for the TVF.

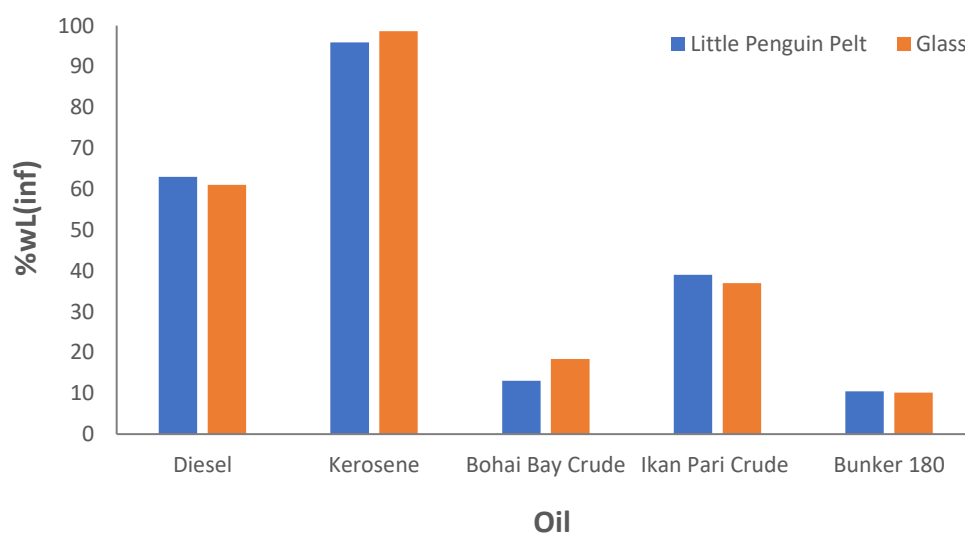


Figure 5.17. Comparative %wL(inf) parameter for the evaporation of six oils from Little Penguin Pelt and Glass at ~16 °C up to ~21 days in the Potter Lab – **Experiment 3.**

The relative values of the k and v_0 parameters with respect to evaporation from Little Penguin Pelt and Glass for the three experiments, as derived from the data in **Tables 5.2 to 5.4**, is shown in **Figures 5.18 to 5.23**.

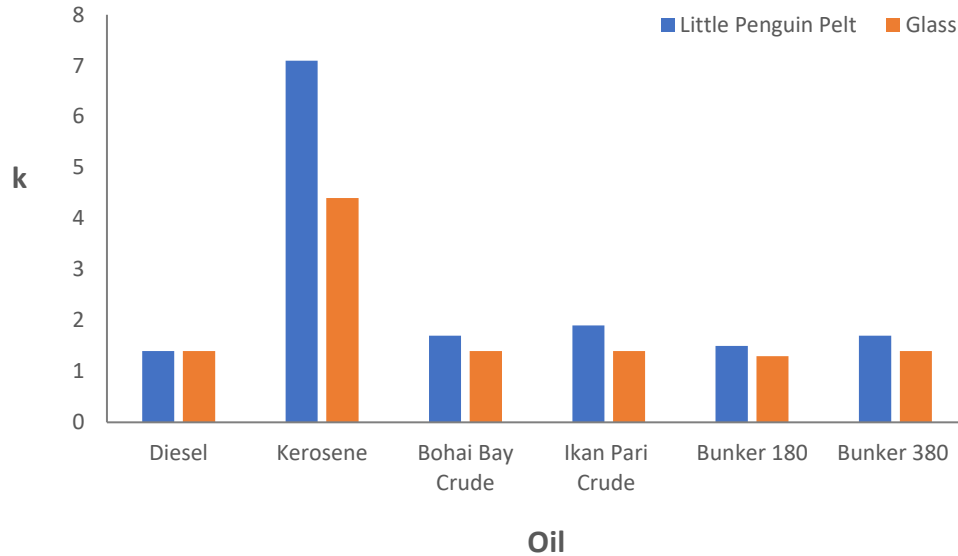


Figure 5.18. Comparative k parameter with reference to the evaporation profile for Little Penguin Pelt and Glass at ~ 20 °C - **Experiment 1**.

The data for **Figure 5.18** shows that the overall evaporation rate for kerosene, for both substrates - but particularly from pelt, is considerably higher than for all the other oils. This is related to the fact that kerosene is totally volatile under these conditions, with no recalcitrant fraction, **Table 5.6**. For the remaining oils, as with kerosene, the rate of evaporation from pelt is greater than that from the glass control and the magnitudes are comparable. This could be related to the fact that the oil on pelt is evaporating from a greater surface area.

The data for **Figure 5.19** shows that the initial evaporation rate for all oils mirrors the data for the overall evaporation rate, **Figure 5.18**. This is not unexpected and is also probably related to the higher surface area of the pelt.

The comparative data of **Figure 5.20** shows that for eight of the eleven oils, the overall evaporation rate is greater from the glass than from the pelt. This overall evaporation rate for the **HVF** is the opposite of what was observed for the **TVF**, **Figure 5.18**. This is a rather anomalous outcome and is supportive of the notion that the components of the **HVF** have

specific chemical characteristics. This is certainly worth further investigation but is beyond the scope of the current project.

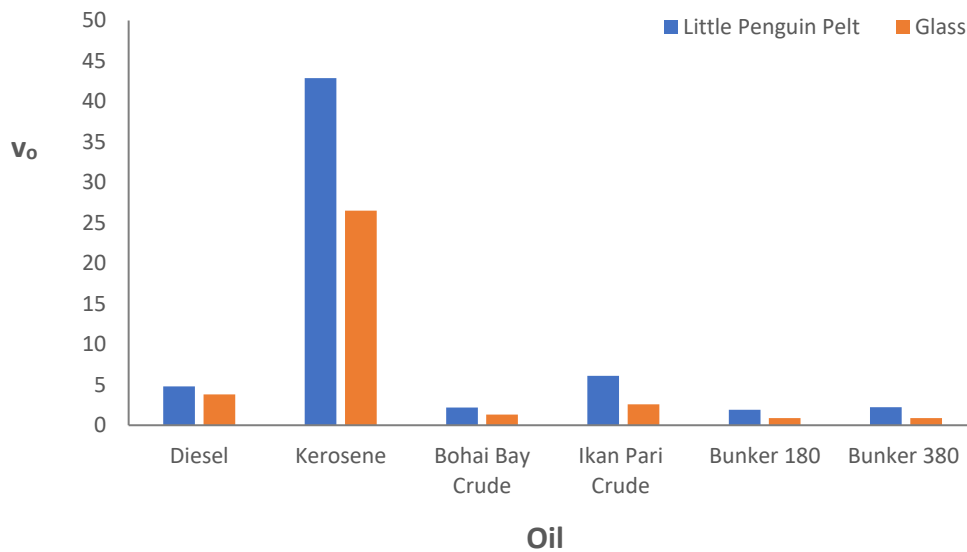


Figure 5.19. Comparative v_0 parameters with reference to the evaporation profile for Little Penguin Pelt and Glass at $\sim 20^\circ\text{C}$ - **Experiment 1.**

The data of **Figure 5.21** to some extent mirrors that of **Figure 5.20**. However, there are some interesting differences. For example, the initial evaporation rates for Diesel and Kerosene are now less for pelt, although Ikan Pari remains the same. A complete explanation of this data would require a consideration of the chemical composition of these oils, which is beyond the scope of this thesis.

The data for **Figure 5.22** demonstrates that, at a lower temperature, the overall rate of evaporation for kerosene is now greater from glass than from pelt compared to the higher temperature experiments, **Figure 5.19**. It may also be seen that the overall evaporation rates for the other oils are similar from both surfaces, demonstrating that for a lower temperature the overall evaporation rate from both surfaces tends to equalize. The same hold true for the initial evaporation rate shown in **Figure 5.23**.

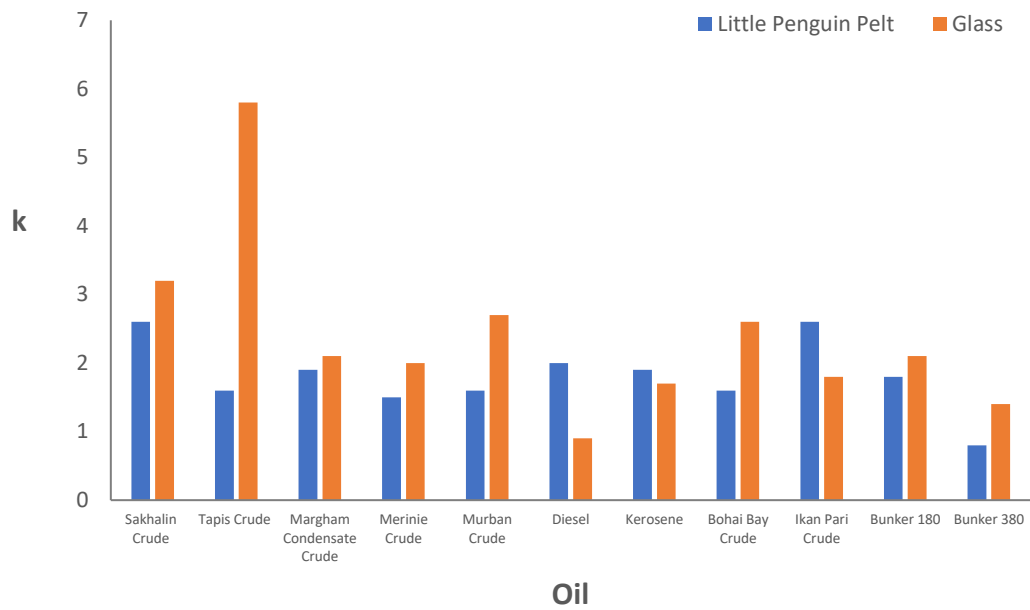


Figure 5.20. Comparative k parameter with reference to the evaporation profile for Little Penguin Pelt and Glass at ~ 21 °C.

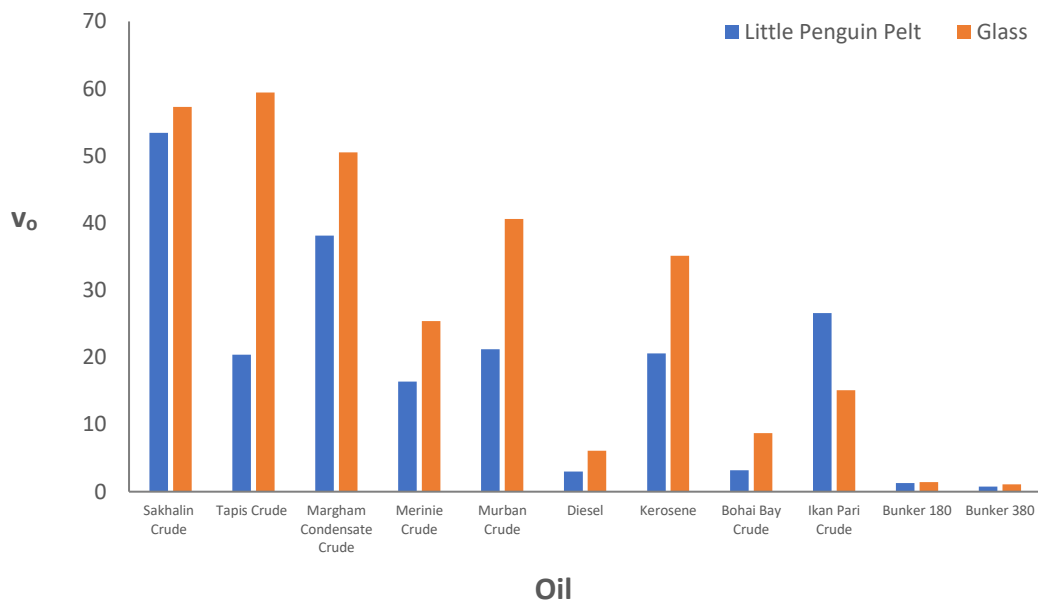


Figure 5.21. Comparative v_0 parameter with reference to the evaporation profile for Little Penguin Pelt and Glass at ~ 21 °C - Experiment 2.

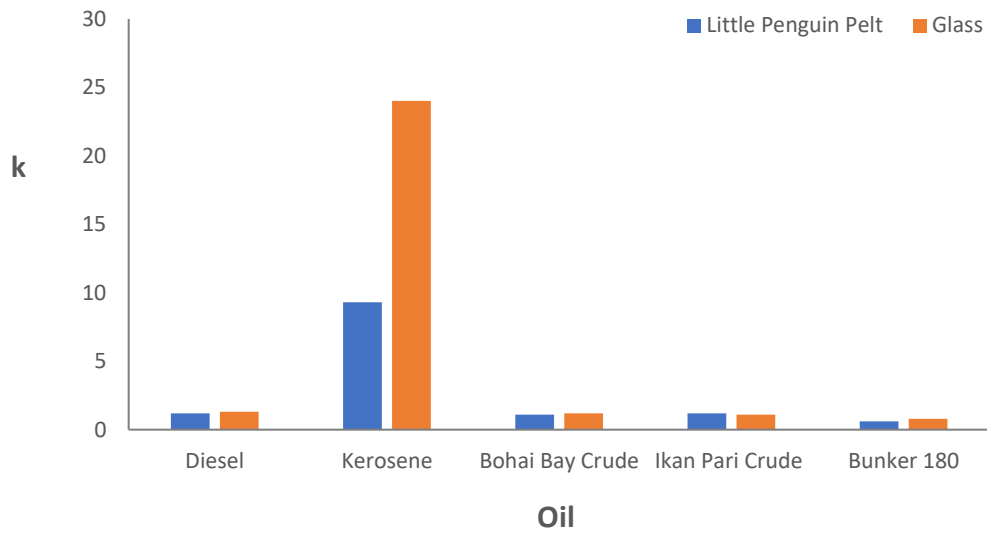


Figure 5.22. Comparative k parameter with reference to the evaporation profile for Little Penguin Pelt and Glass at $\sim 16^\circ\text{C}$ – Experiment 3.

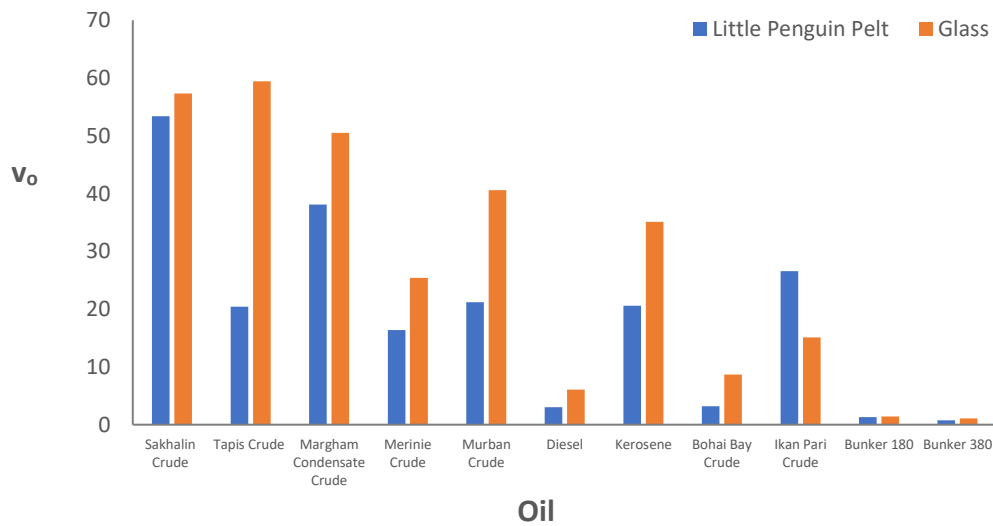


Figure 5.23. Comparative v_0 parameter with reference to the evaporation profile for Little Penguin Pelt and Glass at $\sim 16^\circ\text{C}$.

5.5.1 Block 1 (Experiments 1 & 2)

It should be recognized that the volatile components that are likely to be of particular concern, are the ones that are present on the plumage for shorter periods of time, e.g., less than a day. Although these may well evaporate over a period of hours, they represent volatiles that are particularly toxic and corrosive, and this makes it imperative to remove them as soon as possible¹⁷. We are also interested to investigate to what extent such volatiles become trapped in the plumage¹⁸. In order to answer these research questions, the above experiments were designed to investigate the evaporation of these volatiles during the first 10 hours at ~20 °C, i.e., to resolve the first 10 hours of the evaporation profiles that are measured over an ~21-day period. The data from these experiments are given in **Tables 5.2 and 5.3**. Representative curves for these (nested) evaporation experiments are given in **Figure 5.9 to 5.12**. All other such (nested) curves are provided in the **Appendix**.

Thus, the data represented in **Table 5.2** were from experiments conducted over ~21 days at ~20 °C, **Experiment 1** and were aimed at investigating the extent of evaporation of volatiles from penguin pelt (**TVF**) and the amount of residual oil (**RF**) remaining on the plumage, after two to three weeks. The data represented in **Table 5.3** were from experiments conducted over ~10 hours at ~20 °, **Experiment 2** and were aimed at resolving the initial evaporation profile. These two sets of data are therefore complementary with respect to the six oils that they these experiments have in common.

Interestingly, the evaporation experiments tracked specifically over a period of hours reveal that there is an *initial* evaporation phase followed by a latency period. During this phase, it is evident that for some oils, the evaporation rate is lower for these components, suggesting that they are effectively trapped or retained within the plumage. This situation is reversed after the latency period, where the retained heat within the plumage now leads to a higher rate of evaporation from the plumage compared to the glass control, and the evaporation process continues to a new plateau.

¹⁷ The highly portable magnetic cleansing technology (the “wand”) developed by this group can remove 100% of such volatiles in a matter of minutes.

¹⁸ Evidence for volatiles being trapped in the plumage is when the evaporation from the glass control surface exceeds that from the pelt.

Thus, for the evaporation of a crude oil from a given substrate at a given temperature, this current research has demonstrated for the first time that there is a unique initial evaporation phase that occurs over a matter of hours, whereby certain volatile components may become “trapped” within the plumage. Notably, the phenomenon is observed for a wide range of oils and is described in more detail in **Section 5.2 and Section 5.3**.

5.5.2 Block 2 (Experiments 1 & 3)

The data summarized in **Table 5.3** were from (**Experiment 3** conducted over ~21 days at ~16 °C and were designed to investigate the effect of a lower temperature on evaporation profiles. Thus, these data may be compared with the data of **Experiment 1**, conducted over ~21 days at ~20 °C. Comparative TVF values for evaporation from pelt are tabulated in **Table 5.6** and histogrammed in **Figure 5.24**.

Table 5.6. The **Total Volatile Fraction (TVF)** for evaporation of the oils shown from Penguin Pelt after 21 days, at ~20 °C compared to ~16 °C.

	TVF 20 °C - Pelt	TVF 16 °C - Pelt
Diesel	56.2	63
Kerosene	99.9	95.9
Bohai Bay	21.9	13.1
Ikan Pari	53	39
Bunker 180	21.4	10.5

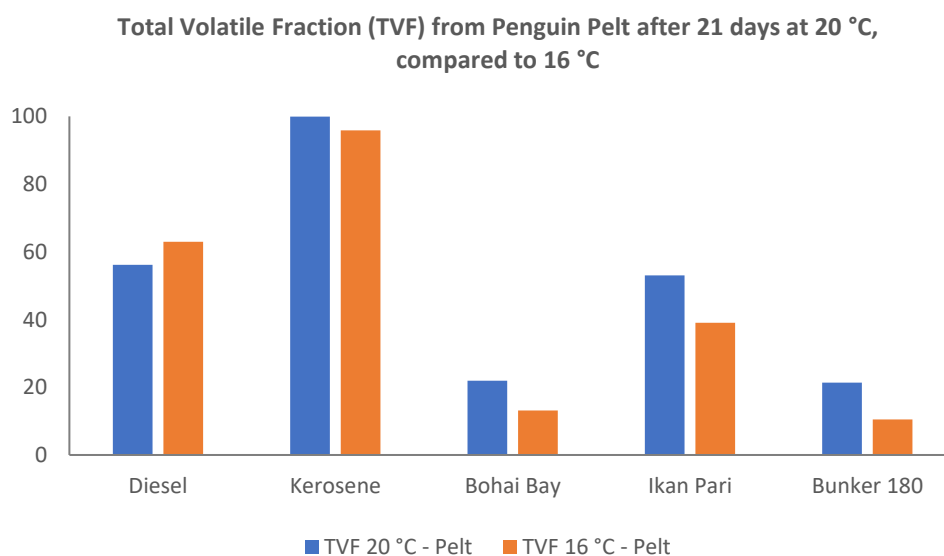


Figure 5.24. Comparative **Total Volatile Fraction (TVF)** profiles of light, medium and heavy crude oils from penguin pelt after 21 days, at controlled temperatures of 20 °C and 16 °C.

As can be seen from **Table 5.6** and **Figure 5.24** more evaporation occurs from pelt at 20 °C than at 16 °C, except for Diesel. This suggests a propensity for Diesel to be trapped in the plumage. An analogous comparison from a glass control substrate is shown in **Table 5.7** and **Figure 5.25**.

Table 5.7. The **Total Volatile Fraction (TVF)** for the evaporation of the oils shown from Glass after 21 days at 20 °C, compared to 16 °C.

	TVF 20 °C - Glass	TVF 16 °C - Glass
Diesel	46.8	61
Kerosene	99.9	98.6
Bohai Bay	15	18.4
Ikan Pari	31.5	37
Bunker 180	11.2	10.2

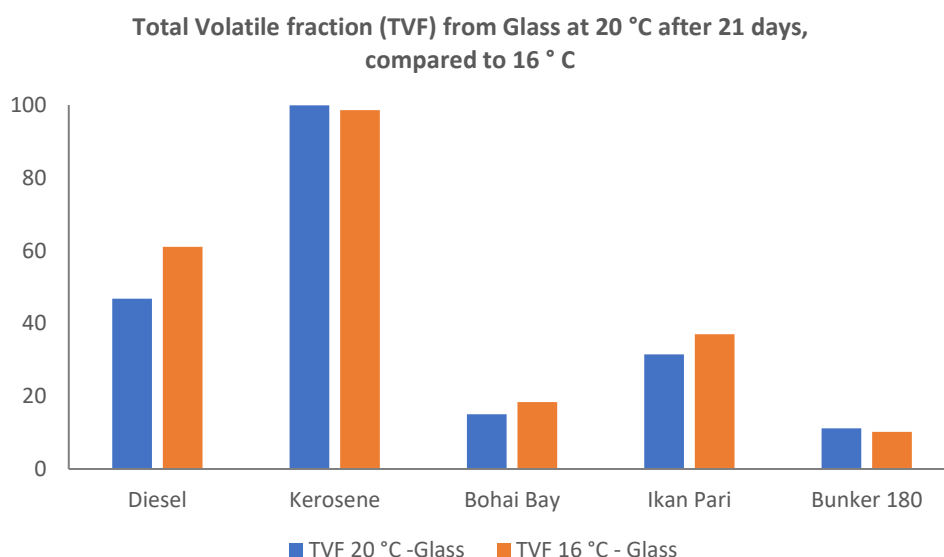


Figure 5.25. Comparative **Total Volatile Fraction (TVF)** profiles of light, medium and heavy crude oils from Glass after 21 days, at a controlled temperature of 20 °C and 16 °C.

It can be seen from **Table 5.7** and **Figure 5.25** that evaporation from glass at these two temperatures is essentially equivalent, except for Diesel and perhaps Bohai Bay and Ikan Pari.

Table 5.8. Total Volatile Fraction (TVF) from Penguin Pelt after 21 days at 20 °C, compared to Glass.

	TVF 20 °C - Pelt	TVF 20 °C - Glass
Diesel	56.2	46.8
Kerosene	99.9	99.9
Bohai Bay	21.9	15
Ikan Pari	53	31.5
Bunker 180	21.4	11.2

The results of the TVF from Penguin Pelt after 21 days at 20 °C, compared to Glass are shown in **Figure 5.26**.

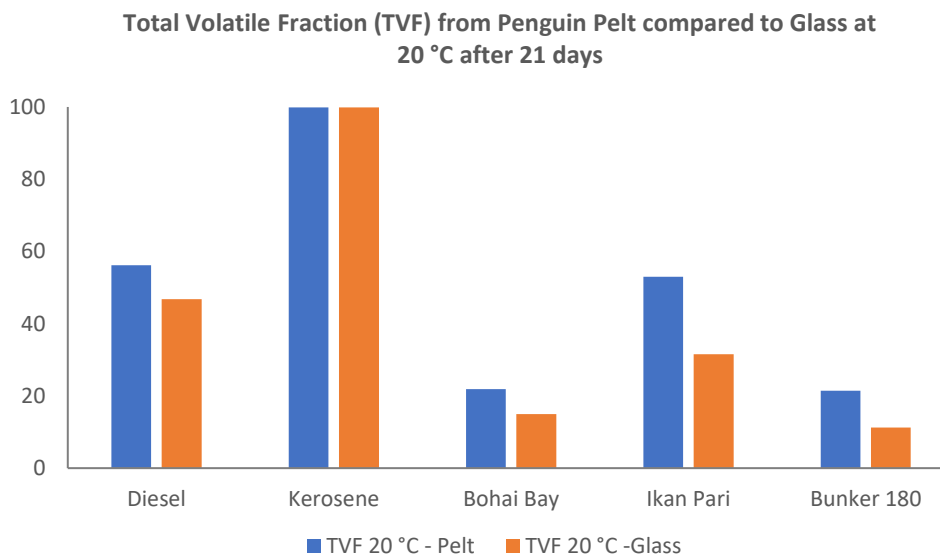


Figure 5.26. Comparative Total Volatile Fraction (TVF) profiles of light, medium and heavy crude oils from Penguin Pelt and Glass after 21 days, at a controlled temperature of 20 °C.

The results from **Table 5.8** and **Figure 5.26** show that at 20 °C there is more evaporation from pelt than from glass, except for Kerosene where it is equivalent (almost 100% in both cases).

Table 5.9. Total Volatile Fraction (TVF) from Penguin Pelt after 21 days at 16 °C, compared to Glass.

	TVF 16 °C - Pelt	TVF 16 °C - Glass
Diesel	63	61
Kerosene	95.9	98.6
Bohai Bay	13.1	18.4
Ikan Pari	39	37
Bunker 180	10.5	10.2

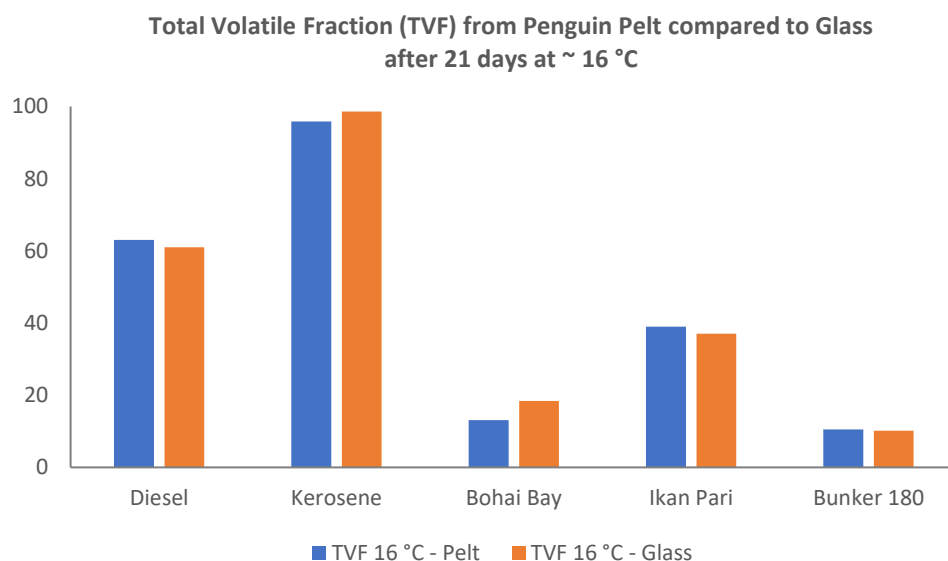


Figure 5.27. Comparative Total Volatile Fraction (TVF) profiles of light, medium and heavy crude oils from Penguin Pelt and Glass after 21 days, at a controlled temperature of 16 °C.

The results of the TVF from Penguin Pelt after 21 days at 16 °C, compared to Glass are shown in **Figure 5.27**.

As can be seen from **Table 5.9** and **Figure 5.27** at 16 °C evaporation from pelt and glass is essentially the same, except for Bohai Bay, that is slightly less from pelt.

5.6. The discovery of the “Highly Volatile Fraction” (HVF)

The plateau for an evaporation curve, represented by $\%wL(\text{inf})$, is where no more evaporation of volatiles from the surface occurs for a given oil type, substrate, and temperature, over a prolonged period. *In these experiments, for each curve, there are two different kinds of plateau that have been discovered.*

For the experiments where measurements are taken daily up to 21 days (**Experiments 1 and 3**), this parameter represents the “Total Volatile Fraction” (TVF) under these conditions. Note that $(100 - \text{TVF})\%$ may be considered to represent a “Recalcitrant (non-volatile) Fraction” (RF). The RF is that fraction of the that remains on the substrate under these conditions, **Figure 5.28**. For the experiments that are conducted up to ~10 hours, where measurements are taken every 10 minutes or so, and where the first part of the complete evaporation profile may be resolved, an *initial plateau* is observed over a shorter period - before the main evaporation process resumes, **Figure 5.28**. This phenomenon has been observed in all the oils studied and, to the best of our knowledge, has not been reported before. Thus, within the first ~ 10 hours of evaporation, there is a distinct category of volatiles that evaporate first, followed by a latency period, after which the evaporation process resumes. We refer to this fraction of volatiles as the **Highly Volatile Fraction (HVF)**, **Figure 5.28**. The remaining volatiles are then referred to as the **Normal Volatile Fraction (NVF)**, such that: **TVF (Total Volatile Fraction) = HVF + NVF**. The overall evaporation phenomenon is represented schematically in **Figure 5.29**.

An experiment was conducted to estimate the duration of the “latency period” associated with the **Highly Volatile Fraction (HVF)** for the evaporation of diesel from a glass surface. The outcome of this experiment is shown in **Figure 5.30**. In this case, the evaporation of the HVF takes ~ 500 min (~ 8.3 h) and the actual latency period (plateau) is ~130 min (~ 2.2 h). Latency period is estimated to be up until the evaporation profile merges with the long-term profile. At the end of the latency period there is a sharp resumption involving the evaporation of the remaining volatile fraction, the NVF, eventually to reach the TVF plateau.¹⁹

¹⁹ This experiment was conducted in the “Ambient Temperature Lab” where the temperature was 23 – 24 °C on that day. Therefore, the actual magnitudes of parameters such as HVF will differ from experiments conducted at 22 - 21 °C. Similar latency periods are observed for the evaporation of all eleven oils studied, both from pelt and from glass.

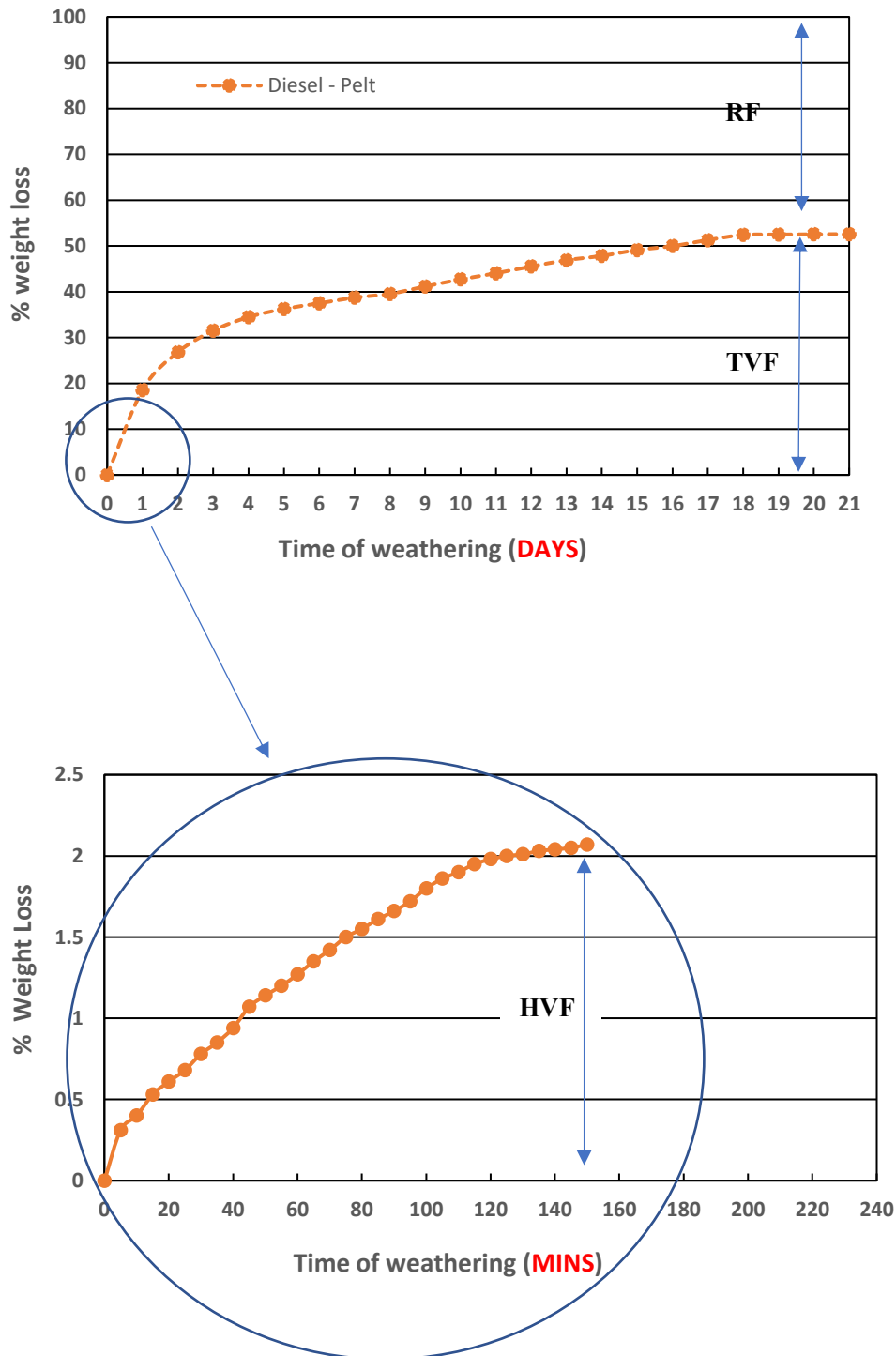


Figure 5.28 The above two graphs provide a representative example of the existence of the **Highly Volatile Fraction (HVF)** for the initial evaporation of Diesel from Little Penguin pelt. The top graph shows the evaporation profile over a long period of time (up to 21 days) whereas the bottom graph shows the evaporation profile over the first three hours; hence resolving the initial stage of the long-term evaporation curve. These experiments were conducted at $\sim 20^{\circ}\text{C}$. The **HVF** typically displays its own plateau and a defined latency period. Notably, some of the components involved in the **HVF** have been shown to become trapped in the plumage, *vide infra*.

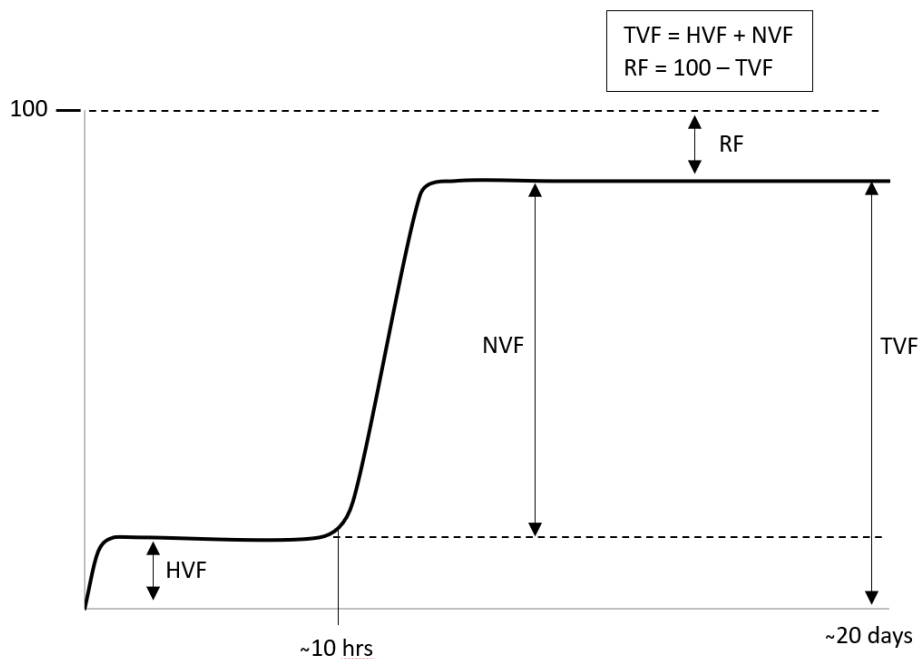


Figure 5.29. A schematic representation of the various fractions during the evaporation of a crude oil from a given surface. **HVF = Highly Volatile Fraction, NVF = Normal Volatile Fraction, TVF = Total Volatile Fraction, RF = Recalcitrant Fraction.** Note that $TVF = HVF + NVF$ and $RF = 100 - TVF$.

The discovery of the “Higher Volatile Fraction” (HVF) in oil contamination, that can remain trapped in plumage for up to 8-9 hours, makes it even more imperative to include an effective “quick clean” into existing stabilization protocols. The presence of such volatiles (both types) for prolonged periods of time is likely to affect the animal's long-term survivability and/or reproductive success.

A tabulation of all the derived **TVF, HVF, NVF and RF** parameters for the evaporation of six oils; namely, Diesel and Kerosene (light), Bohai Bay and Ikan Pari (medium) and, Bunker 180 and Bunker 380 (heavy), is given in **Table 5.10**. Note that these parameters are derived from the **Tables 5.2 and 5.3**.

A set of pie charts comparing the relative **NVF/RF/HVF** values for the three pairs of light, medium and heavy oils; namely, Diesel/Kerosene; Bohai Bay/Ikan Pari; Bunker 180/Bunker 380, is provided in **Figure 5.31**. These comparative pie charts demonstrate, for a given temperature and substrate, the evaporation characteristics for a particular oil. For example, it may be seen that the proportion of the HVF varies considerably and is, perhaps, the most

important consideration for the evaporation from pelt. Thus HVF (Kerosene, 17.8 %) > HVF (Ikan Pari, 16.9 %) > HVF (Bohai Bay, 3.4%) > HVF (Diesel, 2.5 %) > HVF (Bunker 380, 1.5 %) > Bunker 180, 1.2%). This inequality ordering reflects the evaporation from the glass control surface, although the individual magnitudes vary.

Notably, the RF values are quite diverse, but the inequality ordering is not unexpected with RF (heavy oils) > RF (medium oils) > RF (light oils), with kerosene being totally volatile under these conditions (no RF). Kerosene, due to its relatively high HVF and plumage trapping, **Table 5.10** (and to a lesser extent Ikan Pari that also has a relatively high HVF) warrants special attention with respect to providing a quick clean utilizing MPT.

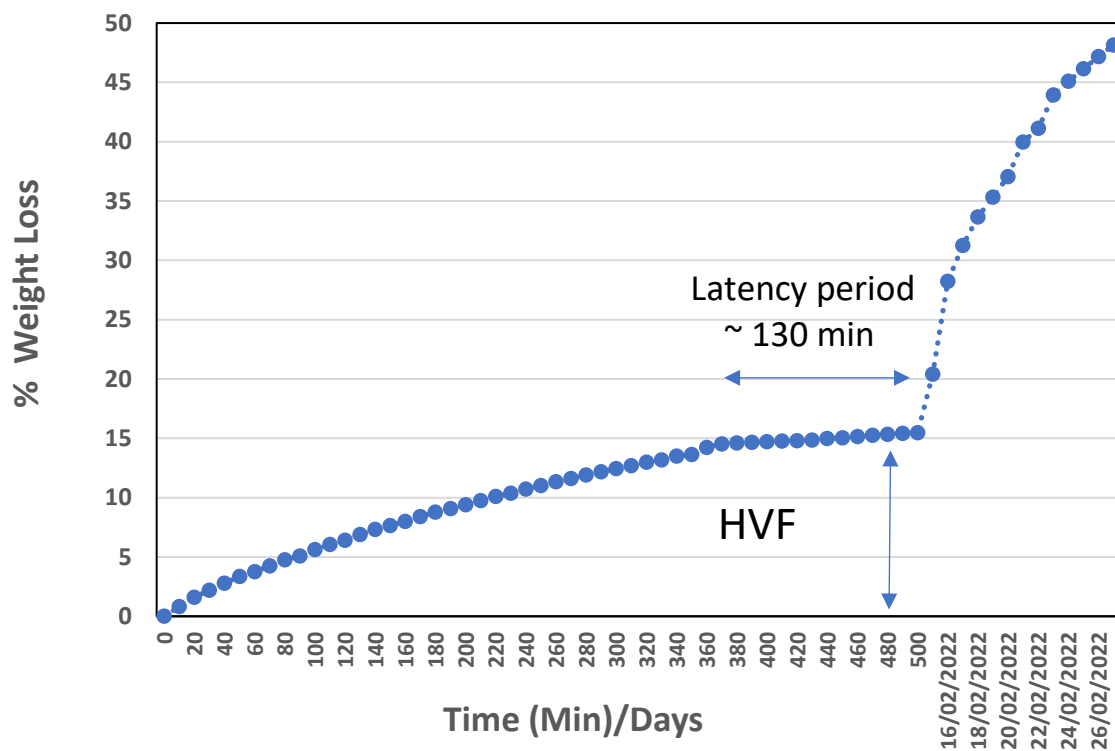


Figure 5.30. Results of an experiment to estimate the duration of the “latency period” associated with the Highly Volatile Fraction (HVF) for the evaporation of diesel from a glass surface. Similar latency periods are observed for the evaporation of all eleven oils studied, both from pelt and from glass. Note how the evaporation resumes to the long-term profile after ~ 500 min (~ 8.3 h). Note: the above experiment was conducted in the “Ambient Temperature Lab” where the temperature was 23 – 24 °C on that day. Therefore, the actual magnitudes of parameters such as HVF will differ from experiments conducted at ~20 °C.

Table 5.10. A tabulation of the relative parameters (derived from **Tables 5.2** and **5.3**) relating to the evaporation of Diesel, Kerosene, Bohai Bay, Ikan Pari, Bunker 180 and Bunker 380 contaminants from Little Penguin Pelt (P) and Glass (G). TVF = Total Volatile Fraction; RF = Recalcitrant Fraction; NVF = Normal Volatile Fraction; HVF = Highly Volatile Fraction. The % of the HVF that is trapped in the plumage during the first evaporation phase is shown in the **right-hand** column. **HVF = Highly Volatile Fraction, NVF = Normal Volatile Fraction, TVF = Total Volatile Fraction, RF = Recalcitrant Fraction. Note that TVF = HVF + NVF and RF = 100 – TVF.**

Oil	TVF (G - 20 °C)	TVF (P - 20 °C)	RF (G - 20 °C)	RF (P - 20 °C)	NVF (G - 20 °C)	NVF (P - 20 °C)	HVF (G - ~21°C)	HVF (P - ~21 °C)	%Trapping by Pelt
Diesel	46.8	56.2	53.2	43.8	35.3	53.7	11.5	2.5	78.1
Kerosene	99.9	99.9	0.1	0.1	64.7	82.1	35.2	17.8	49.4
Bohai Bay	15	21.9	85	78.1	9.4	18.5	5.6	3.4	38.9
Ikan Pari	31.5	53	68.5	47	17.3	36.1	14.2	16.9	-18.6
Bunker 180	11.2	21.4	88.8	78.6	10.1	20.2	1.1	1.2	-4.7
Bunker 380	10.6	22	89.4	78	9.3	20.5	1.3	1.5	-16.2

Figure 5.31. Comparative values of NVF, RF and HVF for the evaporation the light, medium and heavy pairs of oil from plumage and glass at ~20 °C. Note that: **HVF = Highly Volatile Fraction, NVF = Normal Volatile Fraction, TVF = Total Volatile Fraction, RF = Recalcitrant Fraction. Note that TVF = HVF + NVF and RF = 100 – TVF.**

Diesel	Pelt
NVF	53.7
RF	43.8
HVF	2.5

Kerosene	Pelt
NVF	82.2
RF	0.1
HVF	17.8

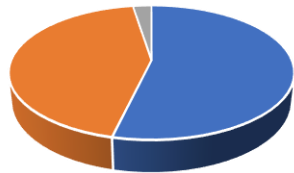
Bohai Bay	Pelt
NVF	18.5
RF	78.1
HVF	3.4

Ikan Pari	Pelt
NVF	36.1
RF	47
HVF	16.9

Bunker 180	Pelt
NVF	20.2
RF	78.6
HVF	1.2

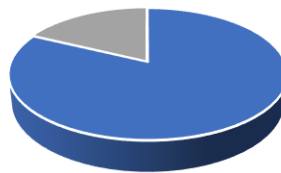
Bunker 380	Pelt
NVF	20.5
RF	78
HVF	1.5

Diesel - Pelt



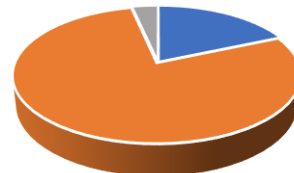
■ NVF ■ RF ■ HVF

Kerosene - Pelt



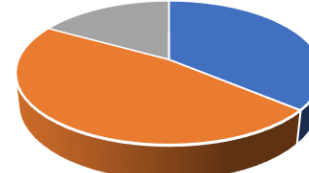
■ NVF ■ RF ■ HVF

Bohai Bay - Pelt



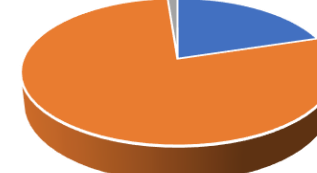
■ NVF ■ RF ■ HVF

Ikan Pari - Pelt



■ NVF ■ RF ■ HVF

Bunker 180 - Pelt



■ NVF ■ RF ■ HVF

Bunker 380 - Pelt



■ NVF ■ RF ■ HVF

Diesel	Glass
NVF	35.3
RF	53.2
HVF	11.5

Kerosene	Glass
NVF	64.7
RF	0.1
HVF	35.2

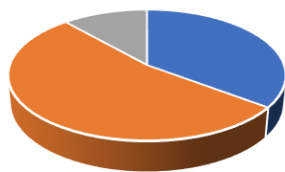
Bohai Bay	Glass
NVF	9.4
RF	85
HVF	5.6

Ikan Pari	Glass
NVF	17.3
RF	68.5
HVF	14.2

Bunker 180	Glass
NVF	10.1
RF	88.8
HVF	1.1

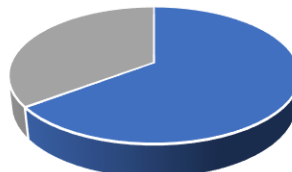
Bunker 380	Glass
NVF	9.3
RF	89.4
HVF	1.3

Diesel - Glass



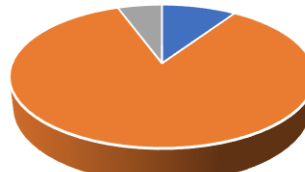
■ NVF ■ RF ■ HVF

Kerosene - Glass



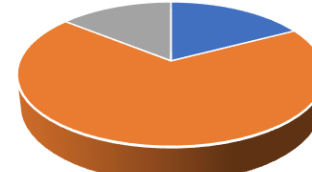
■ NVF ■ RF ■ HVF

Bohai Bay - Glass



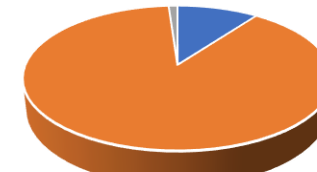
■ NVF ■ RF ■ HVF

Ikan Pari - Glass



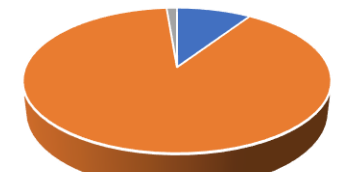
■ NVF ■ RF ■ HVF

Bunker 180 - Glass



■ NVF ■ RF ■ HVF

Bunker 380 - Glass



■ NVF ■ RF ■ HVF

Comparisons of evaporation parameters such as those shown in Table 5.10 and Figure 5.31, would provide useful information in relation to the urgency of providing a quick clean to contaminated wildlife in the field in terms of the different characteristics of different oils, such as extent of volatile trapping, the relative extent of volatile contamination and the relative amounts of expected recalcitrant contamination.

5.7 References

Adofo, YK, Nyankson, E, Agyei-Tuffour 2002, 'Dispersants as an oil spill clean-up technique in the marine environment: A review', *Heliyon*, vol. 8, no. 8, pp. 2-4.

Aeppli, C, Reddy, CM, Nelson, RK, Kellermann, MY, Valentine, DL 2013, 'Recurrent oil sheens at the Deepwater Horizon disaster site fingerprinted with synthetic hydrocarbon drilling fluids', *Environ. Sci. Tech.*, vol. 47, pp. 8211-8219.

Arey, JS, Nelson, RK, Plata, DL, Reddy, CM 2007, 'Disentangling oil weathering using GC×GC: Part 2. Mass transfer calculations', *Environ. Sci. Tech.*, vol. 41, pp. 5747-5755.

ASCE Task Committee 1996, 'State-of-the-art review of modeling transport and fate of oil spills', *Journal. Hydraul. Eng.*, vol. 122, no.11, pp. 594-609.

Asif, Z, Chen, Z, An, C, Dong, J 2022, 'Environmental Impacts and Challenges Associated with Oil Spills on Shorelines', *J. Mar. Sci. Eng.*, vol. 10, no. 6, p. 762.

Azevedo, A, Oliveira, A, Fortunato, AB, Zhang, J, Baptista, AM 2014, 'A cross-scale numerical modeling system for management support of oil spill accidents', *Mar. Pollut. Bull.*, vol. 80, no.1, pp. 132-147.

Bacosa, HP, Ancla, SMB, Arcadio, CGLA, Dalogdog, JRA, Ellos, DMC, Hayag, HDA, Jarabe, JGP, Karim, AJT, Navarro, CKP, Palma, MPI, Romarate, RA 2022, 'From surface water to the deep sea: a review on factors affecting the biodegradation of spilled oil in marine environment', *J. Mar. Sci. Eng.*, vol. 10, no. 3, p. 426.

Beyer, J, Trannum, HC, Bakke, T, Hodson, PV, Collier, TK 2016, 'Environmental effects of the Deepwater Horizon oil spill: A review', *Mar. Pollut. Bull.*, vol. 110, no. 1, pp. 28-51.

Brutsaert, W 1982, *Evaporation into the Atmosphere*, Reidel Publishing Company, Dordrecht, Holland, p. 299.

Chizaba, MD 2021, 'Bioremediation of crude oil-polluted agricultural soil using biosurfactant-producing bacterial isolates, PhD Dissertations, Nnamdi Azikiwe University, Awka.

Dao, HV, Ngeh, LN, Bigger, SW, Orbell, JD, Healy, M, Jessop, Dann, P 2006a, 'Magnetic cleansing of weathered/tarry oiled feathers – The role of pre-conditioners', *Marine Pollution Bulletin*, vol. 52, pp. 1591-1594.

Dao, HV, Maher, LA, Ngeh, LN, Bigger, SW, Orbell, JD, Healy, M, Jessop, R., Dann, P 2006b, 'Removal of petroleum tar from bird feathers utilizing magnetic particles', *Environ. Chemistry Letters*, vol. 4, no. 2, pp. 111-113.

Dao, HV 2007, 'An investigation into factors affecting the efficacy of oil removal from wildlife using magnetic particle technology', PhD Thesis, Victoria University, Melbourne Australia.

DeMarco, J 2022, *Types of Crude Oil*, viewed on 30 December 2023, <<https://www.thebalancemoney.com/the-basics-of-crude-oil-classification-1182570>>.

Fernandes, R 2018, *Risk Management of Coastal Pollution from Oil Spills Supported by Operational Numerical Modelling* (Doctoral dissertation, INSTITUTO SUPERIOR TÉCNICO).

Fingas, MF 1995, 'A literature review of the physics and predictive modelling of oil spill evaporation, *J. Hazard. Mater.*, vol. 42, pp. 157-175.

Fingas, MF 1995, 'The evaporation of oil spills', *In Proceedings of the Eighteenth Arctic and Marine Oilspill Program Technical Seminar*, Environment Canada, Ottawa, Ontario, pp. 43-60.

Fingas, MF 1997, 'Studies on the Evaporation of Crude Oil and Petroleum Products: I. The Relationship between Evaporation Rate and Time', *J. Hazard. Mater.*, vol. 56, pp. 227-236.

Fingas, MF 1999, 'The evaporation of oil spills: development and implementation of new prediction methodology', *In International Oil Spill Conference*, American Petroleum Institute, vol. 1999, no. 1, pp. 281-287.

Fingas, M, Fieldhouse, B, Wang, Z 2003, 'The long-term weathering of water-in-oil emulsions', *Spill. Sci. Technol. Bull.*, vol. 8, no. 2, pp.137-143.

Fingas, MF 2004, 'Modeling evaporation using models that are not boundary-layer regulated', *J. Hazard. Mater*, vol. 107, no. 1-2, pp.27-36.

Fingas, M 2011, 'Evaporation modeling', *Oil spill science and technology*, Gulf Professional Publishing, pp. 201-242.

Fingas, M & Brown, CE 2011, 'Oil spill remote sensing: a review', *Oil spill science and technology*, pp. 111-169.

Fingas, MF 2011, Oil and Petroleum Evaporation, *Proceedings of the 34th Arctic and Marine Oilspill Program Technical Seminar*, pp. 426-459.

Fingas, MF 2014, 'Water-in-oil emulsions: formation and prediction', *J. Pet. Sci. Res.*, vol. 3, no. 1, pp. 38-49.

Fingas, M 2014, 'Oil and petroleum evaporation', *Handbook of oil spill science and technology*, pp. 205-223.

Gin, KYH, Huda, MK, Lim, WK, Tkalic, P 2001, 'An oil spill – food chain interaction model for coastal waters', *Mar. Pollut. Bull.*, vol. 42, no. 7, pp. 590-597.

Gros, J, Nabi, D, Wurz, B, Wick, LY, Brussaard, CPD, Huisman, J, Meer, JR, Reddy CM, Arey, JS 2014, 'First day of an oil spill on the open sea: Early mass transfers of hydrocarbons to air and water', *Environ. Sci. Tech.*, vol. 48, pp. 9400-9411.

Hubbe, MA, Rojas, OJ, Fingas, M, Gupta, BS 2013, 'Cellulosic Substrates for Removal of Pollutants from Aqueous Systems: A Review. 3. Spilled Oil and Emulsified Organic Liquids', *BioResources*, vol. 8, no. 2, pp. 3038-3097.

Jones, FE 1992, *Evaporation of Water*, Lewis Publishers, Chelsea, Michigan, p. 188.

Kennish, MJ 1997, 'Pollution impacts on marine biotic communities', *CRC Press*, pp. 3-31.

Kennish, MJ 2002, 'Environmental threats and environmental future of estuaries', *Environ. Conserv.*, vol. 29, pp. 78-107.

Keramea, P, Kokkos, N, Zodiatis, Sylaios, G 2023, 'Modes of Operation and Forcing in Oil Spill Modeling: State-of-Art, Deficiencies and Challenges', *J. Mar. Sci. Eng.*, vol. 11, no. 6, p. 1165.

Khan, ZH, AbuSeedo, F, Al-Besharah, J, Salman, M 1995, 'Improvement of the quality of heavily weathered crude oils', *Fuel*, vol. 74, no. 9, pp. 1375-1381.

King, MD, Elliott, JE, Williams, TD, 2021, 'Effects of petroleum exposure on birds: A review', *Sci. Total Environ.*, vol. 755, p.142834.

Lehr, WJ 2001, 'Review of modeling procedures for oil spill weathering behavior', *Adv. Ecol. Sc.*, vol. 9, pp. 51-90.

Mackay, D & Shiu, WY 1976, 'Aqueous solubilities of weathered northern crude oils', *Bull. Environ. Contam. Toxicol.*, vol. 15, pp. 101-109.

Michel J & Fingas M 2016, 'Oil Spills: Causes, consequences, prevention, and countermeasures', *Fossil Fuels*, pp. 159-201.

Mishra, AK & Kumar, GS 2015, 'Weathering of oil spill; modeling and analysis', *Aquatic Procedia*, vol. 4, pp. 435-442.

Monteith, JL & Unsworth, MH 2008, *Principles of Environmental Physics*, Hodder and Stoughton.

Monteith, J & Unsworth, M 2013, *Principles of environmental physics: plants, animals, and the atmosphere*, Academic Press.

Morandin, LA & O'Hara, PD 2016, 'Offshore oil and gas, and operational sheen occurrence: is there potential harm to marine birds?', *Environmental Reviews*, vol. 24, no. 3, pp. 285-318.

Mullin, JV & Champ, MA 2003, 'Introduction/overview to in situ burning of oil spills', *Spill Sci. & Technol. Bull.*, vol. 8, no. 4, pp. 323-330.

Murty, KG & Kaufman, D 2020, Blending Operations in Crude Oil Refineries, *Models for Optimum Decision Making: Crude Oil Production and Refining*, pp. 51-62.

National Research Council 2003, '*Oil in the sea III: inputs, fate, and effects*', The National Academies Press, Washington, D.C.

Ndimele, PE 2017, *The political ecology of oil and gas activities in the Nigerian aquatic ecosystem*, Academic Press, Lagos, Nigeria.

Ngeh, LN 2002, 'The development of magnetic particle technology for application to environmental remediation', PhD Thesis, Victoria University, Melbourne, Australia.

National Oceanic Atmospheric Administration (NOAA) 1997, *Open-water response strategies: In-situ burning*, viewed 30 December 2023, <<http://response.restoration.noaa.gov/oilands/ISB/Guidelines/ISBatPST.pdf>>.

Orbell, JD, Dao, HV, Ngeh, LN, Bigger, SW, Healy, M, Jessop, R, Dann, P 2005, 'Acute temperature dependency in the cleansing of tarry feathers utilizing magnetic particles', *Environ. Chem. Letters*, vol. 3, no. 1, pp. 25-27.

Orbell, JD, Dao, HV, Ngeh, LN, Bigger, SW 2007, 'Magnetic particle technology in environmental remediation and wildlife rehabilitation', *Environmentalist*, vol. 27, pp. 175-182.

O'Rourke, D & Connolly, S 2003, 'Just Oil? The distribution of environmental and social impacts of oil production and consumption', *Annu. Rev. Environ. Resour.*, vol. 28, pp. 587-617.

Pete, AJ, Bharti, B, Benton, MG 2021, 'Nano-enhanced bioremediation for oil spills: a review', *ACS ES&T Engineering*, vol. 1, no. 6, pp. 928-946.

Reed, M, Johansen, O, Brandvik, PJ, Daling, P, Lewis, A, Fiocco, R, Prentki, R 1999, 'Oil spill modeling towards the close of the 20th century: overview of the state of the art', *Spill Sci. Technol. Bull.*, vol. 5, no. 1, pp. 3-16.

Sebastiao, P & Soares, CG 1995, 'Modeling the fate of oil spills at sea', *Spill Sci. Technol. Bull.*, vol. 2, no. 2, pp. 121-131.

Silva, IA, Almeida, FC, Souza, TC, Bezerra, KG, Durval, IJ, Converti, A, Sarubbo, LA 2022, 'Oil spills: impacts and perspectives of treatment technologies with focus on the use of green surfactants', *Environ. Monit. Assess.*, vol. 194, no. 3, p.143.

Singh, VP & Xu, CY 1997, 'Evaluation and generalization of 13 mass-transfer equations for determining free water evaporation', *Hydrological Processes*, vol. 11, no. 3, pp. 311-323.

Tarr, MA, Zito, P, Overton, EB, Olson, GM, Adhikari, PL, Reddy, CM 2016, 'Weathering of Oil Spilled in the Marine Environment', *Oceanography*, vol. 29, no. 3, pp. 126-135.

Thakur, A & Koul B 2022, 'Impact of oil exploration and spillage on marine environments', *Advances in Oil-Water Separation*, pp. 115-135.

The No. 1 Source for Oil and Energy News 2009, *A detailed guide on the many different types of crude oil*, viewed 2 February 2022, <<https://oilprice.com/Energy/Crude-Oil/A-Detailed-Guide-On-The-Many-Different-Types-Of-Crude-Oil.html>>.

United States Environmental Protection Agency 2021, *Types of Crude Oil*, viewed 30 December 2023, <<https://www.epa.gov/emergency-response/types-crude-oil>>.

Urum, K, Pekdemir, T, Copur, M 2004, 'Surfactants treatment of crude oil contaminated soils', *J. Colloid & Inter. Sci.*, vol. 276, pp. 456-464.

Urum, K, Pekdemir, T, Ross, D, Grigson, S 2005, 'Crude oil contaminated soil washing in air sparging assisted stirred tank reactor using bio-surfactants', *Chemosphere*, vol. 60, pp. 334-343.

Wang, Z, Hollebone, BP, Fingas, M, Fieldhouse, B, Sigouin, L, Landriault, M, Smith, P, Noonan, J, Thouin, G, Weaver, JW 2003, 'Characteristics of spilled oils, fuels, and petroleum products: 1. Composition and properties of selected oils', *United States Environmental Protection Agency*, pp. 1-28.

Warnock, AM, Hagen, SC, Passeri, DL 2015, 'Marine Tar Residues: a Review', *Water, Air & Soil Pollution*, vol. 226, no. 68, pp. 1-24.

Xie, H, Yapa, PD, Nakata, K 2007, 'Modeling emulsification after an oil spill in the sea', *J. Mar. Syst.*, vol. 68, no. 3-4, pp. 489-506.

Xu, CY & Singh, VP 2000, 'Evaluation and generalization of radiation-based methods for calculating evaporation', *Hydrological processes*, vol. 14, no. 2, pp. 339-349.

Zhang, B, Matchinski, EJ, Chen, B, Ye, X, Jing, L, Lee K 2019, 'Marine oil spills – Oil pollution, sources and effects', *World seas: an environmental evaluation*, vol. 3, pp. 391-406.

Zolfaghari, R, Fakhru'i-Razi, A, Abdullah, LC, Elnashaie, SSEH, Pendashteh, A 2016, 'Demulsification techniques of water-in-oil and oil-in-water emulsions in petroleum', *Sep. Purif. Technol.*, vol. 170, pp. 377-407.

Chapter 6: Overview

The title of this thesis, namely, “Improving Magnetic Particle Technology (MPT) for the Rehabilitation of Oiled Wildlife” builds upon the invention by the Animal Rehabilitation Technology (ART) group at Victoria University, in collaboration with the Phillip Island Nature Parks, of a novel dry-cleaning method for removing oil contamination from wildlife, i.e., “magnetic cleansing”. After several decades of fundamental research and development, the ART group is now at the forefront of this technology worldwide and has published numerous high-ranking publications in Q1 journals, plus conference presentations and media output. This research has also attracted considerable research funding, including from the Australian Research Council (ARC) and the Australian Maritime Safety Authority (AMSA). Notably, this research was awarded the 2013 Banksia Sustainability Award - in partnership with the Phillip Island Nature Parks and the 2014 Google Impact Challenge Award (with \$250,000), in partnership with the Penguin Foundation. These awards were in relation to the development and implementation of the “magnetic wand” for providing a “quick clean” to contaminated wildlife in the field, upon first encounter. This technology is now available for use by wildlife rehabilitators as an important addition to existing stabilization protocols and, due to its portability, allows for the removal of the most toxic and corrosive volatile components within minutes, upon first encounter in the field. It is anticipated that the eventual widespread implementation of this technology will greatly improve the survival prospects of contaminated wildlife. Within this context, this PhD project has successfully defined and tested new methods for establishing the logistics for the use of this technology in the field, and for understanding the physical science that underpins oil contamination of wildlife and this novel cleansing approach.

Chapter 2 has exploited an existing database, created by the ART Group in 2007 (Orbell et al., AMSA Report, 2007), based on quantifying the magnetic cleansing of different coverages of diesel oil from the carcasses of the Little Penguin, to establish a “scenario-based” approach for quantitatively estimating the logistics involved in providing an MPT “quick clean” to contaminated wildlife in the field. This necessarily provides only an estimation of the resources required since the data is currently limited to the contaminant being diesel oil and to Little Penguin plumage as the “substrate”. The critical parameters that have been assessed for a given scenario include the number of birds, the average % oil coverage per bird, the number of

treatments required for a “quick clean” (1 or 2), the time required for 1 or 2 treatments, the weight of magnetic particles required for 1 or 2 treatments, the weight of contaminant-laden particles required for disposal and the number of 2-person teams required for a given scenario. This approach clearly demonstrates that a “quick clean” using existing MPT is feasible for certain scenarios, in terms of the available logistical data. Future work here would involve collecting more experimental data involving different contaminant types and different bird species. An exciting prospect for this “scenario-based” approach, based on experimental data, is the development of a software package whereby the relevant parameters for a given pollution event could be entered (e.g., species involved, contaminant involved, number of birds, average % coverage) and the software would provide a logistical analysis for a “quick clean”.

Chapter 3 investigates the possibility of synthesizing oil absorbing magnetic particles that are lighter in weight than the zero-valent iron powder that is currently employed but will retain the required magnetic cleansing capability for a “quick clean” in the field. This requires them to, not only have a high contaminant absorbance, but also a high magnetic susceptibility. Although this experimental work was limited by the COVID lockdowns, it has been demonstrated that it is indeed possible to create such particles. This is an important proof of principle and promises to enhance the logistics of applying such technology in the field.

Chapter 4 focuses on the use of MPT to provide a quantitative assay of contaminant removal from a particular substrate²⁰. A standard gravimetric method, developed by the ART group, has been employed, whereby experiments have been conducted in five-fold replicate and results compared at the 95% level of confidence. These experiments typically show a high level of reproducibility. Such assays provide essential quantitative information on the relative recalcitrance of different oils, with respect to their initial and final removal, from a given substrate. It can also provide valuable information on the relative difficulty in removing a particular contaminant from different substrates (for example, back versus breast feathers, feathers versus fur, feathers/fur of different animal species). Another potential application is the quantification of the effectiveness of different pre-treatment agents (PTAs) for the removal of heavy and recalcitrant contaminants from a given substrate. This is an extension of the work

²⁰ An important consideration in the application of MPT to oil removal “assays” is the extent to which the oil removal efficacy, as determined by MPT, carries over with fidelity to the detergent-based removal efficacy. Previous work by this group (Kasup et al., 2015) has addressed this problem and has shown that there is an excellent correspondence between MPT and detergent based efficacies ($r^2 > 90\%$ correlation).

carried out by the ART Group under an ARC Linkage grant: 2009-2011. To carry out such assays, the main stumbling block is the choice of substrate. Ideally, removal experiments should be carried out on live animals, but this is not practical. Therefore, an approximate substrate must be used. Three substrates are employed in practice, namely: feather clusters, pelt and whole bird models (carcasses). Feather clusters, although convenient and easily obtained, are only approximations of plumage and tend to overestimate removal efficacy. On the other hand, carcasses are a limited resource and present many experimental difficulties. For example, they must be refrigerated, thawed, and prepared to remove excess moisture and to prevent orifice leakage for subsequent gravimetric experiments. Furthermore, the amount of applied oil compared to the weight of the carcass itself is relatively small, resulting in large experimental errors. This chapter has investigated the use of Little Penguin pelt, supplied by the Phillip Island Nature Parks, as a substrate for such assays and has compared this to the use of feather clusters and carcasses as substrates. The experiments conducted here show *definitively* that pelt is the substrate of choice for such assays. Hence, it has been shown, within experimental error, that pelt effectively mimics the plumage of a whole bird model (carcass) and is a relatively renewable resource. In this regard, it has also been demonstrated, within experimental error, that pelt can be effectively recycled for this purpose. Furthermore, it has been demonstrated that such experiments may be carried out at pelt temperatures that mimic the body temperature of the bird, ~ 40 °C. Again, this represents an important proof of principle study that will enhance future research into oil removal from wildlife.

Chapter 5 aims to systematically characterise the physics involved in the evaporation of a range of crude oils from plumage. Thus, evaporation (i.e. “weathering”) profiles from Little Penguin pelt and a glass surface (as a control) have been determined for up to 11 different oils and for time periods of up to 21 days. These evaporation profiles have been analysed via customized modelling software²¹ that has been developed within the ART group. Although such profiles have been studied by other researchers in this field, no previous studies have been directed towards pelt as a substrate and no previous studies have focused on the initial (up to 10 hours) of the evaporation process. This detailed analysis has resulted in characterizing four relative fractional components for each of six common crude oil contaminants, namely Diesel and Kerosene (‘light’ oils), Bohai Bay and Ikan Pari (‘medium’ oils), and Bunker 180 and Bunker 380 (‘heavy’ oils). A new convention has been defined for describing these fractions, namely:

²¹ OilVap-v1 software developed by Professor Stephen Bigger of Victoria University.

HVF = Highly Volatile Fraction, NVF = Normal Volatile Fraction, TVF = Total Volatile Fraction, and RF = Recalcitrant Fraction. Note that $TVF = HVF + NVF$ and $RF = 100 - TVF$. Evaporation experiments conducted up to the first 10 hours reveal that, for all oils, there is a unique *initial* evaporation phase, the HVF, followed by a latency period. During this phase, the evaporation rate from the pelt is lower for these components than from a glass control, meaning that are effectively trapped or retained within the plumage during this phase. This situation is reversed after the latency period when the evaporation process resumes. This is an important discovery that emphasizes the need to remove such volatiles as soon as possible and makes it imperative to include an effective “quick clean” into existing stabilization protocols to remove the volatiles. Previous research has demonstrated that a “quick clean” utilizing MPT (the “wand”) can remove up to 100% of such volatiles in a matter of minutes. The presence of such trapped (and non-trapped) volatiles for prolonged periods of time is likely to affect the animal's long-term survivability and/or reproductive success.

Appendix 1

Table 1.1: North America Spill Statistics (Michel and Fingas, 2016).

Source	Percentage of total spills	
	Volume	Numbers
Land spills (85% volume, 90% numbers)		
Pipelines	40	20
Wells, production and storage facilities	25	25
Storage refineries	12	25
Retail and delivery	5	10
Trucks	6	11
Rail	7	4
other	5	5
On-water spills (15% volume, 10% numbers)		
Non tank vessels	25	30
Tank barges	15	10
terminals/refineries	25	30
tankers	20	20
platforms and pipelines	15	10
Types of oil spilled		
Crude oil	35	
Diesel and No. 2 fuel oils	20	
Bunkers	15	
Marine	10	
Gasoline	8	
Condensates	3	
Waste and residuals	3	
Other oils	6	

Table 1.2: Major tanker spills since 1967 (ITOPF, 2022).

Position	Shipname	Year	Location	Spill size (tonnes)
1	ATLANTIC EMPRESS	1979	Off Tobago, West Indies	287,000
2	ABT SUMMER	1991	700 nautical miles off Angola	260,000
3	CASTILLO DE BELLVER	1983	Off Saldanha Bay, South Africa	252,000
4	AMOCO CADIZ	1978	Off Brittany, France	223,000
5	HAVEN	1991	Genoa, Italy	144,000
6	ODYSSEY	1988	700 nautical miles off Nova Scotia, Canada	132,000
7	TORREY CANYON	1967	Scilly Isles, UK	119,000
8	SEA STAR	1972	Gulf of Oman	115,000
9	SANCHI*	2018	Off Shanghai, China	113,000
10	IRENES SERENADE	1980	Navarino Bay, Greece	100,000
11	URQUIOLA	1976	La Coruna, Spain	100,000
12	HAWAIIAN PATRIOT	1977	300 nautical miles off Honolulu	95,000
13	INDEPENDENTA	1979	Bosphorus, Turkey	95,000
14	JAKOB MAERSK	1975	Oporto, Portugal	88,000
15	BRAER	1993	Shetland Islands, UK	85,000
16	AEGEAN SEA	1992	La Coruna, Spain	74,000
17	SEA EMPRESS	1996	Milford Haven, UK	72,000
18	KHARK 5	1989	120 nautical miles off Atlantic coast of Morocco	70,000
19	NOVA	1985	Off Kharg Island, Gulf of Iran	70,000
20	KATINA P	1992	Off Maputo, Mozambique	67,000
21	PRESTIGE ⁺	2002	Off Galicia, Spain	63,000
36	EXXON VALDEZ ⁺	1989	Prince William Sound, Alaska, USA	37,000
132	HEBEI SPIRIT ⁺	2007	South Korea	11,000

Table 1.3: Historical major oil spills in or near Australian waters, and several smaller offshore spills (AMSA, 2020).

Date	Vessel	Location	Oil amount
28 November 1903	Petriana	Port Phillip Bay, Victoria	1,300 tonnes
03 March 1970	Oceanic Grandeur	Torres Strait, Queensland	1,100 tonnes
26 May 1974	Syigna	Newcastle, New South Wales	700 tonnes
14 July 1975	Princess Anne Marie	Offshore, Western Australia	14,800 tonnes
10 September 1979	World Encouragement	Botany Bay, New South Wales	95 tonnes
29 October 1981	Anro Asia	Bribie Island, Queensland	100 tonnes
22 January 1982	Esso Gippsland	Port Stanvac, South Australia	unknown
03 December 1987	Nella Dan	Macquarie Island	125 tonnes
06 February 1988	Sir Alexander Glen	Port Walcott, Western Australia	450 tonnes
20 May 1988	Korean Star	Cape Cuvier, Western Australia	600 tonnes
28 July 1988	Al Qurain	Portland, Victoria	184 tonnes
21 May 1990	Arthur Phillip	Cape Otway, Victoria	unknown
14 February 1991	Sanko Harvest	Esperance, Western Australia	700 tonnes
21 July 1991	Kirki	Western Australia	17,280 tonnes
30 August 1992	Era	Port Bonython, South Australia	300 tonnes
10 July 1995	Iron Baron	Hebe Reef, Tasmania	325 tonnes

28 June 1999	Mobil Refinery	Port Stanvac, South Australia	230 tonnes
26 July 1999	MV Torungen	Varanus Island, Western Australia	25 tonnes
03 August 1999	Laura D'Amato	Sydney, New South Wales	250 tonnes
18 December 1999	Sylvan Arrow	Wilson's Promontory, Victoria	less than 2 tonnes
02 September 2001	Pax Phoenix	Holbourne Island, Queensland	less than 1000 litres
25 December 2002	Pacific Quest	Border Island, Queensland	greater than 70 km slick
24 January 2006	Global Peace	Gladstone, Queensland	25 tonnes
11 March 2009	Pacific Adventurer	Cape Moreton, Queensland	270 tonnes
21 August 2009	Montara Wellhead oil platform	NW Australian coast	Approx 4,750 tonnes
03 April 2010	Shen Neng 1	Great Keppel Island, Queensland	4 tonnes
09 January 2012	MV Tycoon	Christmas Island	102 tonnes

Table 1.4: The number of Little Penguins treated annually at the animal rehabilitation facility of PINP from 1994 to 2000 (Healy, 1999).

Year	Little Penguins treated for oil contamination/annually	Little Penguins treated for other conditions/annually
1994-1995	118	106
1995-1996	301	205
1996-1997	24	128
1997-1998	36	142
1998-1999	23	92
1999-2000	236	110

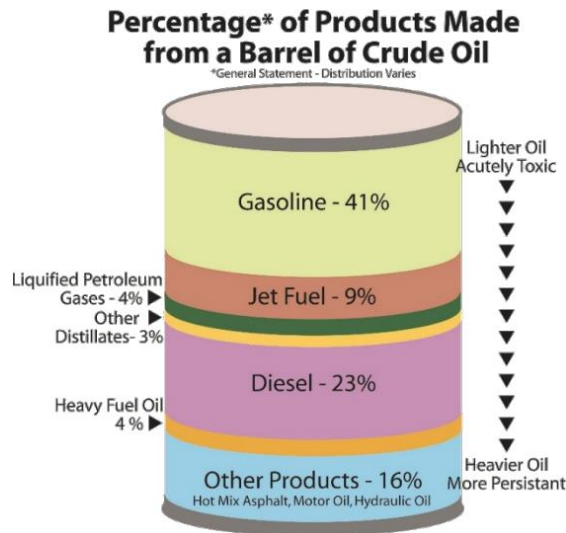


Figure 1.1: Percentage of Products made from a Barrel of Crude Oil (Department of Ecology State of Washington, 2019).

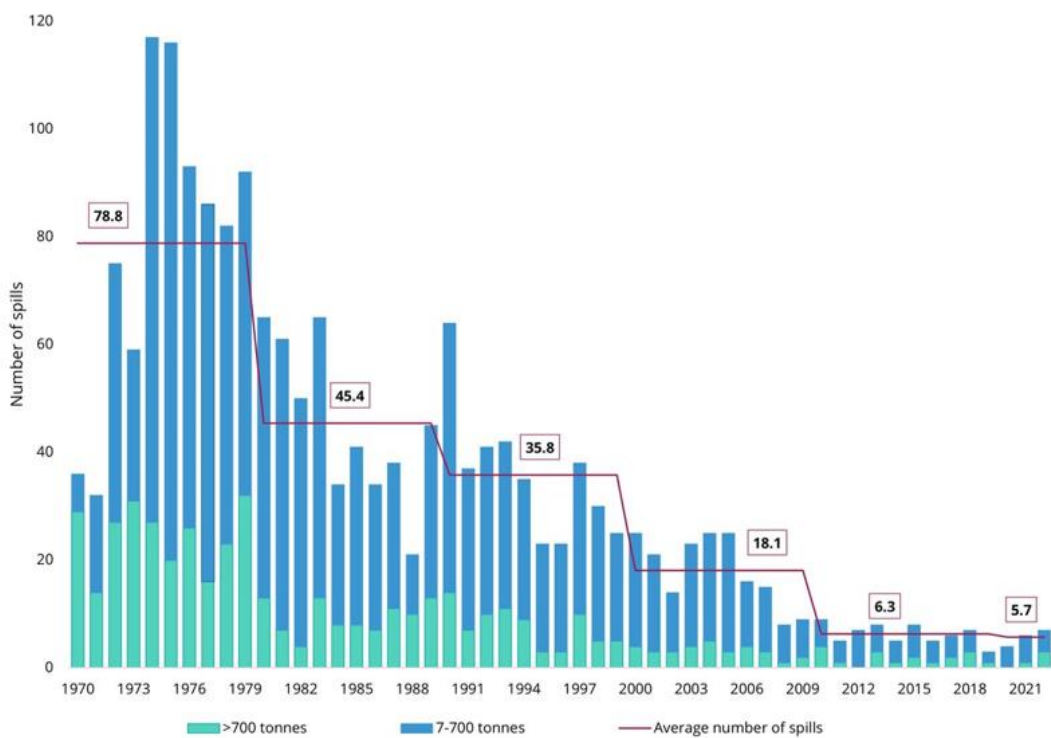


Figure 1.2: Number of medium (7-700 tonnes) and large (>700 tonnes) tanker spills from 1970-2021 (ITOPF, 2022).

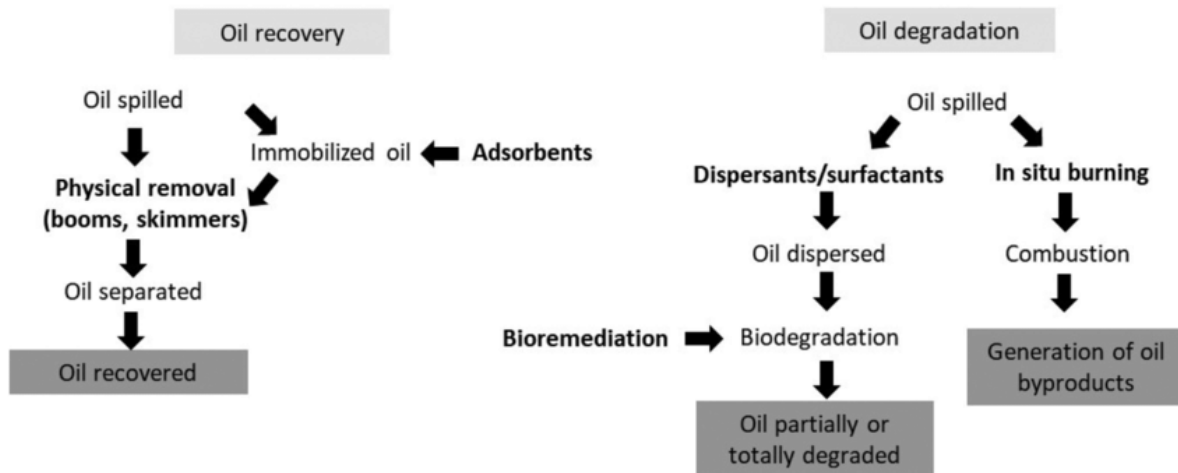


Figure 1.3: Methods for treating oil spills depending on oil recovery or degradation (Silva *et al.*, 2022).

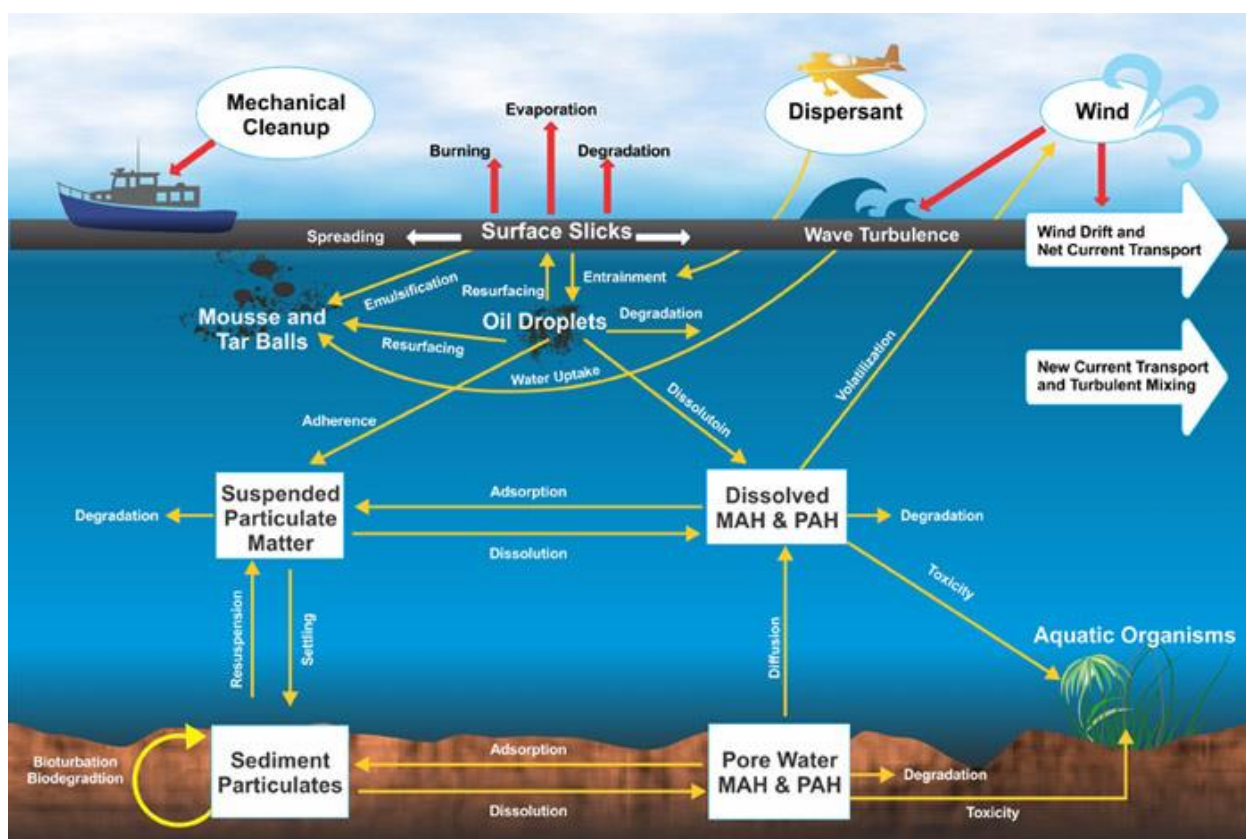


Figure 1.4: State of the art review and future directions in oil spill modeling (Spaulding, 2017).

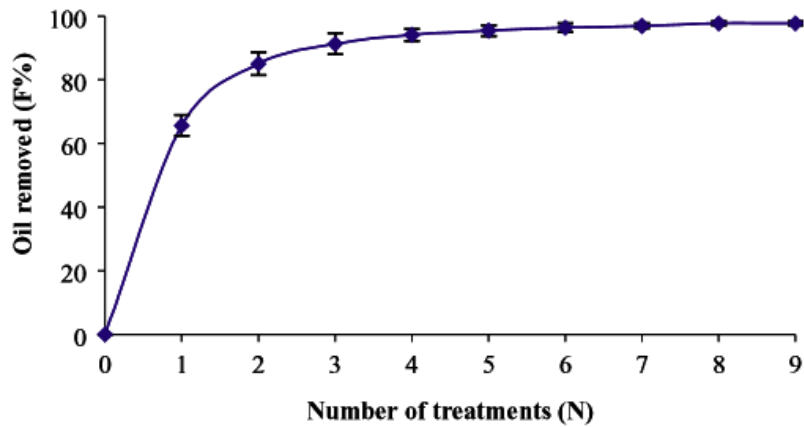


Figure 1.5: Percentage (F%) of oil removed from duck feather clusters as a function of the number of treatments. Error bars represent 95% confidence intervals for five replicates (Orbell *et al.*, 2007).

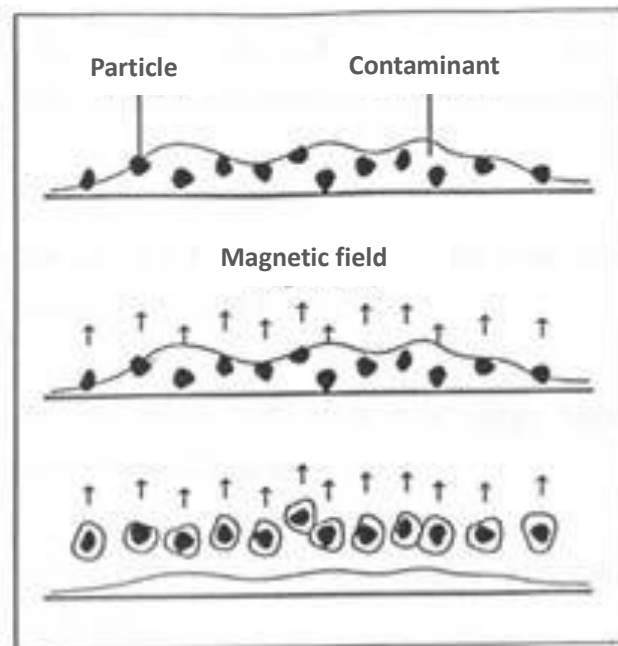


Figure 1.6: (Ngeh 2002), provides a schematic representation of the utilization of magnetic particles to remove a contamination from a substrate.

Appendix 2

Table 2.1 (blue – one treatment; red – two treatments)

Birds	10	100	1000
Cumulative time (h)	0.8 (1.6)	7.7 (15.4)	78.5 (157.0)
Total mass of powder (kg)	2.3 (4.5)	23.4 (45.1)	234.3 (450.9)
Total mass of waste (kg)	2.9 (5.4)	28.7 (54.2)	287.4 (542.1)

Suggest 1 team

Suggest 4 teams

Suggest 10 teams

Table 2.2: Logistical analysis – “In the field” scenario based on 10 birds.

Coverage	10%		20%		50%		70%		100%	
Treatment	Treatment 1	Treatment 2								
Number of birds	10	10	10	10	10	10	10	10	10	10
Coverage (%)	10	10	20	20	50	50	70	70	100	100
Treatments per bird	1	2	1	2	1	2	1	2	1	2
Cumulative time per treatment per bird (min)	2.3	5.4	2.3	4.2	2.5	6.2	3.1	6.4	4.7	9.4
Cumulative mass of powder used per treatment per bird (g)	20.6	41.2	28.1	52.0	39.9	80.4	50.8	101.9	234.3	450.9
Cumulative oil removal per treatment per bird (%)	32.7	56.0	29.5	46.0	19.6	32.7	17.1	31.3	37.2	63.8
Cumulative mass of oil removed per bird (g)	4.4	7.6	8.4	13.2	14.0	23.4	17.1	31.3	53.1	91.2
Cumulative time for 10 birds (min)	23.1	53.7	23.2	42.5	24.5	62.4	30.5	63.7	46.6	94.1
Total mass of powder (kg)	0.21	0.41	0.28	0.52	0.39	0.80	0.50	1.01	2.34	4.50
Total mass of oil removed (kg)	0.04	0.08	0.08	0.13	0.14	0.23	0.17	0.31	0.53	0.91
Total mass of waste (kg)	0.25	0.49	0.36	0.65	0.53	1.03	0.67	1.33	2.87	5.42

Table 2.3: Logistical analysis – “In the field” scenario based on 100 based birds.

Coverage	10%		20%		50%		70%		100%	
Treatment	Treatment 1	Treatment 2								
Number of birds	100									
Coverage (%)	10	10	20	20	50	50	70	70	100	100
Treatments per bird	1	2								
Cumulative time per treatment per bird (min)	2.3	5.4	2.3	4.2	2.5	6.2	3.1	6.4	4.7	9.4
Cumulative mass of powder used per treatment per bird (g)	20.6	41.2	28.1	52.0	39.9	80.4	50.8	101.9	234.3	450.9
Cumulative oil removal per treatment per bird (%)	32.7	56.0	29.5	46.0	19.6	32.7	17.1	31.3	37.2	63.8
Cumulative mass of oil removed per bird (g)	4.4	7.6	8.4	13.2	14.0	23.4	17.1	31.3	53.1	91.2
Cumulative time for 100 birds (hr)	3.85	8.94	3.87	7.09	4.09	10.4	5.08	10.6	7.7	15.6
Total mass of powder (kg)	2.06	4.12	2.81	5.2	3.98	8.04	5.08	10.19	23.43	45.09
Total mass of oil removed (kg)	0.44	0.76	0.84	1.32	1.40	2.34	1.71	3.13	5.31	9.11
Total mass of waste (kg)	2.5	4.88	3.65	6.51	5.39	10.38	6.79	13.32	28.74	54.21

Table 2.4: Logistical analysis – “In the field” scenario based on 1000 based birds.

Coverage	10%		20%		50%		70%		100%	
Treatment	Treatment 1	Treatment 2								
Number of birds	1000	1000	1000	1000	1000	1000	1000	1000	1000	1000
Coverage (%)	10	10	20	20	50	50	70	70	100	100
Treatments per bird	1	2	1	2	1	2	1	2	1	2
Cumulative time per treatment per bird (min)	2.3	5.4	2.3	4.2	2.5	6.2	3.1	6.4	4.7	9.4
Cumulative mass of powder used per treatment per bird (g)	20.6	41.2	28.1	52.0	39.9	80.4	50.8	101.9	234.3	450.9
Cumulative oil removal per treatment per bird (%)	32.7	56.0	29.5	46.0	19.6	32.7	17.1	31.3	37.2	63.8
Cumulative mass of oil removed per bird (g)	4.4	7.6	8.4	13.2	14.0	23.4	17.1	31.3	53.1	91.2
Cumulative time for 1000 birds (hr)	38.5	89.5	38.7	70.9	40.9	104.0	50.8	106.1	77.7	156.8
Total mass of powder (kg)	20.6	41.2	28.1	52.0	39.9	80.4	50.8	101.9	234.3	450.9
Total mass of oil removed (kg)	4.4	7.6	8.4	13.2	14.0	23.4	17.1	31.3	53.1	91.2
Total mass of waste (kg)	25.0	48.9	36.5	65.1	53.9	103.8	67.9	133.2	287.4	542.1

Table 2.5: Cumulative time (hr), total mass of powder (kg) and total mass of waste (kg) as a function of 1 treatment for 10% Diesel Oil coverage based on 10, 100 and 1000 birds.

Birds	10	100	1000
Cumulative time (hr)	0.4	3.9	39
Total mass of powder (kg)	0.2	2.1	21
Total mass of waste (kg)	0.3	2.5	25

Table 2.6: Cumulative time (hr), total mass of powder (kg) and total mass of waste (kg) as a function of 1 treatment for 20% Diesel Oil coverage based on 10, 100 and 1000 birds.

Birds	10	100	1000
Cumulative time (hr)	0.4	3.9	39
Total mass of powder (kg)	0.3	2.8	28
Total mass of waste (kg)	0.4	3.7	37

Table 2.7: Cumulative time (hr), total mass of powder (kg) and total mass of waste (kg) as a function of 1 treatment for 50% Diesel Oil coverage based on 10, 100 and 1000 birds.

Birds	10	100	1000
Cumulative time (hr)	0.4	4.1	41
Total mass of powder (kg)	0.4	4.0	40
Total mass of waste (kg)	0.5	5.4	54

Table 2.8: Cumulative time (hr), total mass of powder (kg) and total mass of waste (kg) as a function of 1 treatment for 70% Diesel Oil coverage based on 10, 100 and 1000 birds.

Birds	10	100	1000
Cumulative time (hr)	0.5	5.1	51
Total mass of powder (kg)	0.5	5.1	51
Total mass of waste (kg)	0.7	6.8	68

Table 2.9: Cumulative time (hr), total mass of powder (kg) and total mass of waste (kg) as a function of 1 treatment for 100% Diesel Oil coverage based on 10, 100 and 1000 birds.

Birds	10	100	1000
Cumulative time (hr)	0.8	7.7	78
Total mass of powder (kg)	2.3	23.4	234
Total mass of waste (kg)	2.9	28.7	287

Table 2.10: Cumulative time (hr), total mass of powder (kg) and total mass of waste (kg) as a function of 2 treatments for 10% Diesel Oil coverage based on 10, 100 and 1000 birds.

Birds	10	100	1000
Cumulative time (hr)	0.9	8.9	90
Total mass of powder (kg)	0.4	4.1	41
Total mass of waste (kg)	0.5	4.9	49

Table 2.11: Cumulative time (hr), total mass of powder (kg) and total mass of waste (kg) as a function of 2 treatments for 20% Diesel Oil coverage based on 10, 100 and 1000 birds.

Birds	10	100	1000
Cumulative time (hr)	0.7	7.1	71
Total mass of powder (kg)	0.5	5.2	52
Total mass of waste (kg)	0.7	6.5	65

Table 2.12: Cumulative time (hr), total mass of powder (kg) and total mass of waste (kg) as a function of 2 treatments for 50% Diesel Oil coverage based on 10, 100 and 1000 birds.

Birds	10	100	1000
Cumulative time (hr)	1.0	10.4	104
Total mass of powder (kg)	0.8	8.0	80
Total mass of waste (kg)	1.0	10.4	104

Table 2.13: Cumulative time (hr), total mass of powder (kg) and total mass of waste (kg) as a function of 1 treatment for 70% Diesel Oil coverage based on 10, 100 and 1000 birds.

Birds	10	100	1000
Cumulative time (hr)	1.1	10.6	106
Total mass of powder (kg)	1.0	10.2	102
Total mass of waste (kg)	1.3	13.3	133

Table 2.14: Cumulative time (hr), total mass of powder (kg) and total mass of waste (kg) as a function of 2 treatments for 100% Diesel Oil coverage based on 10, 100 and 1000 birds.

Birds	10	100	1000
Cumulative time (hr)	1.6	15.7	157
Total mass of powder (kg)	4.5	45.1	451
Total mass of waste (kg)	5.4	54.2	542

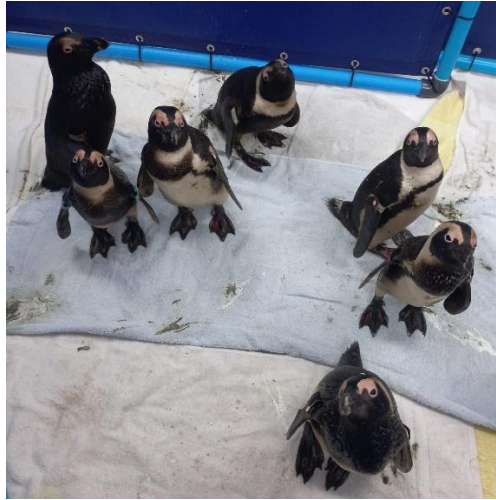


Figure 2.1: Contaminated Little Penguins in holding bays (SANCCOB, 2024).

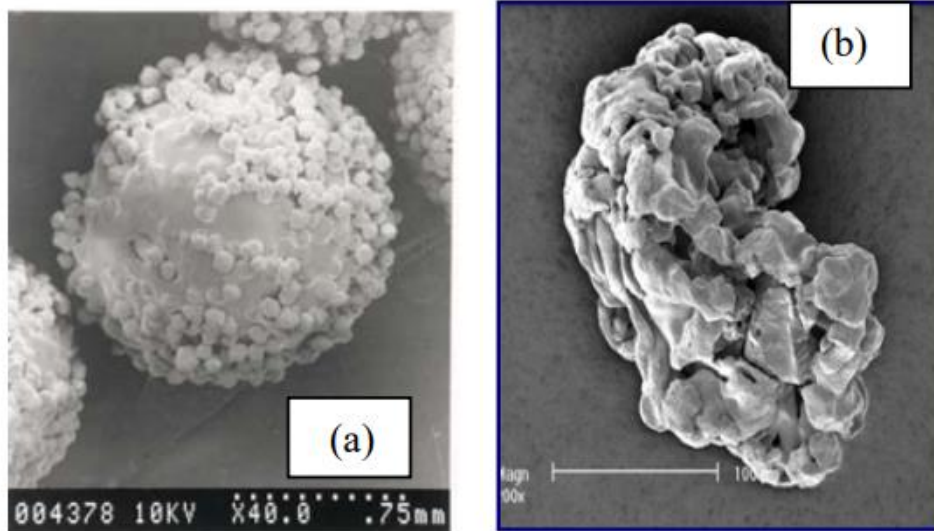


Figure 2.2: Electron micrographs of oil sequestering particles (a) polymer-coated and (b) finely divided iron powder (Ngeh *et al.*, 2012).



Figure 2.3: Magnetic “wand” (Ngeh, 2012).

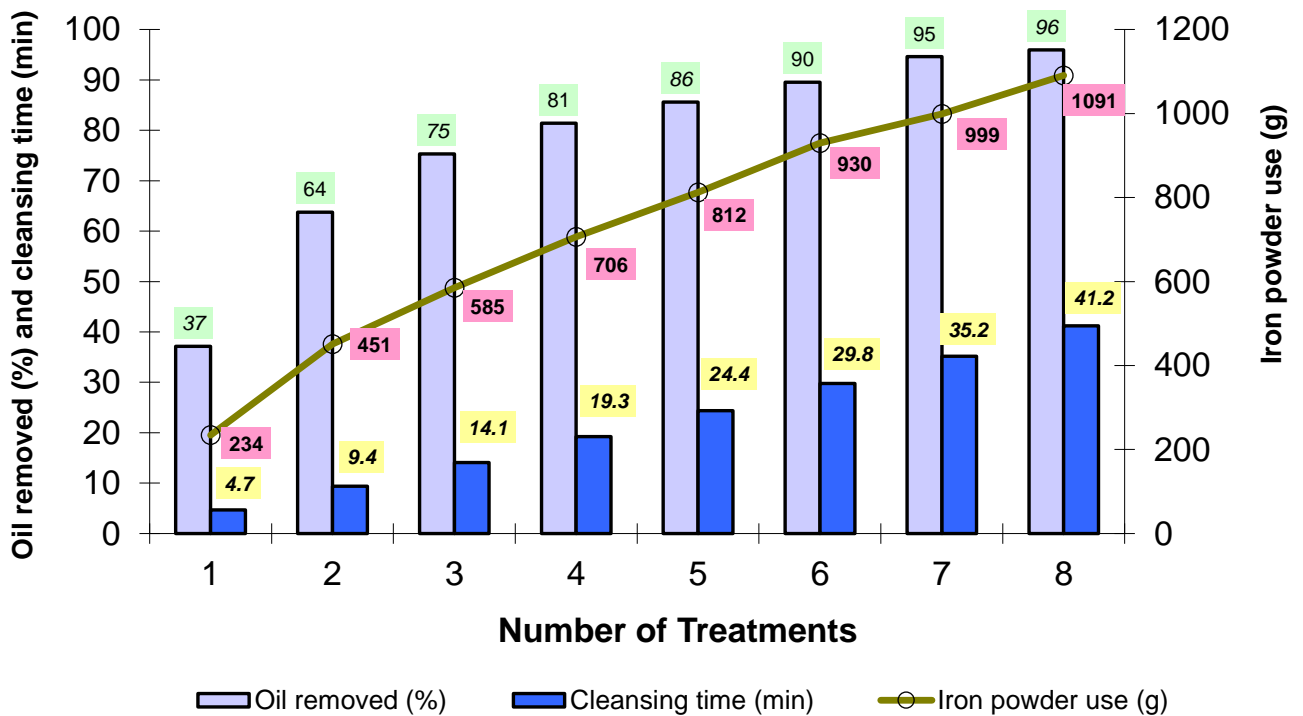


Figure 2.4: An illustration of the removal of Diesel oil (100% coverage – worst case scenario) from a Little Penguin carcass. It should be noted that in this experiment, a “first generation” magnetic tester was utilized, and that 37% removal could be accomplished in 4.7 minutes and 64% removal in 9.4 minutes (Orbell., 2007).

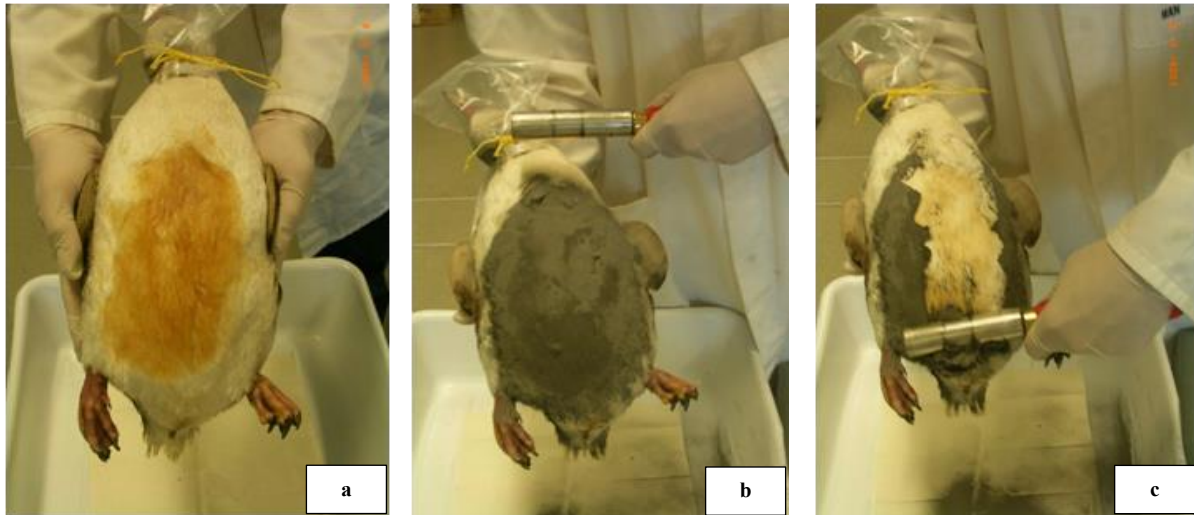


Figure 2.5: Simulating a “quick wash” for a Little Penguin Carcass contaminated with (a) 20% coverage (by mass) of engine oil (b) after magnetic particle application (c) 82% removal is achieved (Orbell., 2007).

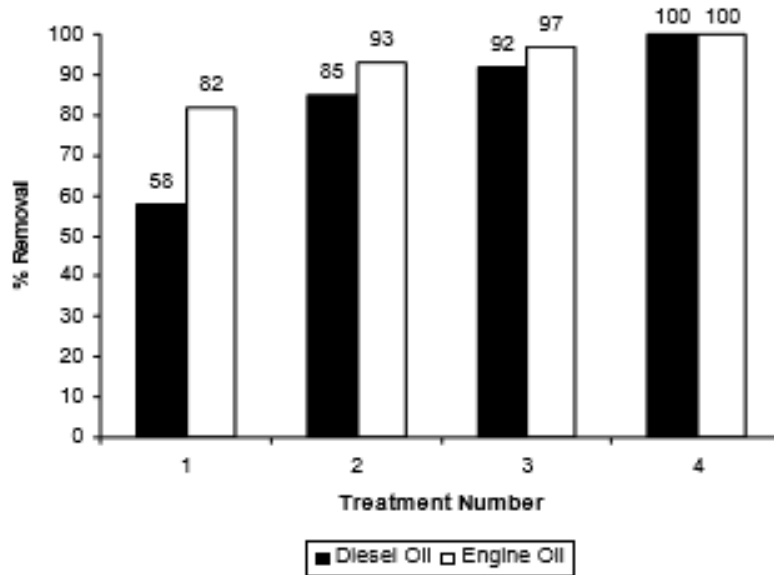


Figure 2.6: Representative data for the “magnetic wand” removal of Diesel and engine oil from carcass of the Little Penguin to the extent of 20% (by mass) (Ngeh *et al.*, 2012).



Figure 2.7: The “backpack” design, based on MPT, for a portable “Quick Clean” Kit (Orbell *et al.*, 2022).

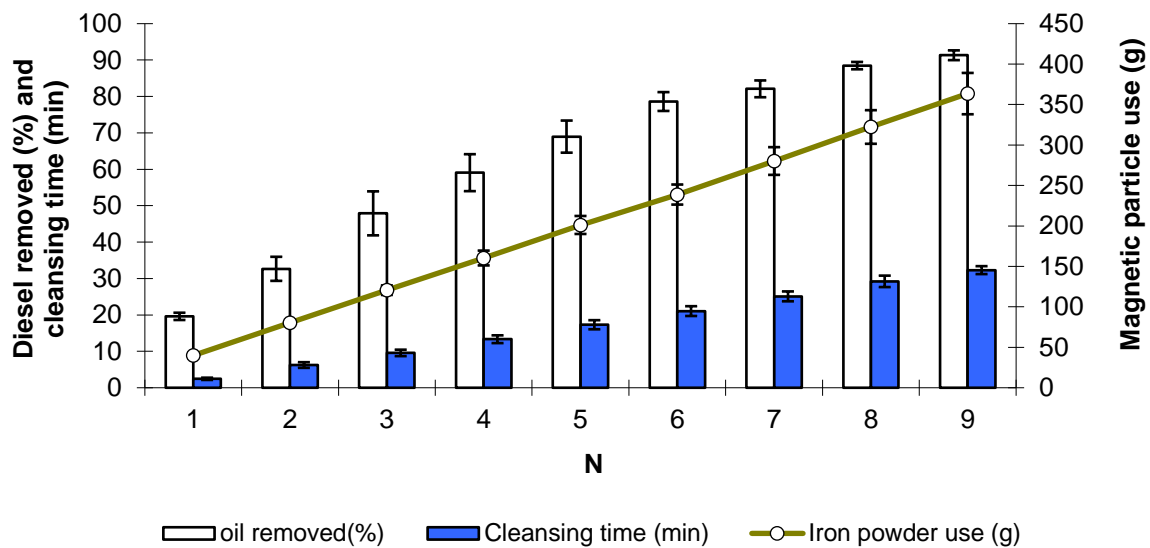


Figure 2.8: Histogram of Diesel removal (%) versus number of treatments (N), cleansing time (min) and magnetic particle consumption (g) as a function of the number of treatments, for the removal of **50% Diesel Oil coverage** (by mass) from plumage. Error bars represent the standard error for three replicates (Orbell *et al.*, 2007).



Figure 2.9: A potential pollution event scenario. Ten fully contaminated (100% coverage) brown pelicans from the Deepwater Horizon oil spill being held, awaiting treatment in a small holding bay (Encyclopedia Britannica, 2010; 2023).

Appendix 3

Schematic Methodology

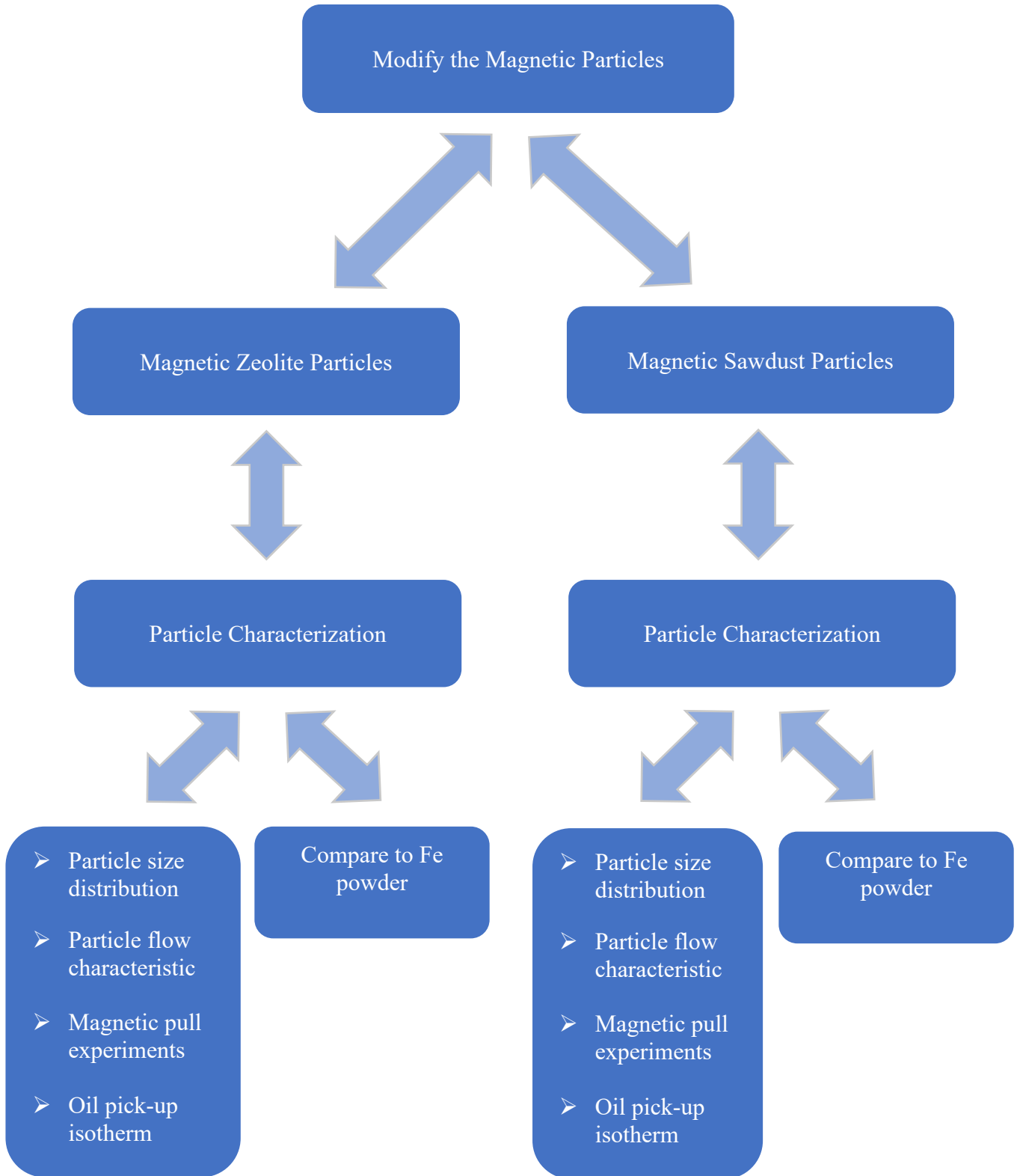


Table 3.1: Composition of the eight magnetic zeolite (MZ) particle types and the two magnetic sawdust (MS) particle types that were formulated, see **Section 3.2.2/3**.

Magnetic Zeolites (MZ)	Mass of iron oxide nanoparticles (g)	Mass of crushed zeolite or sawdust (g)	Total mass of composite (g)	% by weight of the iron oxide nanoparticles	% by weight of crushed zeolite or sawdust
Control (no zeolite)	9.2	0	9.2	100	0
MZ 1	9.2	1	10.2	90.19	9.80
MZ 2	9.2	2	11.2	82.14	17.85
MZ 3	9.2	3	12.2	75.40	24.59
MZ 4	9.2	4	13.2	69.69	30.30
MZ 5	9.2	5	14.2	64.78	35.21
MZ 6	9.2	6	15.2	60.52	39.47
MZ 7	9.2	7	16.2	56.79	43.20
MZ 8	9.2	8	17.2	53.48	46.51
MS 1	1	10	11	9.09	90.90
MS 2	2	10	12	16.66	83.33

Table 3.2: Parameters measured by the PSA instrument, together with their definitions.

Parameters	Definition
D₁₀	Percentile value, D ₁₀ indicates the size below which 10% of all particles are found. The length unit, D ₁₀ , represents the 10% of particles in a powder that are smaller than this size (Microtrac, 2023).
D₅₀	Percentile value, D ₅₀ indicates the size below which 50% of all particles are found. The length unit, D ₅₀ , represents the 50% of particles in a powder that are smaller than this size (Microtrac, 2023).
D₉₀	Percentile value, D ₉₀ indicates the size below which 90% of all particles are found. The length unit, D ₉₀ , represents the 90% of particles in a powder that are smaller than this size (Microtrac, 2023).

Mean size	This is the value of the particle size which divides the population exactly into two equal halves (i.e., there is 50% of the distribution above this value and 50% below) (Microtrac, 2023).
Span	Volume-based size distribution is defined as $\text{span} = (D_{90} - D_{10})/D_{50}$ (Burgess <i>et al.</i> , 2004; Microtrac, 2023). The span value denotes the degree of consistency in the particle size. If the span approaches zero, it indicates that the granularity is more uniform, and the size consistency is better (ACTTR Technology, 2020).
Obscuration	The detector measures the reduction in light intensity and, employing a calibration curve, processes the signal to determine particle size (Bettersize Instruments, 2022).

Table 3.3: Interpretation of the Carr index and Hausner ratio with respect to flowability (Powder Process, 2023).

Flowability expected	Hausner Ratio	Carr Index
Excellent / Very Free Flow	1.00 - 1.11	<10
Good / Free Flow	1.12 - 1.18	11-15
Fair	1.19 - 1.25	16-20
Passable	1.26 - 1.34	21-25
Poor Flow / Cohesive	1.35 - 1.45	26-31
Very Poor Flow / Very Cohesive	1.46 - 1.59	32-37
Approximatively no flow	> 1.60	> 38

Table 3.4: PSA output parameters for the Fe powder control (blue), the MZ particles (black) and the MS particles (red).

Magnetic particle type	D10 (µm)	D50 (µm)	D90 (µm)	“Mean” Size (µm)	Span	Obscuration (%)
Fe powder	18.263	37.997	71.280	44.127	1.395	1.56
MZ 1	1.4574	8.968	42.234	17.601	4.547	5.76
MZ 2	1.3837	8.777	42.563	17.597	4.692	2.14
MZ 3	1.2898	9.802	49.943	21.240	4.964	0.01
MZ 4	0.7699	8.284	40.801	17.764	4.832	0.01
MZ 5	1.0270	8.338	40.655	17.192	4.752	0.61
MZ 6	0.9359	7.595	39.743	16.606	5.110	0.81
MZ 7	0.8078	7.523	48.596	20.141	6.352	4.67
MZ 8	0.3018	5.765	35.902	14.993	6.175	0.18
MS 1	2.791	40.293	123.517	66.075	2.996	0.10
MS 2	5.294	37.387	124.771	62.227	3.196	0.56

Table 3.5: Compressibility and flow parameters calculated as described in **Section 3.2.4.2** for the Fe powder and the Fe₃O₄ nanoparticle controls, pastes MZ 1 – 5 and MS 1 – 2. Note that the sawdust data is in red.

Magnetic Powder	Mass of particles (g)	Unsettled Volume, V _B (mL)	Tapped Volume, V _T (mL)	d _B = m/V _B g/mL	d _T = m/V _T g/mL	Hausner Ratio	Carr Index, (%)	Flow
Fe Powder	13.62 (97.14)	4.7 (32.0)	3.8 (26)	2.9 (3.0)	3.6 (3.7)	1.2 (1.0)	19 (19)	Fair (Fair)
Fe ₃ O ₄ Nanoparticles	4.65 (12.67)	4.8 (32)	3.9 (22)	1.0 (0.4)	1.2 (0.6)	1.2 (1.5)	17 (33)	Fair (Poor)
MZ 1	4.36	4.7	3.7	0.9	1.2	1.3	25	Passable
MZ 2	4.26	4.9	4.0	0.9	1.1	1.1	18	Fair
MZ 3	5.60	5.0	4.0	1.1	1.4	1.3	21	Fair
MZ 4	4.33	4.7	3.8	0.9	1.1	1.2	20	Fair
MZ 5	4.39	5.1	4.1	0.9	1.1	1.2	20	Fair
MS 1	10.52	32	21	0.33	0.49	1.5	33	(Poor)
MS 2	11.73	33	22	0.35	0.53	1.5	34	(Poor)

Table 3.6: Magnetic pull parameters were determined as described in **Section 3.2.4.2** for the Fe powder, the Fe₃O₄ nanoparticle controls and pastes M 1 – 5.

Magnetic Powder	Magnetic Pull (kg)	Mass of Powder (g)	Pull per g (x 10 ⁻³)
Fe Powder	0.045	13.62	3.3
Fe ₃ O ₄ nanoparticles	0.030	4.65	6.5
MZ 1	0.030	4.36	6.9
MZ 2	0.030	4.26	7.0
MZ 3	0.035	5.60	6.3
MZ 4	0.025	4.33	5.8
MZ 5	0.025	4.39	5.7

Table 3.7: A comparative tabulation of the isotherm data from **Figure 3.17** (yellow – glass substrate) and **Figure 3.18** (green – feather clusters) respectively. $P_0 - P_3\%$ is the oil removal (%), N_0 is the total number of treatments.

Powder	$P_0\%$	P_0	P_1	P_2	P_3
Fe	98.1	10	70.0	82.9	87.7
MZ 1	92.1	8	70.2	87.2	89.7
MZ 2	96.7	8	66.4	87.3	88.0
MZ 3	96.3	8	65.2	83.9	88.3
MZ 4	96.4	8	84.9	87.6	91.3
MZ 5	98.0	8	76.3	88.0	92.6
MZ 6	93.8	8	72.5	80.4	84.1
MZ 7	92.8	8	67.7	79.8	85.1
MZ 8	90.6	8	57.7	70.2	84.2

Powder	$P_0\%$	P_0	P_1	P_2	P_3
Fe	99.4	12	65.7	86.9	92.0
MZ 1	99.5	13	19.7	41.7	66.6
MZ 2	95.8	16	36.1	50.8	59.7
MZ 3	95.6	15	20.8	42.7	56.4
MZ 4	91.1	14	27.6	49.2	60.4
MZ 5	98.3	12	41.9	73.8	86.1
MZ 6	83.0	14	51.7	64.0	68.0
MZ 7	90.8	14	20.2	56.6	64.1
MZ 8	85.5	17	22.4	37.5	51.5

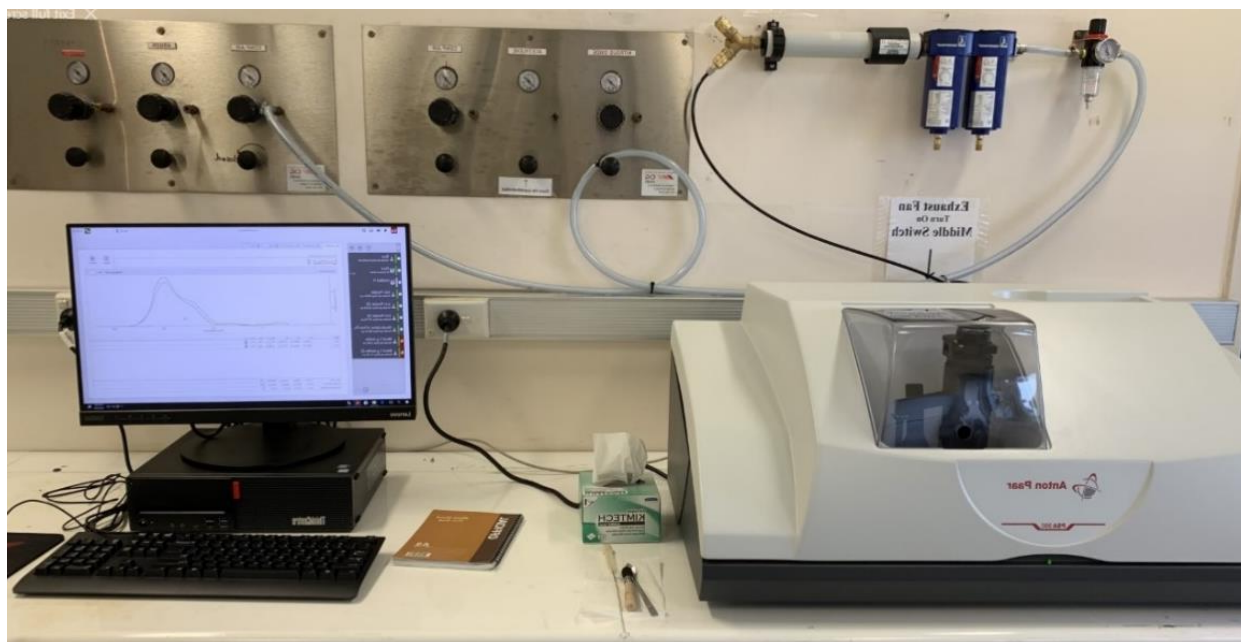


Figure 3.1: Anton Paar PSA 990 Particle Size Analyzer (PSA).

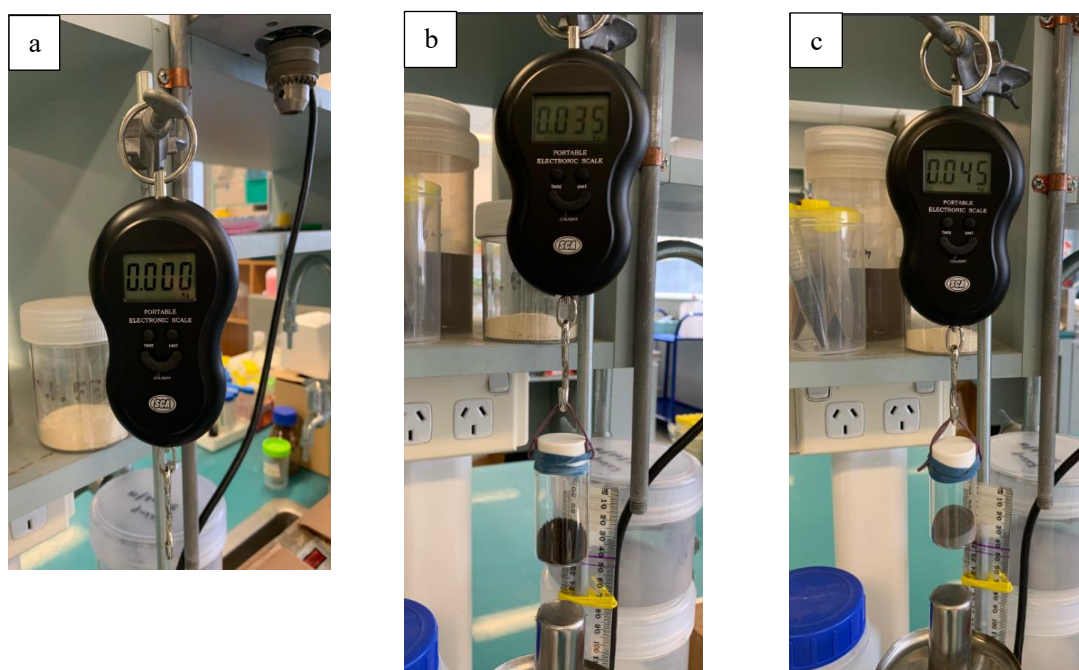
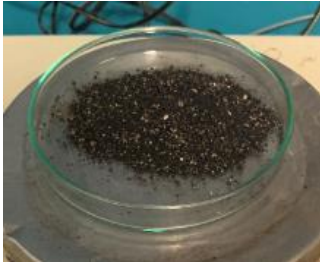


Figure 3.2: Magnetic “pull” experiments (a) portable electronic weighing scale (b) for “magnetic zeolite” and (c) for iron powder (control). Note that the iron powder presents a greater pull (0.045 vs 0.035 kg) than an equivalent settled volume of the magnetic zeolite sample.

<p>Iron oxide nanoparticles - no zeolite added</p>			
<p>MZ 1</p>			
<p>MZ 2</p>			
<p>MZ 3</p>			
<p>MZ 4</p>			

MZ 5	
MZ 6	
MZ 7	
MZ 8	

Figure 3.3: The formulated MZ particles.

<p>Iron oxide nanoparticles with no sawdust added</p>	
<p>MS 1</p>	
<p>MS 2</p>	

Figure 3.4: The formulated MS particles.

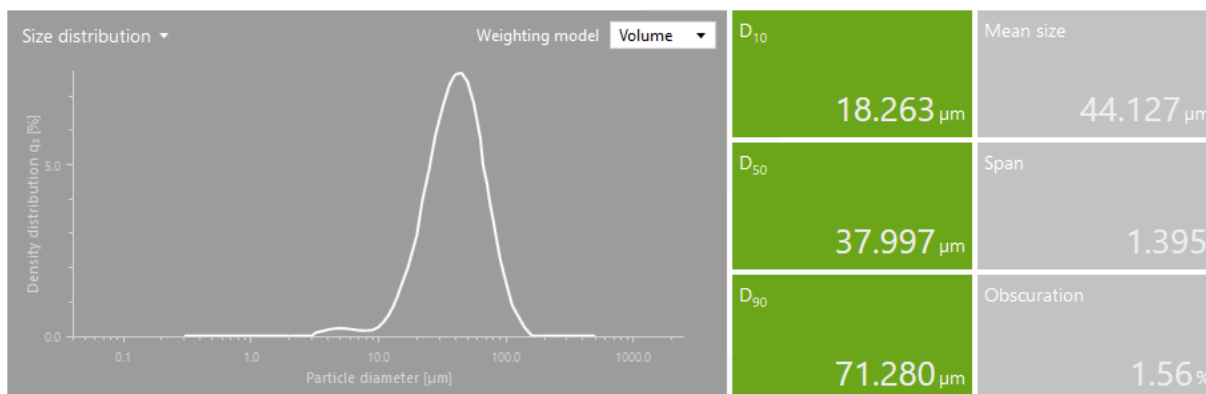


Figure 3.5: Particle size measurement for iron powder.

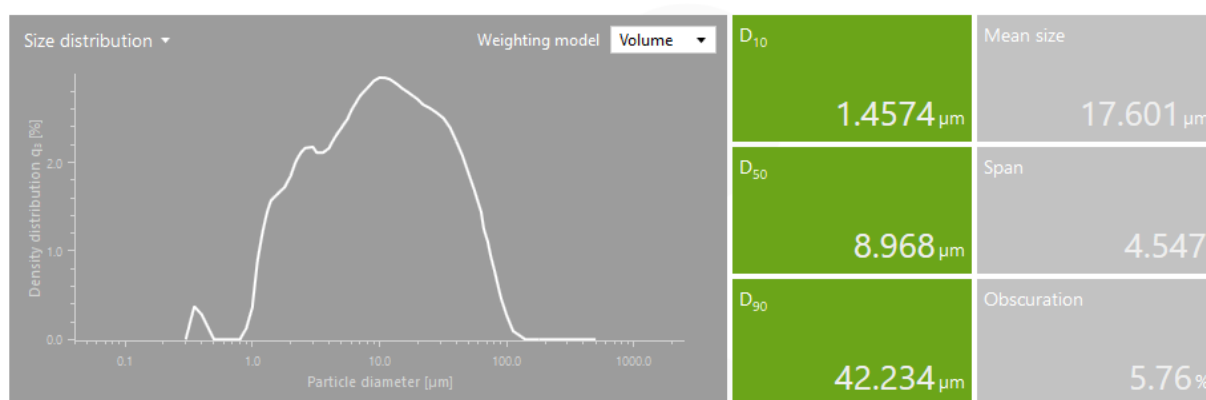


Figure 3.6: Particle size measurement for developed iron oxide nanoparticle with 1 gram zeolite added.

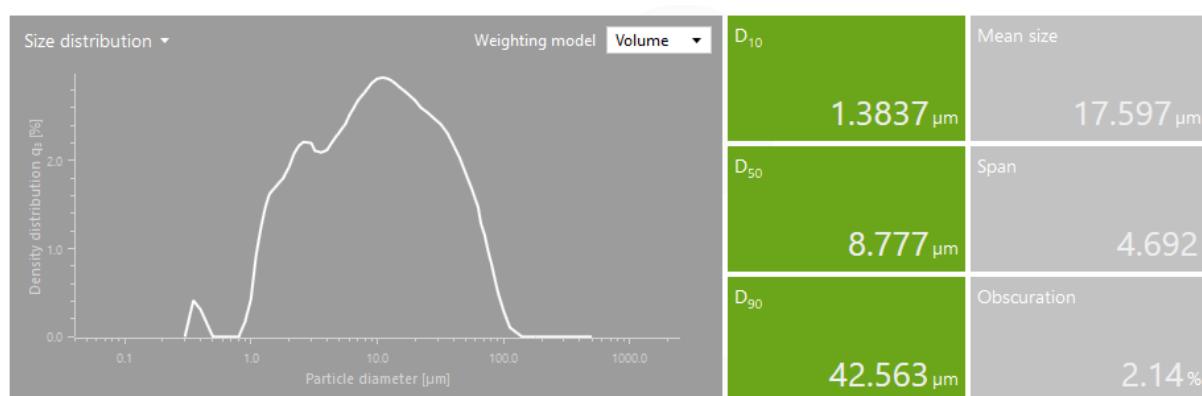


Figure 3.7: Particle size measurement for developed iron oxide nanoparticle with 2 grams zeolite added.

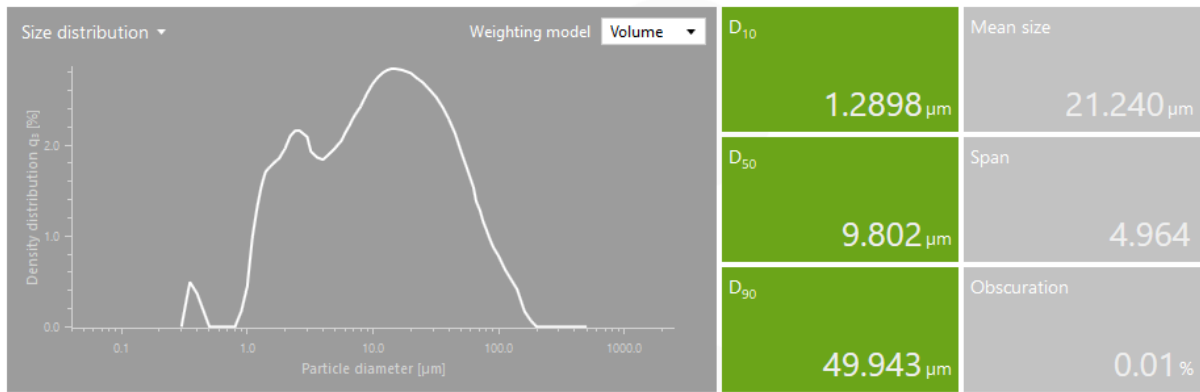


Figure 3.8: Particle size measurement for developed iron oxide nanoparticle with 3 grams zeolite added.



Figure 3.9: Particle size measurement for developed iron oxide nanoparticle with 4 grams zeolite added.

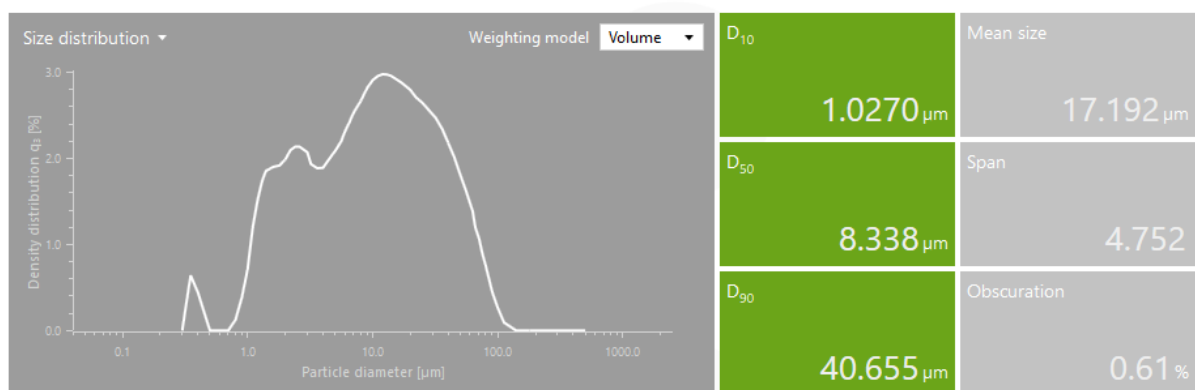


Figure 3.10: Particle size measurement for developed iron oxide nanoparticle with 5 grams zeolite added.

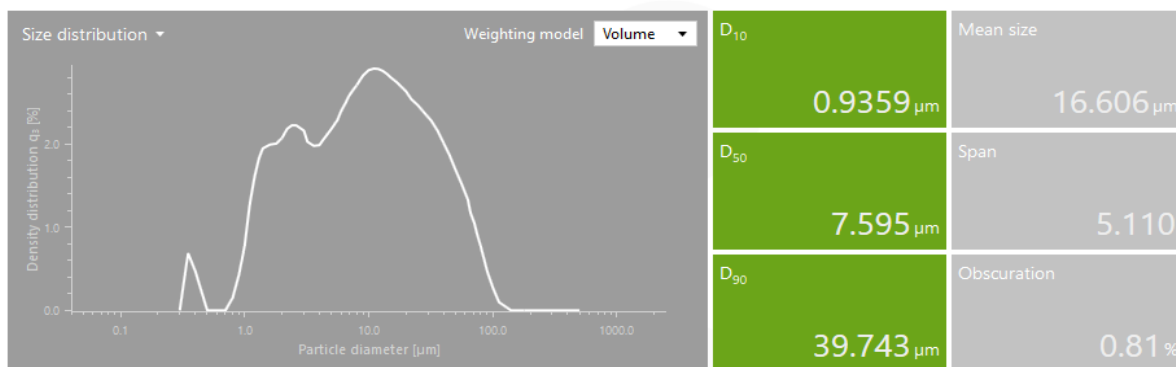


Figure 3.11: Particle size measurement for developed iron oxide nanoparticle with 6 grams zeolite added.

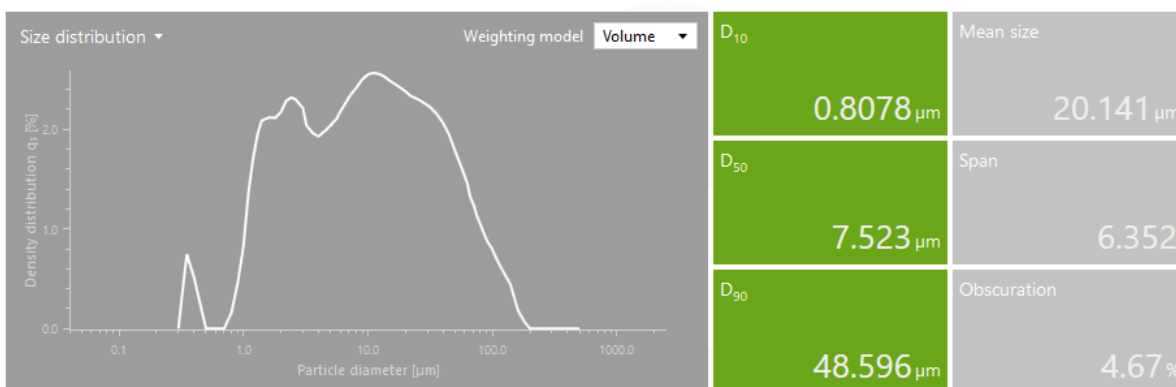


Figure 3.12: Particle size measurement for developed iron oxide nanoparticle with 7 grams zeolite added.

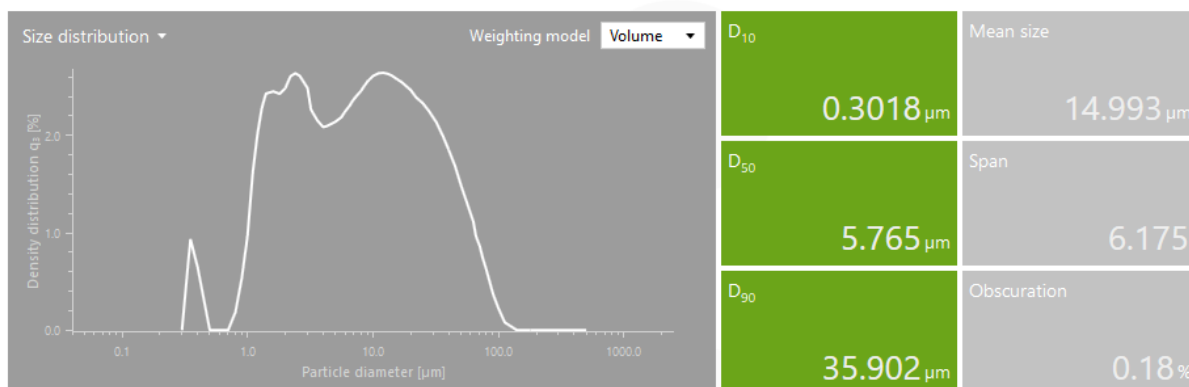


Figure 3.13: Particle size measurement for developed iron oxide nanoparticle with 8 grams zeolite added.

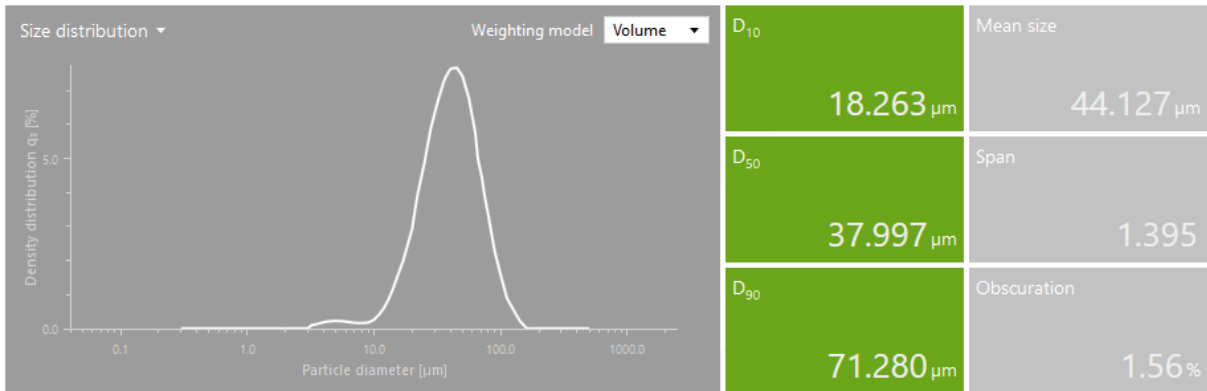


Figure 3.14: Particle size measurement for iron powder.

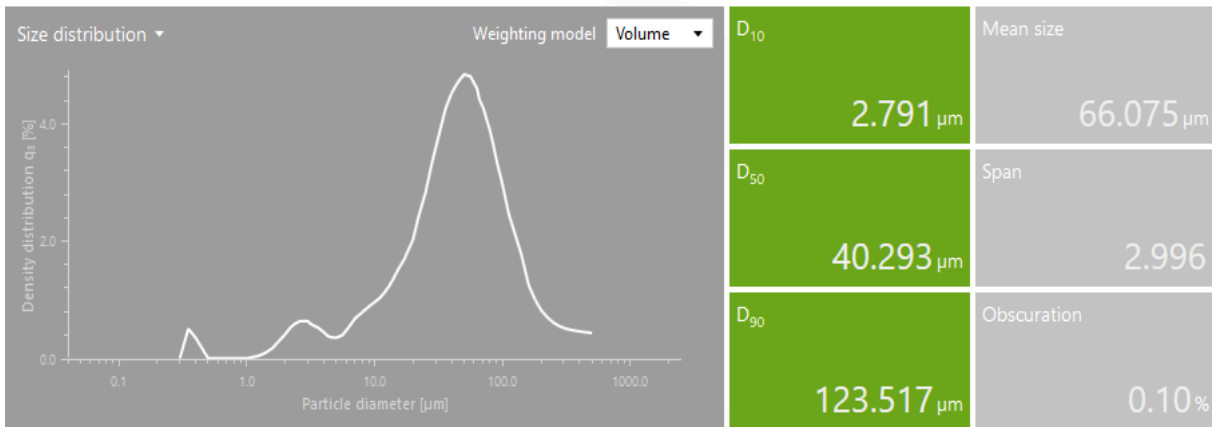


Figure 3.15: Particle size measurement for developed iron oxide nanoparticle with 1 gram sawdust added.

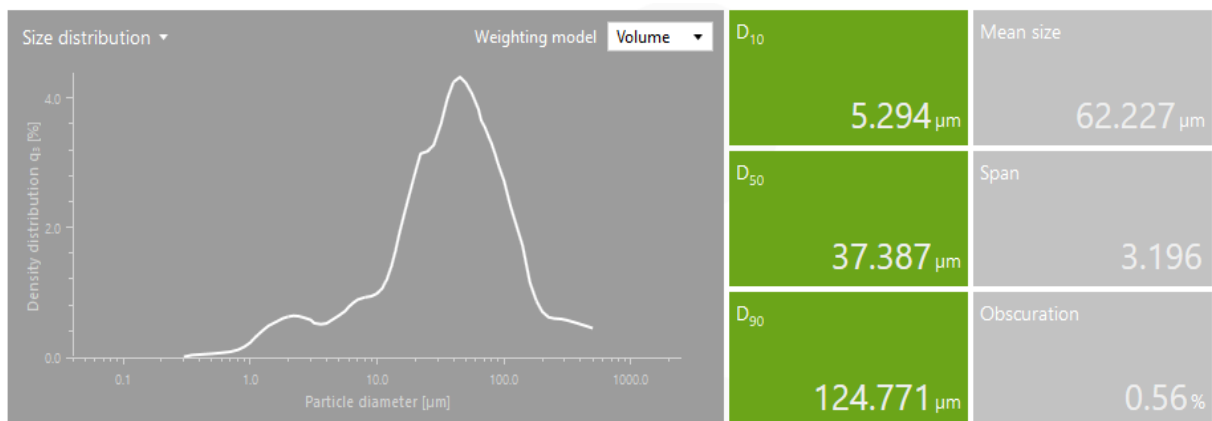


Figure 3.16: Particle size measurement for developed iron oxide nanoparticle with 2 grams sawdust added.

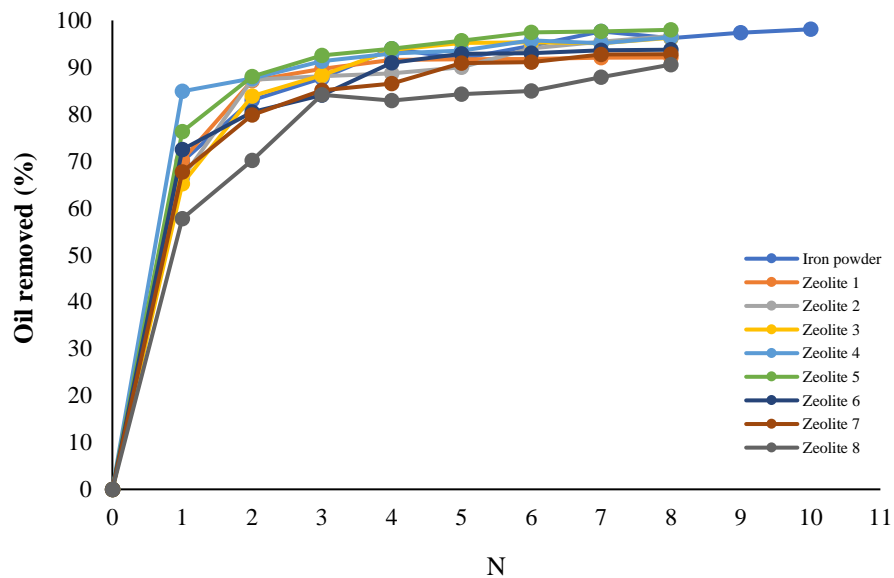


Figure 3.17: Comparison of the oil pick-up, P (%), from a glass substrate as a function of the number of treatments, N, amongst different powder compositions.

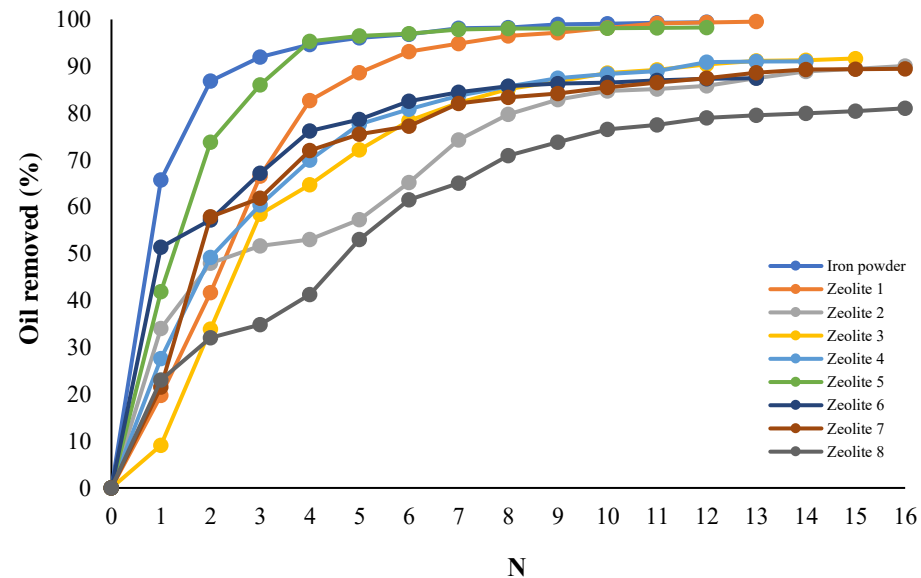


Figure 3.18: Comparison of the oil removal (%), from duck feathers as a function of the number of treatments, N, amongst different powder compositions.

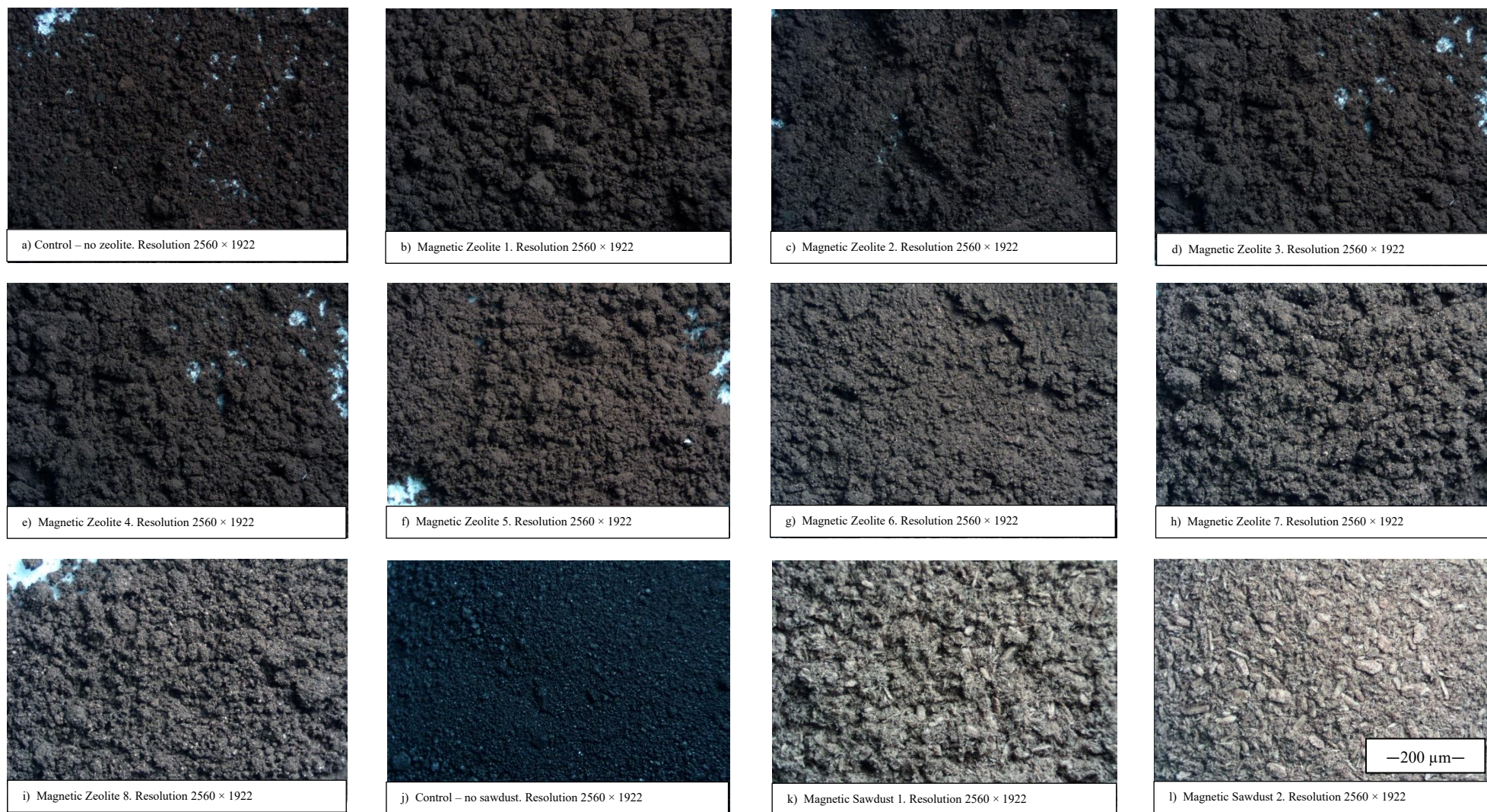


Figure 3.19: Examining the developed Magnetic Particles under an optical microscope (Olympus) of: **(a)** Control – no zeolite (only Fe_3O_4 added), **(b)** Magnetic Zeolite 1, **(c)** Magnetic Zeolite 2, **(d)** Magnetic Zeolite 3, **(e)** Magnetic Zeolite 4, **(f)** Magnetic Zeolite 5, **(g)** Magnetic Zeolite 6, **(h)** Magnetic Zeolite 7, **(i)** Magnetic Zeolite 8, **(j)** Control – no sawdust (only Chitosan and Fe_3O_4 added), **(k)** Magnetic Sawdust1 and **(l)** Magnetic Sawdust 2. The approximate scale (overall) is shown in Box l).

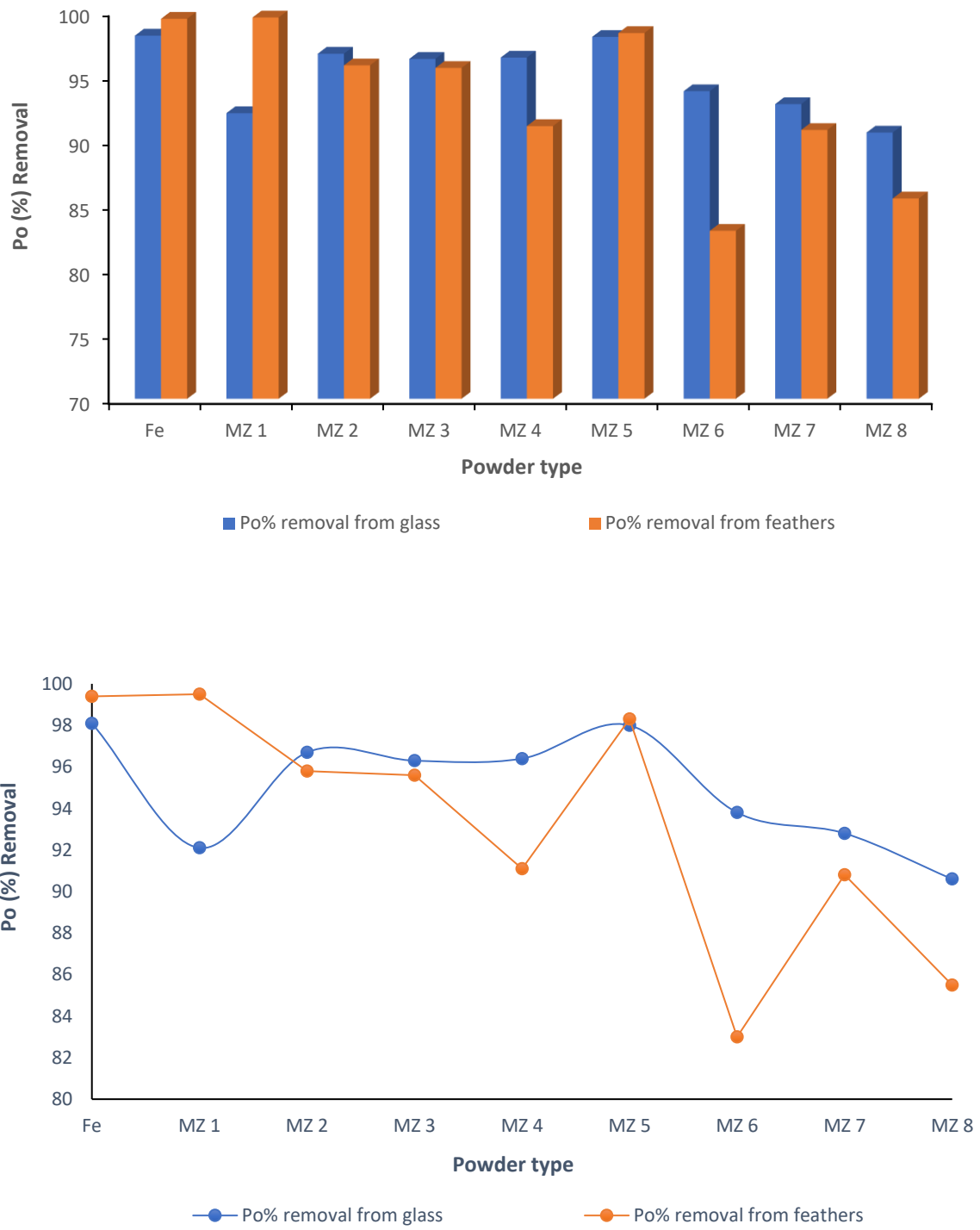


Figure 3.20: The Po% oil pick-up from a glass and feathers for different powder compositions.

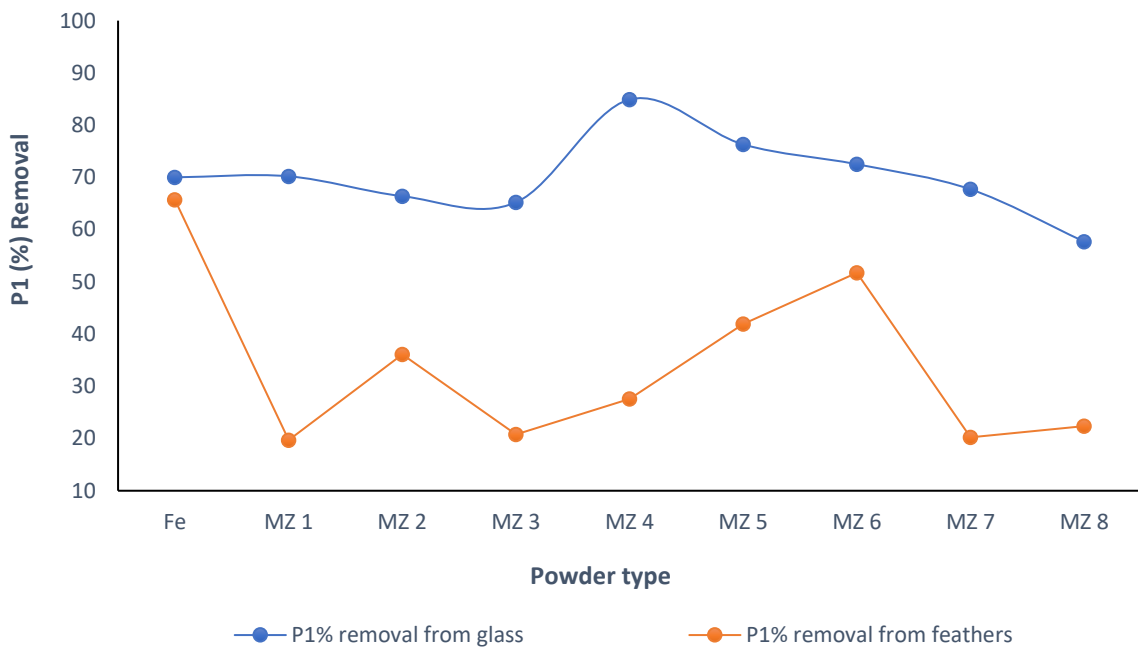
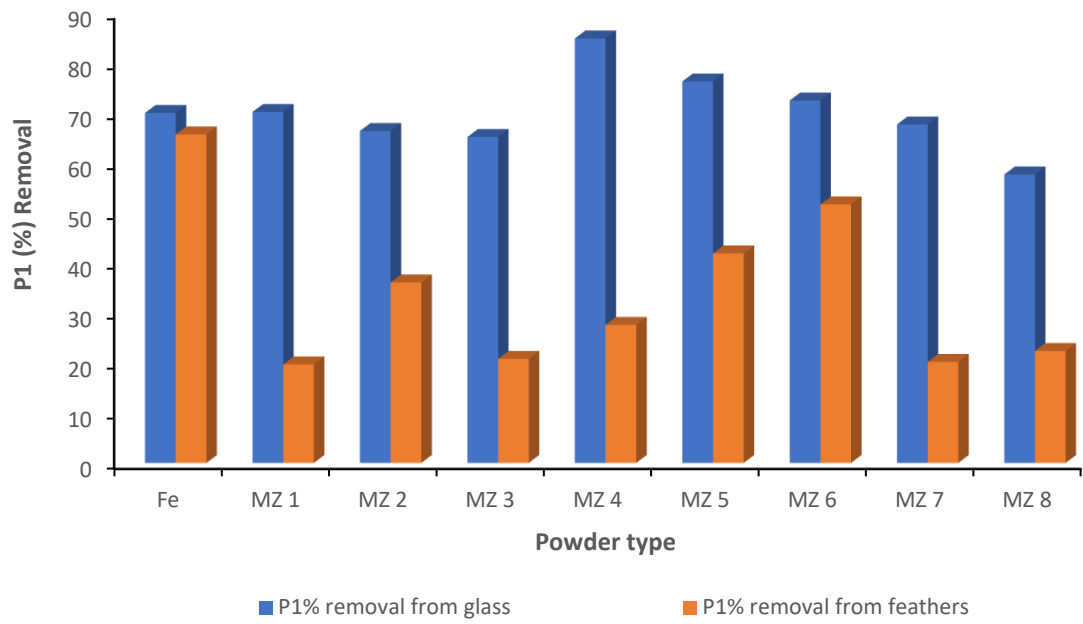


Figure 3.21: The P₁% oil pick-up from a glass and feathers for different powder compositions.

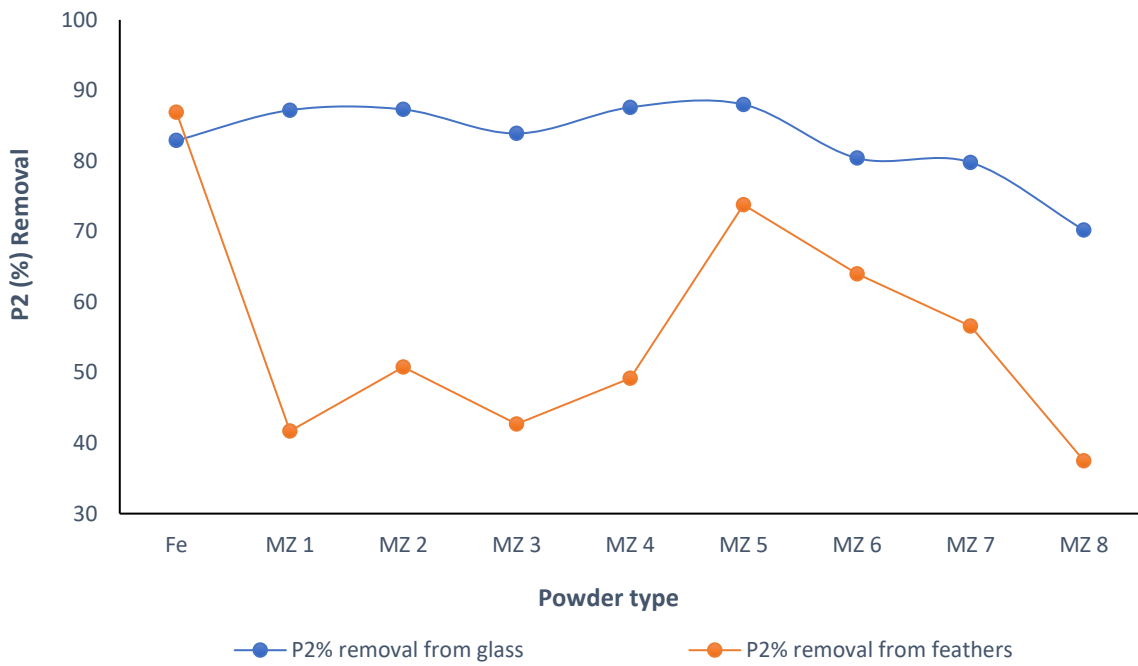
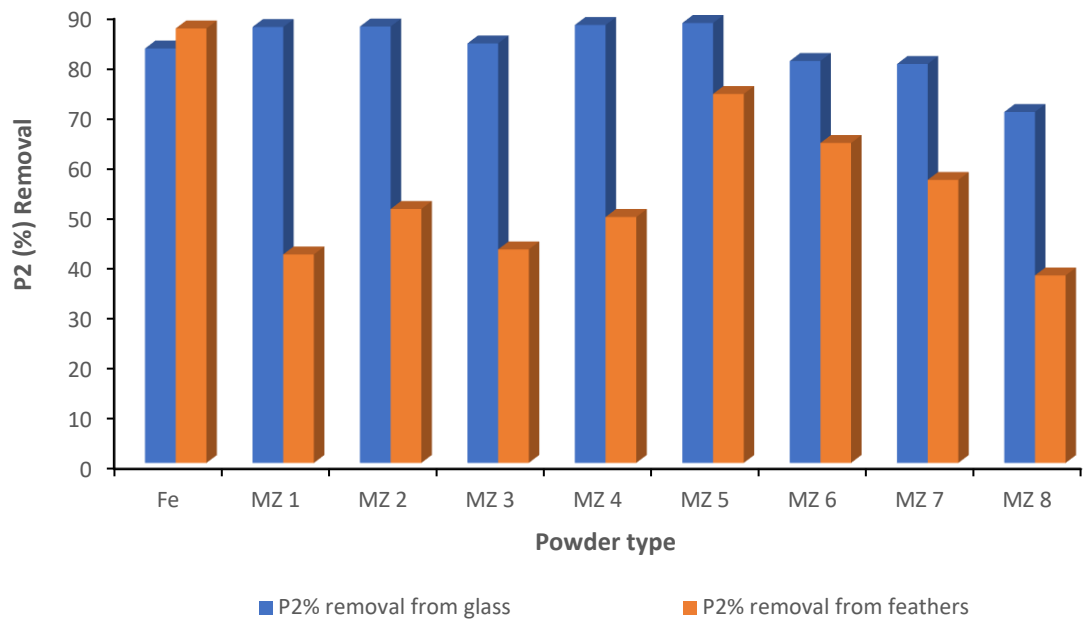


Figure 3.22: The P₂% oil pick-up from a glass and feathers for different powder compositions.

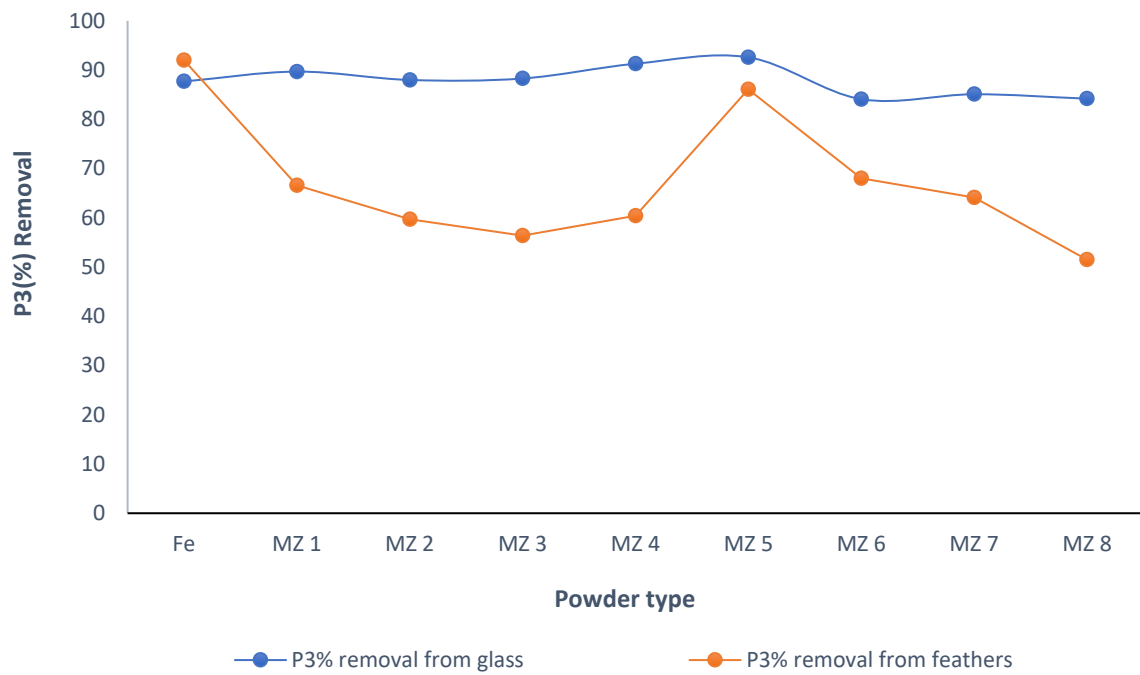
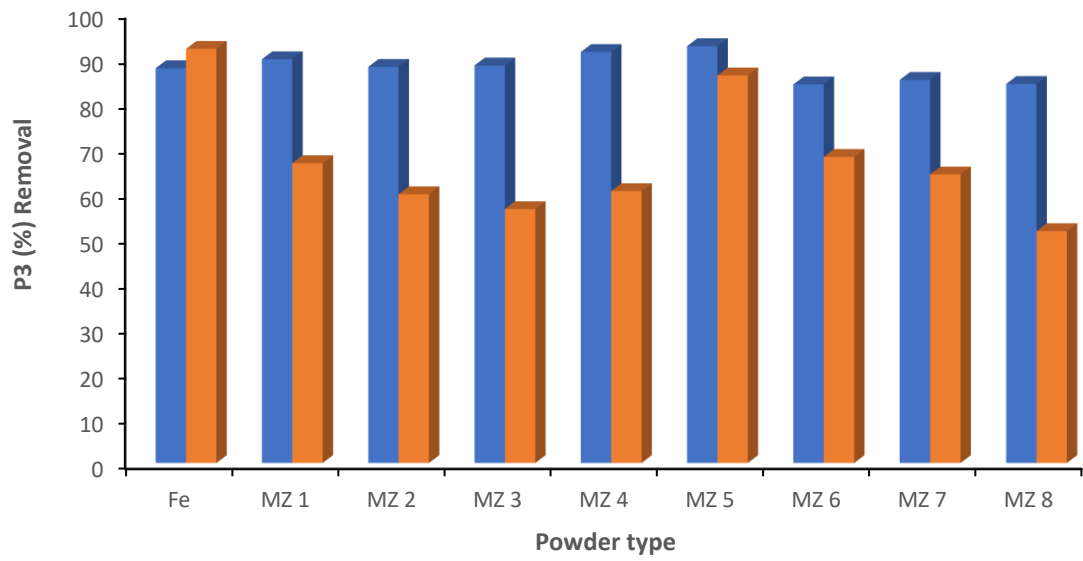


Figure 3.23: The P₃% oil pick-up from a glass and feathers for different powder compositions.

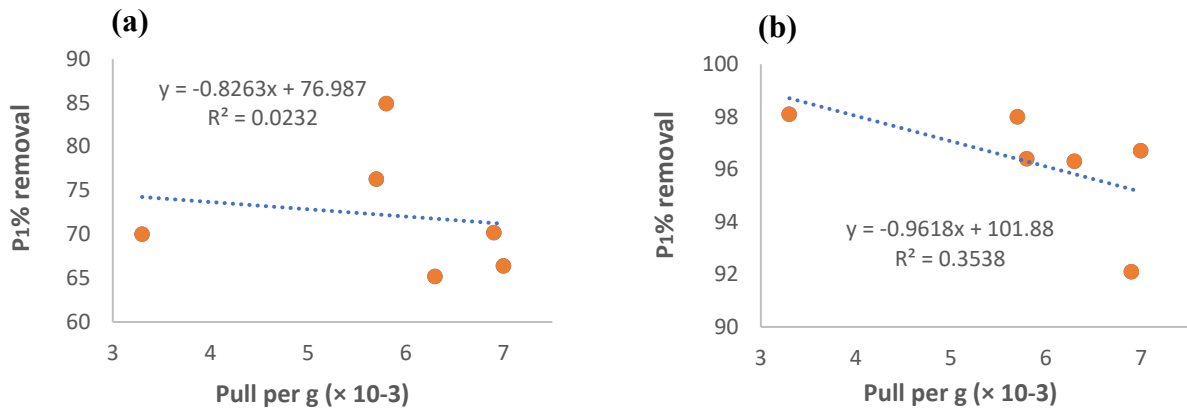


Figure 3.24: (a) Comparison of the P₁% removals versus Pull per gram ($\times 10^{-3}$) for glass and (b) Comparison of the P₁% removals versus Pull per gram ($\times 10^{-3}$) for feathers.

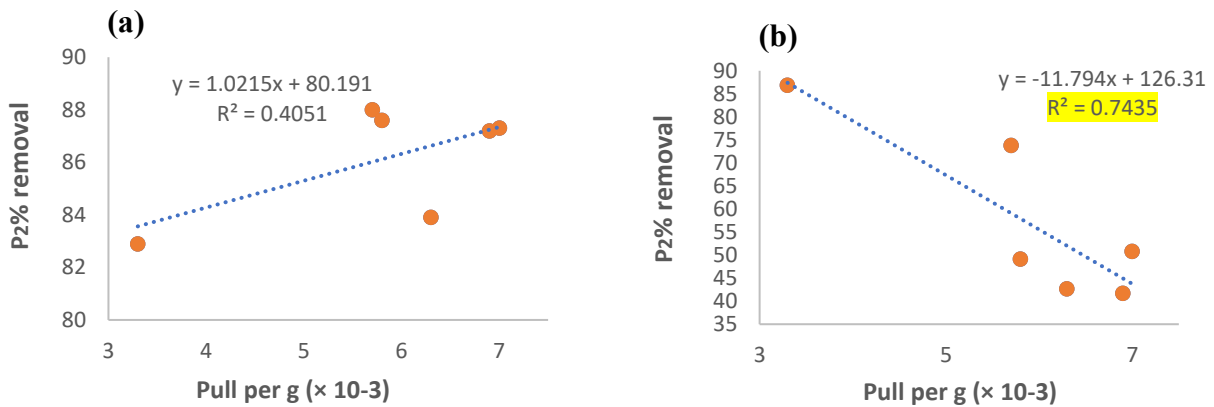


Figure 3.25: (a) Comparison of the P₂% removals versus Pull per gram ($\times 10^{-3}$) for glass and (b) Comparison of the P₂% removals versus Pull per gram ($\times 10^{-3}$) for feathers.

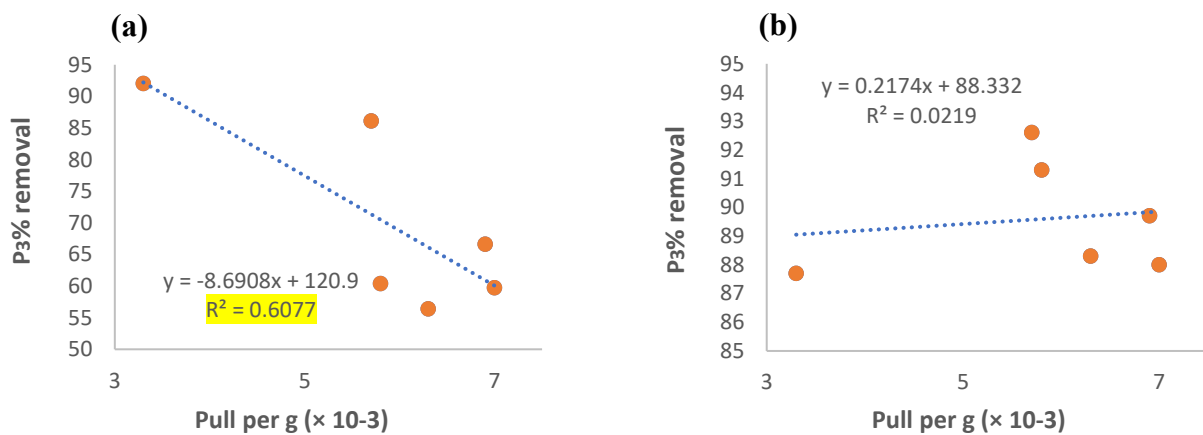


Figure 3.26: (a) Comparison of the P₃% removals versus Pull per gram ($\times 10^{-3}$) for glass and (b) Comparison of the P₃% removals versus Pull per gram ($\times 10^{-3}$) for feathers.

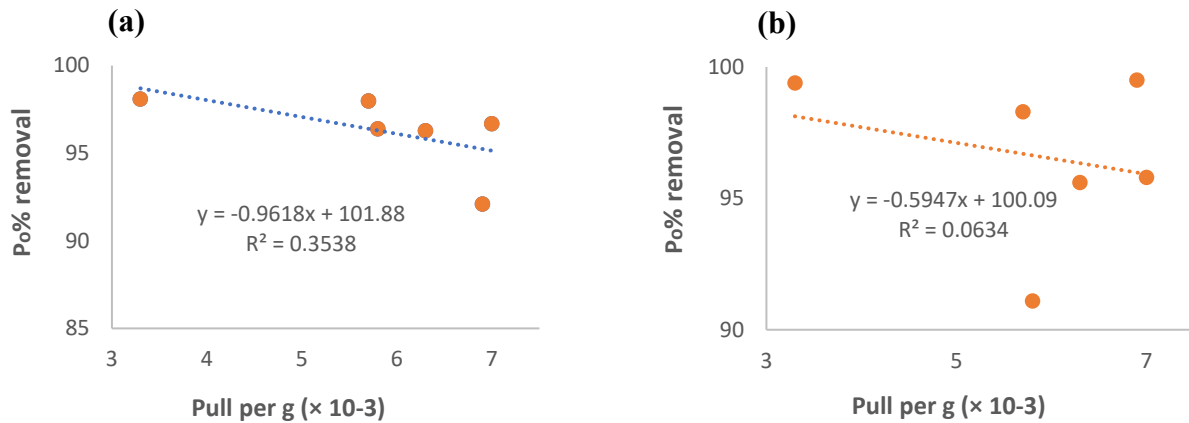


Figure 3.27: (a) Comparison of the $P_0\%$ removals versus Pull per gram ($\times 10^{-3}$) for glass and (b) Comparison of the $P_0\%$ removals versus Pull per gram ($\times 10^{-3}$) for feathers.

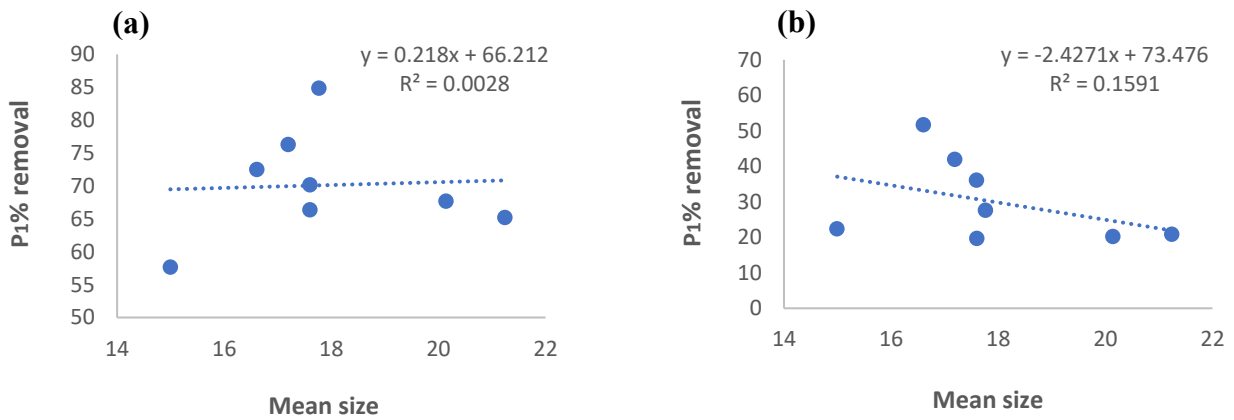


Figure 3.28: (a) Comparison of the $P_1\%$ removals versus Mean size for glass and (b) Comparison of the $P_1\%$ removals versus Mean size for feathers.

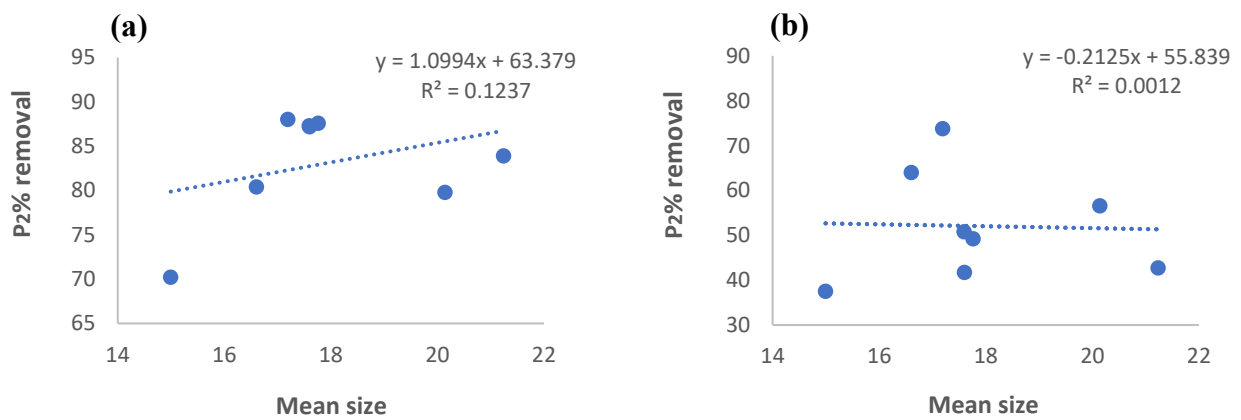


Figure 3.29: (a) Comparison of the $P_2\%$ removals versus Mean size for glass and (b) Comparison of the $P_2\%$ removals versus Mean size for feathers.

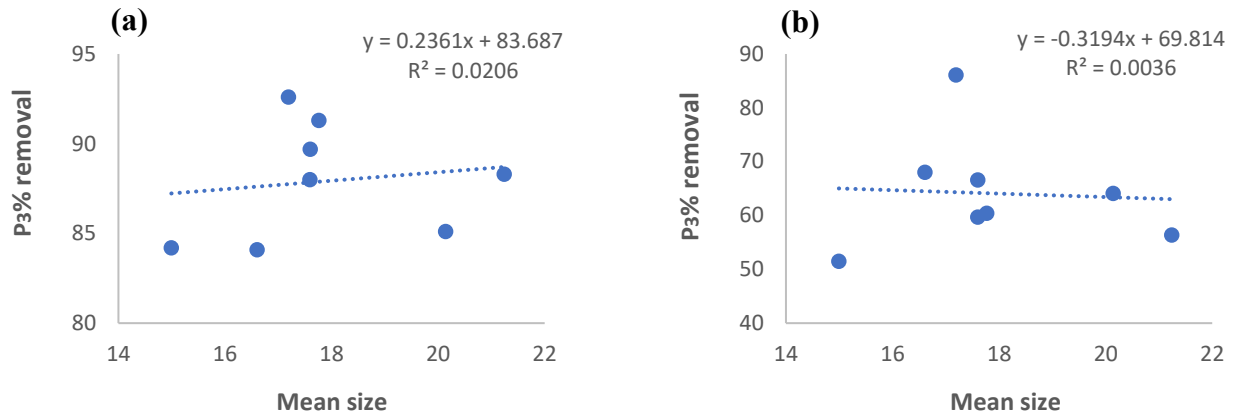


Figure 3.30: (a) Comparison of the P₃% removals versus Mean size for glass and (b) Comparison of the P₃% removals versus Mean size for feathers.

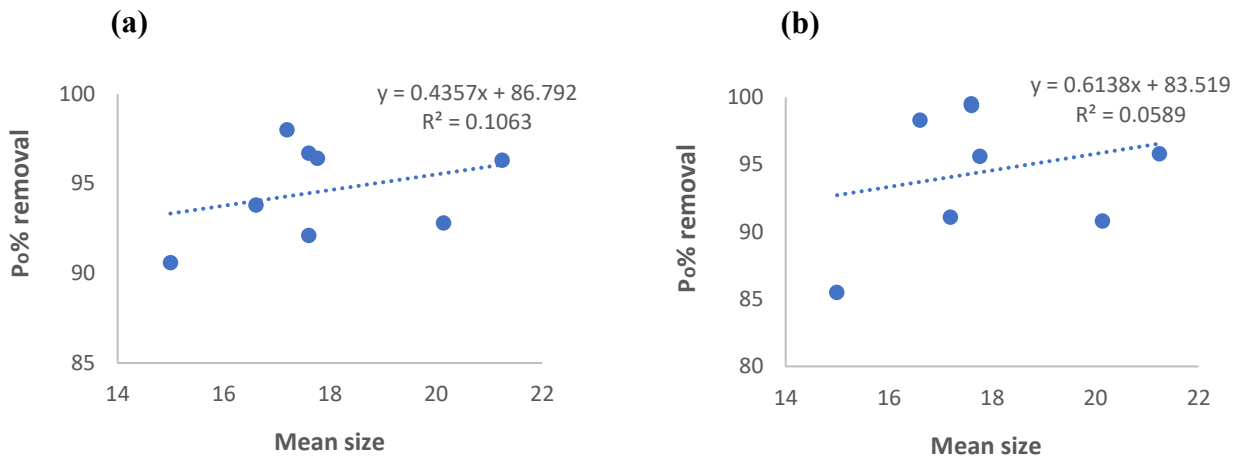


Figure 3.31: (a) Comparison of the P₀% removals versus Mean size for glass and (b) Comparison of the P₀% removals versus Mean size for feathers.

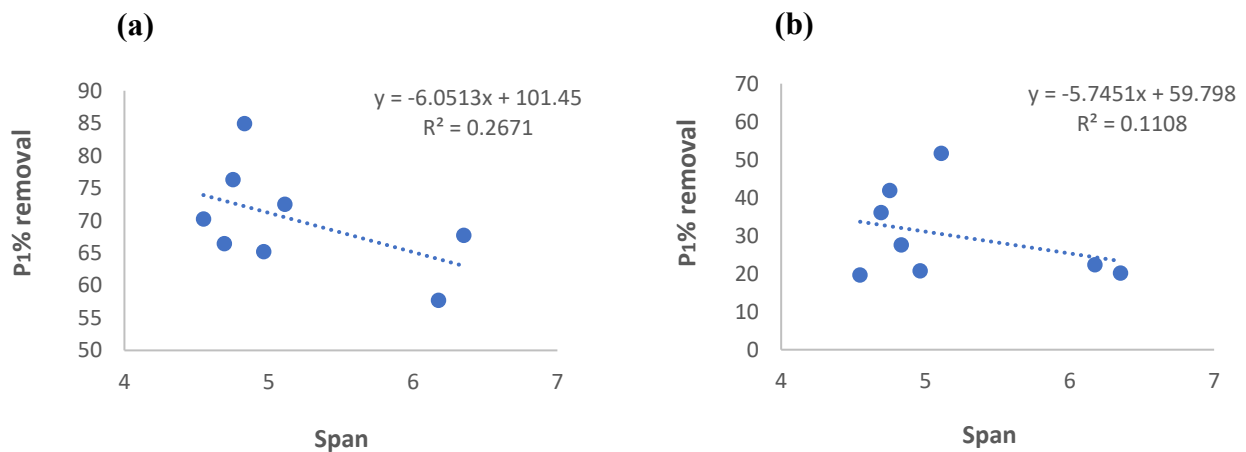


Figure 3.32: (a) Comparison of the P₁% removals versus Span for glass and (b) Comparison of the P₁% removals versus Span for feathers.

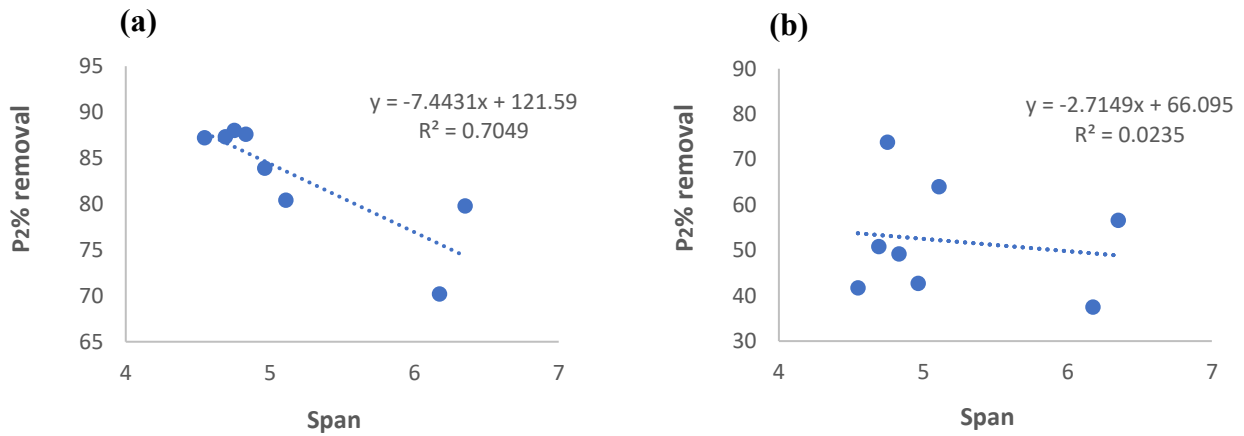


Figure 3.33: (a) Comparison of the P₂% removals versus Span for glass and (b) Comparison of the P₂% removals versus Span for feathers.

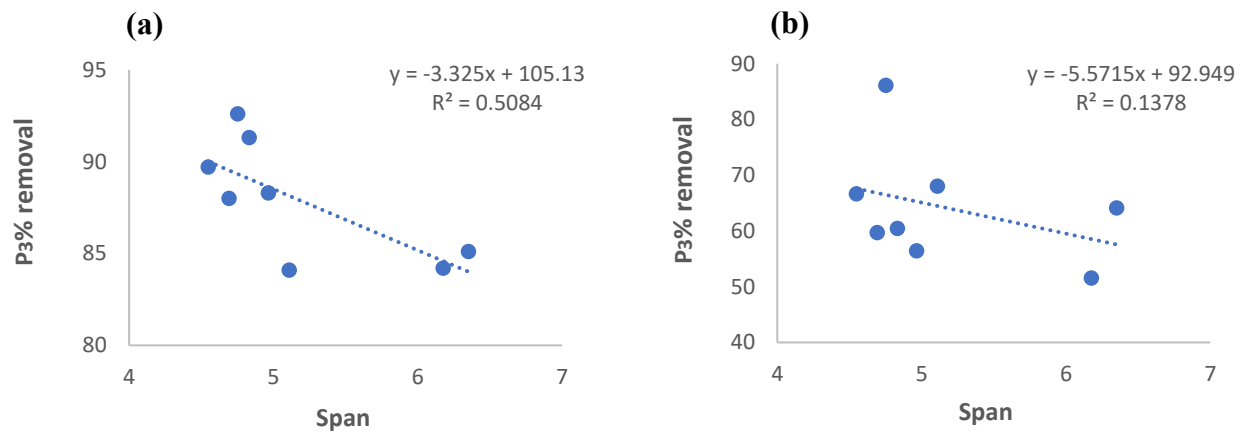


Figure 3.34: (a) Comparison of the P₃% removals versus Span for glass and (b) Comparison of the P₃% removals versus Span for feathers.

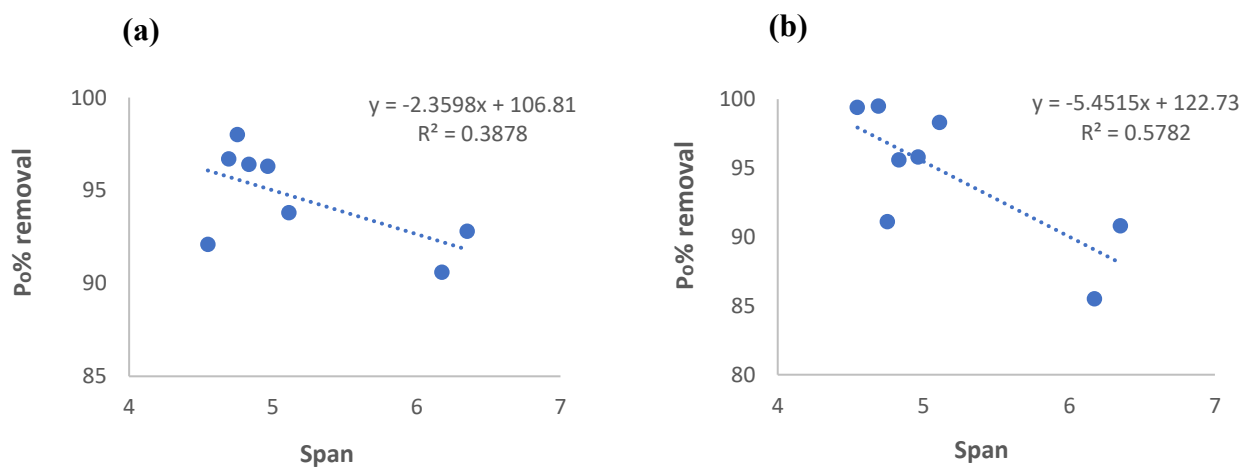


Figure 3.35: (a) Comparison of the P₀% removals versus Span for glass and (b) Comparison of the P₀% removals versus Span for feathers.

Appendix 4

Table 4.1: Oil contaminants utilised in the experiment.

Light Oils	Heavy Oils
Gippsland crude oil (GCO)	Engine oil (EO)
Diesel Oil (DO)	Bunker Oil 1 (BO1)

Table 4.2: Comparison of the removal of Gippsland Crude Oil between plumage, pelt (large and small size) and feather cluster.

N	Plumage		Pelt (large size)		Pelt (small size)		Feather cluster	
	P%	95%	P%	95%	P%	95%	F%	95%
1	41.37	4.34	67.90	4.12	85.51	1.49	98.12	0.16
2	61.96	6.74	73.12	3.31	87.62	0.69	98.54	0.10
A 3	72.94	5.72	78.04	2.53	89.38	0.98	98.84	0.18
4	80.50	4.20	82.34	3.09	90.34	1.09	99.03	0.12
5	86.01	1.91	87.27	2.88	91.75	0.97	99.11	0.20
6	89.84	1.69	91.65	2.36	92.88	1.22	99.12	0.12
7	93.11	2.01	94.05	1.82	94.54	0.79	99.16	0.11
8	95.18	1.33	95.44	1.55	95.27	2.31		
9	96.76	0.96	96.68	2.09	95.30	2.31		
10	97.60	0.97	97.27	2.18				

Table 4.3: Comparison of the removal of Diesel oil between plumage and pelt (large and small size).

N	Plumage		Pelt (large size)		Pelt (small size)	
	P%	95%	P%	95%	P%	95%
1	27.19	10.65	23.23	2.17	78.59	5.56
2	45.93	17.65	36.54	2.18	81.22	3.46
3	60.35	14.24	53.27	3.16	83.32	3.65
4	70.23	10.76	64.17	4.68	84.59	3.43
5	77.26	7.52	73.81	3.26	86.47	3.95
6	82.95	5.05	80.68	2.44	88.47	4.50
7	87.21	5.69	85.15	2.61	90.11	4.33
8	90.76	3.68	89.39	1.83	92.16	2.89
9	93.11	2.36	90.75	1.35	93.35	3.21
10			91.55	1.19	93.75	3.25

Table 4.4: Comparison of the removal of Engine oil between plumage, pelt (large and small size) and feather cluster.

N	Plumage		Pelt (large size)		Pelt (small size)		Feather cluster	
	P%	95%	P%	95%	P%	95%	F%	95%
1	38.23	4.80	40.23	2.20	48.34	1.63	96.65	2.14
2	53.97	11.64	54.27	4.86	61.33	2.79	99.18	0.67
3	66.23	8.11	67.00	5.39	72.32	3.34	99.43	0.43
4	75.23	5.52	78.50	3.51	80.81	3.94	99.53	0.35
5	81.44	5.02	85.87	3.73	86.01	3.33	99.63	0.27
6	86.58	4.91	89.23	4.15	89.98	2.27	99.71	0.21
7	90.88	3.65	91.31	3.30	92.92	1.69	99.74	0.21
8	93.74	2.40	93.99	1.33	94.81	1.70		
9	95.89	1.30	95.48	0.79	96.17	2.24		
10	96.98	1.45	95.94	1.16	97.47	2.27		
10	96.98	1.45	95.94	1.16	97.47	2.27		

Table 4.5: Comparison of the removal of Bunker oil 1 (BO1) between plumage, pelt (large and small size) and feather cluster.

N	Plumage		Pelt (large size)		Pelt (small size)		Feather cluster	
	P%	95%	P%	95%	P%	95%	F%	95%
1	35.07	5.46	38.38	6.04	45.44	3.09	82.23	5.38
2	51.80	7.67	52.62	7.71	56.35	1.85	94.26	1.78
3	66.99	3.40	69.33	3.36	66.73	3.40	97.01	1.88
4	75.03	2.83	77.10	3.12	75.80	2.18	98.25	1.39
5	84.30	2.94	85.61	3.76	84.37	3.45	98.91	0.63
6	88.66	2.88	88.52	2.93	89.93	1.67	99.01	0.37
7	91.16	2.66	92.85	2.22	91.79	0.98	99.26	0.40
8	93.61	2.27	94.21	1.82	93.30	1.42		
9	95.0	1.70	94.76	1.72	93.95	1.94		
10	95.98	1.79	95.15	1.67	94.28	1.98		
11					94.41	2.00		
12					94.49	1.98		

Table 4.6: The removal of Gippsland crude oil, P (%), comparison between original pelt and recycled pelt. Recycling of the pelt experiments were conducted in five replicates.

N	Original	Five replicates (P%)					P% (mean)	95%
1	68.06	63.95	69.34	68.61	65.32	72.30	67.90	4.12
2	73.45	69.93	74.44	73.81	70.94	76.49	73.12	3.31
3	79.19	76.97	80.25	77.51	75.49	79.99	78.04	2.53
4	83.89	81.88	84.82	81.21	79.0	84.79	82.34	3.09
5	88.03	86.2	90.40	86.24	84.63	88.88	87.27	2.88
6	92.35	90.92	94.89	90.89	89.96	91.60	91.65	2.36
7	93.95	92.97	95.91	93.16	92.86	95.38	94.05	1.82
8	95.92	95.11	96.30	94.92	93.85	97.05	95.44	1.55
9	97.19	97.20	97.26	95.80	94.35	98.82	96.68	2.09
10	98.02	97.34	98.84	96.12	94.98	99.09	97.27	2.18

Table 4.7: The removal of Diesel Fuel Oil, P%, comparison between original pelt and recycled pelt. Recycling of the pelt experiments were conducted in five replicates.

N	Original	Five replicates (P%)					P% (mean)	95%
1	23.42	25.7	24.23	21.25	22.2	22.78	23.23	2.17
2	36.73	38.5	37.36	33.81	37.0	36.07	36.54	2.18
3	53.41	55.01	54.4	49.22	55.4	52.36	53.27	3.16
4	64.67	67.57	66.58	58.31	62.58	65.83	64.17	4.68
5	73.19	76.29	75.09	69.49	73.36	74.82	73.81	3.26
6	79.25	82.76	81.26	77.48	81.43	80.5	80.68	2.44
7	84.5	86.97	86.75	81.72	85.02	85.33	85.15	2.61
8	88.98	89.82	91.56	87.5	89.19	88.9	89.39	1.83
9	91.48	91.52	92.22	89.5	90.21	90.33	90.75	1.35
10	91.71	91.94	92.7	90.06	91.59	91.46	91.55	1.19

Table 4.8: The removal of Engine oil, P (%), comparison between original pelt and recycled pelt. Recycling of the pelt experiments were conducted in five replicates.

N	Original	Five replicates (P%)					P% (mean)	95%
1	41.22	40.81	39.83	37.35	41.34	41.83	40.23	2.20
2	57.77	55.63	54.14	47.61	56.62	57.39	54.27	4.86
3	68.52	69.14	67.04	59.49	69.31	70.04	67.00	5.39
4	77.86	78.32	82.18	74.25	78.7	79.06	78.50	3.51
5	83.33	83.21	90.8	83.67	85.8	85.91	85.87	3.73
6	87.79	89.55	94.87	86.41	87.96	87.39	89.23	4.15
7	89.44	92.67	95.15	90.83	89.48	88.45	91.31	3.30
8	92.14	94.08	95.78	93.01	93.79	93.33	93.99	1.33
9	95.09	95.31	96.14	94.63	95.23	96.12	95.48	0.79
10	95.29	95.59	96.48	94.67	95.83	97.15	95.94	1.16

Table 4.9: The removal of bunker oil 1 (BO1), P (%), comparison between original pelt and recycled pelt. Recycling of the pelt experiments were conducted in five replicates.

N	Original	Five replicates (P%)					P% (mean)	95%
1	37.17	38.26	39.01	30.61	43.95	40.09	38.38	6.04
2	53.88	52.07	57.1	42.25	54.13	57.56	52.62	7.71
3	66.89	67.09	71.83	65.81	70.6	71.36	69.33	3.36
4	75.53	75.67	80.16	74.21	76.2	79.28	77.10	3.12
5	84.41	84.02	87.44	81.1	86.95	88.58	85.61	3.76
6	87.88	88.85	89.44	84.51	89.06	90.77	88.52	2.93
7	91.36	91.28	93.64	90.67	93.86	94.84	92.85	2.22
8	93.66	93.55	95.56	91.95	94.88	95.13	94.21	1.82
9	94.95	95.18	95.83	92.32	95.17	95.32	94.76	1.72
10	95.27	95.82	96.18	92.8	95.35	95.61	95.15	1.67

Table 4.10: Magnetic cleansing experiments with different levels of Diesel fuel oil coverage.

N	10% Coverage		20% Coverage		50% Coverage		70% Coverage		100% Coverage	
	P%	95%	P%	95%	P%	95%	P%	95%	P%	
1	32.69	9.30	29.47	8.39	19.60	4.288	17.05	10.65	37.15	
2	55.97	10.10	46.02	9.11	32.66	14.21	31.28	16.71	63.75	
3	67.94	11.37	59.69	3.41	47.90	25.99	50.91	13.86	75.32	
4	75.69	13.80	69.44	7.84	59.07	21.82	65.58	8.69	81.38	
5	79.45	13.51	77.16	4.23	68.97	18.98	75.14	5.20	85.57	
6	83.33	10.51	81.94	4.02	78.60	11.11	81.31	11.96	89.56	
7	87.17	13.38	85.55	2.64	82.09	9.93	86.61	12.01	94.61	
8	90.07	7.86	89.10	2.20	88.47	4.32	90.26	10.72	95.91	
9	92.46	5.37	91.79	1.45	91.32	5.76	93.99	9.79	96.01	

Table 4.11: Magnetic cleansing experiments with different levels of Diesel fuel oil coverage including the average of 10%, 20%, 50%, 70% and 100% and average of percentage error.

N	10% Coverage		20% Coverage		50% Coverage		70% Coverage		100% Coverage		Average of % Coverage	Average of Percentage Error
	P%	95%	P%	95%	P%	95%	P%	95%	P%			
										0	0	
1	32.69	9.30	29.47	8.39	19.60	4.28	17.05	10.65	37.15	27.19	35.32	
2	55.97	10.10	46.02	9.11	32.66	14.21	31.28	16.71	63.75	45.93	33.70	
3	67.94	11.37	59.69	3.41	47.90	25.99	50.91	13.86	75.32	60.35	25.99	
4	75.69	13.80	69.44	7.84	59.07	21.82	65.58	8.69	81.38	70.23	19.93	
5	79.45	13.51	77.16	4.23	68.97	18.98	75.14	5.20	85.57	77.26	14.23	
6	83.33	10.51	81.94	4.02	78.60	11.11	81.31	11.96	89.56	82.95	11.59	
7	87.17	13.38	85.55	2.64	82.09	9.93	86.61	12.01	94.61	87.21	11.10	
8	90.07	7.86	89.10	2.20	88.47	4.32	90.26	10.72	95.91	90.76	6.99	
9	92.46	5.37	91.79	1.45	91.32	5.76	93.99	9.799	96.01	93.11	6.03	

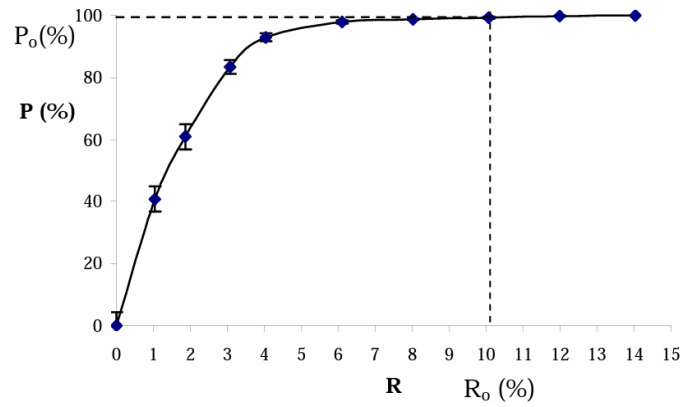


Figure 4.1: Isotherm for oil removal from a glass substrate. The contaminant is Arab medium oil, and the ideal grade of iron powder used for such experiments is Höganäs MH300.29. The 95% confidence intervals are shown by error bars, for five replicates.

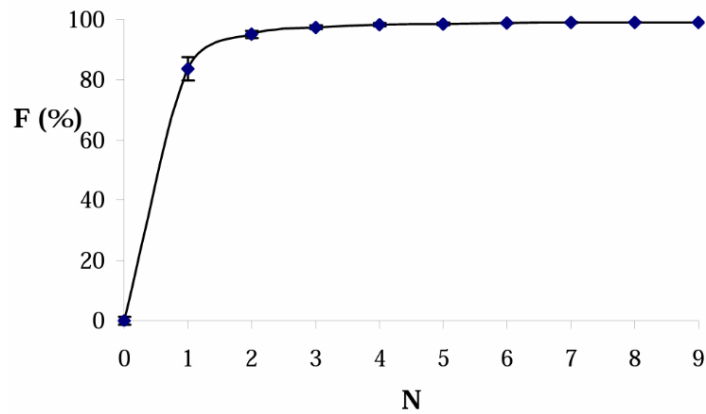


Figure 4.2: Typical ab(d)sorption isotherm for oil removal from a cluster of feathers. The contaminant is Arab medium oil. The confidence intervals are 95% for five replicates.

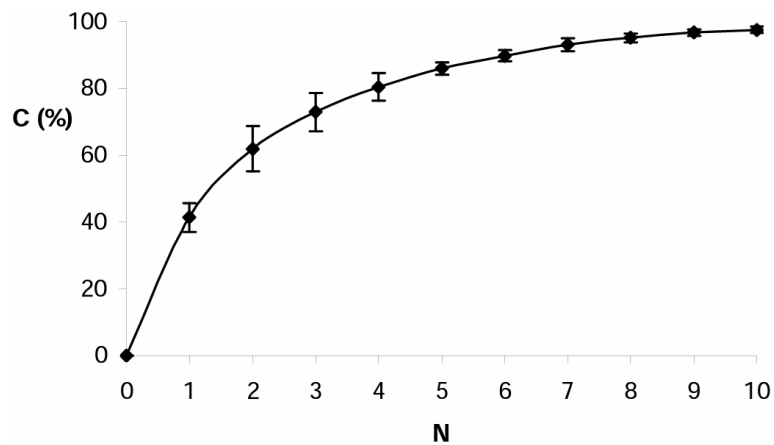


Figure 4.3: The sorption isotherm for oil pick-up from plumage. The contaminant used is Gippsland crude oil, and the iron powder is grade MH300.29. The confidence intervals are 95% for five replicates.

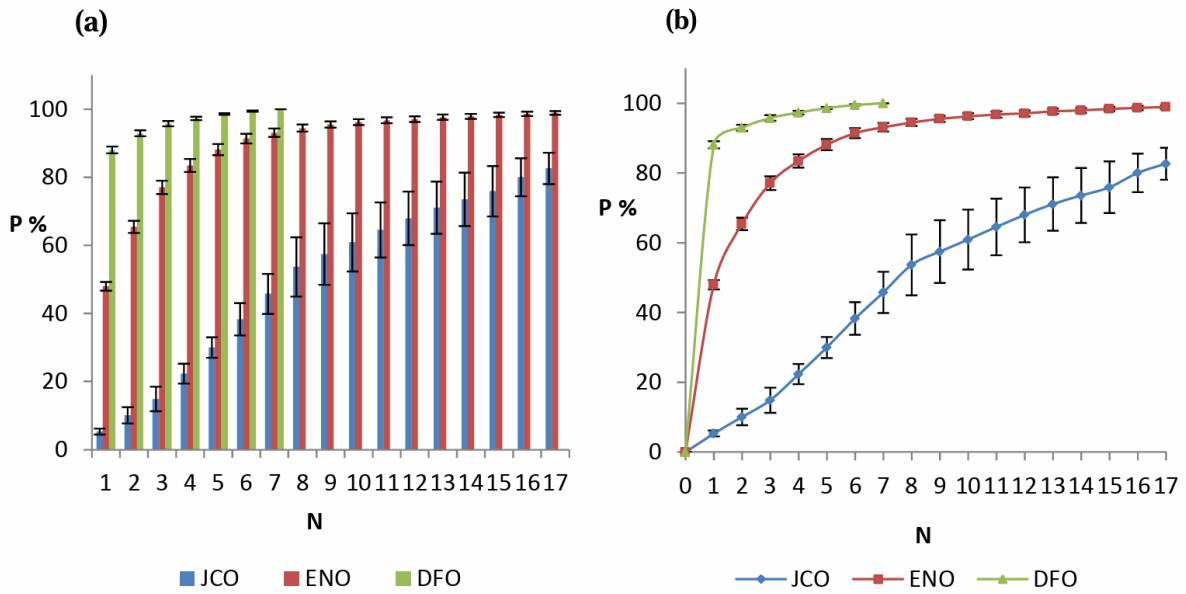


Figure 4.4: (a) Histogram representation (b) Curve representation comparing the removal percentages (P%) of three different contaminants (Jasmine Crude Oil, Engine Oil and Diesel Fuel Oil) from rabbit fur (RF) as a function of the number of treatments (N). The SE for five replicates is shown by error bars (Munaweera, 2015).

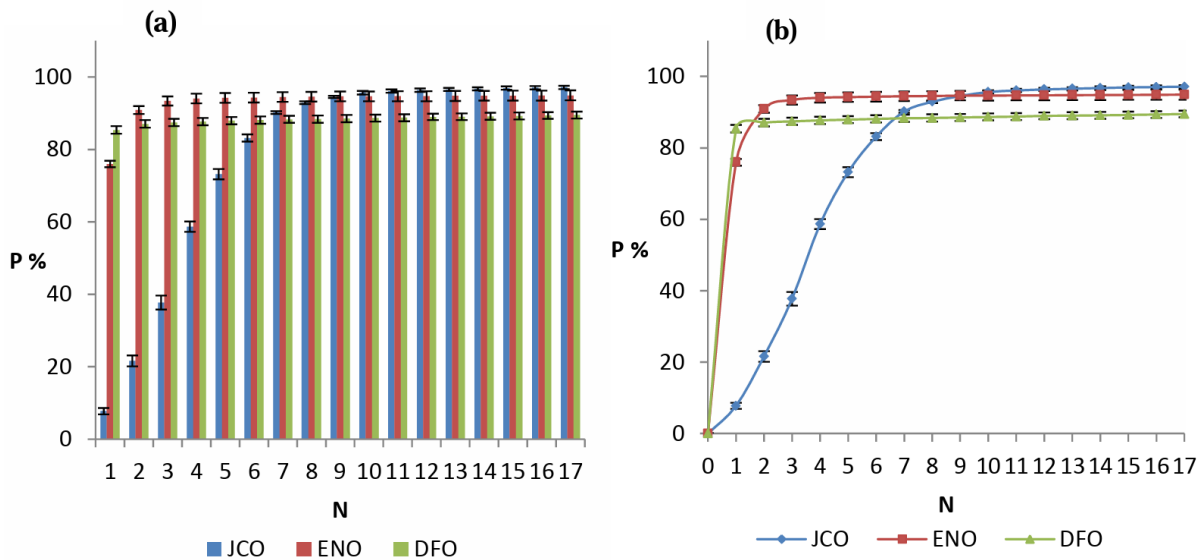


Figure 4.5: (a) Histogram representation (b) Curve representation comparing the removal percentages (P%) of three different contaminants (Jasmine Crude Oil, Engine Oil and Diesel Fuel Oil) from seal fur (SF) as a function of the number of treatments (N). The SE for five replicates is shown by error bars (Munaweera, 2015).



Figure 4.6: Breast pelt and back pelt from Little Penguin (*Eudyptula minor*).



Figure 4.7: Magnetic Tester employed for performing MPT oil removal experiments.

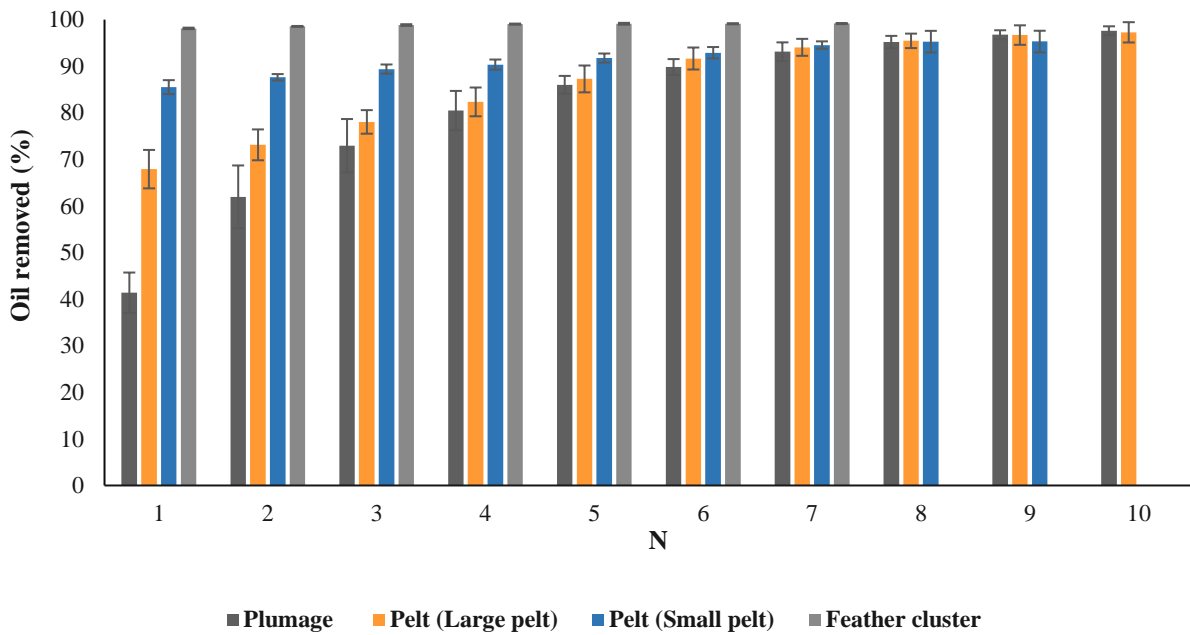


Figure 4.8: Comparison between penguin carcass (plumage), large penguin pelt size, small penguin pelt size and a penguin feather cluster for the removal of Gippsland crude oil as a function of the number of treatments, N. Error bars represent the 95% confidence intervals for five replicates.

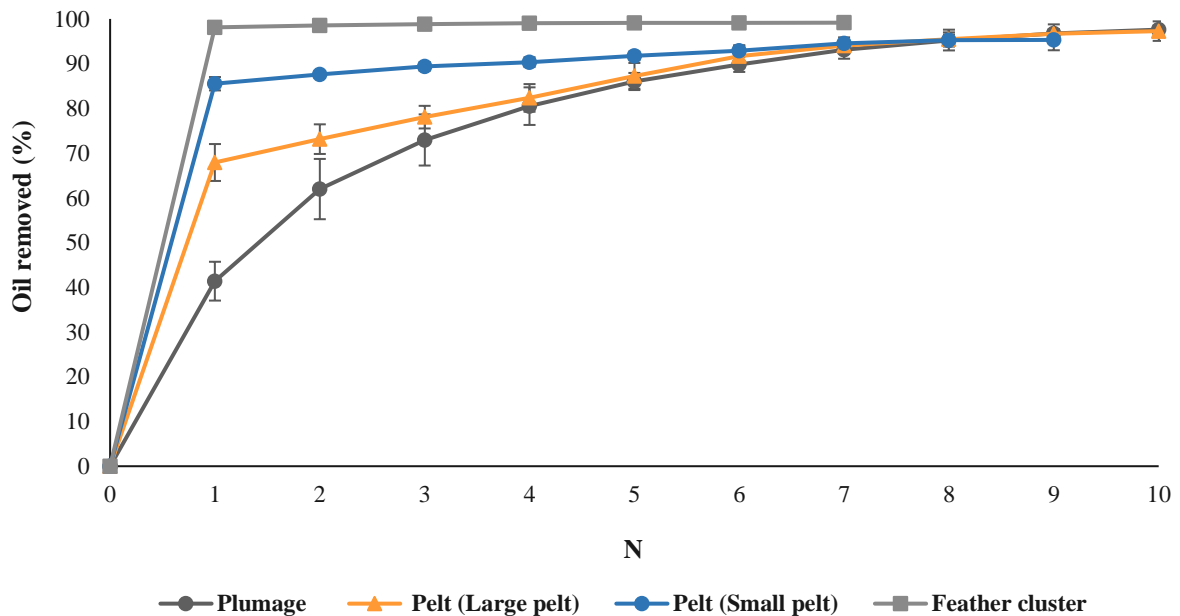


Figure 4.9: Comparison between penguin carcass (plumage), large penguin pelt size, small penguin pelt size and a penguin feather cluster for the removal of Gippsland crude oil as a function of the number of treatments, N. Error bars represent the 95% confidence intervals for five replicates.

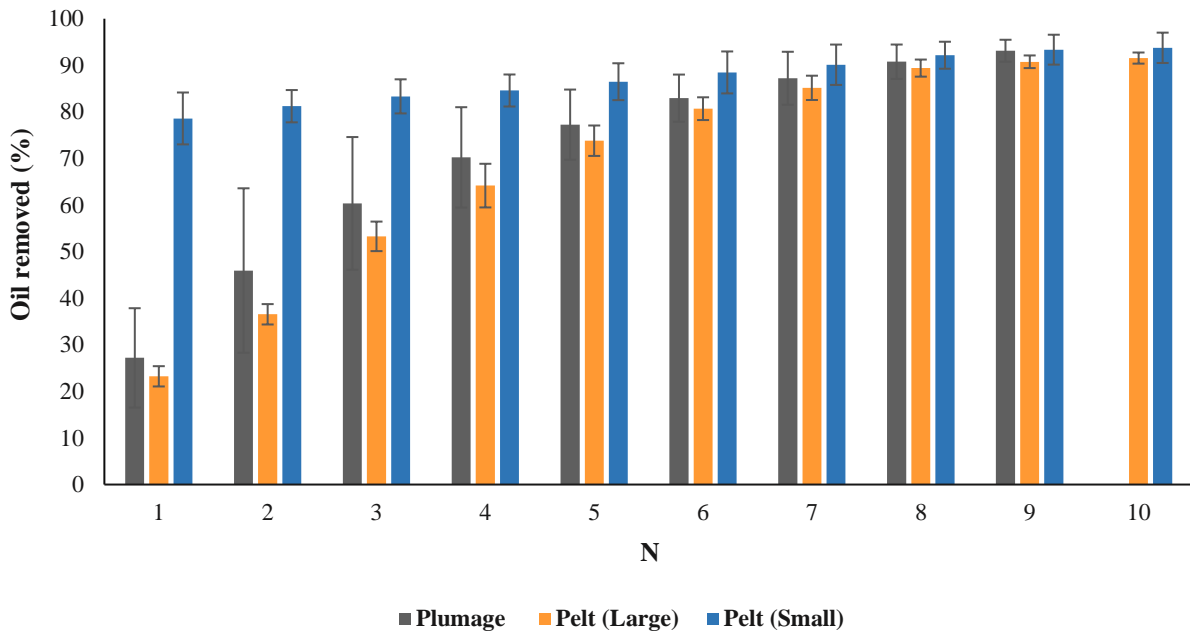


Figure 4.10: Comparison between penguin carcass (plumage), large penguin pelt size and small penguin pelt size for the removal of Diesel oil as a function of the number of treatments, N. Error bars represent the 95% confidence intervals for five replicates.

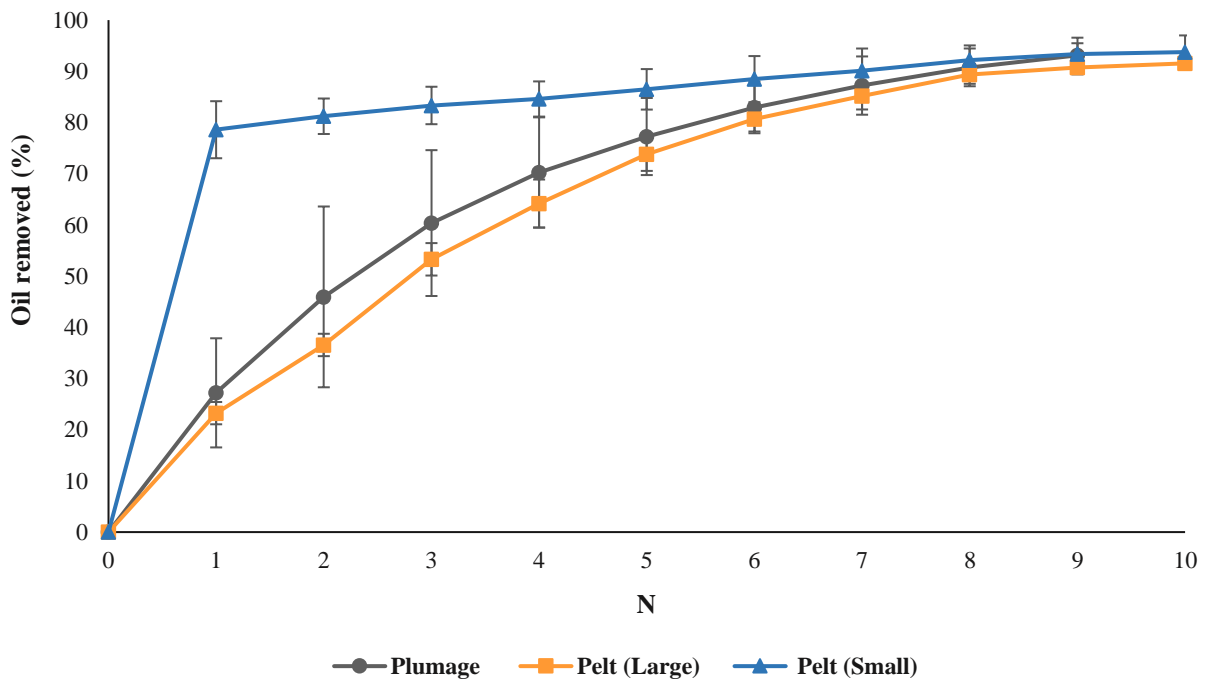


Figure 4.11: Comparison between penguin carcass (plumage), large penguin pelt size and small penguin pelt size for the removal of Diesel oil as a function of the number of treatments, N. Error bars represent the 95% confidence intervals for five replicates.

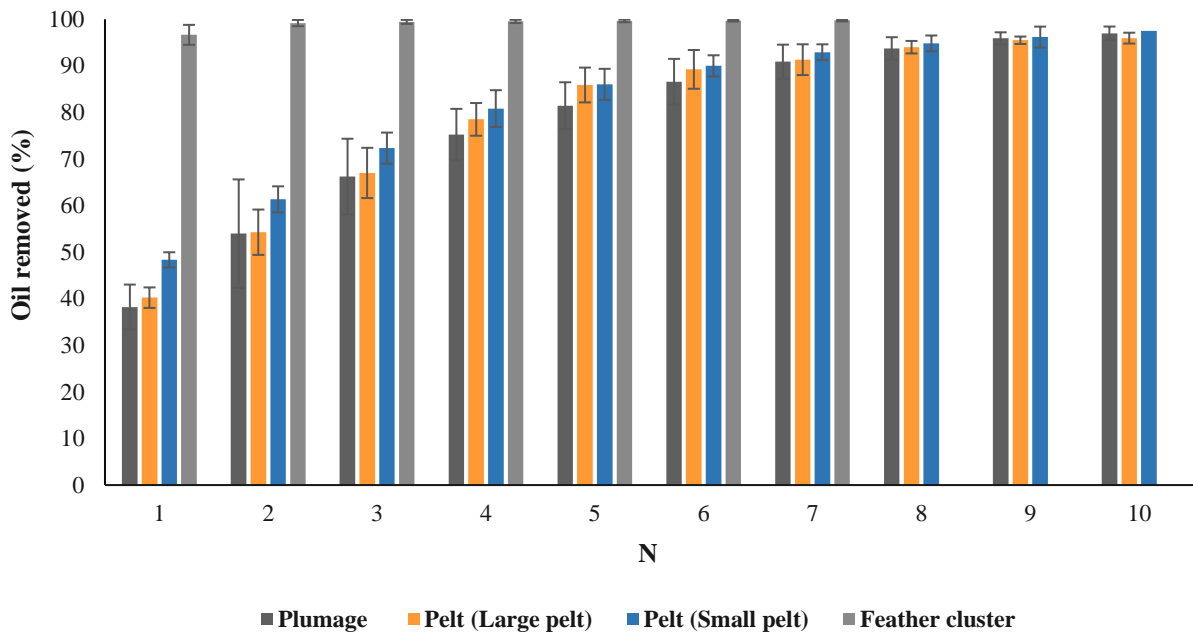


Figure 4.12: Comparison between penguin carcass (plumage), large penguin pelt size, small penguin pelt size and a penguin feather cluster for the removal of Engine oil as a function of the number of treatments, N. Error bars represent the 95% confidence intervals for five replicates.

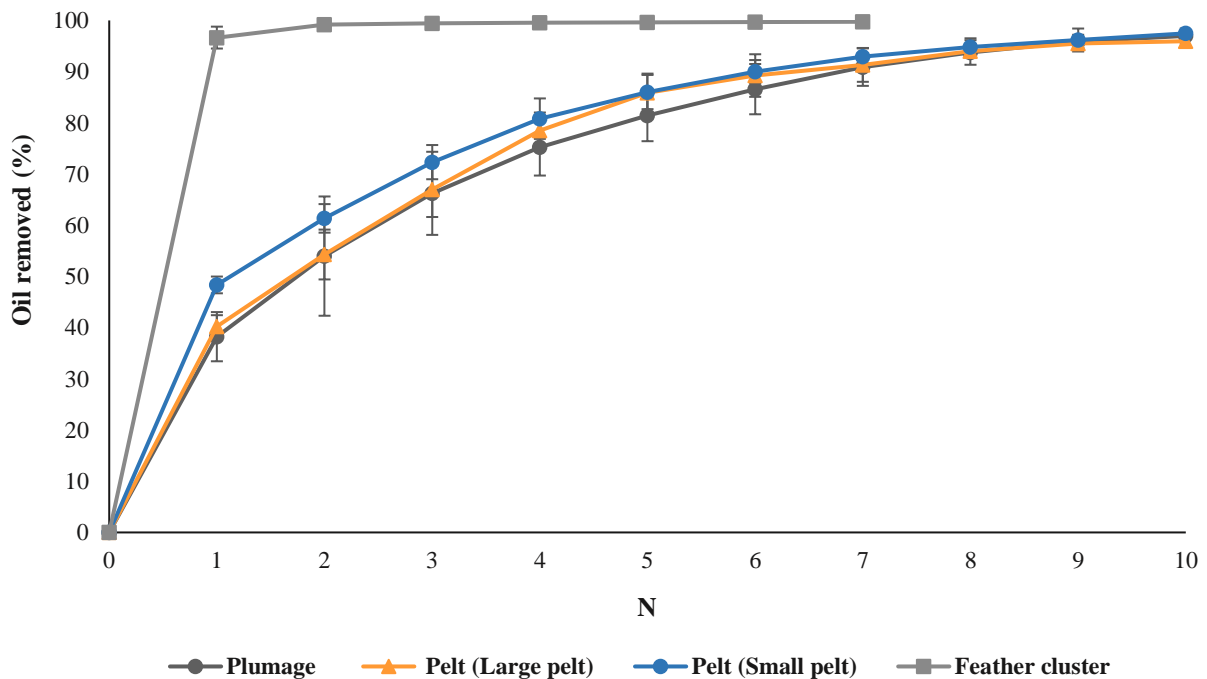


Figure 4.13: Comparison between penguin carcass (plumage), large penguin pelt size, small penguin pelt size and a penguin feather cluster for the removal of Engine oil as a function of the number of treatments, N. Error bars represent the 95% confidence intervals for five replicates.

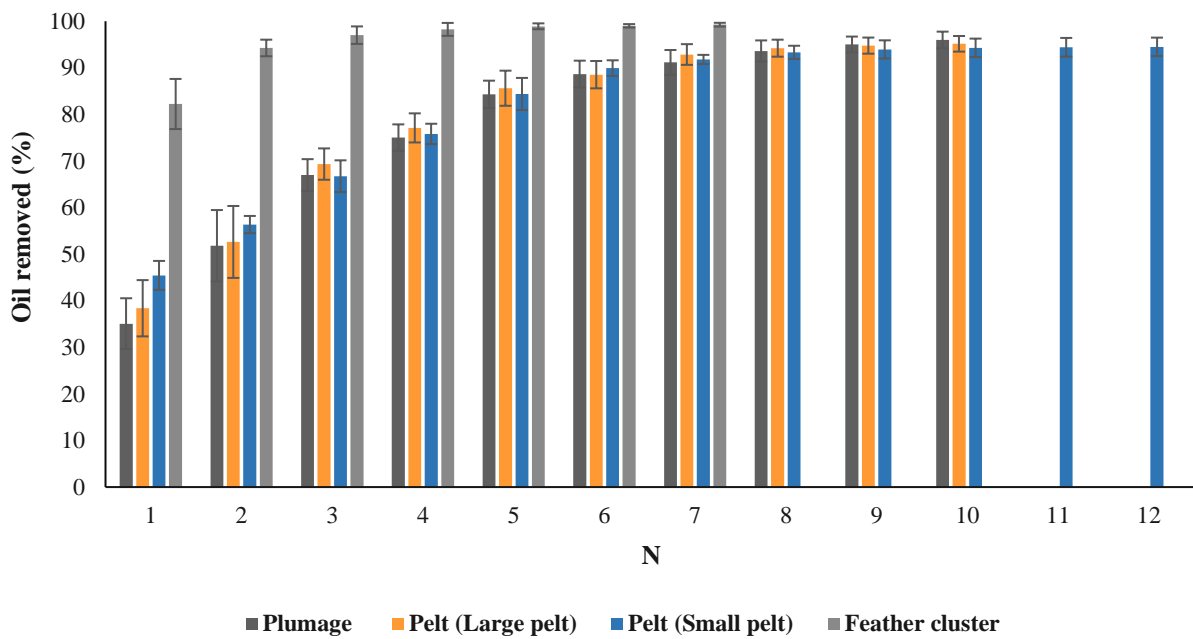


Figure 4.14: Comparison between penguin carcass (plumage), large penguin pelt size, small penguin pelt size and a penguin feather cluster for the removal of Bunker oil 1 (BO1) as a function of the number of treatments, N. Error bars represent the 95% confidence intervals for five replicates.

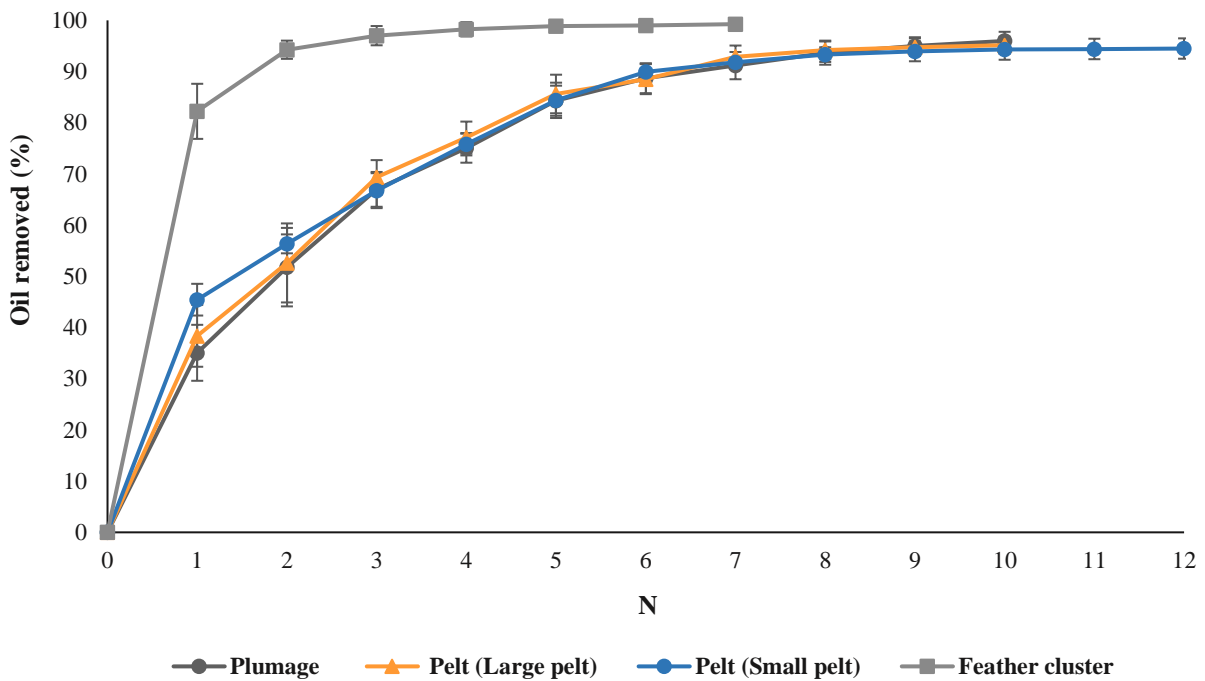


Figure 4.15: Comparison between penguin carcass (plumage), large penguin pelt size, small penguin pelt size and a penguin feather cluster for the removal of Bunker oil 1 (BO1) as a function of the number of treatments, N. Error bars represent the 95% confidence intervals for five replicates.

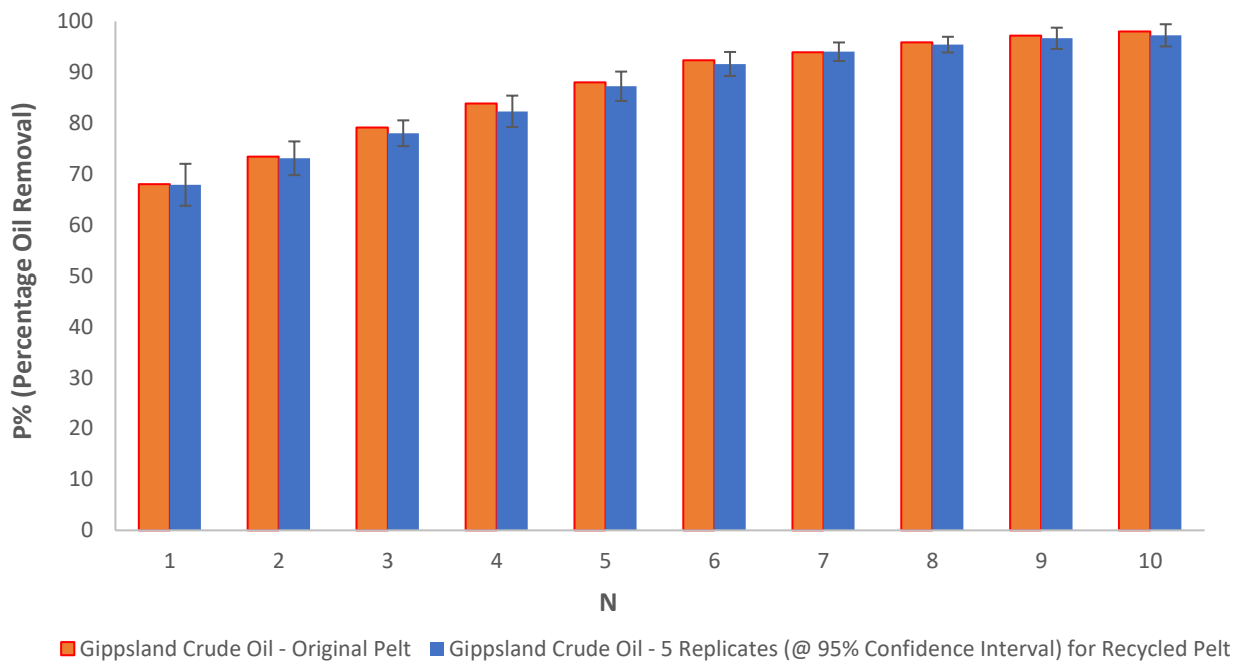


Figure 4.16: Comparison between original pelt and recycled pelt for the removal of Gippsland crude oil as a function of the number of treatments, N. Error bars represent the 95% confidence intervals for five replicates.

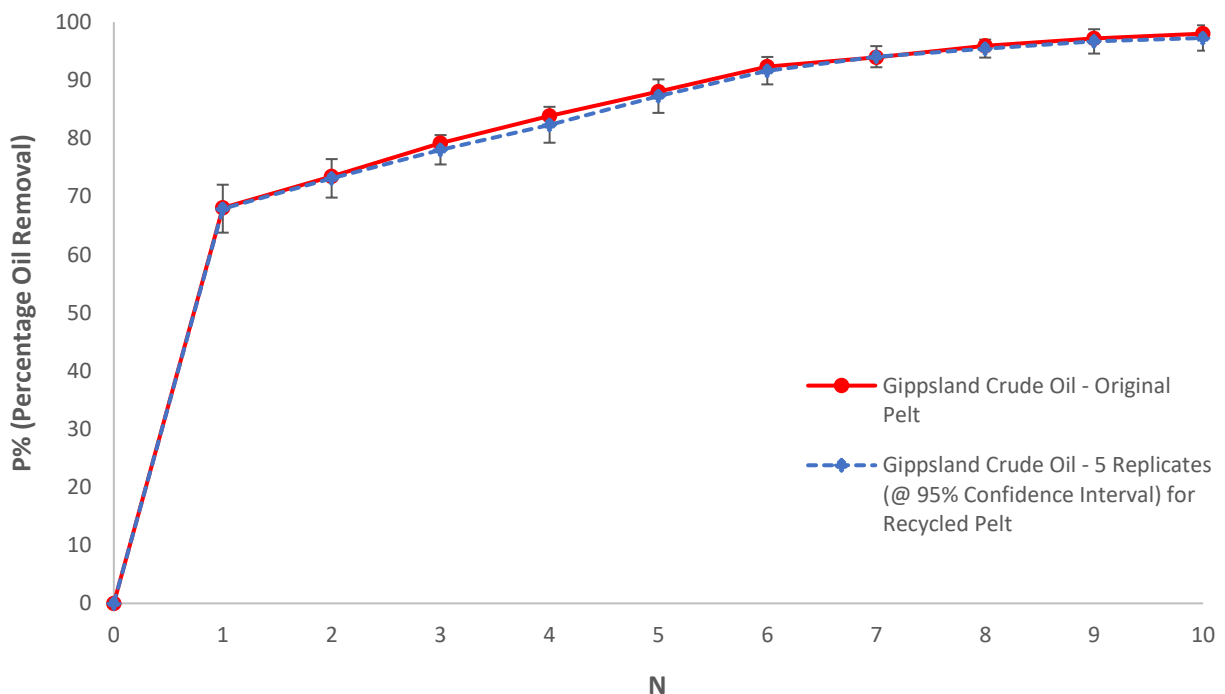


Figure 4.17: Comparison between original pelt and recycled pelt for the removal of Gippsland crude oil as a function of the number of treatments, N. Error bars represent the 95% confidence intervals for five replicates.

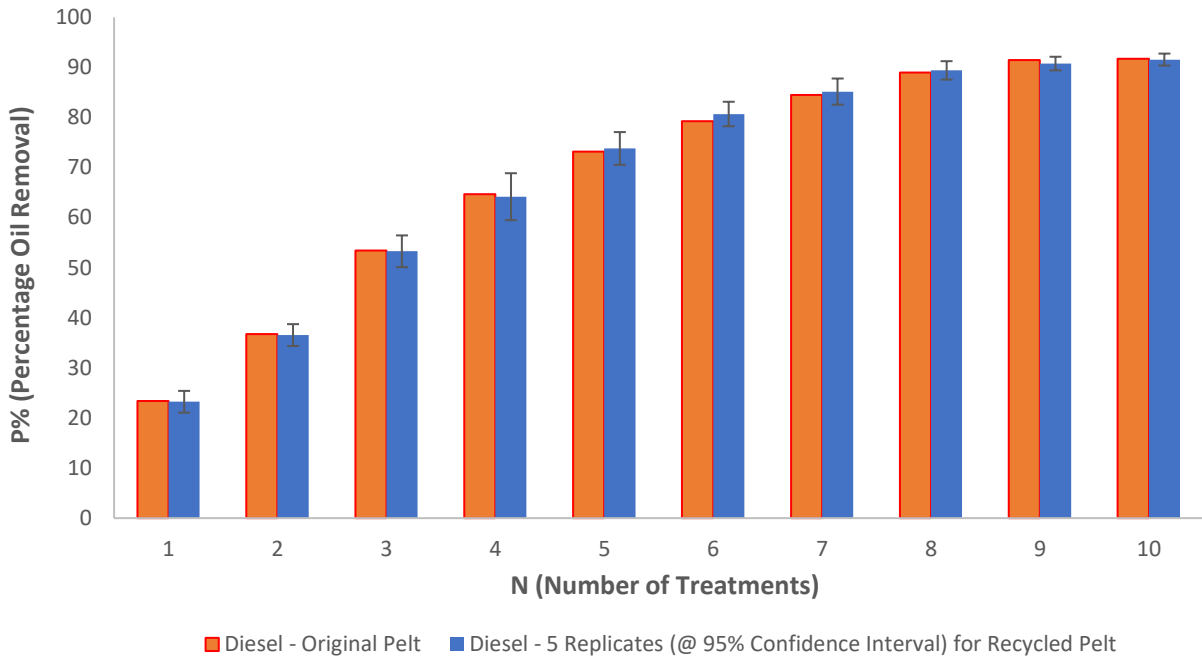


Figure 4.18: Comparison between original pelt and recycled pelt for the removal of Diesel Fuel Oil as a function of the number of treatments, N. Error bars represent the 95% confidence intervals for five replicates.

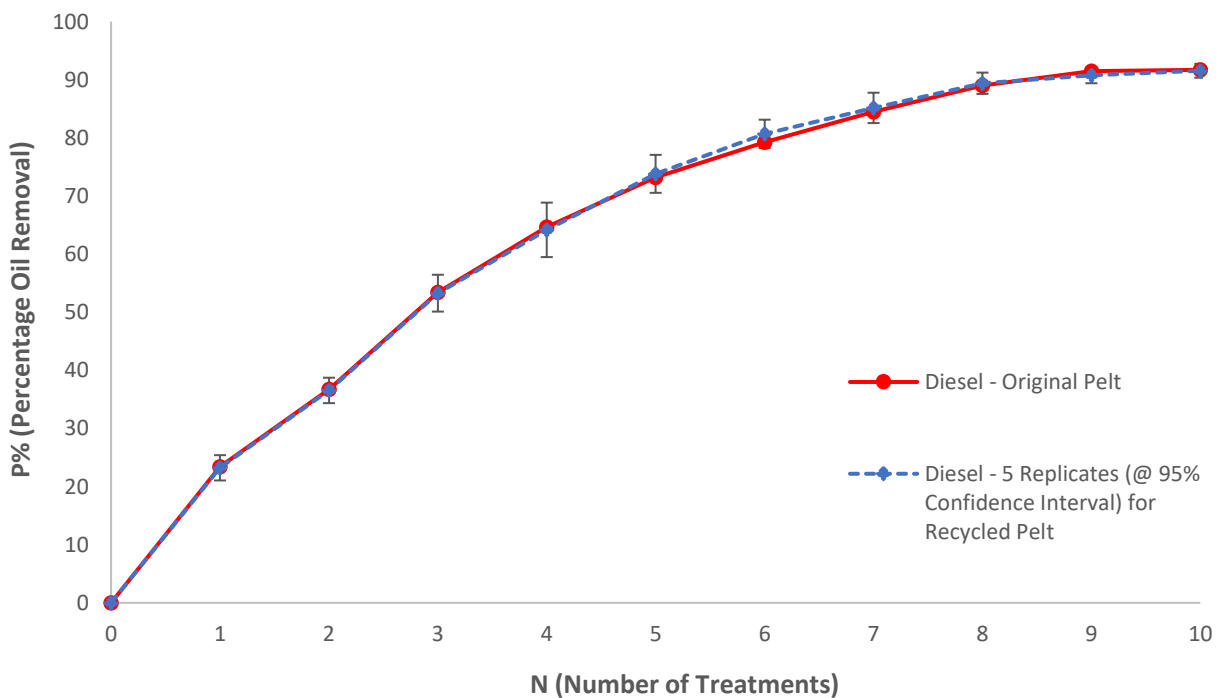


Figure 4.19: Comparison between original pelt and recycled pelt for the removal of Diesel Fuel Oil as a function of the number of treatments, N. Error bars represent the 95% confidence intervals for five replicates.

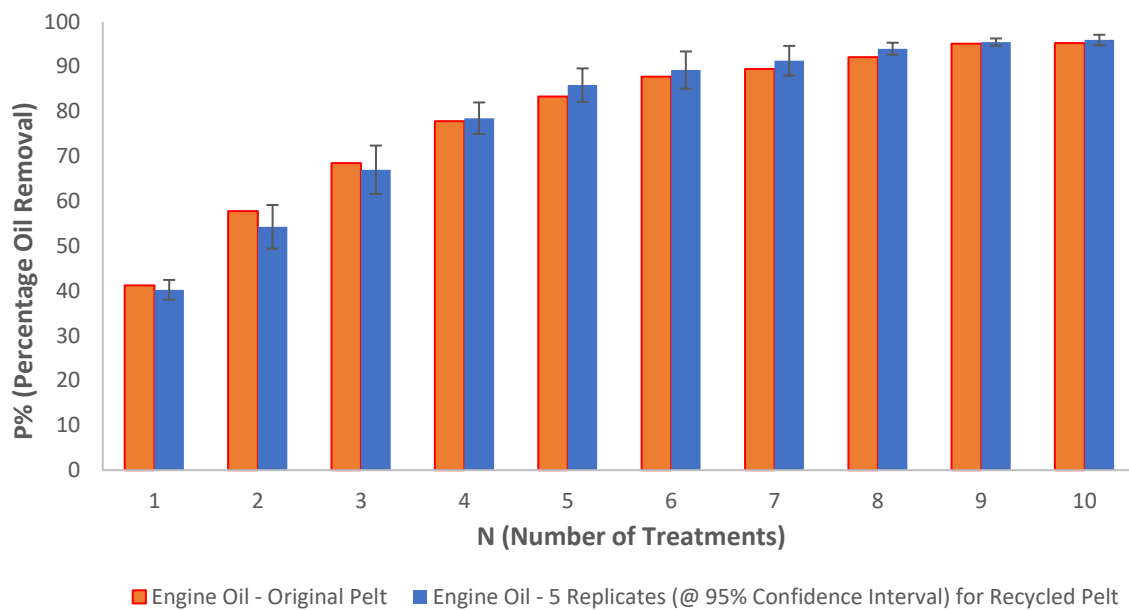


Figure 4.20: Comparison between original pelt and recycled pelt for the removal of Engine oil as a function of the number of treatments, N. Error bars represent the 95% confidence intervals for five replicates.

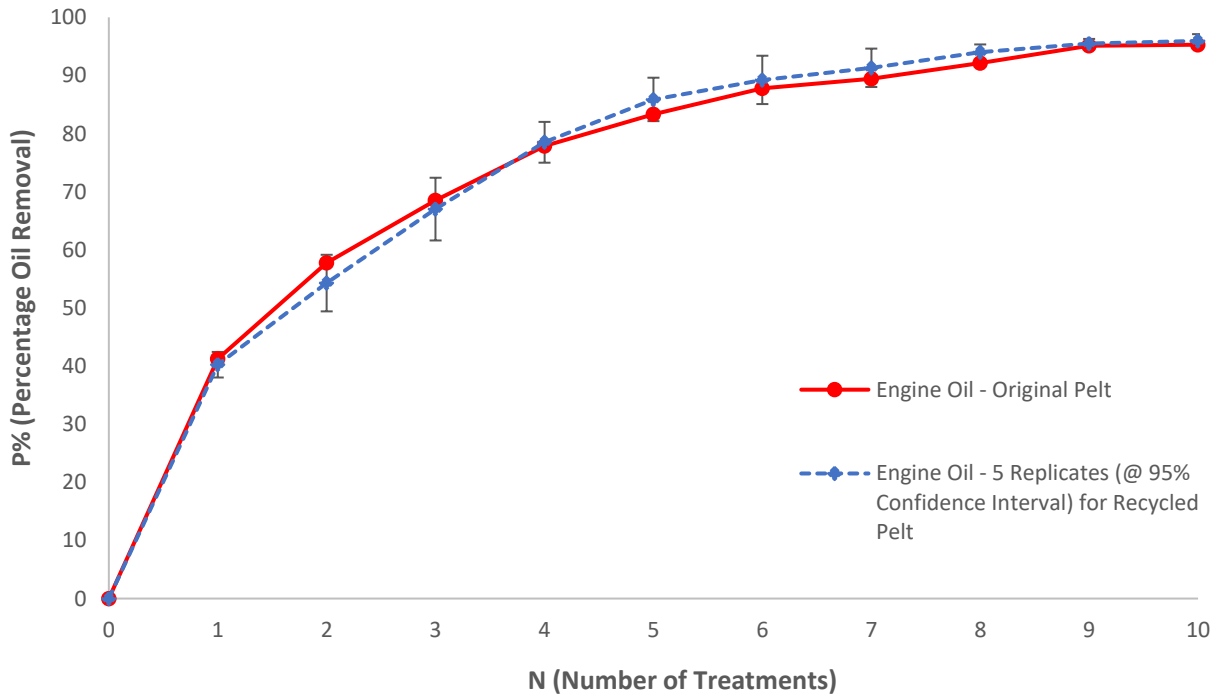


Figure 4.21: Comparison between original pelt and recycled pelt for the removal of Engine oil as a function of the number of treatments, N. Error bars represent the 95% confidence intervals for five replicates.

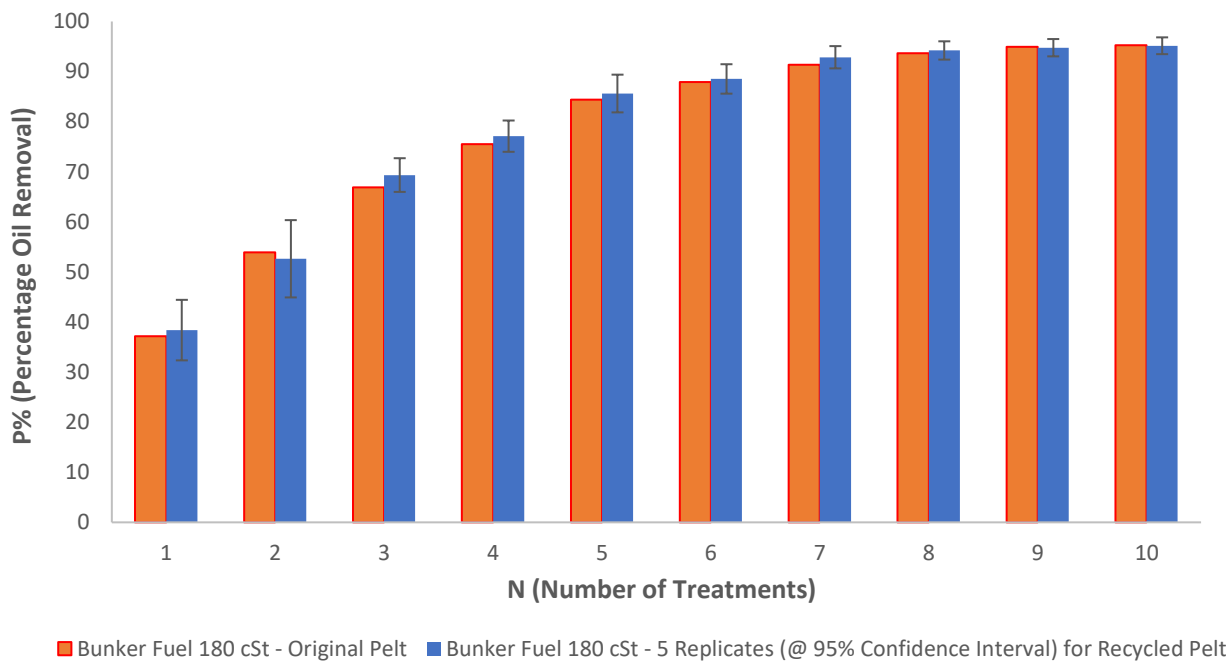


Figure 4.22: Comparison between original pelt and recycled pelt for the removal of Bunker Oil 1 (BO1) as a function of the number of treatments, N. Error bars represent the 95% confidence intervals for five replicates.

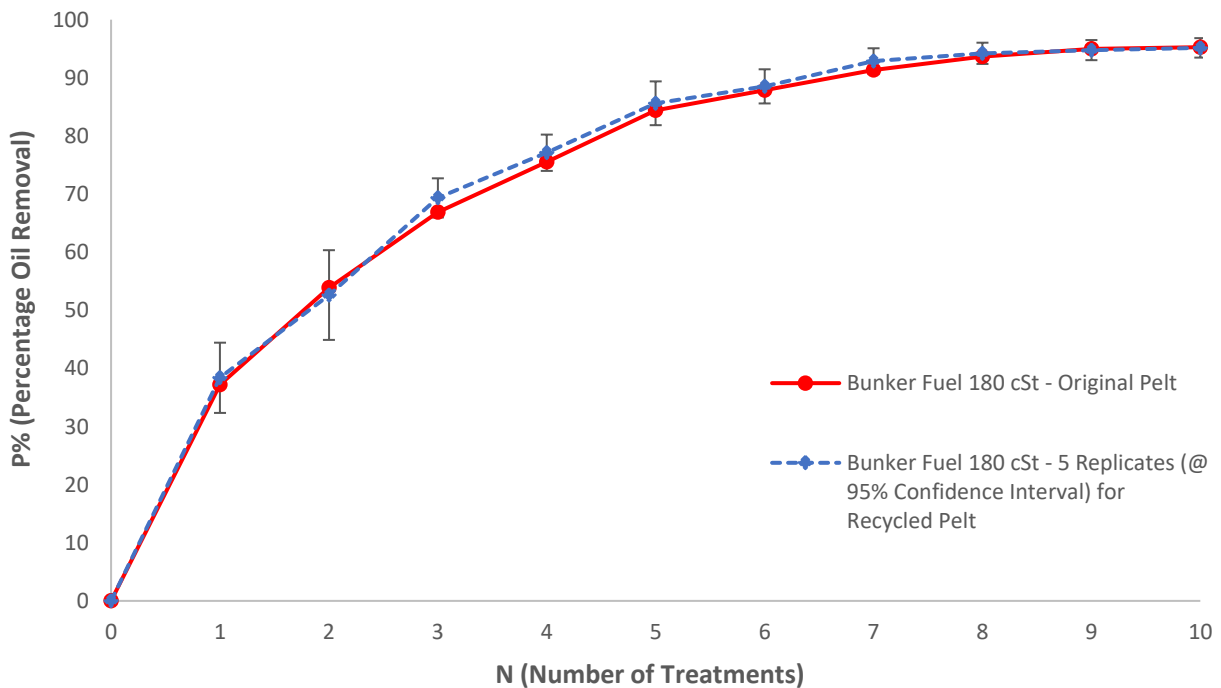


Figure 4.23: Comparison between original pelt and recycled pelt for the removal of Bunker Oil 1 (BO1) as a function of the number of treatments, N. Error bars represent the 95% confidence intervals for five replicates.

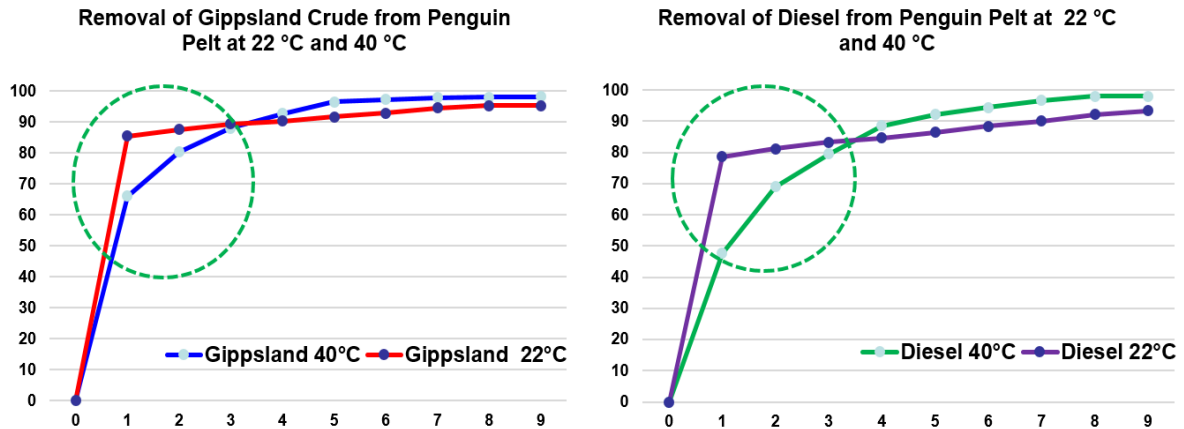


Figure 4.24: Nested isotherms for the removal of Gippsland Crude Oil (left) and Diesel Fuel Oil (right) from penguin pelt at pelt temperatures of 40 °C and 22 °C.

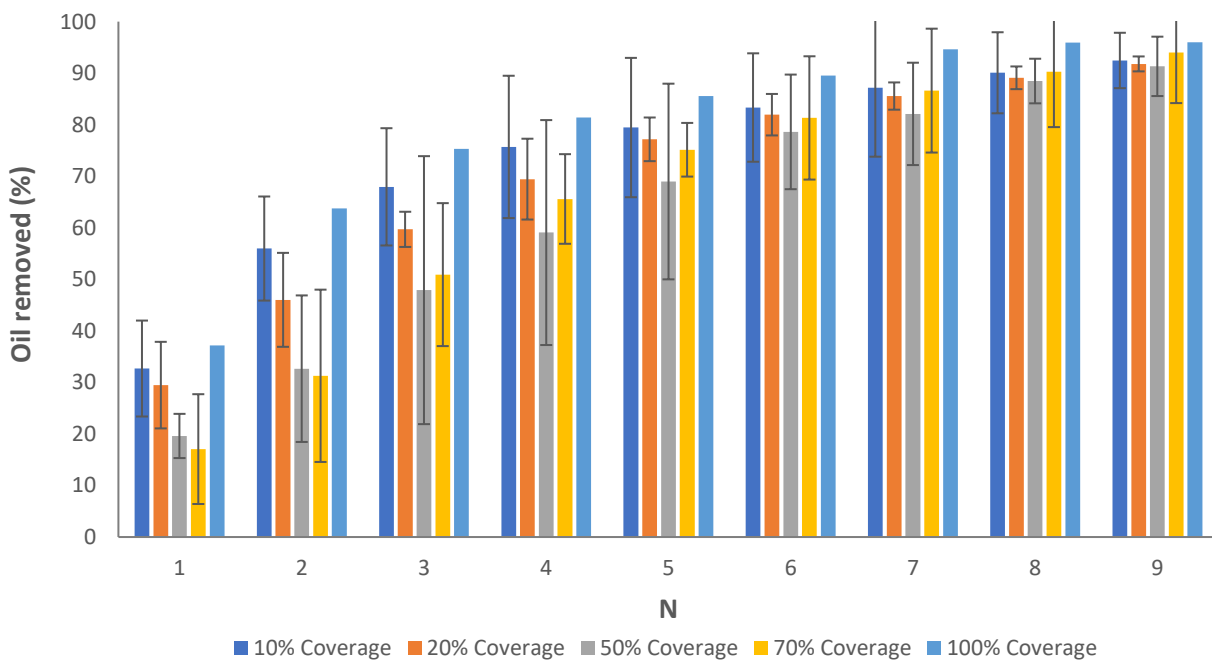


Figure 4.25: Histograms of Diesel Fuel Oil removal (%), as a function of the number of treatments, N; for the removal of 10%, 20%, 50%, 70% and 100% Diesel Oil coverage (by mass) from plumage. Error bars represent the standard error for three replicates for the removal of 10%, 20%, 50% and 70% Diesel Oil coverage (by mass) from plumage.

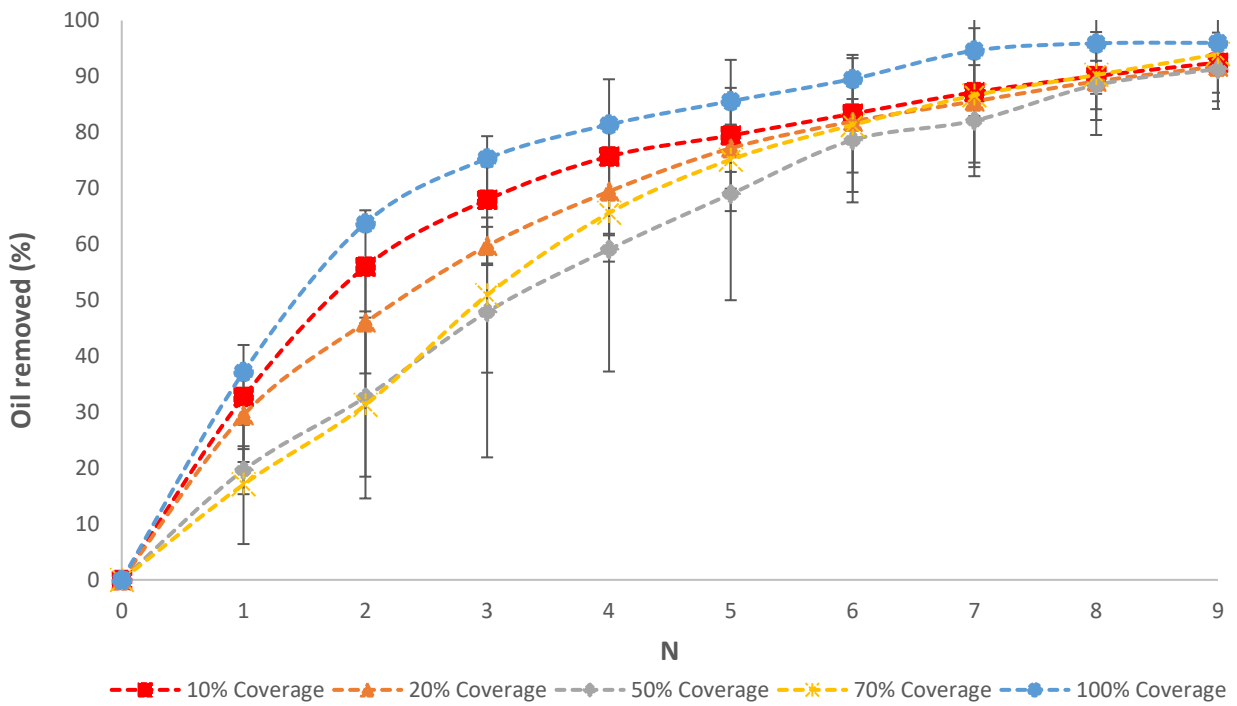


Figure 4.26: Sorption isotherm of oil removal (%), as a function of the number of treatments, N, for the removal of 10%, 20%, 50%, 70% and 100% Diesel Oil coverage (by mass) from plumage. Error bars represent the standard error for three replicates for the removal of 10%, 20%, 50% and 70% Diesel Oil coverage (by mass) from plumage.

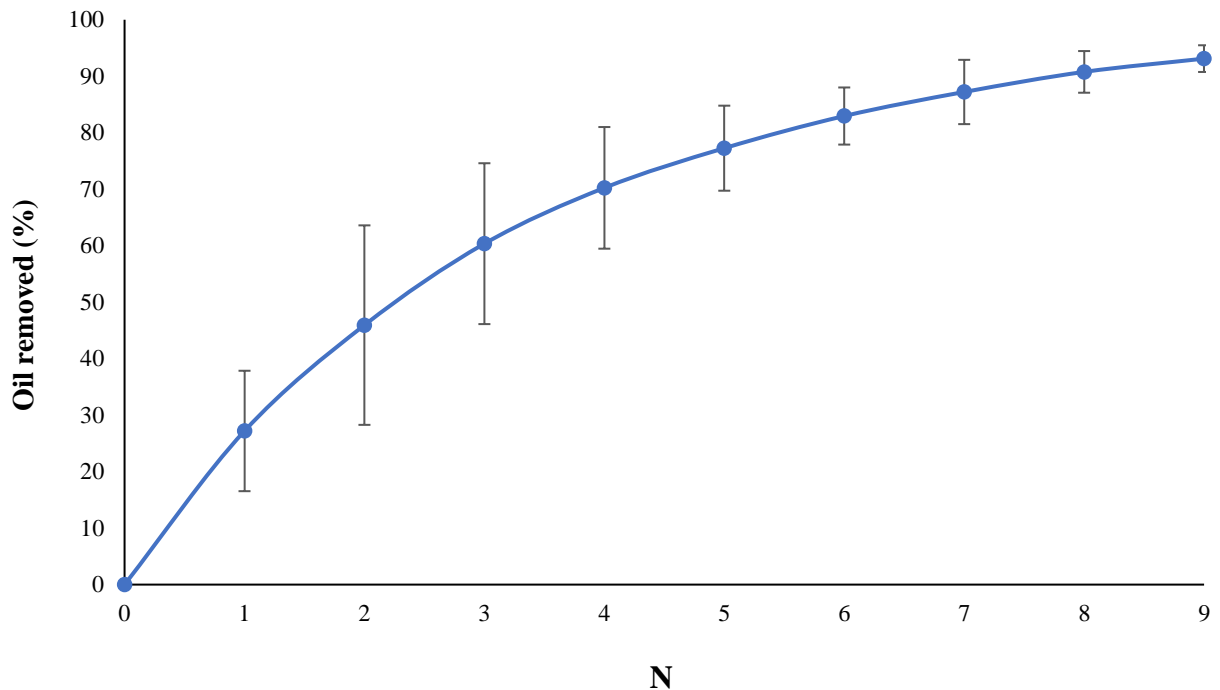


Figure 4.27: Oil removal (%), as a function of the number of treatments, N, for the average removal of 10%, 20%, 50%, 70% and 100% Diesel Oil coverage (by mass) from plumage. Error bars represent the average standard error for three replicates.

Appendix 5

Table 5.1: Crude oils used in the evaporation experiments, showing their sources and relative viscosities. For the experiments conducted at ~20 °C and at ~16 °C in the “Potter Lab”, over a period of up to 21 days, the six oils used are marked with an asterisk and highlighted in green. For the experiments conducted at ~20 °C in the “Ambient Lab”, over a period of up to 10 hours, all eleven oils were used.

	Oil	Source	Viscosity (cP)
Light	Sakhalin	Lytton Oil Refinery, Caltex Australia Ltd., Lytton, QLD 4178	7
Light	Tapis	Lytton Oil Refinery, Caltex Australia Ltd., Lytton, QLD 4178	6
Light	Margham Condensate	Lytton Oil Refinery, Caltex Australia Ltd., Lytton, QLD 4178	4
Light	Merine	Exxon/Mobil Oil Pty. Ltd., Australia	9
Light	Murban	Lytton Oil Refinery, Caltex Australia Ltd., Lytton, QLD 4178	8
Light	Diesel*	Shell local service station	7
Light	Kerosene*	Diggers brand, Recochem Inc., Australian Division, Brisbane, QLD.	1.64
Medium	Bohai Bay Crude*	Lytton Oil Refinery, Caltex Australia Ltd., Lytton, QLD 4178	394
Medium	Ikan Pari Crude*	Lytton Oil Refinery, Caltex Australia Ltd., Lytton, QLD 4178	46
Heavy	Bunker Oil 180*	Industrial and Bearing Supplies (IBS), Gulf Western Oil, Australia.	32040
Heavy	Bunker Oil 380*	Industrial and Bearing Supplies (IBS), Gulf Western Oil, Australia.	70320

Table 5.2. OilVap Parameters for ~20 °C “Potter Lab” **Experiment 1** for Little Penguin Pelt and (Glass), experiments up to 21 days.

Oil	%wL(inf)	k (e-06 s-1)	-c (e-01)	r ²	v ₀ (e-03 wt% s-1)
Diesel	56.200 (46.800)	1.409 (1.367)	2.945 (2.873)	0.9773 (0.9842)	4.750 (3.839)
Kerosene	99.923 (99.891)	7.154 (4.425)	9.487 (4.027)	0.9012 (0.9975)	42.89 (26.52)
Bohai Bay Crude	21.900 (15.000)	1.655 (1.434)	7.189 (6.483)	0.9312 (0.9576)	2.174 (1.291)
Ikan Pari Crude	53.0000 (31.500)	1.922 (1.364)	7.101 (3.978)	0.9429 (0.9757)	6.112 (2.578)
Bunker 180	21.400 (11.200)	1.459 (1.325)	4.680 (3.521)	0.9559 (0.9733)	1.873 (0.8906)
Bunker 380	22.000 (10.600)	1.682 (1.382)	5.184 (3.892)	0.9467 (0.9801)	2.220 (0.8790)

Table 5.3. OilVap Parameters for ~21 °C Ambient Lab Experiments for Little Penguin Pelt and (Glass). **Experiment 2** up to ~ 10 hours.

Oil	%wL(inf)	k (e-04 s-1)	-c (e-01)	r ²	v ₀ (e-02 wt% s-1)
Sakhalin Crude	33.781 (29.919)	2.636 (3.194)	1.472 (2.187)	0.9908 (0.9943)	53.42 (57.34)
Tapis Crude	21.692 (17.127)	1.570 (5.778)	0.9971 (4.849)	0.9940 (0.9725)	20.44 (59.37)
Margham Condensate Crude	32.697 (39.653)	1.943 (2.123)	1.312 (2.308)	0.9951 (0.9965)	38.12 (50.50)
Merinie Crude	18.233 (21.577)	1.497 (1.958)	1.140 (3.253)	0.9983 (0.9917)	16.38 (25.35)
Murban Crude	21.800 (24.800)	1.622 (2.725)	1.459 (3.848)	0.9953 (0.9870)	21.22 (40.55)
Diesel	2.522 (11.493)	1.988 (0.8865)	0.2254 (0.2763)	0.9934 (0.9942)	3.008 (6.113)
Kerosene	17.823 (35.200)	1.922 (1.661)	0.08949 (0.2791)	0.9930 (0.9875)	20.55 (35.08)
Bohai Bay Crude	3.393 (5.511)	1.588 (2.621)	1.012 (0.7424)	0.9947 (0.9960)	3.233 (8.668)
Ikan Pari Crude	16.857 (14.212)	2.632 (1.770)	0.01683 (1.078)	0.9888 (0.9958)	26.63 (15.09)
Bunker 180	1.193 (1.134)	1.796 (2.071)	0.1503 (0.5708)	0.9989 (0.9945)	1.286 (1.409)
Bunker 380	1.500 (1.291)	0.8206 (1.449)	0.08321 (0.07270)	0.9982 (0.9983)	0.7386 (1.122)

Table 5.4. OilVap Parameters for 16 °C “Potter Lab” **Experiment 3** for Little Penguin Pelt and (Glass), experiments up to ~21 days.

Oil	%wL(inf)	k (e-06 s-1)	-c (e-01)	r ²	v ₀ (e-03 wt% s-1)
Diesel	63.000 (61.000)	1.171 (1.313)	3.018 (4.086)	0.9864 (0.9840)	4.427 (4.806)
Kerosene	95.900 (98.600)	9.268 (24.04)	3.696 (0.1358)	0.9830 (0.9999)	53.33 (142.2)
Bohai Bay Crude	13.100 (18.400)	1.124 (1.234)	3.149 (7.559)	0.9514 (0.9552)	0.8832 (1.362)
Ikan Pari Crude	39.000 (37.000)	1.248 (1.119)	3.735 (2.652)	0.9810 (0.9889)	2.921 (2.485)
Bunker 180	10.500 (10.200)	0.5885 (0.8105)	0.6472 (1.093)	0.9475 (0.9965)	0.3708 (0.4960)
Bunker 380	-	-	-	-	-

Table 5.5. A summary of the average -c and r² parameters for **Experiments 1 to 3** extracted from the data provided in **Tables 5.2 to 5.4**.

Experiment 1 - Table 5.2			
Parameter	Little Penguin Pelt	Glass	
-c	0.61	0.41	Ideally 0
r ²	0.94	0.98	Ideally 1.0
Experiment 2 - Table 5.3			
	Little Penguin Pelt	Glass	
-c	0.07	0.18	Ideally 0
r ²	1.00	0.99	Ideally 1.0
Experiment 3 - Table 5.4			
	Little Penguin Pelt	Glass	
-c	0.29	0.31	Ideally 0
r ²	0.97	0.99	Ideally 1.0

Table 5.6. The **Total Volatile Fraction (TVF)** for evaporation of the oils shown from Penguin Pelt after 21 days, at ~20 °C compared to ~16 °C.

	TVF 20 °C - Pelt	TVF 16 °C - Pelt
Diesel	56.2	63
Kerosene	99.9	95.9
Bohai Bay	21.9	13.1
Ikan Pari	53	39
Bunker 180	21.4	10.5

Table 5.7. The **Total Volatile Fraction (TVF)** for the evaporation of the oils shown from Glass after 21 days at 20 °C, compared to 16 °C.

	TVF 20 °C - Glass	TVF 16 °C - Glass
Diesel	46.8	61
Kerosene	99.9	98.6
Bohai Bay	15	18.4
Ikan Pari	31.5	37
Bunker 180	11.2	10.2

Table 5.8. Total Volatile Fraction (TVF) from Penguin Pelt after 21 days at 20 °C, compared to Glass.

	TVF 20 °C - Pelt	TVF 20 °C - Glass
Diesel	56.2	46.8
Kerosene	99.9	99.9
Bohai Bay	21.9	15
Ikan Pari	53	31.5
Bunker 180	21.4	11.2

Table 5.9. Total Volatile Fraction (TVF) from Penguin Pelt after 21 days at 16 °C, compared to Glass.

	TVF 16 °C - Pelt	TVF 16 °C - Glass
Diesel	63	61
Kerosene	95.9	98.6
Bohai Bay	13.1	18.4
Ikan Pari	39	37
Bunker 180	10.5	10.2

Table 5.10. A tabulation of the relative parameters (derived from **Tables 5.2** and **5.3**) relating to the evaporation of Diesel, Kerosene, Bohai Bay, Ikan Pari, Bunker 180 and Bunker 380 contaminants from Little Penguin Pelt (P) and Glass (G). TVF = Total Volatile Fraction; RF = Recalcitrant Fraction; NVF = Normal Volatile Fraction; HVF = Highly Volatile Fraction. The % of the HVF that is trapped in the plumage during the first evaporation phase is shown in the **right-hand** column. **HVF = Highly Volatile Fraction, NVF = Normal Volatile Fraction, TVF = Total Volatile Fraction, RF = Recalcitrant Fraction. Note that TVF = HVF + NVF and RF = 100 – TVF.**

Oil	TVF (G - 20 °C)	TVF (P - 20 °C)	RF (G - 20 °C)	RF (P - 20 °C)	NVF (G - 20 °C)	NVF (P - 20 °C)	HVF (G - ~21°C)	HVF (P - ~21 °C)	%Trapping by Pelt
Diesel	46.8	56.2	53.2	43.8	35.3	53.7	11.5	2.5	78.1
Kerosene	99.9	99.9	0.1	0.1	64.7	82.1	35.2	17.8	49.4
Bohai Bay	15	21.9	85	78.1	9.4	18.5	5.6	3.4	38.9
Ikan Pari	31.5	53	68.5	47	17.3	36.1	14.2	16.9	-18.6
Bunker 180	11.2	21.4	88.8	78.6	10.1	20.2	1.1	1.2	-4.7
Bunker 380	10.6	22	89.4	78	9.3	20.5	1.3	1.5	-16.2

Environmental Weathering of Crude Oil

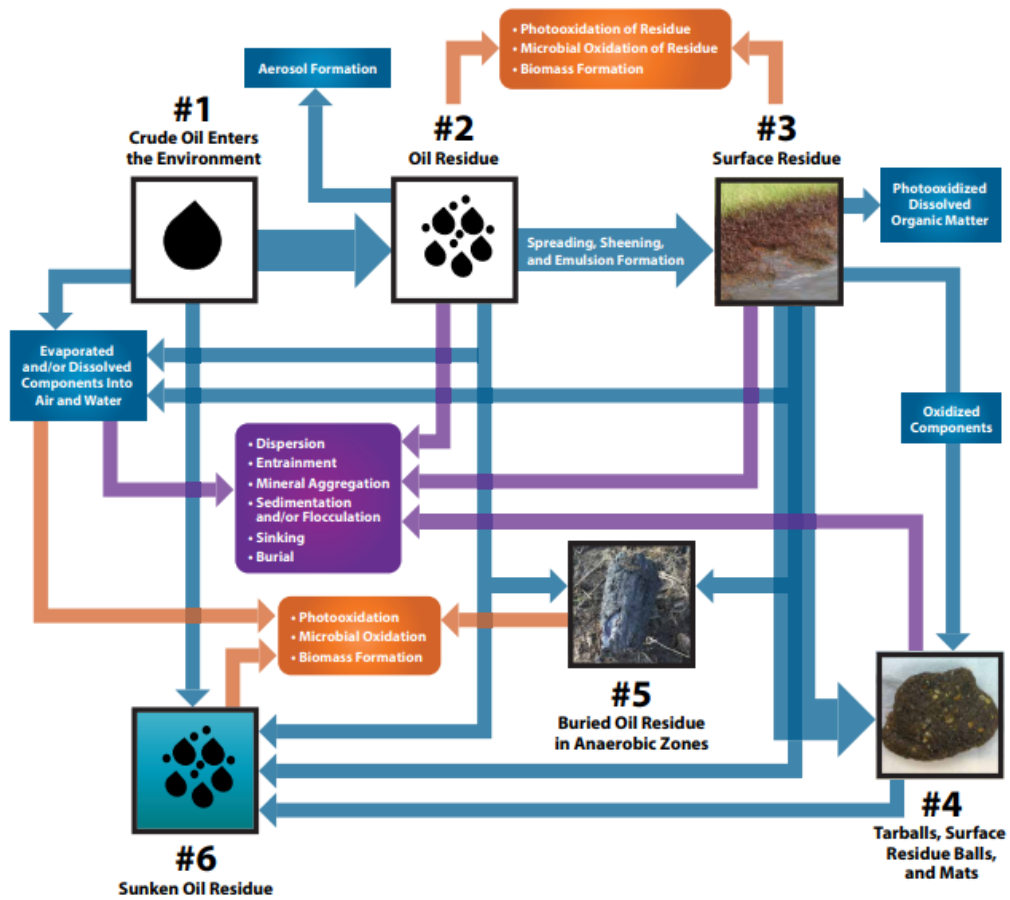


Figure 5.1: Weathering of oil spilled in the marine environment (Tarr *et al.*, 2016).

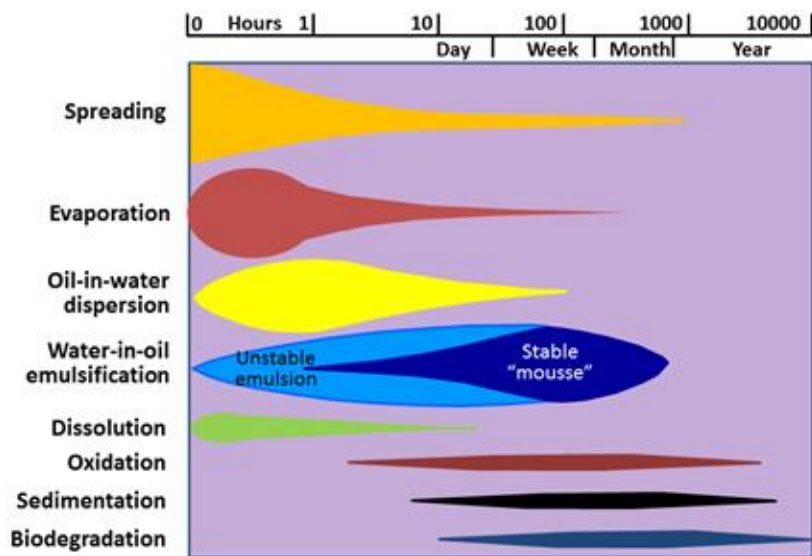


Figure 5.2: Weathering process of a typical crude oil (Fernandes *et al.*, 2018).

Evaporation limited by diffusion rate into the air therefore air boundary layer regulated

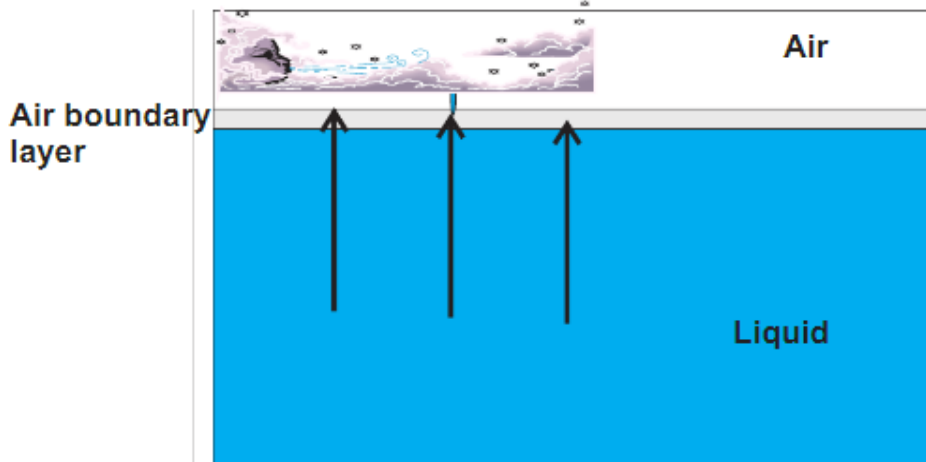


Figure 5.3: Here, the air boundary layer regulating method is depicted. The rate of evaporation is regulated by diffusion into the air layer, which is the limiting factor. Turbulence in the air affects this rate by increasing the transport of molecules over the boundary layer. For pure liquids with a high evaporative rate, this regulation mechanism is true. Water is the most commonly help concept and is an example of such a liquid (Fingas, 2015).

Evaporation limited by diffusion rate through liquid and through surface layer - therefore diffusion regulated

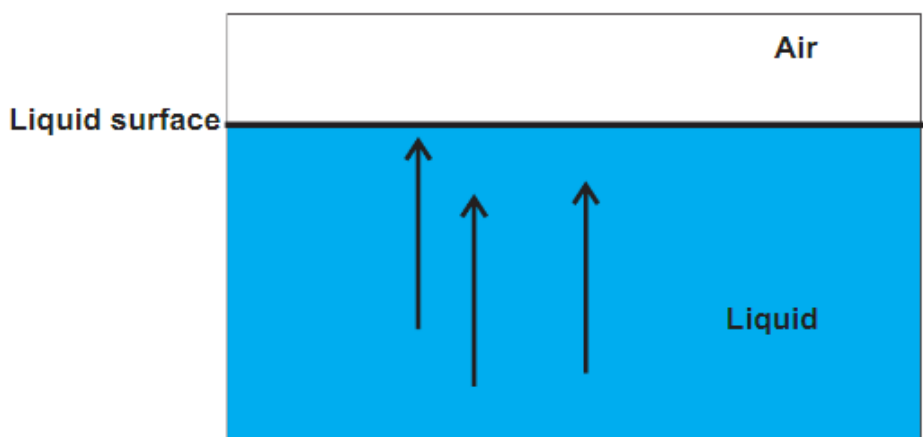


Figure 5.4: Here, the diffusion-controlled regulatory mechanism is depicted. The limiting factor and thus the regulation mechanism is diffusion through the evaporating liquid. This technique applies to oils, fuels, and a variety of other liquid mixes that both evaporate more slowly than water (Fingas, 2015).

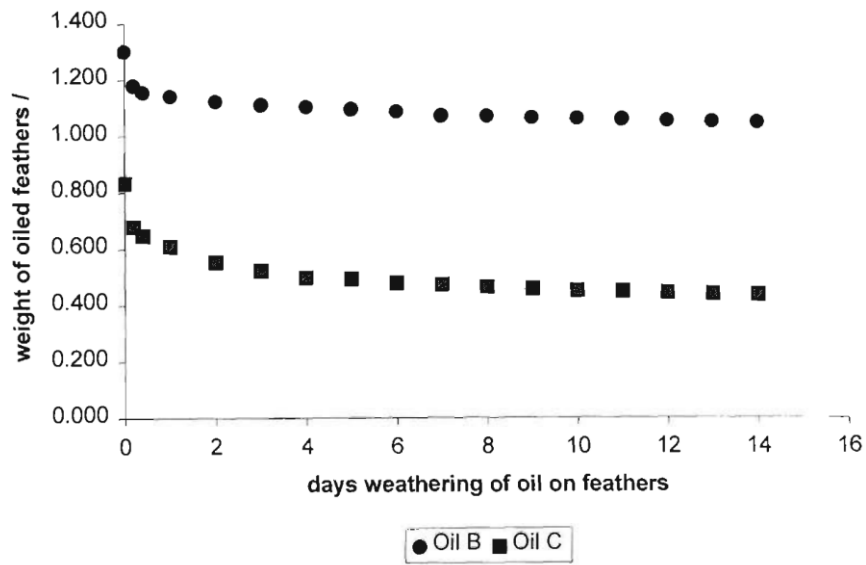


Figure 5.5: Weight of oiled breast feathers of the domestic duck (*Ana platyrhychos*) over time (Ngeh, 2002).

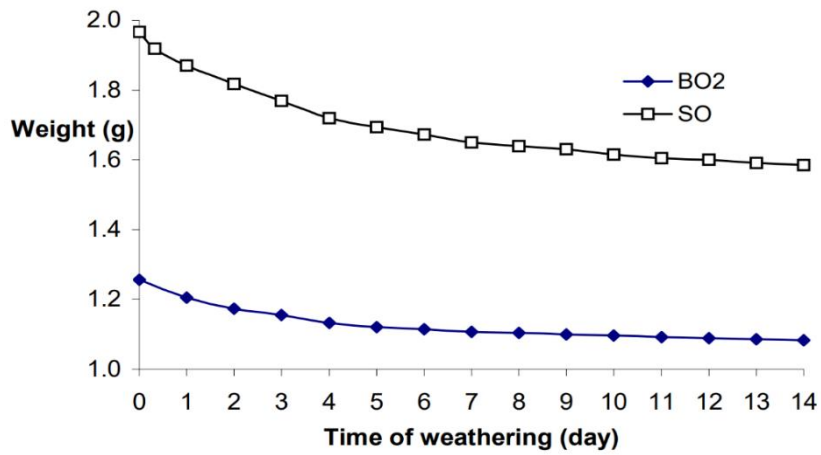


Figure 5.6. Weight versus time of weathering for oiled duck feather clusters (Dao, 2007).

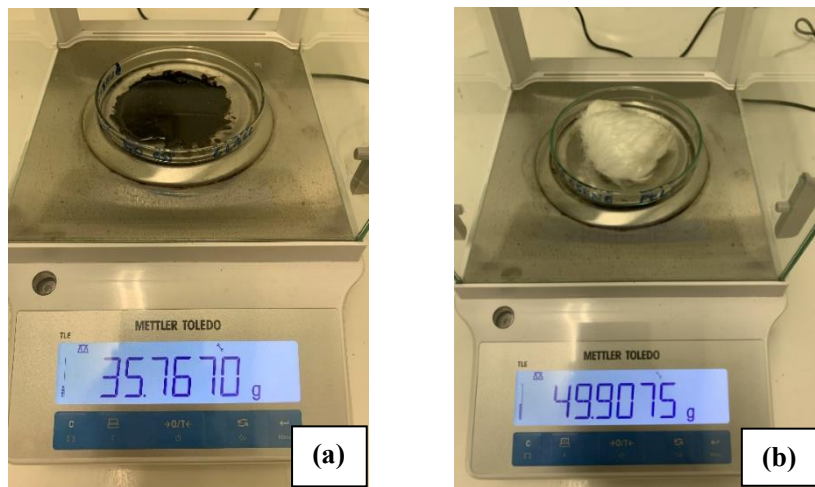


Figure 5.7. Typical weighing experiments, showing (a) an oil sample on a glass substrate (Petri dish) and (b) an oiled pelt sample, contained in a petri dish.



Figure 5.8. Breast and back pelt from Little Penguin (*Eudyptula minor*) were supplied by the Phillip Island Nature Parks.

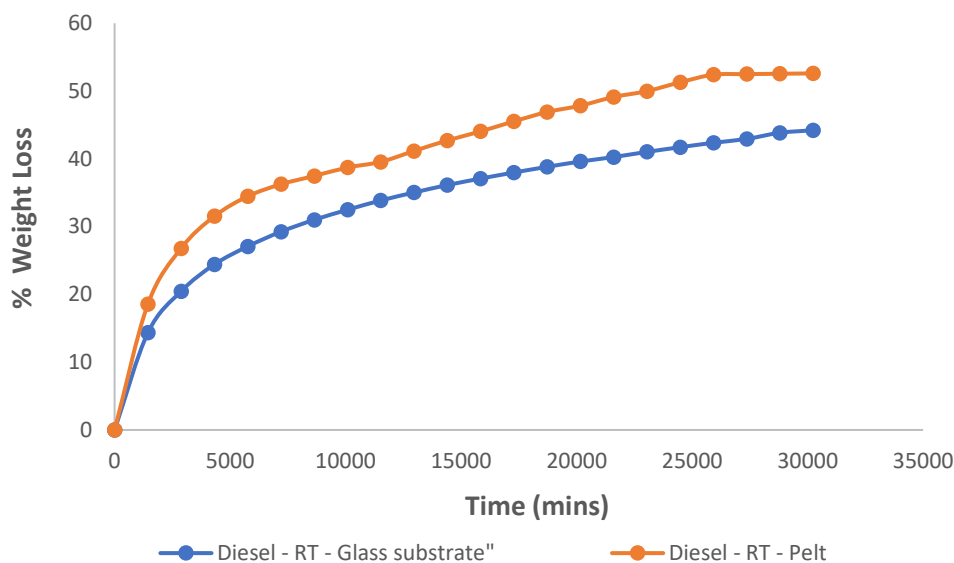


Figure 5.9. Comparative evaporation profiles of Diesel from pelt and glass over ~21 days, at a controlled temperature of 20 ± 1 °C, in the “Potter Lab”. Note that 1 day = 1,440 minutes, 21 days = 30,240 min.

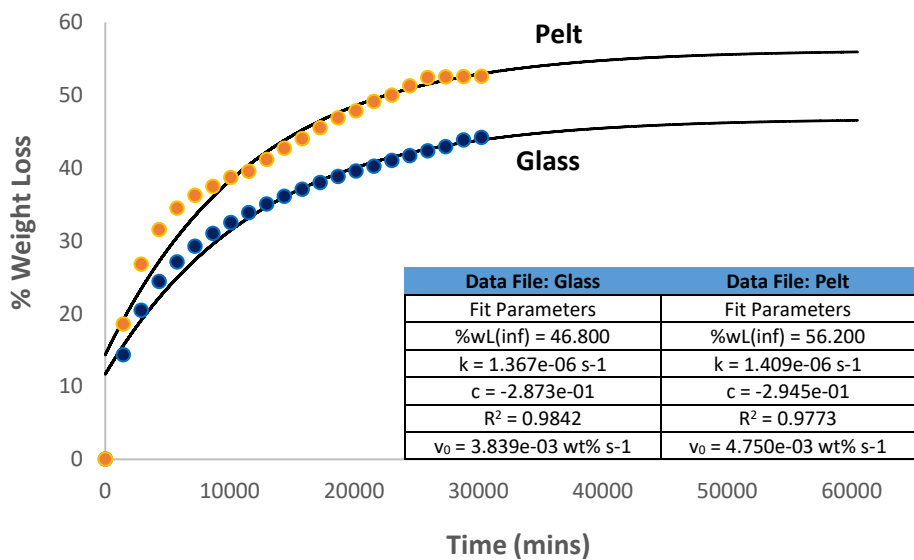


Figure 5.10. Comparative evaporation profiles of Diesel from glass and pelt over ~21 days, at a controlled temperature of 20 ± 1 °C, in the “Potter Lab”, showing the OilVap fit curves for the data presented in **Figure 5.9**. Note that 1 day = 1,440 minutes, 21 days = 30,240 min. The inset gives the OilVap output data for the relevant: plateau, fit and rate parameters for each curve. This is discussed further in the text in Section 5.4.

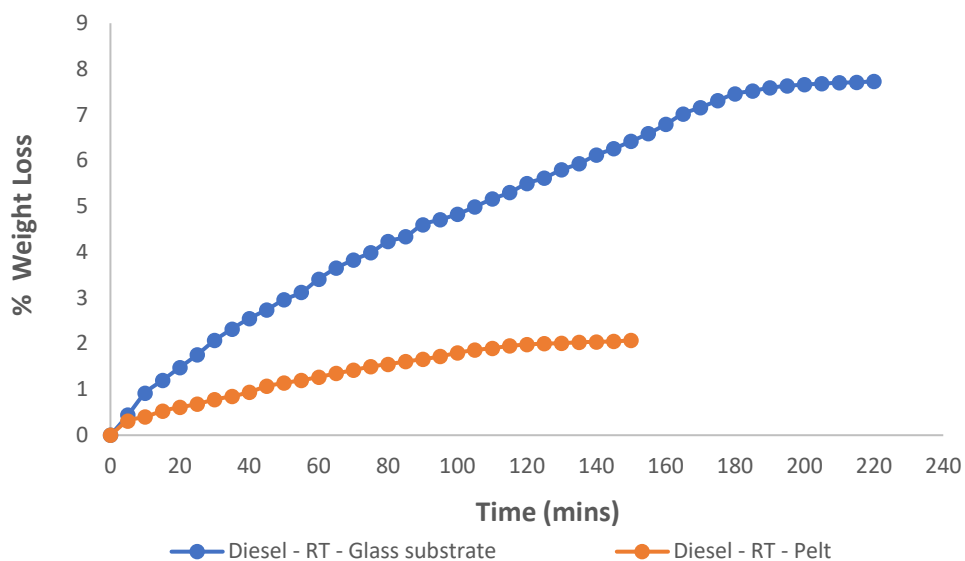


Figure 5.11. Comparative evaporation profiles of Diesel from pelt and glass over hours, at a controlled temperature of 21 ± 1 °C. Note that 10 hours = 600 min.

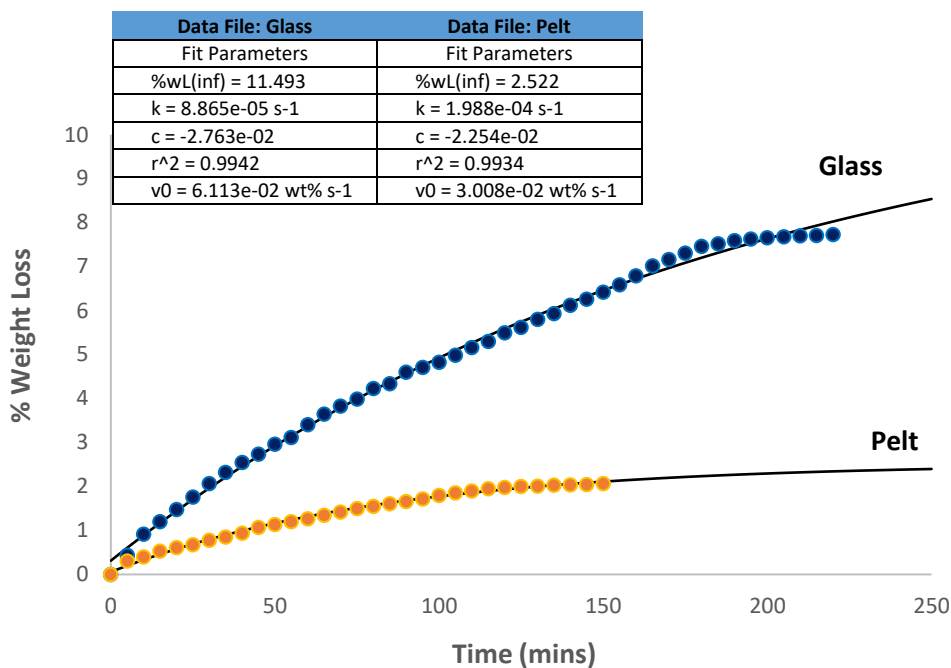


Figure 5.12. Comparative evaporation profiles of Diesel from glass and pelt over hours, at a controlled temperature of 21 ± 1 °C, showing the OilVap fit curves for the data presented in **Figure 5.11**. The inset gives the OilVap output data for the relevant plateau, fit and rate parameters for each curve. This is discussed further in the text in Section 5.4.

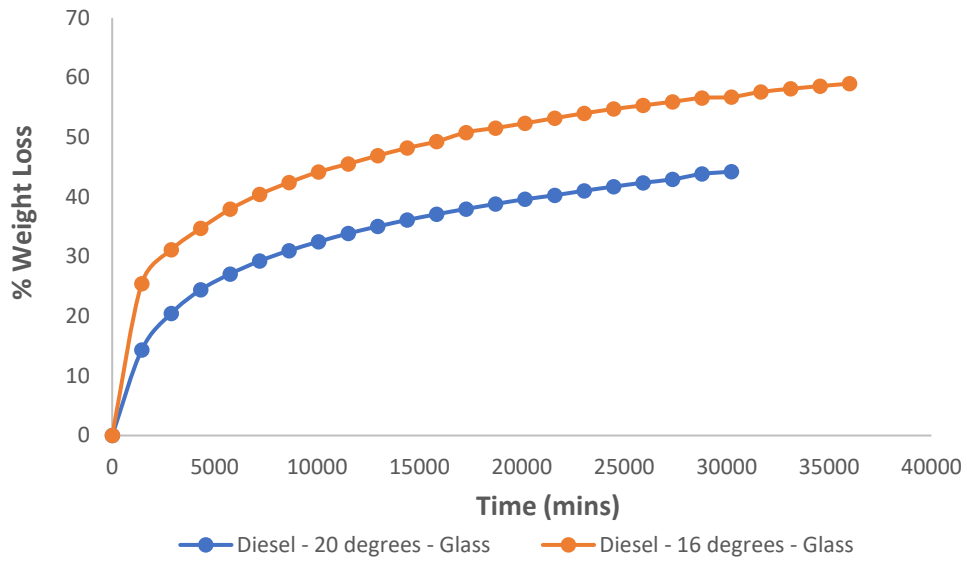


Figure 5.13. Comparative evaporation profiles of Diesel from glass over ~21 days, at a controlled temperature of 20 ± 1 °C and 16 ± 1 °C. Note that 1 day = 1,440 minutes, 21 days = 30,240 min.

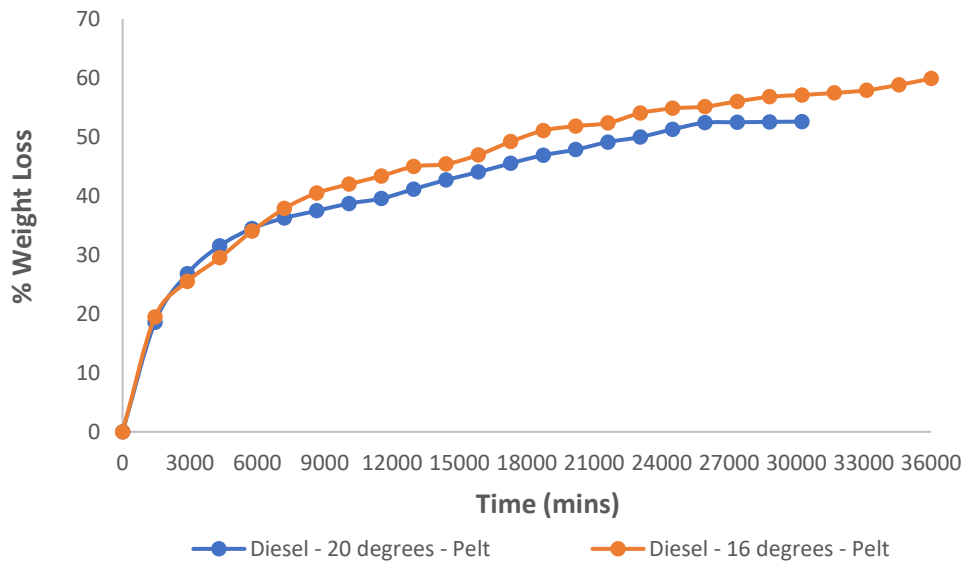


Figure 5.14. Comparative evaporation profiles of Diesel from pelt over ~21 days, at a controlled temperature of 20 ± 1 °C and 16 ± 1 °C. Note that 1 day = 1,440 minutes, 21 days = 30,240 min.

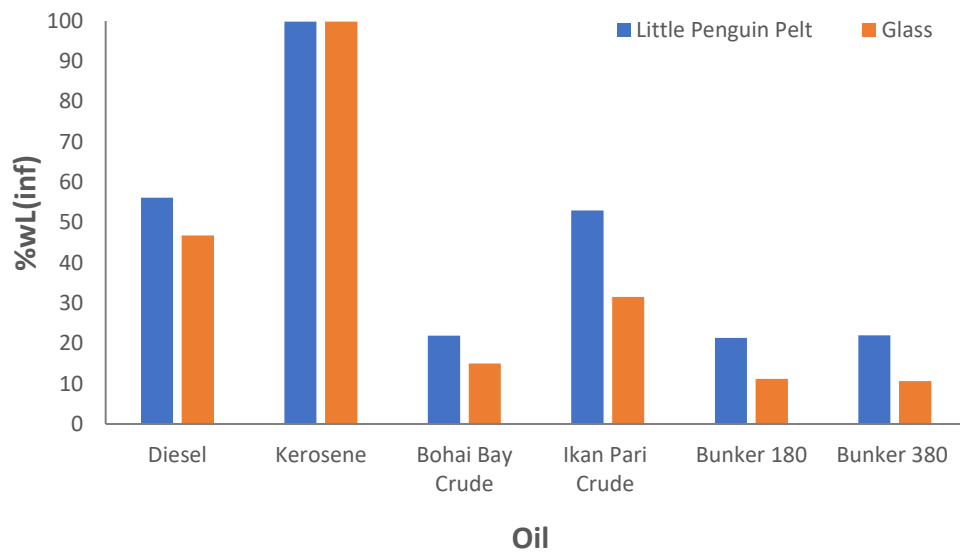


Figure 5.15. Comparative %wL(inf) (plateau) parameters for the evaporation of six oils from Little Penguin Pelt and Glass at ~20 °C up to ~21 days in the Potter Lab – **Experiment 1.**

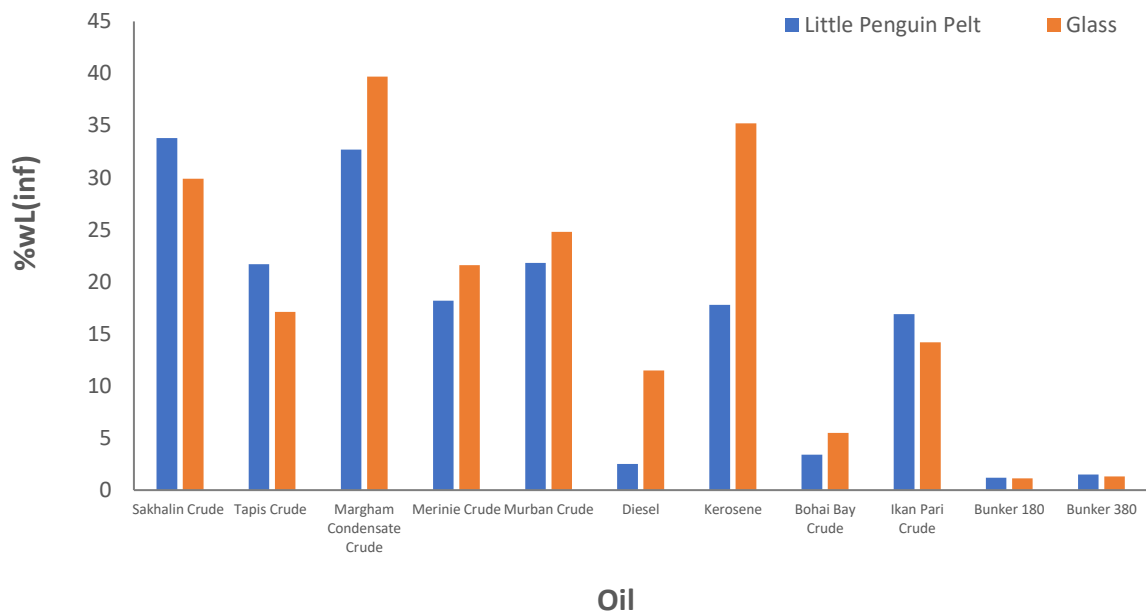


Figure 5.16. Comparative %wL(inf) parameter for the evaporation of all eleven oils from Little Penguin Pelt and Glass at ~21 °C up to 10 hours in the “Ambient Lab” – **Experiment 2.**

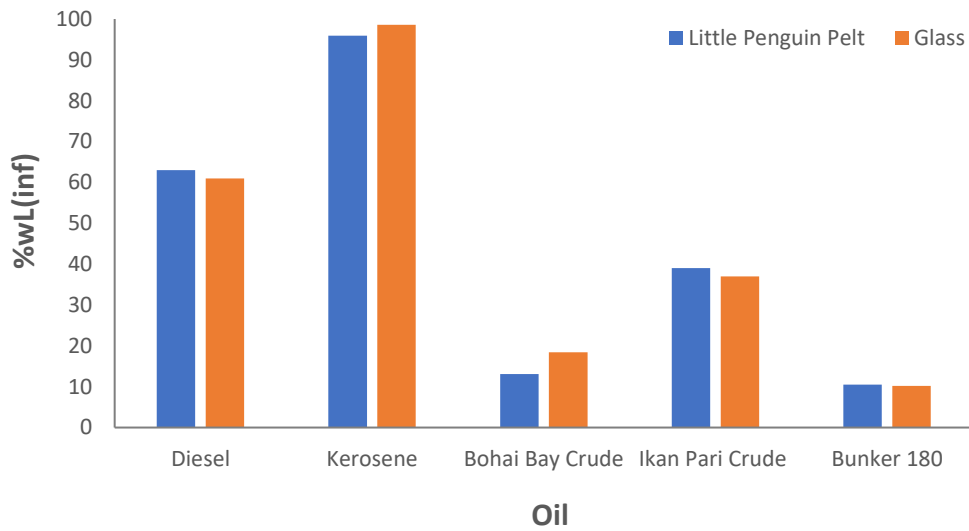


Figure 5.17. Comparative %wL(inf) parameter for the evaporation of six oils from Little Penguin Pelt and Glass at ~16 °C up to ~21 days in the Potter Lab – **Experiment 3.**

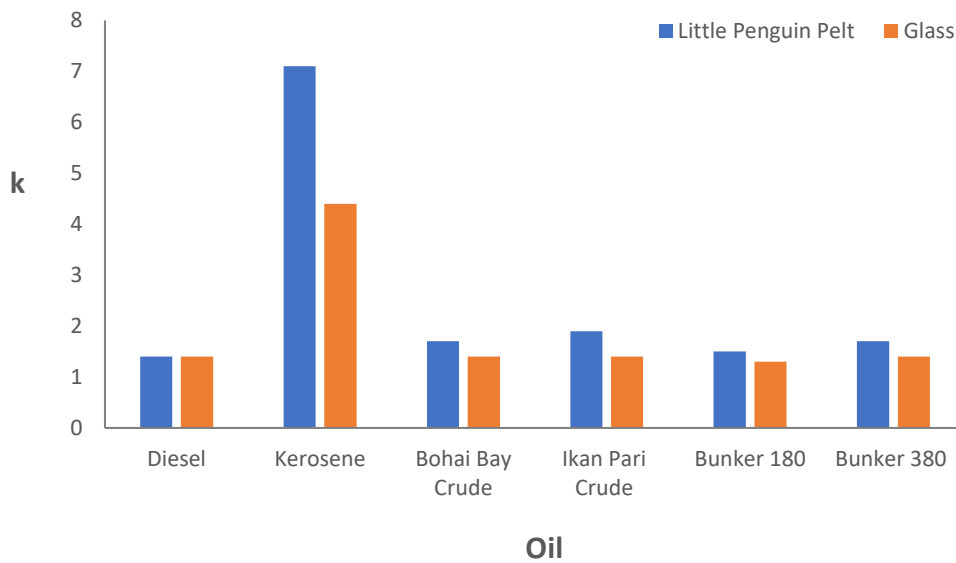


Figure 5.18. Comparative k parameter with reference to the evaporation profile for Little Penguin Pelt and Glass at ~20 °C - **Experiment 1.**

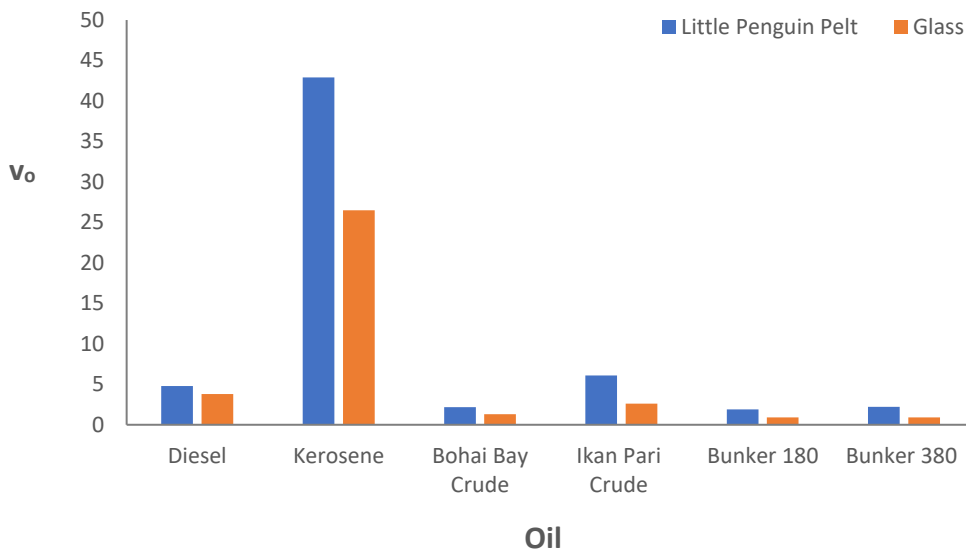


Figure 5.19. Comparative v_0 parameters with reference to the evaporation profile for Little Penguin Pelt and Glass at ~ 20 °C - **Experiment 1.**

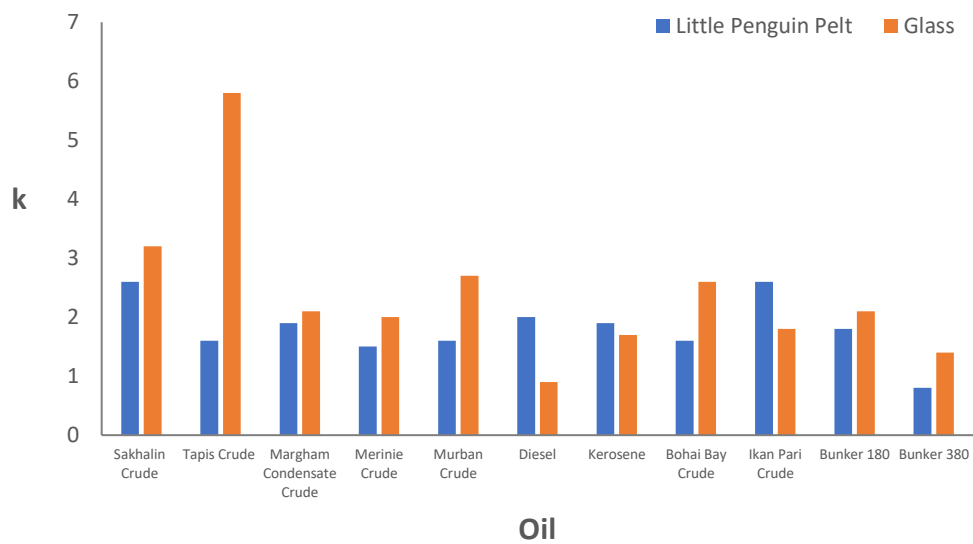


Figure 5.20. Comparative k parameter with reference to the evaporation profile for Little Penguin Pelt and Glass at ~ 21 °C.

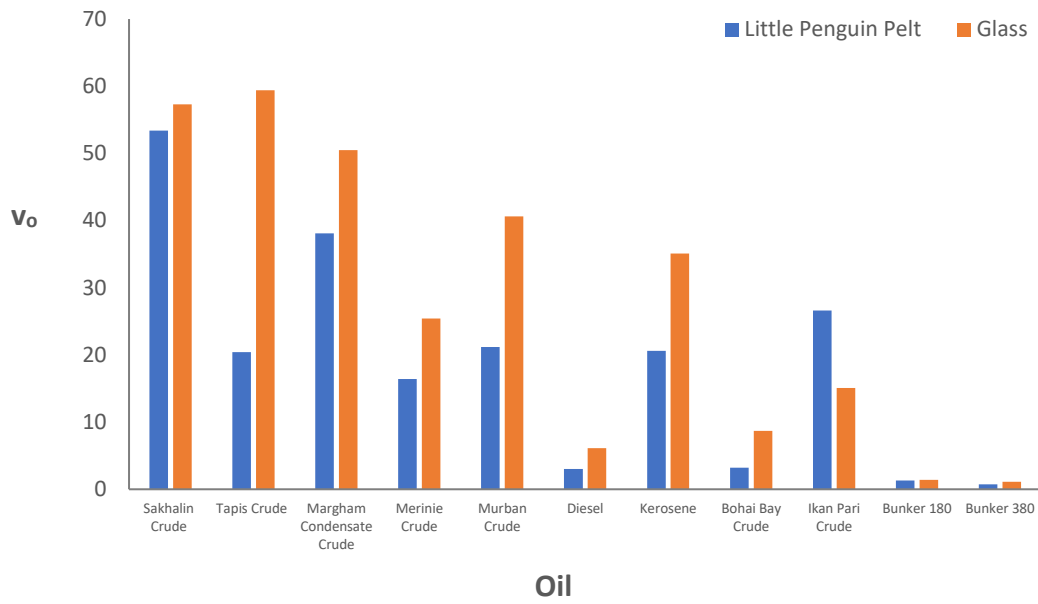


Figure 5.21. Comparative v_0 parameter with reference to the evaporation profile for Little Penguin Pelt and Glass at ~ 21 °C - **Experiment 2.**

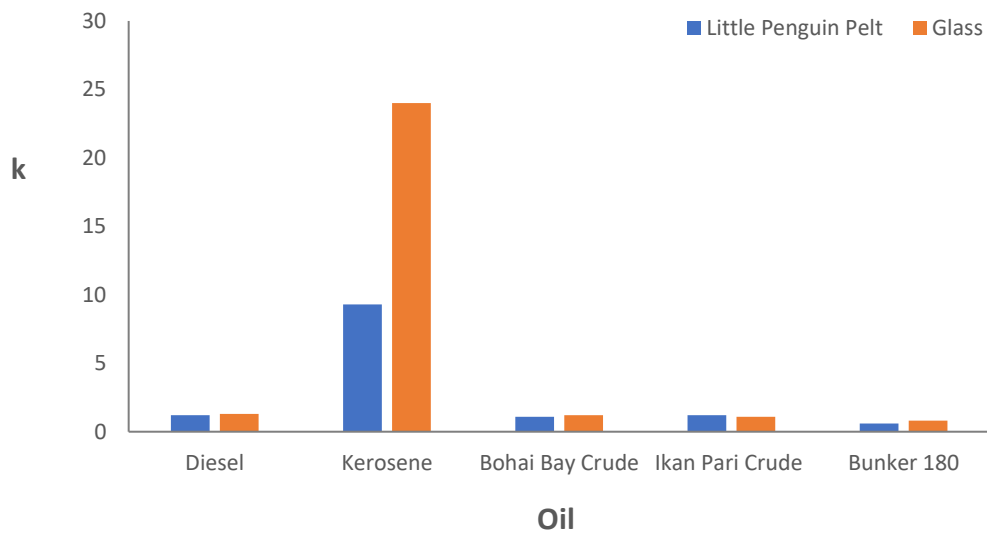


Figure 5.22. Comparative k parameter with reference to the evaporation profile for Little Penguin Pelt and Glass at ~ 16 °C - **Experiment 3.**

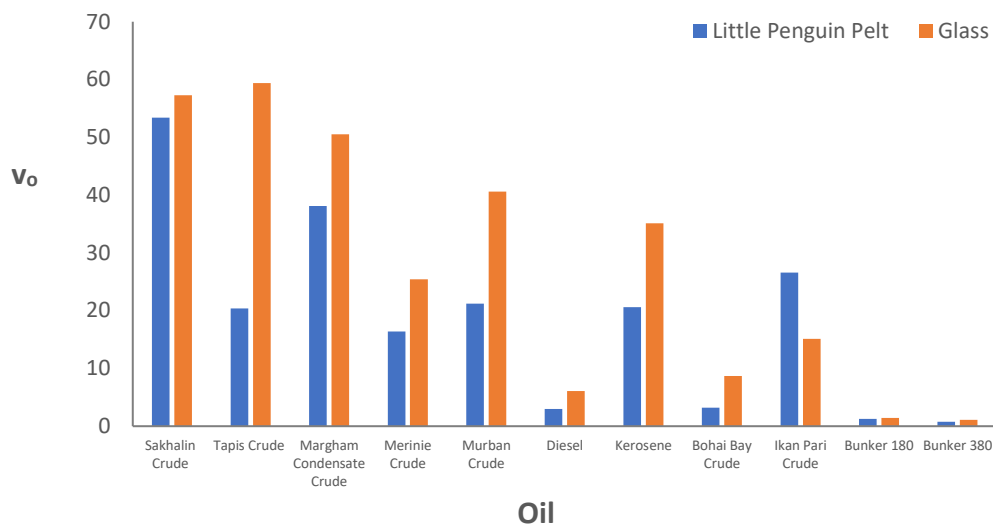


Figure 5.23. Comparative v_0 parameter with reference to the evaporation profile for Little Penguin Pelt and Glass at ~ 16 °C.

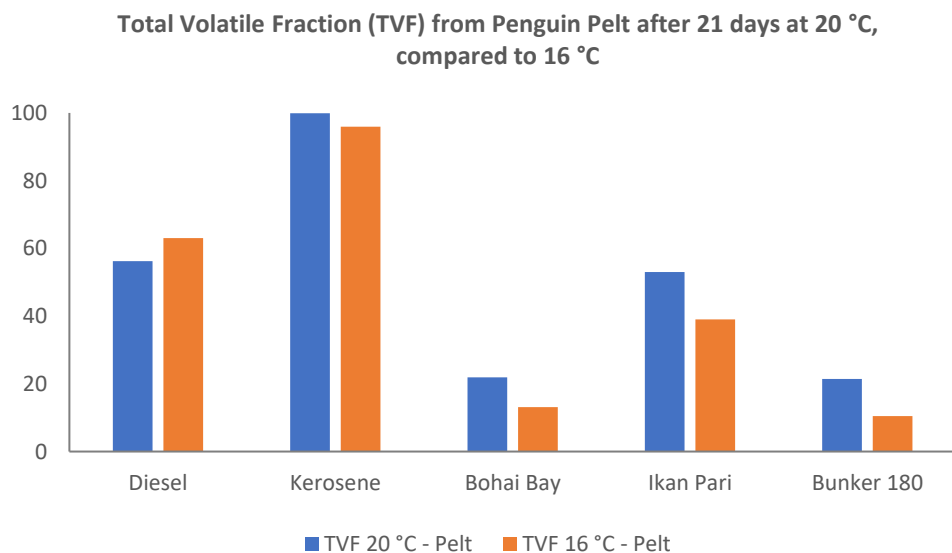


Figure 5.24. Comparative Total Volatile Fraction (TVF) profiles of light, medium and heavy crude oils from penguin pelt after 21 days, at controlled temperatures of 20 °C and 16 °C.

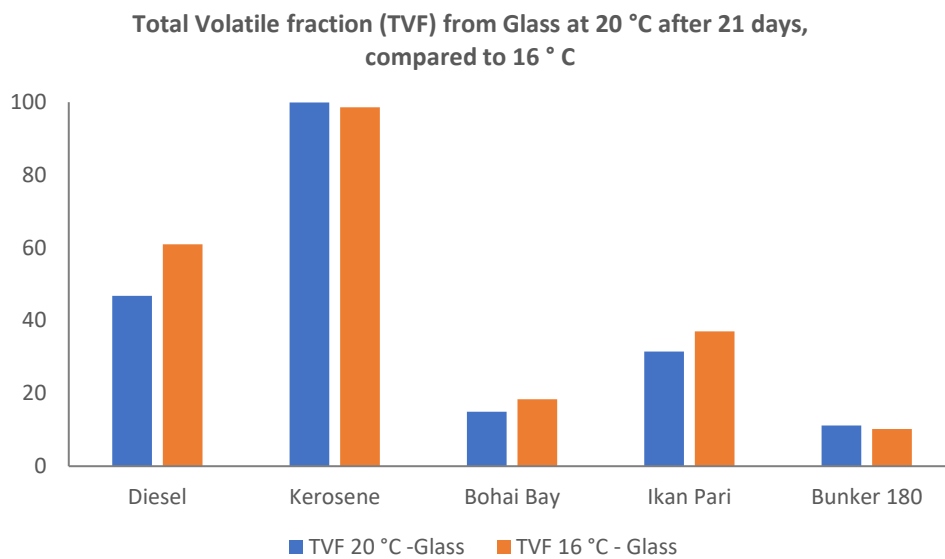


Figure 5.25. Comparative Total Volatile Fraction (TVF) profiles of light, medium and heavy crude oils from Glass after 21 days, at a controlled temperature of 20 °C and 16 °C.

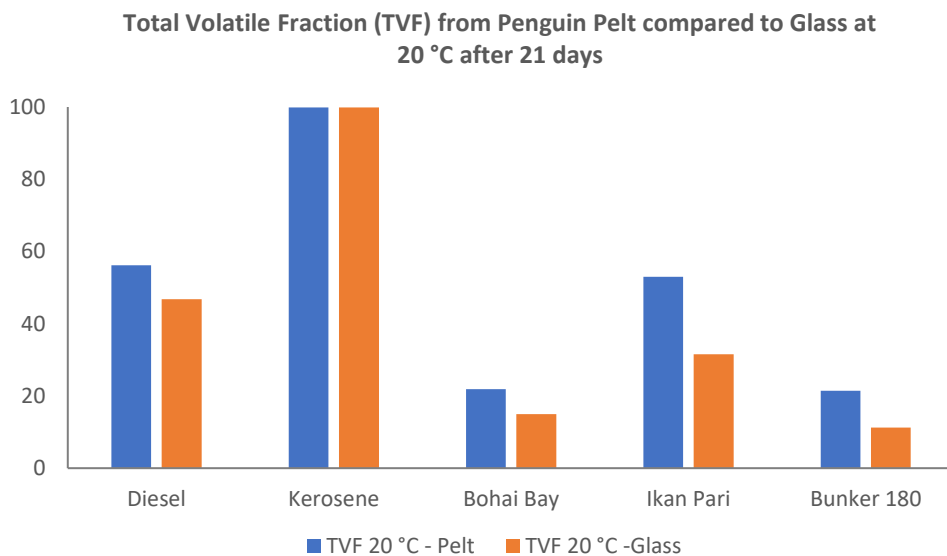


Figure 5.26. Comparative Total Volatile Fraction (TVF) profiles of light, medium and heavy crude oils from Penguin Pelt and Glass after 21 days, at a controlled temperature of 20 °C.

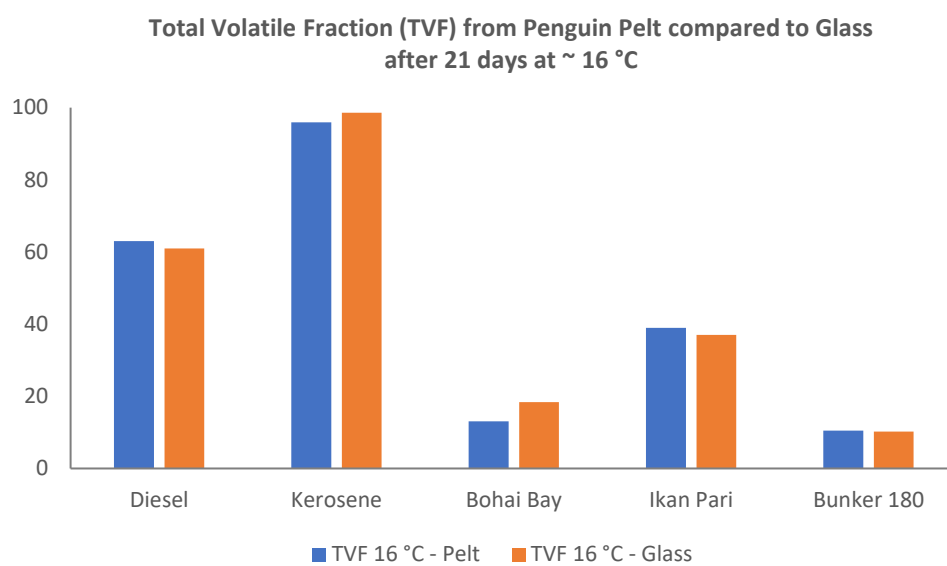


Figure 5.27. Comparative Total Volatile Fraction (TVF) profiles of light, medium and heavy crude oils from Penguin Pelt and Glass after 21 days, at a controlled temperature of 16 °C.

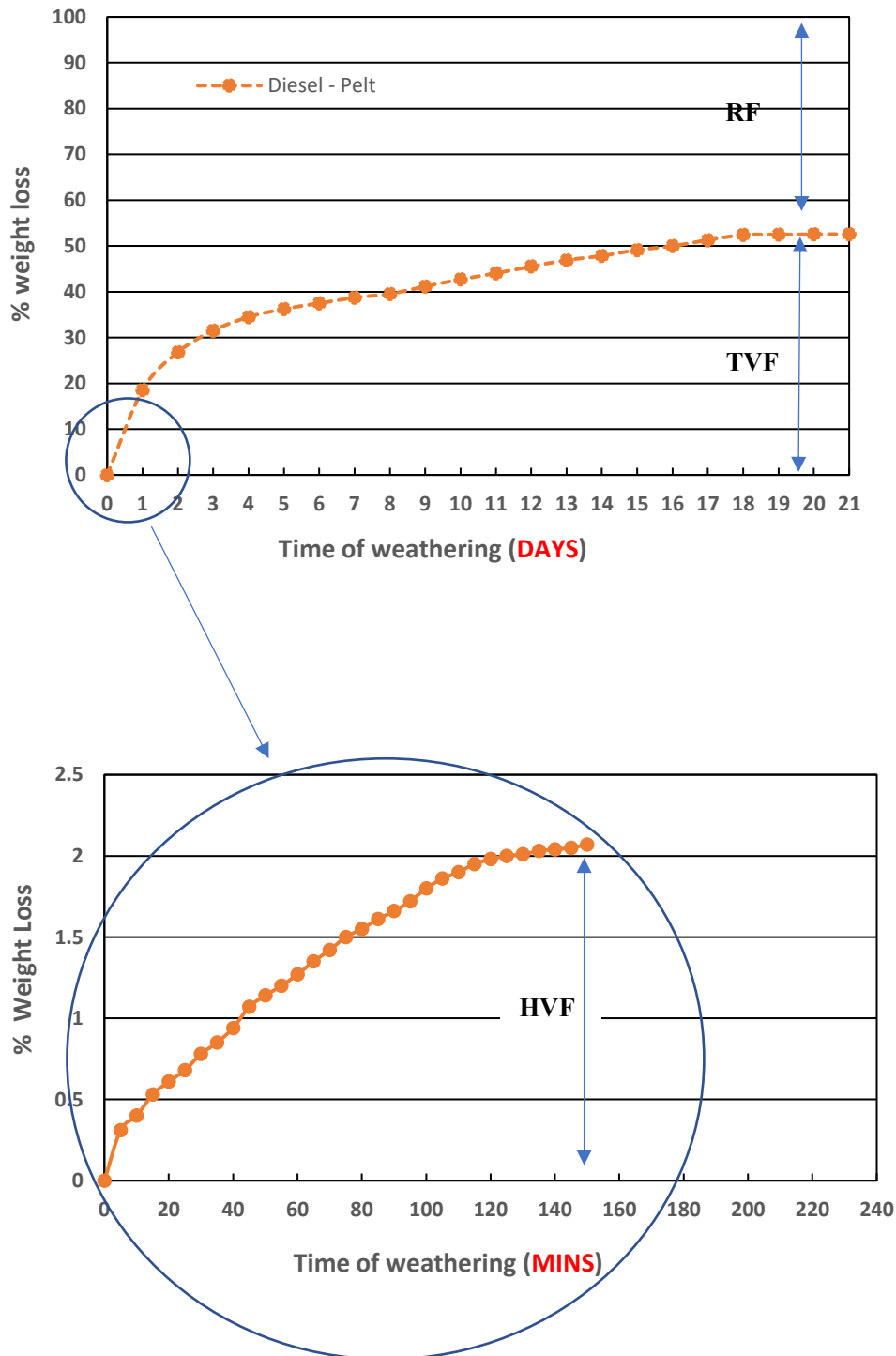


Figure 5.28 The above two graphs provide a representative example of the existence of the **Highly Volatile Fraction (HVF)** for the initial evaporation of Diesel from Little Penguin pelt. The top graph shows the evaporation profile over a long period of time (up to 21 days) whereas the bottom graph shows the evaporation profile over the first three hours; hence resolving the initial stage of the long-term evaporation curve. These experiments were conducted at $\sim 20^\circ\text{C}$. The **HVF** typically displays its own plateau and a defined latency period. Notably, some of the components involved in the **HVF** have been shown to become trapped in the plumage, *vide infra*.

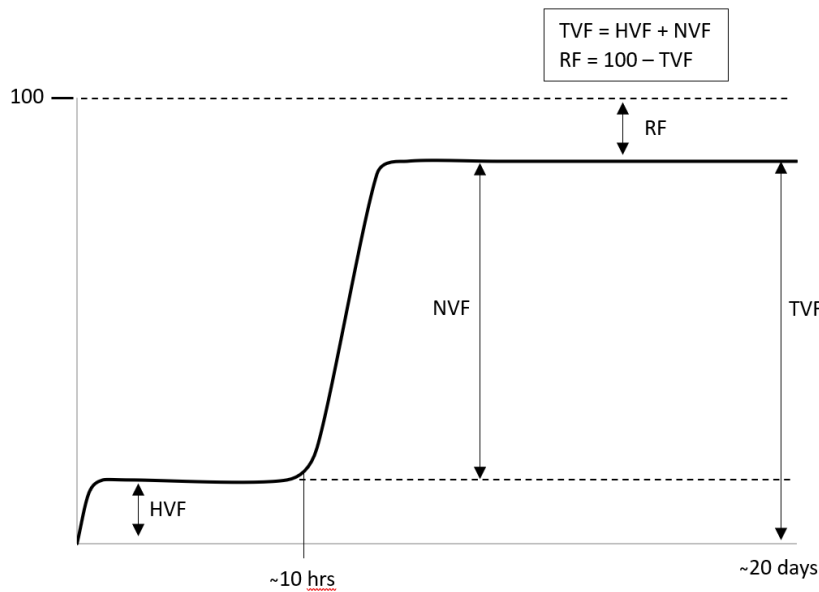


Figure 5.29. A schematic representation of the various fractions during the evaporation of a crude oil from a given surface. **HVF = Highly Volatile Fraction, NVF = Normal Volatile Fraction, TVF = Total Volatile Fraction, RF = Recalcitrant Fraction.** Note that $TVF = HVF + NVF$ and $RF = 100 - TVF$.

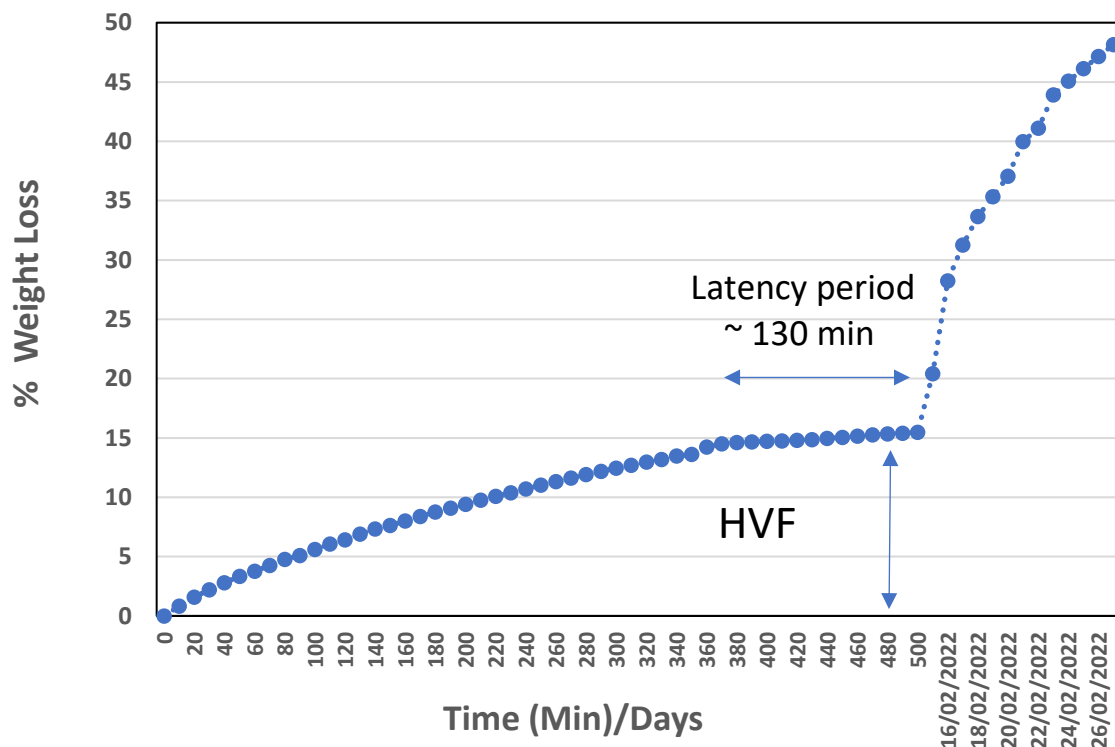


Figure 5.30. Results of an experiment to estimate the duration of the “latency period” associated with the Highly Volatile Fraction (HVF) for the evaporation of diesel from a glass surface. Similar latency periods are observed for the evaporation of all eleven oils studied, both from pelt and from glass. Note how the evaporation resumes to the long-term profile after ~ 500 min (~ 8.3 h).

Figure 5.31. Comparative values of NVF, RF and HVF for the evaporation the light, medium and heavy pairs of oil from plumage and glass at ~20 °C. Note that: **HVF = Highly Volatile Fraction, NVF = Normal Volatile Fraction, TVF = Total Volatile Fraction, RF = Recalcitrant Fraction. Note that TVF = HVF + NVF and RF = 100 – TVF.**

Diesel	Pelt
NVF	53.7
RF	43.8
HVF	2.5

Kerosene	Pelt
NVF	82.2
RF	0.1
HVF	17.8

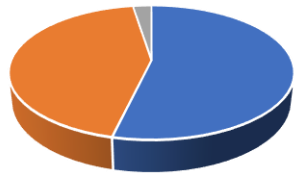
Bohai Bay	Pelt
NVF	18.5
RF	78.1
HVF	3.4

Ikan Pari	Pelt
NVF	36.1
RF	47
HVF	16.9

Bunker 180	Pelt
NVF	20.2
RF	78.6
HVF	1.2

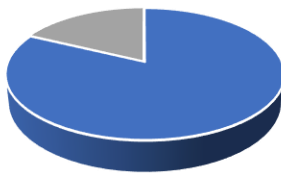
Bunker 380	Pelt
NVF	20.5
RF	78
HVF	1.5

Diesel - Pelt



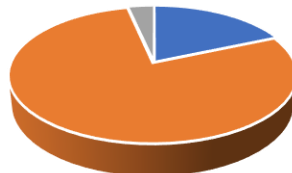
■ NVF ■ RF ■ HVF

Kerosene - Pelt



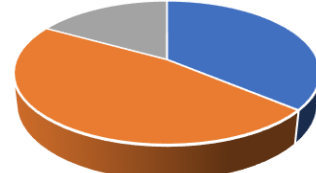
■ NVF ■ RF ■ HVF

Bohai Bay - Pelt



■ NVF ■ RF ■ HVF

Ikan Pari - Pelt



■ NVF ■ RF ■ HVF

Bunker 180 - Pelt



■ NVF ■ RF ■ HVF

Bunker 380 - Pelt



■ NVF ■ RF ■ HVF

Diesel	Glass
NVF	35.3
RF	53.2
HVF	11.5

Kerosene	Glass
NVF	64.7
RF	0.1
HVF	35.2

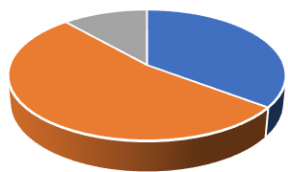
Bohai Bay	Glass
NVF	9.4
RF	85
HVF	5.6

Ikan Pari	Glass
NVF	17.3
RF	68.5
HVF	14.2

Bunker 180	Glass
NVF	10.1
RF	88.8
HVF	1.1

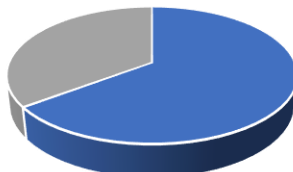
Bunker 380	Glass
NVF	9.3
RF	89.4
HVF	1.3

Diesel - Glass



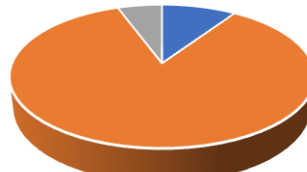
■ NVF ■ RF ■ HVF

Kerosene - Glass



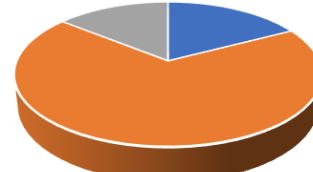
■ NVF ■ RF ■ HVF

Bohai Bay - Glass



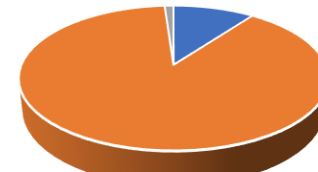
■ NVF ■ RF ■ HVF

Ikan Pari - Glass



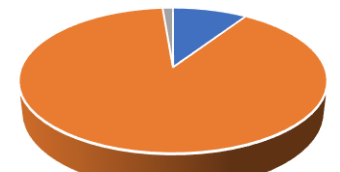
■ NVF ■ RF ■ HVF

Bunker 180 - Glass



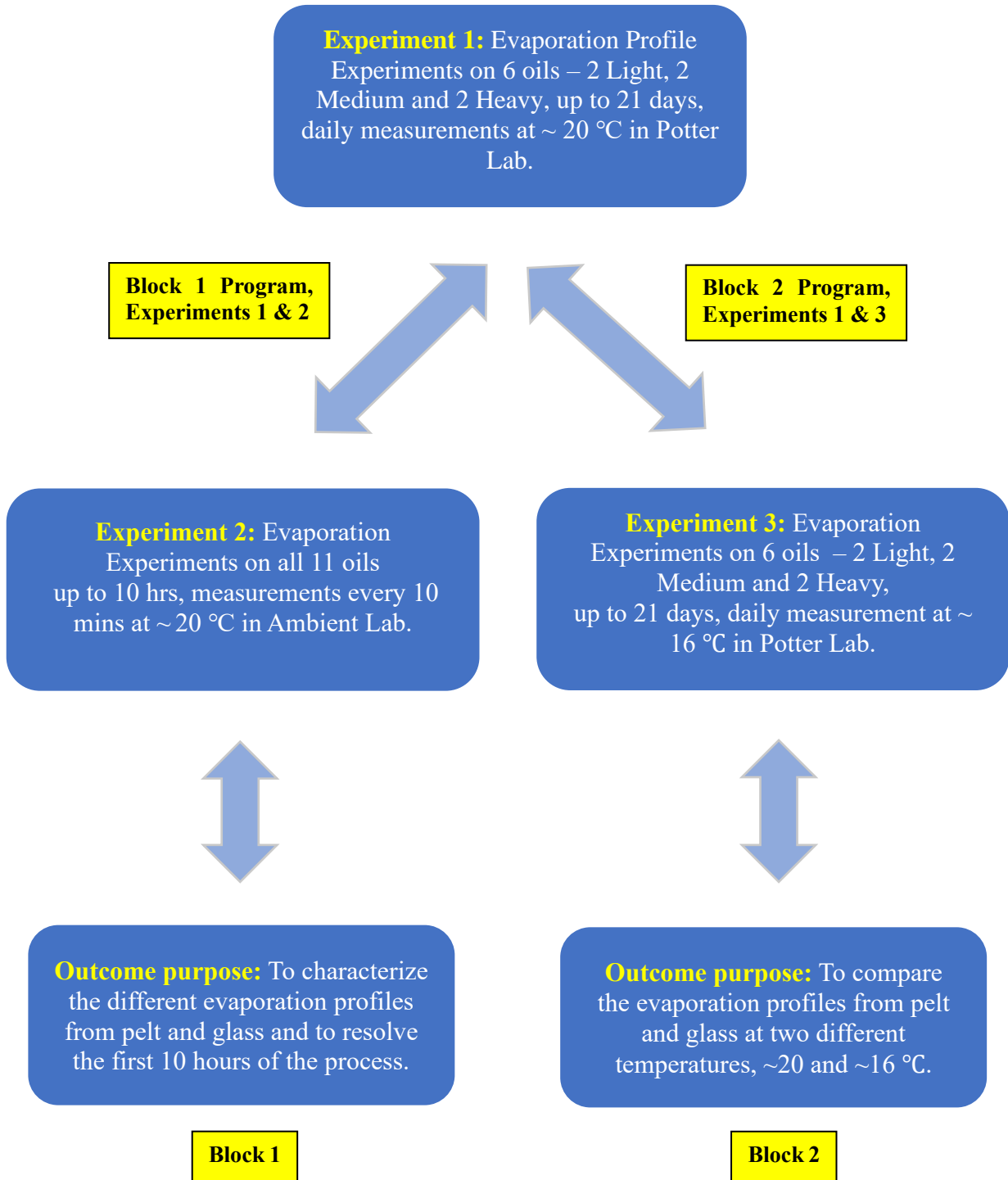
■ NVF ■ RF ■ HVF

Bunker 380 - Glass



■ NVF ■ RF ■ HVF

Experimental Design Schematic



OilVap v1.1

BACKGROUND

The program *OilVap* is an iterative curve-fitting software routine that fits input percentage weight loss, %wL, versus time, t, data in accordance with the equation:

$$\%wL = \%wL_{inf}[1 - \exp(-kt + c)] \quad (1)$$

where $\%wL_{inf}$ is the asymptotic value of the percentage weight loss after infinite time, k is the first-order rate constant, and c is a constant that reflects how close the fit is to first-order kinetics. Whence, if $c = 0$ the fit is described perfectly by the first-order kinetic equation:

$$\%wL = \%wL_{inf}[1 - \exp(-kt)] \quad (2)$$

For a given set of $\{t, \%wL(t)\}$ data the program enables the user to calculate the fit of the input data to Equation (2) over a range of $\%wL_{inf}$ values (i.e. $\%wL_{inf}(L)$ to $\%wL_{inf}(U)$) at a given step interval, $d\%wL_{inf}$. Each of these values is input by the user. During execution, the program displays the linear regression coefficient for the data fitted in accordance with Equation (2) at each of the $\%wL_{inf}$ values calculated within the range, thereby enabling the user to eventually converge upon the value of $\%wL_{inf}$ that produces the optimum fit.

When the optimum fit is achieved the program calculates $\{t, \%wL(t)\}$ values of the fitted curve at 1 min intervals up to a default time limit of 250 min that can be changed by the user. The fitted curve along with the original data are transferred to the Clipboard and these data can then be pasted into a spreadsheet program such as Excel for the convenient plotting of the original data and the fitted curve.

In addition to the original data and curve fit data, the software appends to the Clipboard data the various fit parameters k , c and r^2 where r^2 is the linear regression coefficient obtained from the regression analysis using Equation (2). The initial loss rate, v_0 , is also calculated in accordance with Equation (3):

$$v_0 = k \times \%wL_{inf} \quad (3)$$

where the parameters were obtained from the linear regression analysis using Equation (2).

DATA INPUT

There are a number of different options available to input the data. These can be accessed by using either the "Read Data File" or the "Enter Data" button.

Read Data File Button

The "Read Data File" button enables the program to read in tab-delimited text files that can be created, say, using MS Word or Excel. When this button is clicked the program will display the file list from which the required input file may be selected in the usual way.

MS Word Text File

- Use Microsoft Word to create a text (.txt) file of the $\{t, \%wL(t)\}$ data pairs for input.
- The data pairs should have each t value listed first and the $\%wL(t)$ value listed second.
- The t and $\%wL(t)$ data in each pair should be delimited using a "tab" character, e.g. 20.0 <tab key> 16.08.
- There should be n lines of text in the file, each line containing a $\{t, \%wL(t)\}$ pair of data.
- There should be no other data lines in the file such as headers, etc.
- Ensure that the data file is saved as a text (.txt) file by MS Word before proceeding.

Excel Text File

- Use Microsoft Excel to create a text (.txt) file of the $\{t, \%wL(t)\}$ data pairs for input
- Enter the time, t , values into Column A of a new spreadsheet.
- Enter the corresponding $\%wL(t)$ values into Column B of the spreadsheet
- Select "Save As..." from the "File" menu and select the "Tab-delimited (.txt)" option from the "File Format" menu before clicking the "Save" button.

Enter Data Button

The "Enter Data" button enables the user to enter data directly into the Output field of the software. When the "Enter Data" button is clicked, the Output field is opened for data entry and the user may enter data either directly from the keyboard or by pasting tab-delimited data pairs from the Clipboard.

The "Data File" field can be accessed upon manual data input for the user to provide an associated label for the data.

Direct Keyboard Data Entry

- Click the "Enter Data" button.
- Enter each $\{t, \%wL(t)\}$ data pair on a separate line in the field with a "tab" character between them and a "return" character at the end of each line (e.g. 20.0 <tab key> 16.08 <return>).
- When all data pairs have been entered click the "OK" button.

Pasting Data

- Tab-delimited data from a spreadsheet program such as Excel can be pasted directly into the Output field after the "Enter Data" button has been clicked.
- If the $\{t, \%wL(t)\}$ data are in Columns A and B of the spreadsheet respectively, select all of these data and copy these into the Clipboard.
- Click into the first line of the Output field of the software and paste the data using the "Control V" (windows) or "Command V" (Mac) key combinations.

Calculate Button

When all input data have been entered, the software calculates and displays the maximum values of the percentage weight loss (%wL(max)). This value is used in setting the lower limit of the %wL_{inf} range to be investigated to find the optimum value of %wL_{inf}.

- Choose a value of %wL_{inf}(L) that is slightly above the indicated value of %wL(max).
- As a first trial, set the %wL_{inf}(U) value that is about 20% above the %wL_{inf}(L) value and a step interval (dwL_{inf}) of, say, 0.5.
- Note the lower limit of %wL_{inf} must not be less than %wL(max) and the upper limit of %wL_{inf} must not be greater than 100% otherwise an error message will be generated.
- Click the "Calculate" button.
- If an optimum value of %wL_{inf} exists within the range that has been set this will be indicated in the Output field by values of the regression coefficient being calculated and displayed against the corresponding values of %wL_{inf}. The optimum values appear in red font.
- The range of %wL_{inf} can then be successively narrowed and the step interval successively decreased until the optimum %wL_{inf} value is obtained to a within a precision of 0.001% if required.
- If no optimum value of %wL_{inf} exists within the selected range, then the range should be expanded by increasing the %wL_{inf}(U) setting and/or the lowering the limit %wL_{inf}(L) setting to a value closer (but greater than) the %wL_{inf}(max) value.

Curve Fit Button

After each set of iterations is performed when the "Calculate" button is clicked, the optimum value of along with the corresponding fit parameters k , c , r^2 and v_0 are transferred to the respective fields in the vicinity of the "Curve Fit" button.

When the optimum value of %wL_{inf} has been found to the required precision, the software can be used to generate data that enables the curve of optimum fit to the experimental data to be generated from the optimum fit parameters.

The "Curve Fit" button places the following in the clipboard which can be immediately pasted into a spreadsheet program such as Excel for plotting:

- The original $\{t, \%wL(t)\}$ data pairs.
- The $\{t, \%wL(t)\}$ curve fit data calculated a 1 min intervals up to a default maximum (250 min) that can be changed by the user.
- Appended data: filename; fit parameters k , c , r^2 and v_0 .

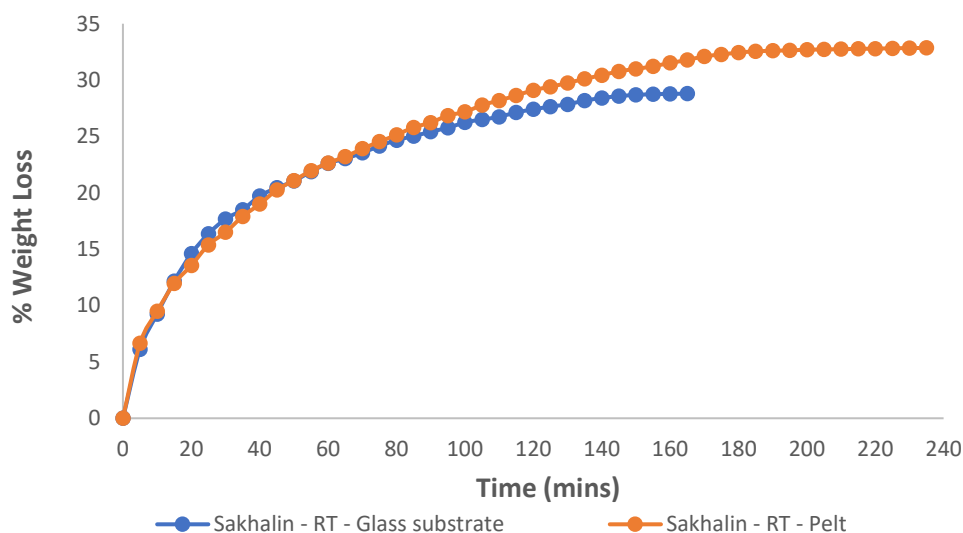


Figure 1. Comparative evaporation profiles of Sakhalin from pelt and glass over ~ 4 hours, at room temperature of 21-23 °C.

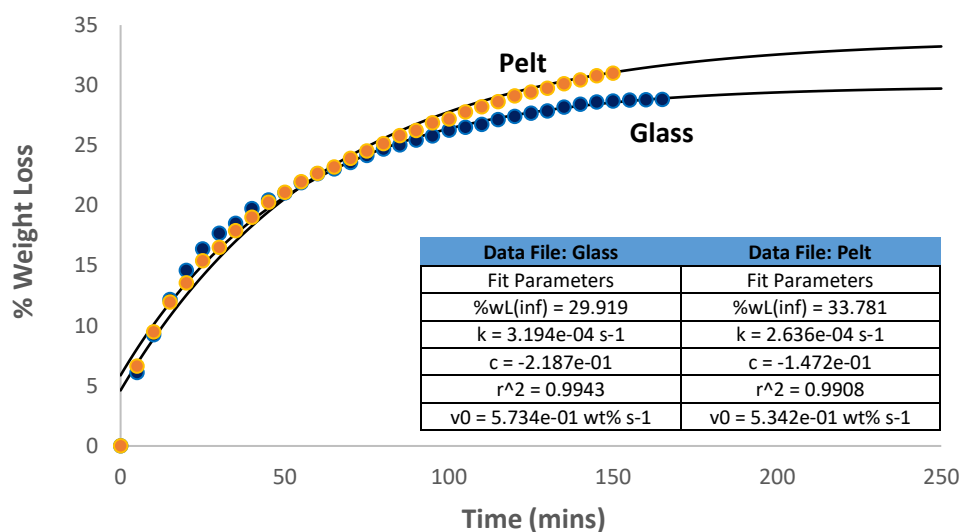


Figure 2. Comparative evaporation profiles of Sakhalin from pelt and glass over ~ 4 hours, at room temperature of 21-23 °C, showing the OilVap fit curves for the data presented in **Figure 1**. The inset gives the OilVap output data for the relevant plateau, fit and rate parameters for each curve.

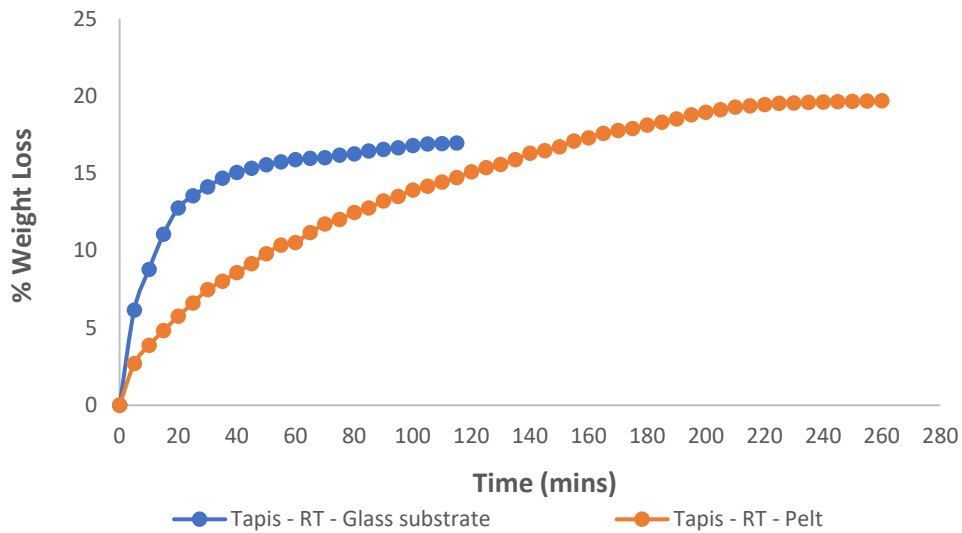


Figure 3. Comparative evaporation profiles of Tapis from pelt and glass over ~ 4 hours, at room temperature of 21-23 °C.

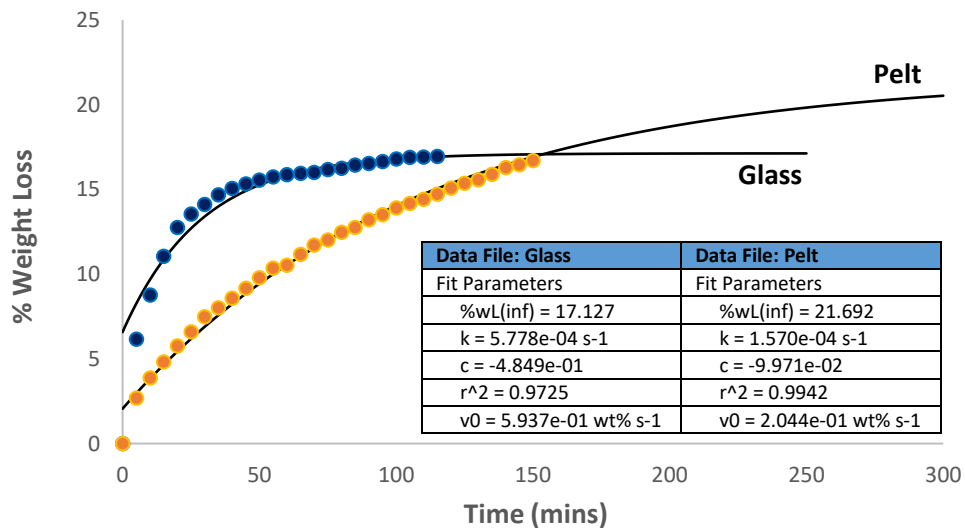


Figure 4. Comparative evaporation profiles of Tapis from pelt and glass pelt and glass over ~ 5 hours, at room temperature of 21-23 °C, showing the OilVap fit curves for the data presented in **Figure 3**. The inset gives the OilVap output data for the relevant plateau, fit and rate parameters for each curve.

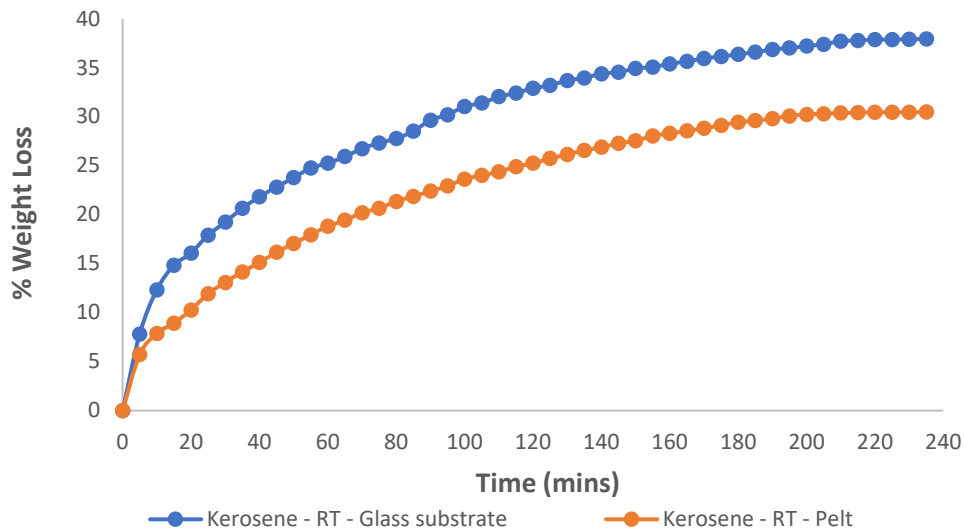


Figure 5. Comparative evaporation profiles of Margham Condensate from pelt and glass over ~ 4 hours, at room temperature of 21-23 °C.

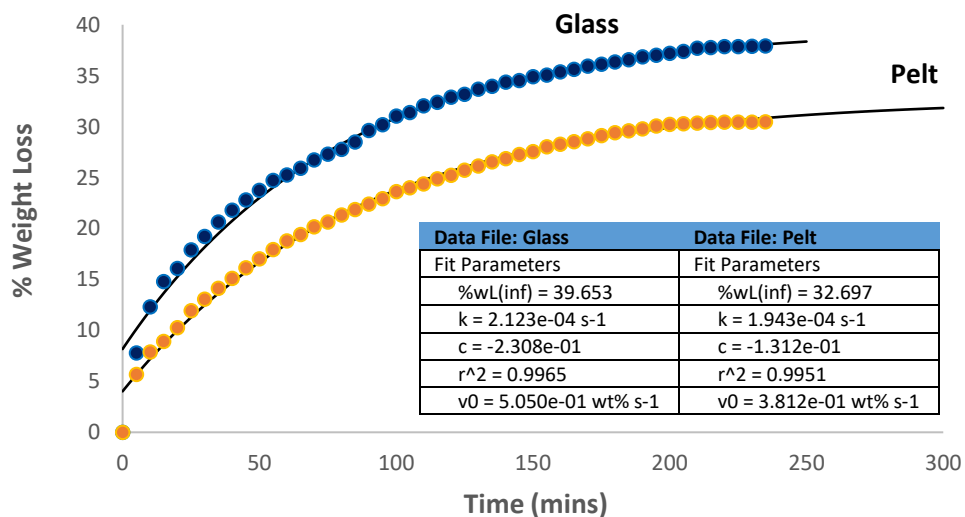


Figure 6. Comparative evaporation profiles of Margham Condensate from pelt and glass over ~ 5 hours, at room temperature of 21-23 °C, showing the OilVap fit curves for the data presented in **Figure 5**. The inset gives the OilVap output data for the relevant plateau, fit and rate parameters for each curve.

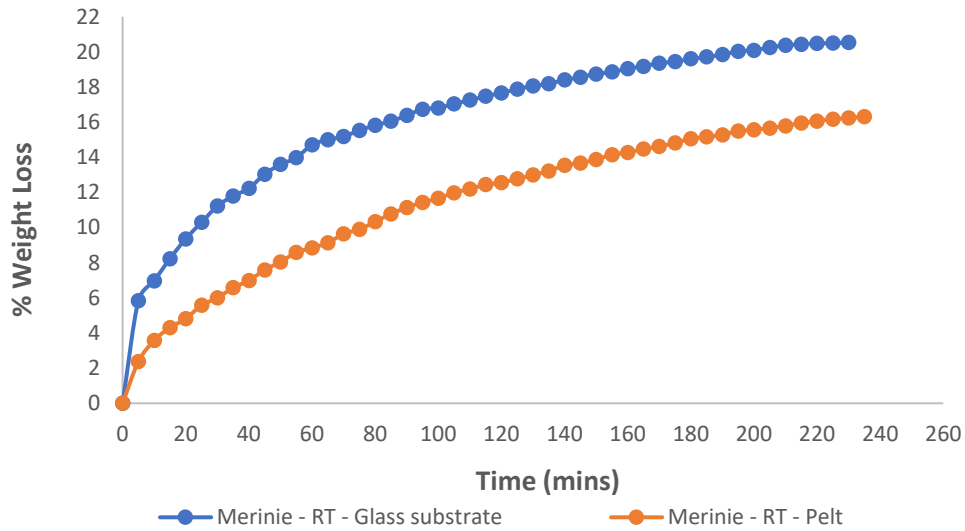


Figure 7. Comparative evaporation profiles of Merinie from pelt and glass over ~ 4 hours, at room temperature of 21-23 °C.

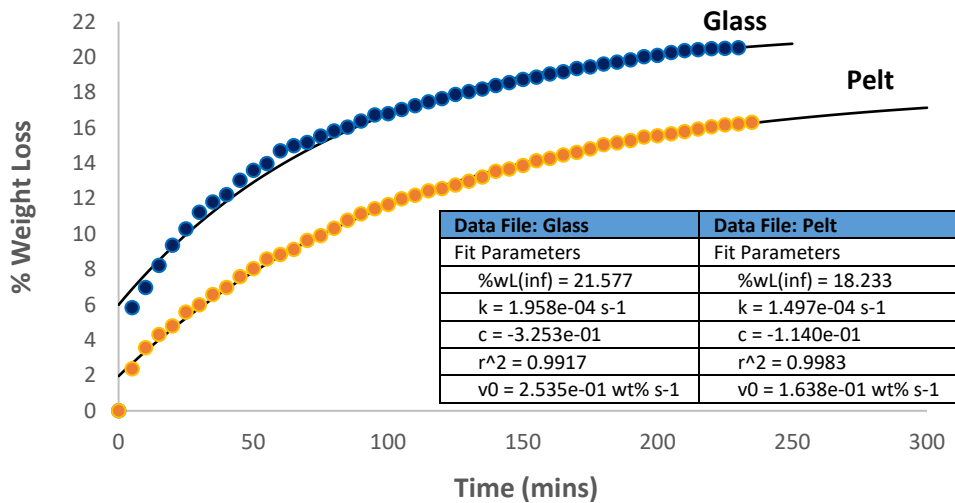


Figure 8. Comparative evaporation profiles of Merinie from pelt and glass over ~ 5 hours, at room temperature of 21-23 °C, showing the OilVap fit curves for the data presented in **Figure 7**. The inset gives the OilVap output data for the relevant plateau, fit and rate parameters for each curve.

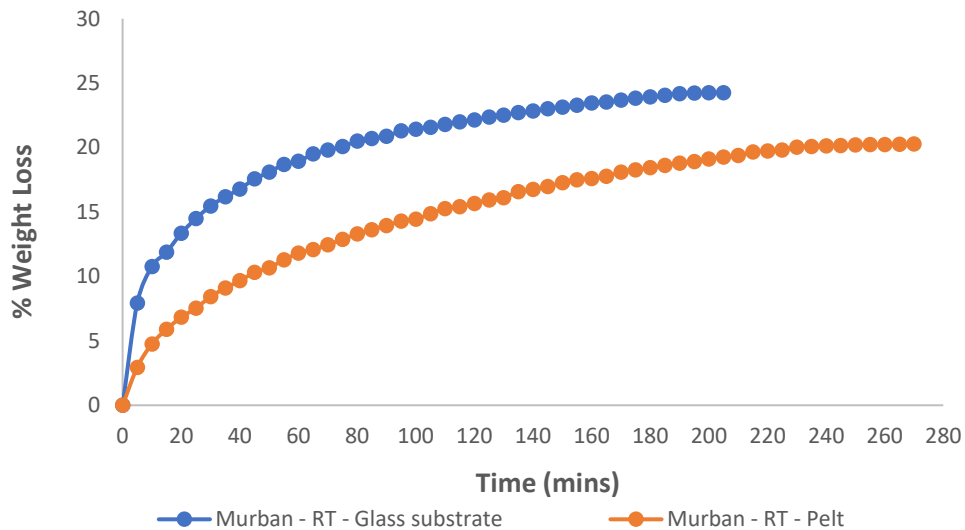


Figure 9. Comparative evaporation profiles of Murban from pelt and glass over ~ 4 hours, at room temperature of 21-23 °C.

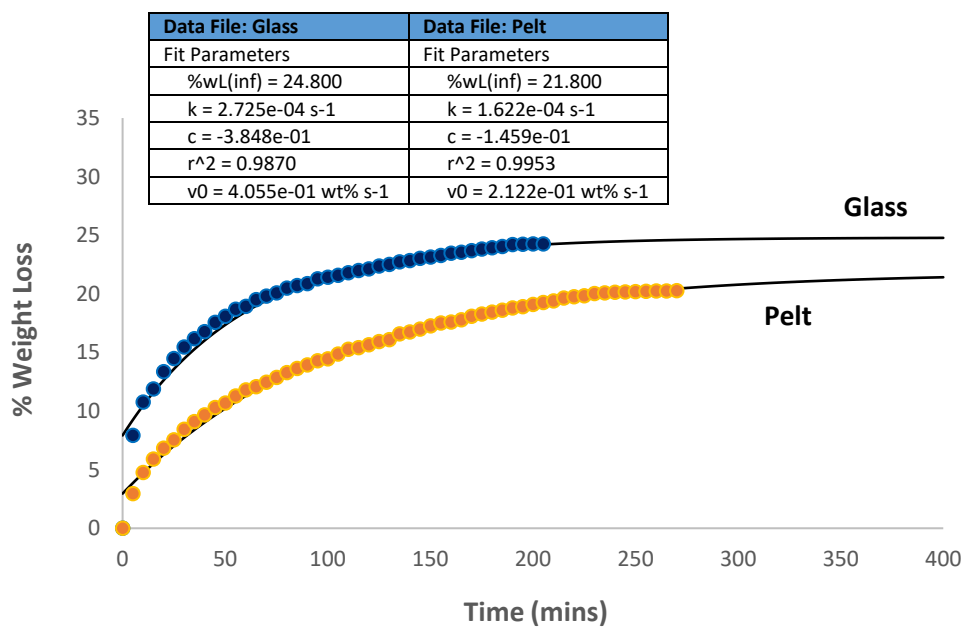


Figure 10. Comparative evaporation profiles of Murban from pelt and glass over ~ 6 hours, at room temperature of 21-23 °C, showing the OilVap fit curves for the data presented in **Figure 9**. The inset gives the OilVap output data for the relevant plateau, fit and rate parameters for each curve.

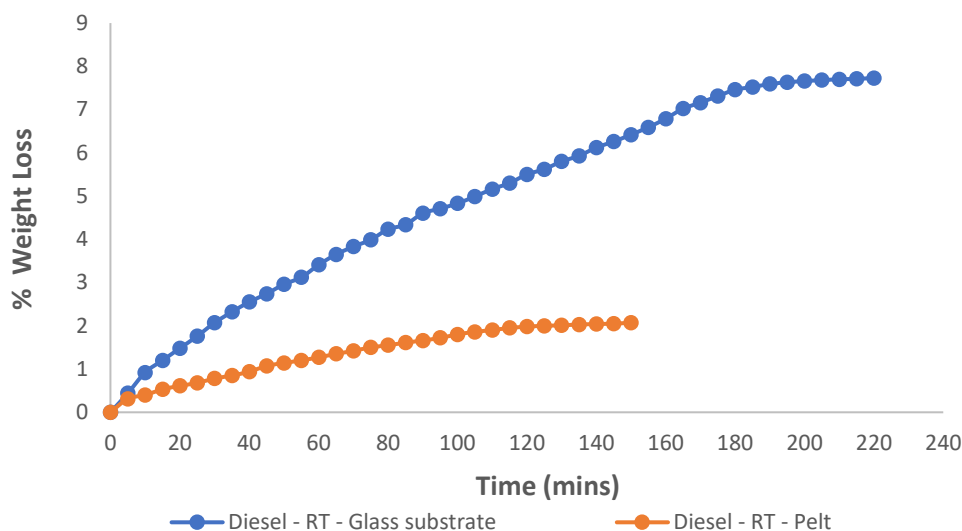


Figure 11. Comparative evaporation profiles of Diesel from pelt and glass over ~ 4 hours, at room temperature of 21-23 °C.

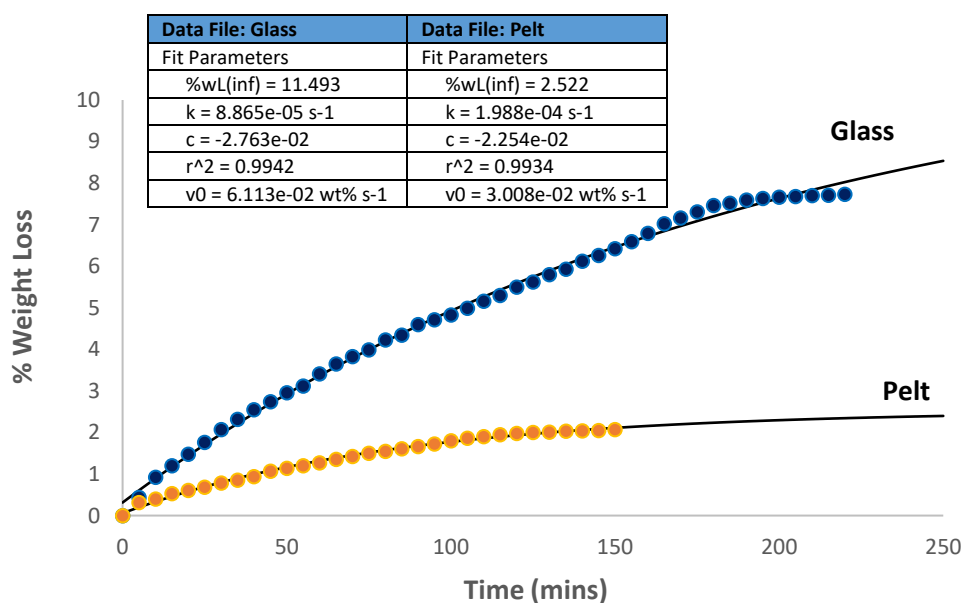


Figure 12. Comparative evaporation profiles of Diesel from pelt and glass pelt and glass over ~ 4 hours, at room temperature of 21-23 °C, showing the OilVap fit curves for the data presented in **Figure 11**. The inset gives the OilVap output data for the relevant plateau, fit and rate parameters for each curve.

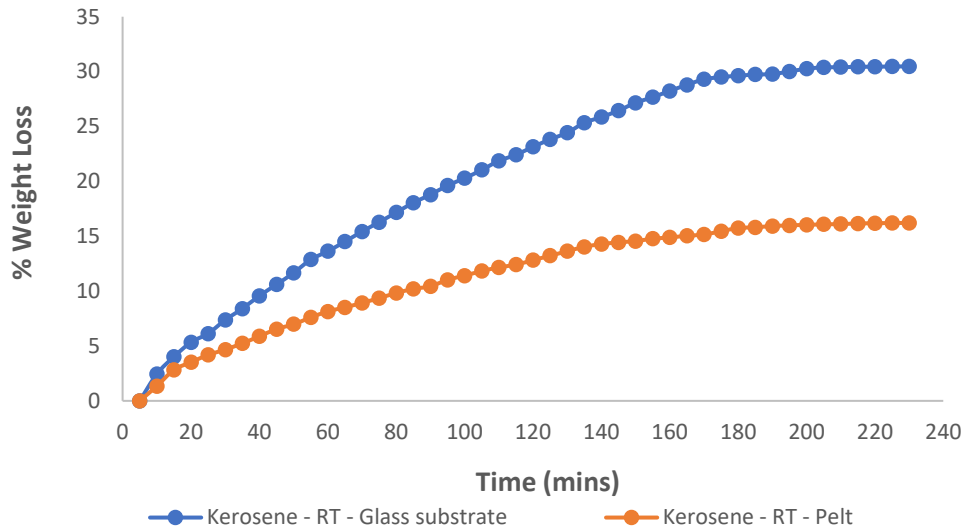


Figure 13. Comparative evaporation profiles of Kerosene from pelt and glass over ~ 4 hours, at room temperature of 21-23 °C.

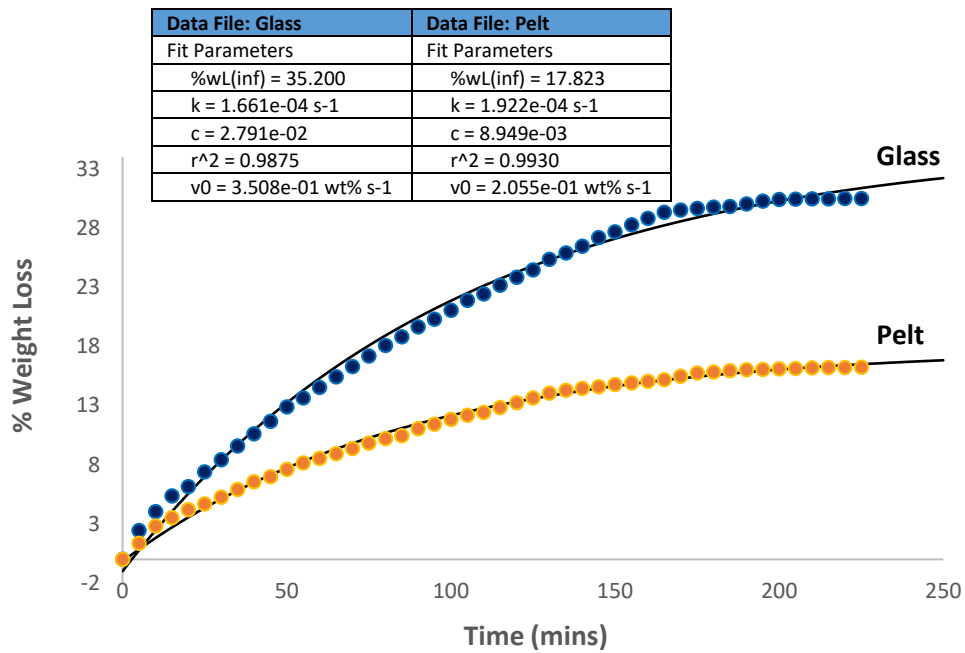


Figure 14. Comparative evaporation profiles of Kerosene from pelt and glass pelt and glass over ~ 4 hours, at room temperature of 21-23 °C, showing the OilVap fit curves for the data presented in **Figure 13**. The inset gives the OilVap output data for the relevant plateau, fit and rate parameters for each curve.

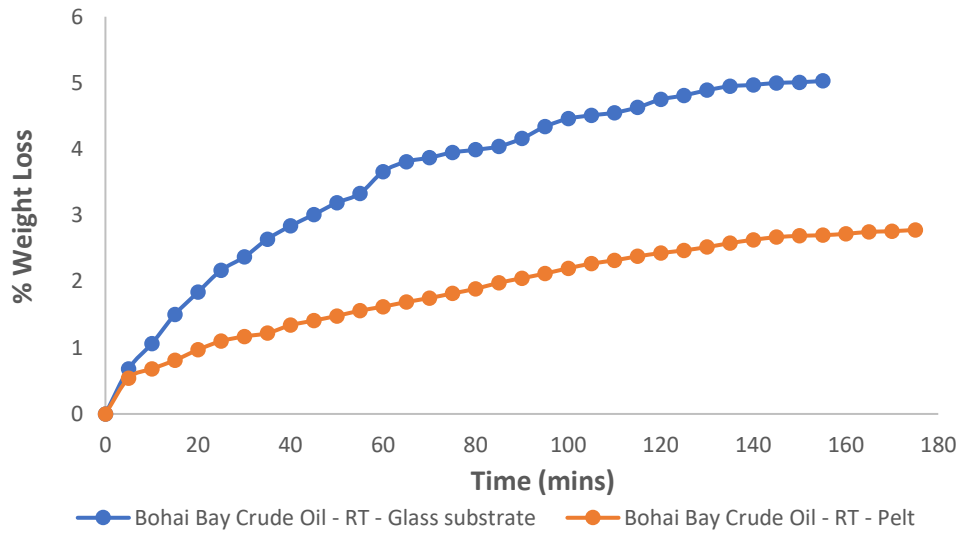


Figure 15. Comparative evaporation profiles of Bohai Bay from pelt and glass over ~ 3 hours, at room temperature of 21-23 °C.

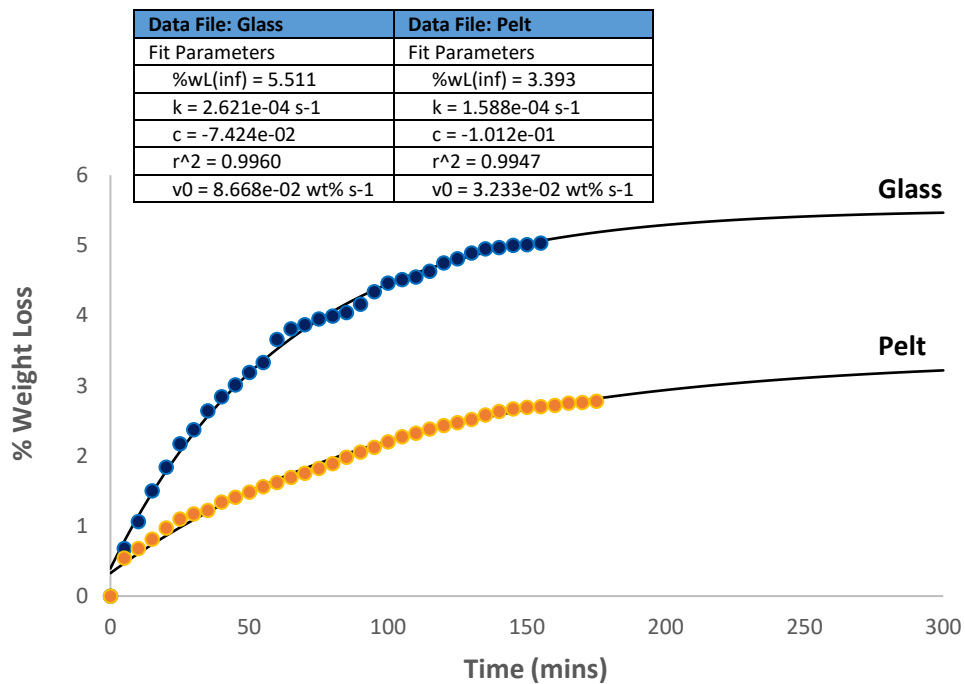


Figure 16. Comparative evaporation profiles of Bohai Bay from pelt and glass over ~ 5 hours, at room temperature of 21-23 °C, showing the OilVap fit curves for the data presented in **Figure 15**. The inset gives the OilVap output data for the relevant plateau, fit and rate parameters for each curve.

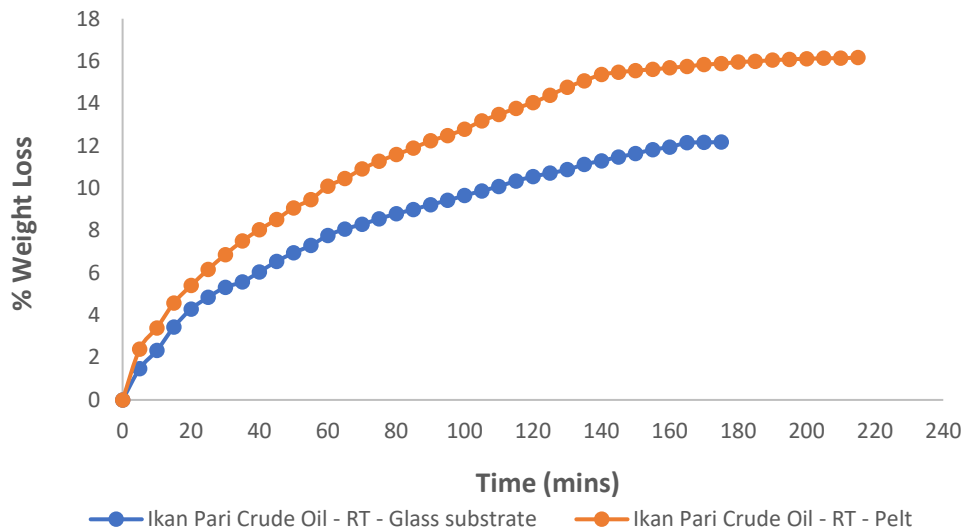


Figure 17. Comparative evaporation profiles of Ikan Pari from pelt and glass over ~ 4 hours, at room temperature of 21-23 °C.

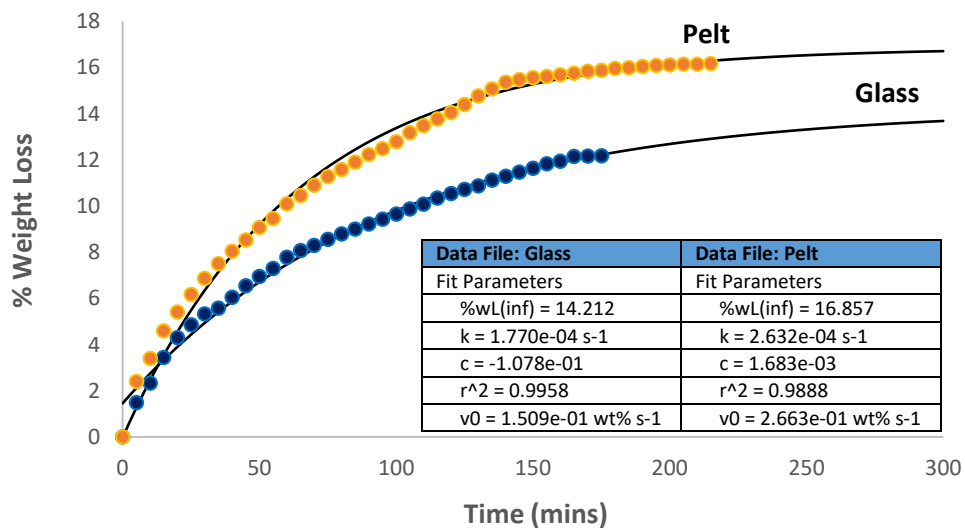


Figure 18. Comparative evaporation profiles of Ikan Pari from pelt and glass over ~ 5 hours, at room temperature of 21-23 °C, showing the OilVap fit curves for the data presented in **Figure 17**. The inset gives the OilVap output data for the relevant plateau, fit and rate parameters for each curve.

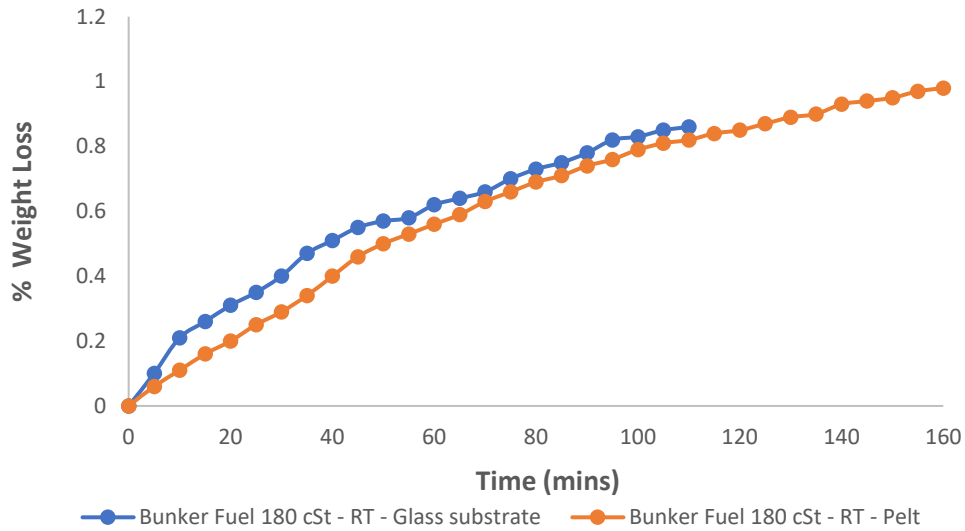


Figure 19. Comparative evaporation profiles of Bunker Fuel 180 cSt from pelt and glass over ~ 2 hours, at room temperature of 21-23 °C.

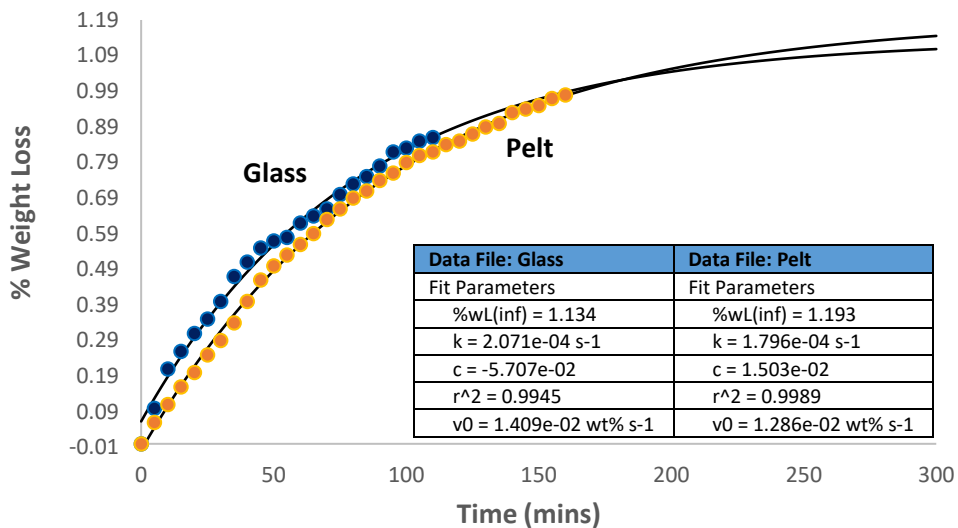


Figure 20. Comparative evaporation profiles of Bunker Fuel 180 cst from pelt and glass over ~ 5 hours, at room temperature of 21-23 °C, showing the OilVap fit curves for the data presented in **Figure 19**. The inset gives the OilVap output data for the relevant plateau, fit and rate parameters for each curve.

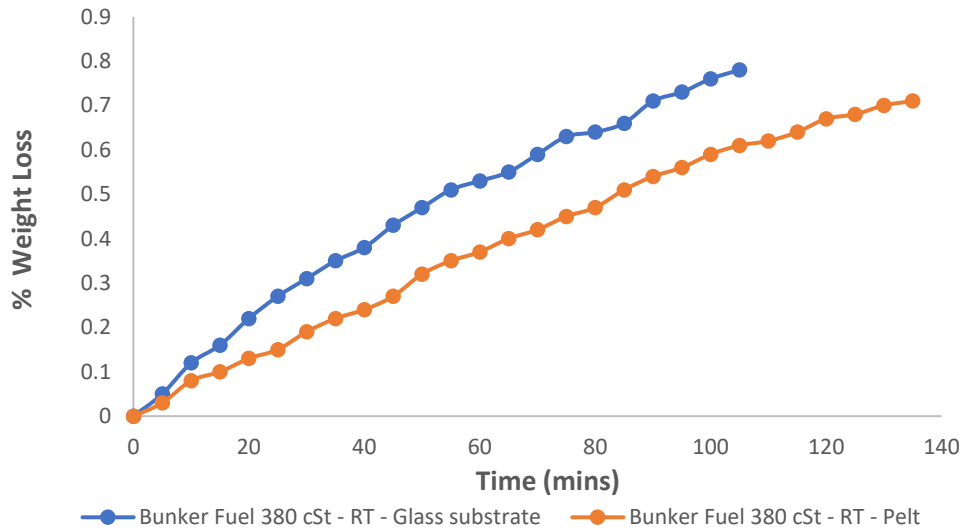


Figure 21. Comparative evaporation profiles of Bunker Fuel 380 cSt from pelt and glass over ~ 2 hours, at room temperature of 21-23 °C.

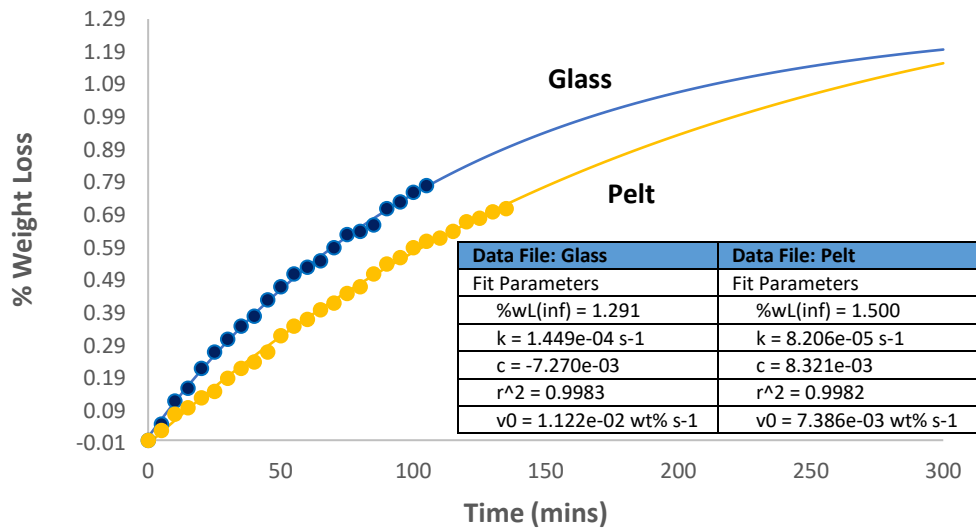


Figure 22. Comparative evaporation profiles of Bunker Fuel 380 cst from pelt and glass over ~ 5 hours, at room temperature of 21-23 °C, showing the OilVap fit curves for the data presented in **Figure 21**. The inset gives the OilVap output data for the relevant plateau, fit and rate parameters for each curve.

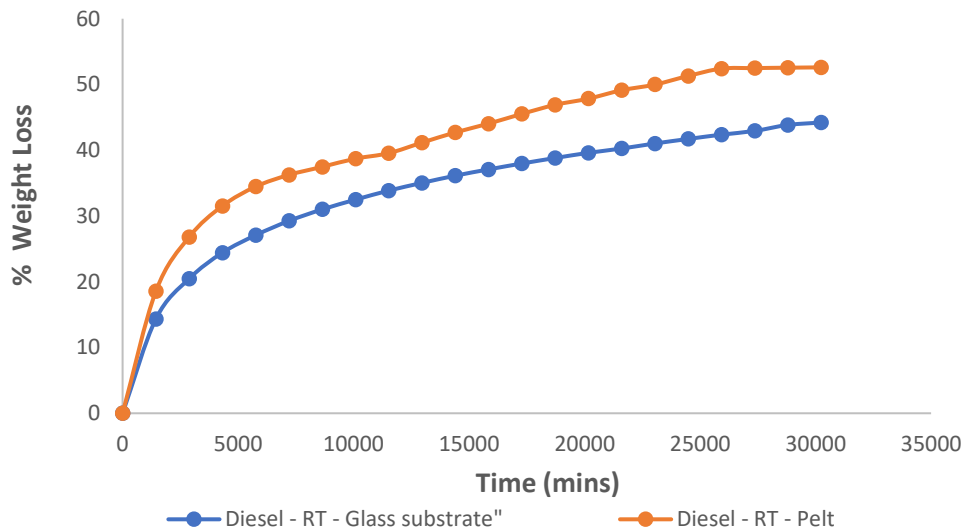


Figure 23. Comparative evaporation profiles of Diesel from pelt and glass over ~21 days, at a controlled temperature of 20 ± 1 °C. Note that 1 day = 1,440 minutes.

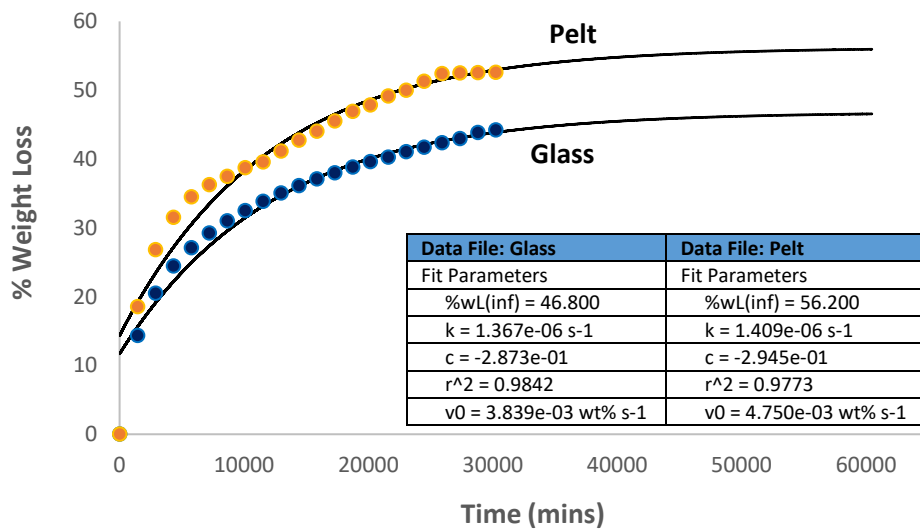


Figure 24. Comparative evaporation profiles of Diesel from glass and pelt over ~21 days, at a controlled temperature of 20 ± 1 °C, showing the OilVap fit curves for the data presented in **Figure 23**. Note that 1 day = 1,440 minutes. The inset gives the OilVap output data for the relevant plateau, fit and rate parameters for each curve.

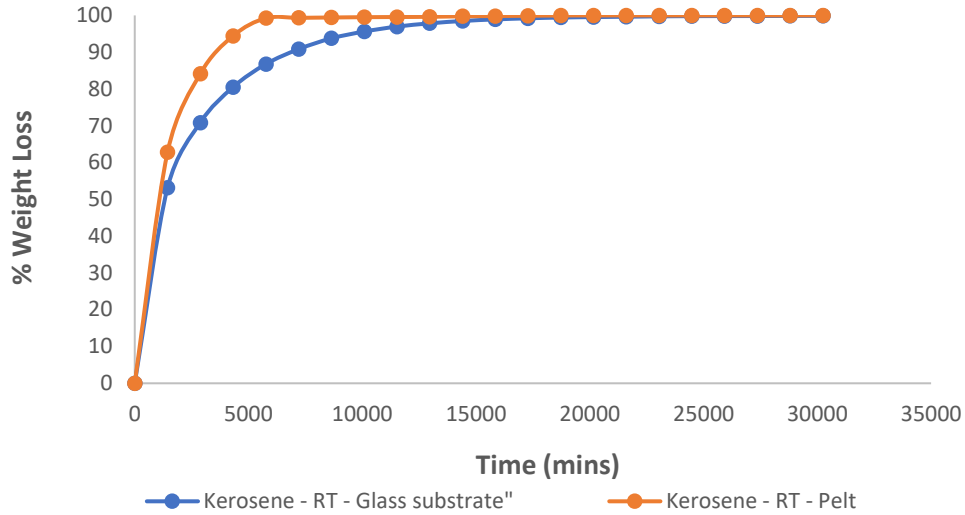


Figure 25. Comparative evaporation profiles of Kerosene from pelt and glass over ~21 days, at a controlled temperature of 20 ± 1 °C. Note that 1 day = 1,440 minutes.

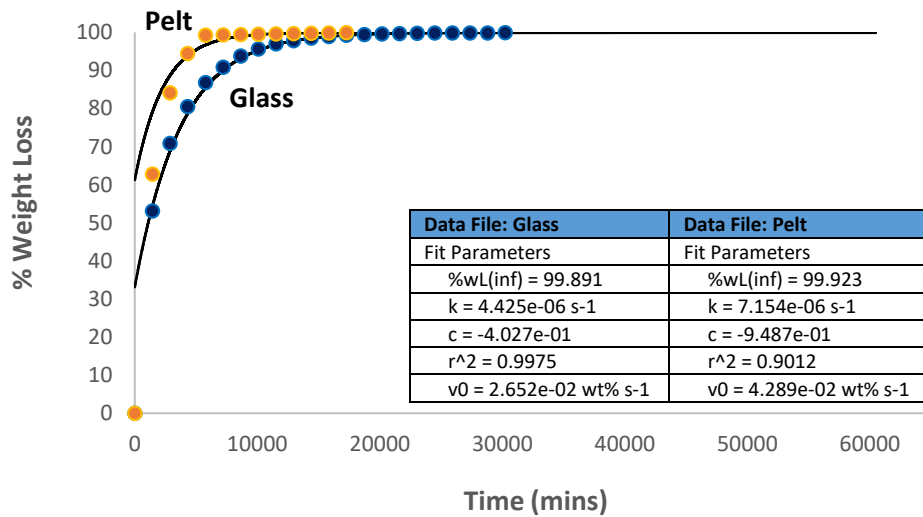


Figure 26. Comparative evaporation profiles of Kerosene from glass and pelt over ~21 days, at a controlled temperature of 20 ± 1 °C, showing the OilVap fit curves for the data presented in **Figure 25**. Note that 1 day = 1,440 minutes. The inset gives the OilVap output data for the relevant plateau, fit and rate parameters for each curve.

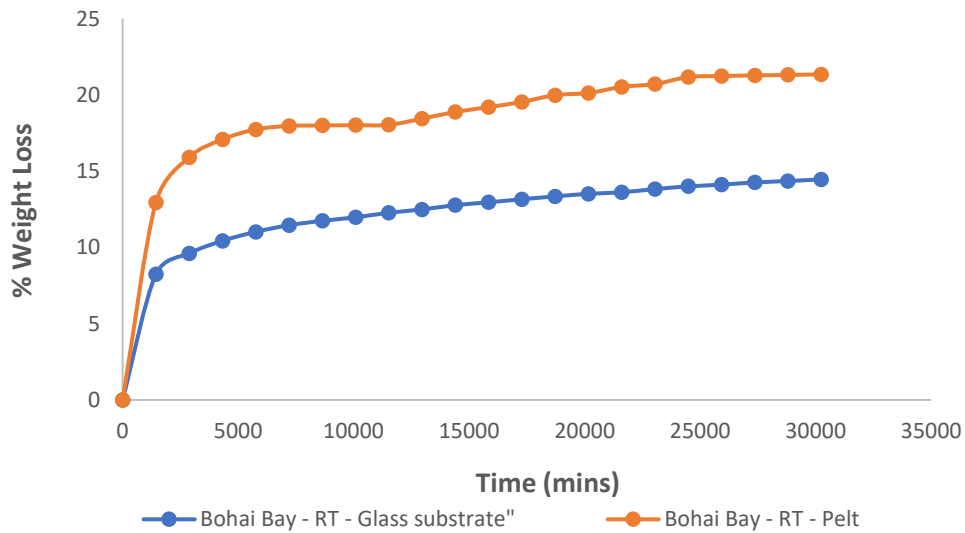


Figure 27. Comparative evaporation profiles of Bohai Bay from pelt and glass over ~21 days, at a controlled temperature of 20 ± 1 °C. Note that 1 day = 1,440 minutes.

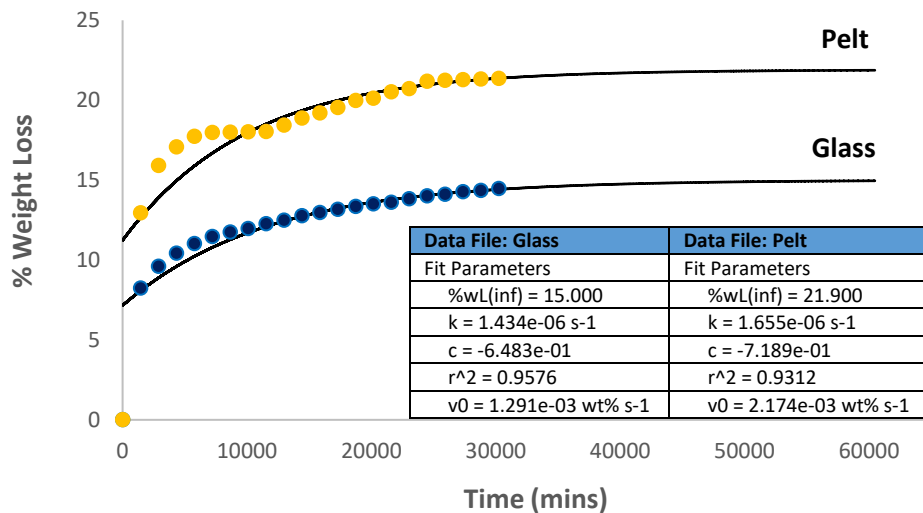


Figure 28. Comparative evaporation profiles of Bohai Bay from glass and pelt over ~21 days, at a controlled temperature of 20 ± 1 °C, showing the OilVap fit curves for the data presented in **Figure 27**. Note that 1 day = 1,440 minutes. The inset gives the OilVap output data for the relevant plateau, fit and rate parameters for each curve.

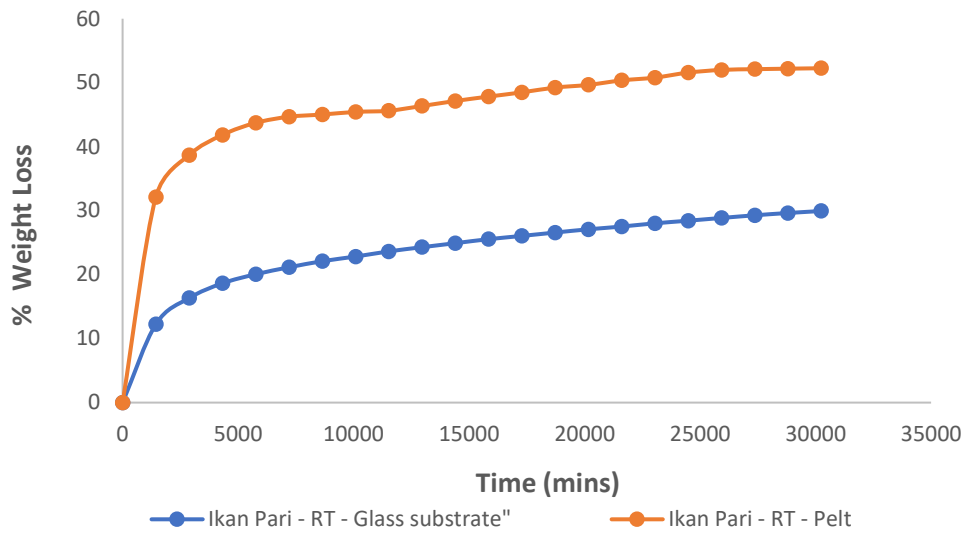


Figure 29. Comparative evaporation profiles of Ikan Pari from pelt and glass over ~21 days, at a controlled temperature of 20 ± 1 °C. Note that 1 day = 1,440 minutes.

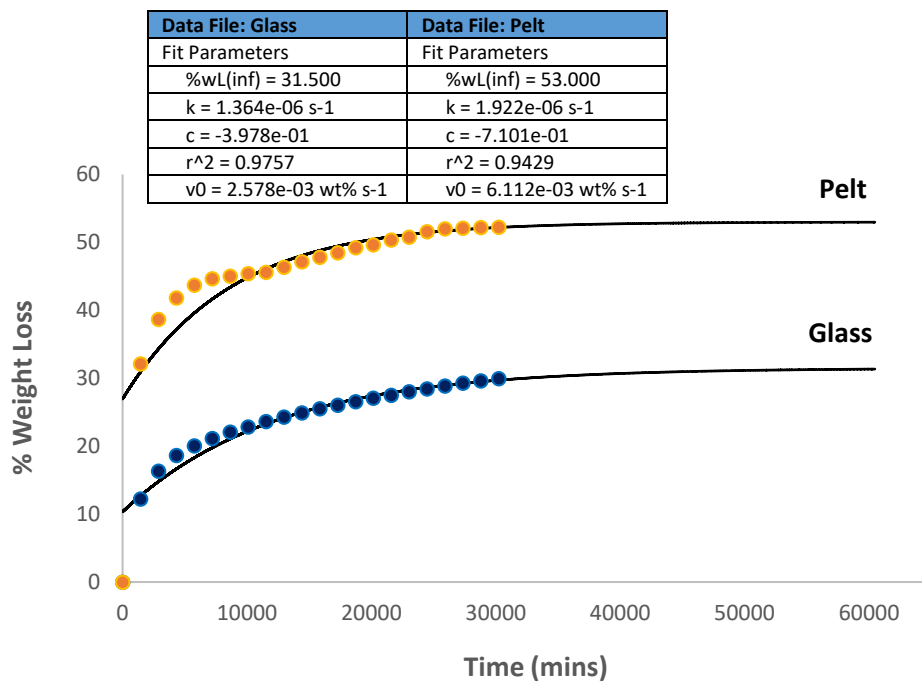


Figure 30. Comparative evaporation profiles of Ikan Pari from glass and pelt over ~21 days, at a controlled temperature of 20 ± 1 °C, showing the OilVap fit curves for the data presented in **Figure 29**. Note that 1 day = 1,440 minutes. The inset gives the OilVap output data for the relevant plateau, fit and rate parameters for each curve.

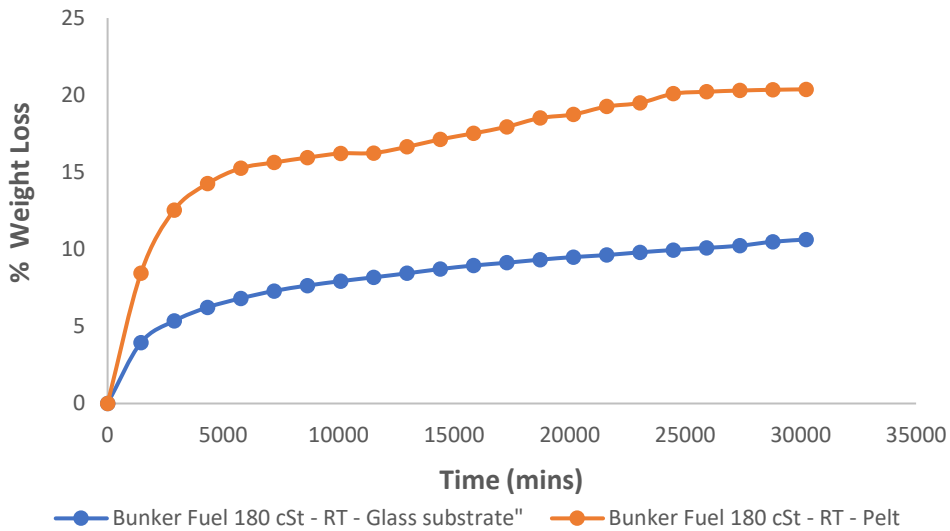


Figure 31. Comparative evaporation profiles of Bunker Fuel Oil 180 cSt from pelt and glass over ~21 days, at a controlled temperature of 20 ± 1 °C. Note that 1 day = 1,440 minutes.

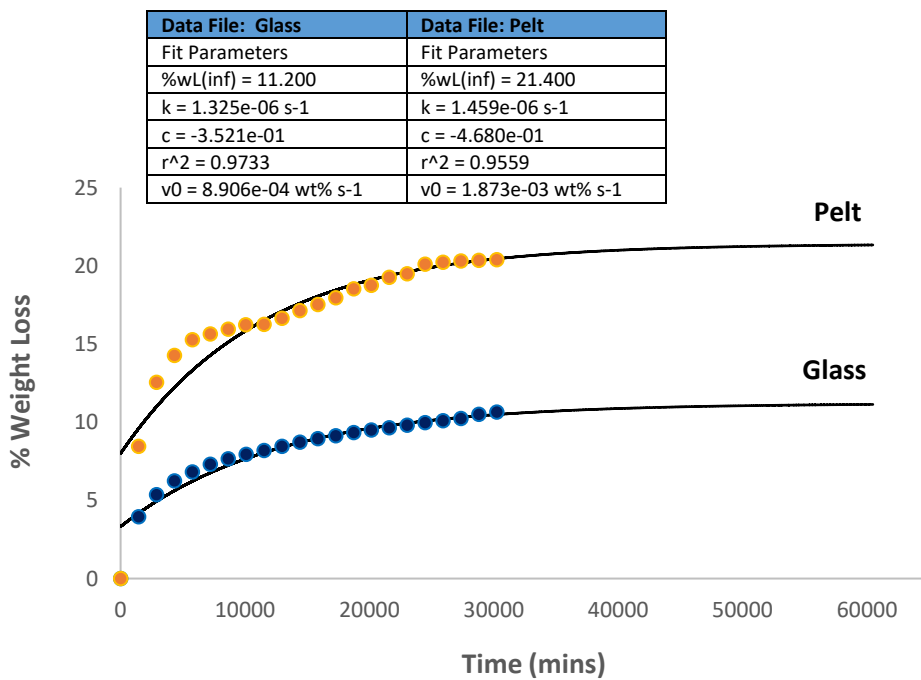


Figure 32. Comparative evaporation profiles of Bunker Fuel Oil 180 cSt from glass and pelt over ~21 days, at a controlled temperature of 20 ± 1 °C, showing the OilVap fit curves for the data presented in **Figure 31**. Note that 1 day = 1,440 minutes. The inset gives the OilVap output data for the relevant plateau, fit and rate parameters for each curve.

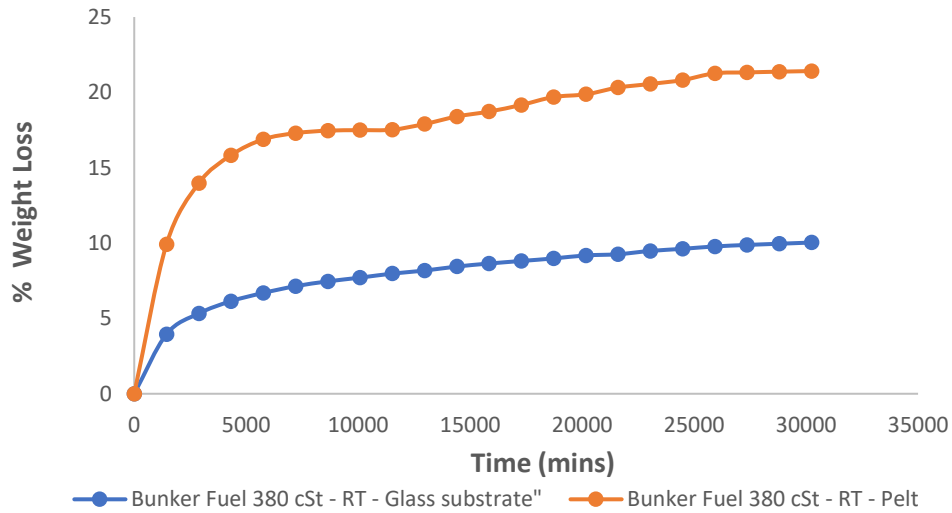


Figure 33. Comparative evaporation profiles of Bunker Fuel Oil 380 cSt from pelt and glass over ~21 days, at a controlled temperature of 20 ± 1 °C. Note that 1 day = 1,440 minutes.

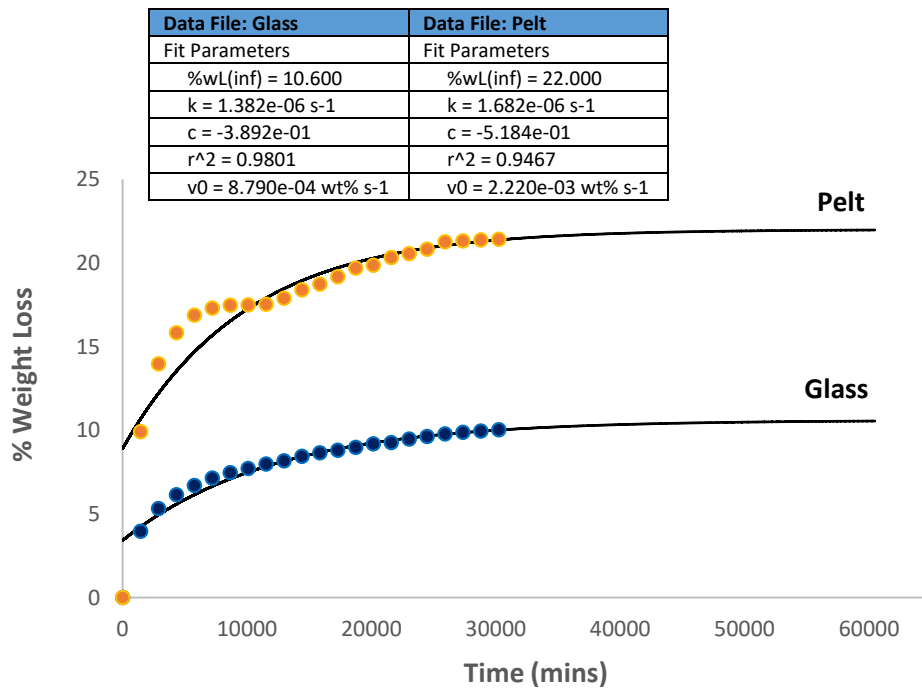


Figure 34. Comparative evaporation profiles of Bunker Fuel Oil 380 cSt from glass and pelt over ~21 days, at a controlled temperature of 20 ± 1 °C, showing the OilVap fit curves for the data presented in **Figure 33**. Note that 1 day = 1,440 minutes. The inset gives the OilVap output data for the relevant plateau, fit and rate parameters for each curve.

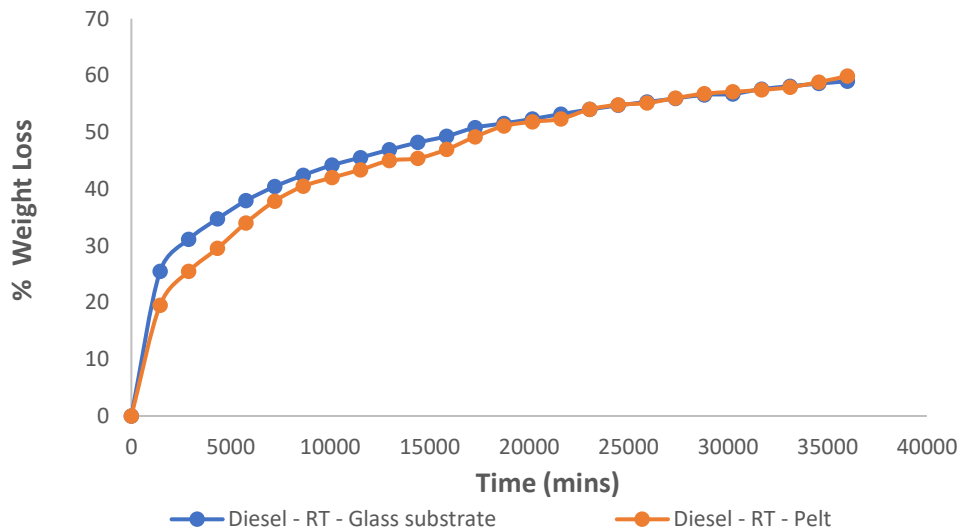


Figure 35. Comparative evaporation profiles of Diesel from pelt and glass over ~21 days, at a controlled temperature of 16 ± 1 °C. Note that 1 day = 1,440 minutes.

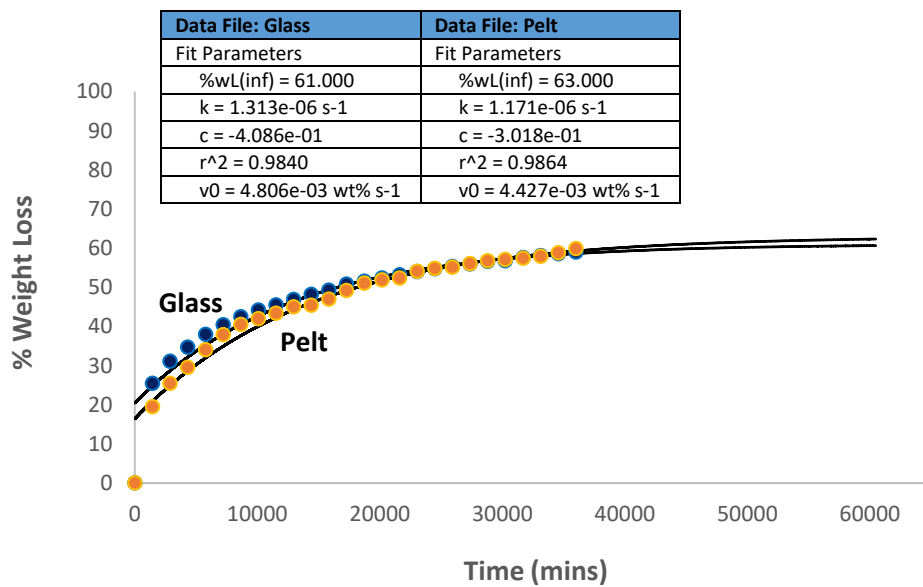


Figure 36. Comparative evaporation profiles of Diesel from glass and pelt over ~21 days, at a controlled temperature of 16 ± 1 °C, showing the OilVap fit curves for the data presented in **Figure 35**. Note that 1 day = 1,440 minutes. The inset gives the OilVap output data for the relevant plateau, fit and rate parameters for each curve.

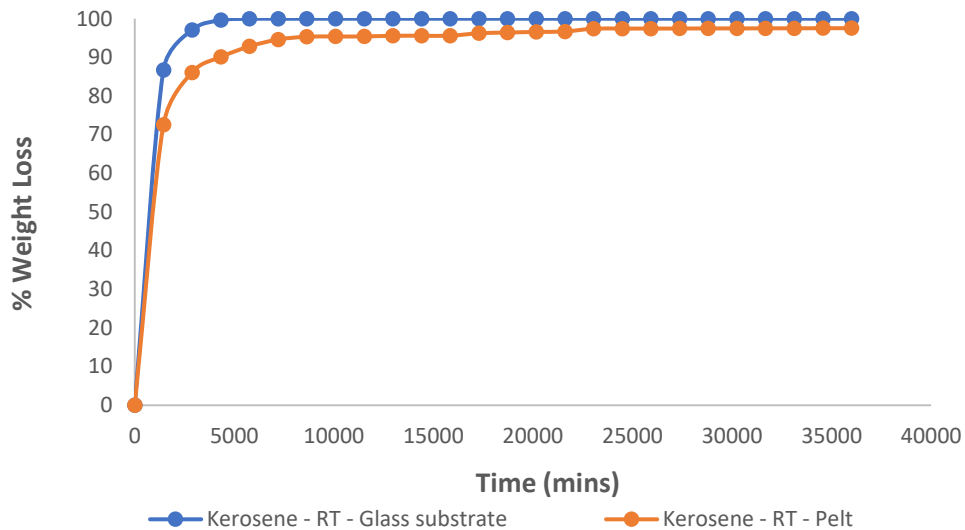


Figure 37. Comparative evaporation profiles of Kerosene from pelt and glass over ~21 days, at a controlled temperature of 16 ± 1 °C. Note that 1 day = 1,440 minutes.

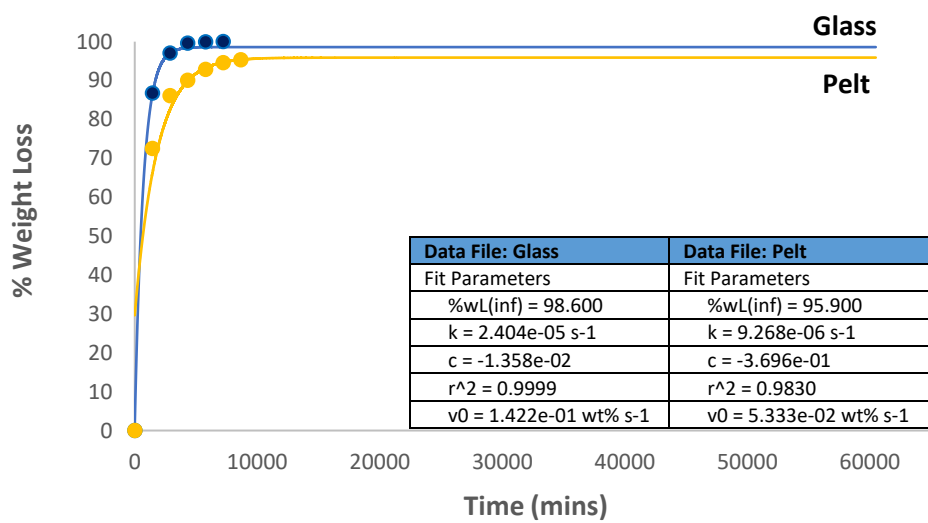


Figure 38. Comparative evaporation profiles of Kerosene from glass and pelt over ~21 days, at a controlled temperature of 16 ± 1 °C, showing the OilVap fit curves for the data presented in **Figure 37**. Note that 1 day = 1,440 minutes. The inset gives the OilVap output data for the relevant plateau, fit and rate parameters for each curve.

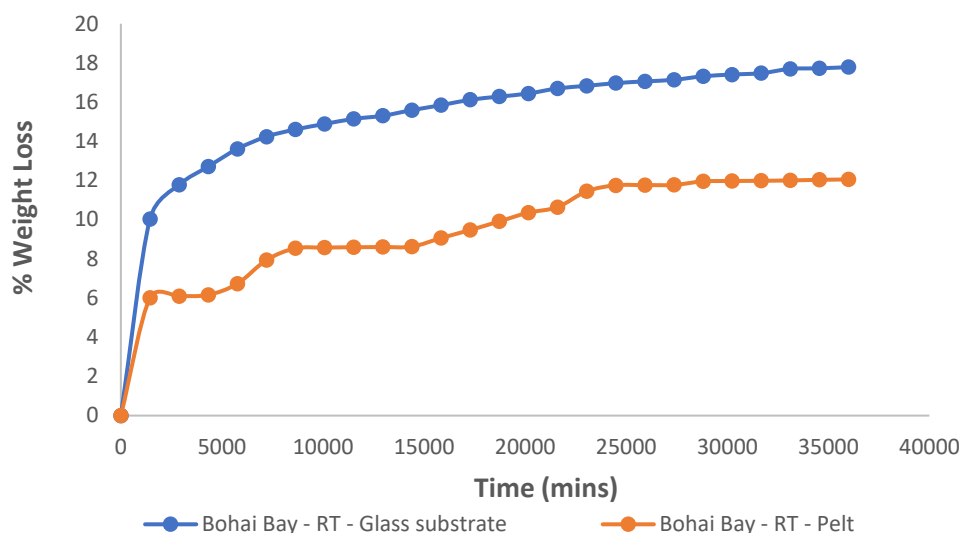


Figure 39. Comparative evaporation profiles of Bohai Bay from pelt and glass over ~21 days, at a controlled temperature of 16 ± 1 °C. Note that 1 day = 1,440 minutes.

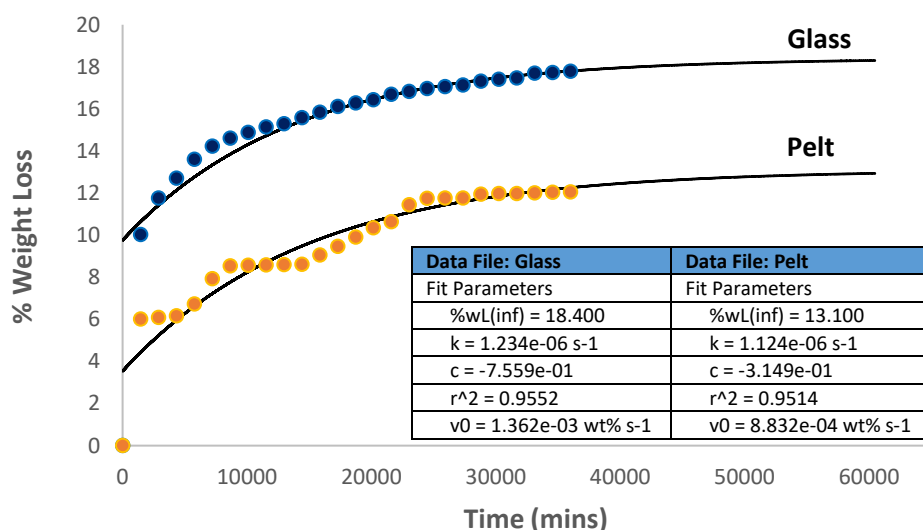


Figure 40. Comparative evaporation profiles of Bohai Bay from glass and pelt over ~21 days, at a controlled temperature of 16 ± 1 °C, showing the OilVap fit curves for the data presented in **Figure 39**. Note that 1 day = 1,440 minutes. The inset gives the OilVap output data for the relevant plateau, fit and rate parameters for each curve.

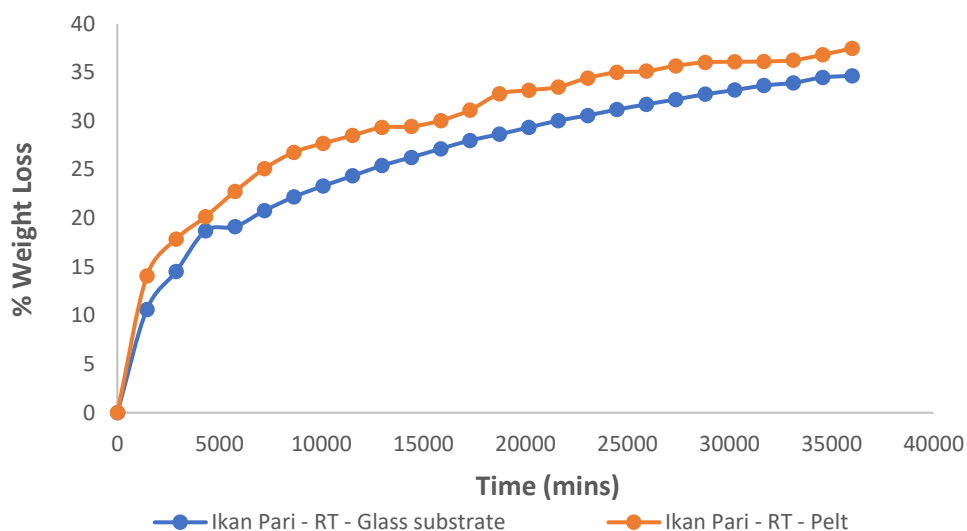


Figure 41. Comparative evaporation profiles of Ikan Pari from pelt and glass over ~21 days, at a controlled temperature of 16 ± 1 °C. Note that 1 day = 1,440 minutes.

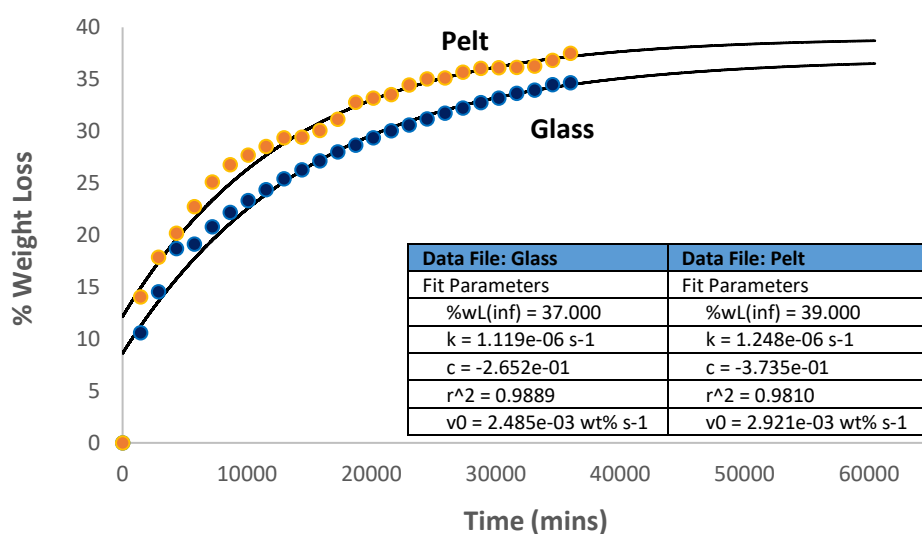


Figure 42. Comparative evaporation profiles of Ikan Pari from glass and pelt over ~21 days, at a controlled temperature of 16 ± 1 °C, showing the OilVap fit curves for the data presented in **Figure 41**. Note that 1 day = 1,440 minutes. The inset gives the OilVap output data for the relevant plateau, fit and rate parameters for each curve.

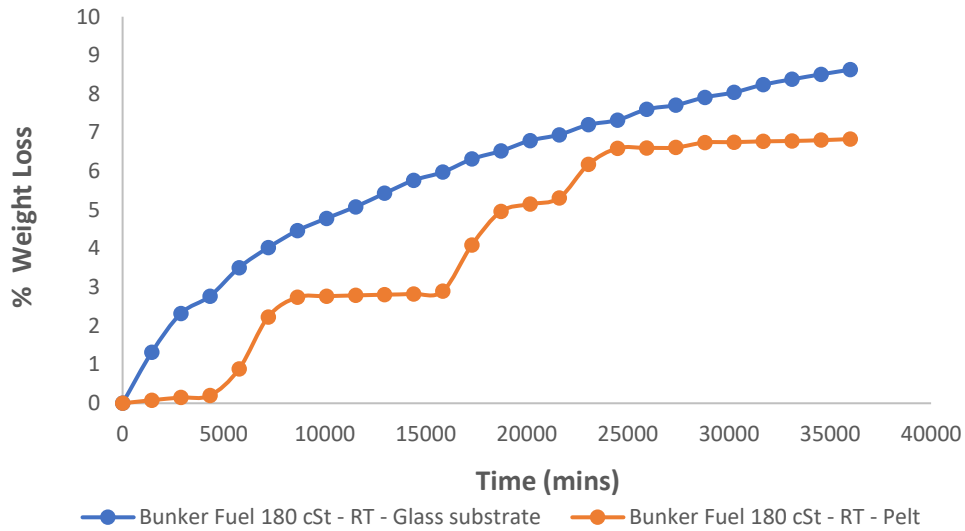


Figure 43. Comparative evaporation profiles of Bunker Fuel 180 cSt from pelt and glass over ~21 days, at a controlled temperature of 16 ± 1 °C. Note that 1 day = 1,440 minutes.

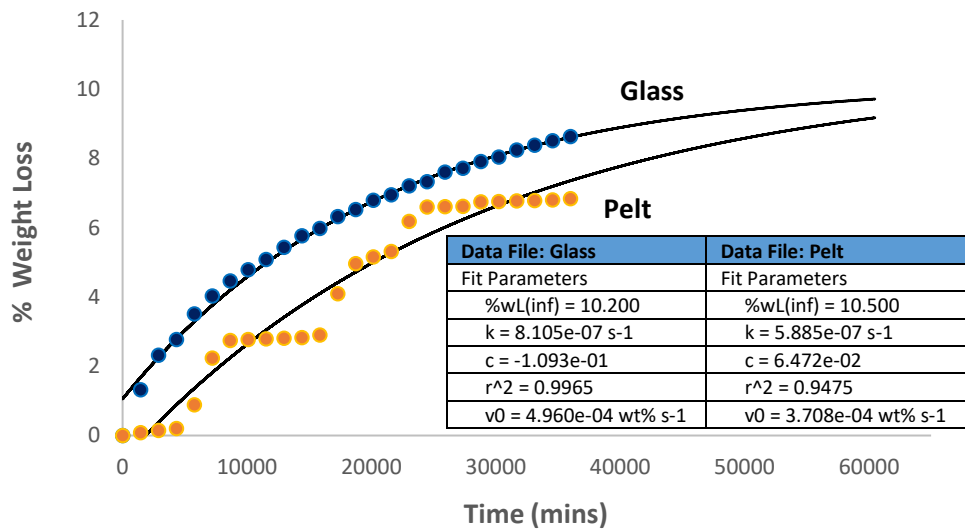


Figure 44. Comparative evaporation profiles of Bunker Fuel 180 cSt from glass and pelt over ~21 days, at a controlled temperature of 16 ± 1 °C, showing the OilVap fit curves for the data presented in **Figure 43**. Note that 1 day = 1,440 minutes. The inset gives the OilVap output data for the relevant plateau, fit and rate parameters for each curve.